Acta Geologica Hungarica

VOLUME 37, NUMBERS 1–2, 1994

Akadémiai Kiadó, Budapest

ACTA GEOL. HUNG. 37(1–2) 1–185 (1994) HU ISSN 0236–5278

ACTA GEOLOGICA HUNGARICA

A QUARTERLY OF THE HUNGARIAN ACADEMY OF SCIENCES

Acta Geologica Hungarica publishes original studies on geology, crystallography, mineralogy, petrography, geochemistry, and paleontology.

Acta Geologica Hungarica is published in yearly volumes of four numbers by

AKADÉMIAI KIADÓ
Publishing House of the Hungarian Academy of Sciences

H–1117 Budapest Prielle Kornélia u. 19–35

Manuscripts and editorial correspondence should be addressed to the

ACTA GEOLOGICA HUNGARICA

Dr. János Haas
Academical Research Group, Department of Geology, Eötvös Loránd University of Sciences
H–1088 Budapest, Múzeum krt. 4/a, Hungary
E-mail: haas@ludens. elte. hu

Orders should be addressed to

AKADÉMIAI KIADÓ
H–1519 Budapest, P.O. Box 245, Hungary

Subscription price for Volume 37 (1994) in 4 issues US$ 84.00, including normal postage, airmail delivery US$ 20.00.

Acta Geologica Hungarica is abstracted/indexed in Bibliographie des Sciences de la Terre, Biological Abstracts, Chemical Abstracts, Chemie-Information, Hydro-index, Mineralogical Abstract

Acta Geologica Hungarica, Vol. 37/1–2, pp. 1–15 (1994)

Geologist József Fülöp

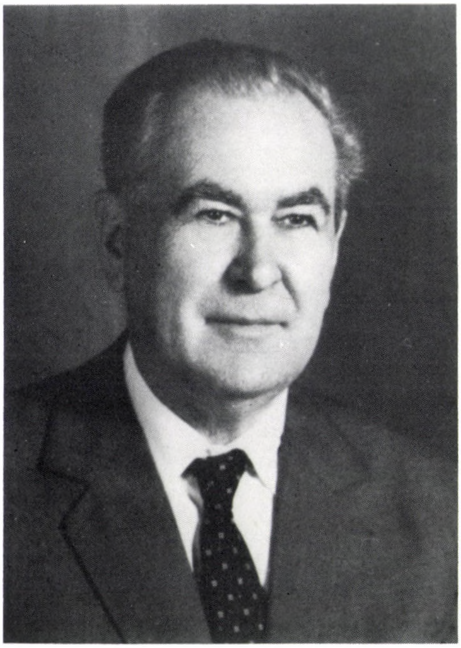

20 January 1927 – 13 April 1994

With the death of József Fülöp the Hungarian and international earth science communities have lost an outstanding scientist, and the higher levels of Hungarian geological education a school-creating teacher. Apart from his family, friends, colleagues, and students, his memory will also be kept alive by Hungarian and international earth sciences scholars.

He was born in Bük, Vas County, Hungary as the first child of joiner József Fülöp. He attended secondary school in the higher elementary school at Kapuvár and in the Sopron commercial grammar-school between 1938 and 1946.

In 1946, he registered at the geography-economics teaching faculty of the Pázmány Péter University of Sciences; thereafter, his interest turned more and more toward mineralogy and later on toward geology, and he finished his studies as a geologist in 1952.

At the Department of Geology of the Eötvös Loránd University of Sciences (ELTE), he began his profession as an assistant. His fascinating scientific career was initiated by professor Vadász Elemér's supporting inspiration and guidance.

Because of his interest in stratigraphy, as an aspirant he received the task of investigating the Cretaceous formations of the Gerecse Mountains. He presented a summary of the results of his work in a monograph published in the series of Geologica Hungarica (Ser. Geol. Tom. 11, 1958) and was awarded a candidate's degree in 1957. He showed continued interest for the Cretaceous of the Gerecse Mountains throughout his entire life (it was just one day before his death that he received with great pleasure the exceptionally rich fossil material found during the explosions of the mine at Berzsekhegy and collected by one of his colleagues working there).

0236–5278/94/$ 4.00 © 1994 *Akadémiai Kiadó, Budapest*

Later, he extended his investigations over other areas of Cretaceous formations of Hungary as well. The monography "Lower Cretaceous (Berriasian–Aptian) formations of the Bakony Mountains" (Unterkreide-Bildungen (Berrias–Apt) des Bakony-gebirges) (Geologica Hungarica Ser. Geol. Tom. 15, 1964) was compiled on the basis of his academic doctoral dissertation (1962). Besides the monographs "Cretaceous formations of the Villány Mountains" (Les formations crétacées de la Montagne Villány) (Geologica Hungarica Ser. Geol. Tom. 15, 1966) and "The Mesozoic Basement Horst Blocks of Tata" (Geologica Hungarica Ser. Geol. Tom. 16, 1975; in English: Geologica Hungarica Ser. Geol. Tom. 16, 1976), his studies describing the Jurassic and Cretaceous formations of Tata, the Vértes and Bakony Mountains, his papers revealing the boundary problems of the Triassic, Jurassic, and Cretaceous, as well as his works summing up the results of the investigation of the Mesozoic of Hungary, show his desire to widen the range of his quest for knowledge more and more, both in time and in space.

He considered it natural, beside elaborating the principles of earth sciences, to exploit his enormous knowledge for economic purposes, i.e. the exploration of mineral resources. While studying the younger Mesozoic formations, he realized the necessity of conducting palaeoenvironmental investigations, palaeoreconstructions, and of preparing palaeogeographic maps explaining the genesis of mineral resources. In the area of the Transdanubian Range, he strived for a graphic (map) representation of the palaeogeographic - genetic connections of bauxite formation and for the scientific foundation of regional bauxite prognostications. Resulting from this inner demand, he and his colleagues constructed the maps "Map of usable mineral materials of Hungary" (1966) and "Uncovered geological map of Palaeozoic and Mesozoic formations of Hungary" (1967) at 1:500 000 scale, the first to be supported by an extensive database. Later, this ambition led (far beyond the call of his official duty) to the compilation of the volumes evaluating the raw material resources of the country. His richly-documented works, of treatise character and of continued value even to this day: "The black coal resources of Hungary" (1980), "The hydrocarbon resources of Hungary" (1982), "The iron ore, manganese ore, as well as, copper ore, lead ore, and zinc ore resources of Hungary" (1983), "The bauxite resources of Hungary" (1984), are fundamental in the scientifically established recognition and evaluation of the raw material potential of Hungary. Assuming tremendous scientific and economic/political responsibility, he was the first to publish data on the mineral resources of Hungary – senselessly qualified top secret at that time.

In the course of time, his scientific life-work extended to the methodology of geologic activity, the investigation of the major tectonic settings of Hungary, the theoretical questions of stratigraphic classification, questions of geology related to the history of science, the palaeoarchaeological connections of geology, and the timeliness of environmental protection; he made his mark as a scholar in all of these fields.

He regarded as a fundamental method of geological research, geologic surveying work and the even more valuable geologic field mapping, map plotting, and map publishing. The results of his research activity in this direction are documented by the director's reports of the Hungarian Geological Institute (1958–1969), his papers on the history of geologic mapping (1959, 1968, 1969), his essays urging the investigation of sedimentary formations (1954, 1967, 1969), the series of maps and atlases constructed by him, or under his vocational guidance and upon which he left his mark as Editor-in-Chief or Responsible Editor.

The novelty and pioneering character of this grandiose work on a global scale are represented by:

– the depth of preparation (evaluation of all previous literature and data on mapping);

– the network of completed surveys based on map-sheet sections, and its detailed scale (in mountainous areas at 1:10 000 or 1:25 000, in hilly country and flatland at 1:100 000);

– the precisely documented surveying work, always supported by studies of surface outcrops, by shallow, structural, exploratory and geological key boreholes, later enriched by geophysical mapping methods (1963), and by regular air photo and space image interpretations (1968); along with the surveys, his conclusions on agricultural, building geology, hydrogeologic, raw material exploration, environmental protection and nature conservation matters;

– the expansive testing of geologic concepts and material, which established the stratigraphical, structure geologic, magmatic, genetic, faciological, and applied geologic conclusions, with a database of suitable density;

– the permanent separation of documentable, objective, and observed data from the subjective, conceptual, and constructed elements, by means of map sheets covering the entire spectrum of the surveying work, and the final publishing, for each map sheet area, of at least two, and as many as 21, varieties, of atlas quality;

– the recording of surface sample material and drilling core material, to ensure the reproducibility of the entire research programme and the subsequent accomplishment of further, specialized investigations;

– the publishing of explanatory notes for map sheets at different scales, as well as producing the related monographic summary, according to regions, periods, and disciplines.

The simultaneous application of these seven points was considered a real novelty in the methodology of geological mapping.

The basic research-level investigation of stratigraphic questions in Hungary passes through the scientific life-work of József Fülöp like a thread. Besides his initial research, as Chairman of the Hungarian Stratigraphic Committee (1970–1991) he took part in the work of stratigraphic revision relating to international programmes (f.i. as the Editor-in-Chief of the volume "Lexique Stratigraphique International Europe - Hongrie" - Paris, 2nd edition 1978). His theoretical activity in Hungary is documented by papers on this subject (1972, 1984), the proceedings "Guide of stratigraphic classification, nomenclature, and their usage" (1976), the 286 formation-rank units of the comprehensive table "Lithostratigraphic formations of Hungary" (1st edition 1983) initiated by him, and the bulk of background material unpublished to the present day. His main intention was the establishment of the conceptual and content unity of equivalent litho-, bio-, and chronostratigraphic systems, established on reliable foundations. This aim was served by the National Key Section Project which he initiated, as a result of which, in 1994, 357 surface sections and 261 key borehole sections were established. He personally put enormous effort into the completion of this complex elaboration, now considered a standard of its kind.

The variety of his scientific activity is demonstrated by his essays on the history of science, on the occasion of the 90th anniversary, then the centenary, of the Hungarian Geological Institute (1959, 1969), on the life-works of geologists Lajos Lóczy Sr. and Elemér Vadász, regarded as models of their kind (1970, 1977 and 1960, 1970, 1983 respectively), and on the history of raw material exploration in Hungary (1978, 1982, 1984). He discovered the first palaeolithic chert quarries of Hungary on Kálváriadomb Hill near Tata and Mogyorósdomb Hill near Sümeg (1958); he elaborated and published the material of these localities, of outstanding importance from the point of view of palaeo-archaeology and the history of the mining industry (1971, 1973, 1975). Ahead of his time, he already recognized in 1954 the necessity of the protection of natural geologic sites (1954, 1960, 1967, 1984). Following his proposal, in 1958 the Tata, and in 1976 the Sümeg area were declared nature conservation areas. He also supported the protection of the areas near Darvastó, Ipolytarnóc, and Rudabánya. His results of less glamorous but of all the greater significance are the declaring as protected of 368 geological exposures (mostly geological key sections or reference sections) of local, regional, or national importance in the territory of Hungary.

One of the objectives of his scientific research career (perhaps the most important one) was the composition of a "Geology of Hungary". He was partly encouraged to fulfill the task by professor Elemér Vadász, who was critical of his own manual on this subject (1953, 2nd revised edition 1960). From the beginning of his career as a geologist, József Fülöp had prepared consciously for this task, by means of literature studies, field and material investigations, and synthesizing work. His objectives were the critical evaluation of the knowledge accumulated during the decades, the systematic filling of knowledge gaps by key section exploration, collecting, material investigation, evaluation work and correlation programmes (also beyond the national boundaries), and finally the publishing of a comprehensive, monograph-like, detailed series of books for use both as manuals and text-books.

His activity of almost two and a half decades in this field, which he usually pursued after finishing his daily routine with preterhuman diligence and endurance, was characterized by the aims of completeness and extreme particularity in the course of investigating, writing, compiling, typographical preparation, and the typographical technical operations. He drew into this activity excellent representatives of the earth sciences: a series on outstanding partial studies, specialized monographs, and professional articles were published under the inspiring influence of this co-operation. Because of his early and sudden death, only the first four volumes of the work planned for eight volumes could appear ("The history of mineral resources in Hungary", Műszaki Kiadó, 1984; "Introduction to the geology of Hungary", Akadémiai Kiadó, 1989; "Geology of Hungary, Palaeozoic I." Hungarian Geological Institute 1989; "Geology of Hungary, Palaeozoic II." Akadémiai Kiadó, 1994), the latest some days before his death. The humility and respect for his profession, his working method and life-style are reflected by the tragic end. He was eager that his friends and colleagues should possess this book as soon as possible. He died while personally presenting it in the Museum of Natural Sciences. His life-work is unique and irreproducible, truncated as it is. His books will still be used by generations as fundamental works. The co-authors he had called upon can only make an attempt at writing the further supplemental volumes.

Apart from his already mentioned qualifications, the recognition of his scientific results is hallmarked by the corresponding (1967), then ordinary (1976) membership of the Hungarian Academy of Sciences (H.A.S.), the Szabó József medal (1969) and the Hantken Miksa medal (1981) of the Hungarian Geological Society; the corresponding membership (1975) of the Geologische Bundesanstalt (Austrian Geologic Survey), the corresponding membership of the Austrian Academy of Sciences (1980), as well as the honorary membership of the Association of Hungarian Geophysicists (1971), Hungarian Geologic Society (1981), Hungarian Geographic Society (1981), Austrian Geologic Society (1980), and the Bulgarian Geologic Society (1981). For his outstanding work performed in the cause of geological research he received the title of Eminent Worker of Geologic Research (1957), for his distinction gained in the field of exploring for raw materials he won the State Prize (1983), for his achievements in the field of geologic environmental protection he was honoured with the Pro Natura Prize (1976).

This rich course of life makes it incumbent upon us to present the activity of József Fülöp in organizing research – without making any claims to completeness.

This field of his activity, in which he also left his mark as a scholar, resulted partly from a sense of responsibility towards his beloved profession, animated by inner motives and the wish for the application of the results of geology for the public good, and partly from the role in public life demanded by the age and society.

The state tasks, the organization and the financing of geological research of which had fallen into disarray during the hard times of the two world wars, economic crises, and changes of regime, returned to normal following the decisions of the Research Council in 1955. For a short time, József Fülöp, as the Geologic Clerk of the Secretariat of the Council of Ministers, could contribute significantly to the preparation of the decisions regarding these tasks over a longer term. As the Assistant Director (1956–1958), then the Director (1958–1969) of the Hungarian Geological Institute he could further formulate the guiding principles of Hungarian geologic research and the classification of the fields of research. In the Institute, he set as an objective the regional concentration of research activities, the increase of sample testing, and the modernization of documentation work in the trinity of analysis-synthesis-publishing. As fundamental scientific method, he urged long-range planned work, geologic mapping and the regional geophysical research promoting it, complex material testing, as well as the compiling of comprehensive, thematic monographs.

He had field mapping designated as the principal task, carried out in the areas (of primary importance from a raw material exploration point of view) of the Eastern Mecsek Mountains (coal, lignite, uranium ore), Northern Bakony Mountains (bauxite, manganese ore, lignite), Dorog Basin (lignite), Mátra Mountains (non-ferrous ores), Tokaj Mountains (mixed mineral material), as well as of the Hungarian Great Plain (water, agriculture, building geology). He found solutions to necessary laboratory developments (sedimentology, petrophysics, soil mechanics) and to the problems of storing field documentation material and drilling core samples, the quantity of which was rapidly increasing (Rákóczibányatelep, Szolnok, Pécs-Vasas, Szépvizér).

Simultaneously, he was able to improve and continuously modernize his own conceptions. This is shown by the introduction of geochemical research in the Institute (1962) and the conceptual establishment of engineering geological-building geological mapping programmes (1963).

On the basis of the efforts made by him to utilize the scientific results of the Institute, under his directorship (lasting little more than 10 years) 149 geological maps, almost 50 individual volumes, and more than 350 papers and studies were issued as publications of the Institute. The system of reporting sessions he called into life in 1961 aimed at initiating the wider professional community into the programmes of the Institute. Through his activity, the Institute became the scientific workshop of a wide spectrum of Hungarian basic and applied geologic research. Thanks to this activity, a large number of the research staff obtained scientific qualifications under his inspiration. Also, by this activity, he ensured for more than three decades the primacy of the work of the Research Institute in the field of geology in Hungary.

Between 1968 and 1984, as the Chairman of the Central Geologic Office he had the possibility to execute and at least partly improve the National Long-Term Research Plan (1965, 1966, 1967), the first such plan in the history of geologic research, elaborated by him in 1961. Besides defining long-term conceptions, he urged the preparation and scholarly discussion of long-term and middle-range research programmes, to be worked out professionally and in detail, as well as concentrating on the restricted financial means imposed even then on the most important matters.

His efforts also met with support in the circles of his fellow-scientists in the Hungarian Academy of Sciences (H.A.S.). Between 1977 and 1980, as the Vice-Chairman of the Academy, then as member of the Presidium, he was one of the initiators and leaders of elaborating the ministry-level research proposal "Researching and exploring the Natural Resources of Hungary", later raised to national rank (1970, 1975, 1977, 1979, 1982, 1983). The situation report brochures, richly illustrated and presenting the geologic resources of the country, were edited by him. Between 1985 and 1991, he was the Chairman of the Geological Scientific Committee of the 10th Department (Earth Sciences) of the H.A.S. Under his guidance, the Committee constructed and published detailed analytical reports on the situation of Hungarian geology, searching for new directions of activity.

As Editor-in-Chief, then from 1985 until his death as the Chairman of the Editorial Board, he initiated and carried through the modernization in content and form of the quarterly Acta Geoogica Hungarica and the reformation of its editing (1983). József Főlöp displayed significant research- organizing activity in the Committee on Interdisciplinary Problems of the Presidium of the H.A.S., in the Energetical Scientific Committee of the Academy, in the Committee on the Social Effects of Science and Technology, as Chairman of the Subcommission on Natural Sciences of Hungarian UNESCO Committee and the National Commission on Mineral Reserves. From 1971 until his death, he was the head of the Geologic Research Group of the H.A.S. in the Geology Department of the ELTE, which had been established by him and which he regarded as his own personal workshop, where his creativity could finally emerge in all its admirable integrity.

Outstanding results also accompany the course of his life in the field of international cultivation and organization of the earth sciences. The international programmes he organized in honour of the 90th anniversary (1959), and then the centenary (1969), of the Hungarian Geologic Institute, made several hundreds of dignified foreign experts decisively acquainted with the so far less- known results of Hungarian earth science. He also established a whole series of extensive personal and institutional connections, which have survived him. Personally, he was most active in the pursuit of Rumanian, French (1964), Austrian (1978), and German (1984) professional co-operations. He played a decisive role in bringing into existence the Cuban-Hungarian geologic mapping expeditions (1972-1990) initiated by the H.A.S. He was an active participant of the Jurassic Colloqium in Luxembourg (1962), the Early Cretaceous Colloqium in Lyon (1964), the Late Jurassic Symposium in Moscow (1967), the Mediterranean Jurassic Colloqium in Budapest (1969) and a member of three Geologic World Congresses (1960, Copenhagen; 1964, New-Delhi; 1968, Prague). He represented Hungary, between 1960 and 1968, as the Chairman of the Committee on the Mediterranean Mesozoic of the International Geologic

Congress, between 1960 and 1964 on the Editorial Board of "Tectonic Map of Europe" (at 1:2,500,000 scale) of the Geologic World Map Committee, and between 1958 and 1978 on the Editorial Board of the International Stratigraphic Lexicon (Lexique Stratigraphique International).

His efforts to promote interest in science were reinforced by the desire to make known and public property the scientific achievements of geology, by publishing popularizing articles, making presentations on the locations of the treasures of nature (Tata, Sümeg), organizing a series of open reporting sessions, conferences, and displaying enormous publicistic activity. His fundamental objective was to modernize and raise Hungarian geology to an international level; by doing this, he wished to promote the national utilization of the scientific results and natural resources, especially on the level of those decisions which relate to long-term planning, raw material policy, agriculture, building geology, nature conservation and practical economic life. Characteristically for the age, his gigantic efforts were sometimes crowned with spectacular success, at other times his impetus was broken by the strongholds of bureaucracy, lack of professionalism or of understanding, and occasionally maliciousness and human frailty.

However, his life-work is complete. As a natural-born teacher, he could give full vent to his innermost desires, and forget his failures. The desire for the conveying and handing on of knowledge set him on his way as an assistant at the Geology Department of the ELTE. In 1953, he kicked off the summer teaching field exercises, the culmination of which (since 1978) has been constituted by the one-month intensive teaching courses in summer at the world-level educational center he established in the Sőmeg nature conservation area. These courses were attended not only by students of geology and geophysics from ELTE, Budapest, but also by those from the Heavy Industries Polytechnic University of Miskolc, and the József Attila University of Sciences of Szeged.

In 1970, as a university professor, he took over the teaching of the subject "Geology of Hungary" from his professor, Elemér Vadász. His teaching activity was characterized by the extremely accurate conveyance of knowledge, reaching back to the roots, the self-confident, systematic and critical-minded manner of lecturing of a practicing geologist, and the high quality of his textbooks. In spite of his varied occupations as the Chairman of the Central Geologic Office, his intense relationship with education never ceased. Besides the professional questions of higher education, he showed great concern about the general educational role and situation of geology, and the necessity of teaching earth sciences in secondary schools. In the interest of this goal, he put together a large collection of foreign secondary school books on the subject of natural sciences. For him, education and university life were vital elements, active forms of relaxation, and the most important way of establishing and maintaining human relations.

He was appointed Rector of the ELTE in 1984. The main stations of his self-sacrificing work, performed throughout the duration of two terms, are as follows: the organization of the 350-year jubilee celebration of the University, the visible achievements of university expansion at Lágymányos, within the framework of the reconstruction of the University, the establishment of the Rectors' Conference, the (mostly) successful solving of pressing problems, and the accomplishment of daily tasks in an extremely difficult period of time. A rare and gratifying pleasure for him was the honouring of his teaching and university-developing activity, with the Gold Medal of ELTE (1990). A more imperishable recognition is represented by the number of his disciples. Two of his close colleagues work as professors and heads of department, and three of them, as titular university professors, continue his teaching work, trying to transmit his fanatic love for his profession, his exactitude and his creativity to future generations, and, what is next to impossible, to show the wonderful variety and grandeur of the puritan, self-denying, constructive, creative, instructing, scientific MAN, tirelessly investigating the world of nature.

Literary life-work of József Fülöp (1954-1994)

1. – 1954: A tatai mezozóos alaphegységrög földtani vizsgálata (Examen géologique de la motte mésozoique de Tata. In Hungarian with French and Russian abstracts.). – Földt. Közl., 84, 4, pp. 309–325.
2. – et al. 1954: A bakonybéli glaukonitos terület földtani és kémiai vizsgálata (The geological and chemical investigation of the glauconitic area at Bakonybél. In Hungarian.). – Földt. Közl., 84, 4, pp. 326–330.
3. – 1958: A Gerecsehegység krétaidőszaki képződményei (Die Kretazischen bildungen des Gerecse Gebirges. In Hungarian and German with Russian abstract). – Geol. Hung. Ser. Geol., 11, pp. 1–122.
4. – et al. 1958: Hongrie – Ungarn. "Lexique Stratigraphique International" Európa. – Fasc. p. Paris, pp. 69–70, 74–74, 134.
5. – et al. 1959: Les formations cretacees de la Hongrie Congreso. – Geologico International XX Sesion – Ciudad de Mexiko, 1956. Simposium del Cretacico pp. 221–251.
6. – 1959: A Magyar Állami Földtani Intézet által rendezett Nemzetközi Mezozóos Konferencia (Die internationale Mesozoische Konferenz der Ungarischen Geologischwn Austalt. In Hungarian, French, German, and Russian.). – MÁFI Évk., XLIX, 1, p. 4.
7. – 1959: A Magyar Állami Földtani Intézet kilenc évtizede. pp. 11–23. (Neun Jahrzente der Ungarischen Geologischen Anstalt In Hungarian, French, German, and Russian.). – MÁFI kiadv., pp. 45–51.
8. – 1959: Magyarország kréta időszaki képződményei. (Formations crétecées de le Hongrie. In Hungarian, French, and Russian.). – MÁFI Évk., XLIX, 3, pp. 577–731.
9. – et al. 1959: A Gerecse-, Vértes- és Bakonyhegység mezozóikuma. Kirándulás a Magyarországi Mezozóos Konferencia résztvevői számára (Das Mesozoikum des Gerecse-, Vértes- und Bakony-Gebirges. Führer den Ausflügen für die Teilnehmer der Konferenz über das Ungarische Mesozoikum. In Hungarian, French, and German.). – Guide, pp. 23–27.
10. – et al. 1959: A Mecsek- és Villányi hegység mezozóikuma (Das Mesozoikum des Mecsek- und Villányer Gebirges. In Hungarian, French, German, and Russian.). – Guide, pp. 52–59.

11. – et al. 1960: A Vértes-hegység juraidőszaki képződményei. (Über die Jurabildungen des Vértesgebirges. In Hungarian with German and Russian abstracts.). – Földt. Közl., 90, 1, pp. 15–26.
12. – 1960: Vadász Elemér 75 éves! (Au soixante-quinziéme aniversaire du Professor Elemér Vadász. In Hungarian and French.). – Földt. Közl., 90, 1, pp. 3–7.
13. – 1960: Őstengerek állatvilágának maradványai a Dunántúlon. In: "Védett természeti ritkaságaink" (Remnants of the fauna of palaeoseas in Transdanubia. In: "Our protected natural rarities". In Hungarian.). – Mezőgazdasági Kiadó, pp. 113–120, Budapest.
14. – 1960: A Föld kialakulása, fejlődése és az ásványkincsek keletkezése. (Development and evolution of Earth, and the formation of mineral resources. In Hungarian.). – TIT kiadv., pp. 1–24, Budapest.
15. – 1961: Igazgatói jelentés az 1957–58. évről, (Compte rendu du directeur sur les Années 1957–58. In Hungarian, French, and Russian.). – MÁFI Évi Jel., 1957–58 -ról, pp. 3–5.
16. – 1961: A bakonyhegységi alsó-kréta (Le crétacé inférieur de la montagne Bakony. In Hungarian with French and Russian abstracts.). – MÁFI Évi Jel., 1961 -ről, I, pp. 228–246.
17. – et al. 1962: Mezsdunaródnaja tektonicseszkaja karta Evropi. 1:2,500.000. – Moszkva 1962.
18. – 1962: Igazgatói jelentés az 1959. évről. (Compte rendu du directeur sur l'année. In Hungarian, French, and Russian.). – MÁFI Évi Jel., 1959. -ról, pp. 3–5.
19. – 1962: A Magyar Állami Földtani Intézet tevékenysége az 1961. évben (Activity of the Hungarian Geological Institute in 1969. In Hungarian.). – Földt. Közl., 92, 3, pp. 337–338.
20. – 1963: Igazgatói jelentés az 1960. évről. (Compte rendu du directeur sur l'année 1960. In Hungarian, French, and Russian.). – MÁFI Évi Jel., 1960 -ról, pp. 3–5.
21. – 1964: A Bakonyhegység alsó-kréta (berriazi–apti) képződményei (Unterkreide-Bildungen (Berrias-Apt) des Bakony-gebirges. In Hungarian and German with Russian abstract.). – Geol. Hung. Ser. Geol., 13, pp. 1–194.
22. – 1964: A Magyar Állami Földtani Intézet tevékenysége az 1961. évben. (Activité de l'Institut Géologique de Hongrie an 1961. In Hungarian, French, and Russian). – MÁFI Évi Jel. 1961 -ről, I, pp. 3–8.
23. – 1964: A Magyar Állami Földtani Intézet 1962. évi működése. (Activité de l'Institut Géologique de Hongrie 1962. In Hungarian, French, and Russian.). – MÁFI Évi Jel. 1962 -ről, pp. 3–8.
24. – et al. 1964: Javaslat az alsó triász nevezéktanával és a raeti emelet hovatartozásával kapcsolatban (Reccommendation in connection with the nomenclature of the Lower Triassic and the assignment of the Rhaetian stage. In Hungarian.). – Földt. Közl., 44, 2, pp. 267–268.
25. – et al. 1964: Résolutions au sujet des recommendations du Colloque du Jurassique tenu á Luxembourg. Comité du Mésozoique Méditerranéen, Sous-Copmmission du Jurassique de Hongrie. – Colloque du Jurassique a Luxembourg 1962. pp. 923–925.
26. – et al. 1964: Határozat a Luxemburgi jura kollokvium javaslatának tárgyában (Decision on the subject of the recommendations of the Jurassic Colloqium held in Luxembourg. In Hungarian.). – Földt. Közl., 44, 1, pp. 152–153.
27. – 1964: Alsókréta rétegtani konferencia Lyonban (Conference on Lower Triassic stratigraphy in Lyon. In Hungarian.). – Földt. Közl., 44, 1, pp. 153–154.
28. – 1964: Tektonika Evropi. – Objasznyityelnaja zapicka k mezsdunarodnoj tektonicseckoj karte Evropi macstaba 1:2.500.000, Moszkva, 1964.
29. – et al. 1965: Teljes jura szelvény a Vértes-hegységből (Ein Juraprofil im Vértesgebirge. In Hungarian with German abstract.). – Földt. Közl., 45, 1, pp. 54–61.
30. – 1965: Earth Sciences. In: "Science in Hungary". – Corvina, pp. 48–62, Budapest,
31. – 1965: A Földtani és Geofizikai Intézet együttműködéséről. (Sur la cooperation entre lInstitut Géologique de Hongrie et l'Institut de Géophysique Roland Eötvös. In Hungarian, French, and Russian.). – MÁFI Évi Jel. 1963 -ról, pp. 9–18.
32. – 1965: Az ország átfogó geofizikai vizsgálata (Comprehensive geophysical investigation of the country. In Hungarian.). – Földt. Kut., 8, 3, pp. 3–7.

33. – 1965: Az ország átfogó geofizikai vizsgálata (Comprehensive geophysical investigation of the country. In Hungarian.). – Magyar Tud., 1965/1, pp. 38–41.
34. – 1966: A Villányi-hegység krétaidőszaki képződményei (Les formations crétacées de la Montagne de Villány. In Hungarian with French and Russian abstracts.). – Geol. Hung. Ser. Geol., 15, pp. 1–95.
35. – 1966: Gazdasági szempontból legjelentősebb hegységeink és medencéink átfogó, sokoldalú és részletes földtani vizsgálata (L'étude geologique compréhensive, complexe et détaillée des bassins et montagnes aux plus grands potentiels économiques de la Hongrie. In Hungarian, French, and Russian.). – MÁFI Évi Jel. 1964 -ről, pp. 11–12.
36. – 1966: A XXII. Nemzetközi Földtani Kongresszusról (International Geological Congress XXIIrd Session. In Hungarian.). – Földt. Kut., 9, 1, pp. 71–72.
37. – et al. 1966: Magyarország hasznosítható ásványos anyagainak térképe. 1:500 000. I. Az energiahordozók lelőhelyei és prognózisa (Map of usable mineral materials of Hungary. I. Localities and prognosis of energy sources. In Hungarian.). – MÁFI.
38. – et al. 1967: Magyarország paleozóos és mezozóos képződményeinek fedetlen földtani térképe (Uncovered geological map of Palaeozoic and Mesozoic formations of Hungary with Hungarian, English, and Russian legends). – MÁFI.
39. – 1967: Üledékes képződményeink kifejlődési törvényszerűségeinek vizsgálata (Investigation of the facies regularities of our sedimentary formations. In Hungarian.). – MTA X. Oszt. Közl., 1, pp. 281–293.
40. – 1967: A jura–kréta határ kérdéseiről (On the Problem of the Jurassic–Cretaceous Boundary. In Hungarian, English, and Russian.). – MÁFI kiadv., pp. 1–16.
41. – 1967: Időszerű földtudomány–szervezési feladatok (Actual tasks relating to the organization of earth science. In Hungarian.). – MTA X. Oszt. Közl., 1, pp. 141–143.
42. – 1967: Hozzászólás az Osztálytitkári beszámolóhoz (Contribution to the Departmental Secretary's report. In Hungarian.). – MTA X. Oszt. Közl., 1, pp. 164–166.
43. – 1967: A Földtani Bizottság Beszámolója (1965–1967) (Report of the Geological Committee. In Hungarian). – MTA X. Oszt. Közl., 1, pp. 349–352.
44. – 1967: A Magyar Állami Földtani Intézetre háruló feladatok és azok megoldása (Le programme de l'Institut Géologique de Hongrie et l'état de son exécution. In Hungarian, French, and Russian.). – MÁFI Évi Jel. 1965 -ről, pp. 9–15.
45. – 1967: Földtani természetvédelmi területeink helyzete és a további feladatok ezen a téren (The situation of our geologic nature conservation areas and the future tasks in this field. In Hungarian.). – MTA Földt. Biz. kiadv., pp. 1–36.
46. – et al. 1968: Geology of the Transdanubian Central Mountains. Guide to Excursion 39 C, Hungary. – International Geological Congress XXIIIrd Session, Prague 1968. Budapest, pp. 1–50.
47. – 1968: A földtani térképezés története, helyzete és feladatai Magyarországon (History, situation, and tasks of geological mapping in Hungary. In Hungarian.). – MTA X. Oszt. Közl., 2, pp. 27–45.
48. – 1968: Igazgatói jelentés a Magyar Állami Földtani Intézet 1966. évi munkájáról (On the Work of the Hungarian Geological Institute: Director's Report 1966. In Hungarian.). – MÁFI Évi Jel. 1966 -ról, pp. 16–22.
49. – 1969: 100 éves a Magyar Állami Földtani Intézet. In. "100 éves a Magyar Állami Földtani Intézet" (Hundred Years of the Hungarian Geological Institute. In: "One Hundred Years of the Hungarian Geological Institute". In Hungarian). – MÁFI kiadv., pp. 8–36.
50. – 1969: Hundred Years of the Hungarian Geological Institute. In: "One Hundred Years of the Hungarian Geological Institute"). MÁFI kiadv., pp. 9–39.
51. – 1969: Centenáriumát ünnepli a Magyar Földtani Intézet. (Hundred years' history of the Hungarian Geological Institute. In Hungarian with English and Russian abstracts.) – Földt. Kut., 10, 1, pp. 1–7.

52. – 1969: Száz éves a Magyar Állami Földtani Intézet (Hundred Years of the Hungarian Geological Institute. In Hungarian.). – Bányászati és Kohászati Lapok, Bányászat, 102, 8, pp. 505–508.
53. – 1969: The day of the Geological Institute (Surveys) Opening adress 100 Year celebrations of the Hungarian Geological Institute (In English and Russian.). – Ann. Inst. Geol. Publ. Hung., LIV, 1, pp 17–24.
54. – 1969: A földtani térképezés története, helyzete és feladatai Magyarországon. In: "100 éves a Magyar Állami Földtani Intézet" (Geological Mapping in Hungary: past, presence and future. In Hungarian and English.). – MÁFI 1969, pp. 82–101.
55. – 1969: Colloque du Jurassique méditerranéen (In French and Russian.). – Ann. Inst. Geol. publ. Hung., LIV, 2, pp. 27–30.
56. – 1969: Magyarország juraidőszaki képződményei (Les formations jurassiques de la Hongrie. In French and Russian.). – Ann. Inst Geol. publ. Hung., LIV, 2, pp. 31–61.
57. – et al. 1969: Földtani kirándulás a Mecsek-hegységben, a Villányi-hegységben és a Dunántúli Középhegységben (Geologische Exkursion im Transdanubischen Mittelgebirge, im Mecsek–Gebirge und im Villanyer–Gebirge. In Hungarian, English, French, German, and Russian). – Mediterrán Jura Kollokvium, Budapest, 1969. Guide, pp. 1–70.
58. – 1969: Conference on Bauxite Geology (In English, French, and Russian). Budapest, 4–8. IX. 1969. – Ann. Inst. Geol. publ. Hung., LIV, 3, pp. 9–17.
59. – et al. 1969: Bauxitföldtani kirándulás a Dunántúli-középhegységben. (English, French, and Russian, Guide d'excursion. Le géologie de bauxite de la Montagne Centrale de Transdanubie. In Hungarian.). – Bauxitföldtani Konferencia, Budapest, 1969, pp. 1–61.
60. – et al. 1969: A Dunántúli-középhegység eocénje (Guided' excursion. L'Éocéne de la Montagne Centrale de Transdanubie. In Hungarian, French, and Russian.). – Eocén Rétegtani Kollokvium, Budapest, 1969, Abstract, pp. 5–17.
61. – 1969: Die Tendenzen der geologischen Untersuchungen sedimenterer Komplexe und die Notwendigkeit der Durchführung ihrer zusammenfassenden Auswertung (In German). – International Geological Congress. Bull. of the IXth Congress of the Carpatho-Balkan Geological Association, Budapest, (1973) IV, pp. 479–486.
62. – et al. 1969: Földtani kirándulás a Dunántúli-középhegységben (Guide to Excursion Geology of the Transdanubian Central Mountains. In Hungarian, English, and Russian.). – A Kárpát-Balkán Földtani Asszociáció IX. Kongresszusa, Budapest, 196,. pp. 1–60.
63. – et al. 1969: Putyevogyityely k ekckurcii geologija everovoctocsnoj csaszti zadunajszkovo Szrednyegorja i Sopronszkih gor. – Sopron. MÁFI 1969. pp. 1–25.
64. – 1969: A centenárium éve (The centenary year. In Hungarian, English, and Russian.). – MÁFI Évi Jel. 1969 -ről, pp. 11–36.
65. – 1969: A Magyar Állami Földtani Intézet 1967 évi munkája (The activity of the Hungarian Geological Institute: Director's report 67. In Hungarian, English, and Russian.) – MÁFI Évi Jel. 1967 -ről, pp. 7–19.
66. – 1970: Lóczy eszméinek időszerűsége (Actuality of the ideas of Professor Lóczy. In Hungarian.). – Földt. Közl., 50, 4, pp. 337–342.
67. – 1971: Dr. Vadász Elemér akadémikus emlékezete (1885–1970) (In Memory of Academician Dr. Elemér Vadász. In Hungarian.). – Földt. Közl., 51, 4, pp. 342–350.
68. – 1971: Dr. Vadász Elemér akadémikus emlékezete (1885–1970) (In Memory of Academician Dr. Elemér Vadász. In Hungarian.). – Magyar Tud., uj folyam, XVI, pp. 251–254.
69. – 1970: Az ország természeti erőforrásainak feltárásának perspektívái (Perspectives of exploring the natural resources of the country. In Hungarian.). – MTA X. Oszt. Közl., 3, 4, pp. 377–381.
70. – 1970: Igazgatói jelentés a Magyar Állami Földtani Intézet 1968. évi munkájáról (Activities of the Hungarian Geological Institute: Director's report 68. In Hungarian, English, and Russian.). – MÁFI Évi Jel. 1968 -ról, pp. 7–15.
71. – 1971: Búcsu az Intézettől (Farewell to the Institute. In Hungarian, English, and Russian.). – MÁFI Évi Jel. 1969 -ről, p. 9, 23–24, 37–38.

72. – 1972: Tudományos és technikai forradalom a földtanban és a hozzá kapcsolódó területeken. (Naucsno-tehnyicseszkaja revoljucija v geologii i na prilegajuscsih territorijah. In Hungarian with Russian abstract.). – Földt. Kut., 15, 3, pp. 1–6.
73. – 1972: A rétegtan alapvető kérdései tanulmányozásának időszerűsége (elnöki vitaindító) (Actuality of studying the fundamental questions of stratigraphy (Chairman's paper introducing a discussion). In Hungarian.). – Őslénytani Viták, 19, pp. 5–9.
74. – 1972: Committee on Mediterranean Mesozoic Stratigraphy. – International Geological Congress XXII. Report of the Twenty-Second Session India 1964. Part XVII. General Proceedings, pp. 102–105.
75. – 1973: Funde des Prehistorischen Silexgrubenbaues am Kálvária-Hügel von Tata. – Acta Archaeol. Ac. sc. Hung., 25, pp. 3–25.
76. – 1973: A földtudományok és a közműveltség (Earth sciences and general education. In Hungarian.). – Magyar Tud., 1973/2. pp. 65–73.
77. – 1973: A geológiai és metallurgiai kutatás feladatai a hazai ritkafém-források bővítésére (The tasks of geologic and metallurgic research, in order to expand Hungarian sources of rare metals. In Hungarian.). – II. Országos Ritkafém Konferencia, Pécs, 1973, MÁFI kiadv., pp. 200–208.
78. – 1973: Geological research and social-economic progress in Hungary. – Studies on the Material and Energy Flows of the Earth Budapest, pp. 398–400.
79. – 1973: Az elmúlt 10 év geológiai kutatásainak eredményei Magyarországon a KGST együttműködés tükrében Results of the last 10 years' geologic investigations in Hungary in the light of COMECON co-operation. (In Hungarian.). – Földt. Kut., 16, 4, pp. 12–14.
80. – 1974: A földtani kutatás és a társadalmi gazdasági haladás (Geologic research and social economic progress. In Hungarian.). – Földt. Közl., 54, 2, pp. 167–173.
81. – 1974: Tudománypolitikai irányelvek és a hazai bauxitkutatás helyzetképe (Political guiding principles of science and general survey of Hungarian bauxite exploration. In Hungarian.). – Geonómia és Bányászat, 7, 1–2, pp. 53–62.
82. – 1974: A magyar aluminiumipar szerepe a hazai ritkafémkutatásban és termelésben (Role of the Hungarian aluminium industry in the domestic rare metal exploration and exploitation. In Hungarian.). – III. Országos Ritkafém Konferencia, Ajka, 1974, I. pp. 1–7.
83. – 1975: A tatai mezozóos alaphegységrögök (The Mesozoic Basement horst Blocks of Tata. In Hungarian and English). – Geol. Hung. Ser. Geol., 16, pp. 1–121.
84. – 1975: Earth Sciences In: "Science and scholarship in Hungary". – Ed. Corvina, Budapest, pp. 81–97.
85. – 1975: Új perspektívák a hazai földtani kutatás előtt (New perspectives ahead of Hungarian geologic research. In Hungarian.). – Földt. Kut., 18, 1–2, pp. 1–4.
86. – 1975: Új perspektívák a hazai földtani kutatás előtt (New perspectives ahead of Hungarian geologic research. In Hungarian.). – Földt. Közl., 105, pp. 565–570.
87. – et al. 1975: A föld- és bányászati tudományok szerepe ásványkincseink feltárásában (Role of earth and mining sciences in the exploration of our mineral resources. In Hungarian.). – Geonómia és Bányászat, 8, 1–2. pp. 145–149.
88. – et al. (szerk.) 1976: A rétegtani osztályozás, nevezéktan és gyakorlati alkalmazásuk irányelvei (Stratigraphic classification, nomenclature and guides of their practical application. In Hungarian.). – Magyar Rétegtani Bizottság, pp. 1–32.
89. – 1976: Ásványi nyersanyagforrásaink kutatása a IV. és V. ötéves tervidőszakban (Exploration of our mineral raw material sources in the 4th and 5th Five-Year Plan-period. In Hungarian). – Földt. Kut., 19, 3, pp. 6–12. Bányászati és Kohászati Lapok, Bányászat, 109, 12, pp. 801–807.
90. – 1976: Ásványi nyersanyagszükségletünk alakulása és a kielégítés forrásai (Tendency of our mineral raw material needs and the sources of its fulfillment. In Hungarian.). – Magyar Tud., 6, pp. 351–363.
91. – 1976: A geológiai kutatás perspektívái és időszerű feladatai. (Ásványi nyersanyagaink igénybevételének alapvető problémái. (Die Perspektiven und zeitgemsäsen Aufgaben der

geologischen (Forschungen). In Hungarian with German abstract.). – Bányászati és Kohászati Lapok, Bányászat, 109, 4, pp. 245–248.
92. – 1977: Vijvoj surovinovych potrieb v Madarskej ludovej republike a zdroje ich zabezpecenia (In Slovakian). – Geologicky pruzkom 10/1977, pp. 307–309.
93. – 1978: Hongrie – 2. édition. – Lexique Stratigraphique International I. Europe, Fasc., 9, pp. 7–8. Paris, 1978.
94. – 1978: Magyarország földtana, egy új szintézis irányelvei (Geology of Hungary, guides of a new synthesis. In Hungarian.). – Geonómia és Bányászat, 11, 1–2, pp. 7–12.
95. – 1978: Az energiahordozó ásványi nyersanyagok hasznosításának története Magyarországon (The history of the utilization of energy-producing mineral raw materials in Hungary. In Hungarian.). – Bányászati Kohászati Lapok, Bányászat, 112, 1, pp. 34–40.
96. – 1978: Geologische Beziehungen zwischen Österreich und Ungarn (Aus den Sitzungsberichten der Österr. Akademia der Wissenschaften.). – Mathem.–naturw. Kl. Abt. I. 187. Bd. 6. bis 10. Heft, pp. 223–231.
97. – 1978: Ausztria és Magyarország geológiai kapcsolatai (Geological connections of Austria and Hungary). – Földt. Kut., 22, 1–2, pp. 1–4.
98. – 1979: Az ország természeti erőforrásainak átfogó, tudományos vizsgálata (Interdisciplinary Research for Assessing the Country's Natural Resources. In Hungarian with English and Russian abstracts.). – Geonómia és Bányászat, 12, pp. 1–13.
99. – 1980: A földtani kutatás helyzete és feladatai (The situation and tasks of geologic research. In Hungarian.). – Földt. Közl., 109, 3–4, pp. 319–326.
100. – 1980: Magyarország kőszénvagyona (The black coal resources of Hungary. In Hungarian). – KFH, 1980. január, pp. 1–18. KFH, 1980. február, pp. 1–20.
101. – 1980: A földtani kutatás helyzete (The situation of the geological research. In Hungarian.). – KFH, 1980. március, pp. 1–48.
102. – 1981: Szotrudnyicsesztvo geologov Vengrii i drugih sztran-cslenov SzEV. Ekonomicseszkoe Szotrudnyicsesztvo sztran–cslenov SzEV. Szovjet Ekonomicseszkoj Vzaimopomoscsi. – Szekretarieat. Moszkva, 1981, 2, pp. 6–19.
103. – 1981: Eredményekben gazdag évek (1976–1980) és jövőt alapozó feladatok (1981–1985) (Years reach in results (1976–1980) and tasks of laying the foundation of the future. In Hungarian.). – Földt. Kut., 24, 2, pp. 4–8.
104. – 1981: Magyarország kőszénvagyona (tanulmány) (The black coal resources of Hungary (an essay). In Hungarian.). – KFH., Budapest, 1981. október. MÁFI pp. 1–24.
105. – 1982: Az ország természeti erőforrásainak átfogó tudományos vizsgálata (Comprehensive scientific investigation of the natural resources of the country. In Hungarian.). – MTA X. Oszt. Közl., 15, 1–2, pp. 113–121.
106. – 1982: Közlemények a magyarországi ásványi nyersanyagok történetéből I. (Selections from the history of Hungarian mineral raw materials. In Hungarian.). – Nehézipari Műszaki Egyetem Központi Kiadványtárának kiadványai, 20, pp. 3–4, Miskolc.
107. – 1982:Geological Mapping in Hungary: Past, Present and Future – X. INHIGEO Sympozium 16–22 August 1982, Programme, pp. 20–41. Budapest, 1982, MÁFI 1982.
108. – 1982: Magyarország szénhidrogén vagyona 1982 (The hydrocarbon resources of Hungary 1982. In Hungarian.). – KFH., Budapest, 1982. november., pp. 1–29.
109. – 1983: Neves elődeink. Vadász Elemér (Our renowned predecessors. Elemér Vadász. In Hungarian). – Pécsi Műszaki Szemle, 27, 1, pp. 16–17.
110. – 1983: Magyarország vasérc-, mangánérc-, valamint réz-, ólom- és cinkércvagyona 1982 (The iron ore, manganese ore, as well as, copper ore, lead ore, and zinc ore resources of Hungary 1982. In Hungarian.). – KFH., Budapest, 1983. október.
111. – 1983: Editorial. – Acta Geol. Hung., 26, 1–2, pp. 3–5.
112. – 1983: Az ország természeti erőforrásainak átfogó tudományos vizsgálata (Comprehensive scientific investigation of the natural resources of the country. In Hungarian). – Természeti Erőforrások, 1983, pp. 3–6.

113. – 1984: 25 Jahre Bundesanstalt für Geowissenschaften und Rohstoffe und Niedersechsishes Landesamt für Bodenforschung. – Geologisches Jahrbuch, R., A, 73, p. 50.
114. – 1984: Magyarország Bauxitvagyona (The bauxite resources of Hungary. In Hungarian). – KFH., Budapest, 1984. május., pp. 1–29. MÁFI 1984.
115. – 1984: Az ásványi nyersanyagok története Magyarországon (The history of mineral resources in Hungary. In Hungarian.). – Műszaki Könyvkiadó, Budapest.
116. – 1984: Országos jelentőségű földtani természetvéfelmi terület Tatán (A geologic nature conservation area of national importance at Tata. In Hungarian). – Tata Barátai Körének Tájékoztatója VI., Tata, 1984, pp. 78–85.
117. – 1984: Natural lithologic units and lithostratigraphy. – 27th International Geological Congress, Moscou, Abstracts,. 1, Sections Olto 03., pp. 45–46.
118. – 1989: Bevezetés Magyarország geológiájába (Introduction to the geology of Hungary. In Hungarian.). – Akadémiai Kiadó, Budapest.
119. – 1990: Magyarország geológiája. Paleozoikum I (Geology of Hungary, Palaeozoic I. In Hungarian.). – MÁFI, Budapest.
120. –1994: Magyarország geológiája. Paleozóikum II (Geology of Hungary, Palaeozoic II. In Hungarian). – Akadémiai Kiadó, Budapest.
126. – et al. 1995: A Föld mint folyamatosan változó dinamikus egyensúlyi rendszer (Earth as a continuously changing dynamic system of equilibrium. In Hungarian). – Magyar Tud., 95/2., pp. 156–163.

About 60 popular scientific papers and newspaper articles are not included into the above list.

Acta Geologica Hungarica, Vol. 37/1–2, pp. 17 (1994)

8th Meeting of the European Geological Societies

19–26 September, 1993

The Association of European Geological Societies (AEGS) was formally established in 1987. It has been granted the status of an affiliated organization of the International Union of Geological Sciences (IUGS).

Periodical Meetings of the European Geological Societies have taken place since 1975. (MEGS–1: Reading, England, 1975; MEGS–2: Amsterdam, the Nederlands, 1978; MEGS–3: Erlangen, Germany, 1983; MEGS–4: Edinburgh, Scotland, 1985; MEGS–5: Dubrovnik, Yugoslavia, 1987; MAEGS–6: Lisbon, Portugal, 1990; MAEGS–7: Paris, France. 1991).

MAEGS–8 was held in Budapest, Hungary, 19–26 September 1993, on the occasion of the 145th anniversary of the foundation of the Hungarian Geological Society. Its topic was the evolution of Intramontane Basins, on the Example of the Pannonian Basin.

It was organized jointly by the Hungarian Geological Society and the Association of Hungarian Geophysicists, and sponsored by MOL Rt. (Hungarian Oil Company), the Hungarian National UNESCO Commission, the Hungarian Academy of Sciences, and the European Community.

One pre-meeting and two post-meeting Field trips were held. (Field Trip A: Marginal facies of the Pannonian Basin; Field Trip B: Geology, agriculture, environment, and urban engineering geology in the Pannonian Basin; Field Trip C: Oil and gas subsurface water, and geothermal activity in the Pannonian Basin.)

156 geoscientist from 23 countries attended. Altogether 72 lectures (including 4 keynote ones) and 24 posters were presented.

The authors were requested to send their manuscripts to Acta Geologica Hungarica for publication. Beside the keynote lectures, 28 manuscripts had been received, out of which 21 were accepted by the Editorial Board.

Accordingly, to my sincere regret, the present volume represents only a minor part of what was displayed at the MAEGS–8. For this reason, I would like to point out that the volume of ABSTRACTS and the three Field Guides are still on sale at the Hungarian Geological Society, H–1027 Budapest, Fő u. 68, Hungary.

Assoc. Prof Endre Dudich
President, AEGS

0236–5278/94/$ 4.00 © 1994 *Akadémiai Kiadó, Budapest*

Acta Geologica Hungarica, Vol. 37/1–2, pp. 19–32 (1994)

Oceanic crust in geological history of the Western Carpathian orogeny

Peter Ivan, Štefan Méres
Department of Geochemistry
Comenius University, Bratislava

Dušan Hovorka
Department of Mineralogy and Petrology
Comenius University, Bratislava

Studies performed in the previous years of the Paleozoic and Mesozoic metabasalts of the Western Carpathians allowed the establishment of a preliminary genetic systematic subdivision of the oceanic, and/or semi-oceanic types of crust relics. Geochemical type of metabasalts served as the main criterion for the systematic subdivision, which yielded the classification of relics into two groups: (A) relics of mature crust of back-arc basins with metabasalts of the N-MORB type; (B) relics of initial crust of back-arc basins containing metabasalts similar to E-MORB/OIT or BABB. Metabasalts belonging to the first group are accompanied by small amount of metapelites; the second group, on the other hand, by frequently dominating clastic metasediments. Other members of the ophiolites sequence are to be found in both groups. The subdivision is further based on metamorphic history and on tectonic position. According to the metamorphic history can be discerned relics metamorphosed in (1) low grade conditions and (2) in subduction zone conditions. According to the tectonic position, metabasalts representing the crust of back-arc basins may be further divided into: (a) extensive nappes, (b) olistoliths and enclaves, and (c) pebbles in conglomerates. The most significant relics of immature crust of back-arc basins in the Western Carpathians include the Rakovec Group and the Zlatník Formation of the Dobšiná Group. The relics of the developed crust may be assigned to the Pernek Formation of the Malé Karpaty Mts crystalline (all Paleozoic in age).

Key words: Western Carpathians, Paleozoic and Mesozoic, oceanic crust, systematic subdivision

Introduction

Hitherto tentative models of the geodynamic evolution of the Western Carpathians generally accept the fact that the Western Carpathian orogeny was formed by multiple pre-Alpine extension and compression events, later overlaid by analogical Alpine events (Bajaník and Reichwalder 1979; Grecula 1982; Kozur and Mock 1987; Plašienka 1991). Final extensive compression in the Neogene led to the formation of the nappes of the Carpathian flysch in the outer Western Carpathians; subsequent extension contributed to the creation of intramontane depressions and the Pannonian Basin (Bergerat 1989; Royden and Burchfield 1989; Csontos et al. 1992). Extensions are often accompanied by the generation of oceanic crust, in contrast to compressions, associated with its consumption. For this reason, it is vital to identify the relics of oceanic crust in the Western Carpathians in order to understand the geodynamic development of this region. The systematic geochemical study of metabasalts in both pre-Alpine and Alpine

Addresses: P. Ivan, Š. Méres, D. Hovorka: Mlynská dolina, 84215 Bratislava, Slovak Republic
Received: 12 October, 1993

0236–5278/94/$ 4.00

units of the Western Carpathians enabled us to work out the systematic subdivision of oceanic crust relics in the Western Carpathian orogeny. The aim of this paper is to present a brief characterization of this subdivision, and its main results.

Theoretical background

Plate tectonics confirmed an agreement between complete ophiolite sequences and the oceanic crust. However, continued research has shown that the crust of extensive oceanic basins is usually consumed totally in subduction zones and the ophiolite complexes are generally the relics of back-arc and more seldom also fore-arc basins (Moores 1982; Coleman 1983). Typical oceanic crust with N-MORBs (normal mid-ocean ridge basalt) occurs in back-arc basins only in the mature stage of their evolution and is generated in a rift-type being close to the typical mid-ocean rift. Initial stages of back-arc basin evolution proceeds on the island arc crust, or on the crust of transitional to continental type. These stages are similar to those of continental rifting.

Island arc rifting is usually accompanied by basic or bimodal mildly-alkaline magmatism. Basalts are geochemically close to the E-MORB/OIT (enriched mid-ocean ridge basalt/oceanic island tholeiite) or CT (continental tholeiite; Hawkins and Melchior 1985).

Subsequent evolution causes a gradual change of basalt composition into N-MORB via transitional types, generated by mixing of E-MORB, N-MORB and arc magmas or by melting of mixed mantle sources with these characteristics (Volpe et al. 1988; Ikeda and Yuasa 1989; Hochstaedter et al. 1990). Transitional basalt types differ from typical N-MORB and are usually designated as BABB (back-arc basin basalts, cf. Holm 1985). The change in the geochemical type of metabasalts is connected with the transformation of the crust into typical oceanic crust with complete profile. The crust transformation is a complex process, possibly with variable transition stages. This fact, together with subsequent metamorphism and tectonism, render difficult the reconstruction of the evolution of the back-arc basin in the Western Carpathians.

Principles of the systematic subdivision

A systematic subdivision of oceanic crust relics in the Western Carpathian orogeny relied upon the determination of the geochemical type of all metabasalt occurrences (or metabasites) in Paleozoic and Mesozoic formations of the Western Carpathians. Geochemical typing of metabasalts was determined on the basis of the distribution of incompatible trace elements, as rare earth elements (REE) or high field strength elements (HFSE). We have also used geological and petrographic characteristics of metabasalts, and metamorphism of metabasalts for the subdivision. The presence of other rocks of the ophiolite sequence and/or other accompanying rocks was taken into consideration.

Not only were the relatively extensive remnants of back-arc basin crust included into the system; it also comprises smaller objects representing the initial products of the formation of this crust, and products of its destruction during subsequent evolution. The scheme of the systematic subdivision is presented in Fig. 1.

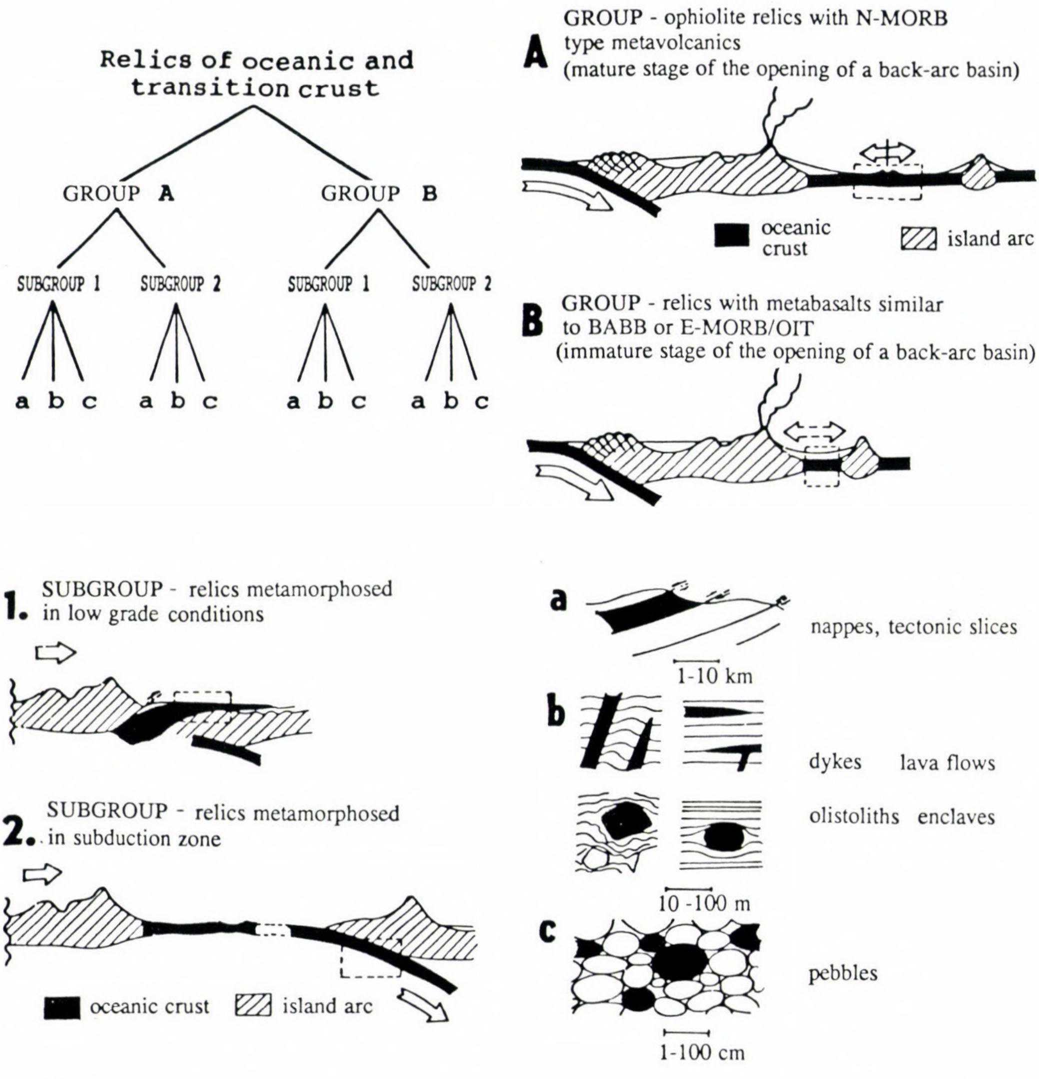

Fig. 1
Scheme of systematic subdivision of the oceanic crust relics in the Western Carpathians

All relics of the oceanic crust (including different transition types) of the Western Carpathians may be distinguished into two groups, A and B, according to the geochemical character of metabasalts. Group A includes relics with metabasalts geochemically similar to the N-MORB. They are usually accompanied by other members of the ophiolite suite. These relics represent the advanced stage of back-arc basin formation (Fig. 1). Group B, on the other hand, contains relics of the crust formed during the initial (immature) stages of the back-arc opening with metabasalts close to E-MORB/OIT or BABB type. Each group may be divided into two subgroups. Subgroup 1 comprises relics metamorphosed in low-grade conditions, not involved in subduction zones. Subgroup 2 is represented by relics metamorphosed in high-pressure conditions in the subduction zone. On the basis of the geological position within each subgroup, three members have been distinguished: a/ relics forming continuous nappes, or tectonic imbrication, b/ relics in the form of dykes, lava flows, olistoliths in melange or enclaves in lower crustal leptyno-amphibolite complexes, and c/ relics as pebbles in conglomerates – i.e. recycled material of the orogeny.

Systematic subdivision of relics of the oceanic crust in the Western Carpathians – results

An outline of oceanic crust relics (including transitional types) hitherto ascertained in pre-Alpine and Alpine units of the Western Carpathians can be found in Table 1. Their type, age, localization and present extent and metamorphic alteration are obvious from Fig. 2 and Fig. 3.

It should be mentioned that the relics of typical oceanic crust, in the form of ophiolite nappes with a complete ophiolite profile, do not occur in the Western Carpathians. Among all the relics containing basalts close to N-MORB, the closest affinity to them is displayed by ophiolites from the Szarvaskő Group (Meliata Group) in the Bükk Mts. It is a sequence consisting of pillow lavas, dolerites and gabbros (Balla et al. 1983; Downes et al. 1990). However, it does not correspond to typical oceanic crust: it is a complex of partly differentiated dykes penetrating the sediments of Triassic age which, in the upper parts, pass into pillow lavas. The whole complex was affected by low-grade oceanic floor metamorphism.

Probably the uppermost part of the typical oceanic crust is represented by the Jaklovce Formation in the Mesozoic Meliata Unit – the complex of basalt flows and dykes intercalated by radiolarites and red deep-sea shales. Basalts are close to N-MORB. The Jaklovce Formation is Triassic in age and was metamorphosed in low-grade conditions (Kozur and Mock 1987; Hovorka and Spišiak 1988, Ivan 1989). The same characteristic is displayed by the Meliata Group of the Meliatic Unit. Complete ophiolites, however, occurring only as pebbles in Cretaceous conglomerates of the Gosau type, were found near the

Table 1
Relics of the oceanic and transitional crust in the Western Carpathians

	Code	Relicts	Unit	Age	Basic magmatite (ophiolite suite)	Sediments	Type of meta-basalts	Metamorphism	Geological position	References
1	A.1.a.	Szarvaskő Group	Meliatic	Jurassic	basalts (pillow lavas), dolerite (dykes), gabbros	shales-turbidites	N-MORB	very low-grade (up to middle grade metamorphism of the oceanic floor type in gabbros)	nappe	Balla et al. (1983) Kozur and Mock (1987) Downes et al. (1990)
2	A.1.b.	Jaklovce Formation	Meliatic	Triassic	basalts (lava flows, dykes?) ultrabasites	radiolarites, red radiolarian shales	N-MORB	low-grade metamorphism	olistoliths?	Kozur and Mock (1987) Hovorka and Spišiak (1988)
3	A.1.b.	Meliata Group	Meliatic	Triassic–Jurassic	basalts	shales, carbonates, cherts	N-MORB	low-grade metamorphism	olistoliths	Hovorka and Spišiak (1988)
4	A.1.b.	Bodva Valley	Meliatic	Triassic (Ladinian)	basalts (pillow lavas), gabbros, ultrabasites	red shales, radiolarites		low-grade metamorphism	olistoliths	Réti (1985) Kozur and Réti (1986)
5	A.1.c	Cretaceous of Gosau Type (Dobšinská Lad. Jaskyňa)	Gemeric	Triassic	basalts, dolerites, gabbros, pyroxenites, peridotites	radiolarites, carbonates, cherts	N-MORB	low-grade (up to middle grade metamorphism of the oceanic floor-type in gabbros)	pebbles	Ivan (1988) Hovorka et al. (1990)
6	A.2.a.	Pernek Formation	Tatric	Early Paleozoic	basalts, dolerites, gabbros	black shales, cherts	N-MORB	polymeta-morphosed probably with early high-pressure stage?	nappe	Cambel (1954) Hovorka (1985) Ivan et al. (1993) Hovorka et al. (1994)

Table 1 cont.

	Code	Relicts	Unit	Age	Basic magmatite (ophiolite suite)	Sediments	Type of meta-basalts	Metamorphism	Geological position	References
7	A.2.b.	Leptyno-amphibolite complex	Gemeric Tatric	Early Paleozoic?	basalts, gabbros?, ultrabasites		N-MORB N-MORB/ BABB	polymetamorphosed with HP/HT stage	enclaves	Hovorka and Méres (1993) Spišiak and Pitoňák (1992) Hovorka et al. (1994) Ivan (1994)
8	A.2.c.	Rudňany Formation	Gemeric	Carboniferous	basalts	hematite shales, gneisses	N-MORB	polymetamorphosed with HP/HT stage	pebbles	Ivan (1994)
9	B.1.a.	Zlatník Formation	Gemeric	Carboniferous?	basalts, dolerites, gabbros	black shales	BABB	low-grade (up to middle grade metamorphism of the oceanic floor-type in gabbros)	nappe	Bajaník et al. (1981) Vozárová and Vozár (1988) Ivan (in prep.)
10	B.1.b.	Darnó Formation	Meliatic	Triassic	basalts (pillow lavas), dolerites, gabbros	radiolarites, red shales	BABB	very low-grade	olistoliths	Downes et al. (1990)
11	B.1.b.	Gelnica Group	Gemeric	Silurian–Devonian	basalts, dolerites	acid volcanoclastics, shales, black shales, cherts, carbonates	E-MORB/ OIT BABB CAB	low-grade	dyckes, necks, olistoliths?	Ivanicka et al. (1989) Ivan (1993) Ivan (1994)
12	B.1.b.	Ochtiná Formation and Črmel Formation	Gemeric	Carboniferous	basalts	black shales, sandstones, carbonates	E-MORB/ OIT - BABB	low-grade	lava flows? olistoliths?	Bajaník et al. (1981) Ivan (in prep.)

Table 1 cont.

	Code	Relicts	Unit	Age	Basic magmatite (ophiolite suite)	Sediments	Type of meta-basalts	Metamorphism	Geological position	References
13	B.2.a.	Rakovec Group	Gemeric	Early Paleozoic	basalts, basaltic andesites	shales	E-MORB/ OIT	polymetamor-phosed probably with early high-pressure stage?	nappe	Bajaník et al. (1981) Hovorka et al. (1988) Ivan (1994)
14	B.2.b.	Bôrka Formation	Meliatic	Triassic	basalts	shales, carbonates	E-MORB/ OIT BABB	blueschist	lava flows (olistoliths)	Leško and Varga (1980) Kozur and Mock (1987) Faryad (1991)
15	B.2.b.	Harmónia Formation	Tatric	Devonian	basalts	sandstones, siltstones, shales, black shales, carbonates	E-MORB/ OIT	polymetamor-phosed probably with early high-pressure stage?	lava flows, dykes	Cambel (1954) Ivan et al. (1993) Hovorka et al. (1994)
16	B.2.b.	Leptyno-amphibolite complex	Veporic	Early Paleozoic	basalts		E-MORB/ OIT	polymetamor-phosed with HP/HT stage	enclaves	Hovorka et al. (1992) Hovorka et al. (1994)
17	B.2.c.	Cretaceous of the Manin development	Klippen belt	?	basalts, dolerites, gabbros	carbonates, cherts	BABB	blueschist	pebbles	Šimová (1985) Ivan and Sýkora (in prep.)

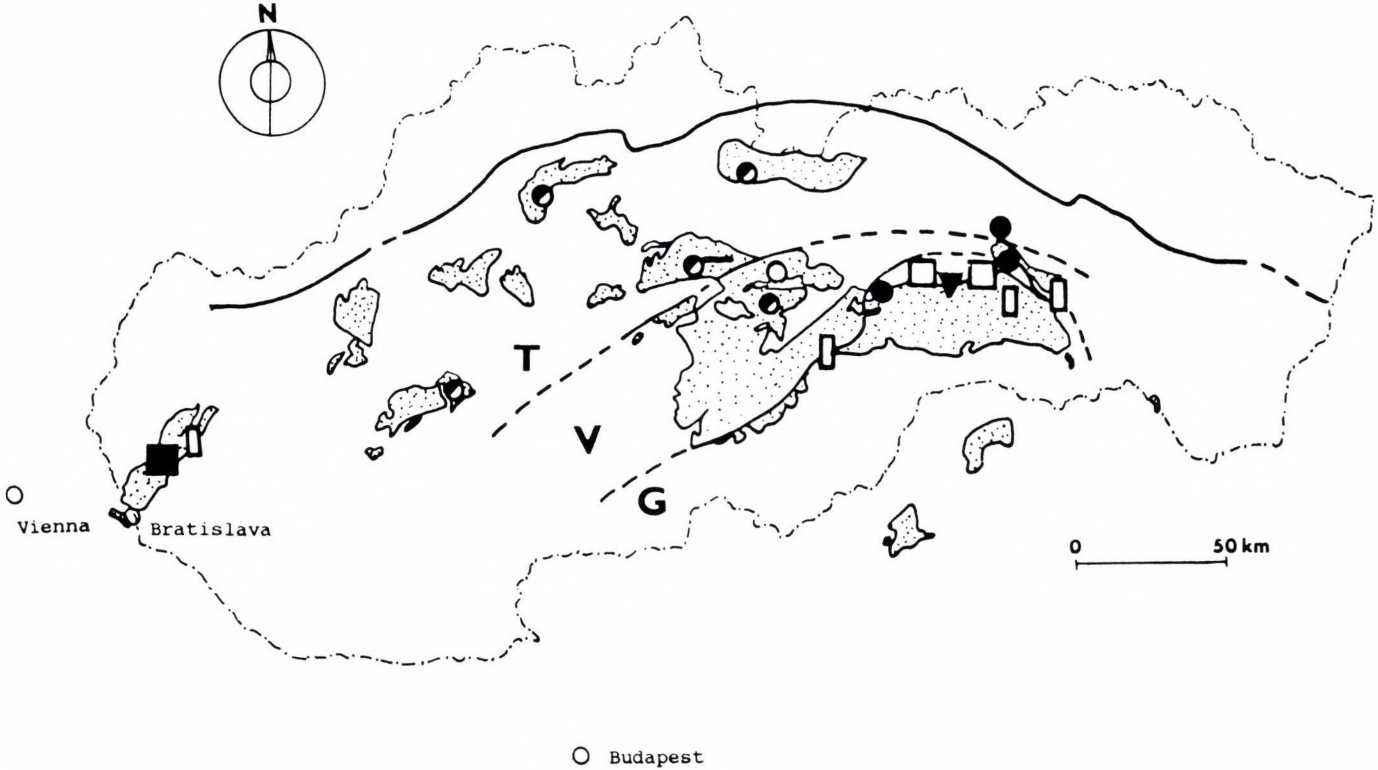

Fig. 2
Distribution of oceanic and transition crust relics in of the Western Carpathians Paleozoic formations. For legend see Fig. 2, circles – enclaves in leptyno-amphibolite complexes, half-filled symbols – metabasites close to N-MORB and BABB

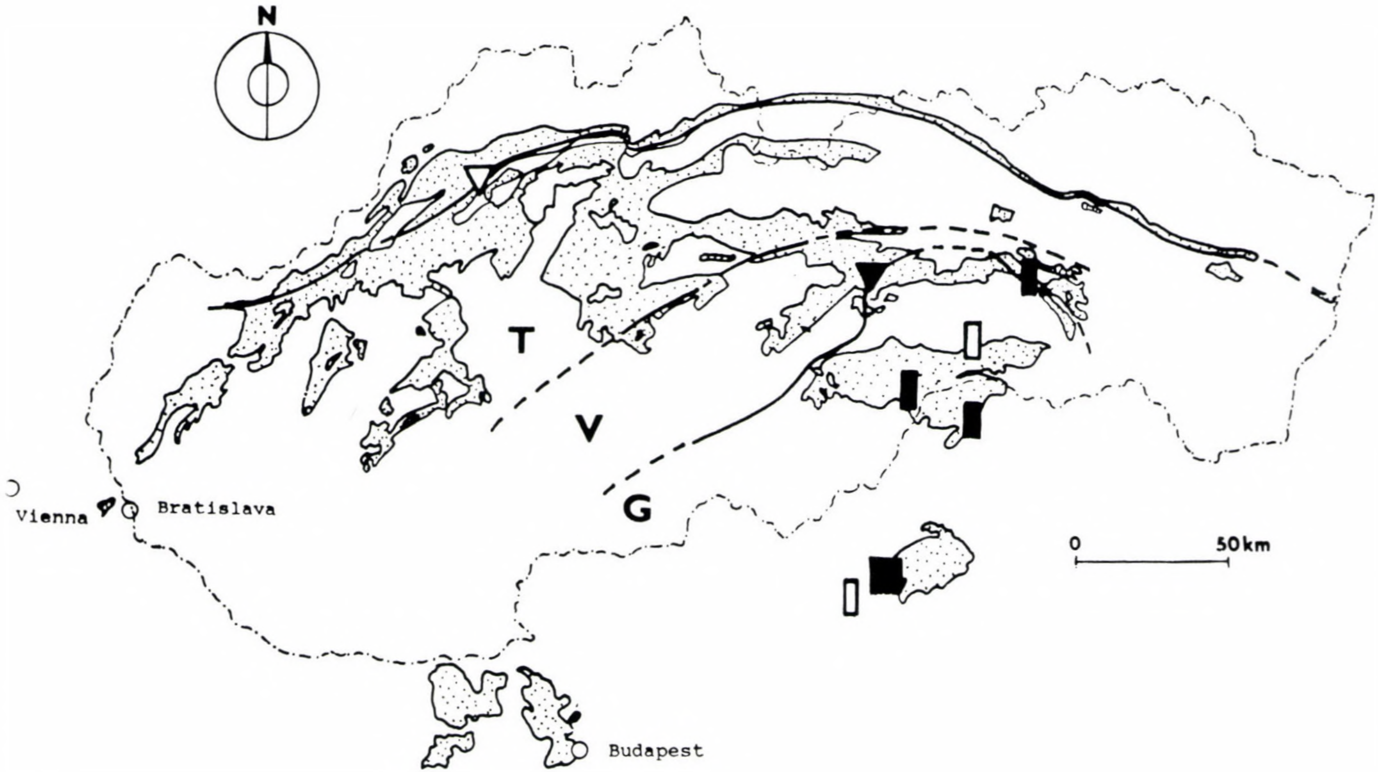

Fig. 3
Distribution of the oceanic and transitional crust relics in the Western Carpathians Mesozoic formations. Filled symbols – relics with metabasalts close to N-MORB, open symbols – relics with metabasalts close to E-MORB/OIT or BABB; squares – nappes or tectonic slices, rectangles – dykes, lava flows or olistoliths, triangles – pebbles in conglomerates; G – Gemeric Unit, V – Veporic Unit, T – Tatric Unit

village Dobšinská Ľadová Jaskyňa and as olistoliths in the Bodva valley (Réti 1985; Kozur and Réti 1986; Ivan 1989; Hovorka et al. 1990).

The most significant relics of the Paleozoic oceanic crust are represented by the complex of basalts and gabbros – the so-called Pernek Formation – in the crystalline complexes of the Malé Karpaty Mts (Ivan et al. 1993). Metabasalts are geochemically close to N-MORB type. Magmatic rocks are accompanied by small amounts of lydites and black shales. This complex suffered multi-stage metamorphic reworking, most probably also in the subduction zone. On the present-day surface it forms a relatively extensive nappe.

Relics of crust representing transitions to the typical oceanic crust were ascertained in pre-Alpine and Alpine sequences. They are the most widespread, with the largest affinity to typical oceanic crust in the Late Paleozoic (?) Zlatník Formation and Early Paleozoic Rakovec Group, both in the Gemeric Unit. The Zlatník Formation is composed of metabasalts with BABB signatures, metadolerites, metagabbros and black shales. This formation was metamorphosed mostly in low-grade conditions; manifestations of LP/HT metamorphism of oceanic floor-type are preserved in some gabbros (Ivan, in prep.). The Rakovec Group contains mainly basalts (lava flows, pillow lavas, dykes, necks), in low amounts basaltic andesites, dacites, rhyolites and pelitic sediments. The Rakovec Group suffered polyphase metamorphism under at least medium-pressure conditions (Hovorka et al. 1988). Both the Zlatník Formation and the Rakovec Group represent independent nappes in the present structure of the Western Carpathians.

Other relics of the transitional crust types of pre-Alpine and Alpine age represent only the initial stages of the process leading to the formation of the oceanic crust, which are manifested by volcanic activity of the basalts of BABB type, or E-MORB/OIT respectively.

A special type of the relics of pre-Alpine oceanic crust is represented by the enclaves of amphibolitized eclogites and metaperidotites in polymetamorphic banded bimodal magmatites of lower crust origin, designated as the leptyno-amphibolite complex. Amphibolitized eclogites usually show greater affinity to N-MORB or BABB; the types close to E-MORB/OIT were also found, but only rarely (Hovorka et al. 1994; Ivan 1994). Similar enclaves from the West European Variscides (Cabo Ortegal Complex, Bernard-Griffiths et al. 1985) were interpreted as the relics of the old oceanic crust which had suffered metamorphism in the subduction zone.

Implications for geodynamic evolution

The systematic subdivision of the oceanic and transitional crust relics in the Western Carpathians indicates relatively intensive extension, as well as compression, connected with subduction in the pre-Alpine and Alpine time span.

Alpine age extension perhaps attained a greater extent in the Western Carpathian realm than in the pre-Alpine age. This is evident from the presence of the relics of typical oceanic crust with N-MORBs and characteristic deep-water sediments. However, the prevalence of pelitic sediments over radiolarites indicates that the width of this oceanic domain might have enabled intensive deposition of pelitic material.

Extension during pre-Alpine (Variscan) time had the character of back-arc basin formation, with only slightly evolved oceanic crust. A more detailed reconstruction is not possible, since the spatial evolution of geochemical characteristics of basalts is very complicated in back-arc basins (cf. Falloon et al. 1992). It seems that during the Paleozoic, two time periods of formation of back-arc basins occurred, the remnants of which might be the Rakovec Group and the Zlatník Formation.

Since exact chronostratigraphic data are not available, it is not possible to explain them as the product of one extensional event.

It is probable that spreading in back-arc basins both, in pre-Alpine and Alpine age, was preceded by the initial stages of back-arc rifting. They were associated with effusions of E-MORB/OIT type basalts into the sedimentary basins filled with clastics, and if the sedimentation was less intensive with limestones. The remnants of these stages of the evolution of the Western Carpathian orogeny are most probably the Early Paleozoic Gelnica Group and Harmónia Formation, Late Paleozoic Ochtiná Formation, or the complexes of the Bôrka nappe of Triassic age, respectively.

The compression connected with the subduction is indicated by the relics of oceanic or transitional crust metamorphosed in medium to high pressure conditions. Metamorphosis of this type, already considerably overprinted by younger regression stages was identified in the Early Paleozoic Rakovec Group and perhaps also in the Pernek Formation. Subduction during the Alpine age is supported by metamorphism in blueschist conditions in the Bôrka nappe complexes, and by glaucophane schists in the detritus of Cretaceous conglomerates near the Dobšinská Ľadová Jaskyňa (the Gemeric Unit) and Považská Bystrica (Klippen belt).

Conclusions

1. Relics of oceanic and/or transitional crust in the Western Carpathians may be positioned in a systematic subdivision (Fig. 1) according to the following criteria: i/geochemical type of basalts, ii/ metamorphic recrystallization and iii/ position in present geological structure.

2. Relics of typical oceanic crust in the form of extensive nappes of complete ophiolites are not present in the Western Carpathians.

3. Sequences with metabasalts of N-MORB type and other members of the ophiolite suite originated in the course of back-arc spreading (mature stage of back-arc basin evolution).

4. Sequences with metabasalts of E-MORB/OIT and/or BABB are the product of back-arc rifting and initial stage of the opening of back-arc basin.

5. Formation of back-arc basins, probably of smaller extent, proceeded during the Early Paleozoic and Carboniferous (?). The extension during the Upper Triassic reached a more advanced stage.

6. Pre-Alpine and Alpine extensions were most probably preceded by a stage of back-arc rifting.

7. The existence of compression connected with subduction is confirmed by high pressure metamorphosis of the relics of the crust of back-arc basins during the course of Alpine and perhaps also pre-Alpine time span.

Acknowledgements

This paper represents a part of the results obtained in the course of work on project 02–1/96/92, financially supported by the Slovak Grant Agency.

References

Balla, Z., D. Hovorka, M. Kuzmin, V. Vinogradov 1983: Mesozoic ophiolites of the Bükk Mountains (North Hungary). – Ofioliti, 8, 1, pp. 5–46.

Bajaník, Š., P. Reichwalder 1979: Outline of the paleotectonic development of the Gemeric and its relation to adjacent tectonic units. – In: Czechoslovak geology and global tectonics. (In Slovak). Veda, pp. 141–154.

Bajaník, Š., A. Vozárová, P. Reichwalder 1981: Lithostratigraphic classification of Rakovec Group and Late Paleozoic in the Spišsko-gemerské rudohorie Mts. (In Slovak). – Geol. Práce, Zpr., 75, pp. 27–56.

Bergerat, F. 1989: From pull-apart to the rifting process: the formation of the Pannonian Basin. – Tectonophysics, 157, pp. 271–280.

Bernard-Griffiths, J., J.J. Peucat, J. Cornichet, M. Iglesias Ponce de Leon, J.I. Gil Ibarguchi 1985: U-Pb, Nd isotope and REE geochemistry in eclogites from the Cabo Ortegal Complex, Galicia, Spain: An example of REE immobility conserving MORB-like patterns during high-grade metamorphism. – Chem. Geol. 52, pp. 217–225.

Cambel, B. 1954: Geological-petrographical problems in the NE part of the Malé Karpaty Mts. crystalline. (In Slovak). – Geol. Práce, Zoš., 36, pp. 3–14.

Coleman, R.G. 1983: Preaccretion tectonic and metamorphism of ophiolites. Ophiolites: oceanic tectonics and metamorphism. – Abstract, Suppl., Ophioliti, 8, 18 p.

Csontos, L., A. Nagymarosi, F. Horváth, M. Kovac 1992: Tertiary evolution of the Intra-Carpathian area - A model. – Tectonophysics, 208, 1–3, pp. 221–242.

Downes, H., Gy. Panto, P. Árkai, M.F Thirlwall 1990: Petrology and geochemistry of Mesozoic igneous rocks, Bükk Mountains, Hungary. – Lithos, 24, 3, pp. 201–216.

Falloon, T.J., A. Malahoff, L.P. Zonenshain, Y. Bogdanov 1992: Petrology and geochemistry of back-arc basin basalts from Lau Basin spreading ridges at 15-degrees, 18-degrees and 19-degrees. – Mineral. Petrology, 47, 1, pp. 1–36.

Faryad, S.W. 1991: Metamorphism of the mafic rocks in the gemericum (In Slovak). – Miner. slov., 23, 2, pp. 109–122.

Grecula, P. 1982: Gemericum - segment of the paleotethyan riftogenous basin (In Slovak). – Alfa, Bratislava, pp. 1–263.

Hawkins, J.W., J.T. Melchior 1985: Petrology of Mariana Trough and Lau Basin. – J. Geophys. Res., Solid Earth Planet. 90, pp. 11431–11468.

Hochstaedter, A.G., J.B. Gill, M. Kusakabe, S. Newman, M. Pringle, B. Taylor, P. Fryer 1990: Volcanism in the Sumisu Rift. 1. Major element, volatile and stable isotope geochemistry. – Earth planet. Sci. Lett., 100, 1–3, pp. 179–194.

Holm, P.E. 1985: The geochemical fingerprints of different tectonomagmatic environments using hydromagmatophile element abundances of tholeiitic basalts and basaltic andesites. – Chem. Geol., 51, 3–4, pp. 303–323.

Hovorka, D. 1985: Pre-Alpine ophiolites and associated complexes of the Western Carpathians. (In Russian) – In: Riphean - Early Paleozoic ophiolites of the northern Eurasia. N. L. Dobrecov edit., Novosibirsk, pp. 148–159.

Hovorka, D., P. Ivan, L. Jilemnická, J. Spišiak 1988: Petrology and geochemistry of metabasalts from Rakovec, the Paleozoic of Gemeric unit, Inner Western Carpathians). – Geol. Zbor. Geol. Carpathica, 39, 4, pp. 395–426.

Hovorka, D., P. Ivan, R. Mock, L. Rozložník, J. Spišiak 1990: Sediments of Gosau type near Dobšiná Ice Cave: ideas for their non traditional interpretation (In Slovak). – Miner. slov., 22, 6, pp. 519–525.

Hovorka, D., Š. Méres 1993: Leptyno-amphibolite complex of the Western Carpathians: occurrences and lithology. (In Slovak) – Miner. slov., 25, pp. 1–9.

Hovorka, D., Š. Méres 1990: Clinopyroxene-garnet metabasites from the Tríbec Mts. (Central Slovakia) (In Slovak). – Miner. slov., 22, pp. 533–538.

Hovorka, D., Š. Méres, P. Ivan 1992: Pre-Alpine Western Carpathians Mts. Basement Complexes: Geochemistry, Petrology, Geodynamic Setting. – Terra nova, 4, Abstract Suppl., 2, p 32.

Hovorka, D., Š. Méres, P. Ivan 1994: Pre-Alpine Western Carpathians Complexes: Lithology and Geodynamic setting. – Mitteil. Österr. Geol. Gesellschaft, 86, V, pp. 33–44.

Hovorka, D., J. Spišiak 1988: Mesozoic Volcanism of the Western Carpathians (In Slovak). – Veda, pp. 1–263.

Ikeda, Y., M. Yuasa 1989: Volcanism in nascent back-arc basins behind the Shichito Ridge and adjacent areas in the Izu-Ogasawara arc, northwest Pacific: evidence for mixing between E-type MORB and island arc magmas at the initiation of back-arc rifting. – Contr. Miner. Petrology, 101, pp. 377–393.

Ivan, P. 1989: Oceanic crust in the Western Carpathians orogen ? Discussion. – Geol. Zbor. Geol. Carpath., 39, 2, pp. 245–253.

Ivan, P. 1993: Geochemistry and petrology of mildly-alkaline metabasalts, Early Paleozoic of Gemeric Unit (Western Carpathians): Implications for lithostratigraphy and geodynamic setting. Abstract. – Geologica Carpath., 44, 4, pp. 258–259.

Ivan, P. 1994: Early Paleozoic of the Gemeric Unit (Inner Western Carpathians) geodynamic setting as inferred from metabasalt geochemistry data. – Mitt. Österr. Geol. Gesell., 86, V, pp. 23–31.

Ivan, P., Š. Méres, M. Putiš, M. Kohút 1993: Geochemistry of the Early Paleozoic metabasalts and metasediments from the Malé Karpaty Mts.; some constraints on the lithostratigraphic division and geodynamic setting. Abstract. – Geologica Carpath., 44, 4, pp. 259–260.

Ivanička, J., L. Snopko, P. Snopková, A. Vozárová 1989: Gelnica Group – lower unit of Spišsko-gemerské rudohorie Mts. (West Carpathians), Early Paleozoic. – Geol. Zborn. Geol. Carpath., 40, pp. 483–501.

Kozur, H., R. Mock 1987: Deckenstructuren im südlichen Randbereich der Westkarpaten (Vorlaufige Mitteilung). – Geol. - paläont. Mitt., 14, 6, pp. 131–155.

Kozur, H., Zs. Réti, Z. 1986: The first paleontological evidence of Triassic ophiolites in Hungary. – N. Jb. Geol. Paläontol., Mh., 5, pp. 284–292.

Leško, B., I. Varga 1980: Alpine elements in the West Carpathian structure and their significance. – Miner. slov., 12, 2, pp. 97–130.

Moores, E.M. 1982: Origin and emplacement of ophiolites. – Rev. Geophys. Space Phys., 20, 4, pp. 735–760.

Plašienka, D. 1991: Mesozoic tectonic evolution of the epi-Variscan continental crust of the Central Western Carpathians - a tentative model. – Miner. slov., 23, 5–6, pp. 447–457.
Réti, Zs. 1985: Triassic ophiolite fragments in an evaporitic melange, northern Hungary. – Ofioliti, 10, 2–3, pp. 411–422.
Royden, L., B.C. Burchfield 1989: Are systematic variations in thrust belt style related to plate boundary processes? - (The Western Alps versus the Carpathians). – Tectonics, 8, 1, pp. 51–62.
Spišiak, J., P. Pitoňák 1992: Banded amphibolic rocks - pre-Variscan basement of the Western Carpathians? – Terra abstr., Suppl., 2 , Terra Nova, 4, p 63.
Šímová, M. 1985: Magmatic rocks from the Cretaceous conglomerates of the western part of Klippen and Mann Belt (In Slovak), – Západ. Karpaty, Sér. Mineral. Petrol. Geochem. Metalog., 10, pp. 9–10.
Volpe, A.M., J.D. Macdougall, J.W. Hawkins 1988: Lau Basin basalts (LBB): trace element and Sr-Nd isotopic evidence for heterogeneity in back-arc basin mantle. – Earth planet. Sci. Lett., 90, 2, pp. 174–186.
Vozárová, A., J. Vozár 1988: Late Paleozoic in West Carpathians. – D. Štúr Geol. Inst., 314 p.

Acta Geologica Hungarica, Vol 37/1–2, pp. 33–44 (1994)

Pressure–temperature conditions and oxidation state of the upper Mantle in southern Slovakia

Monika Huraiová
Department of Mineralogy and Petrology, Bratislava

Patrik Konečný
Dionýz Štúr Institute of Geology Bratislava

Upper mantle rocks in southern Slovakia (northern margin of the Pannonian Basin) are represented by lherzolite xenoliths, accompanied by olivine and clinopyroxene xenocrysts included in Pliocene-Pleistocene alkali basalts. Their dominant protogranular structures are considered to have preserved original equilibrium conditions. Pressure-temperature conditions derived from pyroxene thermobarometry (Wells 1977; Köhler and Brey 1990) cover the intervals 850–1050 °C and 10–27 kbar.

Oxygen fugacity values calculated after Mattioli and Wood (1988) cluster around FMQ oxygen buffer (from FMQ–1.56 to FMQ+1.23, mean value FMQ–0.04). Silicate melt and CO_2 inclusions frequently occur in olivines and clinopyroxenes. Raman spectroscopy has revealed up to 2.4% CO and 0.4% N_2 in fluid inclusions. Oxygen fugacities were calculated for XCO_2=0.976–0.988, inferred from the composition of fluid inclusions, assuming oxidation of CO to CO_2. Values of oxygen fugacity vary around FMQ buffer, supporting the oxidation state derived from mineral assemblages. Maximum fluid pressures obtained from the densest CO_2 inclusions reach up to 8 kbars (~29 km), implying as most probable the upper mantle origin of the trapped fluids. The upper mantle in southern Slovakia shows a high P-T gradient, comparable to regions of volcanic activity of alkaline type (Jones et al. 1982; O'Reilly and Griffin 1985; O'Reilly 1990). The high geothermal gradient most probably resulted from Miocene upper mantle uplifting, overheating, contemporaneous alkali magma generation and thinning of the Earth's crust to approximately 26 km in the Pannonian Basin (Čermak et al. 1986; Stegena 1964, Stegena et al. 1975; Lexa and Konečný 1974, 1979).

Key words: upper mantle, alkali basalts, spinel lherzolites, xenoliths, Pannonian Basin, oxygen fugacity, fluid inclusions

Introduction

Upper mantle xenoliths are common in alkali basalts in the Pannonian Basin. In the Hungarian part of the Pannonian Basin, the post-Sarmatian alkali basalts are well exposed in the Balaton Highlands, and in the northeast in the Salgótarján area (Nógrád County). Upper mantle xenoliths and xenocrysts have been studied by many authors (Embey-Isztin, 1978, 1984; Embey-Isztin et al. 1989; Dobosi 1986, 1989; Downes et al. 1992 and others).

Pliocene to Pleistocene alkaline volcanics in southern Slovakia are associated with those in the Salgótarján area and consist mainly of lava flows with minor cinder cones (Fig. 1). Upper mantle xenoliths were first described by Hovorka

Addresses: M. Huraiová: Mlynská dol. 842 15 Bratislava, Slovakia
P. Konečný: Mlynská dol. 1, 817 04 Bratislava, Slovakia
Received: 15 October, 1993

0236–5278/94/$ 4.00

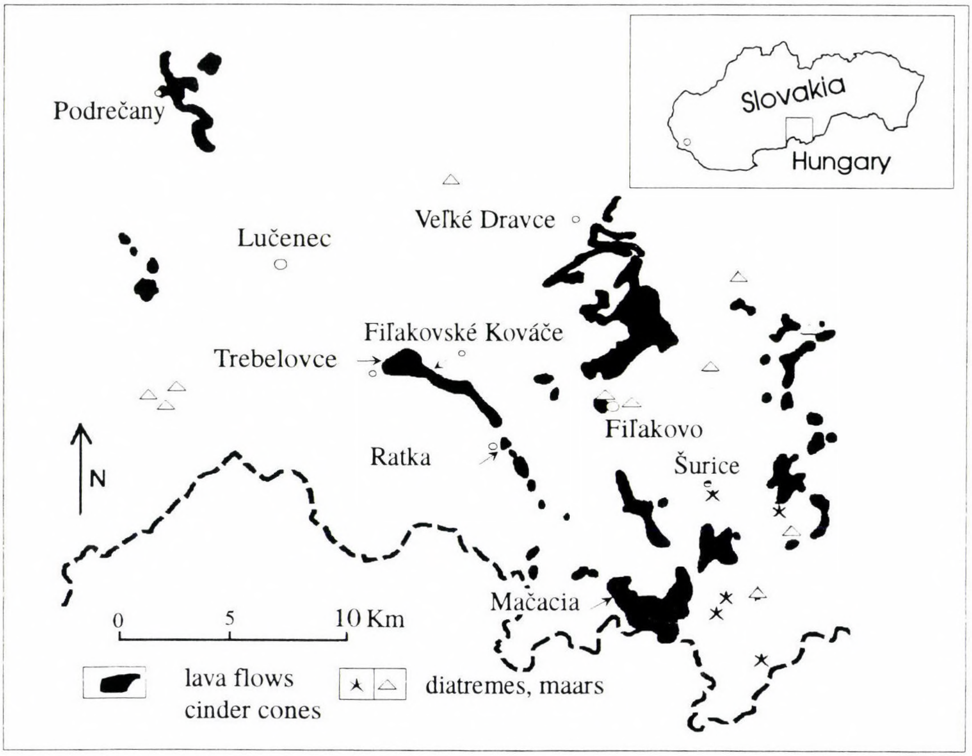

Fig. 1
Distribution of alkali basalts in southern Slovakia

and Fejdi (1987) as spinel lherzolite peridotites. Lherzolite xenoliths are abundant in some alkali basalt lava flows. We have sampled two large lava flows in the following localities: one at Trebelovce, Fiľakovské Kováče and Ratka, and the other lava flow in the Mačacia area.

Lherzolites preserve specific structures depending on re-equilibration conditions. Mercier and Nicolas (1975) recognized succeeding structures: protogranular, porphyroclastic, equigranular and secondary structures. They assume the protogranular structure as the oldest structure. Under increased plastic flow it grades into porphyroclastic and finally into completely recrystallized equigranular structure. Secondary structure is a result of intense heating and recrystallization in the second cycle.

Analytical methods

Chemical analysis of all mineral phases were made using the JEOL-733 electron microprobe. Operating conditions: accelerating voltage 15 KV, beam current 20 nA, beam diameter about 3 µm.

Standards used: albite (Na, Al, Si), wollastonite (Ca), MgO (Mg), willemite

(Mn), chromite (Fe, Cr), TiO_2 (Ti). Counts were recalculated using the ZAF correction method.

Homogenization temperature and melting temperature of two phase (liquid-vapour) fluid inclusions were determined with the CHAIXMECA stage in the ÚUG laboratory in Prague. Two samples were sent to the GREG laboratory in France and were analysed by Raman spectroscopy.

The chemical composition of mineral phases

Spinel lherzolites are typically composed of four-phase assemblages: olivine, orthopyroxene, clinopyroxene and spinel. Microprobe analyses of main mineral phases are given in Table 1. We have identified the following structures:

- protogranular
- transitional to porphyroclastic
- porphyroclastic
- secondary protogranular

The protogranular structures prevail over the others. Olivines are forsterite-rich (from Fo_{86} to Fo_{92}, average Fo_{90}). The chemical composition of orthopyroxenes (Fig. 2) is limited to boundary enstatite-bronzite ($Wo_{1.4}$, $En_{89.4}$, $Fs_{9.2}$). Clinopyroxenes (Cr-diopsides) exhibit the composition $Wo_{56.1}$, $En_{48.9}$, $Fs_{4.8}$. The composition of spinels is related to lherzolite structures (Fig. 3). The lowest abundances of Cr_2O_3 have spinels from transitional structure (10–15 wt.%), and an intermediate content in those from protogranular structure (16–22 wt.%); spinels from secondary structures are extremely rich in Cr_2O_3 (34–40 wt.%).

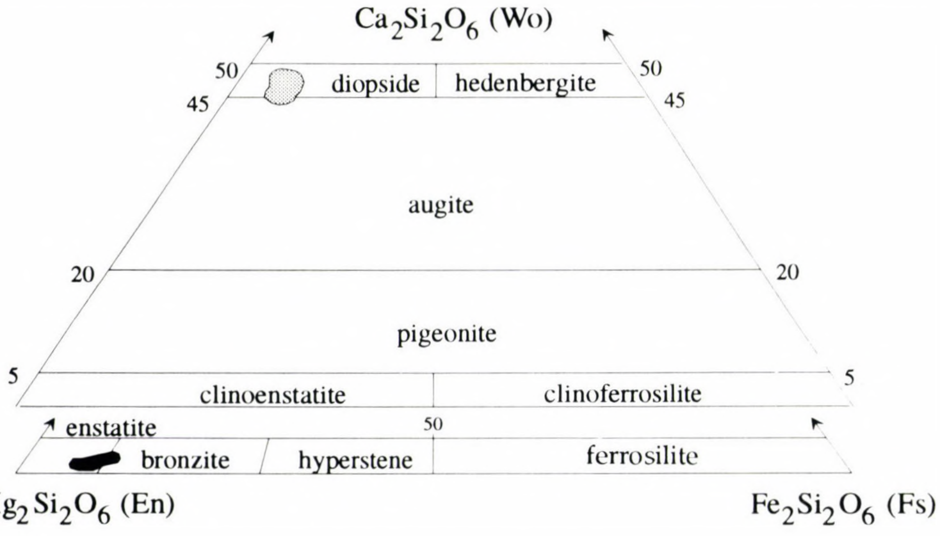

Fig. 2
Chemical composition of pyroxenes after Morimoto (1988). Wo – wollastonite; En – enstatite; Fs – ferrosilite; the dotted area refers to orthopyroxenes and the dark one comprises clinopyroxenes

Table 1
Selected microprobe analysis of coexisting spinel (sp) + orthopyroxene (opx) + clynopyroxene (cpx) + olivine (ol) and recalculation to given oxygen basis (ox)

Locality	RATKA I				MAČACIA				TREBELOVCE				FIĽAKOVSKÉ KOVÁČE			
Sample	lhz1/33	lh1/4	lhz1/8	lhz1/5	lhz16/28	lhz16/15	lhz16/16	lhz16/21	mr2/4	mr2/12	mr2/13	mr2/14	m7/1	m7/30	m7/33	m7/32
Structure	protogranular				transitional to porphyroclastic				prophyroclastic				secondary protogranular			
Wt %	sp	opx	cpx	ol	sp	opx	cpx	ol	sp	opx	cpx	ol	sp	cpx	cpx	ol
SiO_2	0.00	55.18	52.34	39.78	0.00	55.92	52.41	40.81	0.06	55.68	51.00	40.91	0.05	56.32	52.18	41.68
TiO_2	0.03	0.09	0.21	0.03	0.00	0.08	0.39	0.00	0.25	0.10	0.06	0.02	0.00	0.00	0.23	0.09
Al_2O_3	47.94	3.64	4.10	0.02	54.75	4.11	6.41	0.00	53.37	4.00	4.31	0.00	26.72	2.45	3.58	0.01
FeO	13.32	5.97	2.78	9.55	10.68	5.56	2.71	9.35	12.30	5.79	2.71	9.62	13.81	4.90	2.23	7.12
MnO	0.11	0.01	0.09	0.09	0.07	0.21	0.02	0.13	0.06	0.25	0.06	0.31	0.10	0.07	0.12	0.14
MgO	19.28	33.54	16.98	49.68	20.27	33.76	15.64	49.47	20.73	33.26	17.01	49.03	17.34	35.02	16.58	50.85
CaO		0.71	22.31	0.05		0.75	20.98	0.10		0.67	23.03	0.13		0.83	21.58	0.11
Na_2O		0.00	0.54	0.02		0.10	1.46	0.00		0.00	0.50	0.00		0.01	1.29	0.03
K_2O		0.01	0.00	0.00		0.01	0.00	0.00		0.00	0.01	0.01		0.00	0.00	0.00
NiO	0.28	0.00	0.00	0.55	0.42	0.13	0.09	0.40	0.43	0.00	0.00	0.00	0.16	0.00	0.00	0.00
Cr_2O_3	18.33	0.53	1.03	0.19	12.87	0.28	0.92	0.10	12.83	0.28	0.51	0.12	41.01	0.74	1.35	0.02
Total	99.29	99.68	100.37	99.96	99.06	100.93	101.03	100.36	100.03	100.01	99.19	100.17	99.19	100.35	99.13	100.06
	coexisting minerals															
	4 ox	6 ox	6 ox	4 ox	4 ox	6 ox	6 ox	4 ox	4 ox	6 ox	6 ox	4 ox	4 ox	6 ox	6 ox	4 ox
Si	0.000	1.910	1.896	0.979	0.000	1.909	1.879	0.996	0.002	1.917	1.876	1.001	0.001	1.930	1.913	1.007
Ti	0.001	0.002	0.006	0.000	0.000	0.002	0.010	0.000	0.005	0.002	0.002	0.000	0.000	0.000	0.006	0.002
Al	1.540	0.149	0.175	0.000	1.703	0.166	0.271	0.000	1.659	0.162	0.187	0.000	0.943	0.099	0.155	0.000
Fe^{2+}	0.304	0.173	0.084	0.197	0.236	0.159	0.081	0.191	0.271	0.167	0.083	0.197	0.346	0.140	0.068	0.144
Mn	0.002	0.000	0.003	0.002	0.002	0.006	0.001	0.003	0.001	0.007	0.002	0.007	0.002	0.002	0.004	0.003
Mg	0.784	1.731	0.917	1.823	0.797	1.718	0.836	1.801	0.815	1.708	0.933	1.788	0.774	1.789	0.906	1.831
Ca	0.000	0.026	0.866	0.001	0.000	0.027	0.806	0.003	0.000	0.025	0.908	0.003	0.000	0.031	0.848	0.003
Na	0.000	0.000	0.038	0.001	0.000	0.007	0.102	0.000	0.000	0.000	0.036	0.000	0.000	0.000	0.091	0.002
K	0.000	0.000	0.000	0.000	0.000	0.000	0.000	0.000	0.000	0.000	0.000	0.000	0.000	0.000	0.000	0.000
Ni	0.006	0.000	0.000	0.011	0.009	0.004	0.003	0.008	0.009	0.000	0.000	0.000	0.004	0.000	0.000	0.000
Cr	0.395	0.014	0.029	0.004	0.268	0.008	0.026	0.002	0.268	0.008	0.015	0.002	0.971	0.020	0.039	0.000
Total	3.032	4.006	4.015	3.019	3.014	4.006	4.013	3.003	3.030	3.995	4.040	2.998	3.042	4.011	4.030	2.992

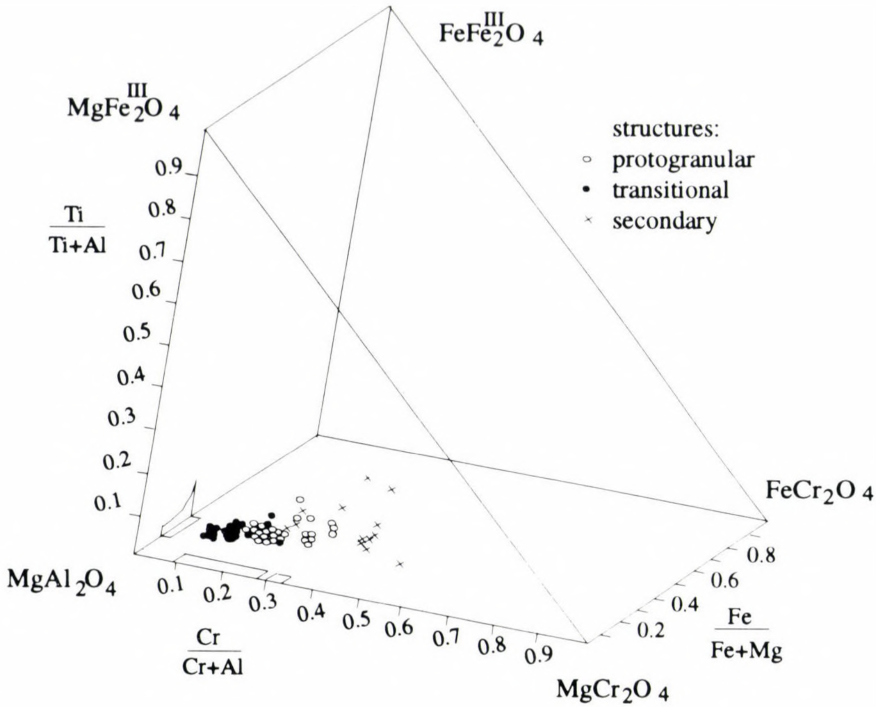

Fig. 3
Spinel composition depends on the structure of lherzolites and varys from Al to Cr spinel

Oxygen fugacity

The oxygen state of the upper mantle in conjunction with pressure, temperature, composition of fluids and mineral phases defines the state of the upper mantle. Oxygen fugacity is buffered by the reaction:

$6Fe_2SiO_4 + O2 = 3Fe_2Si_2O_6 + 2Fe_3O_4$

where Fe_2SiO_4 is the fayalite content in olivine, $Fe_2Si_2O_6$ is the ferrosilite content in orthopyroxene and Fe_3O_4 is the magnetite component in spinel. We have applied calibration after Mattioli and Wood (1988), with calculation of magnetite activity in spinel after Nell (1989). Pressure was normalized to 15 kbars and temperature was determined by means of the semi-empiric two-pyroxene thermometer after Wells (1977). The crucial point in the whole procedure was to determine the ferric iron content in spinel as precisely as possible. We have measured unknown spinels and consequently also spinel standards with known Fe^{3+} content evaluated by Mössbauer spectroscopy (kindly sent us by Mr. Wood); thereafter, the ferric iron was corrected for unknown (detailed information in Wood and Virgo, 1989).

Oxygen fugacity in relation to the FMQ oxygen buffer spans the interval from FMQ–1.56 to FMQ+1.23, with an average FMQ–0.04 (Fig. 4). The succession of oxygen fugacity for diverse geotectonic settings is given in Table 2. The oxygen state of our continental xenoliths from southern Slovakia projects between two assessments for continental xenoliths after Amundsen and Neumann (1992) and Bryndzia and Wood (1990), respectively.

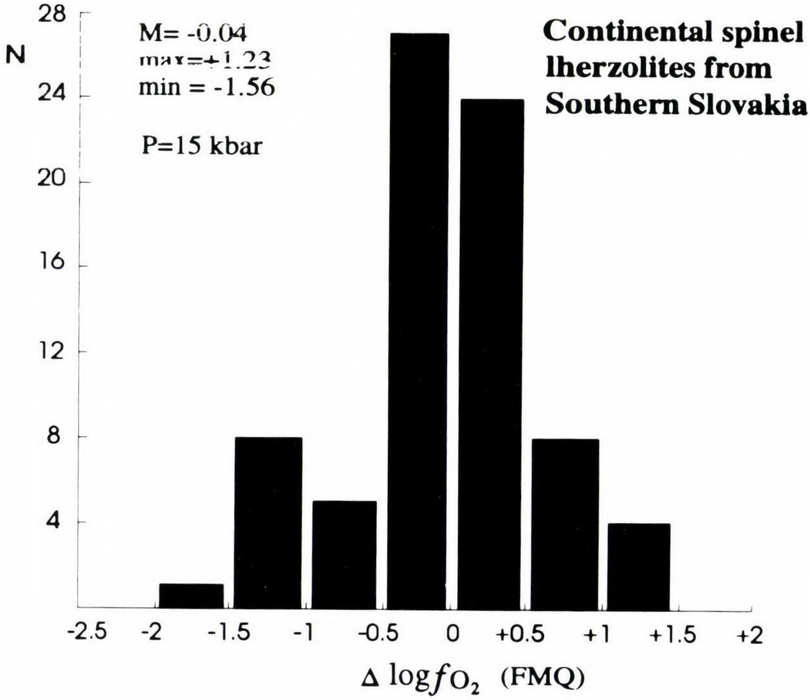

Fig. 4
Histogram of oxygen fugacity calculated from spinel lherzolites

Oxygen fugacity systematically decreases from ocean island lherzolites through subcontinental, to suboceanic (abyssal); the most reduced are orogenic lherzolites. The oxygen state of the upper mantle displays heterogeneity due to subduction, ocean crust recycling, generating of partial melts and metasomatic changes caused by penetrating magma or fluids (Mattioli and Wood 1986; Wood and Virgo 1989; Ballhaus et al. 1991; Bryndzia and Wood 1990; Woodland et al. 1992; Amundsen and Neumann 1992). Lherzolites from southern Slovakia are also variably oxidized according to their structures. Lherzolites with protogranular structures comprise a wide range; those with transitional structure are essentially reduced (under FMQ) and secondarily reheated ones are considerably oxidized (over FMQ).

Table 2
Oxygen fugacity of dry spinel lherzolites for diverse geotectonic settings. Arrows denote the position of mean value (M). 1, 2. Woodland et al. (1992); 3. Bryndzia and Wood (1990); 4. Amundsen and Neumann (1992); 5. this study; 6. Wood and Virgo (1989), Bryndzia and Wood (1990); 7. Amundsen and Neumann (1992)

Oxygen fugacity of dry lherzolites relative to FMQ

orogenic lherzolites:	Beni Bousera 1)	-3.3 — -0.1	M= -1.5
orogenic lherzolites:	Ronda 2)	-2.3 — +0.2	M= -1.1
abyssal peridotites:	mid-Atlantic, central Indian, SW Indian, American-Antarctic ocean ridges 3)	-2.5 — +0.5	M= -0.9
continental xenoliths:	NW Spitsbergen, Riogrande rift, SE Australia 4)	-5.3 — +0.8	M= -0.5
continental xenoliths:	Southern Slovakia 5)	-1.6 — +1.2	M= -0.04
continental xenoliths:	Japan, San Carlos, Massif Central, Kilbourn Hole 6)	-1.7 — +1.2	M= +0.24
ocean islands:	Canary Islands, Hawaii, Tahiti 7)	-0.7 — +2.1	M= +1

-6 -5 -4 -3 -2 -1 0 +1 +2 +3

Pressure is normalized to 15 kbar except for Ronda = 9 kbar, and ocean ridges = 10 kbar

Pressure–temperature conditions

Equilibrium temperatures after Wells (1977) extend from 840 °C to 1088 °C, yielding typically subsolidus values. The temperature decreases from the oldest protogranular structures to transitional and porphyroclastic ones, indicating the origin of metamorphic structures under increasing pressure while temperature change ceases. The extreme temperature range of secondary lherzolites suggests an additional reheating.

The problem of pressure estimation for spinel lherzolites was successfully solved by Köhler and Brey (1990). Their P_{KB} combined with T_{BKN} (Brey and Köhler 1990) gives a good approach to experimentally-derived equilibrium conditions. Pressure–temperature estimations tend to scatter around high temperature geotherms (Fig. 5). The South Australian geotherm exhibits heat flows of 90–100 mW/m^2. A comparable heat flow was estimated in the Pannonian basin (90 mW/m^2) by geophysical research (Cermak 1986). The proposed heat flow is supported by the higher P–T conditions of upper mantle lherzolites.

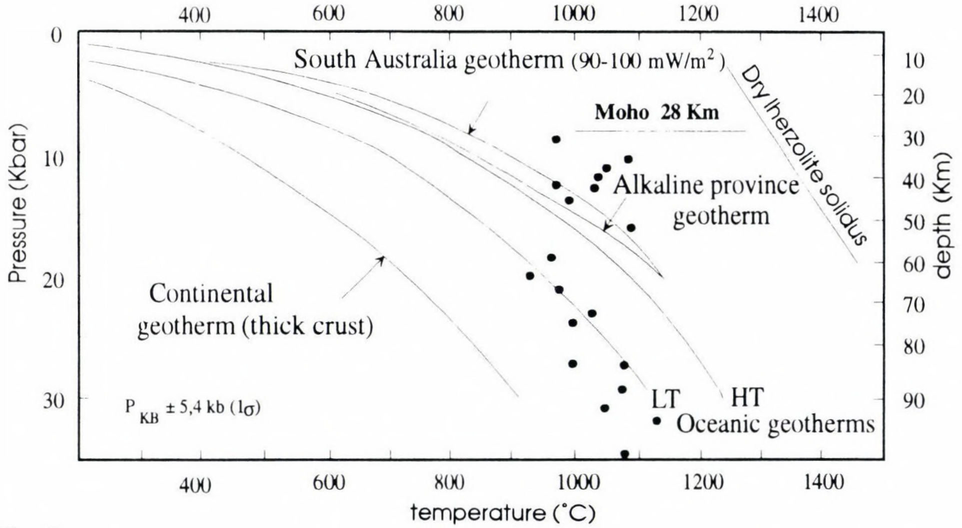

Fig. 5

Pressure–temperature conditions of spinel lherzolites. Pkb vs Tbkn plots are scattered around high-temperature geotherms. Geotherms adopted: continental and oceanic geotherms after Mercier-Carter (1975, 1990), South Australia geotherm after O'Reilly and Griffin (1985, 1990), alkaline province geotherm Jones et al. (1982), dry lherzolite solidus, Kushiro (1973)

Fluid inclusions

Silicate melt or fluid inclusions frequently occur in olivines and clinopyroxenes. Almost all monophase fluid inclusions are formed by nearly pure CO_2. Raman spectra revealed minor amounts of N_2 (0.4%) and CO (2.4%).

Oxygen fugacity is preserved by the reaction:

$CO_2 = 1/2\ O_2 + CO$

Fugacity coefficients of pure gases were taken from Saxena-Fei (1988) and equilibrium constants from Ohmoto and Kerrick (1977). Pressure was normalized to 15 kbar and a negligible amount of N_2 was added to CO_2.. Oxygen fugacity values inferred from fluid inclusions are in good agreement with those obtained from mineral assemblages (Fig. 6). Both independent methods confirm that the oxygen state of upper mantle lherzolites clusters around FMQ.

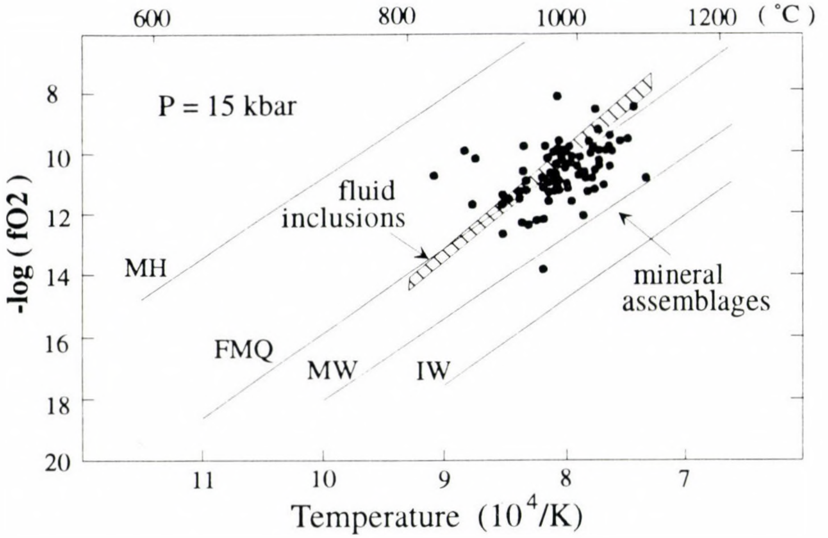

Fig. 6
Oxidation state of spinel peridotites inferred from mineral assemblages and fluid inclusions cluster around FMQ oxygen buffer.

State of the upper mantle

The pressure-temperature conditions of the upper mantle lherzolites in southern Slovakia imply a higher geothermal gradient, which is in agreement with geophysical measurements of heat flow in the Pannonian basin (Čermák et al. 1985). The proposed heat flow and thinning of the lithospheric crust is attributed to upper mantle upwelling during the Miocene (Stegena 1964, Stegena et al. 1975; Lexa and Konečný 1974, 1979). P–T projections are oriented across geotherms (Fig. 5), indicating adiabatic ascent of the upper mantle. The structures of lherzolites are sensitive to P–T conditions of the upper mantle. The protogranular structures (the oldest ones) prevail prior to transitional ones, and secondary structures are rare. This type of structure might be related to small-scale diapiric uprise. Careful studies in the Massif Central (e.g. Nicolas et al. 1987) have shown that metamorphic structures (porphyroclastic, equigranular) dominate in the centre of diapirs (due to high strain), and the protogranular structures on the margins. The paleomorphological study evidenced uplifting of the whole studied area during Pliocene to Pleistocene times, resulting in a change from a marine environment to a continental one (V. Konecny, personal communication). Considering the distribution of lherzolite structures, the centre of uplifting might be represented in the Mačacia locality, and the margins in the other areas.

Similarly, the Balaton area is the center of upper mantle uplifting, in contrast to undisturbed mantle in Kapfenstein (Austria) as reported by Kurat et al. (1991).

Upper mantle in southern Slovakia is oxidized in the same degree as normal subcontinental mantle. Oxygen fugacity inferred from mineral assemblages and fluid inclusions concentrates around FMQ. Subduction and metasomatic changes shift the oxygen fugacity towards more oxidizing conditions. No metasomatic influence has been observed within lherzolites (no hornblende, phlogopite, etc.); this is also supported by the oxidation state (around FMQ). The majority of fluid inclusions are CO_2 rich, but a minor amounts of N_2 (0.4%) and CO (2.4%) were determined by Raman spectroscopy. The densest fluid inclusions indicate pressures up to 8 kbar, corresponding to a depth of 29 km, suggesting perhaps their upper mantle origin, if we assume an average Moho boundary at 26 Km in the Pannonian Basin (Stegena 1964, Stegena et al. 1975; Čermák et al. 1985).

Acknowledgements

Prof. B. Wood is thanked for providing spinel standards used in the estimation of oxygen fugacity. We thank Dr. Dubessy for providing the Raman spectra which were used in this study, supported by the grant: "Geodynamic model of Western Carpathians".

References

Amundsen, H.E.F., E.R. Neumann 1992: Redox control during mantle/melt interaction. – Geoch. et Cosmoch. Acta, 56, pp. 2405–2416.

Ballhaus, C., R.F. Berry, D.H. Green 1991: High pressure experimental calibration of the olivine-orthopyroxene-spinel oxygen geobarometer: implications for the oxidation state of the upper mantle. – Contrib. Mineral. Petrol., 107, pp. 27–40.

Brey, G.P., T. Köhler 1990: Geothermobarometry in four-phase lherzolites II. new thermobarometers, and practical assessment of existing thermobarometers. – J. Petrology, 31, 6, pp. 1353–1378.

Bryndzia, L.T., B.J. Wood 1990: Oxygen thermobarometry of abyssal spinel peridotites: the redox state and C-O-H volatile composition of the Earth's sub-oceanic upper mantle. – Am. J. Science, 290, pp. 1093–1116.

Cermak, V. 1985: Geofyzikální model litosféry. – In: Blízkovsky, M. et.al 1982-85: Geotermicky model zemské kúry na územ strední a vychodny Evropy. – Záverecná správa, pp. 271–298.

Dobosi, G. 1986: Clinopyroxene composition of some Mesozoic igneous rocks of Hungary: the possibility of identification of their magma and tectonic setting. – Ofioliti, 11, 1, pp. 19–34.

Dobosi, G. 1989: Clinopyroxene zoning patterns in the young alkali basalts of Hungary and their petrogenetic significance. – Contrib. Mineral. Petrol., 101, pp. 112–121.

Downes, H., A. Embey-Isztin, M.F. Thirlwall 1992: Petrology and geochemistry of spinel peridotite xenoliths from the western Pannonian Basin (Hungary): evidence for an association between enrichment and the texture in the upper mantle. – Contrib. Mineral. Petrol., 109, pp. 340–354.

Embey-Isztin, A. 1978: On the petrology of spinel lherzolite nodules in basaltic rocks from Hungary and Auvergne, France. – Annls. Hist-nat Mus. Hung., 70, pp. 27–40.

Embey-Isztin, A. 1984: Texture types and their relative frequencies in ultramafic and mafic xenoliths from Hungarian alkali basaltic rocks. – Annls Hist-nat Mus. Hung., 76, pp. 27–42.

Embey-Isztin, A., H.G. Scharbert, H. Dietrich, H. Poultidis 1989: Petrology and geochemistry of peridotite xenoliths in alkali basalts from the Transdanubian volcanic region, West Hungary. – J. Petrology, 30, 1, pp. 79–105.

Griffin, W.L., S.Y. O'Reilly 1987: The composition of the lower crust and the nature of the continental moho-xenolith evidence – In: P.H. Nixon (Ed.) Mantle, Xenoliths J. Wiley & Sons Ltd., pp. 29–433.

Hovorka, D., P. Fejdi 1980: Spinel peridotite xenoliths in the Western Carpathian late cenozoic alkali basalts and their tectonic significance. – Bull. Volcanol., 31, 1, pp. 95–107.

Jones, A.P., J.V. Smith, J.B. Dawson, E.C. Hansen 1982: Metamorphism, partial melting, and K-metasomatism of garnet-scapolite-kyanite granulite xenoliths from Lashaine, Tanzania. – J. Geol., 91, pp. 143–165.

Köhler, T., G.P. Brey 1990: Calcium exchange between olivine and clinopyroxene as a geothermobarometer for natural peridotites from 2 to 60 kb with applications. – Geochim. Cosmochim. Acta, 54, pp. 2375–2388.

Kurat, G., A. Embey-Isztin, A. Kracher, H.G. Scharbert 1991: The upper mantle beneath Kapfenstein and the Transdanubian volcanic region, E. Austria and W. Hungary: a comparison. – Miner. and Petrol., 44, pp. 21–38.

Kushiro, I. 1973: Partial melting of garnet lherzolites from kimberlite at high pressures. – In P.H. Nixon (Ed.) Mantle Xenoliths. J. Wiley & Sons Ltd. pp. 249–299.

Lexa, J., V. Konečný 1974: The Carpathian volcanic arc: a discussion. – Acta Geol. Acad. Sci. Hung., 18, 3–4, pp. 279–293.

Lexa, J., V. Konečný 1979: Relationship of the Carpathian volcanic arc to the geodynamic evolution of the Pannonian Basin. – Geodynamic Invest. in Czechoslovakia, Bratislava.

Mattioli, G.S., B.J. Wood 1986: Upper mantle oxygen fugacity recorded by spinel lherzolites. – Nature, 322, pp. 626–628.

Mattioli, G.S, B.J. Wood 1988: Magnetite activities across the metric estimates of upper mantle

oxygen fugacity. – Contrib. Mineral. Petrol., 98, pp. 148–162.
Mercier, J.C.C., A. Nicolas 1975: Textures and fabrics of upper-mantle peridotites as illustrated by xenoliths from basalts. – J. Petrol., 15, 2, pp. 454–487.
Nell, J. 1989: High temperature cation distributions and thermodynamic properties of (Fe^{2+}, Mg)(Fe^{3+}, Al, Cr)2O_4 spinels. Ph.D. Dissertation, Nothwestern University, Evanston, IL, 148 in: Woodland et al., 1992.
Nicolas, A., F. Lucazeau, R. Bayer 1987: Peridotite xenoliths in Massif Central, France: textural and geophysical evidence for astenopheric diapirism. in: P.H Nixon (Ed.) Mantle Xenoliths, J. Wiley & Sons Ltd. pp. 29–433.
Ohmoto, H., D.M. Kerrick 1977: Devolatilization equilibria in graphitic systems. – Am. J. Sci., 277, 8, pp. 1013–1044.
O'Reilly, S.Y., W.L. Griffin 1985: A xenolith-derived geotherm for southeastern Australia and its geophysical implications. – Tectonophysics, 111, pp. 41–63.
O'Reilly, S.Y. 1990: Equilibration temperatures and elastic wave velocities for upper mantle rocks from eastern Australia: implications for the interpretation of seismological models. – Tectonophysics, 185, pp. 67–82.
Saxena, S.K., Y. Fei 1988: Fluid mixtures in the C-H-O system at high pressure and temperature. – Geochim. et Cosmochim. Acta, 52, pp. 505–512.
Stegena, L. 1964: The structure of the Earth's crust in Hungary. – Acta Geol. Acad. Sci. Hung., 8, 1, p. 413.
Stegena, L., B. Géczy, F. Horváth 1975: Late Cenozoic evolution of the Pannonian Basin. – Tectonophysics, 26, pp. 71–90.
Wells, P.R.A. 1977: Pyroxene thermometry in simple and complex systems. – Contrib. Mineral Petrol., 62, pp. 129–139.
Woodland, A.B., J. Kornprobst, B.J. Wood 1992: Oxygen thermobaometry of orogenic lherzolite massifs. – J. Petrol., 33, 1, pp. 203–230.
Wood, B.J., D. Virgo 1989: Upper Mantle Oxidation State: Ferric iron contents of lherzolite spinels by 57Fe Mössbauer spectroscopy and resultant oxygen fugacities. – Geochim. Cosmochim. Acta, 53, pp. 1277–1291.

Acta Geologica Hungarica, Vol. 37/1–2, pp. 45–66 (1994)

The Velence Mts granitic rocks: geochemistry, mineralogy and comparison to Variscan Western Carpathian granitoids

Pavel Uher, Igor Broska
Geological Institute of the Slovak Academy of Sciences, Bratislava

A geochemical and mineralogical study of the Velence granitic rocks indicates the features of a post-orogenic suite tending to A-type granites. They show clear geochemical and geotectonic differences in comparison to Carboniferous orogenic calc-alkaline granitoids of the Central Western Carpathians on the one hand, and on the other have some similar features to several small, post-orogenic (Permian) granitic rocks in the Western Carpathians as well as in Eastern Alps. New results permit us to assume that the Velence granitoids were generated in a deep fault in a post-collision extensional environment; the granite magma was relatively hot, showed increased alkalinity and intruded into shallower crustal levels.

Key words: granitoids, Velence Mts, Western Carpathians, zircon, REE-bearing minerals, trace elements

Introduction

The more recent studies of the Western Carpathian Variscan granitoids have provided new ideas on their classification, petrogenesis and geotectonic position (Broska and Uher 1991; Hovorka and Petrík 1992; Petrík et al. 1994; Buda 1985 and others), which have brought about the necessity of a wider correlation among granitoids of the Western Carpathians, the Pannonian region and the Eastern Alps.

The granitoids of the Velence Mts, situated south of the Central Western Carpathians in the contact zone with the Eastern Alps, represent the more extensive occurrence of Variscan acid intrusive rocks along the Balaton Line area. From this viewpoint their study also appears to be important for the understanding of the evolution of granitoids over a wider region.

The aim of our work was to contribute to the problem of the position, classification and petrogenesis of the Velence granitic rocks on the basis of geochemical and mineralogical examination.

Addresses: P. Uher, I. Broska: Dúbravská cesta 9, 842 26 Bratislava, Slovakia
Received: 22 October, 1993

0236–5278/94/$ 4.00

Geological position

The Velence granitoid massif is situated in the Bakony Unit of the Transdanubian Central Range. To the south the granitoids and the younger rocks are tectonically separated by the Balaton Lineament. Hidden granitoids analogical to the Velence granitic rocks are known from boreholes and geophysical measurement along the Balaton Lineament at a distance of up to 150 km (Wein 1969, see Buda 1975, 1981, Fülöp and Dank 1987).

The Velence granitoid massif is exposed near the town of Székesfehérvár, over an area of approximately 20 x 5–7 km. Petrographically they represent granites, to a lesser extent veins of granite porphyries, microgranites, and rarely kersantites, aplites and pegmatites (Vendl 1914, Jantsky 1957, Vadász 1964, Buda 1969, 1975, 1985, 1987a, b, 1990a, b, 1992, 1993, Embey-Isztin 1974). The granitoid pluton intruded into Lower Paleozoic, (Lower Ordovician to Lower Carboniferous) sediments, with a predominance of phyllites (Vadász 1964; Balla and Dudko 1993). On the basis of geological and geochronological data it has been assumed that they are of late to post-Variscan (most probably Upper Carboniferous to Permian) age (Földvári and Vogl 1961 ex. Buda l.c.; Buda 1981; Balogh et al. 1983).

Methods

The material for the geochemical, petrographical as well as mineralogical study was obtained from 5–7 kg field samples (Ve-1 to Ve-10). The macroelements were determined by wet chemical analysis, and trace elements by spectrochemical analysis (OES), except for Li, Rb and Zn, which were determined by atomic absorption spectroscopy (AAS). The accessory minerals were extracted by standard methods: crushing, sieving, treatment on a concentrated table, concentration in bromoform and electromagnetic separation according to magnetic properties in an isodynamic magnetic separator. The zircon morphology was studied using a TESLA BS 300 scanning microscope (50 to 100 grains in each sample) and additionally under a binocular microscope. The inner structure zoning of zircon crystals was investigated with a JEOL 840A – scanning electron microscope. Microprobe analyses of zircons were carried out on the X-ray electron microanalyser JEOL JCXA-733 Superprobe with accelerating voltage of 25 kV, specimen current of 40 nA, beam diameter of 5 μm with the use of natural zircon (for Zr, Hf, Si) and YAG (for Y) standards.

Petrography

On the basis of modal analyses, according to IUGS classification, the Velence granitoids are mostly monzogranites, with lesser granodiorites (sample Ve-1) (Fig. 1a). Some samples represent alkaline – feldspar granites according to the Q'-ANOR diagram (Fig. 1b).

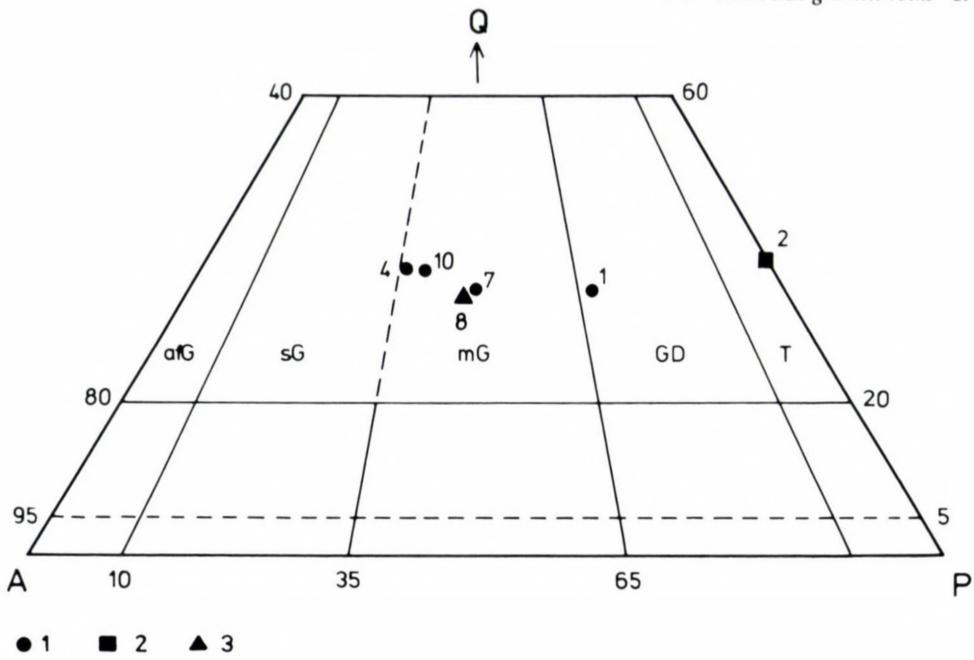

Fig. 1a
QAP diagram according to the IUGS classification of the Velence granitoids. Explanations for Figs 1–5 and 9: 1. granitoids; 2. magmatic enclave; 3. granite porphyries

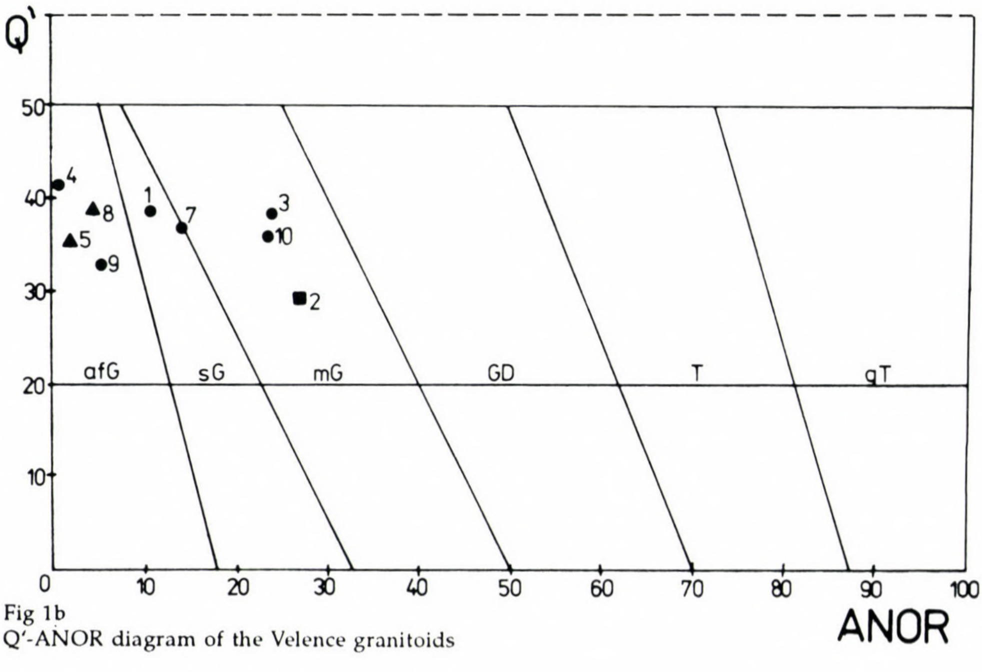

Fig 1b
Q'-ANOR diagram of the Velence granitoids

The most frequent types (Ve-1, Ve-7, Ve-10) are represented by medium- to coarse-grained and sometimes porphyritic granites to granodiorites. They contain subhedral to anhedral, often intensively sericitized plagioclase (centre of crystals An_{34-36}, rim An_{22} – Ve-1), with an average size of 0.7 to 3 mm (max. 7 mm), and intersticial, mainly subhedral biotites reaching 1–2 mm in size. Pink subhedral to euhedral, often perthitic orthoclase with an average size of 1 to 8, max. 10 mm, and Karlsbad twins are sometimes developed. Buda (1993) described relatively high temperatures for these Velence granitoid K-feldspars (680 °C).

Pink, coarse-grained granodiorite (Ve-1) contains numerous X0 cm-large enclaves of dark-grey, fine-grained rocks of leucotonalite composition (Plg+Qtz+Bt), with magmatic structure (Ve-2, M-7 highway near Sukoró).

The granite porphyries, forming veins with a thickness of 0.X to X m, can be divided into two colour types: pink Sukoró (Ve-8, 9) and greyish-green Pátka (Ve-5 Dunkl, pers. communication).

Geochemical characteristics

Increased SiO_2 contents and relatively reduced contents of Al_2O_3, MgO, CaO and P_2O_5 are characteristic of the chemical composition of the Velence granitoids (Table 1). On the other hand, the contents of alkalis are slightly increased (Buda 1985). The granitoids are slightly peraluminous (A/CNK = 1.03–1.27) and they display a trend especially analogous to post-orogenic granites (sensu Maniar and Piccolli 1989 – Fig. 2). The R1-R2 multicationic diagram (de la Roche et al. 1980, Batchelor and Bowden 1985), with a clear trend analogous to post-orogenic to anorogenic suites (Fig. 3), provide a more persuasive indication of the geotectonic position of the Velence granitoids.

We have not registered significant anomalous values in comparison with average concentrations for Ca-poor granites (Turekian and Wedepohl 1961), in the range of trace elements studied (Table 1). There are only slightly increased values of Li, Rb and Zn contents, and in some cases Y and Zr. However, the contents of Sr, Ba, Ni, Co and Cr are relatively reduced. Increased Rb/Sr ratios indicate a higher differentiation level of the granitic melt. The 10 000 Ga/Al vs. Zr, Y, Zn, A.I. discrimination diagrams (Whalen et al. 1987) indicate a transitional position for the Velence granitoids between the S- and the I-types on one side, and A-type on the other (Figs 4a, b). Incomplete spider-diagram of trace elements also indicate a relationship of the Velence granitoids with the post-collision granite group (Pearce et al. 1984 – Fig. 5).

The normalized patterns of rare-earth elements in the Velence granitoids reflect their relatively lower contents, slight enrichment of HREE and marked negative Eu-anomalies (Eu/Eu^* average = 0.43 – Fig. 6), corresponding with the data of Pantó (1980) and Buda (1985). The HREE enrichment in the Velence granites (La_N/Yb_N average = 6.99) is also reflected in the accessory mineral assemblages, especially by an increased concentration of xenotime in some cases (sample Ve-4).

Table 1
Chemical composition of the Velence granitoids (major elements in wt. % – analyst Dr. B. Toman, trace elements in ppm - analyst Dr. Puškelová)

	Ve-1	Ve-2	Ve-3	Ve-4	Ve-5	Ve-7	Ve-8	Ve-9	Ve-10
SiO2	72.95	67.84	71.72	77.48	70.84	72.84	70.66	68.94	73.66
TiO2	0.40	0.61	0.47	0.18	0.48	0.34	0.47	0.49	0.34
Al2O3	13.47	15.87	13.80	12.43	14.76	13.78	14.45	14.85	13.26
Fe2O3	0.94	0.55	2.00	0.25	1.08	0.66	1.56	1.69	0.38
FeO	1.19	2.59	0.47	0.22	1.76	1.40	1.08	1.62	1.44
MnO	0.06	0.08	0.04	0.01	0.05	0.06	0.05	0.05	0.06
MgO	0.43	0.71	0.46	0.04	0.88	0.43	0.74	0.94	0.34
CaO	0.70	1.52	1.43	0.05	0.21	0.72	0.35	0.39	1.37
Na2O	3.43	4.27	3.27	3.16	3.95	3.64	3.68	4.36	3.52
K2O	4.45	3.98	3.97	4.89	4.51	4.37	4.32	3.93	4.24
P2O5	0.08	0.13	0.03	0.01	0.12	0.07	0.10	0.12	0.05
H2O+	1.28	1.18	1.54	0.48	1.56	1.14	1.58	1.79	0.90
H2O-	0.32	0.37	0.29	0.16	0.44	0.44	0.63	0.54	0.28
TOTAL	99.70	99.70	99.49	99.36	100.64	99.89	99.67	99.71	99.84
Li	80.0	118.0	33.0	43.0	55.0	38.0	78.0	68.0	63.0
Rb	225.0	243.0	175.0	263.0	170.0	190.0	215.0	180.0	203.0
Sr	141.0	269.0	148.0	26.0	47.0	115.0	74.0	133.0	100.0
Ba	370.0	500.0	500.0	141.0	420.0	288.0	590.0	320.0	257.0
Be	4.1	5.4	404.0	4.8	~2	4.1	~2.6	~2.6	3.4
B	34.0	35.0	8.0	17.0	9.0	17.0	19.0	10.0	10.0
Sc	7.4	9.6	7.9	<3	8.9	7.8	8.3	11.5	
Y	34.0	66.0	17.0	34.0	30.0	37.0	26.0	30.0	38.0
Zr	210.0	410.0	186.0	62.0	170.0	182.0	174.0	239.0	148.0
Ga	20.0	28.0	18.0	14.0	17.0	17.0	16.0	20.0	20.0
Zn	60.0	85.0	57.0	23.0	104.0	45.0	57.0	77.0	37.0
Sn	<3	3.3	<3	<3	3.7	<3	<3	5.2	<3
Mo	~1.4	~1.7	~1.1	<1	<1	~1.1	<1	~1.1	~1.8
Cu	<3	<3	<3	<3	<3	<3	<3	<3	18.0
Ni	3.7	4.3	6.3	<3	4.5	<3	4.3	5.0	6.3
Co	3.3	5.3	4.6	<3	3.6	3.2	4.7	5.1	3.3
V	16.0	20.0	20.0	<3	29.0	16.0	28.0	43.0	15.0
Cr	<3	<3	<3	<3	9.3	<3	8.3	6.8	<3
Pb	29.0	36.0	19.0	37.0	34.0	19.0	5.0	16.0	28.0
Rb/Sr	1.60	0.90	1.18	10.12	3.62	1.65	2.91	1.35	2.03
Ga/Al	2.80	3.33	2.46	2.13	2.18	2.33	2.09	2.54	2.85
A/CNK	1.15	1.13	1.12	1.17	1.25	1.15	1.27	1.22	1.03

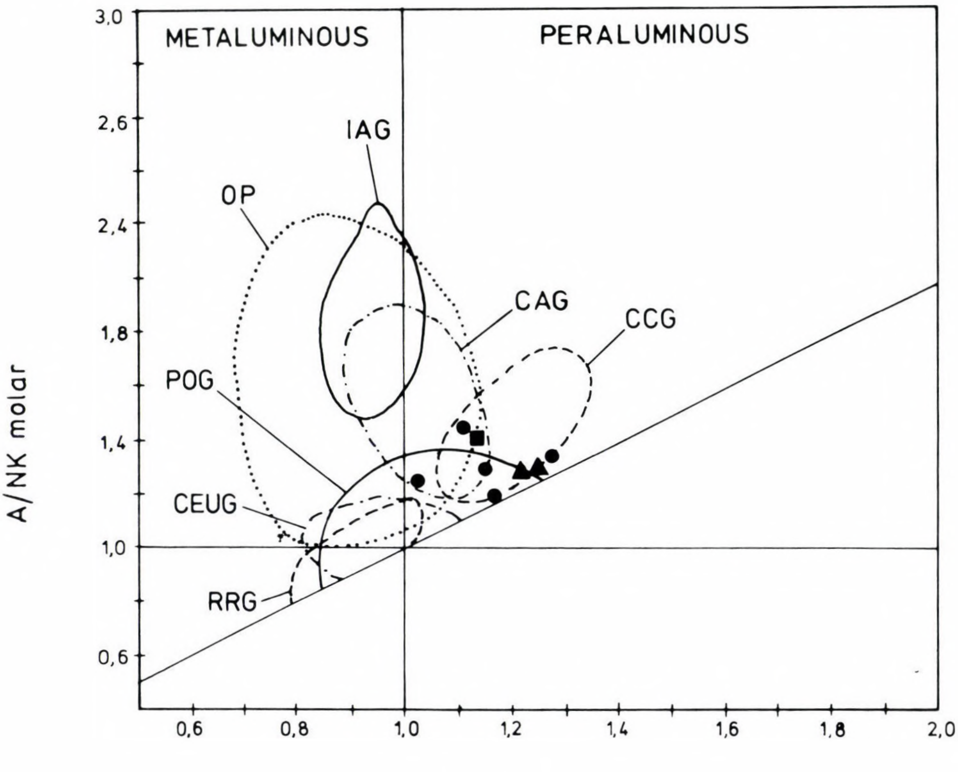

Fig. 2
Shand's index (Maniar and Piccoli 1989). The position of points reflect the slight peraluminous character of the Velence granitoids

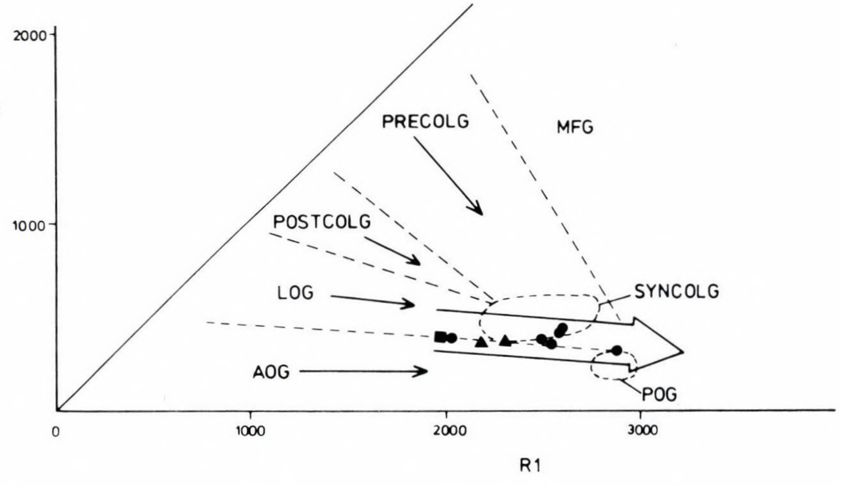

Fig. 3
R1–R2 diagrams (de la Roche et al. 1980, Batchelor and Bowden 1985) of the Velence granitoids

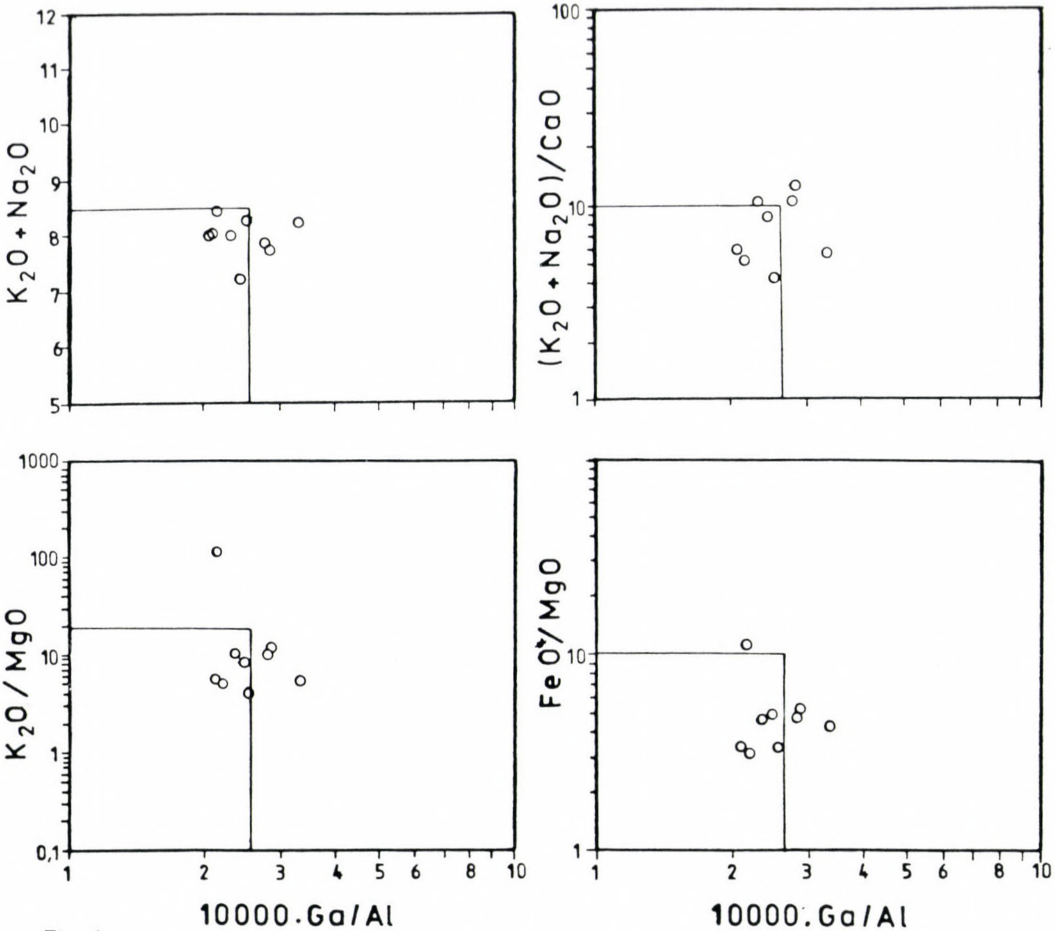

Fig. 4a
10000 * Ga/Al vs. (K_2O+Na_2O), (K_2O+Na_2O)/CaO, K_2O/MgO and FeO*/MgO (Whalen et al. 1987) of the Velence granitoids. The rectangles in the left corner-field of I- and S-types, the rest A-type

Accessory mineral assemblage

The Velence granitoids are characterized by qualitatively (in terms of the number of determined mineral phases – 14) as well as quantitatively (180-1180 g/t) poor accessory mineral assemblages, with zircon and apatite as the most frequently occurring minerals (Table 2). Allanite (Fig. 7a) occurs as the principal REE-bearing mineral phase, with the exception of altered granite from the Aranybulla quarry near Székesfehérvár, where monazite occurs instead of allanite, and xenotime is also abundant (Figs 7 b, c). The occurrence of xenotime, less so of allanite and rarely monazite, in the Velence granitoids has also been

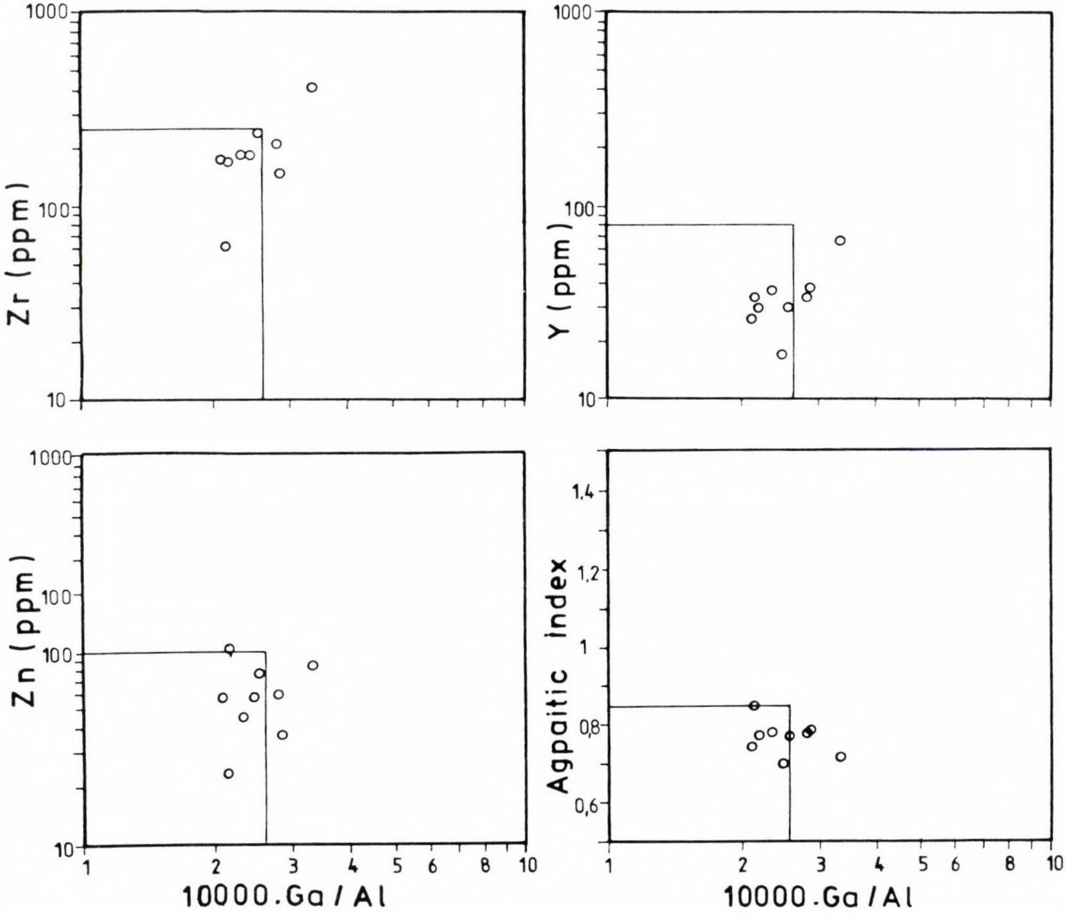

Fig. 4b
10000 * Ga/Al vs. Zr, Y, Zn and agpaitic index (Whalen et al. 1987) of the Velence granitoids. Explanations as in Fig. 4a

mentioned by Pantó (1975, 1980) and Pantó et al. (1988). The contents of Fe-Ti oxides are low; ilmenite is predominant, whereas magnetite is practically absent in the examined samples, and a noteworthy amount of anatase was registered (200 g/t - Pátka Fig. 7d, Ve-5). The Velence granitoids are characterized by an absence, or very low content of Al-rich minerals, and only garnet is sporadically present. Among the sulfides pyrite was present (especially at the Sukoró locality - Ve-9, 10), and the occurrence of molybdenite is sporadic (Ve-1).

The most informative accessory mineral – zircon – was examined in great detail. The zircon occurs as perfect and transparent light-pink 0.0X to 0.3 mm-long crystals. The position of the typological mean points of zircon in the I.A vs. I.T diagram (Pupin 1980) indicates relatively high temperature and an

Table 2
Distribution of accessory minerals in the Velence granites and granite porphyries (in g/t)

	Ve-1	Ve-2	Ve-3	Ve-4	Ve-5	Ve-7	Ve-8	Ve-9	Ve-10
zircon	480	820	370	120	340	360	350	480	300
apatite	80	170	1.5	1.5	260	130	180	350	360
allanite	15	tr.	n.o.	10	0.2	150	3	30	310
monazite	n.o.	n.o.	15	n.o.	n.o.	n.o.	n.o.	n.o.	n.o.
xenotime	n.o.	n.o.	n.o.	50	n.o.	n.o.	n.o.	n.o.	n.o.
rutile	n.o.	n.o.	tr.	tr.	n.o.	n.o.	n.o.	n.o.	n.o.
anatase	n.o.	n.o.	n.o.	n.o.	200	tr.	tr.	n.o.	n.o.
magnetite	tr.	n.o.	n.o.	n.o.	n.o.	n.o.	n.o.	tr.	n.o.
ilmenite	0.6	150	60	0.3	tr.	10	tr.	0.3	10
garnet	0.4	tr.	10	n.o.	1	n.o.	2	1	n.o.
tourmaline	n.o.	tr.	tr.	tr.	n.o.	n.o.	n.o.	n.o.	n.o.
epidote	tr.	tr.	25	tr.	n.o.	n.o.	n.o.	tr.	tr.
pyrite	35	8	n.o.	tr.	1.5	tr.	tr.	220	200
molybdenite	tr.	n.o.	n.o.	n.o.	n.o.	n.o.	n.o.	n.o.	n.o.

comment: n.o. - no observed, tr. - trace content

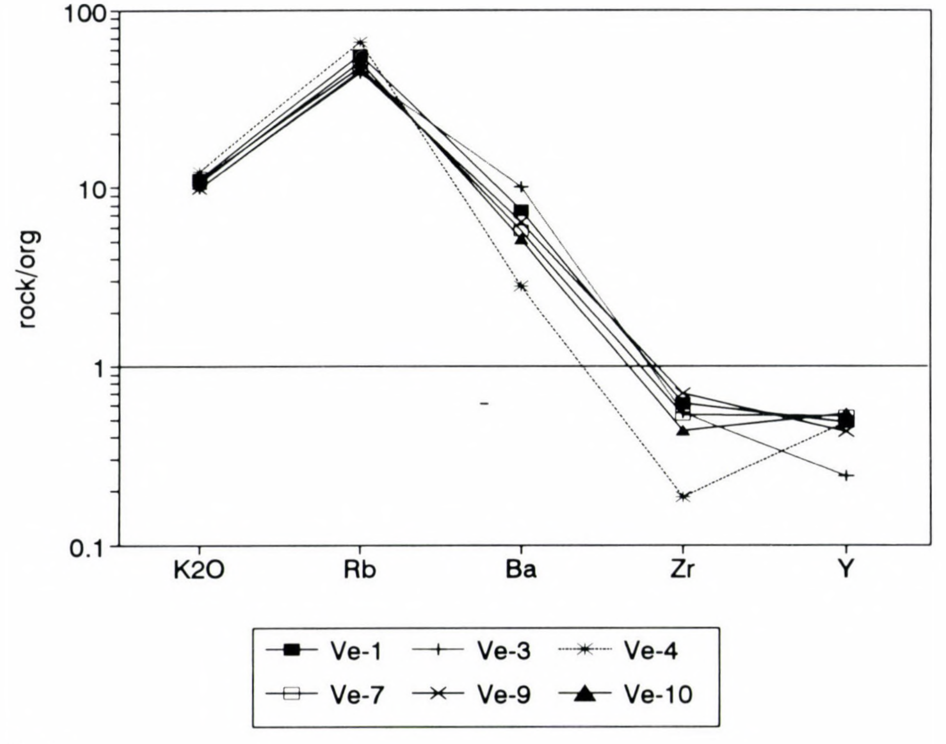

Fig. 5
Incomplete spider-diagram (Pearce et al. 1984) of the Velence granitoids

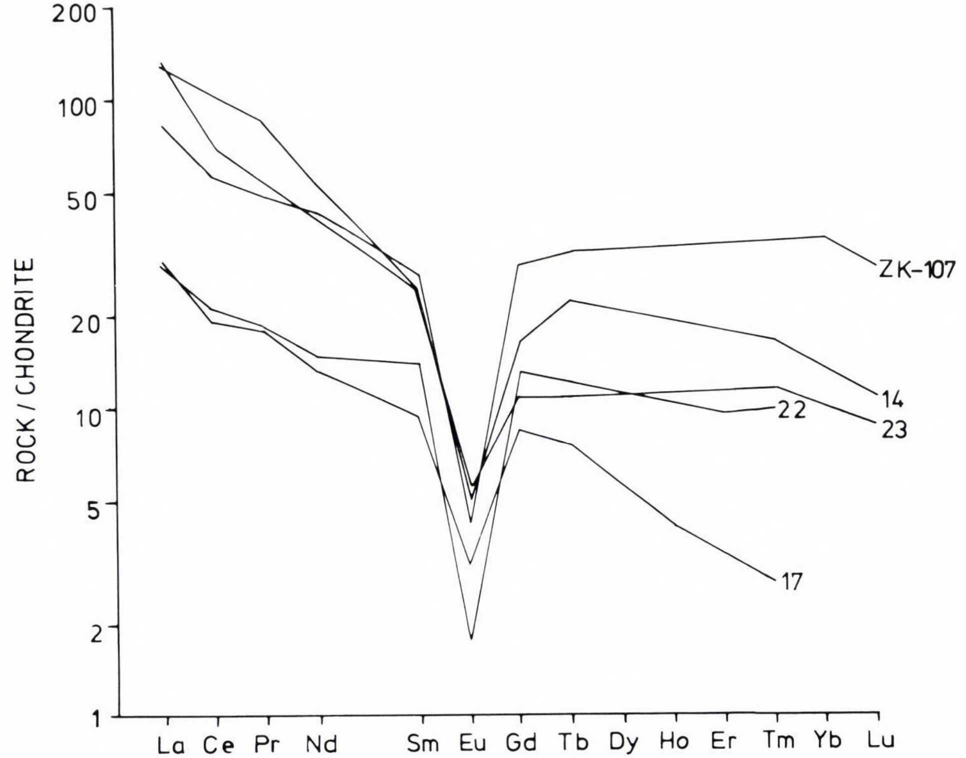

Fig. 6
REE rock/chondrite normalized patterns of the Velence granitoids. Comments: Specimens 14, 23, 22, 17 taken from Pantó (1980), ZK-107 (Aranybulla) unpublished material of Prof. Cambel

alkaline trend in the Velence granitoids (Figs 8, 9). The highest zircon temperature index (I.T) has been recorded in a mafic enclave of leucotonalite composition entrapped in coarse-grained granodiorite (Ve-2, Sukoró); on the other hand, the lowest I.T value is found in granite with a high xenotime content (Ve-4, Székesfehérvár). Two granite porphyries (a green one from Pátka, Ve-5, and a pink one from Sukoró, Ve-8) display a significantly different typologic position of the mean points (Figs 8c, d). Their position on the typogram is almost identical with high I.T, but the clearly lower I.A indices bring them into a position comparable to the calc-alkaline suite of granitic rocks (Pupin, l.c.).

The internal structure of the zircon crystals shows regular oscillation zoning, with slight to considerable variations of the Zr/Hf weight ratios (Fig. 10). However, the hafnium contents generally increase from the centre to rim of crystals, while yttrium, on the other hand, decreases (Table 3). At the same time, the Zr/Hf_{wt} ratios in the centres of crystals vary between 50.8 and 64.7 (average 56.4), and in the rims between 35.1 and 49.9 (average 43.1 - Table 3).

Table 3
Representative analyses of zircon from the Velence granites (wt. %)

	VG-1					VG-6				
	1C	1R	1R	2C	2R	1C	1M	1R	2C	2R
SiO2	32.71	32.65	32.87	32.36	32.66	33.04	32.86	33.29	32.99	32.67
ZrO2	66.79	66.73	65.93	67.13	65.53	65.93	65.33	65.75	67.02	67.20
HfO2	1.11	1.47	1.26	1.10	1.26	0.89	1.04	1.18	1.05	1.67
Y2O3	0.15	0.01	0.01	0.44	0.06	0.33	0.32	0.21	0.07	0.02
TOTAL	100.76	100.86	100.07	101.03	99.51	100.19	99.55	100.43	101.13	101.56
Zr/Hf	52.5	39.6	46	53.3	45.4	64.7	54.8	48.6	55.7	35.1

	Tac-1					Szfvt-6					
	1C	1R	3C	3M	3R	1C	1R	2C	2R	3C	3R
SiO2	33.25	32.59	32.89	33.00	32.78	32.54	32.36	32.50	32.77	32.22	32.24
ZrO2	65.69	64.92	65.22	66.16	65.70	65.72	65.90	66.76	67.27	65.76	66.37
HfO2	1.13	1.27	1.02	1.23	1.15	0.91	1.30	1.09	1.38	0.98	1.65
Y2O3	0.04	0.03	0.14	0.00	0.28	0.30	0.01	0.27	0.02	0.30	0.02
TOTAL	100.11	98.81	99.27	100.39	99.91	99.47	99.57	100.62	101.44	99.26	100.28
Zr/Hf	50.8	44.6	55.8	47	49.9	63.1	44.3	53.5	42.6	58.6	35.1

Fig. 7
Morphology of accessory minerals of the Velence granitoids (SEM - secondary electron images – photo Dr. I. Holický): a – allanite, loc. Ve-7 (real wide 0.18 mm); b – monazite, loc. Ve-3 (real length 0.14 mm); c – xenotime, loc. Ve-4 (real size 0.12 mm); d – anatase, loc. Ve-5 (real. size 0.10 mm)

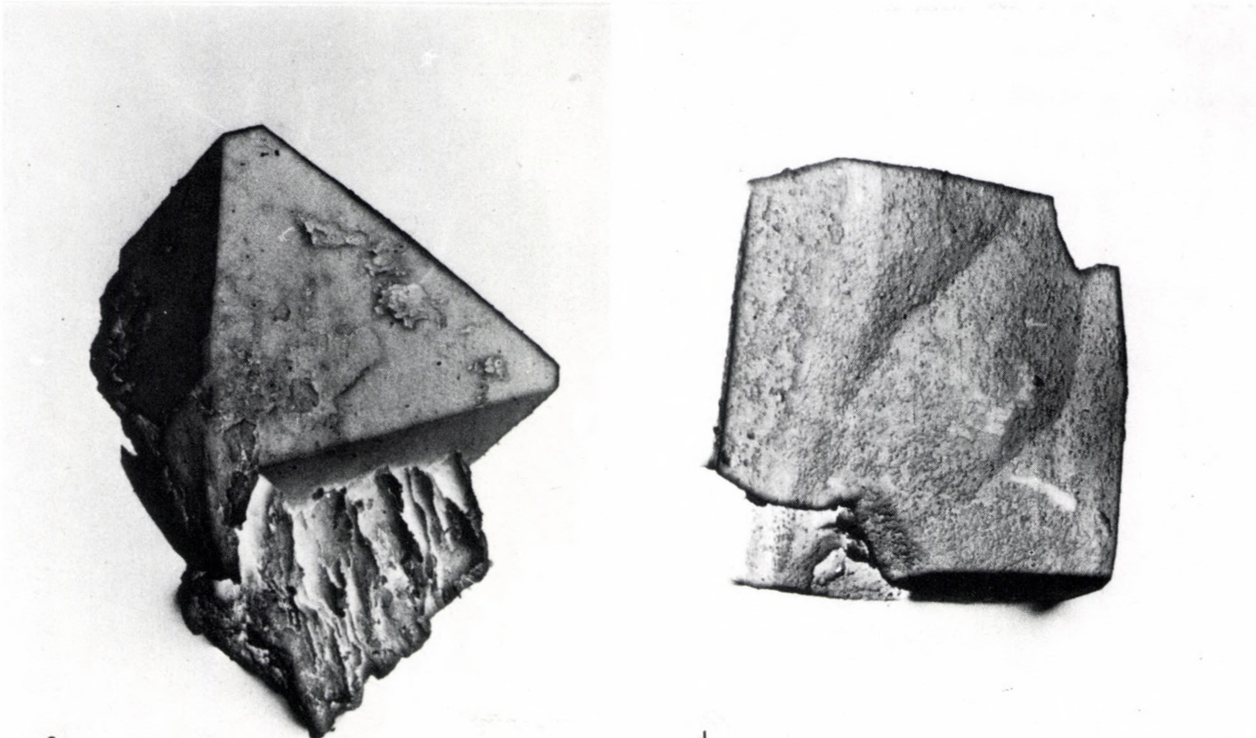

c d

Fig. 7 cont.

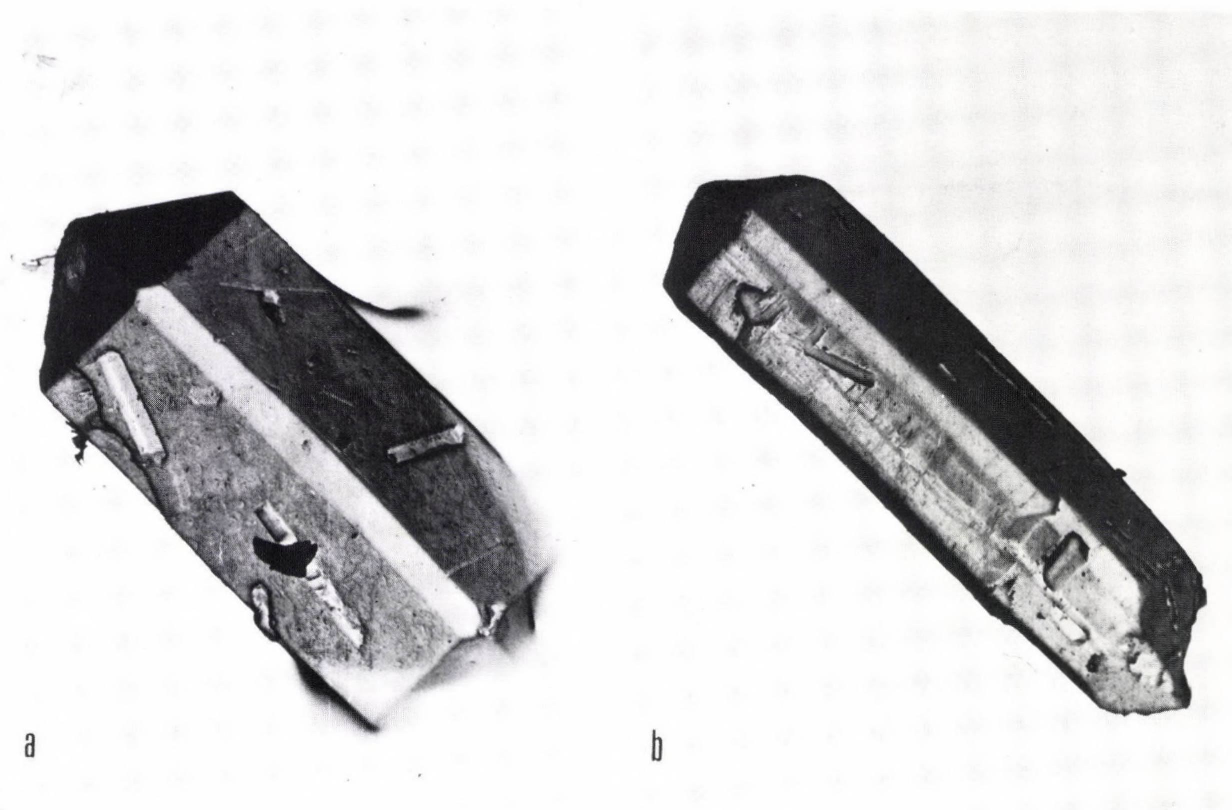

Fig. 8
Zircon morphology of the Velence granitoids (SEM – photo Dr. I. Holický). a, b – P_5 subtype, loc. Ve-10 (real length both 0.25 mm); c – S_{20} subtype, loc. Ve-8, (real length 0.28 mm); d – S_{12} subtype, loc. Ve-8 (real length 0.38 mm)

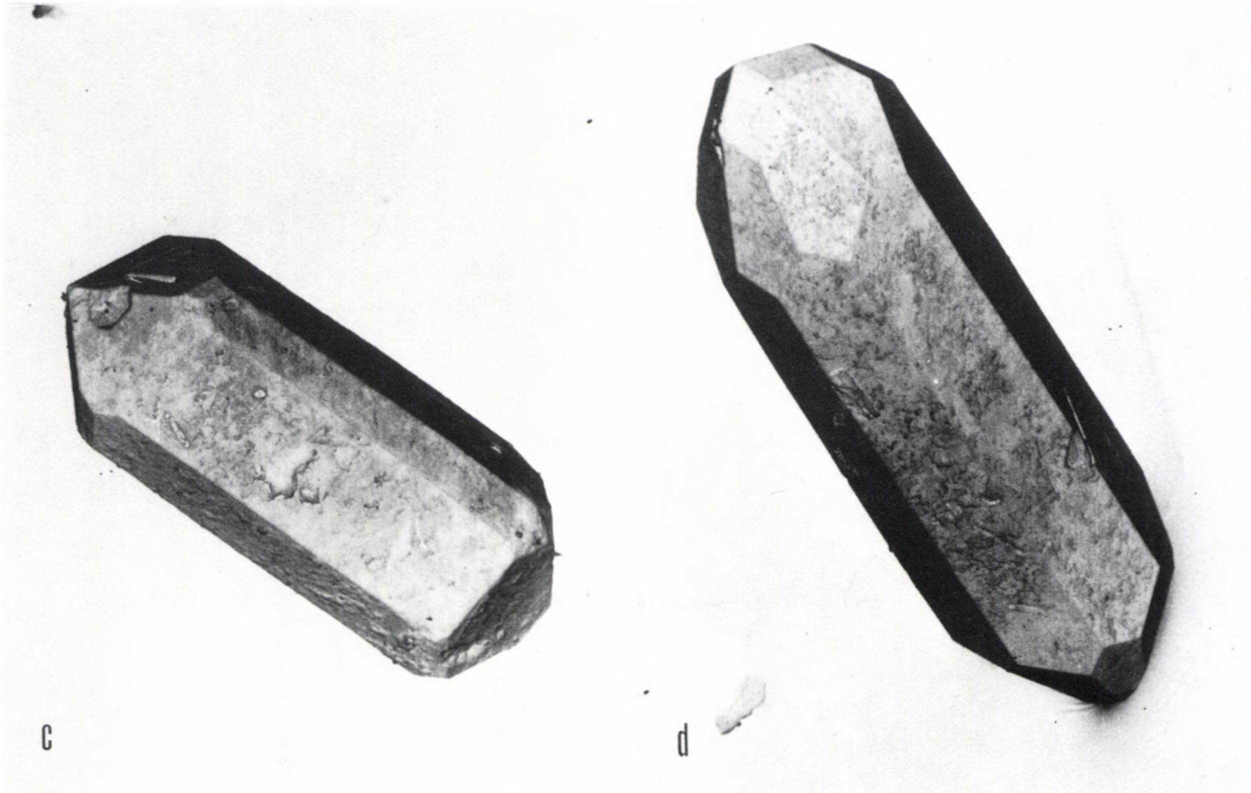

Fig. 8 cont.

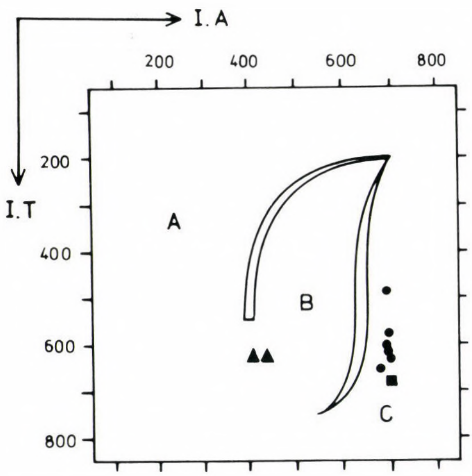

Fig. 9
Zircon typological mean points (Pupin 1980) of the Velence granitoids

Average Zr/Hf values in the centres of crystals are best compared with the Zr/Hf values of hypersolvus alkaline granites (Pupin 1992).

Discussion

On the basis of geochemical analysis (main and trace elements (Figs 2–6) the Velence granites show a certain affinity to post-orogenic, slightly peraluminious granitic suites tending towards A-type granites (sensu Pitcher 1983, Whalen et al. 1987 etc.). These features correspond to the zircon typology and zircon chemistry data: high temperature I.T and agpaicity indices I.A (Fig. 9, earlier data from Gbelský and Határ 1982, Dunkl unpubl. data), higher Zr/Hf ratios and Y contents (Table 3). We agree with Buda (1985, 1987a, b, 1992, 1993) that, just as in other areas where such types of granite occur, the Velence granite magma was probably generated at great depths (high magma temperature, presence of magmatic enclaves), and that it ascended into the shallow to hypabyssal levels of the crust. This is also documented by petrographic features (porphyric development of the granites, dykes of granite porphyries). Crystallization at a shallow crustal level (4–5 km) was also assumed by Buda (1980 ex Balogh et al. 1983, Buda 1993). During this long ascent the granite melt became considerably differentiated in respect to its relatively leucocratic character (QAP and Q'-ANOR diagrams – Figs 1a, b), normalized REE patterns with marked negative Eu-anomalies (Fig. 6), low accessory mineral contents (Table 2) and relatively high Hf contents in the marginal parts of zircons (Table 3).

The geochemical description of the Velence granitoids is not yet unambiguous: they have been described as I-type (Pantó et al. 1988), as well as S-type (Buda 1985, 1992). Our data show that Velence granites present more the features of an immature A-type granitic suite.

Similar post-orogenic suites are typical of a geotectonic regime after the main orogenic collisional events, where a compressional regime had been replaced by extension, which was reflected in changes in the character of acid magmatism from the calc-alkaline to alkaline type (Lameyre 1988, Bonin 1990). The Rb/Sr geochronological data of the Velence Mts. granitic rocks in fact indicate early Permian age (280 Ma – Buda 1985) at the peak of the period of formation of post-orogenic alkaline intrusions in post-Variscan Europe (Bonin l.c.).

The Velence Mts have been ranked geologically with the Bakony Unit in the Transdanubian Central Range, which at present occupies a geographic position between the Eastern Alps and Western Carpathians. If we compare the Velence granitoids with the main mass of Variscan (especially Carboniferous) orogenic granitic intrusion of the central Western Carpathians (Tatric and Veporic Units), we can state that the main differences are in their geochemical characteristics as well as their geotectonic position. The Tatric and Veporic orogenic granitoids are generally characterized as calc-alkaline, metaluminous to peraluminous suites with lower I.A and I.T zircon indices and having other geochemical and mineralogical features ranking with continental collision granites (S>I-types or monazite-bearing granites), or even the volcanic arc granitoids of active continental margins (I>S-type, or allanite-bearing granites) – Broska and Uher 1991; Hovorka and Petrík 1992; Petrík and Broska 1994; Petrík et al 1994.

The Velence granites also do not resemble the Sn-bearing leucogranites and porphyries of probable Permian age (Cambel et al. 1990) in the Gemeric Unit of the Central Western Carpathians, in that they have a different trace element geochemistry and zircon typology data (Jakabská and Rozložník 1989, unpublished data of authors). Besides these, however, small intrusions of post-orogenic (especially Permian) to A-type-tending granites and granite porphyries have also recently been distinguished in the Western Carpathian area (mainly the Turčok and Upohlav granites - Uher and Gregor 1992, Uher and Broska 1992). They are leucocratic granites with increased K-feldspar contents and several geochemical features analogous to A-type granites: increased alkali contents, SiO_2, Zr, REE, Y, Nb and Zn, and reduced contents of Al_2O_3, MgO, CaO, P_2O_5, Sr, Ba, V and Cr. Their zircon typologic characteristic (high I.A, I.T) confirm the assumption of their belonging to hot and dry alkalic melts (sensu Pupin 1980). These post-orogenic Western Carpathian granites thus have many features in common with the studied Velence granitic rocks. Moreover, probably similar types of Permian granitic rocks have also recently described in the Tauern Window of the Penninic Unit in the Eastern Alps (Finger et al. 1992).

Conclusions

The granitoids of the Velence Mts. belong to leucocratic, slightly peraluminous (A/CNK = 1.0–1.3) granite suites, with features of post-orogenic types.

The distribution of major and trace elements, as well as the chemical composition of zircon, indicate their post-orogenic character, with a trend tending from I or S to A-type granites. Typological analysis of zircon indicates relatively high temperatures of magma crystallization (approx. 800 °C) and increased alkalinity of the magma environment.

The Velence granitoids were generated in deep faults in a post-collision extensional tectonic environment, of the post-Variscan, probably Lower

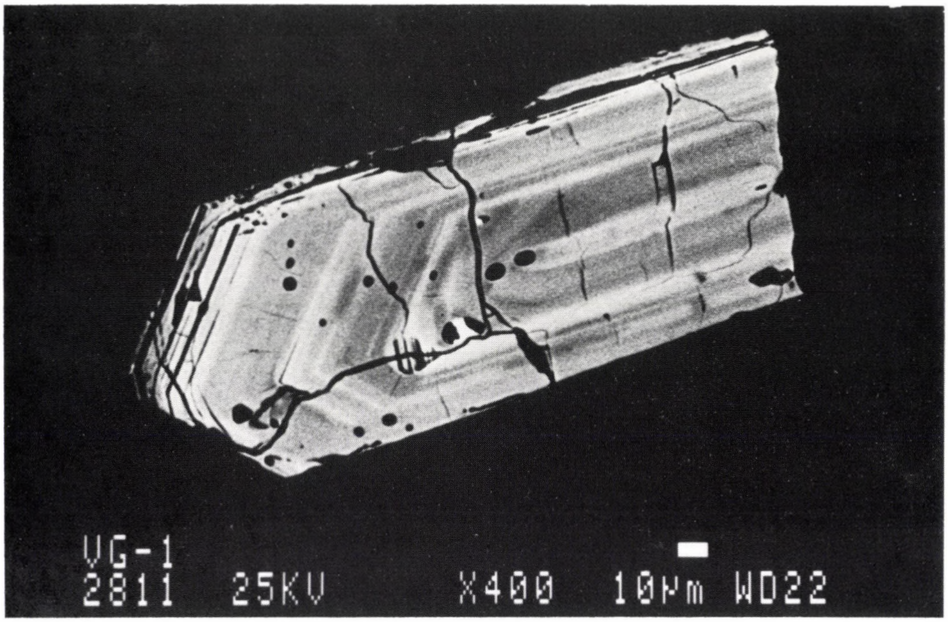

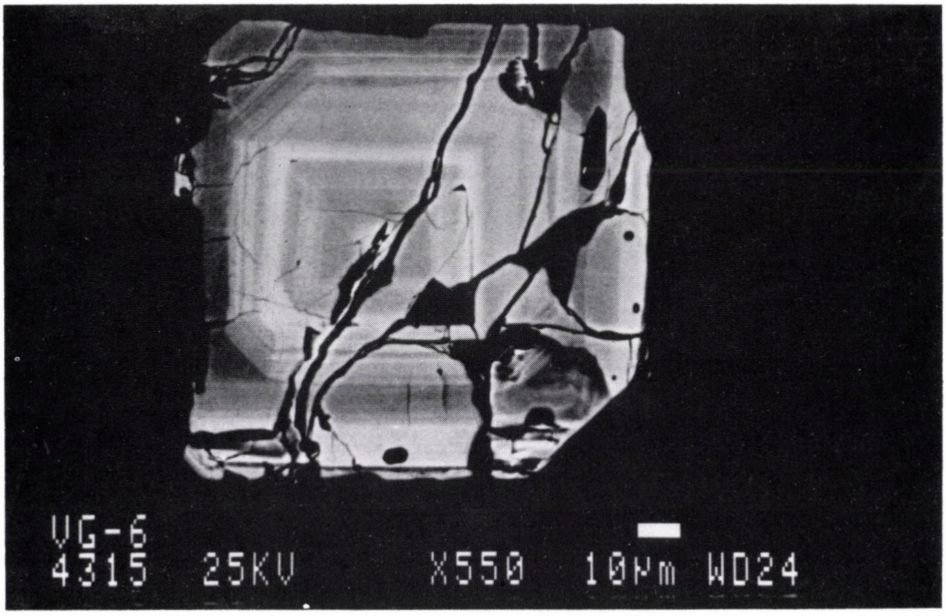

Fig. 10
Internal structure of zircon crystals in back-scattered electron images (BEI – Dr. J. Stankovič). Note zonal structure of zircon

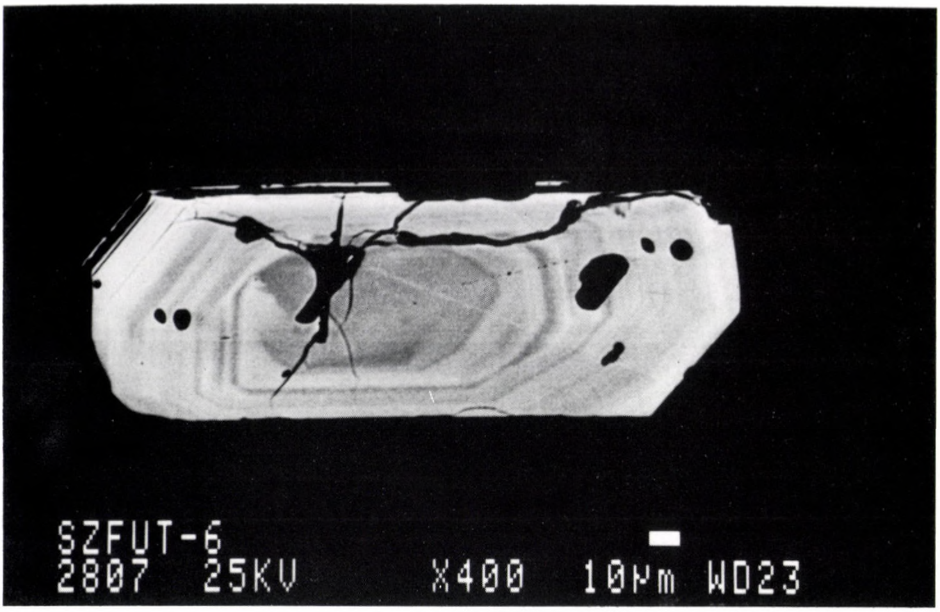
SZFUT-6
2807 25KV X400 10µm WD23

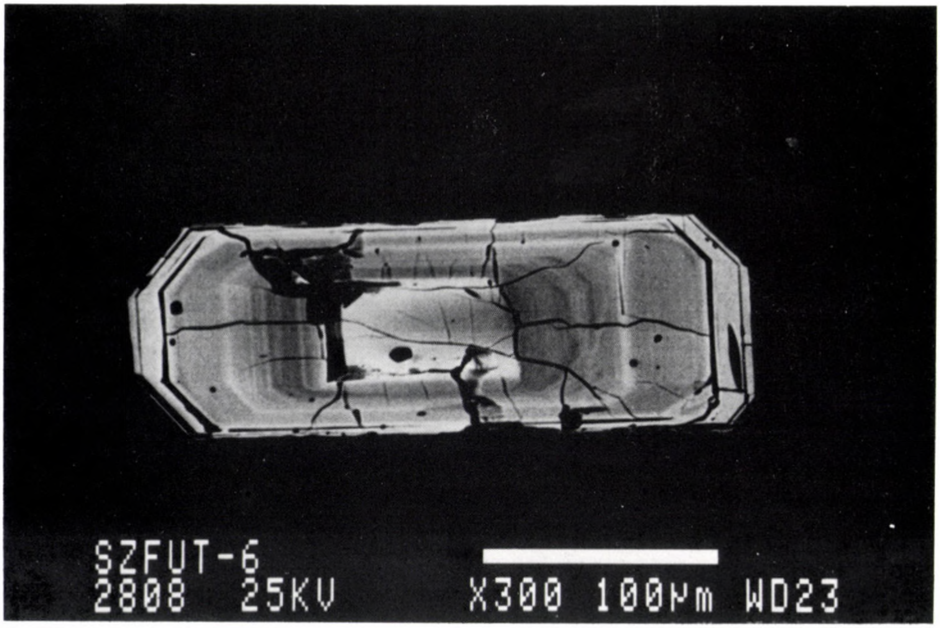
SZFUT-6
2808 25KV X300 100µm WD23

Fig. 10 cont.

The Velence granitoids were generated in deep faults in a post-collision extensional tectonic environment, of the post-Variscan, probably Lower Permian, early consolidated Pangea; their magma intruded into shallower crustal levels. In their basic geochemical as well as mineralogical features, the granitoids of the Velence Mts. are different from the Carboniferous orogenic granitic rocks of the Western Carpathians. On the contrary, they display a certain similarity to some post-orogenic Permian leucocratic granitic rocks of the Western Carpathians.

Acknowledgements

We are grateful to Dr. I. Dunkl, who accompanied us in the field and familiarized us with the details of the geological structure of the Velence Mts, and to Prof. Gy. Buda for many important comments and references. We thank also to Dr. I. Petrík for his critical comments on the manuscript of the paper, as well as to Dr. Cano and Dr. Siman for the zircon microprobe analyses. The research was supported by Grant No 118 (GA Slov. Acad. of Sci.).

Appendix

List of the samples:

Ve-1 leucocrate biotite granodiorite. 1.5 km SW of Sukoró village, NW part of the Velence Mts Outcrop on the M7 highway.

Ve-2 biotite leucotonalite. Fine-grained magmatic enclaves in the Ve-1 granodiorite. Locality as Ve-1.

Ve-3 biotite monzogranite (weathered rock). Székesfehérvár, Aranybulla quarry.

Ve-4 leucocrate biotite monzogranite. Székeshehérvár, Aranybulla quarry.

Ve-5 granite porphyry. Pátka quarry.

Ve-7 leucocrate biotite monzogranite. Pátka quarry.

Ve-8 leucocrate biotite monzogranite. Sukoró, Rigó-hegy quarry.

Ve-9 granite porphyry. Sukoró, Rigó-hegy quarry.

Ve-10 leucocrate biotite monzogranite. Sukoró, Rigó-hegy quarry.

VG-1 Zircons from granite – Pákozd. (Granite with fluorite vein).

VG-6 Zircons from granite – Pákozd. (Granite with monchiquite vein).

Tác-1 Zircons from granite – Tác (borehole core).

Szfvt-6 Zircons from granite – Székesfehérvár.

Comment: Specimens VG-1, VG-6, Tác-1 and Szfvt-6 were provided by Dr. I. Dunkl.

References

Balla, Z., A. Dudko 1993: Tectonics of the Transdanubian Range. In: Balla Z. ed.: Geological problems of the East Alpine–West Carpathian–Pannonian junction area. – Excursion guide. Budapest pp. 3–24.

Balogh, K., E. Árva-Sós, Gy. Buda 1983: Chronology of granitoid and metamorphic rocks of Transdanubia (Hungary). – Ann. Inst. Geol. Geofiz., 61 – Contrib. of 12. Congress of CBGA, Bucuresti, Metamorf. Magmat. Isot. Geol., pp. 359–364.

Batchelor, R.A., P. Bowden 1985: Petrogenetic interpretation of granitic rock series using multicationic parameters. – Chem. Geol., 48, pp. 43–55.

Bonin, B. 1990: From orogenic to anorogenic settings: evolution of granitoid suites after a major orogenesis. – Geol. J., 25, pp. 261–270.

Broska, I., D. Uher 1991: Regional typology of zircon and its relationship to allanite-monazite antagonism (on an example of Hercynian granitoids of Western Carpathians). – Geol. Carpath. 43, pp. 271–277.

Buda, Gy. 1969: Genesis of the granitoid rocks of the Mecsek and Velence Mountains on the basis of the investigation of the feldspar. – Acta Geol. Acad. Sci. Hung., 13, pp. 131–155.

Buda, Gy. 1975: Classification of the Hungarian granitoid rocks on the basis of feldspar investigation. – Carpatho-Balkan Geol. Assoc. Tect. (sec. III), pp. 67–74.

Buda, Gy. 1981: Genesis of the Hungarian granitoid rocks. – Acta Geol. Acad. Sci. Hung., 24, 2-4, pp. 309–318.

Buda, Gy. 1985: Origin of collision-type Variscan granitoids in Hungary, West-Carpathian and Central Bohemian Pluton. – vol. I–II, Unpublished Ph.D. thesis (in Hungarian).

Buda, Gy. 1987a: Variscan granitoids in Hungary and their relation to the West Carpathian. Abstracts. – In: Structural evolution of the Carpathian–Balcan orogenic belt, Bratislava, p. 26.

Buda, Gy. 1987b: The genesis and tectonic settings of the Hungarian Variscan granitoids compared with West-Carpathian and South Alpine ones. – Abstract. Orogeny, Magmatism and Metallogeny in Europe. 5th Meeting of European Geol. Soc. Dubrovnik, p. 8.

Buda, Gy. 1990a: Biotite composition as an indicator of the origin of granitoids. – Abstracts v. 2. IMA Beijing. China, pp. 772–773.

Buda, Gy. 1990b: REE in Hungarian and West-Carpathian Variscan granitoids. – Abstracts v. 2 IMA. Beijing. China, pp. 983–984.

Buda, Gy. 1992: Tectonic settings of the Variscan granitoids occurring in Hungary and some other surrounding areas. – Terra abstract (ALCAPA - Geological evolution of the internal Eastern Alps, Carpathians and of the Pannonian basin, Graz July 1–3) p. 10.

Buda, Gy., 1993: Enclaves and fayalite-bearing pegmatitic "nests" in the upper part of the granite intrusion of the Velence Mts. Hungary. – Geol. Carpath., Bratislava, 44, 3, pp. 143–153.

Cambel, B., Král, J., Burchart, J., 1990: Isotopic geochronology of the Western Carpathian crystalline complex with catalogue of data. – Veda SAV Bratislava 183 p. (in Slovak with English summary).

de la Roche, H., J. Leterrier, P. Grand Claude, M. Marchal 1980: A classification of volcanic and plutonic rocks using R1-R2 diagrams and major element analyses - its relationships with current nomenclature. – Chem. Geol., 29, pp. 183–210.

Embey-Isztin, A. 1974: Petrochemistry of the dike-rocks in the Velence Hills (Hungary). – Ann. His. Nat. Mus. Nat. Hungarici, 66, 23-32.

Finger, F., G. Frasl, B. Haunschmidt, A. von Qandt, A. Schermaier, A. Schindlmayr, H.P. Steyrer, 1992: Late Paleozoic plutonism in the Eastern Alps. – ALCAPA - field guide, Graz, pp. 37–45.

Fülöp, J., V. Dank 1987: Magyarország földtani térképe a kainozoikum elhagyásával (Geological map of Hungary without Cenozoic). – Hungarian Geological Survey, Budapest

Gbelský, J., J. Határ 1982: Zircon from some granitic rocks of the Velence and Mecsek Mountains (Hungary). – Geol. Zbor. Geol. Carpath., 33, pp. 343–363.

Hovorka, D., I. Petrík 1992: Variscan granitic bodies of the Western Carpathians: the backbone of the mountain chain. – Spec. vol. IGCP 276, pp. 57–66.

Jakabská, K., L. Rozložník 1989: Zircons of Gemeric granites (West Carpathians – Czechoslovakia). – Geol. Zbor. Geol. Carpath., 40, pp. 141–169.

Jantsky, B. 1957: A Velencei-hegység földtana (Geology of the Velence Mts). – Geol. Hung. ser. Geol,. 10, pp. 1–170.

Lameyre, J. 1988: Granite settings and tectonics. – Rend. Soc. It. Min. Petrol., 43, 2, pp. 215–234.

Maniar, P.D., P.M. Piccoli 1989: Tectonic discrimination of granitoids. – Geol. Soc. Am. Bull., 101, pp. 635–643.

Pantó, Gy. 1975: Trace minerals of the granitic rocks of the Velence and Mecsek mountains. – Acta Geol. Acad. Sci. Hung., 19, 1-2, pp. 59–93.

Pantó, Gy. 1980: Genetic significance of rare elements in granitoid rocks of Hungary. – In: Proceedings of the XI congress of Carpathian-Balkan Geological Association. Naukova dumka, Kiev.

Pantó, Gy., V. Jovic, I. Fórizs, M. Vukov 1988: Genetic significance of REE accessory minerals in granitic rocks. – Vesnik (Bull.), 44, Beograd, pp. 89–100.

Pearce, J.A., B.W. Harris, A.G. Tindle 1984: Trace element discrimination diagrams for the tectonic interpretation of granitic rocks. – J. Petrol., 25, 4, pp. 956–983.
Petrík, I., I. Broska 1994: Petrology of two granite types from the Tríbec Mountains, Western Carpathians: an example of allanite (+ magnetite) versus monazite dichotomy. – Geol. J., 29, pp. 59–78.
Petrík, I., I. Broska, P. Uher 1994: Evolution of the Western Carpathian granite magmatism: Age source rock, geotectonic setting and relation to the Variscan structure. – Geol. Carpath., 45, (in press).
Pitcher, W.S. 1983: Granite type and tectonic environment. – In Hsü K. (Ed.) Mountain building processes, Acad. Press. London pp. 19–40.
Pupin, J.P. 1980: Zircon and granite petrology. – Contrib. Mineral. Petrol., 73, pp. 207–220.
Pupin, J.P. 1992: Les zircons des granites océaniques et continentaux: couplage typologie-géochimie des éléments en traces. – Bull. Soc. géol. France, 163, 4, pp. 495–507.
Turekian, K.K., K.H. Wedepohl 1961: Distribution of the elements in some major units of the Earth's crust. – Geol. Soc. Amer. Bull., 72, pp. 175–192.
Uher, P., Broska, I., 1992: Variscan post-orogenic Permian-Triassic granitic rocks in the Western Carpathians and Pannonian area. – Terra abstract (ALCAPA – geological evolution of the internal Eastern Alps, Carpathians and of the Pannonian basin. Graz, 1–3 July), 4, p. 157.
Uher, P., T. Gregor 1992: Turčok granite – product of the A-type post-orogenic magmatism? – Mineralia slov., 24, pp. 301–304 (in Slovak with English summary).
Vadász, E. 1964: Geology of Hungary. – Mir, Moscow, pp. 1–532 (in Russian).
Vendl, A. 1914: A Velencei-hegység geológiai és petrográfiai viszonyai (Geological and petrographical conditions of Velencei Mts). – M. Kir. Földt. Int. Évk., 22, pp. 170.
Wein, Gy. 1969: Tectonic review of the Neogene-covered areas of Hungary. – Acta Geol. Acad. Sci. Hung., 13, 399-436.
Whalen, J.B., L.C. Currie, B.W. Chappell 1987: A-type granites: geochemical characteristics, discrimination and petrogenesis. – Contrib. Mineral. Petrol., 95, pp. 407–419.

Acta Geologica Hungarica Vol. 37/1–2, pp. 67–75 (1994)

Interpretation of buried magnetic anomalous sources in the Transcarpathian Depression (Eastern Slovakia)

Ivan Gnojek
Geofyzika a.s. Brno

Jozef Vozár
Dionýz Štúr Geological Institute, Bratislava

The magnetic map of the East Slovakian Lowland demonstrates a remarkably anomalous pattern, the sources of which pertain to different geological structures situated in various depth levels. The striking short-wave and high-amplitude anomalies belong to the outcropping Miocene–Pliocene neovolcanics, mostly andesites, which border the lowland to the W and NE. They also sporadically outcrop in the South of the lowland. Somewhat different parameters are associated with magnetic anomalies representing covered neovolcanics situated within the Neogene Basin at depths of hundreds of meters or deeper. A specific anomaly was found in the North of the basin. Its source, proven by one borehole, is represented by a spinel chrysotile peridotite with a large amount of secondary magnetite as a product of serpentinization. Recent studies point to a Mesozoic–Paleogene age of the source-rock. The long-wave anomaly filling the entire central part of the East Slovakian Lowland has not been completely proven by drilling yet.

Its source, expected to be involved in the basement of the Neogene Basin, is supposed to occupy the depth interval 3–10 km and to consist of basic to ultrabasic rocks.

Key words: magnetic anomalies, neovolcanics, Neogene Basin, basement, ophiolite complex

Introduction

The new (pseudo-) aeromagnetic map at the scale of 1:100 000 was compiled partly from ground measurement of the vertical (Z) component and partly from airborne total (T) vector data; a special technology was employed to convert original Z-component data via magnetic inclination, as a function of geographical position, to T-data. The latter were further converted to a 100 m level of flying and finally merged into the maps of the areas really flown, using a 1 nT airborne proton magnetometer. The final result showed the completed and comprehensive pattern of magnetic field in the East Slovakian Lowland which occupies the NW part of the Transcarpathian Depression (Fig. 1).

The varied magnetic field presented in the map can be regarded in general as an anomalous effect of at least two types of geological bodies participating in the structure of the East Slovakian Neogene Basin (ESNB), developed in the region of the East Slovakian Lowland (ESL). The two different types of anomalies mentioned above are the following:

Addresses: I. Gnojek: Ječná 29a, 612 46 Brno, Czech Republic
J. Vozár: Mlynská dolina 1, 817 04 Bratislava, Slovak Republic
Received: 25 October,1993

0236–5278/94/$ 4.00

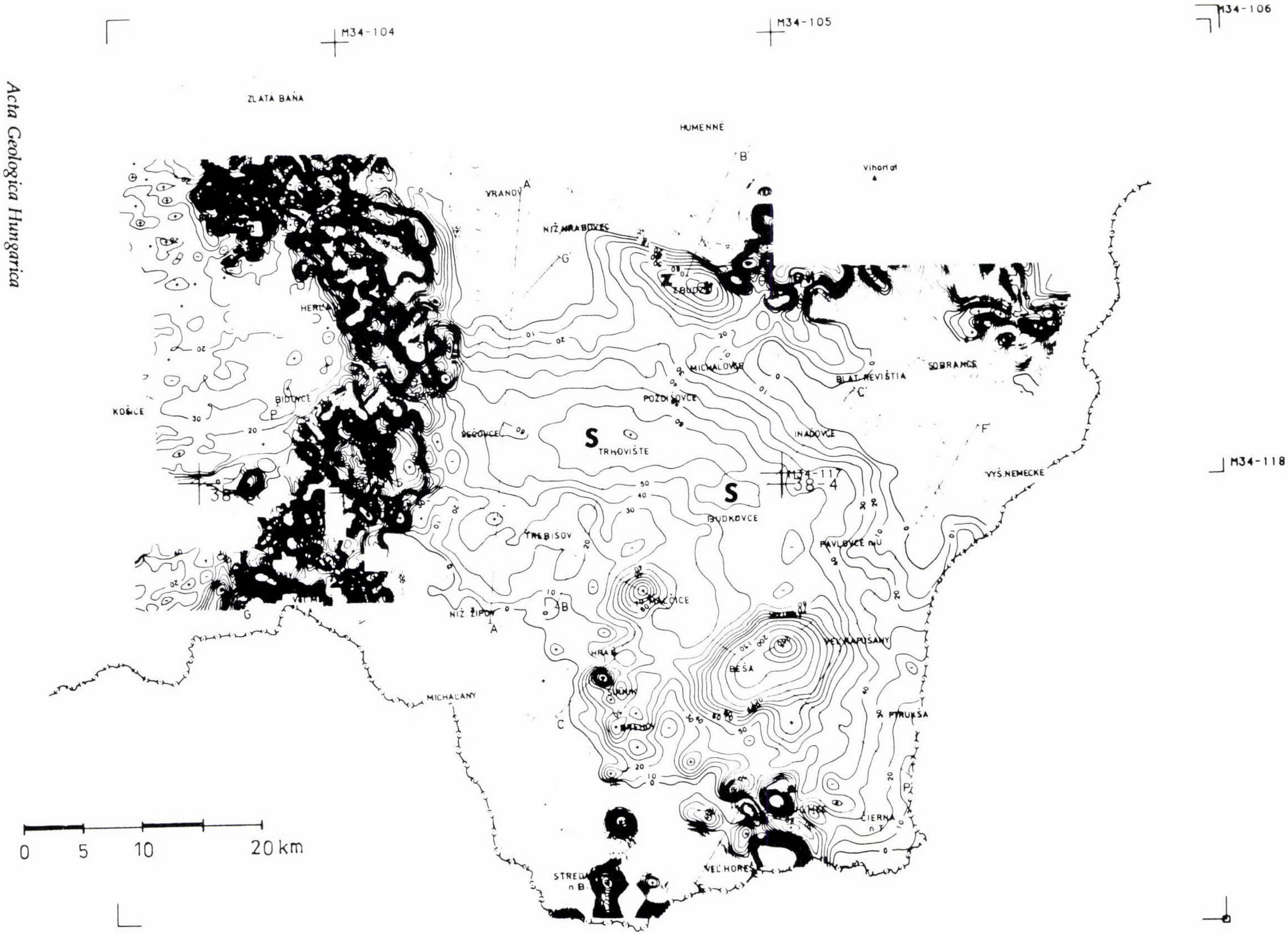
M34-104
M34-105
M34-106
M34-117
M34-118
ZLATÁ BAŇA
HUMENNÉ
Vihorlat
VRANOV
NIŽ. HRABOVEC
ZBUDZA
HERLANY
MICHALOVCE
SOBRANCE
BLAT. REVIŠTIA
KOŠICE
BIDOVCE
POZDIŠOVCE
SEČOVCE
TRHOVIŠTE
INAČOVCE
VYŠ. NEMECKE
BUDKOVCE
TREBIŠOV
PAVLOVCE n. U.
NIŽ. ŽIPOV
VEĽ. KAPUŠANY
BEŠA
MICHAĽANY
PTRUKŠA
ČIERNA n. T.
STREDA n. B.
VEĽ. HOREŠ
0 5 10 20 km

- anomalies caused by neovolcanics – both outcropping and buried
- anomalies the sources of which are incorporated within the basement of the Neogene Basin

Neovolcanics

The most striking mosaic-type short-wave anomalies pertain to the outcropping Miocene–Pliocene neovolcanics, mostly of andesitic character. These outcropping neovolcanics are predominantly concentrated in the western and the northern rims of the ESL, forming the mountain ranges of the Slanské vrchy Mts and the Vihorlatské vrchy Mts. Individual volcanos noted for classical circle-shaped magnetic anomalies could be distinguished in both neovolcanic ranges. Utilizing recently acquired geological knowledge together with the detailed magnetic pattern of the mountain ranges, Gnojek and Kaličiak (1990) were able to study the resulting magnetic polarity – normal and/or reverse – of the dominant volcanic masses in the individual parts of the ranges and, finally, to discuss the sequence of the volcanic events comparing this phenomenon with the latest magnetostratigraphic scale of Harland et al. (1982).

In the southern part of the ESL the outcropping neovolcanics form only several local spots which do not exceed five kilometers in their surfacial sizes. In spite of the small size of the exposed neovolcanic occurrences, the magnetic map shows many medium-wave anomalies, indicating a large amount of buried volcanic rocks in many places in this part of the ESL. Analyzing the magnetic map together with the results of the seismic survey and with the outcome of the individual boreholes (Mořkovský and Novák 1980), the extensive area comprising the buried magnetically anomalous (i.e. intermediate and basic) neovolcanics could be delineated. Although the aggregate area of the outcropping neovolcanics is merely some 20 km^2, an area as large as 350 km^2, filled with buried, mostly andesitic rocks, could be defined there. The general distribution of the buried neovolcanics delineated in the ESL is shown in Fig. 2.

Five volcanic centers were determined in the area. The largest northeastern body occupies an area of about 40 km^2 of buried andesitic rocks. A large amount of the volcanic bodies can be found in the relatively shallow depth of less than 2 km. Their thicknesses, partly proven by drilling and partly estimated by magnetic modelling, vary from hundreds of meters to up to four kilometers. In comparison with this southern part of the ESL, with a fairly concentrated group of buried neovolcanics, another much smaller chain of diminutive, partly acidic and partly intermediate neovolcanic bodies are interpreted to exist in the northern tectonic margin of the ESNB. Almost all neovolcanic bodies

← Fig. 1
(Aero)magnetic map of the East Slovakian Lowland, flown at 100 m above ground level; black contours – positive anomalies; gray contours – negative anomalies; "s" and "z" – anomalies caused by basement sources

detected in the East of Slovakia and pertaining to the Transcarpathian Depression extend into neighbouring countries – Hungary and the Ukraine.

Basement Sources

A substantial part of the northern half of the ESL is occupied by a large and long-wave magnetic anomaly, reaching an amplitude of 70 nT and filling almost the entire W–E dimension of the lowland, from the volcanic range of the Slanské vrchy Mts (W) to the Ukrainian border (E); anomaly "S" in Fig. 1.

This largest anomaly of the ESL is accompanied by a relatively smaller but very distinct (90 nT) and nearly parallel anomaly detected in the northern margin of the ESL; anomaly "Z" in Fig. 1.

Anomaly "Z" was verified by borehole Zb-1 (near the village of Zbudza situated in the western periphery of the Vihorlatské vrchy Mts) – Magyar et al. 1986; here a 170 m thick ultrabasic body was found in the depth interval of 2730–2900 m. Hovorka (in Gnojek et al. 1991) defines the rock as a chrysolite–lizardite variety of peridotite. The large amount of secondary magnetite as a product of serpentinization of this rock yields its extremely high magnetic susceptibilities, reaching up to 240×10^{-3}(SI); the mean value of the susceptibility in the peridotite "layer" drilled is about 120×10^{-3}(SI). This ultrabasic body is believed to account entirely for the existence of anomaly "Z", as was mentioned for the first time by Gnojek (1987). The lowest interval of the Zb-1 borehole from 2900 m to 3705 m was drilled through dark shales to slates.

The largest anomaly ("S") had not yet been proven by drilling. The magnetic modelling applied across this anomaly along several interpretation sections, using the magnetic susceptibilities from 25×10^{-3}(SI) to 50×10^{-3}(SI) – Gnojek et al. 1991 and 1993, shows its source as a 1–2 km thick and slightly vaulted body situated below the northern part of the basin, at a depth of about 3 (2.5) km. From this part of the basin the basement magnetic rocks descend gradually and almost in parallel fashion with the declining basin floor southward. The deepest part of the source-body is expected to be at a depth of about 8 km in places which pertain to the deepest part of the Basin (i.e. 25–30 km ESE of the town of Trebišov; Fig. 3). The detailed analysis of the magnetic field, using also derived maps (such as analytical continuation ones up to a level of 1 km above the ground) suggests the continuation of the magnetic basement source-bodies even below the southern half of the volcanic range of the Slanské vrchy Mts, as was briefly pointed out by Gnojek (1990). The general extent of the magnetic anomalous rocks belonging to the pre-Neogene basement is drawn in Fig. 4.

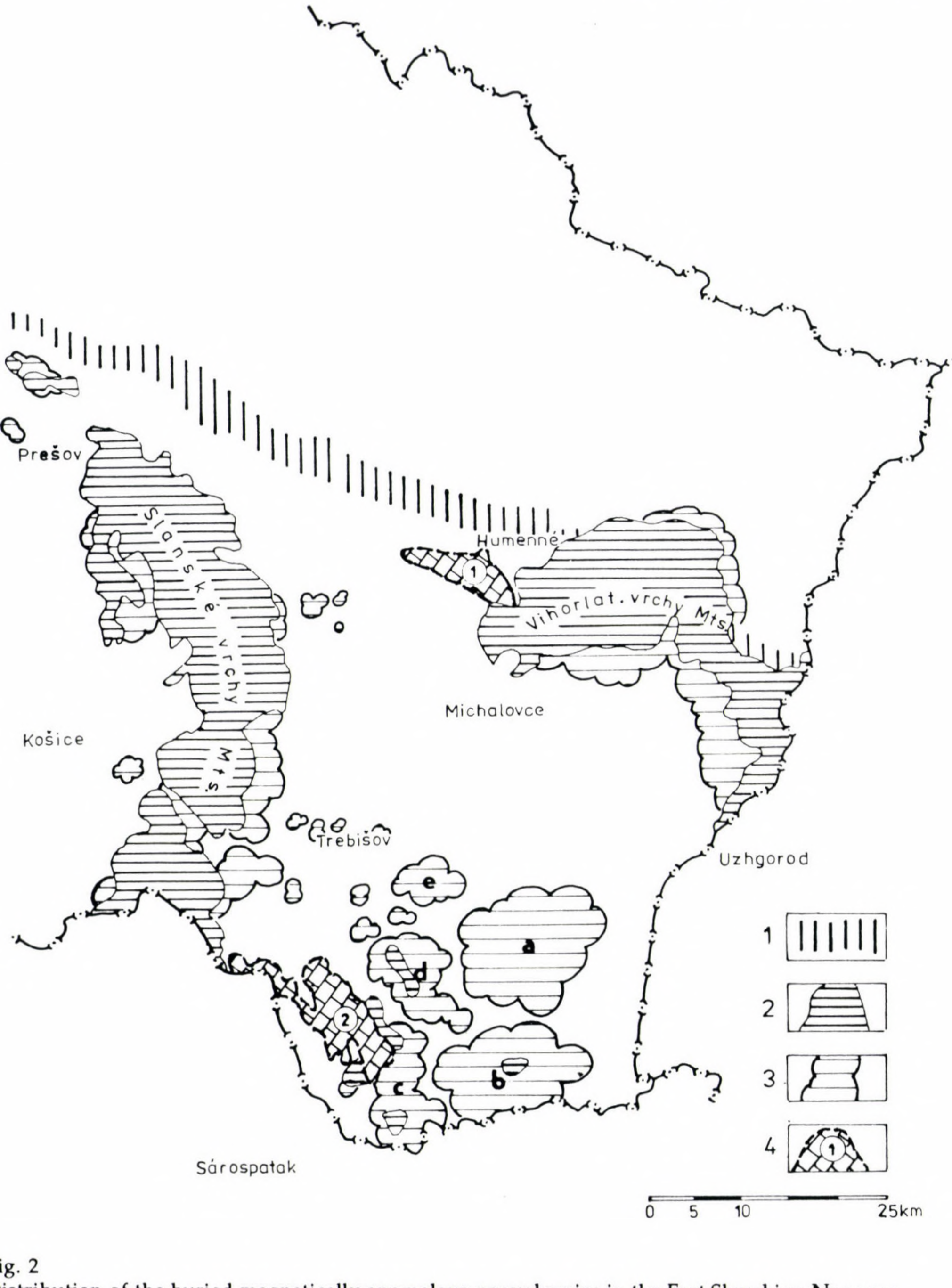

Fig. 2
Distribution of the buried magnetically anomalous neovolcanics in the East Slovakian Neogene Basin. 1. Pieniny Klippen Belt; 2. outcropping neovolcanics; 3. buried magnetically anomalous neovolcanics; 4. outcropping pre-Tertiary basement; ① Mesozoic of Humenné; ② Paleozoic and Mesozoic of the "Zemplín Island"

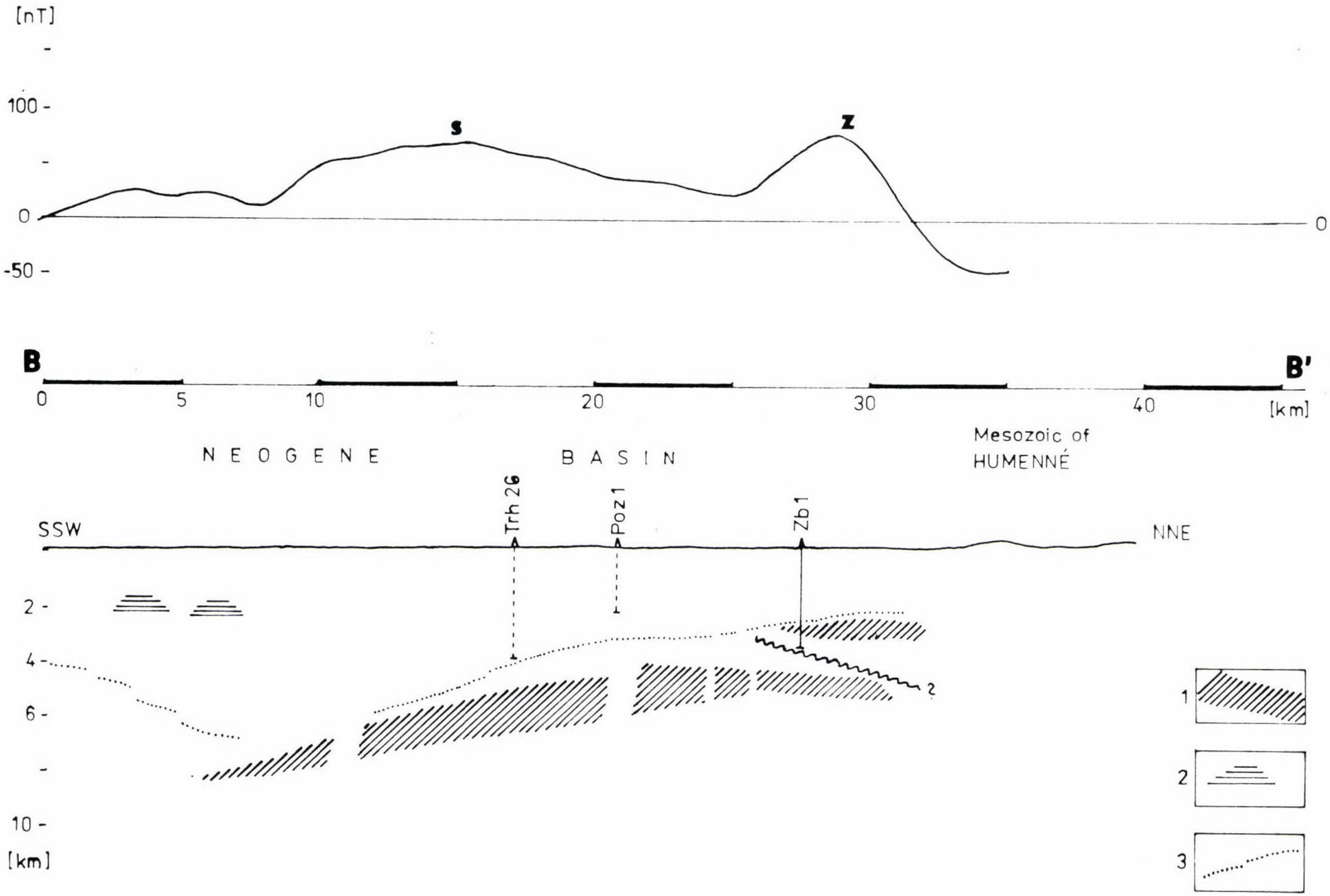

Fig. 3
Interpretation profile and cross-section B–B′, (Trebišov–Humenné). "s" and "z"– anomalies caused by basement bodies; 1. basement source-body; 2. buried neovolcanic source-body; 3. basin bottom mostly defined by seismic survey

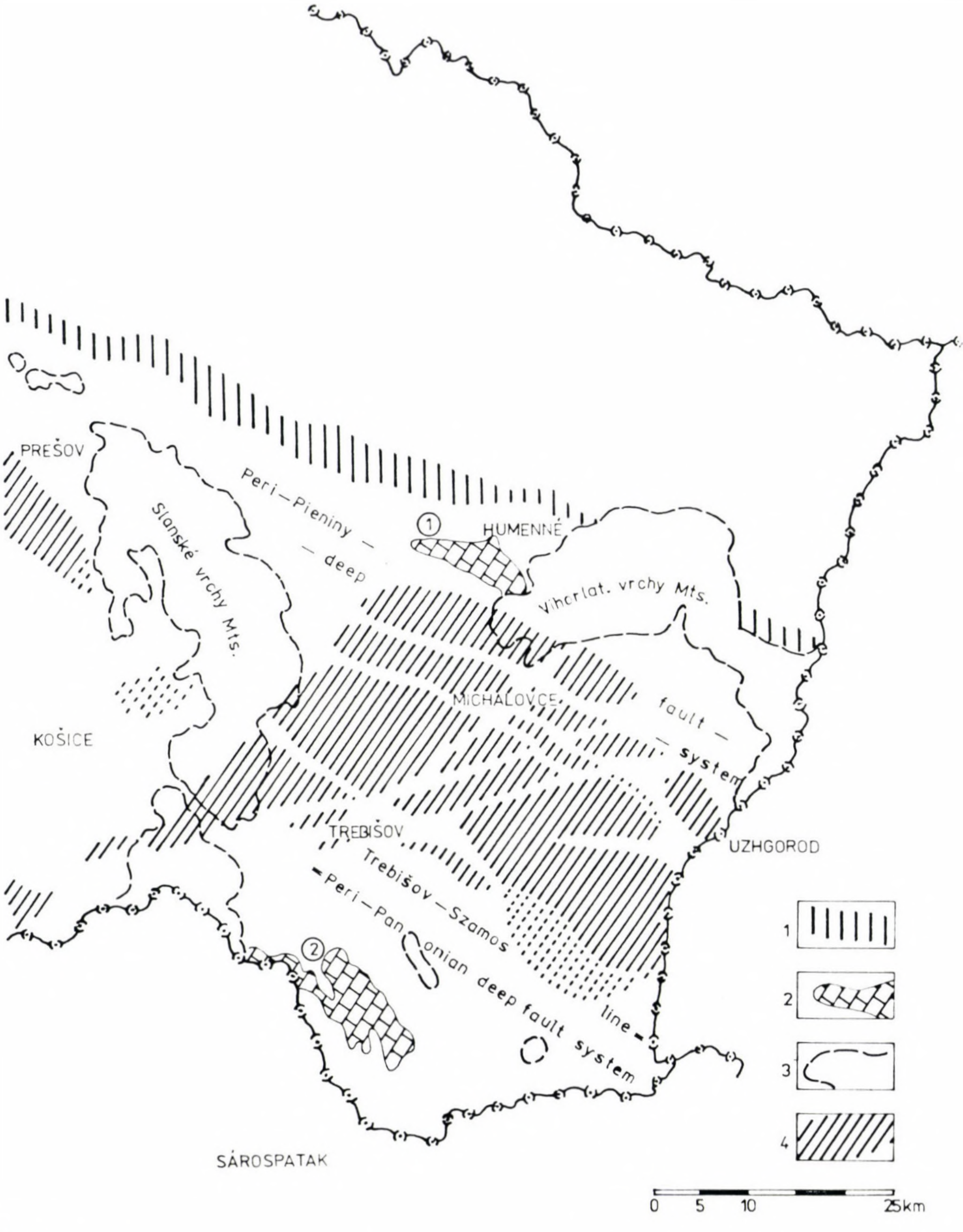

Fig. 4
Delineation of magnetically anomalous basement sources below the East Slovakian Neogene Basin. 1. Pieniny Klippen Belt; 2. outcropping pre-Tertiary basement; ① Mesozoic of Humenné, ② Paleozoic and Mesozoic of the "Zemplín Island"; 3. contour of the outcropping neovolcanics; 4. magnetically anomalous basement source-bodies

Discussion

The ESNB is assumed to have opened between two NW–SE fault systems: a first (northern) one, running out from the Peri-Pienine fault system and passing the town of Michalovce to the town of Uzhgorod, and a second (southern) one, being an element of the Trebišov–Szamos line (the Peri-Pannonian lineament). The above-mentioned fault systems are also interpreted as essential tectonic boundaries delineating the magnetic rocks in the basement. There are likewise young faults of strike-slip character (according to Vass et al. 1988) expected in the ESL region, mostly of SW–NE (W–E) direction, which also complicated the final structure of the magnetic basement.

New outcomes of the geological research in the ESNB were published during the past year – Vozár et al. 1993; Soták et al. 1993.

According to the work of Vozár et al. (1993), the basement substratum of the East Slovakian Neogene Basin is built up of a flysch sequence, which is in direct connection with the flysch series of the Szolnok through in Hungary and with the Krichevo unit in the Ukraine. As far as the relationship to the Inner Carpathians and the Apuseni Mts. is concerned, this flysch sequence is regarded as a relic of a particular subduction zone.

Ultrabasic bodies of the peridotite type were protruded from a mantle source into shallower horizons, exceptionally to the lowest Neogene strata, during the process which formed the Neogene pull-apart basin.

The opinions of Leško (in Leško and Varga 1980); of Mahel (1981) and that of Soták et al. (1993), which consider the pre-Tertiary basement to be a part of the Penninicum, do not seem to be acceptable. We must refute them entirely (1) for the geological reasons mentioned above and (2) and because of the most probable mantle origin of the source of the distinct basement magnetic anomaly.

In spite of the fact that rocks with expressively anomalous magnetic susceptibilities have not yet been found in the boreholes situated within the extension of the "S" anomaly (the boreholes having only reached the uppermost part of the sub-Neogene series), the basement complex in which the basic and ultrabasic rocks are involved is nevertheless considered to be the very source-complex of the large magnetic anomalies. Other large and expressive magnetic anomalies of relatively deep sources were mapped in the territory of the Transcarpathian Depression – the origin of which is probably not only linked to neovolcanics – (i.e. two "deep-source" anomalies W of the Slanské vrchy Mts, the Uzhgorod anomaly in the westernmost part of the Ukraine and the Kisvárda anomaly in the NE Hungary).

References

Gnojek, I. 1990: Areal extent of the basement magnetic source in SE Slovakia. – Mineralia Slov., 22, pp. 191–192. (in Czech with English abstract).

Gnojek, I., M. Kaličiak 1990: Chronological development of the Neogene andesite volcanism in the Eastern Slovakia in the light of magnetostratigraphic scale. – Mineralia Slov., 22, pp. 499–506. (in Slovak with English abstract).

Gnojek, I., D. Hovorka, L. Pospíšil 1991: Sources of magnetic anomalies in the pre-Tertiary basement of the Eastern Slovakia (Czecho-Slovakia). – Geol. Carpath. 42, 3, pp. 169–180.

Gnojek, I., F. Janák, I. Poledňák, A. Mutlová 1993: Geological interpretation of buried sources of magnetic anomalies in the East Slovakian Lowland. – Manuscript, Geofond Bratislava (in Czech).

Harland, W.B., A.V. Cox, P.G. Llevellyn, C.A.G. Pickton, A.G. Smith, R. Walters 1982: A geologic time scale. – Cambridge Univ. Press.

Leško, B., I. Varga 1990: Alpine elements in the West Carpathian structure and their significance. – Mineralia Slov., 12, 2, pp. 97–130.

Mahel, M. 1981: Penninicum in the Western Carpathians from the point of view of the global tectonics. – Mineralia Slov., 13, 4, pp. 289–306.

Magyar, J., R. Rudinec, M. Řeřicha, J. Smetana, G. Tlumač, M. Geci, H. Jánoštíková, J. Krištek, L. Praščák, A. Stanková 1986: Annual report on the geological results of the Michalovce Exploration Company in 1985. – Manuscript, archives of the Moravian Oil Mines, Hodonín (in Slovak).

Mořkovský, M., J. Novák 1980: Some results of reflection seismic measurements in the area of buried volcanic bodies in the SE of the Potiská nižina Lowland (Eastern Slovakia). – Mineralia Slov., 12, 3, pp. 229–239. (in Czech with English abstract)

Soták, J., R. Rudinec, J. Spišiak, J. 1993: The Penninic "pull-apart" dome in the pre-Neogene basement of the Transcarpathian Depression (Eastern Slovakia). – Geol. Carpath., 44, 1, pp. 11–16.

Vass, D., M. Kováč, V. Konečný, J. Lexa 1988: Molasse basins and volcanic activity in West Carpathian Neogene – its evolution and geodynamic character. – Geol. Zbor. Geol. Carpath., 39, 5, pp. 539–561.

Vozár, J., Č. Tomek, A. Vozárová 1993: Reinterpretácia predneogénneho podložia východoslovenskej panvy. – Mineralia Slov., Geovestník, 25, 6, pp. 1–2. (in Slovak).

Acta Geologica Hungarica, Vol. 37/1–2, pp. 77–96 (1994)

The evolution of the intramontane basins at the western edge of the Bohemian Massif during the Permo-Carboniferous: Environment of deposition and economic geology

Harald Gerold Dill
Bundesanstalt für Geowissenschaften und Rohstoffe, Hannover

In southern Germany Permo-Carboniferous clastic, volcaniclastic and volcanic rocks are patchily distributed along the SW border of the Bohemian Massif. These rocks, which may be subdivided into four formations (Bechtsrieth Fm.: Westphalian (?) to Stephanian, Schadenreuth Fm.: Stephanian (?) to Lower Autunian, Weiden Fm.: Upper Autunian–Saxonian, Tiefenbach Fm.: Saxonian to Thuringian) were formed in three major basins named Stockheim, Weiden and Schmidgaden Basins. The Bechtsrieth Fm. is made up of red and grey beds with some volcaniclastic interbeds, and reflects the transition from a proximal alluvial fan to a lacustrine environment. The Schadenreuth and Weiden Fms. are representatives of a playa environment containing red beds with calcretes and freshwater carbonates. The Tiefenbach Fm. is held to be contemporaneous with the Thuringian Zechstein units and is likely to represent a continental equivalent to these marine deposits. Carbonaceous matter deposited in swamps and lacustrine environments throughout the Permo-Carboniferous gave rise to minable hard coal seams and has proven its source rock potential for gaseous and liquid hydrocarbons. This organic matter acted as a reducing agent for hexavalent U, which was derived from the volcanic rocks (calkalkaline suite: mainly dacites to rhyolites) and caused layered uranium deposits to be formed in these troughs. Data from organic chemistry, sedimentology and mineralogy provided the base for modelling four reference basin types which are remarkably distinct with respect to their economic potential of energy resources.

Key words: Permo-Carboniferous, southern Germany, facies analyses, terrigenous clastic depositional system, hydrocarbons, hard coal, uranium, basin model

Introduction

Along the SW edge of the Bohemian Massif Permo-Carboniferous clastic, volcaniclastic and volcanic rocks crop out in narrow troughs and small embayments (Fig. 1) (Emmert 1981; Lützner 1988; Dill 1987; 1989b; Helmkampf et al. 1982; Helmkampf and Waeber 1983).

The Permo-Carboniferous series are bounded towards the NE by basement rocks; towards the SW they dip under Triassic arkoses and conglomerates. Rock exposures at Weidenberg (condensed and reduced facies on the Fichtelgebirge -Erzgebirge Anticline), combined with cutting and drill core examinations of water wells and exploration wells spudded for uranium and coal provide a

Address: 30655 Hannover, P.O. Box 510153, D-30631 Hannover, Germany
Received: 23 September, 1993

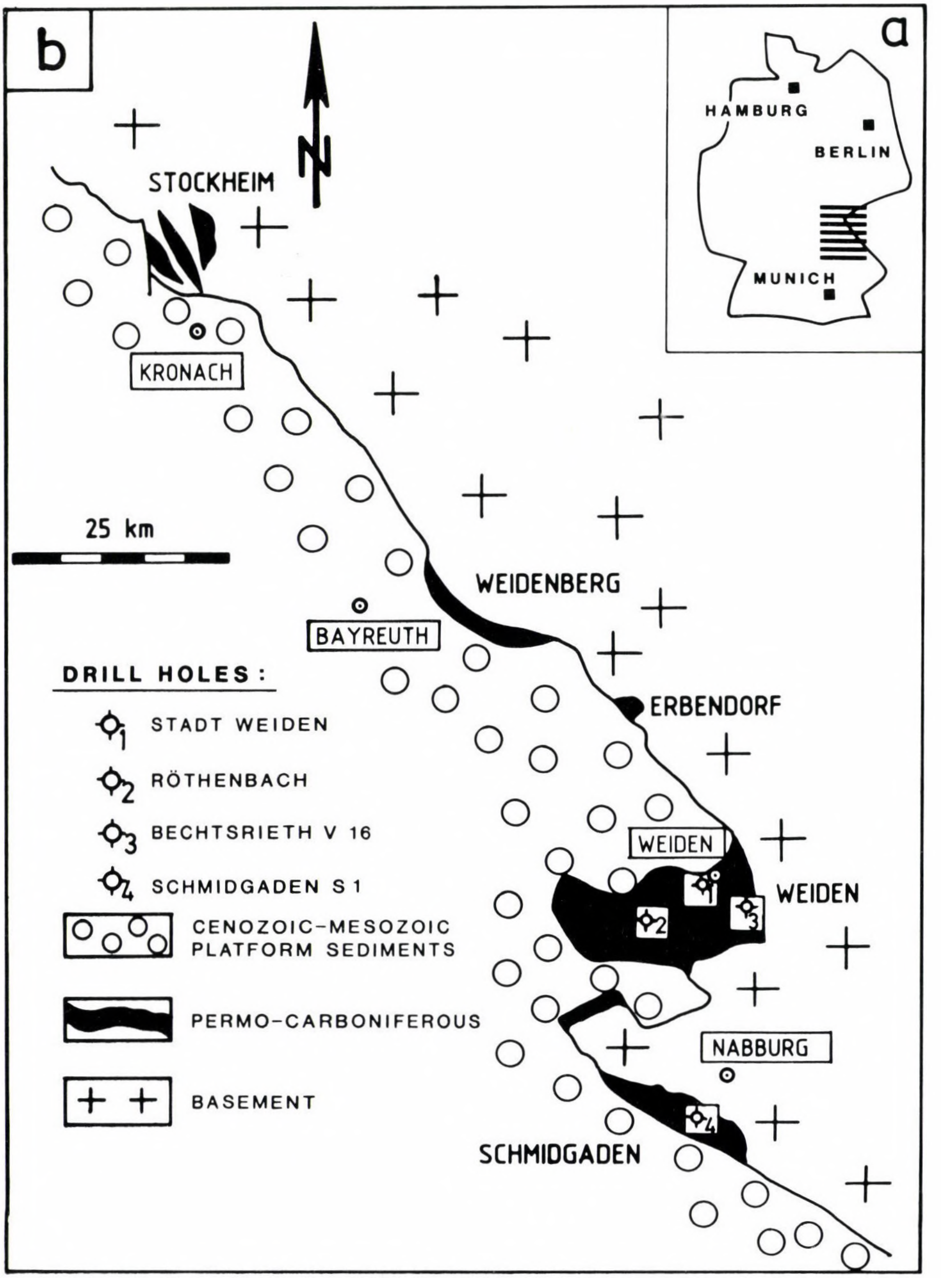

Fig. 1
Map showing the Permo-Carboniferous troughs and embayments alongside the basement boundary fault, and major boreholes (b). The stratigraphic and sedimentary records of these boreholes are illustrated in Fig. 2 ("Stadt Weiden") and Fig. 3 (Röthenbach, Bechtsrieth V16, Schmidgaden S1). Sketchmap showing the location of the area under consideration in southern Germany near the border with the Czech Republic (a)

sound basis for the stratigraphic subdivision (Fig. 2) of the rock series and the interpretation of their environment of deposition. Detailed ore mineralogical studies and investigations concerned with organic chemistry have been performed to assess the source rock potential of the carbonaceous interbeds of these basins with respect to hydrocarbon and uranium potential. Supplementary studies were aimed at unravelling the nature of the volcanic activity during the Permo-Carboniferous (Richter and Villwock 1960; Dill 1991), which has an intermediate control on the enrichment of uranium and associated base metals, as well as having governed the geothermal gradient and maturity of organic matter. The purpose of this paper is to contribute to the depositional environmental analysis of these rock series and the knowledge of its economic geology as a function of facies variations.

Stratigraphy

A tripartite sequence penetrated beneath the Triassic Bunter in a geothermal well at Weiden was taken as reference for the correlation and age-dating of the adjoining basins (Dill with a contribution by Hartkopf-Fröders 1990) (Fig. 2).

It consists of the Bechtsrieth Formation (Upper Carboniferous), Schadenreuth Formation (Upper Carboniferous (?) to Lower Autunian) and Weiden Formation (Upper Autunian to Saxonian). Another unit overlying rhyodacites and dacites was designated Triebenreuth Formation. This rock unit, which is Thuringian in age, was only found in the Erbendorf subbasin (Fig. 3) and consists of prevalently coarse-grained red beds; it is of no particular interest as far as hydrocarbon or metal exploration is concerned.

Lithology and environment of deposition

The greywacke conglomerate member of the Bechtsrieth Fm.

At the base of the Bechtsrieth Fm., polymict, grain to matrix-supported conglomerates with gneissic and volcanic clasts of diameters as large as 10 cm rest unconformably upon Precambrian basement. According to Miall's facies classification (1984) these crudely bedded conglomerates may be coded "GM" (Plate IIIA). Where bedding is discernible it may be termed flaser bedding, according to Reinecke and Singh (1980). The occurrence of dispersed carbonaceous matter may be inferred from the grey to black colour, particularly observed in the fine-grained beds.

The poorly-sorted, extremely coarse-grained deposits originated from landslides. Downslope these boulder beds gradually passed over to aqueous arenaceous deposits of active channels of braided streams. In places dirty, high-ash coal and carbargillites indicate the presence of abandoned channels hosting a swamp environment. These coal seams, which may be correlated with the Westphalian ones from the adjacent Pilsen Basin in the Czech Republic

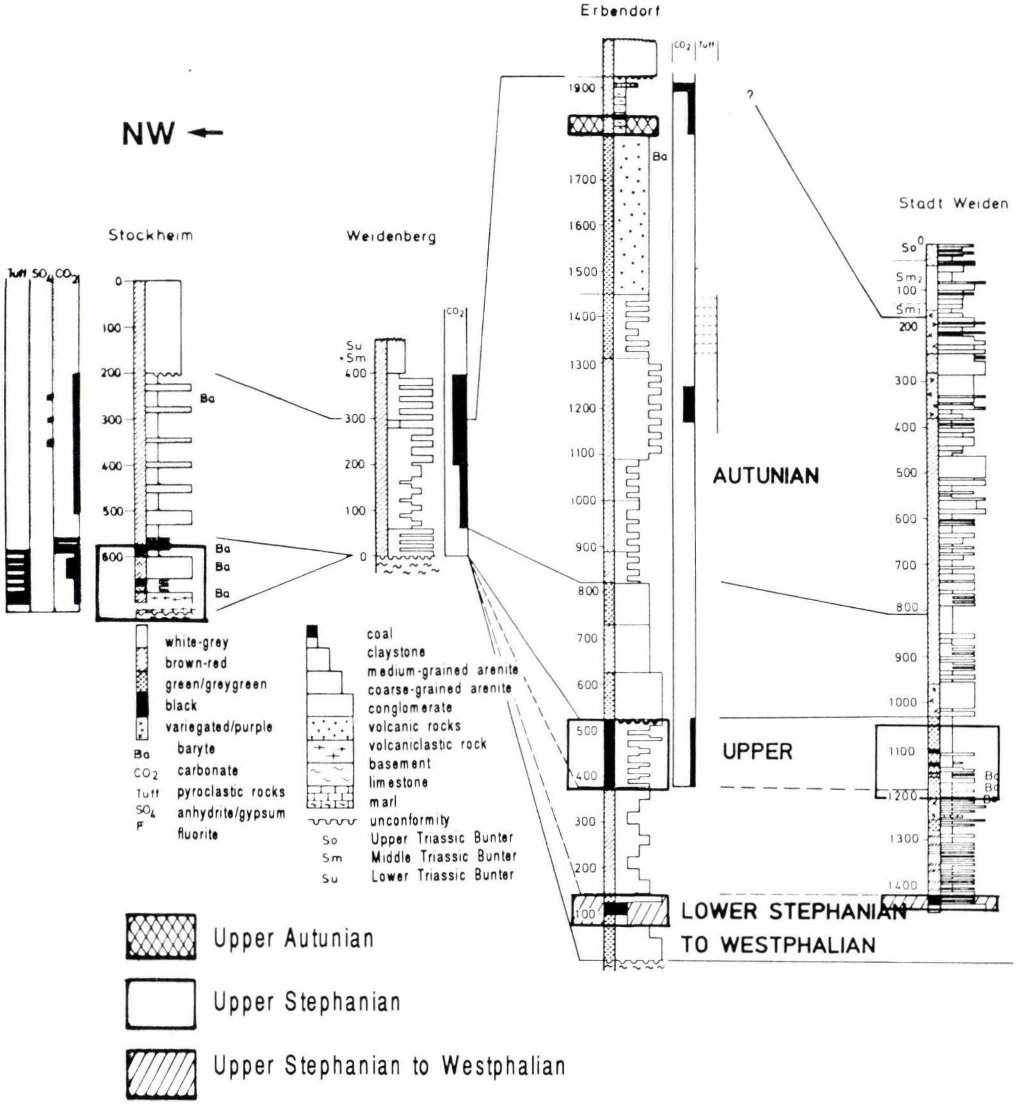

Fig. 2
The "Stadt Weiden" borehole was used as reference for the subdivision of the lower Permo-Carboniferous strata in NE-Bavaria/S-Germany. For stratigraphic correlation with boreholes in the adjacent basins, see Fig. 3

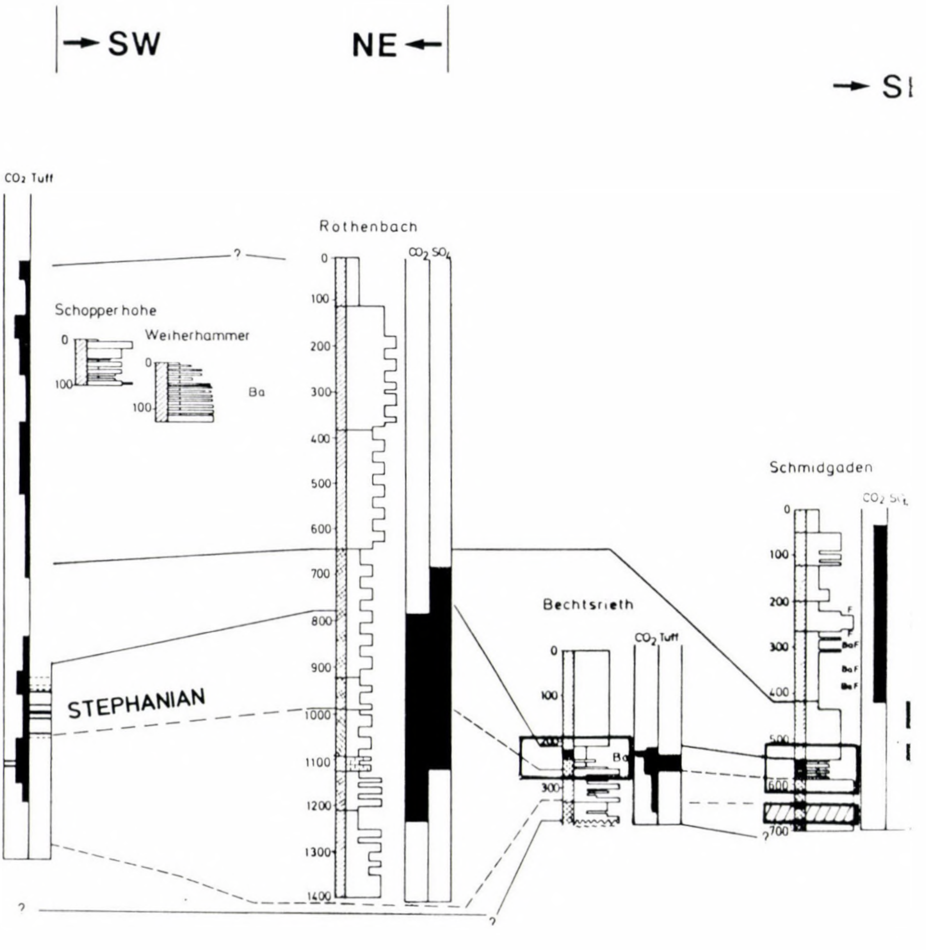
→ SW
NE ←
→ S
CO2 Tuff
Rothenbach
CO2 SO4
Schopper hohe
Weiherhammer
Ba
Schmidgaden
Bechtsrieth
CO2 Tuff
STEPHANIAN
BaF

Fig. 2 cont.

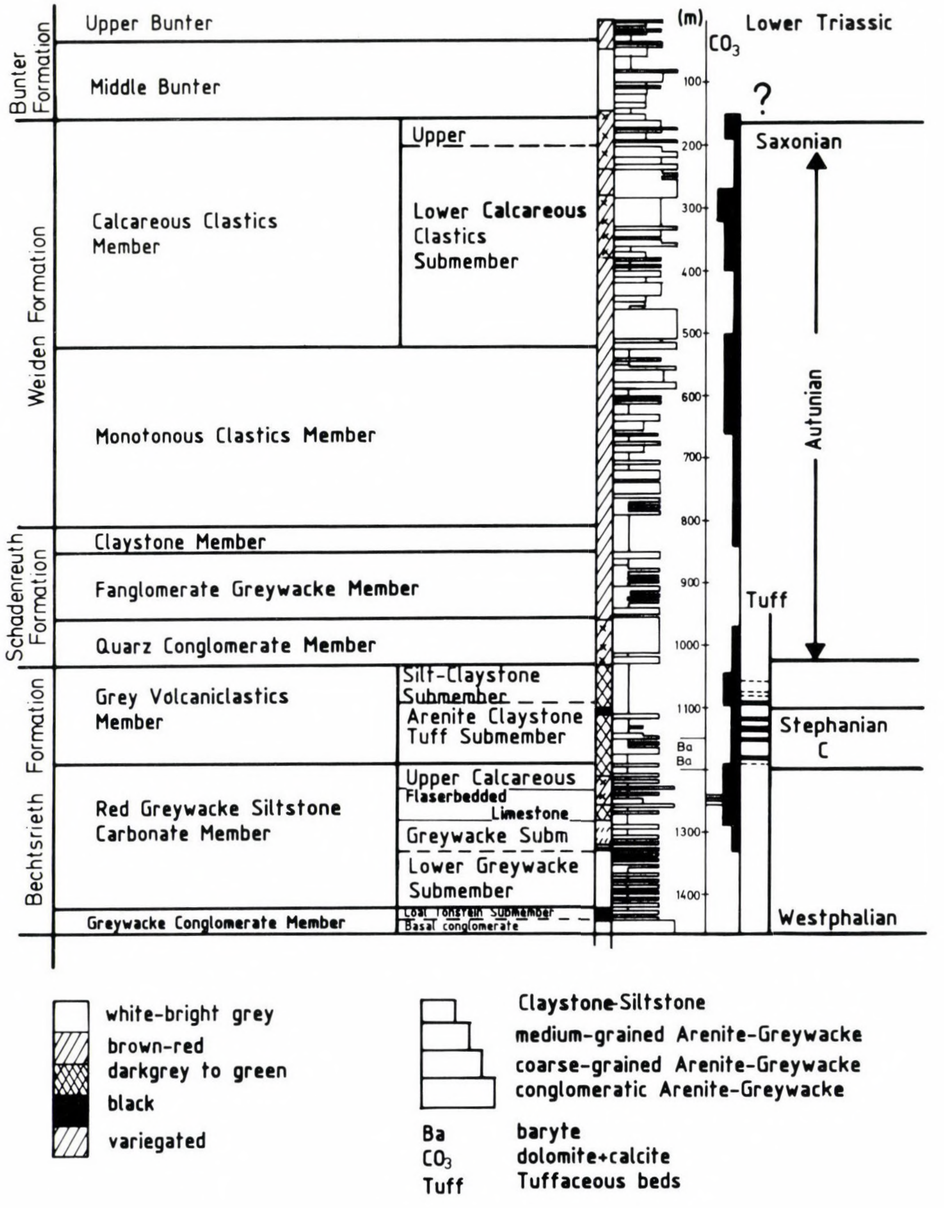

Fig. 3
Subcrop expression of the Permo-Carboniferous basin fill in NE-Bavaria (southern Germany). For locations see Fig. 1. Carbonaceous beds and series of interest for U accumulation are framed with a bold line

(Pesek 1988), pertain to the so-called alluvial fan coals, as they are collectively discussed by Fielding (1987).

The red greywacke siltstone carbonate member of the Bechtsrieth Fm.

In comparison with the footwall member, there is a marked grain-size decrease in the arenaceous rocks, with a conspicuous augmentation of red silt and mudstones (Plate IIIB).

Calcite and dolomite occur in a great variety of facies. Most of these carbonate minerals are concentrated in nodules dispersed in the red siltstones. Upsection these concretions pass into massive flaser-bedded limestones topped by tiny bands of black shales (Plate IIIC, D). In places some shells of an unidentified species of bivalves have been observed in these limestones.

This facies mirrors alternating bed – and suspended – load depositions on an alluvial outwash plain. Arenaceous interbeds may be interpreted as sheet floods over ephemeral flood plains. Rarely, channels gully into the fine-grained substratum which contains some eolinites. Downslope the low sinuosity braided rivers are consequently replaced by meandering streams as indicated by small-scale fining-upward cycles (Plate IIID). Carbonate precipitation on mud flats reflect strong evapotranspiration. Calcretes developed as a result of paleosol formation (see Goudie 1983).

Black shales, associated with flaser-bedded limestones, are likely to have originated from bacterial reduction of sulfate in stagnant waters of an ephemeral saline lake. This part of the fan underwent flooding and drying out, where organic matter was only preserved when the water table did not fall below the sediment surface. Phases of emersion are testified by the reworked freshwater limestones and remnants of calcareous beds scattered on the fan plain. This series is therefore of minor significance, when assessing the potential to generate hydrocarbons.

The grey volcaniclastics member of the Bechtsrieth Fm.

The uppermost Bechtsrieth Fm. shows a pronounced cyclicity, with at least four cyclothems to be traced all over the basins under consideration. All of them bear fine-grained topstrata with coalified matter, which grade down-section into a coarser-grained substratum, fairly different as far as their sedimentological appearance and the mineral associations of rock-forming minerals are concerned.

Schmidgaden cyclothems with basal coarse-grained arenites and carbonaceous siltstones above them attest to changing conditions, from a high-energy to a low-energy regime, as is well represented by modern meandering drainage systems. Clay minerals – illite (Hb rel 214 to 360), kaolinite, chlorite – do not point to a significant contribution of pyroclastic material to the overbank fines in this fluvial environment.

Unlike Schmidgaden, the pyroclastic deposits in the cyclothems of the Weiden

Basin are much more pronounced. "Open illite", smectite-illite mixed layers and smectite besides kaolinite and chlorite bear witness of lapilli-ash tuffs in the fine-grained carbonaceous topstrata, which in places may be denominated as "bentonites" according to the proposals of Fisher and Schmincke (1984) (Plate IA). These air-fall tuffs are likely correlatable to montmorillonite tuffs in the western part of the Czech Republic (Holub 1982). The coarse-grained greywackes at the base of each of these cyclothems contain only few volcaniclasts. The environment of deposition may be interpreted as a permanent lake, as was studied in detail by Haywarth and Lund (1984), Burgis and Morris (1987) and by Kelts (1988).

The fine-grained carbonaceous topstrata are representatives of an off-shore lacustrine, deep water facies with air-fall tuffs; the coarse-grained sandy material mirrors near-shore lacustrine low-density turbidites (Plate IVF, G, H).

In the northwesternmost Stockheim Basin the input of pyroclastic material is very much higher than in the aforementioned basins. According to the classification of Fisher and Schmincke (1984) these tuffaceous host rocks may be categorized as lapilli tuffs, vitric tuffs and tuffaceous mudstones, which contain illite (Hb rel: 240 to 380), "open illite", kaolinite, dickite (Halbach et al. 1984), and chlorite. They are associated with high-ash coals which form seams, discontinuous layers and lenses in the upper fines of each of these cyclothems. Steeply dipping hill slopes, and a more rugged relief than in the Weiden Basin, have given rise to pyroclastic conglomerates and agglomerates ("lahars") which washed a great many plant remains into the depocentre. Unlike the paralic coal seams from the Ruhr district (Jessen 1961), the lack of rootlet beds in the basins under study point to an allochthonous origin of coal seams.

Schadenreuth Formation

This formation is made up of coarse-grained arenaceous and conglomeratic, varicoloured rocks (Kiwitt 1985), which show a conspicuous depletion in biotite and locally increased amounts of anatase in the heavy mineral assemblages. The paleogeography may be explained in terms of a delta-like fan which prograded into the depressions of the "Bechtsrieth Fm." (Plate IVH). Organic matter was not concentrated during deposition of this series; the paleopedological process may have played a significant part when these terrigenous fluvial deposits came into being (see anatase and its interpretation by Schnitzer 1957; Valeton 1983).

Weiden Formation

The majority of redbeds of the Weiden Fm. manifests an alluvial fan plain (Plate IIA) with braided streams ("dry fan"). Sporadically encountered conglomerates attest to catastrophically violent floods, splayed onto the distal fan plain (Kehew 1982). Wind-faceted cobbles frequently found among gravel-sized material point to eolianites (Plate IIB). Calcareous encrustations disseminated in the basin centre (playa) support the idea of duricrust formation during this period. This series is barren of carbonaceous intercalations. A tiny carbonaceous horizon is exclusively encountered on top of a volcanic complex in the Erbendorf Basin. These Upper Autunian carbargillites from Erbendorf were deposited in a narrow volcanotectonic ("caldera-like") depression, with restricted continental run-off on account of a smooth relief – note the contrast with the carbonaceous, coarse-grained sediments of the Stockheim caldera during the formation of the Upper Stephanian (Bechtsrieth Fm.) – ("event lake") (Plate IV,I).

Tiefenbach Formation

These red and brown arkoses and conglomerates do not host organic intercalations. Its overall coarsening-upward grain size distribution reflects a prograding dry fan with fluvial deposits of braided streams.

Chemistry and petrography of Permo-Carboniferous volcanites

The Permo-Carboniferous volcanogenic rocks in the study area may be subdivided as follows: (1) subvolcanic dike swarms, (2) tabular and stock-like volcanic rocks (3) pyroclastic rocks (4) epiclastic-volcaniclastic rocks. Groups (3) and (4) have already been treated in the discussions of lithology and paleoenvironment.

Igneous rocks of categories (1) and (2), based on their modal composition and their Zr, Ti, Nb and Y contents, pertain to the calk-alkaline rock suite (Winchester and Floyd 1977) and may be classified as rhyodacites, and dacites with subordinate amounts of trachyandesites and rhyolites (Dill 1991). Upper Carboniferous volcanic activity commenced contemporaneously with the latest granitic intrusions of the Variscan plutonic complexes. They vented along deep-seated lineaments ("porphyry line") and, at the Westphalian/Stephanian boundary, were eroded for the first time; they are encountered as pebbles in the Bechtsrieth Fm. The Upper Carboniferous series of each of these basins, albeit abundant in volcanites of similar composition, do not show a uniform trend of igneous evolution.

The Stockheim Basin demonstrates its peculiarity in form of a "calderalike depression" with ignimbrites and lahars, whereas to the southeast (Weiden Basin) eruptions expelled vast ash clouds which gave rise to the deposition of 4 to 5 tiny layers of air-fall tuffs which may be equivalent to the so-called "Kaminek" in the Stephanian Kounor Member (Pesek 1975). Recurrent volcanic activity with effusion of dacites and rhydacites took place by the end of the Autunian, as a result of fracturation and venting at the intersection of the Franconian Line (boundary fault) with incipient faults of the Eger Rift.

Economic geology of Permo-Carboniferous basins

Coal Petrography

In the surroundings of Stockheim and Erbendorf coal was mined until the late sixties and early twenties, respectively. Detailed petrographic studies focusing on these dirty, high-ash coals were made by Hoffmann and Hoehne (1969) and by Dill et al. (1991). Vitrinite reflectance falls in the range 0.49 to 1.74%. The coal attained high to medium volatile bituminous ran. In places silica, derived from the decomposition of vitreous tuffs, entered these carbonaceous beds and led to a syndiagenetic silicification. Coalification is attributed to very high temperatures which were achieved during basin subsidence and caused by igneous activity during Permo-Carboniferous times. Coal alteration by radiation damage, produced by the α-particles from uranium decay, had only a microscopic effect. Measurements in some of the brightest zones range between 3.8 and 6.3%, with a 4.75% average.

Uranium mineralogy

All basins have been investigated for their strata-bound and fault-bound (only Stockheim) uranium concentrations (Dill 1987; Halbach et al. 1984; von Borstel 1984). Replacement of organic matter and introduction of metals in the coal seams or plant remains took place in a rather early diagenetic stage. $Fe\ S_2$ especially displays a great variety of textures, being categorized according to Pilgrim (1985) and Wiese and Fyfe (1986) as cell wall pyrite, framboidal pyrite and aggregated pyrite. Marcasite was precipitated, followed by galena and sphalerite. Oxygen isotope studies on cementing calcite and dolomite in the seams furnish evidence of formation temperatures between 43^o and 54^o C. The incipient uranium accumulation came into being as "carburan" or "carburan oxide" through mobilization of uranium from the pyroclastic deposits caused by intrastratal solutions. UO_2+ bearing solutions circulated in the peat swamps where U was adsorbed onto humic acids. Hexavalent U was partly reduced to tetravalent U and concentrated as pitchblende with the formula $UO_{2.6.}$

Hydrocarbons

In addition to the coal petrographic studies, organo-chemical studies have been centered around the carbonaceous beds of all basins in the studied area (Dill et al. 1988; 1991). The composition of organic matter was plotted in a ternary plot using heterocompounds, saturated hydrocarbons and aromatic hydrocarbons. The data arrays of the swamp environments such as Schmidgaden, Stockheim and Erbendorf lie close to the tie-line of heterocompounds and aromatic hydrocarbons.

Lake sediments such as those from the Weiden Basin and the oil extracted from these sediments (Dill et al. 1989) are distinguished from the previously mentioned ones by increased amounts of saturated hydrocarbons (Fig. 4). Another approach to assess the source rock potential of these carbonaceous beds has been attempted by plotting HC contents vs. TOC (Fig. 5).

Basin models and economic geology

During the Westphalian and Lower Stephanian three narrow basins (Schmidgaden, Weiden, Stockheim) subsided in the Variscan basement. They were separated from each other by NE-SW-striking anticlines which reflect the Variscan pre-fold architecture. The carbonaceous series of the lowermost Bechtsrieht Fm. are considered equivalent to the Kladno/Plzen Fm. which is encountered in the Plzen and Central Bohemian Basins (Holub 1982; Pesek 1987). Four basin types may be delineated:

Intramontane fault-bounded basins (Type A) are sites of minable, coal seams. They show, moreover, good source rock qualities for gas, yet do not host heavy metal enrichments of economic interest.

Type B is akin to this type, but basin subsidence was accompanied by the venting of extrusive rocks and deposition of epiclastic-volcaniclastic and pyroclastic fans. There exist volcano-tectonic depressions with carbonaceous rocks, which may be worked for hard coal and may be qualified as "gas prone". The extensive volcanic activity makes the basins a target for uranium exploration.

The Upper Stephanian lacustrine environment evolved in a half-grabenlike depression. A representative of this type C is found in the Weiden Basin. These depressions, with few smectitic tuffaceous interbeds or "bentonites", have good source rock potential for oil, but neither metal enrichments nor coal seams of economic interest were discovered.

Basin type D is only represented by the narrow volcanic depression following the eruption of Erbendorf dacites. Its basin fill has good source rock qualities for oil. This interfingering of carbonaceous rocks and pyroclastic deposits (see also Weiden) can provide favourable conditions for the generation of hydrocarbons.

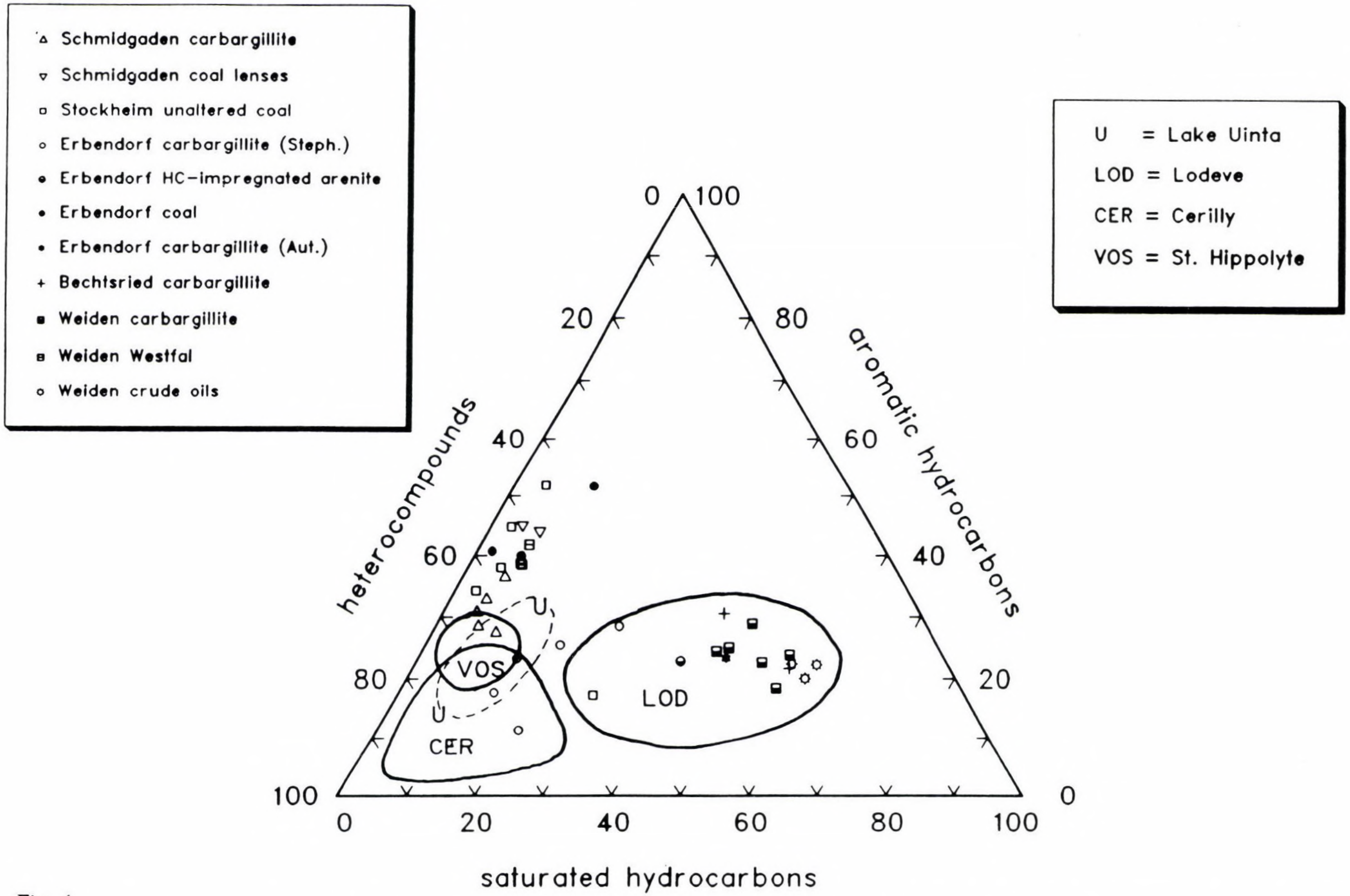

Fig. 4
Composition of carbonaceous matter from Permo-Carboniferous clastic rocks and crude oil of NE-Bavaria. Reference data (after Landais and Connan 1980)

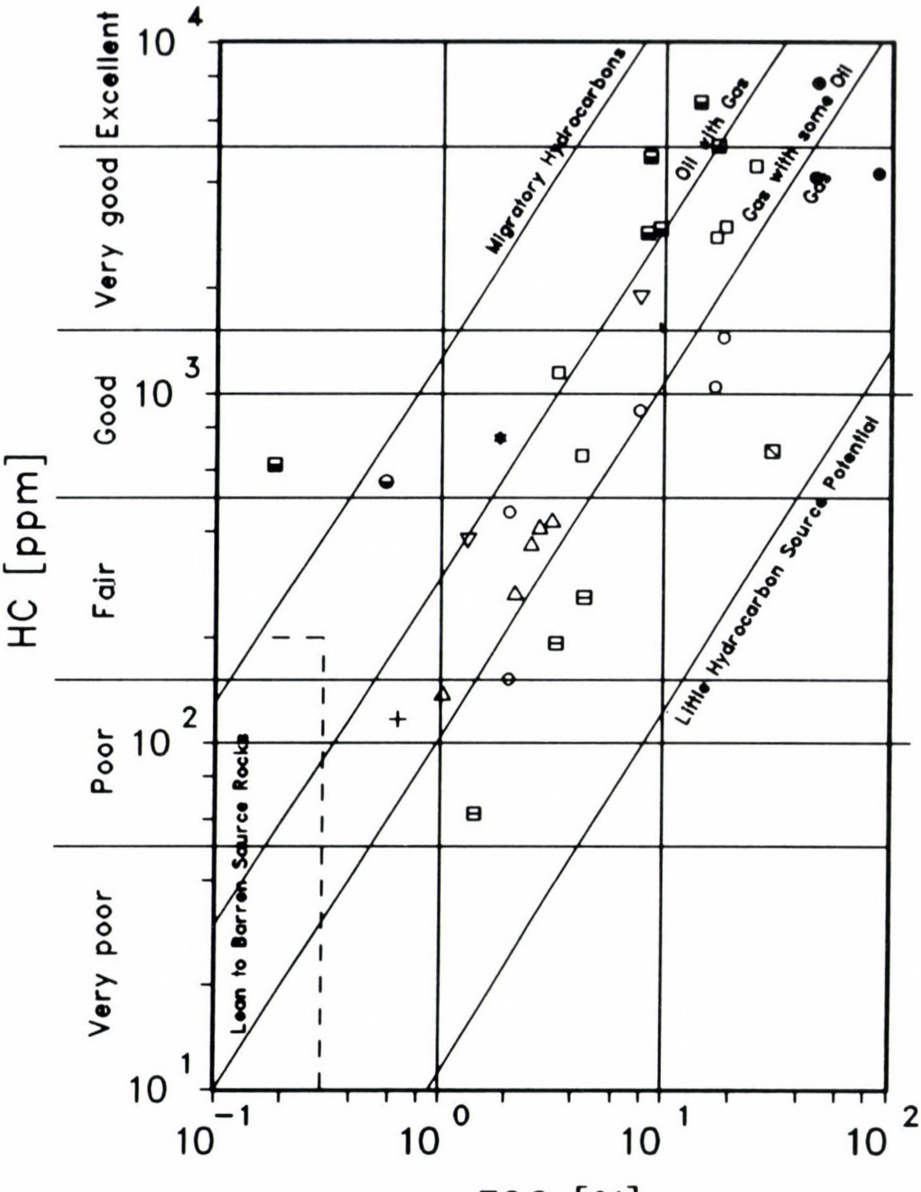

Fig. 5
Hydrocarbon plotted vs. TOC to assess the source rock potential for the Permo-Carboniferous basins in NE-Bavaria

Plate I

A) Conglomeratic to coarse-grained arkose with pore space filled by barite (Ba). Quartz grains (Qz) are replaced along grain boundaries by the sulfate (Stephanian Bechtsrieth Fm. Arenite-Claystone-Tuff Submember (Weiden)) Micrograph, thin section, crossed polars, lower edge 0.8 mm
B) Strongly-welded tuff with illite-smectite mixed layers (Sm) and vermicular kaolinite aggregates (Ka). Stephanian Bechtsrieth Fm. Arenite-Claystone-Tuff-Submember (Weiden) Micro- graph, thin section, crossed polars lower edge 0.4 mm

Plate II

A) Channel sandstone gullying into red siltstones of a flood plain. Autunian Weiden Fm. (Stockheim)
B)Wind-faceted cobble from conglomerates of the Weiden Fm. (Erbendorf) Length: approx. 5 cm

Plate III

A) Weiden well 1455 m: Coarsely-bedded polymict conglomerates with volcaniclasts, gneissic and granitic clasts (= debris flows/braided stream active channels)
B) Weiden well 1315 m: Horizontally and planar crossbedded arenites at sharp angle with an erosional plain, cutting into red claystones (= flood plain or outwash plain of an alluvial plain with incised channels of braided streams).
C) Weiden well 1249 m: Nodular flaser-bedded limestone with tiny black shales on top of it. The topmost part is composed of red claystones (= shallow fresh water lake on a mud flat of the alluvial fan).
D) Weiden well 1235 m: White arkoses cross-bedded at a sharp angle, gradually passing into massive red claystones with some nodular calcareous concretions (= fan plain with meandering streams and minor calcretes).
E) Weiden well 1168 m: Horizontally-bedded, fine to coarse-grained arkoses and silty red claystones (= nearshore fluvio-lacustrine deposits).

Plate IV

F) Weiden well 1132 m: Spontaneous expulsion of oil from coarse-grained arkoses and greywackes (= near-shore lacustrine deposit, low-density turbidites (?)).
G) Weiden well 1125 m: Ash-lapilli tuff with water escape structures giving rise to convolute bedding, overlain by black claystone at an obliquely dipping erosional plane. The tuffaceous material is composed of kaolinite and smectite-illite mixed layers (= offshore lacustrine deep fresh water air-fall tuffs).
H) Weiden well 1064 m: Alternating beds of white arkoses and siltstone underlain by gray-green silty claystones (= deltaic near-shore lacustrine deposits).
I) Erbendorf well 93.82 to 94 m: Black shales overlain by tuffaceous siltstones displaying crinkled bedding (= organic lake sediments on top of dacitic volcanic rocks). Fine to coarse-grained arkoses and silt.

Plate I

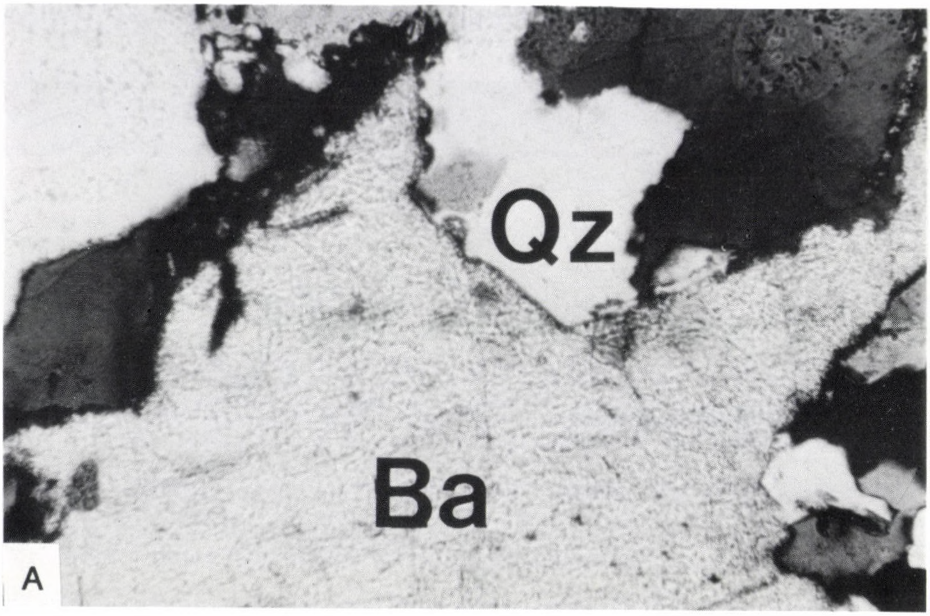

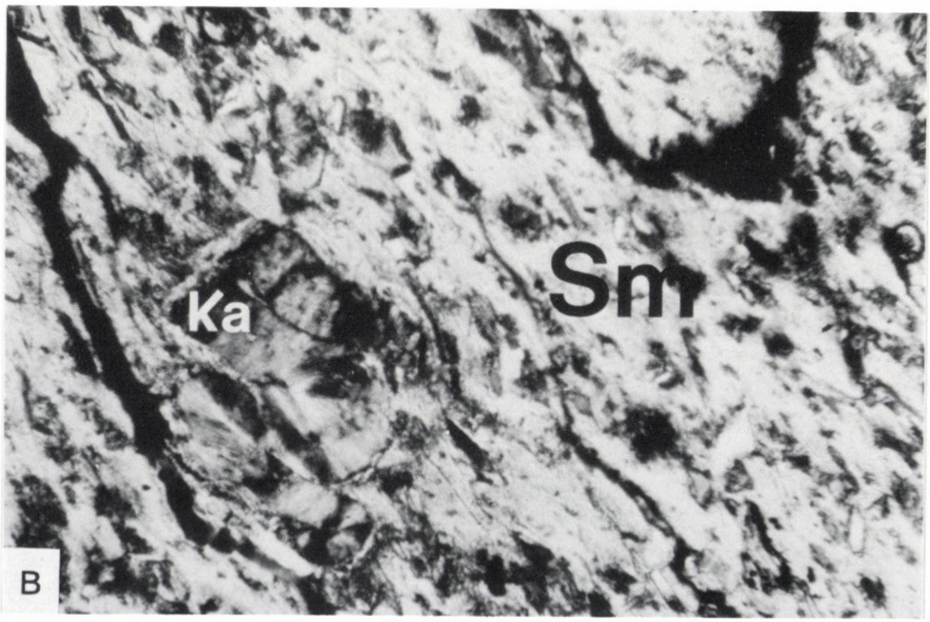

Plate II

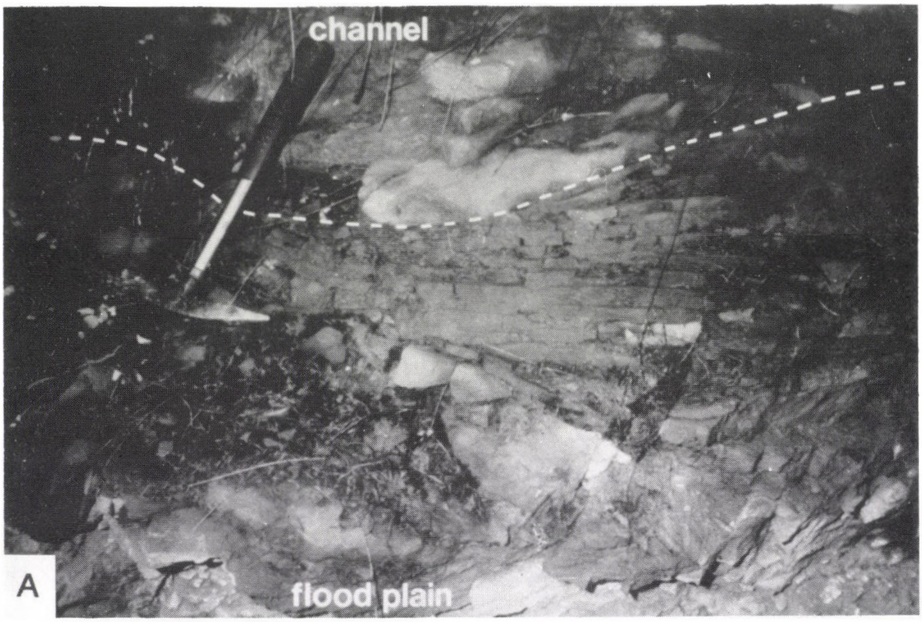

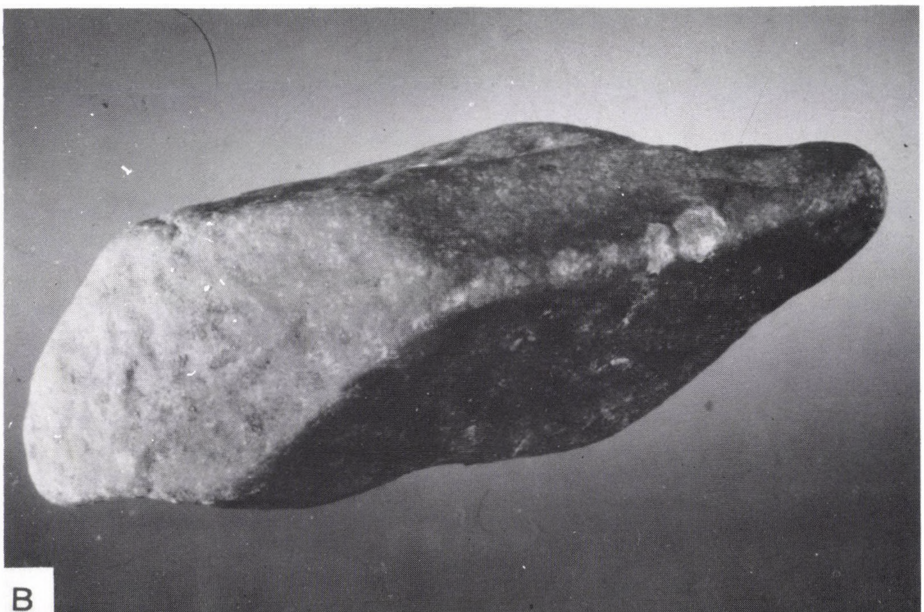

Plate III

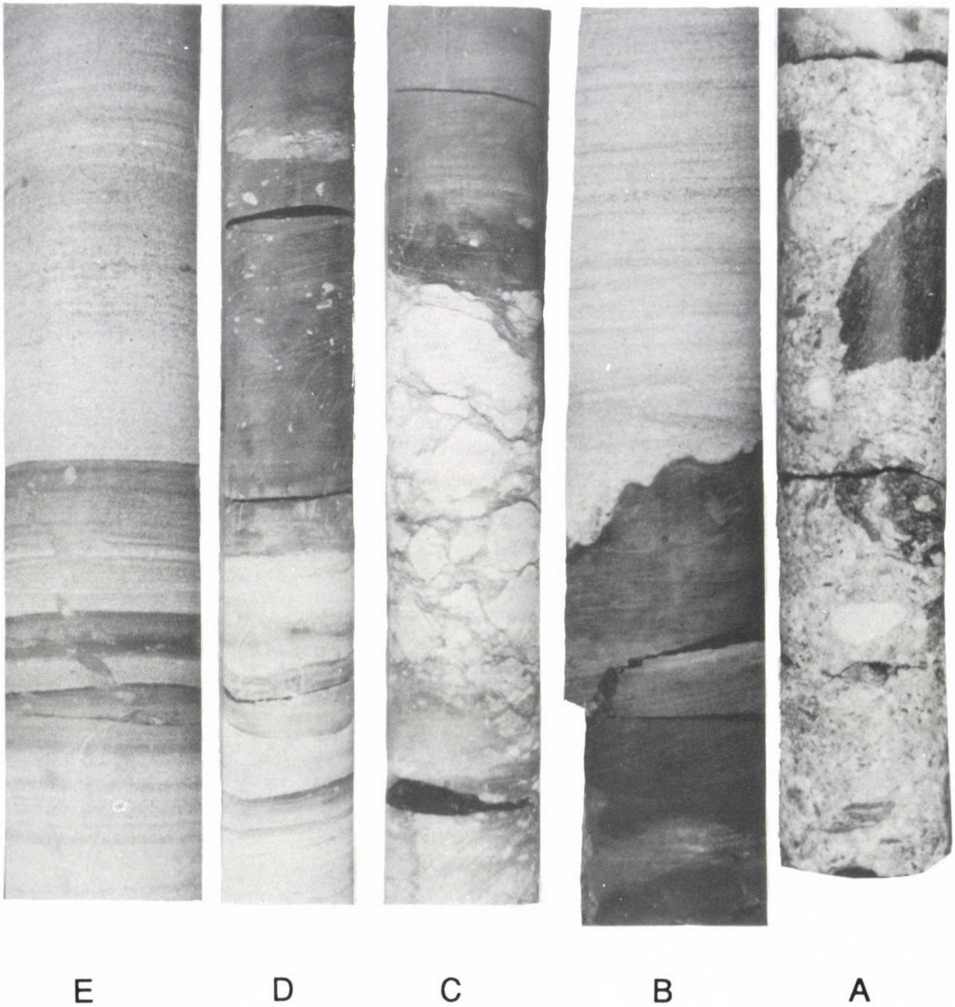

Plate IV

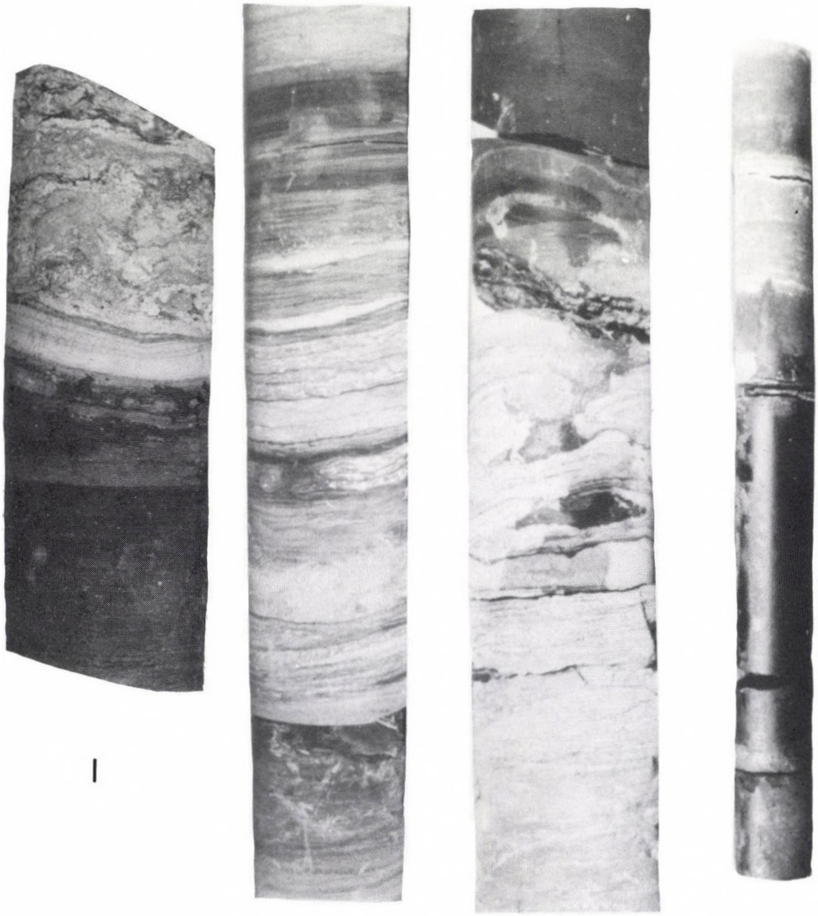

I H G F

References

Borstel, von D., 1984: Bindungsformen von Uran in kohlissgen; Ablagerungen von Sedimenten unterschiedlichen Diagenesegrades. – Ph.D. thesis, Techn. University Clausthal, p. 156.

Burgis, M.J., P. Morris 1987: The natural history of lakes. – Cambridge University Press, Cambridge, p. 232.

Dill, H. 1987: Environmental and diagenetic analyses of Lower Permian epiclastic and pyroclastic fan deposits – Their role for coal formation and uranian metallogeny in the Stockheim Trough (F.R.G.). – Sedimentary Geology, 52, pp. 1–26.

Dill, H., H. Teschner, H. Wehner. 1988: Petrography, inorganic and organic geochemistry of Lower Permian Carbonaceous fan sequences ("Brandschiefer Series") - F.R.G.: Constraints to their paleogeography and assessment of their source rock potential. – Chemical Geology, 67, pp. 307–325.

Dill, H. 1989a: Facies and provenance analysis of Upper Carboniferous to lower Permian fan sequences at a convergent plate margin, using phyllosilicates, heavy minerals and rock fragments (Erbendorf Trough, F.R.G.). – Sedimentary Geology, 61, pp. 95–110.

Dill, H. 1989b: Petrographie und Geochemie der Bunten Basal-sedimente des Permo-Karbons im Weidener Becken. – Geologische Blätter NO-Bayern, 39, pp. 129–160.

Dill, H. with a contribution by Hartkopf-Fröders, C. 1990: Stratigraphie und Lithologie des Permokarbons im Weidener Becken (NO-Bayern, B.R. Deutschland). – Zeitschrift der deutschen geologischen Gesellschaft, 141, pp. 31–47.

Dill, H. 1991: Volcanic and Volcaniclastic rocks at the southwestern edge of the Bohemian Massif. – Zeitschrift für geologische Wissenschaften, 19, pp. 519–537.

Dill, H., J. Koch, M. Teschner, H. Wehner 1991: Permo-Carboniferous beds in the Stockheim Basin/NE-Bavaria. Coalification and organic chemistry. – Erdöl und Kohle, 44, pp. 97–105.

Dill, H., M. Teschner, H. Wehner 1991: Geochemistry and lithofacies of Permo-Carboniferous carbonaceous rocks from the southwestern edge of the Bohemian Massif (Germany). A contribution to facies analysis of continental anoxic environments. – International Journal of Coal Geology, 18, pp. 251–291.

Emmert, H. 1981: Perm nördlich der Alpen. – Erläuterungen zur geologischen Karte von Bayern 1: 500 000, pp. 34–40, Bayer. Geol. Landesamt, München.

Fielding, C.R. 1987: Coal depositional models for deltaic and alluvial plain sequences. – Geology, 15, pp. 601–604.

Fisher, R.V., Schmincke, H.-U. 1984: Pyroclastic Rocks. – Springer, New York, Berlin, Heidelberg, 472 p.

Goudie, A.S. 1983: Calcrete. – In: A.S. Goudie and K. Pye (eds), Chemical sediments and geomorphology, Academic Press, London, pp. 93–131.

Halbach, P., D. Borstel von, A. Janetzke 1984: Carburan oxide in Lower Permian high volatile bituminous coal. – Naturwissenschaften, 71, pp. 41–42.

Haywarth, E.Y., J.W.G. Lund 1984: Lake sediments and environmental lithology. – University Press, Leicester, 411 p.

Helmkampf, K.E., J. Kuhlmann, D. Kaiser 1982: Das Rotliegende im Randbereich der Weidener Bucht. – Geologica Bavarica, 83, pp. 167–186.

Helmkampf, K.E., L. Waeber 1983: Das Rotliegende in der Schmidgadener Senke (Opf.). – Geologische Blätter NO-Bayern, 33, pp. 29–64.

Hoffmann H., K. Hoehne 1960: Petrographische Eigenschaften und archeologisches Verhalten von permischen Steinkohlen, insbesondere der Gondwanaformation. Teil 1. Brennstoff-Chemie, 41, pp. 5–11.

Holub, V. 1982: Explanatory notes to the lithotectonic profile of the Permo-Carboniferous basins of the Central Bohemian Region (CSSR). – Veröffentlichungen des ZIPE – AdW DDR Potsdam, 1982, pp. 301–318.

Jessen, W. 1961: Zur Sedimentologie des Karbons mit Ausnahme seiner festlnädischen Gebiete. – 4. Congress Stratigraphy, Geology Carboniferous Heerlen, 2, pp. 307–327.

Kehew, A.E. 1982: Catastrophic flood hypothesis for the origin of the Souris Spillway, Saskatchewan and North Dakota. – Geol. Soc. Amer. Bull., 93, pp. 1051–1058.
Kelts, K. 1988: Environment of deposition of lacustrine petroleum source rocks: an introduction – Geological society of London Special Publication, 40, pp. 3–26.
Kiwitt, R. 1985: Strukturgeologische und emanometrische Untersuchungen im Gebiet des Erbendorfen Blei-Zink-Reviers Bayern, sowie feinstratigraphische Aufnahme des Rotliegenden bei Erbendorf. – Ms. Thesis, University Mainz, 142 p.
Lützner, H. 1988: Sedimentology and basic development of intramontane Rotliegend basins in Central Europe. – Z. geol. Wiss., 16, pp. 845–863.
Miall, A.D. 1984: Principles of Sedimentary Basin Analysis. – Springer, New York, Berlin, Heidelberg, 423 p.
Pesek, J. 1975: Notes on the geology of Plzen Carboniferous of the Dobre Stesti Mine. – Acta Univ. Carolina Geologica, 2, pp. 139–147.
Pesek, J. 1987: Deposits of bituminous coals of Czechoslovakia. – Geologica, 26, pp. 3–66.
Pesek, J. 1988: The influence of the basement geological structure on the coal-bearing character of the Upper Paleozoic basins in the Central Bohemian Area – Coal-Bearing formations of Czechoslovakia. – IGCP project, 166, pp. 27–36.
Pilgrim, J.C. 1985: The mode of occurrence and distribution of iron sulfides in selected eastern Canadian coals. – Canadian Min. Ass. Ann.Meeting, 1985 Abstract 10, A p. 49.
Reinecke, H.E., J.B. Singh. 1980: Depositional Sedimentary environments – Springer, Berlin, Heidelberg, New York 549 p.
Richter, D., R. Villwock 1960: Die Rotliegenden Vulkanite am Westrand des Fichtelgebirges. – N. Jb. Miner. Abh., 95, pp.
Stephan, W. 1959: Die Gliederung des Rotliegenden und die Stellung seiner Vulkanite am Südwestrand des Frankenwaldes. – Geologische Rundschau, 48, pp. 336–357.
Schnitzer, W.A. 1957: Die Lithologie und Palogeographie des Buntsandsteins am Westrand der Böhmischen Masse. – Erlanger geologische Abhandlungen, 24, pp. 1–130.
Valeton, J. 1983: Klimaperioden lateristischer Verwitterung und ihr Abbild in den synchronen Sedimentationsräumen. – Zeitschrift der deutschen geologischen Gesellschaft, 134, pp. 413–452.
Wiese, R.G., W.S. Fyfe 1986: Occurrence of iron sulfides. – In: Ohio coals - Int. Journ. of Coal Geology, 6, pp. 251–276.
Winchester, J.A., P.O.A. Floyd 1977: Geochemical discrimination of different magma series and their differentiation products using immobile elements. – Chemical Geology, 20, pp. 325–343.

Acta Geologica Hungarica, Vol. 37/1-2, pp. 97–110 (1994)

Diagenetic illitization of smectite from the shales of the Danube Basin

Vladimír Šucha,
Department of Geology of Mineral Deposits, Fac. of Natural Sciences, Comenius University Bratislava

Françoise Elsass
Station de Science du Sol, INRA Versailles

Dionýz Vass
Dionýz Štúr Geological Institute, Bratislava

The conversion of smectite to illite was studied in buried shales of the Danube Neogene Basin using X-ray diffraction analysis and analytical electron microscopy. A good correlation was observed between the content of expandable layers in mixed layer illite/smectite minerals and burial temperature. The illitization in the basin is controlled mainly by temperature. The initial illitization of the original shale materials is due to their pre-sedimentary history.

Key words: shale diagenesis, illite-smectite minerals, burial temperature, Danube Basin

Introduction

Smectite illitization is an important indicator describing the diagenetic evolution of sedimentary basins. This reaction, which is probably the most important diagenetic mineral one, was observed for the first time by Burst (1959) in the Gulf Coast region. Since that time, many investigations have been devoted to this phenomenon (see reviews by Kisch 1983; Środoń and Eberl 1984; Frey 1987).

Several papers also discussed this problem for the Central European region, particularly in the Vienna Basin, Pannonian Basin and East Slovak Basin (Kraus and Šamajová 1978; Kurzweil and Johns 1981; Viczián, 1985, 1992; Francú et al. 1990; Šucha et al. 1993). For the present paper we decided to bring new data from the shales of the Danube basin, describing the mineralogical composition of the clay fraction by X-ray diffraction analyses and analytical electron microscopy.

Addresses: V. Šucha: Mlynská dolina G, 842 15 Bratislava, Slovak Republic
F. Elsass: INRA, 78026 Versailles, France
D. Vass: Mlynská dolina 1, 817 04 Bratislava, Slovak Republic
Received: 25 October, 1993

Geological setting

The Danube basin came into existence during the Neogene. The basin began to open in the North near the Pieniny Klippen belt, as is proven by Lower Miocene deposits in the Pieštány, Bánovce, Horná Nitra depressions, and in some other small ones located along the Klippen belt. During the Middle Miocene the process of basin opening and subsidence migrated to the South.

The opening of the depressions along the Klippen belt were the result of the oblique convergence of the subducting North European platform and the overriding Carpatho-Pannonian Plate (Royden et al. 1982; Royden 1988; Vass et al. 1988; Kovač et al. 1993). Some authors consider these dynamics as the collisional northeastward escape of the Carpathian domain from the Alpine one. The faults originating in the stress field on the margin of the Carpatho-Pannonian Plate were decisive for the opening of the depression. When subduction ceased at the end of Miocene, the fault activity and the subsidence slowed down.

The opening of the southern part of the Danube basin in Hungary during the Middle Miocene was controlled by faults formed by thermal stretching as a result of the Pannonian astenolith rising (tectonic phase of thermal subsidence, Royden and Schlater 1981). The thermal effect probably also affected the South of the Slovak part of the basin (Gabčíkovo sub-basin), where the thermal phase of subsidence began during the Sarmatian. It is manifested by the beginning of the dish-like depression formed in the area between Dunajská Streda and Dunajský Klátov. Later the depression extended over the whole Gabčikovo sub-basin. The intensive sedimentation was controlled by thermal subsidence resulting from brachysynclinal bending of the cooling crust. The fault activity had a subordinate importance.

Because of double genesis of the Slovak part of Danube basin the thickness of the basin filling has two trends. In the northern depressions of the basin the Middle Miocene is thick (up to 3000 m) and the Upper Miocene and Pliocene sediments are relatively thin (approx. 1000 m or less). To the South, in the Gabčíkovo sub-basin, the thickness of the Upper Miocene and Pliocene reaches approximately 5000 m. In this subbasin the cumulative thickness of the basin fill is approximately 6000–7000 m.

The thermal conditions in the Danube basin vary between extremely cold in the Vienna Basin and extremely warm in the East Slovak Basin. The spatial distribution of the temperature up to the depth of 2000 m is variable. The warmest is in the Želiezovce Depression with a heat flow of 90 mW/m^2. Mean temperature at the depth of 1000 m is of 49.5 °C, and mean geothermal gradient is of 39.1 °C/km. The thermal field is influenced mostly by hydrogeological conditions. In the Gabčíkovo sub-basin, at the depth of 6 000 m, the maximum temperature could be approx. 245 °C. This shows that the Danube basin is a geothermally active structure, generated as a result of Neogene geodynamics (Král et al. 1985, Král pers. com.).

Materials and methods

The samples studied were taken from bore-holes yielding pelitic samples. They are situated (Fig. 1) in the Gabčíkovo sub-basin (VTP 11, VDK 15), the Rišňovce Depression (R1) and in the zone separating both depressions (D1). The samples represent depths of 500–3420 m. This interval represents temperatures between 22 and 130 °C (Král et al. 1985).

All the samples were crushed to pass a 0.2 mm sieve and then disintegrated using an ultrasonic probe. Samples were then treated with sodium acetate buffer and H_2O_2. Subsequently, the < 1 μm fraction was separated, and converted to Na form by exchanging three times with 1 M sodium chloride solution, excess salts being removed by dialysis.

X-ray diffraction (XRD) analysis was carried out on a Philips 1075 diffractometer, using CuK_α radiation. Oriented specimens were prepared by sedimentation of clay suspension on a glass slide and analysed in the air-dried state and after saturation by ethylene-glycol vapour for 8 hours at 60 °C. The samples were also saturated by dimethyl sulfoxide vapour for 8 hours at 100 °C.

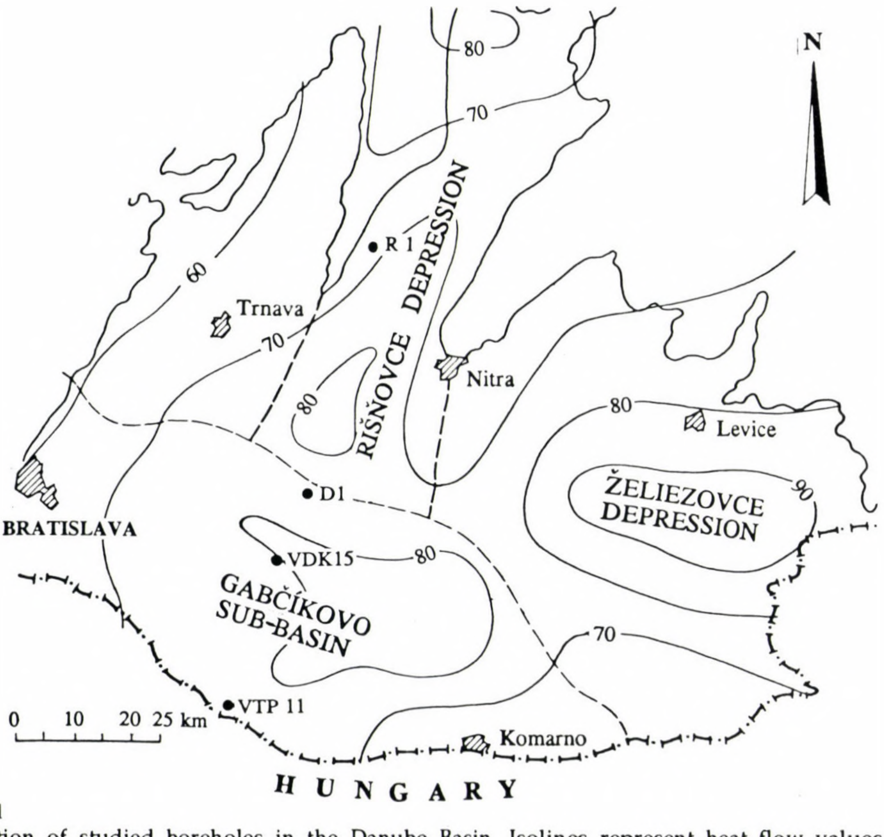

Fig. 1
Location of studied boreholes in the Danube Basin. Isolines represent heat flow values in Mw/m^2

Elemental X-ray microanalyses were performed using a Philips 420 transmission electron microscope equipped with a LINK AN 10000 energy dispersive system and windowless Si-Li detector. The acquisition conditions were 50 seconds lifetime, 1000 cts/s count rate on spots no smaller than 100 nm in diameter so as to limit the overheating and irradiation artefacts of the mineral, thus minimizing element migration and mass loss during the analyses. Lukophyllite from Russia and muscovite from Madagascar were used as standards (Smoljar and Drits 1988; Laperche 1991).

Mineralogical composition

Bulk mineralogy

The mineralogical composition of bulk rock samples was determined by XRD analysis of randomly oriented powder specimens. Quartz, feldspar, calcite, dolomite, biotite, illite, kaolinite, chlorite and mixed layer illite/smectite were identified as major or minor phases. Pyrite, siderite and hematite were identified in some samples as a trace phase. No systematic changes in mineral abundance with depth were observed in any of the bore-holes (Fig. 2).

Mineralogy of the fraction < 1 μm

Quartz and phylosilicates – detritic illite (sometimes associated with biotite), kaolinite, chlorite and mixed layer illite/smectite are the only phases determined in the < 1 μm fraction (Fig. 3).

Kaolinite and chlorite were distinguished using dimethyl sulphoxide treatment (DMSO). Kaolinite intercalation by DMSO molecules causes an increase of its d-parameter from 0.7 nm to 1.14 nm.

Mixed layer illite/smectite

Mixed layer illite/smectite minerals were identified using X-ray diffraction of specimens saturated with ethylene glycol. The proportion of smectitic interlayers in the mixed layer crystals – interlayers which are able to accept ethylene-glycol molecules and to expand in the c* direction – represents expandability. Expandability was determined by the peak position techniques of Środoń (1980, 1981). These techniques are based on the fact that the positions of I/S XRD reflections are shifted due to the changes in the proportions of illite (1.0 nm thick) and smectite (1.7 nm thick) layers (Fig. 4).

Expandability – the proportion of smectite layers – decreases with depth in all studied samples (Fig. 5). The highest identified expandability was about 80%; the lowest obtained value was 25%. This means that a significant part of the smectite layers was converted into illite during the burial history of the investigated shales. This reaction (smectite + Al + K = illite + Si + exchangeable

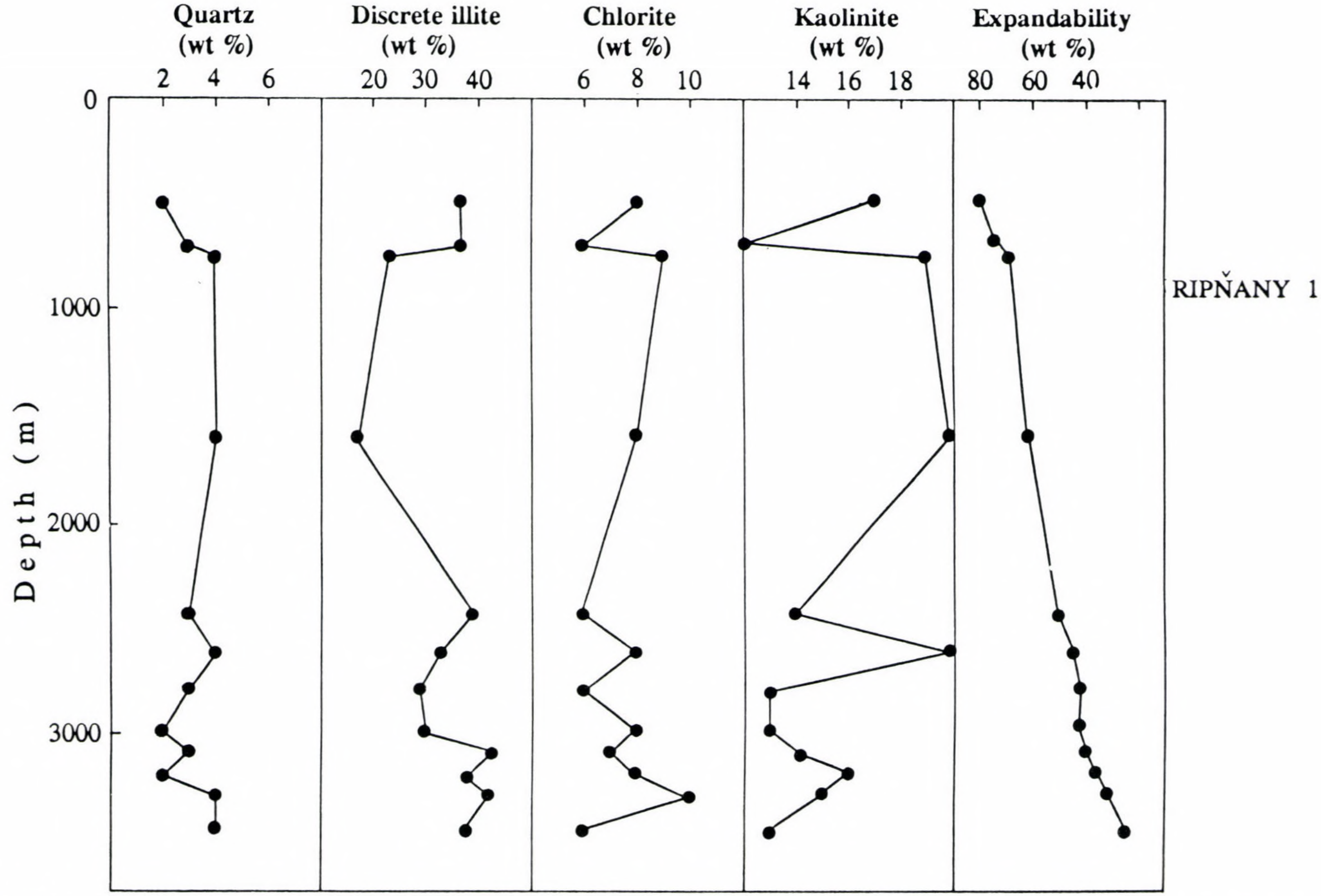

Fig. 2
Relation between semiquantitative mineralogical composition of fraction <1 μm, expandability content and burial depth of borehole R1

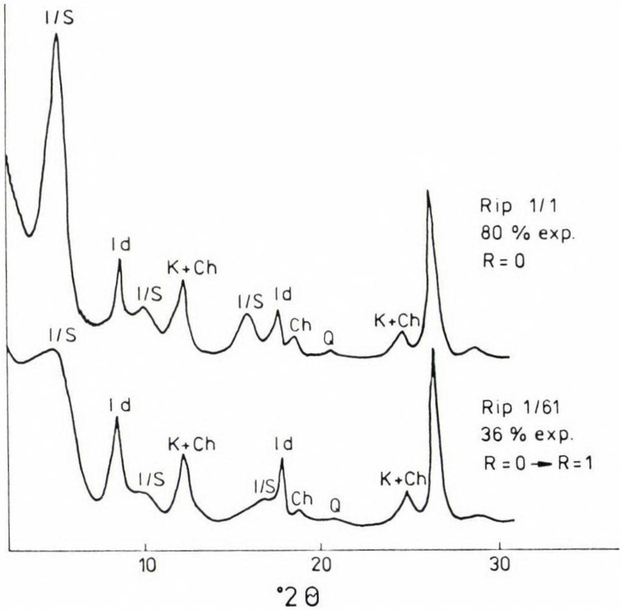

Fig. 3
X-ray diffraction patterns of the <1 μm fraction after ethylene-glycol saturation. I/S=illite/ smectite, Id=detrital illite, K=kaolinite, Ch=chlorite, Q=quartz

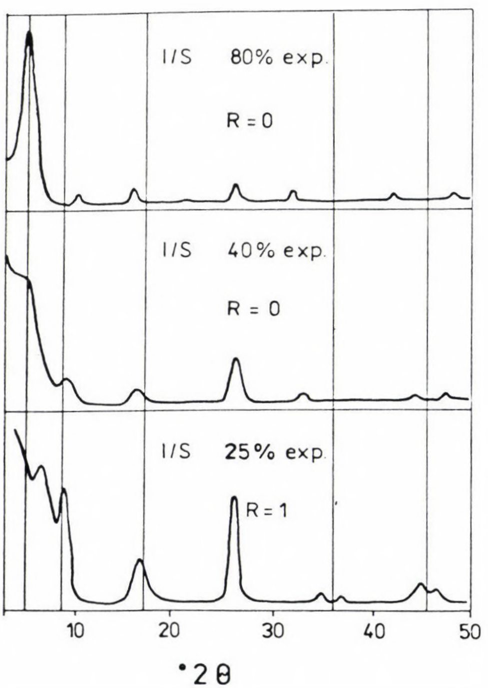

Fig. 4
Theoretical XRD patterns of mixed layer minerals with different expandability calculated using NEWMOD program (Reynolds 1985). First vertical line represents the position of the first smec- tite reflection and other lines represent positions of illite basal reflections (001, 002, 003, 004, 005)

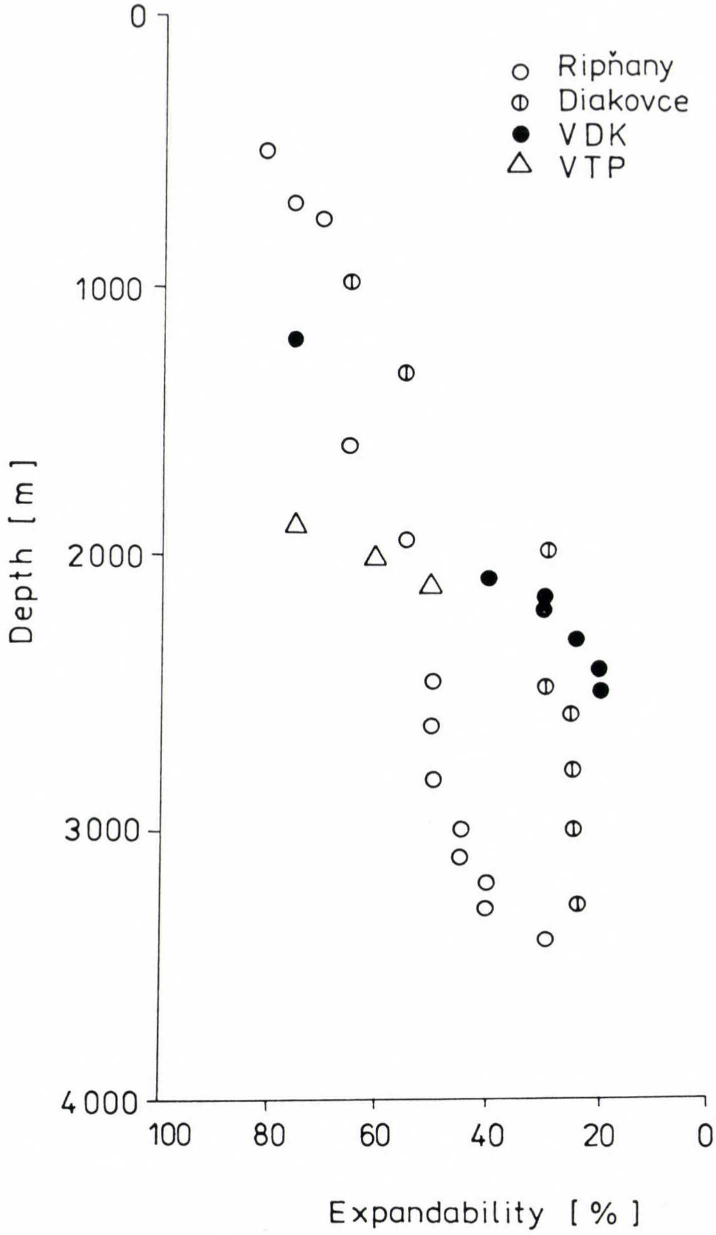

Fig. 5
Plot of expandability of mixed layer illite/smectite measured by XRD versus burial depth

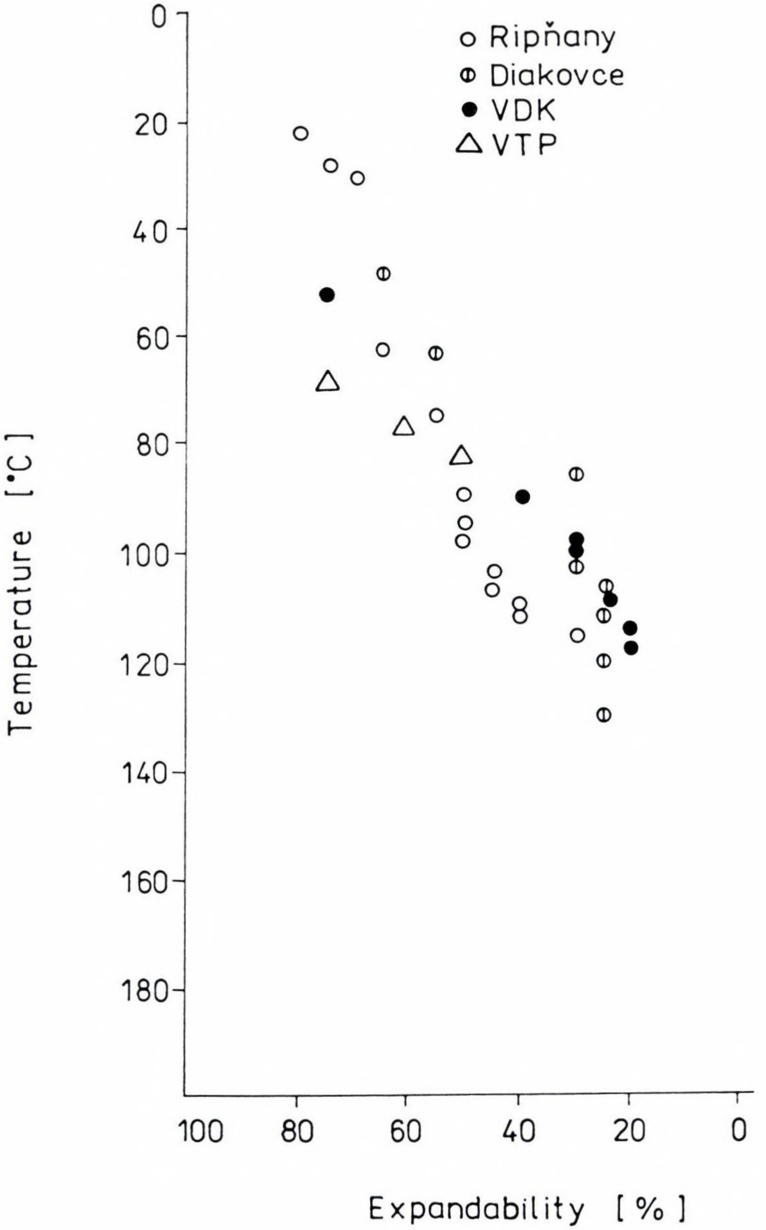

Fig. 6
Plot of expandability of mixed layer I/S measured by XRD versus burial temperature

cations) causes irreversible fixation of potassium in smectitic interlayers and an increase of Al tetrahedral substitution. The mechanism of the reaction is still not clear. At least three different mechanisms were suggested by several authors:

1. Substitution reaction inside the mineral structure (Hower et al. 1976).
2. Dissolution and precipitation of crystals (Nadeau et al. 1985).
3. K-fixation in a low temperature interval and dissolution and precipitation at higher temperature (Inoue et al. 1987).

Most probably, several different mechanisms take part in the smectite illitization process (Šucha et al. 1993).

Two stages of smectite illitization can be defined in the Danube Basin. The first stage begins with the first appearance of illite layers in the smectite structure and ends when the 1.7 nm reflection of smectite disappears from the XRD pattern. This stage is characterized by randomly ordered interstratification and is described by the parameter R (Reichweite), which is equal to 0 (Reynolds 1980). Ordered interstratification (R>0) defines the second stage of illitization. The border between these two stages in the Danube Basin is at an expandability of 35–40%. This value is the same for all studied bore-holes, but does not represent the same burial depth. The disharmony is caused by differences in geothermal gradient. Different illitization trends are also shown in Figure 5 when plotting expandability against burial depth. The only joint trend to appear was expandability versus burial temperature (Fig. 6).

The rate of illitization (amount of illitized layers per temperature unit) in the shales of the Danube Basin fits well with rates obtained for the Vienna Basin and the East Slovak Basin (Francŭ et al. 1990; Šucha et al. 1993).

Data from the shallowest available samples, where the temperature should be 130 °C (Král et al. 1985) show about 20% of illite layers. This remarkable decrease of expandability cannot be interpreted as a diagenetic reaction because smectite to illite conversion begins at a temperature of about 50 °C (Perry and Hower 1970). There are several possible explanations for this phenomenon:

1. The initial material came from source rocks containing some illitic layers.
2. Some smectite layers were collapsed by potassium fixation during the transportation process to the basin (most probably by the wetting and drying cycles described by Eberl et al. 1986; Šucha and Širáňová 1991).
3. The upper part of the basin was eroded.

According to the data published by Vass et al. (1988), we can omit significant erosion, but must still take into account both the first and second explanations.

Chemical composition

The semiquantitative chemical composition of the individual particles was determined by analytical electron microscopy on samples with different expandability from the borehole Ripňany 1 (R1/5 – expandability 75% and R1/57 – expandability 35%; see XRD patterns in Figure 3). Chemical analyses confirmed the mineralogical composition obtained by XRD. It also allowed us to distinguish a small amount of biotite in sample R1/57 which was not recognized by X-ray diffraction.

Chemical data were plotted in two types of triangles: Si-Al-3K and Al/Si-(Fe+Mg)/Si-3K/Si. The Si-Al-3K triangle (Fig. 7) shows Si-Al substitution and potassium content. All the analyzed individual particles are in the field described by the theoretical composition of muscovite, illite (see Środoň et al. 1992), montmorillonite and kaolinite. The sample with high expandability (R1/5) contains many particles with a chemical composition spread along the montmorillonite-muscovite line. Particles close to montmorillonite composition are 1 nm thick smectite fundamental particles (Nadeau et al. 1985). The points close to muscovite composition represent detritic micas which came to the basin from the sediment source rocks and originated in the previous geological cycle. The points between montmorillonite and muscovite belong to authigenic illite fundamental particles. The chemical composition of particles from a high illitic sample (R1/57) is more or less concentrated around an illite-muscovite composition. No smectite fundamental particle was found at this stage of illitization. This means that all particles are thicker than 1 nm and they contain at least one interlayer with potassium. The results also show no changes in Al and Si contents of kaolinite during diagenesis.

Triangles plotting Al/Si, (Fe+Mg)/Si and 3K/Si (Fig. 8) show changes in octahedral Mg and Fe contents during diagenesis. This diagram shows a decrease of Fe+Mg in the illite octahedral position during illitization. It allows us to distinguish very well the points belonging to kaolinites with no K content and no Fe+Mg content, smectites with no K and about 20% Fe+Mg octahedral substitution and chlorites with high Fe, Mg contents. This triangle also shows the biotite particles in sample R1/57 with high Fe+Mg and potassium content.

Conclusions

The diagenetic illitization of smectites was studied in the North-South section of the Danube Basin. The clay fraction (<1 μm) in all the samples contains a mixture of detritic illite (+– biotite), chlorite, kaolinite, mixed layer illite/smectite and a small amount of quartz. No correlation between the quantities of identified mineral phases and burial depth was found. Different positive correlations were found between the amount of illite layers in mixed layer illite/smectite minerals and burial depth in particular boreholes. The joint relation between expandability and burial temperature was determined in all studied boreholes. Approximately 20% of the initial illite layers in the original shale materials are linked to pre-sedimentary history (most probably the combination of illitization in the previous geological cycle and non-diagenetic fixation of potassium in smectites). The chemical compositions of individual illite particles show an increase of K and a decrease of Fe+Mg during diagenesis.

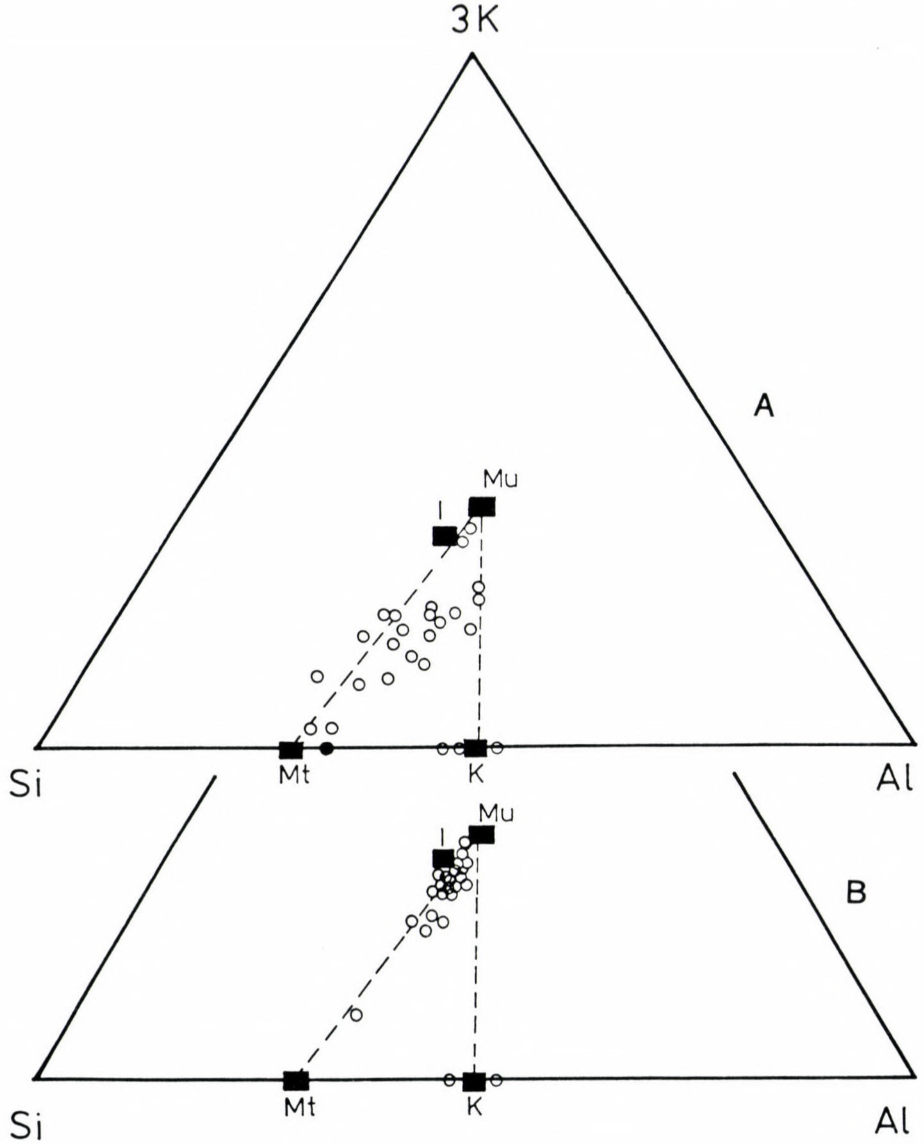

Fig. 7
Chemical composition of individual particles of samples R1/5 (A) and R1/57 (B) plotted in Si-Al-3xK triangle. Mu – muscovite, Mt – montmorillonite, I – illite, K – kaolinite

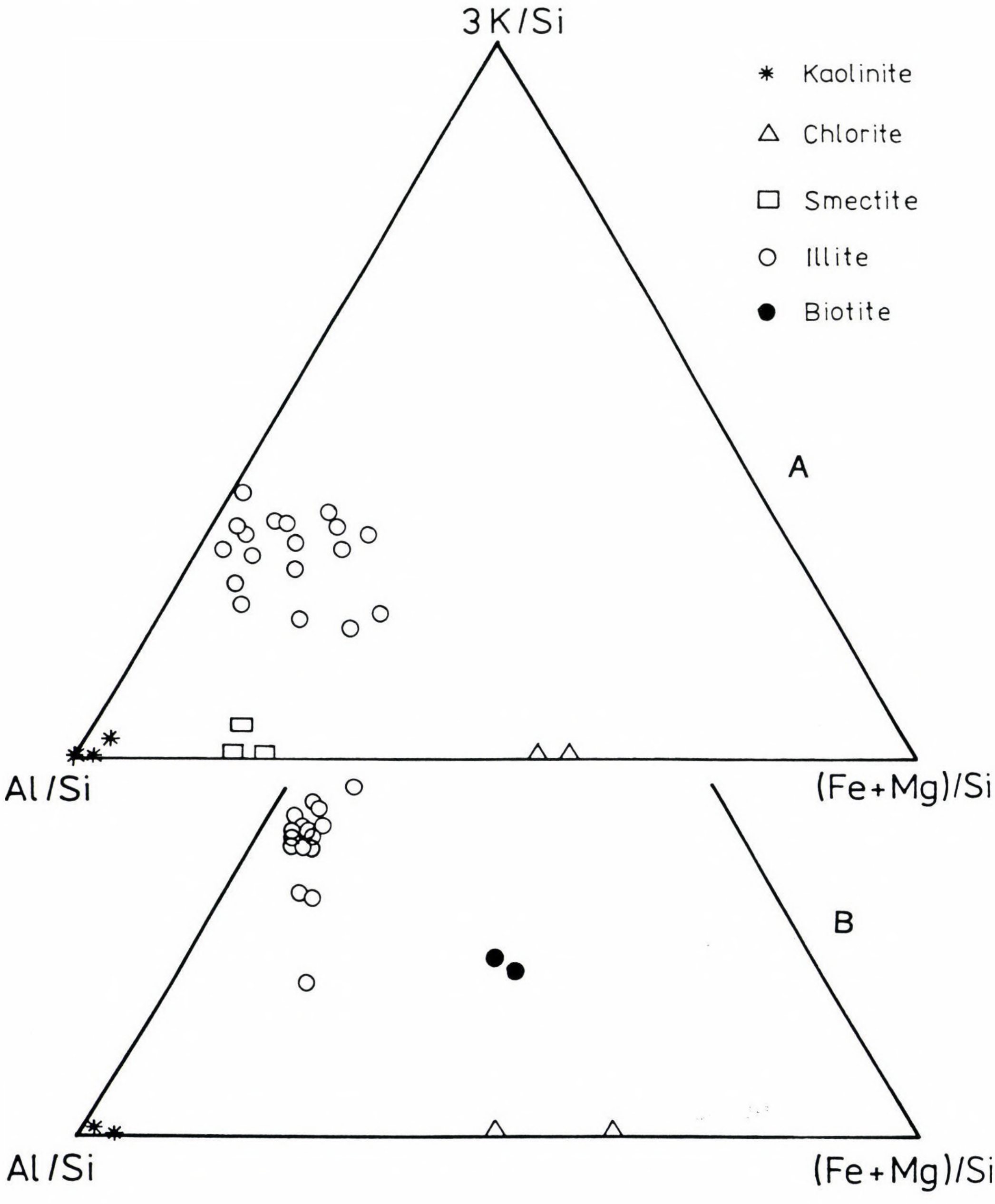

Fig. 8
Chemical composition of individual particles plotted in 3Al/Si-(Fe+Mg)/Si–3xK/Si triangle of samples R1/5 (A) and R1/57 (B)

References

Burst, J.F. 1959: Post diagenetic clay mineral-environment relationship in the Gulf Coast Eocene. – In: Clays and Clay Minerals 6th Conf., pp. 327–341.

Eberl, D.D., J. Srodon, H.R. Northrop 1986: Potassium fixation in smectite by wetting and drying. pp. 296–326 – In: Geochemical processes at Mineral Surfaces (J.A.Davis and K.F. Hayes, editors). Am. Chem. Soc.

Francŭ, J., P. Muller, V. Šucha, V. Zatkalikov 1990: Organic matter and clay minerals as indicators of thermal history in the Transcarpathian depression (East Slovakian Neogene Basin) and the Vienna Basin. – Geol. Zborník-Geol. Carpath. 41, pp. 535–546.

Frey, M. 1987: Very low-grade metamorphism of clastic sedimentary rocks. pp. 9–58 – In: Low Temperature Metamorphism (M. Frey, ed.). Blackie, London

Horton, R.B., W.D. Johns, H. Kurzweil 1985: Illite Diagenesis in the Vienna Basin, Austria. – Tschermaks Min. Petr. Mitt. 34, pp. 239–260.

Hower, J., E.V. Eslinger, M.E. Hower, E.A. Perry 1976: Mechanism of burial metamorphism of argillaceous sediments: 1. Mineralogical and chemical evidence. – Geol. Soc. Amer. Bull. 87, pp. 725–737.

Inoue, A., N. Kohyama, R. Kitagawa, T. Watanabe 1987: Chemical and morphological evidence for the conversion of smectite to illite. – Clays Clay Miner. 35, pp. 111–120.

Kisch, H.J. 1983: Mineralogy and petrology of burial diagenesis (burial metamorphism) and incipient metamorphism in clastic rocks. pp. 289–494. – in: Diagenesis in Sediments and Sedimentary Rocks (G. Larsen, G.V. Chilingar, Eds). Developments in Sedimentology 25B, Elsevier, New York.

Kovač M., A. Nagymarosy, J. Soták, K. Šútovský 1993: Late Tertiary paleogeographic evolution of the Western Carpathians. – Tectonophysics 226, 1–4, pp. 401–416.

Král M., I. Lizoň, J. Jančí 1985: Geothermal Research of Slovakia. – Manuscript, Geofond, Bratislava (in Slovak).

Kraus, I., E. Šamajová 1978: Clay minerals in sediments of the East Slovak Basin. – Zap. Karp. Sr. Min. Petr. Geochem. Metalogen. 5, pp. 29–82 (in Slovak).

Kurzweil, H., W.D. Johns 1981: Diagenesis of Tertiary marlstones in the Vienna basin. – Tschermaks Mineral. Petrogr. Mitt. 29, pp. 103–125.

Laperche V. 1991: Etude de l'état et de la localisation des cations compensateurs dans les phyllosilicates. Ph.D. thesis, Université de Paris VII, 104 pp.

Nadeau, P.H., M.J. Wilson, W.J. McHardy, J.M. Tait 1985: The conversion of smectite to illite during diagenesis: evidence from some illitic clays from bentonites and sandstones. – Miner. Mag. 49, pp. 393–400.

Perry, E.A., J.Hower 1970: Burial diagenesis in Gulf coast pelitic sediments. – Clays Clay Miner. 18, pp. 165–177.

Reynolds, R.C. 1980: Interstatified clay minerals. – In: Crystal Structure of Clay Minerals and their X-ray Identification. (G.W. Brindley and G. Brown, Eds). pp. 248–303. Mineralogical Society, London.

Reynolds, R.C. 1985: Newmod, a computer program for the calculation of basal X-ray diffraction intensities and mixed-layered clays: – R.C. Reynolds, Hanover, New Hampshire.

Royden, L.H. 1988: Late Cenozoic tectonics of the Pannonian Basin system. – In: The Pannonian Basin: a Study in the Basin Evolution. (L.H. Royden, F. Horváth, Eds) AAPG Memoire, 45, pp. 27–48.

Royden, L.H., F. Horváth, B.C. Burchfiel 1982: Transform faulting, extension and subduction in the Carpathian/Pannonian region. – Geol. Soc. Amer. Bull., pp. 717–725.

Royden, L.H., J.C. Schlater, 1981: The Neogene intra-Carpathian Basins. – Phil. Trans. R. Soc. London A 300, pp. 373–381.

Smoljar B.B., V.A. Drits 1988: Relation between b-parameter and basic cell chemistry. – Mineralogicheskij zhurnal 10, 6, pp. 10–16.

Środoń, J. 1980: Precise identification of illite/smectite interstratification by X-ray powder diffraction. – Clays Clay Miner. 28, pp. 401–411.
Środoń, J. 1981: X-ray identification of randomly interstratified illite/smectite in mixture with discrete illite. – Clay Miner. 16, pp. 297–304.
Środoń, J., D.D. Eberl 1984: Illite. pp. 495–544. – In: Micas (S.W. Bailey, Ed.). Mineralogical Society Review in Mineralogy 13, Mineralogical Society of America, Washington, DC.
Środoń, J., F. Elsass, W.J. McHardy, D.J. Morgan 1992: Chemistry of illite-smectite inferred from TEM measurements of fundamental particles. – Clay Miner. 27, pp. 137–158.
Šucha,V., V. Širánová 1991: Ammonium and potassium fixation in smectites by wetting and drying. – Clays Clay Miner. 27, pp. 137–158.
Šucha, V., I. Kraus, H. Gerthofferová, J. Peteg, M. Serekov 1993: Smectite to illite conversion in bentonites and shales of the East Slovak Basin. – Clay Minerals 28, pp. 243–253.
Vass, D., M. Kovác, V. Konečný, J. Lexa 1988: Molasse basins and volcanic activity in West Carpathians Neogene. – Geologica Carpathica 39, pp. 539–561.
Viczián, I. 1985: Diagenetic transformation of mixed-layer illite/smectites in deep zones of the Pannonian Basin (Hungary). – 5th meeting of the European Clay Groups, Prague, 1983, pp. 135–140, Charles University, Prague.
Viczián, I. 1992: Clay minerals of a thick sedimentary sequence in SE part of the Pannonian Basin (Hungary). – Geol. Carpath. Clays 1/1, pp. 27–30.

Acta Geologica Hungarica, Vol. 37/1–2, pp. 111–117 (1994)

The basis of a new optical method for quantitative estimation of total rock porosity (preliminary results)

Alexander Kh. Zilbershtein
A.P. Karpinsky All-Russian Geological Res. Institute (VSEGEI), St. Petersburg, Russia

G.M. Romm
Institute of Earth Physics, Russian Acad. Sci., St.. Petersburg, Russia

The basis of the proposed new method for the quantitative estimation of total rock porosity is the analysis of transmission of monochromatic light passing through samples plates (thin sections). For transparent material, this transmission is determined by light scattering on the heterogeneities of the sample's material (pores, cracks, intergranular spaces). The logarithmic dependence of total porosity (heterogeneity concentration) on light transmittance is obtained theoretically and experimentally (using dolomite samples as an example).

Key words: porosity, light transmission, wave length, scattering, pore size, plate thickness

Introduction

The study of fluid transfers addresses important problems in various fields of geosciences. It has theoretical importance as well as practical applications – the latter because of the fact that mineralized fluid migration leads to ore bed formation. The study of fluid migration processes is especially important in oil and gas prospection.

The investigation of fluid migration processes has been the subject of constant interest of many specialists (see Torgesen 1991; Lockner et al. 1991; etc.). The ability of fluids to move in rock is determined by the rock's physical properties, mainly permeability. Permeability is a function of cavities, such as fractures, pores, intergranular spaces, etc. It has been shown that permeability is directly related to intergranular microporosity (Ehrenberg 1990). However, classical methods for quantitative estimation of porosity (see, for example Milner 1962), as well as modern methods (Dobrynin 1991; Yuan 1991; etc.), are rather difficult to use in practice and are not always adequate. A new, independent method for rock porosity estimation, based on the study of light transmission through thin sections, is proposed.

Addresses: A. Kh. Zilbershtein: Sredny pr. 74, 199226, St. Petersburg, Russia.
G. M. Romm: Bolshoy pr. 50, St. Petersburg, Russia.
Received: 12 October, 1993

0236–5278/94/$ 4.00

Theory

The optical properties of the medium (crystals and/or rocks) are sensitive to its porosity. We take into account the fact that the difference between the optical characteristics of the medium itself and that of pores, fractures and intergranular spaces, may be a reason for light scattering in these cavities.

The intensity of light passed through thin section decreases due to the scattering, as does also the magnitude of light transmittance. The theoretical description of light scattering was presented by Raleigh (1899) and Mie (1908) in a general sense (see Born and Wolf 1968). In the case of transparent, non-absorbing, non-luminescent media of sufficiently small optical thickness, the description may be more simple.

Standard thin sections (with thickness l) of most non-absorbing rocks satisfy this condition and makes it possible to suppose scattering as being non-reiterative.

Thus, light transmittance (T) of rock thin sections with cavities (pores, intergranular spaces, fractures) is described by the Bouguer-Lambert-Beer law:

$$T = I/I_o = \exp\left(-(l/V)\sum_{i=1}^{N} y_i\right) \qquad (1)$$

where l is the thickness of thin section; I_o is the intensity of the incident parallel monochromatic light beam (λ is the wavelength of the light); I is the intensity of light passed through thin section in the incident light direction; V is the analyzed volume of thin section; N is the quantity of cavities in the analyzed volume; y_i is the coefficient of extinction for the cavity "i". If the size of cavities is significantly more than wavelength (λ):

$$r_i >> \lambda \qquad (2)$$

(r_i is the characteristic geometrical size of cavities) and cavity shapes might be supposed as not very anisotropic ones, i.e. if it may be assumed that

$$s_i >> \lambda^2 \qquad (2a)$$

(s_i is the area of cavity or "pore" section in thin section plane), then the extinction coefficient y_i may be expressed in this form:

$$y_i = 2s_i \text{ (see Born and Wolf 1968)} \qquad (3)$$

for different cavities (pores). Using conditions (2), (2a), (3), equation (1) may be expressed as:

$$T = \exp\left(-(2l/V)\sum_{i=1}^{N} s_i\right) \qquad (4)$$

As a rule the total volume of cavities is significantly lower than volume of medium (V). So Eq. (4) may be represented in the linear form:

$$T = \exp\left(-(2l/V)\sum_{i=1}^{N} s_i\right) = 1 - (2l/V)\sum_{i=1}^{N} s_i \tag{5}$$

The total volume (Vp) of cavities (pores) may be expressed as:

$$V_p = \sum_{i=1}^{N} V_i = \sum_{i=1}^{N} s_i r_i = r \sum_{i=1}^{N} s_i \tag{6}$$

where V_i is the volume of cavity "i" and r is the mean geometrical size of cavities in the incident light direction. By definition the total porosity (P) of the medium is:

$$P = V_p / V \tag{7}$$

Then, using Eq. (6), the expression for P may be obtained as:

$$P = (r/V) \sum_{i=1}^{N} s_i \tag{8}$$

The solution of the system of simultaneous equations (4) and (8) may be expressed in this form:

$$P = -(r / 2l) \ln T \tag{9}$$

Equation (9) demonstrates the logarithmic dependence of porosity P on transmittance T. For samples with low porosity, the solution of system Eq.(5) and Eq. (8) may be presented as:

$$P = r(1 - T) / 2l \tag{9a}$$

Equation (9a) shows approximately linear dependence between porosity (P) and light transmittance (T) for samples with low porosity. The transmission depends on all cavities and so P (in equations (9), (9a)) conforms to total porosity.

If the size of pores exceeds the thin section thickness, i.e.

$$r > l \tag{10}$$

then, using measured values of transmittance T, the approximate estimation of total porosity P may be expressed as follows:

$$P = -(1/2) \ln T \text{ (general case)} \tag{11}$$

or

$$P = (1-T)/2 \text{ (for samples with low porosity)} \tag{11a}$$

Equations (9), (9a), (11) and (11a) demonstrate the simple relations between porosity and transmittance and are the main expressions for the application of the theory to the experimental data.

Discussion

The effects of surface roughness of the sample and mineral–mineral interfaces on light transmittance T should be taken into account. These effects induce a decreasing of transmittance by the increase of scattering.

The first effect may be relatively slight for polished sample plates (thin sections).

The second effect is determined by the characteristics of the interfaces (structure, density, geometry) and the difference between refractive indices of the minerals. This effect may be relatively slight for sufficiently coarse-grained polycrystalline aggregates and/or monomineralic aggregates (with optically isotropic minerals or minerals with slight optical anisotropy). In addition, these interfaces often form the intergranular spaces. In this paper, all the above circumstances permit us to ignore both these effects.

The laser macroscope-photometer (λ = 632.8 nm) was used for the measurements of light transmittance (T_e) for thin sections of dolomites from an oil exploration well (North Pechora Plain, Russia) as an example. The setup permits producing one measurement of T during one minute. Rocks of Early Silurian age were extracted from 3.0–3.5 km depth. The analyzed area of the thin sections may reach 3 cm. The thickness (l) of the thin sections was 0.030 mm. This relation between wavelength (λ) and thickness (l) is in accordance with condition (2) if condition (10) is true, and vice versa.

Total porosity P_t was estimated by the well-known method of using a unit weight of dolomite p_m and a dry unit weight of sample p_c :

$$P_t = 1 - p_c / p_m \tag{12}$$

For these estimations we assumed that the majority of cavities (pores) is empty, and that the total unit weight is close to the dry unit weight for all samples under study. The correlation between total porosity P_t and transmittance T_e is presented in Fig. 1 and may be expressed in this form:

$$P_t = C - D \ln T_e \tag{13}$$

($C = -1.25$, $D = 0.22$, correlation coefficient equal to – 0.68). In this case, the logarithmic correlation (13) may be represented in linear form:

$$P_t = A - B\, T_t \tag{13a}$$

($A = 19.83$, $B = -1.78$, correlation coefficient is equal to – 0.71).

Also, the effective porosity, P_e, was measured by the standard method, using kerosene as the impregnating medium. The experimental results permit us to

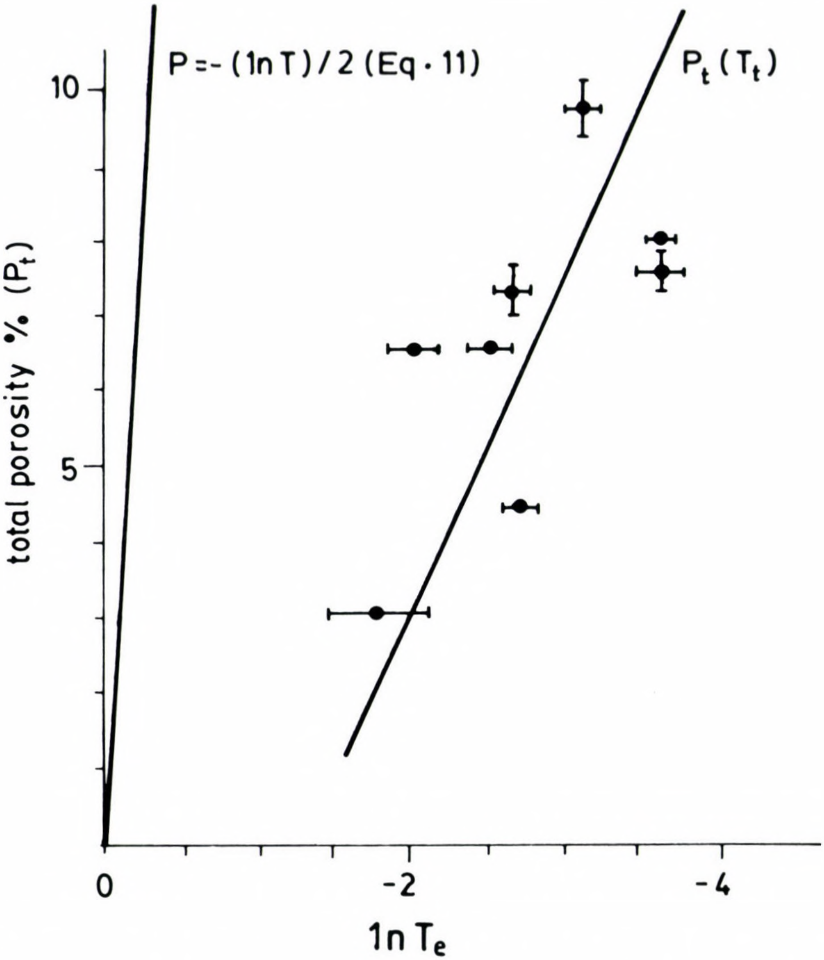

Fig. 1
Dependence of the experimentally determined (P_t) and theoretically estimated (P) (see Eq. (11)) total porosity on the measured light transmittance T_e

obtain the logarithmic correlation between effective porosity P_e and transmittance T_e (Fig. 2):

$$P_e = C' - D' \ln T_e \tag{14}$$

($C' = -1.50$, $D' = 0.23$, correlation coefficient is equal to -0.72). In this case, the logarithmic dependence (14) may be also represented in linear form:

$$P_e = A' - B' T_e \tag{14a}$$

($A' = 18.11$ [%], $B' = 1.88$ [%P/%T], correlation coefficient equal to -0.75).

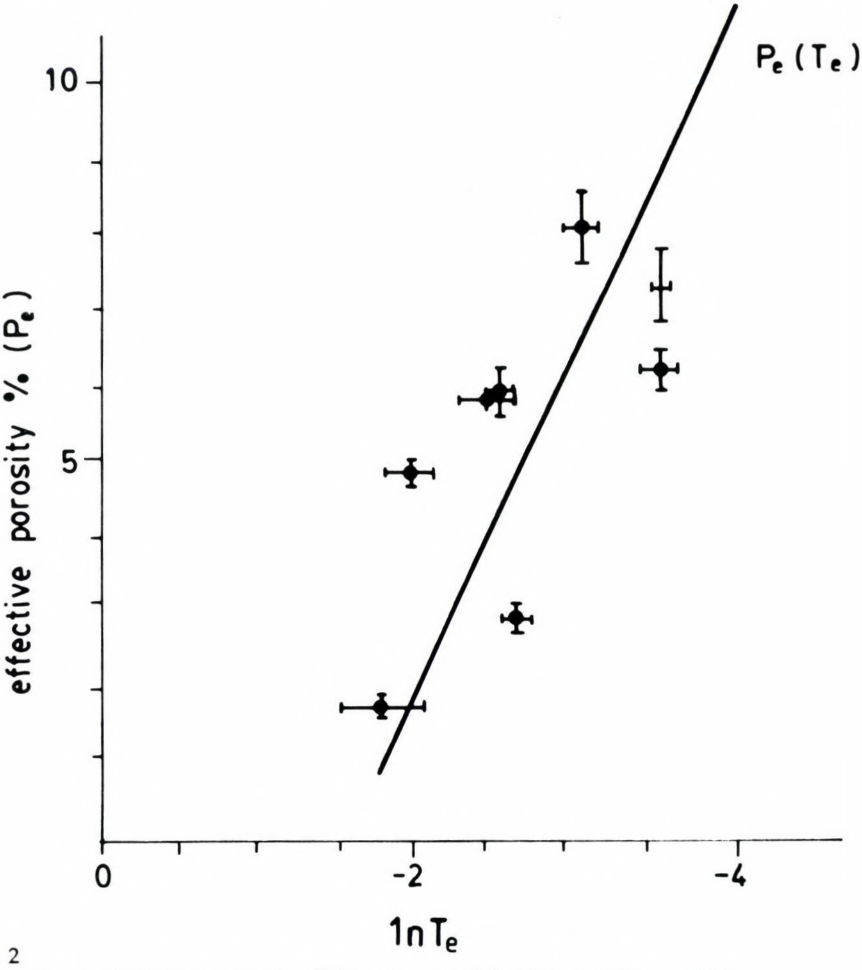

Fig. 2
Dependence of effective porosity (P_e) on measured light transmittance (T_e)

Thus the light transmittance (T_e) of thin sections may be used as a measure of the porosity of materials (see equations (9), (9a), (11), (11a), (13), (13a), (14), (14a)).

It is necessary to take into account that experimentally measured transmittance may be dependent not only on pores (cavities) but also on other optical heterogeneities, and the light absorption of material. Thus, the values of experimentally measured light transmittance (T_e) are lower than the values of (T) in equations (9), (9a) and (11), (11a). This fact determines the difference between theoretical dependences P(T) and experimental ones $P_t(T_e)$, (see Fig. 1).

The applicability of equations (9) and (9a) requires limitations on the relations between wavelength of radiation, size of pores (cavities) and thickness of thin sections only. Limitations on their absolute values are not required. Thus, logarithmic (and linear) dependence of P on T may exist for any magnitude of r. However, measurements of transmittance (T_e) for such variable transparent (non-absorbing for the given radiation) samples requires a corresponding choice of radiation wavelength (λ) and sample thickness (l).

Conclusion

Equations (9), (9a) and (11), (11a) for the light transmittance of transparent, non-absorbing, non-luminescent media with heterogeneities (cavities) were obtained. They demonstrate logarithmic (in the general case) and linear (for low porosity) correlations between porosity and light transmittance. Experimental measurements of porosity and light transmission for the dolomite thin sections confirm the predicated dependence. Thus, light transmittance of thin sections could be used as a measure of rock porosity.

Acknowledgements

The authors wish to thank Dr. M.Bulach for supplying the thin sections and Dr. A.Khudoley for assistance in this study.

References

Born, M., E. Wolf 1968: Principles of Optics. – Pergamon Press, London, p. 720.

Dobrynin, V.M. 1991: Investigation of porosity of composed carbonate collectors. – Geology of Oil and Gas, 5, pp. 30–34.

Ehrenberg, S.N. 1990: Relationship between diagenesis and reservoir quality in sandstone of the Garn Formation, Haltenbanken, mid-Norwegian continental shelf. – AAPG Bulletin, 74, pp. 1538–1578.

Franklin, K. 1990: Study of Nordgren's equation of hydraulic fracturing. – SPL Prod. Eng., 5, pp. 311–314.

Lockner, D., S. Hickman, V.A. Kuksenko 1991: Laboratory determined permeability of cores from the Kola Superdeep well, USSR. - Geophys. Res. Lett., 18, pp. 881–884.

Mie, G. 1908: Beitrage zur Optik trueber Medien, speziell kolloidaler Metallosungen. – Annalen der Physik, 25, pp. 377–445.

Milner, H.B. 1962: Sedimentary Petrography. Vol. 1 Methods in Sedimentary Petrography. – Allen, London, p. 643.

Rayleigh, L. 1899: Transparency and opacity. – Nature, 60, pp. 64–65.

Torgesen, T. 1991: Crustal-scale fluid transport – Geophys. Res. Lett., 18, pp. 917–986.

Yuan, H.H. 1991: Pore-scale heterogeneity from mercury porosimetry data. – SPE Form. Eval., 6, pp. 233–240.

Acta Geologica Hungarica, Vol. 37/1–2, pp. 119–134 (1994)

Assessing the engineering geological factors of the environment in Slovakia

Vlasta Jánová, Miloš Kováčik, Pavel Liščák, Martin Ondrášik,
Dionyz Štúr Institute of Geology, Bratislava

Maria Kováčiková, Lubomir Petro, Zoltan Spišák
Dionyz Štúr Institute of Geology, Bratislava

The authors describe the compilation methodology of a set of engineering geological environmental maps at a scale of 1:50 000. The new methodology and mapping were performed within a larger project of environmental mapping, which began in 1991 in the Slovak Republic. Altogether six regions (with areas of 800 to 2 000 km²) were chosen to test the new methodologies, and to prepare maps. The set consists of the following maps: 1. Engineering geological zoning map, 2. Area landslide susceptibility map, 3. Rock resistance to weathering map, 4. Rock and soil erosion susceptibility map, 5. Geopotentials and geobarriers map, 6. Foundation soil load-bearing capacity map and 7. Area waste disposal suitability map. The choice of maps can be changed (limited or extended) in other regions, which are to be mapped in the next years.

Key words: geological factors, landsliding, weathering, erosion foundation soils, waste disposal

Introduction

In the late 1980's a theoretical engineering geological study was focused on the assessment of the engineering geological factors of the environment in the Slovak Republic. A large project of multidisciplinary environmental mapping in selected regions of Slovakia began in 1991. A set of environmental maps concerning engineering geology is one product resulting from this project.

The methodology of regional investigation and compilation of maps at the scale of 1:50 000 was developed for the following geodynamic phenomena: slope failure, sheet and gully erosion and weathering (Kováčik et al, 1991). These phenomena are of the greatest importance in the selected regions from an economic point of view. Other natural geodynamic phenomena are expected to be studied in different regions of Slovakia (e.g. collapsibility in loess, karst, land subsidence, etc.).

The engineering geological contribution to the set of environmental maps comprises the following: landslide susceptibility of the area, rock and soil erosion susceptibility, rock resistance to weathering, foundation soils load-bearing capacity, and geological potentials and barriers. Figs 1 and 2 assess the present status of the natural processes and the prognosis of future development due to natural or artificial factors. Figs 3 and 4 are special environmental maps which display the present conditions of the area. Figs 1,

Addresses: V. Jánová, M. Kováčik, M. Kováčiková, P. Liščák, M. Ondrašik, L. Petro, Z. Spišák: Mlynská dolina 1, 817 04 Bratislava, Slovakia.
Received: 14 October, 1993

0236–5278/94/$ 4.00

5 and 7 represent synthetic maps. The engineering geological zoning map is constructed according to the standard mandatory methodology for this type of map in force in the Slovak Republic.

These maps were compiled for six areas of Slovakia according to the described methodology. The total surface of each region varies from 800 to 2 000 km^2.

All these special geological maps not only have theoretical importance but are also of practical use to the local authorities for land-use planning and for the protection of the environment.

The set of engineering geological maps

The set of engineering geological maps consists of seven different types of maps. Methodologies of the elaboration of these maps were for the most part established specially for this project. Only Figs 1, 3 and 7 were based on older national or international experience or procedures.

Engineering geological zoning map (Fig. 1)

This kind of map can be characterized as a comprehensive (synthetic) multi-purpose map. The content of the engineering geological zoning map and the amount of information are determined by the purpose and by the scale of this map. The essence of the zoning method is the comprehensive evaluation of the engineering geological environment (geology, geomorphology, hydrogeology and geodynamic phenomena) to a limited number of uniform map units which assess the ground conditions to a limited depth (usually up to 10 m).

Engineering geological zones are determined on the basis of the similarity of the lithological character and the uniformity of the geological formations up to a depth of 10 m. Individual zones are represented by symbols expressing both the genesis and lithology of the rocks and soils. When two superimposed formations occur, symbols can be combined. Subzones are identified by symbols which are formed by grouping the appropriate signs for soils and rocks (type, thickness of Quaternary deposits or the depth of pre-Quaternary basement), according to the vertical sequence of delimited strata (e.g. the symbol p1g2B2 indicates a soil sequence in which sandy soil – p (thickness less than 2m) is underlain by gravels – g (thickness 2–5 m), and pre-Quaternary semi-solid rock – B occurs at a depth of 5–10 m).

The zones on the map are delineated by full black lines and identified by symbols and colours based on our classification system. Subzones are delineated within the zones by dashed black lines.

Groundwater and surface water play a prominent role in the geodynamic processes. Engineering geological properties of rocks and soils are often altered by the presence of groundwater. Hydrogeological data are represented by symbols and numbers (the depth of groundwater level, direction of

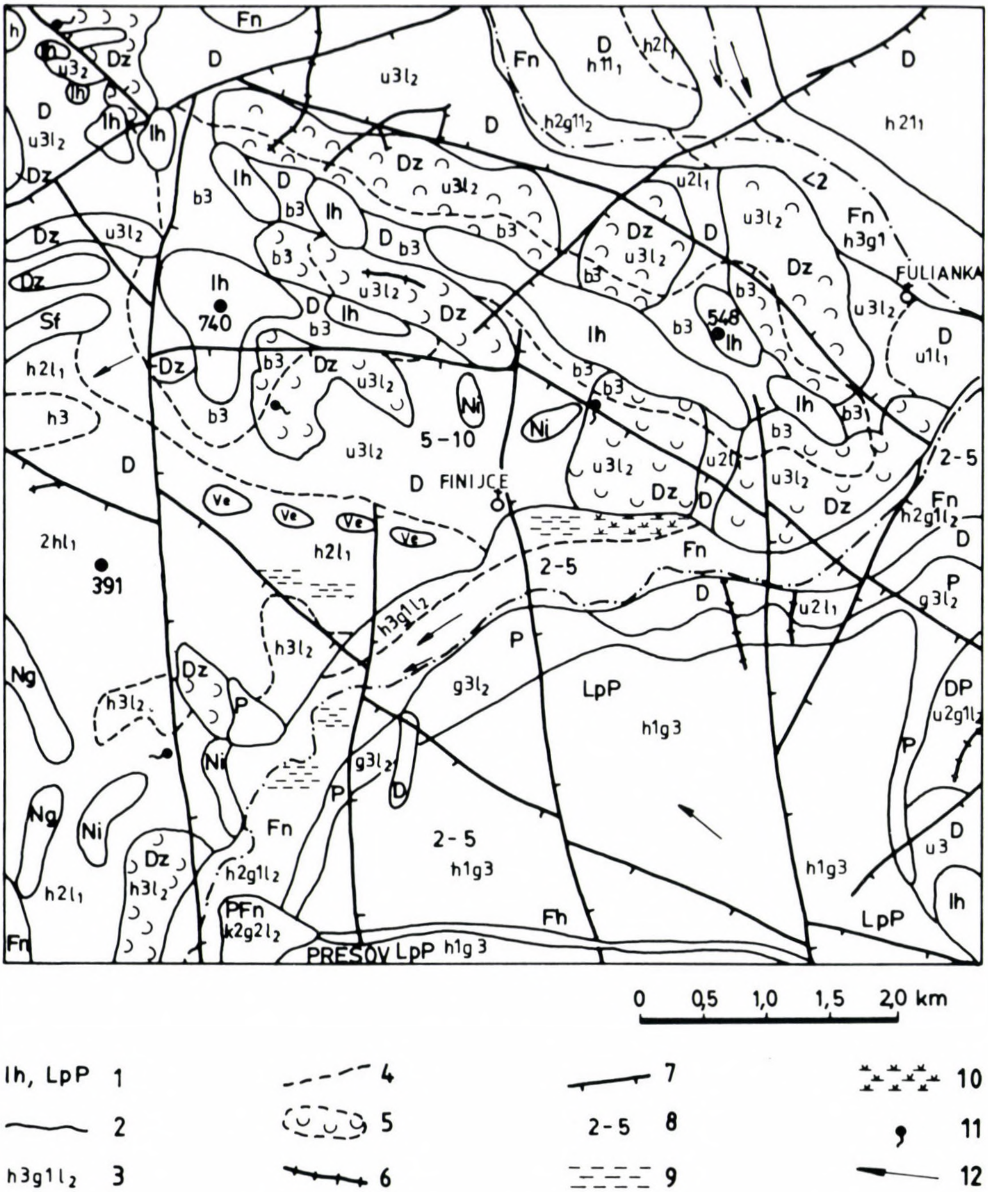

Fig. 1
Engineering geological zoning map of the northern part of the Kosicka kotlina Basin (East Slovakia). 1. symbol of zones; 2. boundaries of zones; 3. symbol of subzones; 4. boundaries of subzones; 5. areas affected by landsliding; 6. gully erosion; 7. significant faults of pre-Quaternary basement; 8. depth of groundwater; 9. waterlogged territory; 10. swamps; 11. significant springs; 12. direction of groundwater flow

groundwater flow, waterlogged terrains, significant springs, corrosiveness of groundwater, etc.).

The occurrence of the most significant geodynamic phenomena (slope deformations of all types, gully erosion, moving sands, karst phenomena, suffusion, loess collapsibility, swelling and shrinkage of soils, mining subsidence, tectonic depressions of Quaternary age and significant faults) is depicted in red on the map.

Documentation marks (e.g. quarries, mines, etc.) have informative character and are depicted in black.

Lithological, geomorphological, hydrogeological and geodynamic conditions of the individual zones are characterized in tabular form, including the physical and mechanical properties of rocks and soils.

Area relative landsliding susceptibility map (Fig. 2)

Landsliding is one of the most important exogenous geodynamic phenomena in large regions of the world which often threatens, or at least negatively influences, human properties or even lives.

There is a great variety of special geological or geomorphological maps in which areas are displayed and evaluated according to the instability of slopes (landslide inventory maps, landslide hazard and risk maps, etc.). Zones and subzones are depicted according to the equal or similar occurrence of slope deformations. The degree of landslide hazard of the delineated zones is normally expressed by denomination, e.g. low – middle – high, or stable – relative stable – unstable.

Such a type of landslide hazard map can be used not only for a simple prognosis of the evolution of unstable slopes, but for urban planning and the choice of alternative communication routes as well.

The elaboration of the map requires taking into account the following factors: 1. geological conditions (lithology of the bedrock, thickness and character of slope sediments, the presence of geological landsliding structures, tectonics, degree of weathering of rocks, orientation of joints and bedding planes in rock masses, etc.), 2. hydrogeological, hydrological and climatic conditions, 3. morphology (slope angles, character of slopes, etc.), 4. existing slope failures, 5. vegetation cover.

Among the above-mentioned aspects geological conditions and existing slope failures seem to be the most important from the viewpoint of slope stability. Other factors (morphology and hydrogeology) are of less importance in comparison with the first two. In general, vegetation cover has only a limited and local importance.

The output of the assessment of these factors is a zoning map entitled "Area relative landsliding susceptibility map". Three zones are differentiated: 1. zone of unstable areas, 2. zone of relatively stable areas, 3. zone of stable areas. Zones

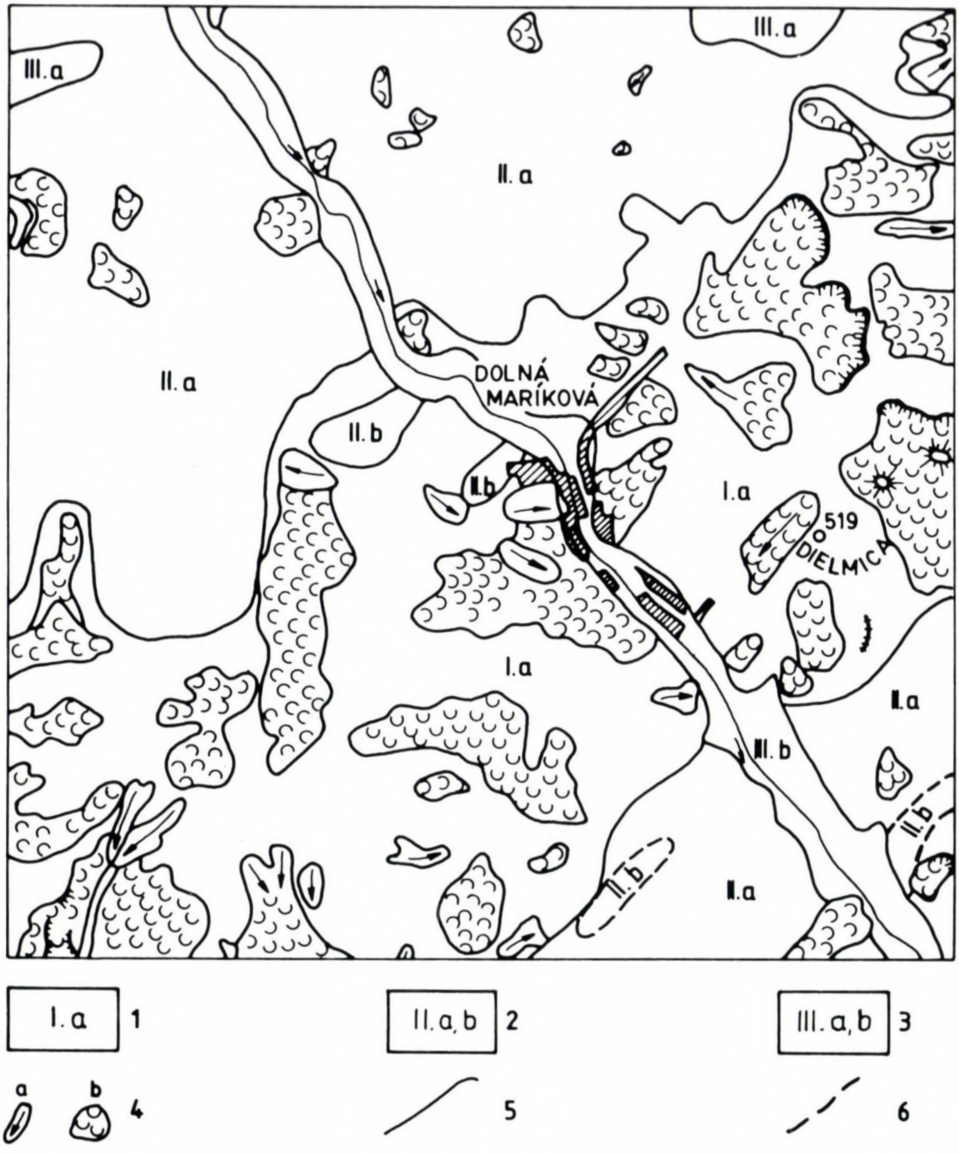

Fig. 2
Part of the area landsliding susceptibility map from the Javorníky Mts. in W-Slovakia (the original map is in colour). 1. zone of unstable areas on flysch strata; 2. zone of relatively stable areas on flysch strata (a), limestónes (b); zone of stable areas on fluvial sediments (a), flysch strata (b); 4. slope deformations: flows (a), slides (b); 5. boundary of the zones; 6. boundary of the subzones

can be subdivided into subzones according to the prevailing geology (e.g. zone of unstable areas on flysch strata, etc.).

The final map offers all the relevant information about conditions and factors which influence the stability of slopes – geology (hatched in gray), existing slope failures and gully and sheet erosion (marked in red for active phenomena, black for dormant ones), hydrogeological data (marked in blue), morphology (isolines in brown). Colours (red, orange, green) and symbols (letters) are used for zoning of the area according to its stability.

Rock and soil erosion susceptibility map (Fig. 3)

Erosion is one of the most powerful natural phenomena which significantly contributes to changes of the environment. Erosion is a very complex natural phenomenon which depends on a variety of factors (e.g. soil and rock properties, climate, precipitation, morphology, vegetation cover, etc.). Many of these vary in time and space. These variations can be regular (e.g. climate changes during the year) or irregular (e.g. alternating of crops, lumbering, construction, etc.).

The compilation of this map is based on the geological map, the engineering geological zoning map, aerial photographs, field survey and additional sampling and laboratory testing in places where required information is missing.

According to these data, the area studied is divided into zones with different predisposition to erosion. The following zones were selected: 1. zone of rocks and soils resistant to erosion, 2. zones of rocks and soils relatively resistant to erosion, 3. zones of rocks and soils sensitive to erosion.

The zones are distinguished from each other by colour (green for resistant, yellow for relatively resistant and red for sensitive rocks and soils). The final map contains not only the depicted zones but also gullies, tectonic faults, solifluction, abrasion, proluvial cones, streams and isolines separating zones with different length of erosion furrows per square kilometer. This last-mentioned phenomenon objectively expresses the real state of erosion of the studied area. The map can be complemented by a brief characterization of the zones (geological, engineering geological and geomorphological conditions, character of erosion and forecasting of erosion due to possible removing of vegetation cover).

The described map is easily readable for anyone who needs brief and clear information and can be used without any special knowledge of geology.

Rock resistance to weathering map (Fig. 4)

Rock weathering interferes considerably with the costs of engineering constructions. The state of weathering and the thickness of weathered rock are very variable even within a single rock mass. Because the mechanical characteristics and chemical composition of rocks can change in a few years,

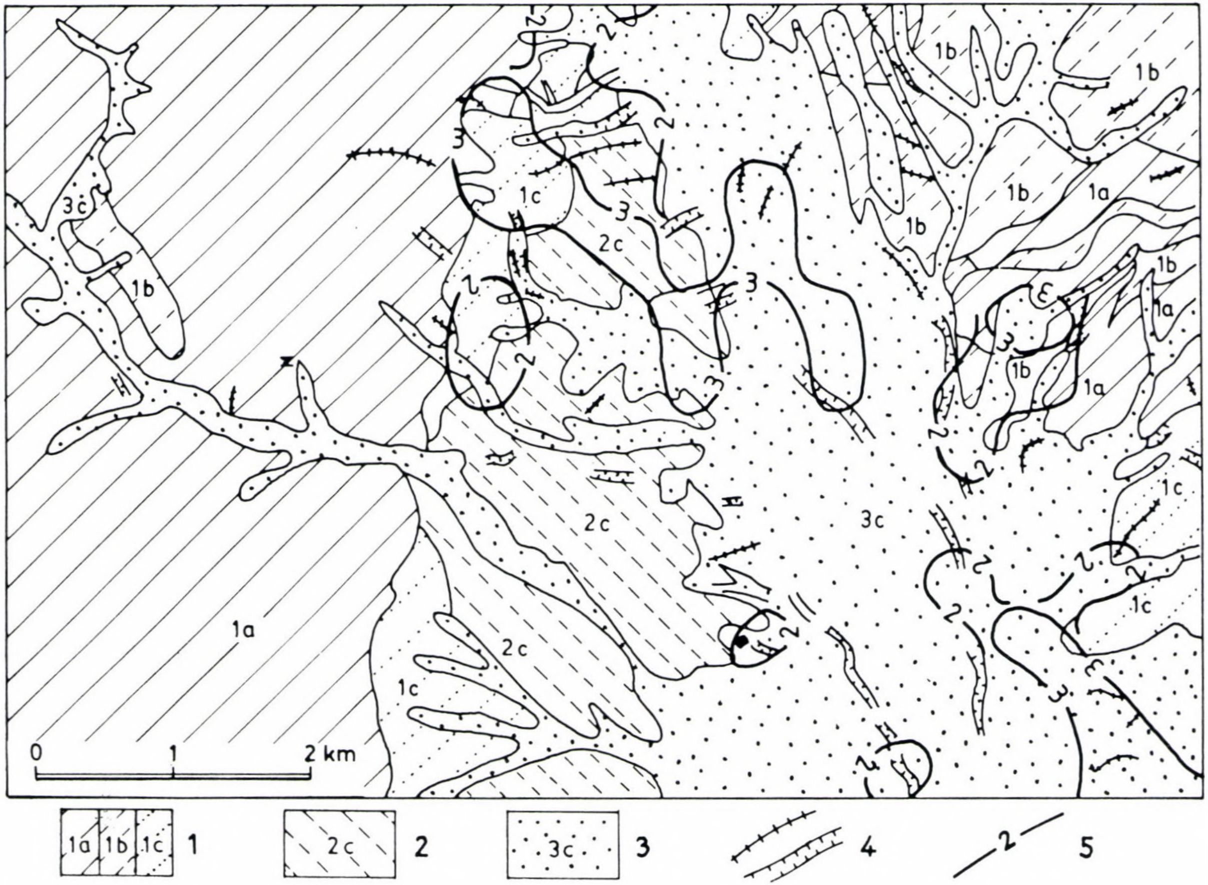

Fig. 3

Part of the rock and soil erosion susceptibility map (Horná Nitra region). 1. zones of resistant rocks and soils to erosion: a. solid rocks (granite, limestone etc.) b. semi-solid rocks (flysch, claystone, marly limestones etc.), c. soil (slope, eluvial, alluvial, colluvial etc.); 2c. zones of relatively resistant rocks and soils to erosion, soil (slope, eluvial, alluvial, colluvial etc.); 3c. zones of sensitive rocks and soils to erosion, soil (slope, eluvial, alluvial, colluvial etc.); 4. erosion furrow; 5. length of erosion furrow per square kilometer (m/km^2)

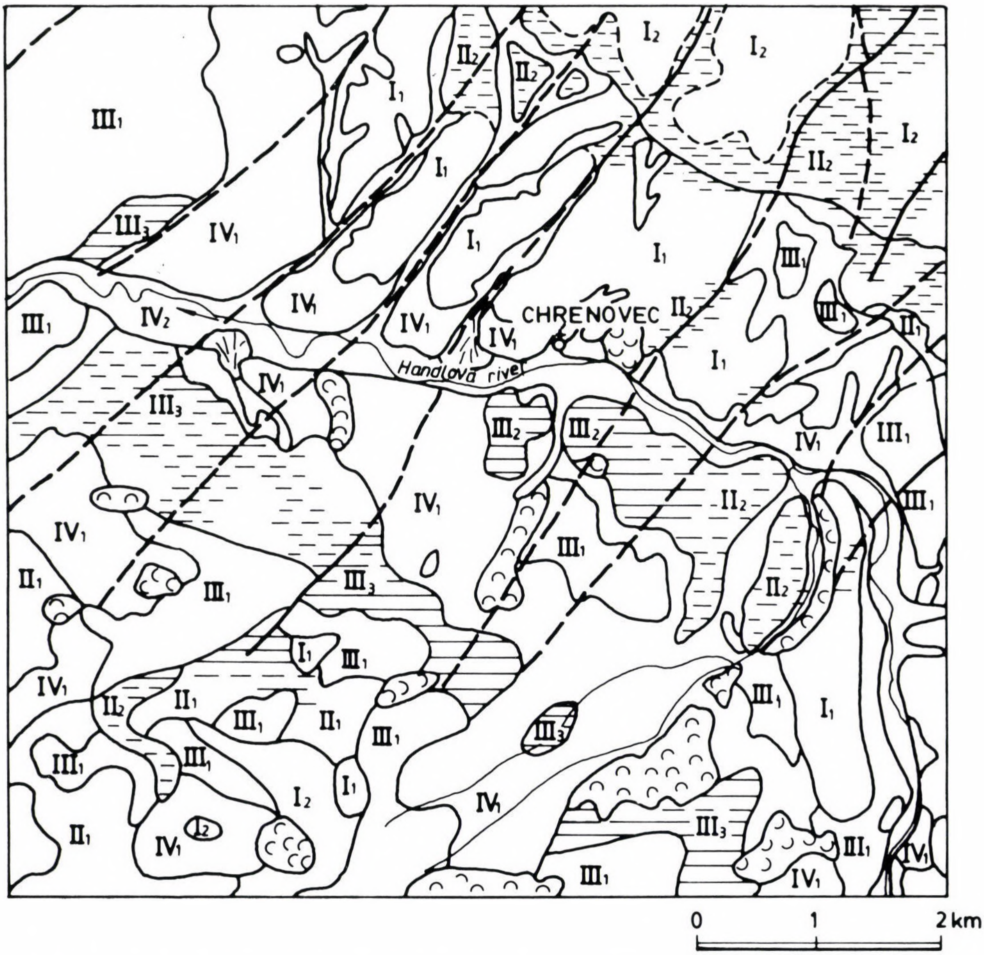

Fig. 4
Part of the rock resistance to weathering map from the Horná Nitra region. (The original map is in colour). Rocks with fair resistance to weathering: I_1. sound solid rocks with extremely high compressive strength (150 MPa), I_2. sound solid rocks with high compressive strength (50–150 MPa); Rocks with moderate resistance to weathering: II_1. sound semisolid rocks, moderate compressive strength (15–50 MPa), II_2. altered rocks of the first category (15–50 MPa); Rocks with low resistance of weathering: III_1. weak rocks, rocks with high content of clay minerals, rocks containing quickly weathering minerals, leachable soils (<15MPa). $III_{2,3}$. highly weathered rocks desintegrated by tectonics or other alterations

months and even days, it is useful to have basic information about the susceptibility of rocks to weathering in the preliminary stages of survey. The map of rock resistance to weathering can be defined as a predictive zoning map that should indicate or predict the hazard of the short-term or long-term engineering interference with the rocks.

Resistance of rocks to weathering is defined as the rock's ability to withstand the destructive action of exogenous agents. This ability depends on the intrinsic parameters of the rocks (mineral composition, texture, porosity, structure, bulk properties, etc.) and on the state of disintegration and decomposition (as a consequence of previous tectonic and morphologic evolution of the rock masses, hydrothermal and other alteration processes). Both these phenomena are evaluated in the map, intrinsic parameters by means of colors and the present state of weathering by use of hatching.

The value of uniaxial compressive strength can be used as the main criterion of the rock classification to compile the maps of the resistance to weathering. This property characterizes to a certain degree the intrinsic composition of the rock as well as its disintegration. Four categories of rocks can be distinguished: 1. Rocks resistant to weathering (sound, solid rocks, with a compressive strength of more than 50 MPa). Solid rocks containing quickly-weathering minerals and leachable salts (carbonates, sulfates, etc.) are excluded from this zone. 2. Rocks moderately resistant to weathering (sound, semisolid rocks and altered rocks of the first category with a compressive strength of 15–50 MPa). Rocks susceptible to slaking and washing out do not belong to this category. 3. Rocks with low resistance to weathering (weak rocks, rocks with a high content of clay minerals, rocks containing quickly-weathering minerals and leachable salts, moderately and highly-weathered rocks of the first two categories, rocks disintegrated by tectonic and other alterations. 4. The fourth category distinguished in the maps are soils.

A range of field and laboratory tests can be used for the study of the rock weathering (e.g. Schmidt hammer test, ultrasonic pulse test, point load test, etc).

Geopotentials and geobarriers map (Fig. 5)

This map is of a synthetic and multi-purpose nature, and provides basic information about all relevant geological factors (geofactors) of the mapped area. The " geofactors", according to Matula and Ondrášik (1990), represent such geological objects and processes which can fundamentally influence (positively or negatively) the quality of the environment and its development. We can divide them into geopotentials and geobarriers. The first ones represent positive and the second ones negative aspects of the environment. It is of importance that the nature of individual geofactors can have a positive or negative impact on human activities. For example, an ore deposit represents geopotential from the industrial utilization point of view; on the other hand, it is a geobarrier in respect of foundation engineering demands (Petro et al. 1989). Taking into account the facts mentioned above, a more appropriate name for this map should be "Map of the important geofactors". If it is necessary (a

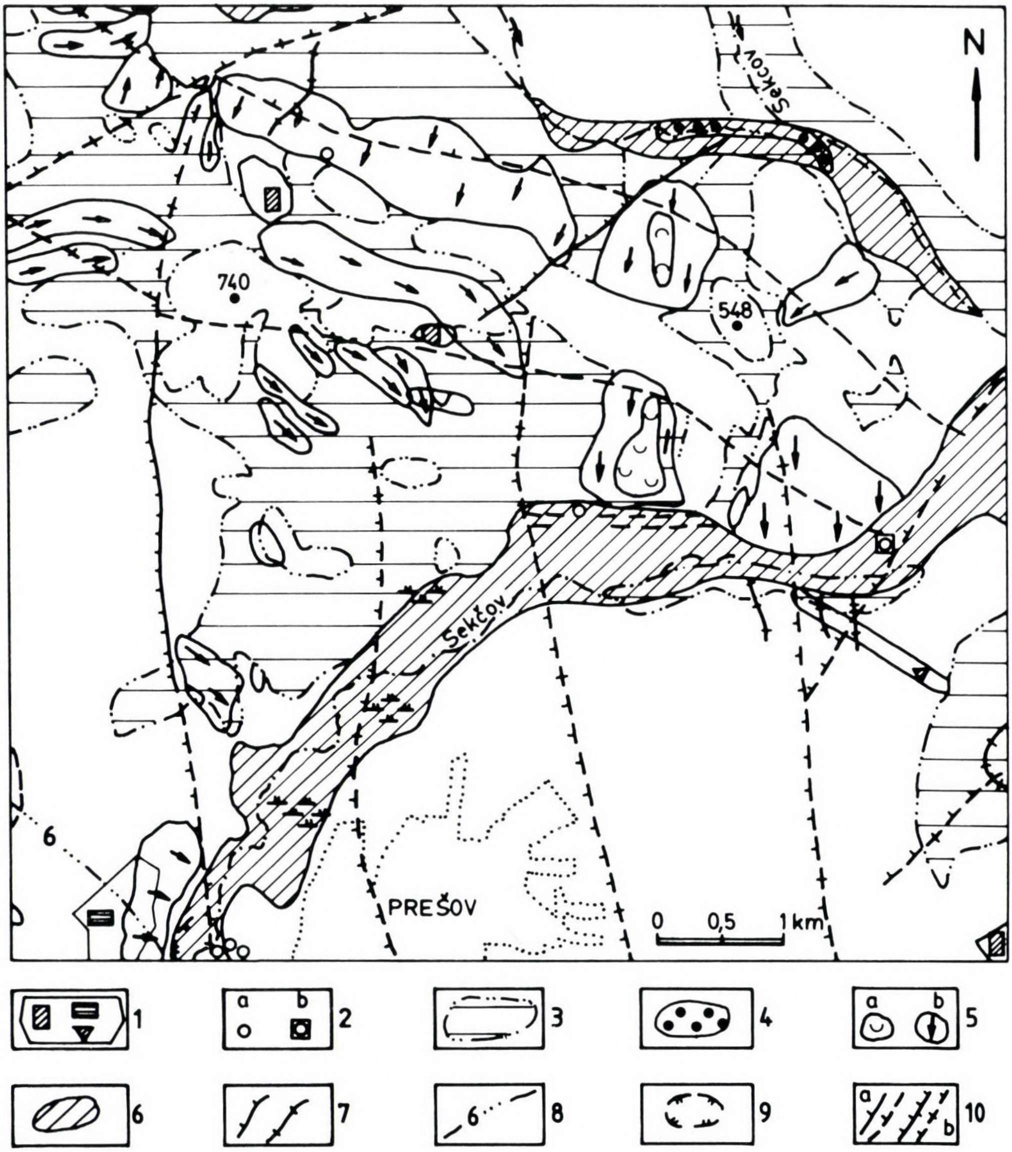

Fig. 5
Part of the geopotentials and geobarriers map from the Košická kotlina depression. (East Slovakia). 1. contours of the raw material deposites; 2. significant resource of groundwater, a. common, b. mineral; 3. areas suitable for waste disposal sites; 4. areas with most fertile agricultural soils; 5. landslides, a, active, b. potential; 6. areas with occurrence of low-bearing capacity soils; 7. guilles; 8. isoseismic lines (≥ 6°MSK); 9. flooded area; 10. tectonic failures, a. active since the late Badenian, b. active before the late Badenian)

large number of various factors), we can divide geofactors into two separate maps (e.g. "geopotential map" and "geobarrier maps"). The most suitable, for practical purposes, is to delineate the geofactors into non-coloured topographic maps of scales of 1:10 000–1:50 000.

The map of the important geofactors contains useful information (from a geological and engineering geological point of view) for land-use planning (e.g. various stages of planning documents, for selection of residential or industrial sites, waste disposal sites, etc.). Information about the geofactors can be extracted from various types of geological, hydrogeological, engineering geological or other maps or from the various geological databases (e.g. register of slope deformations, raw materials, etc.).

The 12 geofactors below are distinguished using colored symbols (areas, lines and point symbols).

1. Raw material deposits – all the important minerals inside the deposit contours and important resources of groundwater (common, mineral, healing, geothermal) inside the protected zones are delineated. It is possible to distinguish underground storage;

2. Geological basement suitability for waste disposal sites – areas with suitable geological or hydrogeological conditions are depicted (in accordance with the special map of this project);

3. Agricultural soil areas with the most fertile soils are delineated;

4. Slope stability is expressed by occurrence of active and potential slope deformations;

5. Foundation soil load-bearing capacity – areas with occurrence of low load-bearing capacity and highly compressive soils are depicted (e.g. weak soils, man-made sediments like communal waste, etc.).

6. Gully erosion – the most expressive (morphologically) active erosion forms (e.g. gullies, furrows) are delineated.

7. Karst-areas with frequent occurrence of subsurface and/or surface karst forms are indicated (e.g. caves, caverns, collapses, sinkholes, karrens).

8. Seismicity is expressed by isoseismic lines (5^o–9^o MSK) and earthquake epicenters (6^o MSK and more with the year of occurrence).

9. Inundation–flooded areas are delineated (e.g. 100-year or maximum recorded flood).

10. Subsidence–undermined areas with influences on surface (e.g. fissures, depressions, failures on buildings) or without them.

11. Tectonic failures - all disjunctive failures with activity (proved or assumed) since the late Badenian and/or older failures of regional importance (lineaments, nappes, reverse faults, seismoactive faults, etc.) are depicted.

12. Other geofactors – if necessary, it is possible to delineate other relevant information, e.g. collapsible soils, soils sensitive to suffusion or to volumetric changes, avalanches, aggressive groundwater, etc.

Foundation soil load-bearing capacity map (Fig. 6)

This map demonstrates the areal extent and quality of foundation soils to a depth of 1.5 m according to the classification of homogeneous stratigraphic and lithological complexes. It evaluates the foundation soils from the viewpoint of the foundation of engineering structures on flat foundations with a width up to 1.0 m and in a depth of 1.5 m, according to Czechoslovak Standard CSN 73 1001.

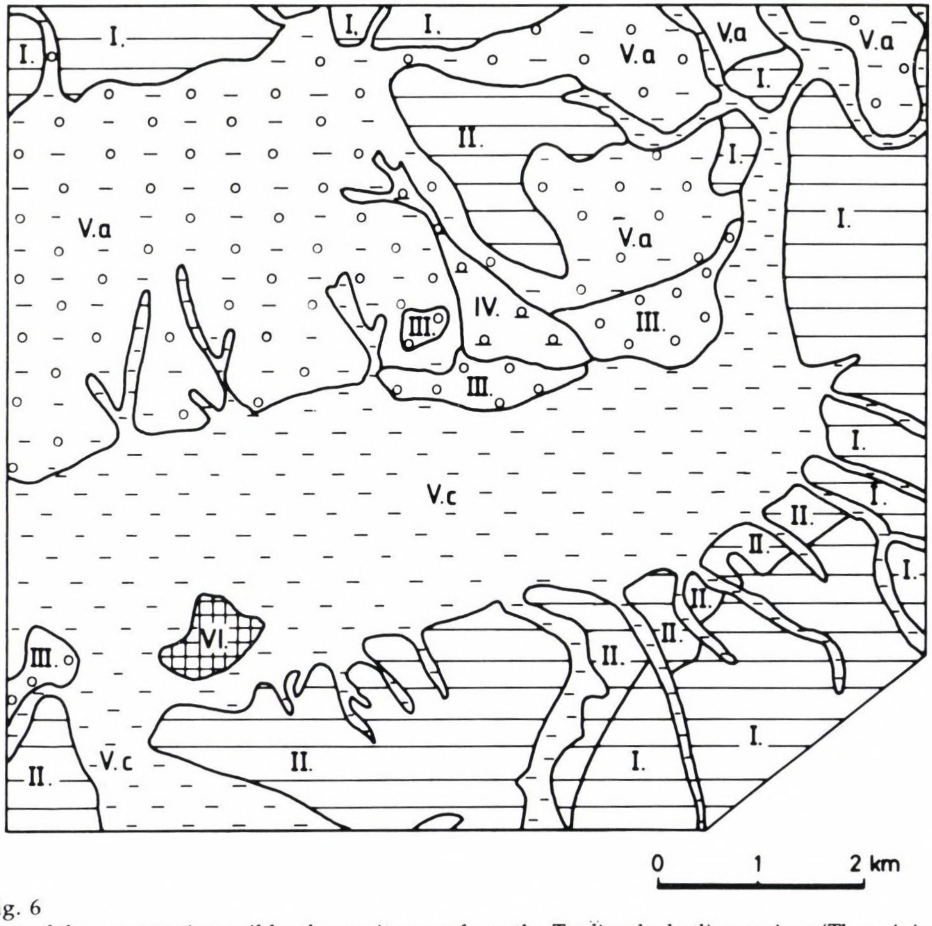

Fig. 6
Part of the construction soil load-capacity map from the Turčianska kotlina region. (The original map is in colour). I. solid rocks (c> 50 MPa), bearing capacity R_{dt} over 0.8 MPa; 2. semisolid rocks (c=1.5–50 MPa), R_{dt}=0.3–0.8 MPa; III. soils with bearing capacity R_{dt}>0.5 MPa; IV. soils with bearing capacity R_{dt}=0.3–0.5 MPa; V. soils with bearing capacity R_{dt}=0.04–0.3 MPa; VI. manmade soils R_{dt} <0.04 MPa

The methodology of creation of the map is based on assessing the geological conditions of the area, the mineralogical and petrological evaluation of rocks and on data about physical and mechanical properties of soils and solid rocks. Field and laboratory investigation and testing of rocks and soils are necessary for the preparation of this map.

Among the geotechnical characteristics of soils, the following ones are important: natural water content, bulk density and specific gravity, plastic and liquid limits, grain size composition, volume of organic and carbonate admixture, volumetric changes of soils (shrinkage and swelling), collapsibility, total shear strength, compressibility for = 0.05; 0.1; 0.2; 0.4 MPa levels.

Tests of rocks are focused on the determination of bulk density, specific gravity, porosity, compressive strength, Schmidt hammer rebound hardness and deformation modules.

The map, at a scale of 1 : 50 000, shows the areal distribution of stratigraphical and lithological complexes of rocks and soils in accordance with the geological map of the same scale, while the lithological types which can be considered to be homogeneous from the point of view of foundation engineering are conjugated. The rules for the conjugations are not strictly determined; they are dependent on the judgement of the author of the map.

Colours, hatchings and symbols are used in the maps to distinguish the types of foundation soils according to their quality.

Soils can be presented in green (R_{dt} value of the foundation soils over 500 KPa), orange (R_{dt} from 301 to 500 KPa), red (R_{dt} from 41 to 300 kPa) and black (R_{dt} value lower than 40 KPa). The lowest values are characteristic mainly for organic and man-made sediments. The black hatching is used to express the granulometric character of the lithological types (gravel, sand, clay, etc.).

Solid or semisolid rocks are distinguished by the color of the hatching. Green hatching represents foundation rocks with an R_{dt} value of 2 MPa, orange is for foundation rocks with R_{dt} from 0.8 up to 1.99 MPa, red for foundation rocks with R_{dt} 0.8 MPa, and black indicates that the foundation rocks are unsuitable for foundation engineering.

The R_{dt} value is determined as the tabular calculated load-bearing capacity of foundation soils according to the procedures defined in Czechoslovak Standard CSN 73 1001. The main criterion for R_{dt} determination for cohesive soils is the degree of consistency, for sands and gravels, compactness and for solid and semisolid rocks, the compressive strength with the spacing of discontinuities.

Area waste disposal suitability map (Fig. 7)

This map represents a special, single-purpose map. Suitability or unsuitability of the area for location of a site for waste disposal results from the evaluation of the following factors:

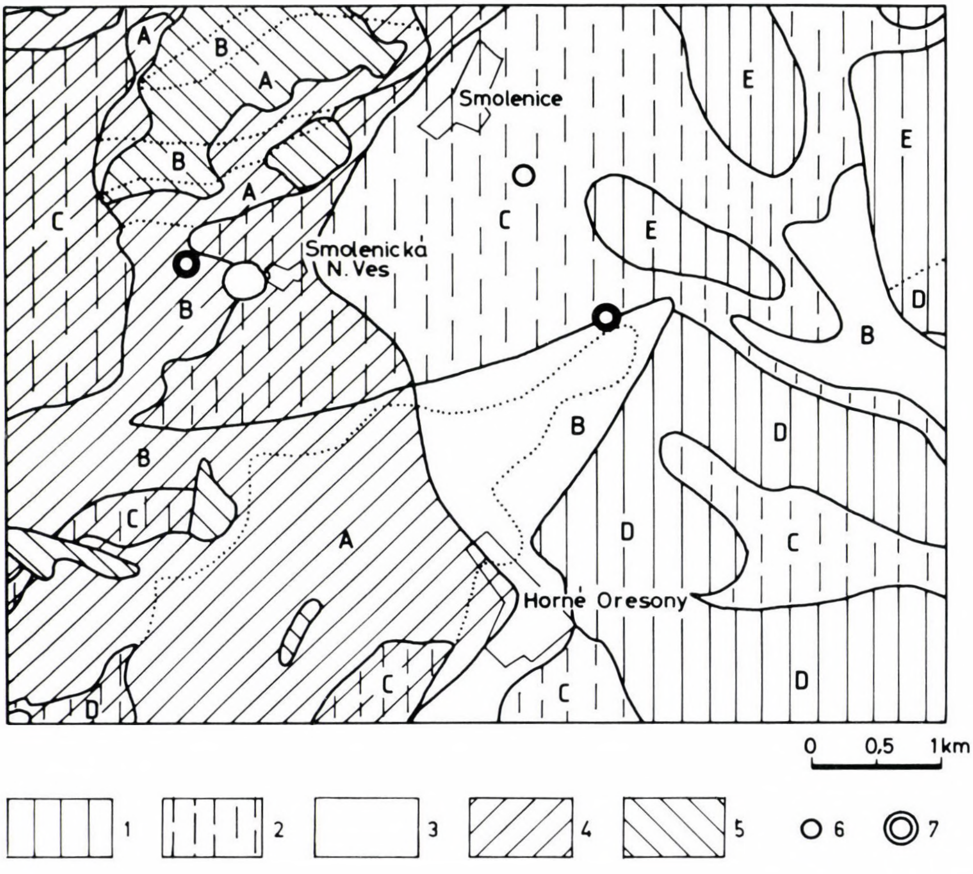

Fig. 7
Part of the area waste disposal susceptibility map from the Danube lowlands. (The original map is in colour). 1. area suitable to waste disposal; 2. area conditionally suitable to waste disposal; 3. area unsuitable to waste disposal; Degree of the protection given by legislation: 4. area limited by legislation for building up of waste disposals; 5. area excluded by legislation for building up of waste disposals; 6. small-scale area limited by legislation for building up of waste disposals; 7. small-scale area excluded by legislation for building up of waste disposals; Exposure of groundwater to danger (investments in protection of groundwater: D, E – very low, low; C – middle; A, B – very high, high

– protected groundwater areas and resources (protected zones of springs of therapeutic water, mineral and thermal water, mineral and thermal hydrogeologic boreholes, inundation areas of water reservoirs in construction, etc.),

– protected areas (national parks, nature reserves, protected gardens and parks, protected forests),

– protected zones with raw materials,

– raw material sites in use,

– geological and hydrogeological factors - (threatening of groundwater, natural geodynamic phenomena like slope deformations, gully erosion, surficial karst phenomena, collapsibility of loess, high seismicity, high level of groundwater, improper direction of the groundwater flow.

The above-mentioned factors have limiting, excluding or informative character. Some of them are governed by law: they are legislatively ordained (it is impossible to omit them). The importance of others should be evaluated by the author of the map. All of these factors are displayed in two documentation maps which are not included in the set of seven environmental maps.

Taking into account all these factors and conditions, the final map – "Area waste disposal suitability map" – shows three zones according to their suitability for establishing waste disposal sites: suitable, conditionally suitable and unsuitable. The main criterion for the zoning of the area into three zones is the presence and importance of the above-mentioned factors, e.g. an unsuitable zone represents the area with at least one of the above-mentioned excluding factors.

The final map also contains information about existing waste disposal sites. The detailed field inventory of all existing waste disposal (at the scale 1:10 000), including a circumstantial description of all relevant information (situation and material disposed of), by using the special inventory sheets is an inevitable part of the preparation of the described map.

Conclusion

This set of seven different engineering geological maps at a scale of 1:50 000 was prepared for a first group of six chosen regions of Slovakia. It is part of a set of various geological, hydrogeological, geochemical maps of the environment, and represents a rather heterogeneous conglomerate of maps.

The first one, the engineering geological zoning map, is a synthetic, multi-purpose map which represents the standard Czechoslovak map of this kind. The final map and report offers information about the geological and hydrogeological conditions, present geodynamic processes and geotechnical properties of soils and rocks. It has a broad usage not only for local authorities and builders, but for urban or environmental planners as well.

Maps 2, 3 and 4 are special maps in which the natural geodynamic phenomena (slope deformations, erosion, weathering) are presented and evaluated according to a methodology prepared specifically for this purpose. Other natural phenomena which have theoretical or economic importance can be evaluated in other regions of Slovakia (e.g. karst phenomena, collapsibility in loess, seismicity, etc.). The methodology of the compilation of the relevant maps remains to be established.

The map of geobarriers and geopotentials represents a special synthetic multipurpose map which refers to all the important geological factors of the area being studied. These factors can involve positive or negative changes of the environment. The data for this map are compiled from various geological, hydrogeological, environmental maps or geodatabases. This kind of map can be prepared fairly easily and is addressed to the same users as the engineering geological zoning map.

The last two maps (6 and 7) have a more "practical" utilization. The Rdt value of rocks and soils is used as the main criterion for the elaboration of the "Construction soil load-bearing capacity map". It demonstrates the quality of the rocks as construction ground. This map can be used by local authorities or builders as a first source of information about the area. It cannot replace a site investigation for engineering construction.

The last map of the set, the "Area waste disposal suitability map", is a single-purpose map based on the assessment of geological, hydrogeological and land-use criteria. Information about the suitability of the area for waste disposal and the location of the present landfills can be obtained from this map.

The experience gained during mapping procedures and compilation of the maps has shown the necessity of certain changes in the methodology of the preparation and elaboration of the proposed set of environmental maps. This will be the task of future work in this field.

References

Kovácik, M., V. Jánová, P. Lišcák, M. Kováciková, I. Modlitba, M. Ondrášik1991: Mapa geofaktorov zivotného prostredia Turcianskej kotliny. – Unpublished report. GÙDŠ Bratislava, 1991.

Petro, L. et al. 1989: Metodické pokyny pre zostavovanie máp geologickch faktorov životného prostredia. – Unpublished report. GÙDŠ Bratislava, 1989.

CSN 73 1001: Základová puda pod plošnými základy. Vyd. ùNM Praha, 1987.

Acta Geologica Hungarica Vol. 37/1–2, pp. 135–151 (1993)

The itinerary of the Transdanubian Central Range: An assessment of relevant paleomagnetic observations

Emő Márton
Eötvös Loránd Geophysical Institute of Hungary

Paleomagnetic data require to subdivide the Mesozoic–Cenozoic displacement history of the Transdanubian Central Range into three main periods. During the first, the Transdanubian Central Range must have moved in close coordination with Africa; the second period (Paleogene early–mid Miocene) is characterized by displacements independent of both Africa and stable Europe; finally, the Transdanubian Central Range welded to stable Europe. This paper deals with the first two periods, paying special attention to the problem of how paleomegnetic data may constrain "escape models" that envisage the Transdanubian Central Range as moving from the southern neighbourhood of the Northern Calcareous Alps into its present position.

As paleomagnetic observations suggest, the Transdanubian Central Range collided with stable Europe in the late Senonian. After the collision it moved to the south with respect to both large plates. In the course of this "escape" the Transdanubian Central Range could have become juxtaposed with the Gemer-Bükk unit. In the Karpatian during a second "escape", the Transdanubian Central Range as part of the North Pannonian unit shifted to its present position.

In relation to tectonic escape models, the second paleomagnetically indicated "esccape" involves an additional movement, a combination of northward shift accompanied by counterclockwise rotation. The implication is that if the Transdanubian Central Range started its last tectonic escape from the area south of the Eastern Alps, it was brought there after the Paleogene. As the different characters of the Cretaceous segments of apparent polar wander curves for the Transdanubian Central Range and the Northern Calcareous Alps indicate, the two tectonic units moved differently even before the Paleogene.

Contrary to the paleomagnetic incompatibility of the Transdanubian Central Range and the Northern Calcareous Alps, there is no such problem between the former and the Southern Alps.

Key words: Transdanubian Central Range, origin, escape, paleomagnetism

Location of the Transdanubian Central Range in pre-Cenozoic times

The first paleomagnetic results obtained from the Mesozoic of the Transdanubian Central Range were interpreted (Márton and Márton 1978, 1981) as conforming with a southern Tethyan origin (Géczy 1973) of the area. Soon, paleomagnetic evidence was capable to demonstrate, independently of any other consideration, that the Transdanubian Central Range was indeed part of the African plate during the Mesozoic opening of the Tethys (Márton and Márton 1983). The same paleomagnetic results had further tectonic implications, namely that the Transdanubian Central Range must have 1. separated from

Address: E. Márton: H–1145 Budapest, Columbus u. 17–23, Hungary
Received: 12 May, 1992

0236–5278/94/$ 4.00

Africa during the Cenozoic, 2. reached its present position by a counter-clockwise rotation of 30–35°, 3. moved in coordination with the "Adriatic microplate".

Márton and Márton (1982) attempted to restore the position of the Transdanubian Central Range (and along with it the whole area defined later as North Pannonian Unit) as part of the "Adriatic microplate" prior to the Cenozoic rotation with respect to Africa (Fig. 1). The reconstruction relied on an averaged Apparent Polar Wander curve, characterizing the overall movement of the Adriatic microplate, and assumed that the net Cenozoic rotation of 30–35° signified a single rotation of post-Paleogene age.

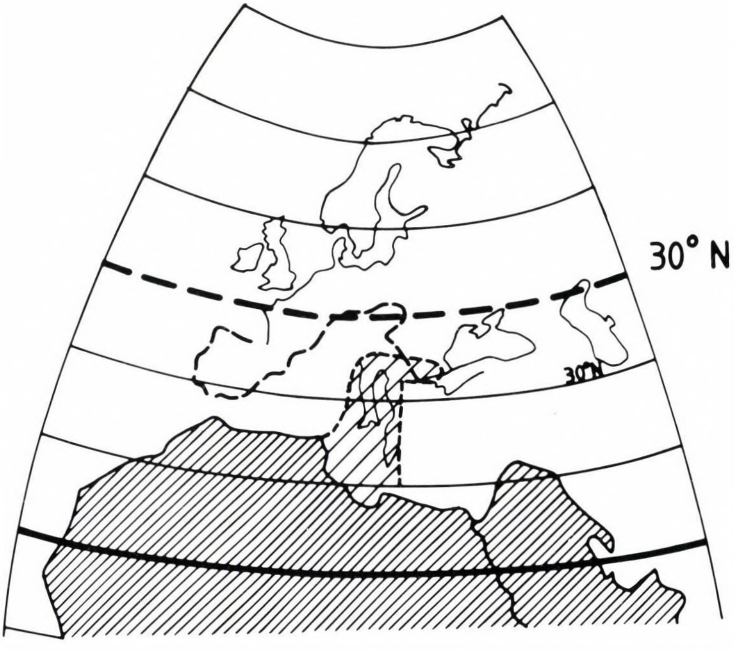

Fig. 1
Reconstructed position at 80 Ma of the "Adriatic microplate" sensu lato (shaded area). The dimensions of the Adriatic microplate were taken from Vanden Berg (1979) and the area, later coined as North Pannonian Unit (Balla 1984) added

While the angle was based on measurements, the pole of rotation (lat. 40°, lon. 18°) was arbitrarily selected, since its exact location (as long as it remained within the area) was not critical from the viewpoint of bringing the "Adriatic" and African polar wander patterns into coincidence. After having corrected for the Cenozoic rotation, and keeping the Transdanubian Central Range in rigid connection with Africa, the position of the Transdanubian Central Range was reconstructed for three time points: 80, 120, 170 Ma, respectively. According to this reconstruction, the North Pannonian Unit shifted, relative to its present location at the margin of stable Europe, in the following way: at 170 Ma it was far to the west. Then, as the relative positions of Africa and stable Europe changed (suggested by plate tectonic reconstructions), the North Pannonian unit shifted to the South-East with respect to the same margin. After 80 Ma, the movement of the African plate became north-westerly directed (Savostin et al. 1986). This, in combination with a counterclockwise rotation independent from Africa, could have brought the Transdanubian Central Range to its present position.

To account for the overlap between the North Pannonian unit and the Moesian Platform, Márton and Márton (1982) suggested that the latter was emplaced after the counterclockwise rotation of the "Adriatic microplate". In view of later developments of tectonic ideas, an alternative solution is to change the geometry of the "Adriatic microplate", e.g. by reconstructing the pre-escape position of the North Pannonian Unit (e.g. Kázmér 1984; Kázmér and Kovács 1985; Balla 1988; Ratschbacher et al. 1989; Csontos et al. 1992). In this case, however, we have to distribute the Cenozoic net rotation of the Transdanubian Central Range between a displacement coordinated with the "Adriatic microplate" and other movements. The reason why we cannot perform it entirely by escape from the area between the Eastern and Southern Alps, as suggested by Balla (1988), or by in situ block rotations, is that paleoinclinations require the creation, together with the counterclockwise rotation, of about 4° difference in latitude between the Transdanubian Central Range and e.g. the Umbrian Apennines (Fig. 2).

Tari (1991) estimated the possible magnitude of in situ rotations in the Transdanubian Central Range and concluded that about 15° counterclockwise declination deviation may be attributed to this mechanism. His estimation is close to the value that may be derived by comparing declinations of different areas of the Central Mediterranean region exhibiting CCW declination rotation with respect to both Africa and stable Europe. For instance, between the Transdanubian Central Range and the Umbrian Apennines the difference is 12° on average, i.e. the former is more rotated to the W (Table 1). With respect to the "autochthonous" region of the "Adriatic microplate", the angle is somewhat larger: if the angle .calculated by Lowrie (1986) for the relative rotation between the "Adriatic autochthonous" and the Umbrian Apennines, is accepted, the rotation angle for the Transdanubian Central Range with respect to the "Adriatic autochthonous" will be about 20°.

Table 1
Differences in declination between the Transdanubian Central Range and the Umbrian Apennines. Declinations recalculated for a common point, lat. 47.5°, long. 17.5°

Late Senonian	12 ° W
Albian	7 ° W
Aptian	20 ° W
Neocomian	10 ° W
average	12 ° W

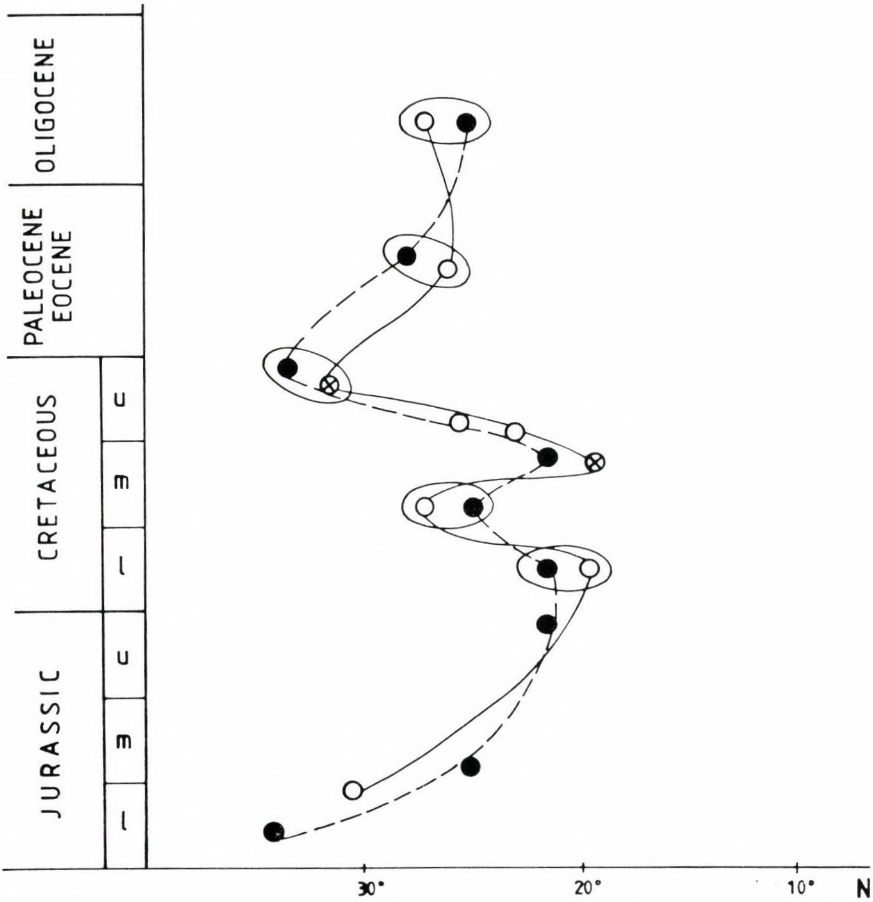

Fig. 2
Paleolatitudes calculated for the Transdanubian Central Range (full circles) and the Umbrian Apennines (hollow circles) from measured inclinations. Jurassic through Paleogene latitudes do not show systematic differences. Data compiled by Márton (1990) with the addition of data on Eocene bauxites and hanging walls (Márton 1990) and Oligocene for the Esztergom area (Márton et al. 1992)

Timing and character of Cenozoic movements

The angle of Cenozoic net rotation of the Transdanubian Central Range with respect to Africa was first derived indirectly, from Mesozoic paleomagnetic data (Márton and Márton, 1981, 1983). When the Cenozoic itself yielded paleomagnetic results from the Transdanubian Central Range, and also from the Gemer-Bükk unit, complications appeared. Some were connected to counterclockwise rotations in excess of 35°, others to latitude relations.

Concerning latitudes, the problem is that paleomagnetic inclinations measured on Paleogene and early Miocene rocks are systematically lower then expected inclinations either in the African or stable European framework (Fig. 3). This feature, which is not unique to the Transdanubian Central Range (Márton 1988), implies that the "Adriatic microplate" shifted to the south after the late Cretaceous with respect to both large plates.

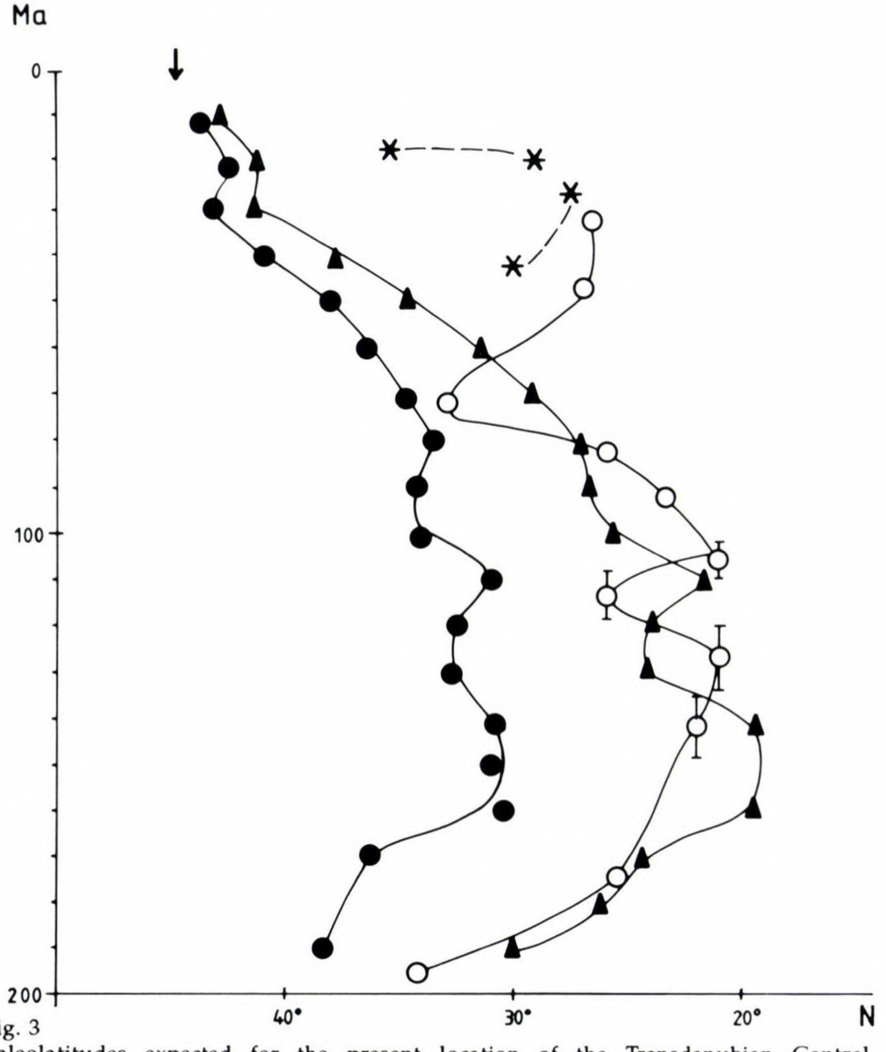

Fig. 3
Paleolatitudes expected for the present location of the Transdanubian Central Range (represented by lat. 47.5° long. 17.5°) in stable European (dots) and African (triangles) framework. Apparent Polar Wander curves defined for the large plates by Besse and Courtillot (1991) served as basis for the calculations. They are compared with paleolatitudes derived from measured inclinations for the Transdanubian Central Range + Umbrian Apennines (circles average of Fig. 3) and Northeast Hungary (asterisks). Error bar on the age is defined by differences between scales by Odin (1982) and by Berggren et al. (1985)

Counterclockwise rotations in excess of 35° (with respect to Africa) were measured in the Transdanubian Central Range as well as in the Gemer-Bükk unit (Fig. 4). However, their timing is different. In the Transdanubian Central Range they were observed on Eocene bauxites and non-marine hanging walls (Fig. 5), but rocks in higher stratigraphic position exhibited not more than 35° (Márton 1990).

In contrast, excess CCW rotation characterizes all pre-Ottnangian sediments in the Gemer-Bükk unit and the volcanic horizon equivalent to the lower ignimbrite at the South Margin of the Bükk. Ottnangian sediments and Karpatian volcanics are characterized by about 30° (Márton and Márton 1991). From these observations, it follows that the North Pannonian unit cannot be treated as a rigid unit throughout the whole Cenozoic.

Paleomagnetic data to date suggest that the difference between the Transdanubian Central Range and the Gemer-Bükk unit is profound: on the one hand, the timing of the excess Cenozoic counterclockwise rotation seems to be different in the two areas; on the other, the Transdanubian Central Range exhibits not only counterclockwise but also clockwise rotation (both within the Eocene!). It may be argued that the differences are simply due to the lack of observations in one or in the other of the areas in the critical intervals (Fig. 5). Indeed, we cannot exclude the possibility that the Gemer-Bükk unit shared the Eocene rotations of the Transdanubian Central Range (the theory is impossible to test for lack of rocks of suitable ages in the Gemer-Bükk unit!), thus eliminating one of the differences by speculation. However, by assuming that the post-Eocene CCW rotations of the Transdanubian Central Range and the Gemer-Bükk unit were the same, we also imply that the former must have rotated in the CW sense after the early–mid Miocene. This is necessary, since the angle we observe on late Eocene–Oligocene in the Transdanubian Central Range is not more than 35°. The conclusion is, therefore, that existing data suffice to prove the basic difference between the Cenozoic movements of the Transdanubian Central Range and the Gemer-Bükk unit.

Escape models in the light of paleomagnetic observations

Escape of continental fragments during continent-continent collision and/or gravity sliding of the North Pannonian Unit from above the Penninicum, seems to account for a large number of the present day geologic features of the Carpathians and the Intra Carpathian basins.

It is generally agreed that the North Pannonian Unit, before the escape, was situated at the northern tip of the African indenter (Adriatic microplate), i.e.

Fig. 4 →
Paleomagnetic sampling localities (asterisk) where excess counterclockwise rotation was observed compared to the angle expected in an African framework for the respective ages plus + 35°. Base map modified after Balla (1988). Note that in Northeast the observations are not confined to one tectonic unit, neither are they connected to tectonic lines

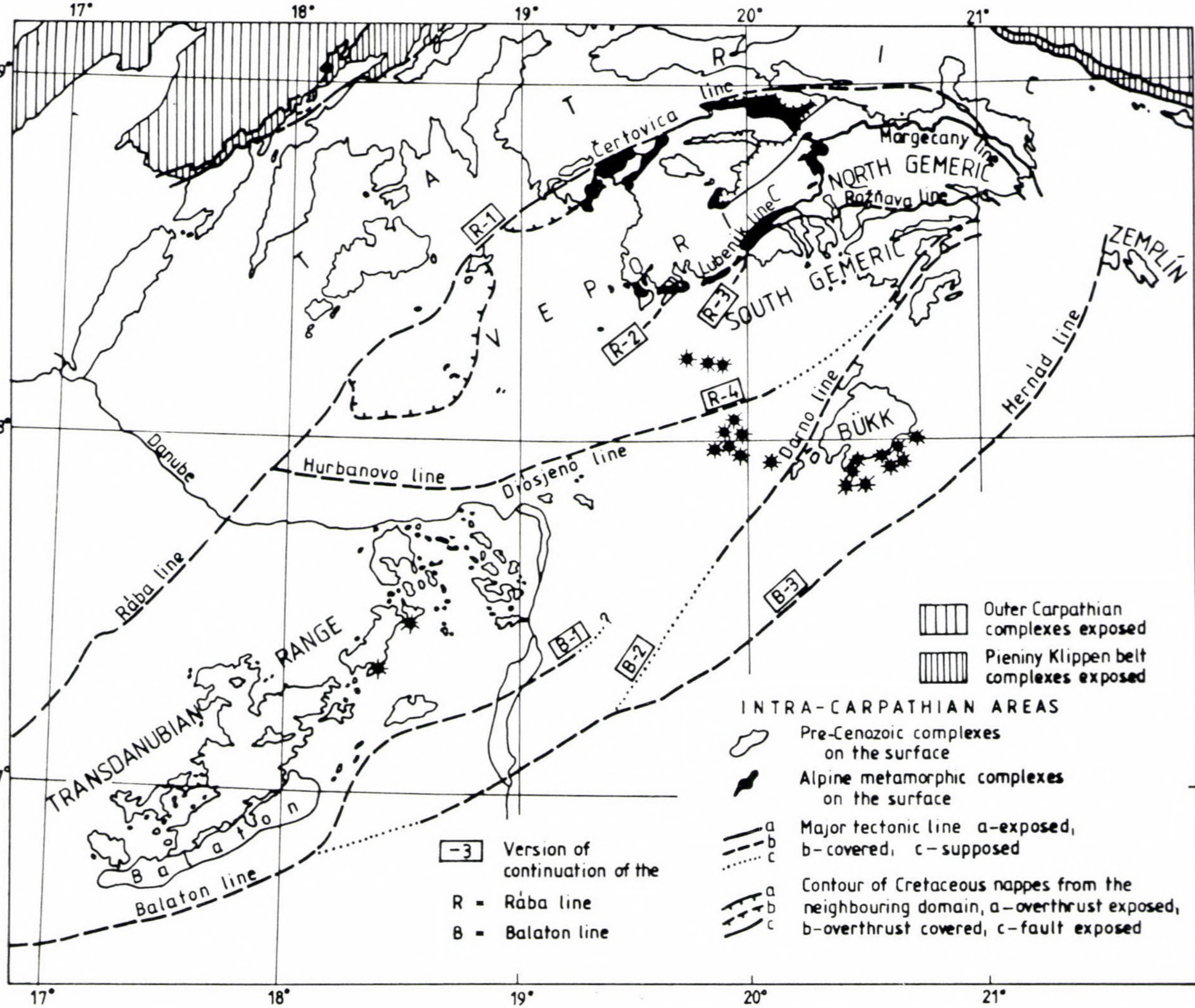
17°
18°
19°
20°
21°
49°
48°
47°
R
I
C
T
A
T
A
P
Čertovica line
Margecany line
NORTH GEMERIC
Rožňava line
Lubeník lineC
SOUTH GEMERIC
V
E
P
O
R
I
ZEMPLÍN
R-1
R-2
R-3
R-4
Darno line
Hernád line
BÜKK
Hurbanovo line
Diósjenő line
Danube
Rába line
TRANSDANUBIAN RANGE
B-1
B-2
B-3
Balaton
Balaton line
Outer Carpathian complexes exposed
Pieniny Klippen belt complexes exposed
INTRA-CARPATHIAN AREAS
Pre-Cenozoic complexes on the surface
Alpine metamorphic complexes on the surface
Major tectonic line a-exposed, b-covered, c-supposed
Contour of Cretaceous nappes from the neighbouring domain, a-overthrust exposed, b-overthrust covered, c-fault exposed
-3 Version of continuation of the
R = Rába line
B = Balaton line

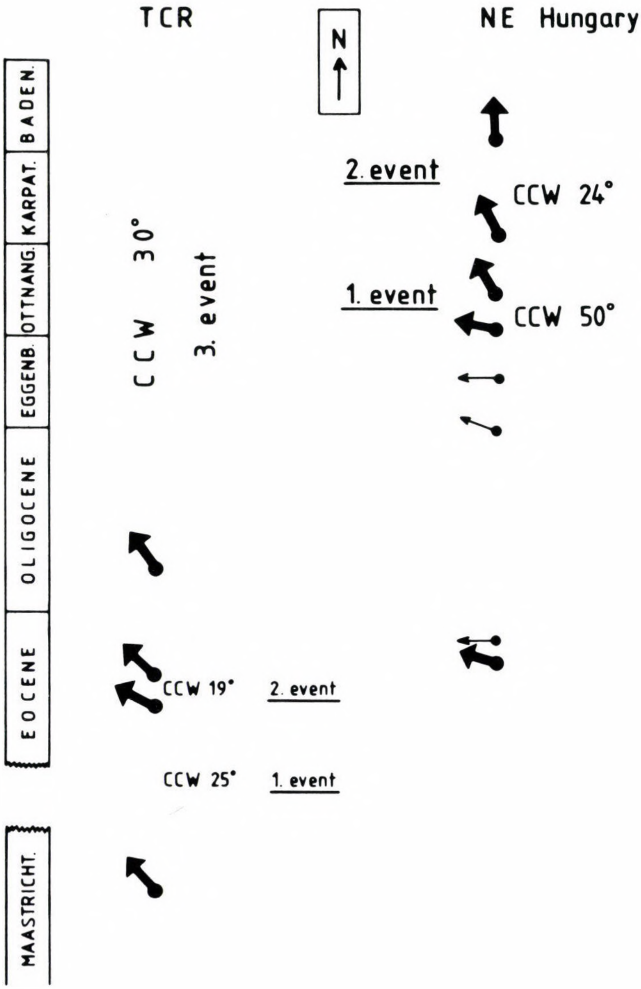

Fig. 5
Declination deviation (arrows) with respect to the present North in the Transdanubian Central Range and Northeast Hungary. It must be remembered that Cenozoic rotations with respect to both Africa and Europe are larger than with respect to the present North. Rotations which are not conform with those of Africa or stable Europe are called events and indicated by sense and angle of rotation. Solid arrows: directions based on a number of sites and localities and often different rock types; light arrows: directions based on one locality

north of the Southern Alps, and south of the Northern Calcareous Alps, in the vicinity of the Bohemian Massif. Opinions differ, however, on the matter of commencement and termination of the eastward movement. Concerning the beginning, it is regarded as late Eocene by some (e.g. Balla 1988; Fodor et al. 1992) or late Oligocene by others (e.g. Ratschbacher et al. 1989). To some, the escape ended with the Paleogene (e.g. Kázmér 1984; Kázmér and Kovács 1985;

Balla 1988), to others in the early Miocene (Ratschbacher et al. 1989; Csontos et al. 1992). Arguments to support the different views are mostly based on stratigraphy and/or tectonics.

The relevance of paleomagnetic observations to escape models of the Alpine-Carpathian Pannonian region is twofold: both the reconstructed pre-escape position and the escape itself may be tested against them.

The escaping North Pannonian Unit

As was already discussed, the Cenozoic declination patterns of the Transdanubian Central Range and the Gemer-Bükk unit are different (Fig. 5). Nevertheless, the last phase of rotation in both areas is manifested in about 30° declination deviation to the west. The age is well constrained in the Gemer-Bükk unit (Karpatian), while for the Transdanubian Central Range it may be placed anywhere between 30 and 6Ma (limited by radiometric ages of the andesite volcanism in the Velence Hills and that of the basalt volcanism in the Balaton Highlands: Balogh pers. comm. and Balogh et al. 1982).

In interpreting the Cenozoic observations in the frame of escape we may follow different lines of reasoning. However, paleomagnetic data do not allow much freedom in the Paleogene. What they suggests is an important event during the Eocene in the Transdanubian Central Range, granted that the age of bauxites at Gánt and Csordakút is indeed Eocene (e.g. Dunkl 1990). The event is seen as a hairpin on the Apparent Polar Wander curve, due to a fast clockwise rotation followed by an equally fast counterclockwise rotation (Fig. 5). Immediately before, during and after these rotations the Transdanubian Central Range must have been at much lower latitudes (as indicated by inclinations) than the southern margin of stable Europe. Earlier, the return of the Transdanubian Central Range to lower latitudes after the Senonian (Fig. 2) was interpreted as evidence for a double collision with Europe, and the Transdanubian Central Range was not separated from Africa during the first (Márton 1988). In the light of intra-Eocene rotations, the shift to the south may be interpreted as indicative of escape during the late Cretaceous collision of Africa and stable Europe. Nevertheless, this escape could not keep the Transdanubian Central Range in the vicinity of stable Europe (low paleolatitudes). On the other hand, by this escape the Transdanubian Central Range could become juxtaposed in the Eocene with the Gemer-Bükk unit, not by a movement to the northwest of the Transdanubian Central Range (e.g. Haas et al. 1990) but just the opposite, by a southeastward shift (Fig. 3). If we assume that the Transdanubian Central Range and the Gemer-Bükk unit moved in coordination from this time on, we can see them, after a couple of ten million years, as meeting stable Europe in a movement which is the combination of northward shift and counterclockwise rotation. During this movement a second escape may have taken place (in the Karpatian); this time possibly from between the Southern and Eastern Alps. This model implies that the first event in the

Gemer-Bükk unit correlates with the third one in the Transdanubian Central Range (Fig. 5). The larger angle in the Gemer-Bükk unit may be due to an additional "escape" of the Gemer-Bükk unit with respect to the Transdanubian Central Range (Csontos et al. 1992). The second rotation event in the Gemer-Bükk unit may be connected to an extensional regime during the thrust of the Outer Carpathian nappes (Csontos et al. 1992).

Alternatively, the Transdanubian Central Range and the Gemer-Bükk unit may have become juxtaposed in the Miocene, after the first rotation event of the Gemer-Bükk unit and could have undergone together a microplate-like rotation plus escape in the Karpatian (late Ottnangian). This latter solution better satisfies paleomagnetic constraints, since shallower than present inclinations were also measured on Ottnangian sediments (Fig. 3).

Paleomagnetic test for the pre-escape position

Kázmér and Kovács (1985) restored the Transdanubian Central Range to its pre-escape position by matching late Permian through late Cretaceous facies zones of the Northern Calcareous Alps, the Transdanubian Central Range and the Southern Alps. According to these authors, the intra-Alpine position of the Transdanubian Central Range corresponded to the place of the Drauzug, since they were able to fit North and South Alpine facies zones across that of the Transdanubian Central Range, replaced in the Drauzug. Balla (1988), treating paleomagnetic data in a peculiar way, argued that paleomagnetic observations also supported such a reconstruction.

An essential feature of most escape models is that, with very few exceptions (e.g. Haas 1987), they preserve the relative positions of the Northern Calcareous Alps, the Transdanubian Central Range and the Southern Alps throughout the Mesozoic. They also insist that the escape was initiated in the Eocene by a squeeze between stable Europe and the African indenter with the Southern Alps on its northern tip.

Reconstructions place the Transdanubian Central Range to match the eastern part of the Southern Alps. From a paleomagnetic point of view the most important feature of the eastern Southern Alps is that declination rotations here roughly correspond to what is expected in an African framework. In other words, there is no direct indication for relative rotation of the Southern Alps with respect to Africa (e.g. Vanden Berg and Wonders 1976; Lowrie 1986). This coincidence with "African" directions, however, cannot be regarded as proof for rigid contact with Africa.

The main reason is that the "autochthon" of the Adriatic region (and less widely recognized, the Southern Alps, West of the Iudicaria line) exhibits signs of Cenozoic relative rotation with respect to Africa, in the counterclockwise sense (Márton and Veljovič, 1987; Vanden Berg 1983; Márton and Nardi 1991). For lack of reliable constraints from the eastern Southern Alps, different opinions were expressed about the situation. Vanden Berg and Zijderveld (1982) suggested that the Southern Alps participated in a counterclockwise rotation with respect to Africa, together with the "Adriatic microplate", in the early Miocene, but the rotation of the Southern Alps was 15° instead of 30°; another 15° of the clockwise deviation of the Southern Alps with respect to the "Adriatic backbone" is due to a late Cretaceous lag. The latter statement is not really supported by data (Table 2), since the rotation during late Cretaceous (Se_2 – Alb) is similar for the Southern Alps, Umbrian Apennines and the Transdanubian Central Range, while there is a more expressed difference for the early Cretaceous (Alb – Ti). Heller et al. (1989), searching for a more plausible solution, sacrificed the autochthony of the core of the "Adriatic microplate" for that of the Southern Alps, thus implicitly returning to the concept of an Adriatic promontory in an unchanged position with respect to Africa.

Table 2
Comparison between paleomagnetic data for the Southern Alps (SA), Umbrian Apennines (UA) and Transdanubian Central Range (TCR). All data referred to a common point lat. 47.5 ° long. 17.5 °

Differences in declination	Se_2–Ti	Se_2–Ce, Tu	Se_2–Alb	Se_2–Apt	Alb–Ti
SA	35°	15°	15o	–	20°
UA		24°	23o	26°	–
TCR	53°	–	18o	28°	35°
Max difference between areas	18°	9o	8°	2°	15°

Expected paleolatitudes	Se_2	Ce–Tu	Alb	Apt	Neocomian	Ti
SA	24.2	22.0	21.6	21.4*		18.6
UA	31.6	21.8	19.4	27.0	18.5	–
TCR	34.2	–	21.8	27.7	21.6	21.3

Symbols: Se_2 – late Senonian; Ce – Cenomanian; Tu – Turonian; Alb – Albian; Apt – Aptian; Ti – Tithonian; * – Barr–Apt average

In the context of available information for Cenozoic rotations in the Alpine and Adriatic realms, Márton (1990) interpreted the Eastern part of the Southern Alps as participating in a Miocene counterclockwise rotation with respect to Africa and tentatively suggested that the area rotated clockwise before, most likely in the Eocene (this may be imagined as occurring in coordination with the Transdanubian Central Range).

Except for the solution by Heller et al. (1989), which has no support by data, the eastern Southern Alps is conceived as rotating in the late Cretaceous or in the Cenozoic, independently of both stable Europe and Africa. This, in combination with the similar late Jurassic–late Cretaceous declination patterns and similar paleolatitudes of the Transdanubian Central Range and the eastern Southern Alps (Table 2), permits joining the Transdanubian Central Range with the eastern Southern Alps (and the Umbrian Apennines) throughout the Mesozoic. However, the orientation (with respect to stable Europe) of the eastern Southern Alps at the time of a Cenozoic escape must have been different from the present situation.

The relationship of the Transdanubian Central Range to the Northern Calcareous Alps is more problematic than to the Southern Alps. Late Senonian-Danian in the Northern Calcareous Alps exhibits (in average) declination close to that of stable Europe, indicating that the Northern Calcareous Alps must have been already emplaced at the south margin of stable Europe by the Cenozoic. Thus the Cenozoic counterclockwise rotation of the Transdanubian Central Range in relation to the Northern Calcareous Alps, agrees with escape models. However, the pre-late Cretaceous paleomagnetic data from the Transdanubian Central Range and the Northern Calcareous Alps cannot be easily reconciled.

From the western part of the Northern Calcareous Alps (west of the western end of the Tauern window), the available observations (Permian–Triassic, see Mauritsch and Becke 1987) indicate counterclockwise rotations; Early-mid–Jurassic (Triassic), east of the western end of the Tauern window, however, was found to behave differently (Mauritsch and Frisch 1980). Large clockwise declination rotations were measured in the Osterhorn nappe units, which were interpreted by the authors of the data as characteristic of the whole eastern Northern Calcareous Alps. Such an interpretation was supported by subsequent studies (Heer 1982; Channell et al. 1991). Based on the enormous differential rotation, Mauritsch and Becke (1985) suggested that the Northern Calcareous Alps was V shaped originally and became East–West trending as a result of bending, i.e. counterclockwise rotation in the West, clockwise rotation in the East. Other views of the situation included the suggestion that the Northern Calcareous Alps belonged to the Northern shelf of the Tethys (Vanden Berg and Zijderveld 1982) and alternatively, that the eastern Northern Calcareous Alps was emplaced before other units of southern Tethyan origin (Márton 1987).

Without reference to the model by Mauritsch and Becke (1985), Balla (1988) revived the bending model for the Northern Calcareous Alps, arguing that the Transdanubian Central Range (paleomagnetic data and structural trends combined) is a perfect match for the Northern Calcareous Alps in its bending pattern.

The author of the present paper thought that, given the geological circumstances, there are two crucial problems that may be addressed with paleomagnetic methods in connection with the Eastern Alps and its relation to the Transdanubian Central Range. One is the search for the late Jurassic–early Cretaceous segment of the Apparent Polar Wander curve (as it was done for the Tisza unit: Márton in press a); the second is a systematic check on the "bending" in the Transdanubian Central Range.

Concerning the second, studies are in progress on late Triassic carbonate platform sediments (Márton 1992), since they are widespread in the

Transdanubian Central Range and also very precisely correlatable. Both properties are very important, for only systematic differences observed on strictly coeval rocks may convincingly show the lack or presence of bending deformation.

In the matter of the late Jurassic–early Cretaceous Apparent Polar Wander curve for the Northern Calcareous Alps, the first results (Table 3) of a joint project between ELGI and the University of Leoben suggest that the Transdanubian Central Range and the Northern Calcareous Alps could not belong together during the late Jurassic–Cretaceous (Fig. 6).

Table 3
Paleomagnetic directions for late Jurassic–early Cretaceous from the Northern Calcareous Alps (area of Salzburg)

	N	D^o D_c^o	I^o I_c^o	k	$\alpha^o{}_{95}$
Lower Rossfeld beds, late Valanginian–early Hauterivian (tectonically corrected directions only) beds are subhorizontal!					
Results by Heer (1982)	10	112	69	119	4
AF cleaning only!	8	58	52	26	11
	8	77	78	27	11
	7	74	41	15	16
Preliminary results by Márton and Mauritsch	2	77	46	–	–
Stepwise thermal cleaning pilot samples	4	65	54	46	14
overall mean	6*	74	58	24	14
Osternhorn group, Oberalm beds, Kimmeridgean–Tithonian					
preliminary data by	3	80	27	33	22
Márton and Mauritsch		85	35		
stepwise thermal demagnetization	3	64	46	536	5
pilot samples		60	40		
	3	235	80	62	16
		61	30		
overall mean					
before tectonic correction	3*	75	57	5	65
after tectonic correction	3*	69	36	42	19

Symbols: N – number of independently oriented cores (sites*); D, I and D_c, I_c – declination, inclination before and after tectonic correction; k and $\alpha^o{}_{95}$ statistical parameters (Fisher 1953)

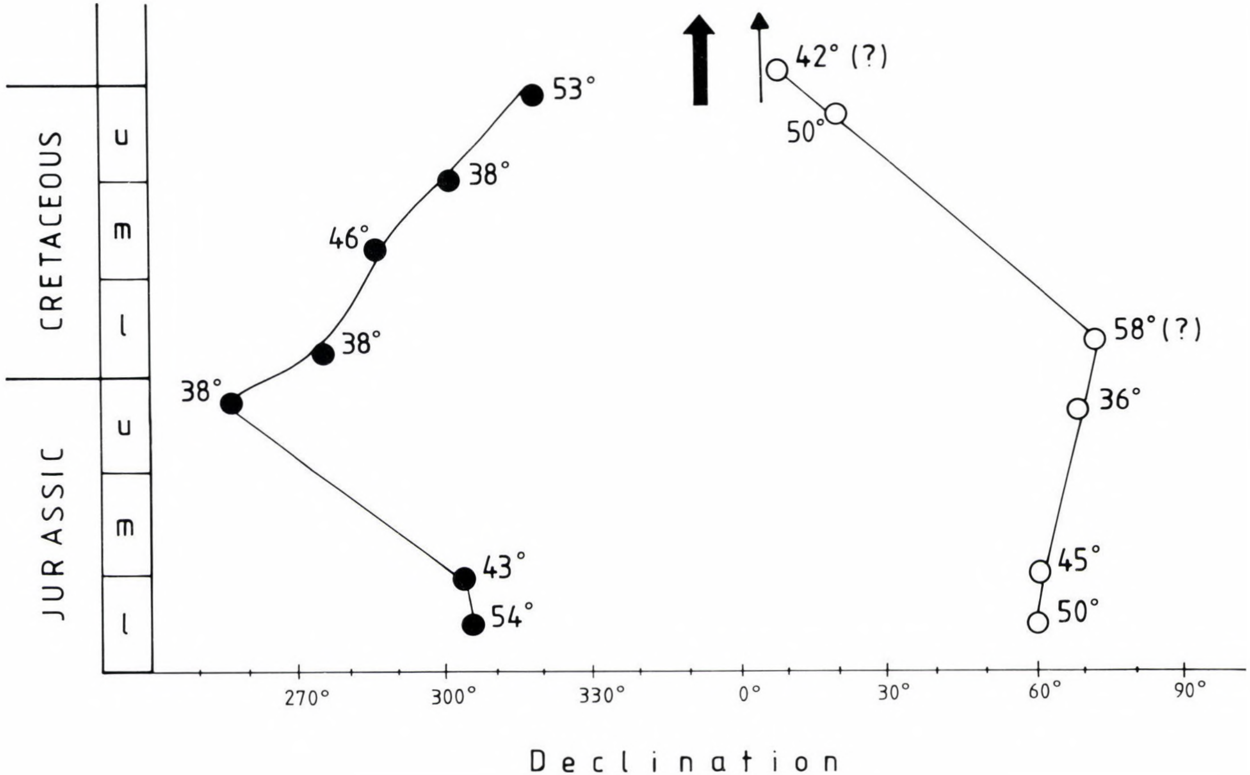

Fig. 6
Jurassic–Cretaceous declinations observed for the Northern Calcareous Alps (hollow circles) and the Transdanubian Central Range (full circles). Respective paleomagnetic inclinations are indicated by numbers. Data as compiled by Márton (1990) with addition of data in Table 3 and Table 4. Expected declinations in stable European and African frameworks, respectively, are shown by light and heavy arrows. Question marks indicate suspected error in inclination

Table 4
Paleomagnetic directions for early–mid Jurassic from the Northern Calcareous Alps

	D°	I°	k	α_{95}
Osternhorn (Lias–Dogger), Mauritsch and Frisch (1988)	62	45	29	11
Early Jurassic, Adnetkalk, Heer (1982), different nappes in the NCA average of 20 sites	57	42	13	9
Liassic average of 17 sites between 12°E and 16°E, Channell et al. (1991)	60	58	18	8

Conclusions

Within the resolution of the African Apparent Polar Wander curve, paleomagnetic observations connect the Transdanubian Central Range to the African plate during the Mesozoic. On the present evidence, it is not possible to reconstruct the exact location of the Transdanubian Central Range at the Southern Tethyan margin, since the displacements of the area must have been complicated during the Cenozoic. The intra-Eocene rotations of the Transdanubian Central Range, combined with a marked shift to the south with respect to both stable Europe and Africa, can be interpreted as an escape from the collision zone of the large plates.

During the Mesozoic, the Transdanubian Central Range could have moved with the Southern Alps, but from the beginning of the opening of the Atlantic, the character of the movements of the Northern Calcareous Alps were different from that of the Transdanubian Central Range. The lack of net overall rotation of the Northern Calcareous Alps with respect to stable Europe in the Cenozoic, as opposed to the mobility of the Transdanubian Central Range, imply that the separation of the Northern Calcareous Alps and the Transdanubian Central Range continued. In addition to the Eocene "escape" of the Transdanubian Central Range, the area suffered counterclockwise rotation after 30 Ma, which may be resolved into two components: one accompanying a microplate-like movement, the second an escape (and/or in situ block rotations). In the context of Cenozoic paleomagnetic data from the Gemer-Bükk unit this escape must be of Ottnangian (Karpatian) age.

Acknowledgement

This work was partially supported by the National Scientific Research Fund (OTKA grant Nos 2671 and 3023).

References

Balla, Z. 1984: The Carpathian loop and the Pannonian basin: A kinematic analysis. – Geophys, Trans., 30, 4, pp. 313–353.

Balla, Z. 1988: Clockwise paleomagnetic rotations in the Alps in the light of the structural pattern of the Transdanubian Range (Hungary). – Tectonophysics, 145, pp. 277–292.

Balogh, K., Á. Jámbor, Z. Partényi, L. Ravasz-Baranyai, G. Solti 1982: K/Ar dating of basaltic rocks in Transdanubia, Hungary. – Földt. Int. Évi Jel. 1980, pp. 243–260.

Berggren, W.A., D.V. Kent, J.J. Flynn, J.A. Van Couvering 1985: Cenozoic Geochronologie. – Geol. Soc. Am. Bull., 11, pp. 1407–1418.

Besse, J., V. Courtillot 1991: Revised and Synthetic Apparent Polar Wander Paths of the African, Eurasian, North American and Indian Plates, and True Polar Wander since 200 Ma. – Journ. Geophys. Research, 96, B3, pp. 4029–4050.

Channell, J.E.T., R. Brandner, A. Spieler, J. Stoner 1991: Paleogeography of the Northern Calcareous Alps: evidence from paleomagnetism and facies analysis. – XX. General Assembly IUGG Vienna, 11–24 August, 1991, Abstract.

Csontos, L., A. Nagymarosy, F. Horváth, M. Kovács 1992: Model for Tertiary evolution of the Intra-Carpathian area. – Tectonophysics, 208, pp. 221–241.

Dunkl, I. 1990: Fission track age of zirkon grains from Eocene-covered bauxites of the Transdanubian Central Range (Hungary): evidence for Early Eocene volcanism. – Ált. Földt. Szemle, 25, pp. 163–177.

Fischer, R.A. 1953: Dispersion on a spere. – Proc Roy. Soc. London, A217, pp. 229–305.

Fodor, L., Á. Magyari, M. Kázmér, A. Fogarasi 1992: Gravity-flow dominated sedimentation on the Buda paleoslope (Hungary): Record of Late Eocene continental escape of the Bakony unit. – Geol. Rundschau, 81, 3, pp. 695–716.

Géczy, B. 1973: Plate tectonics and paleogeography in the East-Mediterranean Mesozoic. – Acta Geol. Sci. Hung., 17, pp. 421–428.

Haas, J. 1987: Position of the Transdanubian Central Range structural unit in the Alpine evolution phase. – Acta Geol. Hung., 30, 3–4, pp. 243–256.

Haas, J., G. Császár, S. Kovács, A. Vörös 1990: Evolution of the western part of the Tethys as reflected by the geological formations of Hungary. – Acta Geod. Geoph. Mont. Hung., 25, 3–4. pp. 325–344.

Heer, L. 1982: Paläomagnetische Testuntersuchungen in den Nördlichen Kalkalpen im Gebiet zwischen Gollig und Kössen. – M. Sc. Thesis, Technical University, Munich.

Heller, F., W. Lowrie, A.M. Hirt, 1989: A review of paleomagnetic and magnetic anisotropy results from the Alps. – Geol. Soc. Spec. Publ., 45, pp. 399–420.

Kázmér, M. 1984: Continental escape of the Bakony-Drauzug unit in the Paleogene. – Ált. Földt. Szemle, 20, pp. 55–102 (in Hungarian with English abstract).

Kázmér, M., S. Kovács 1985: Permian–Paleogene paleogeography along the eastern part of the Insubric–Periadriatic Lineament System: evidence for continental escape of the Bakony–Drauzug Unit. – Acta Geol. Hung. 28, 1–2, pp. 71–84.

Lowrie, W. 1986: Paleomagnetism and the Adriatic promontory: a reappraisal. – Tectonics, 5, pp. 797–807.

Mauritsch, H.J., M. Becke 1985: Die Entwicklung der Nördlichen Kalkalpen aus paläomagnetischer Sicht. – Archiv für Lagerstöttenforschung der Geol. Bundesanst., Wien, 6, pp. 113–116.

Mauritsch, H.J., M. Becke 1987: Paleomagnetic investigations in the Eastern Alps and the Southern Border Zone. – In: Geodynamics of the Eastern Alps. Deuticke, Vienna pp. 282–308.

Mauritsch, H.J., W. Frisch 1980: Paleomagnetic results from the Eastern Alps and their comparison with data from the Southern Alps and the Carpathians. – Mitt. Österr. Geol. Ges., 73, pp. 5–13.

Márton, E. 1987: Paleomagnetism and tectonics in the Mediterranean region. – Journ. of Geodyn., 7, pp. 33–57.

Márton, E. 1988: Paleomagnetic indication for double collision between the Central Mediterranean and stable Europe. – Ann. Geophys. Spec. Issue, Abstract, SI, pp. 6–13.

Márton, E. 1990: Paleomágnesség a középső Mediterráneumban (Paleomagnetism in the Central Mediterraneum). – DSc. Thesis, in Hungarian.

Márton, E. 1992: Triassic carbonate platform sediments: applicability of paleomagnetism to cyclostratigraphy and tectonics. Abstract. – Geol. Carpath., 43, 3, p. 175.

Márton, E. in press: Mecseki és Villányi hegységi mezozoos alapszelvények paleomágnessége (Paleomagnetism of Mesozoic basic sections from the Mecsek and Villány Hills). – Ált. Földt. Szemle, in Hungarian.

Márton, E., P. Márton 1978: Tectonic implication of a new paleomagnetic result from the Jurassic of the Transdanubian Central Mountains. – Tectonophysics, 45, pp. T1–T6.

Márton, E., P. Márton 1981: Mesozoic paleomagnetism of the Transdanubian Central Mountains and its tectonic implications. – Tectonophysics, 72, pp. 129–140.

Márton, E., P. Márton 1982: A litoszféra mozgásainak rekonstrukciója paleomágneses adatok alapján (The reconstruction of the movements of the lithosphere using paleomagnetic data). – Transactions of the Hungarian Academy of Sciences, 15, 3–4, pp. 256–276, in Hungarian.

Márton, E. P. Márton 1983: A refined apparent polar wander curve for the Transdanubian Central Mountains and its bearing on the Mediterranean tectonic history. – Tectonophysics, 98, pp. 43–57.

Márton, E., P. Márton 1991: Tertiary rotations in NE-Hungary. – XX. General Assembly, IUGG Vienna, 11–24 August 1991, Abstract.

Márton, E., G. Nardi 1991: Is it still evidenced paleomagnetically that Apulia region has been part of Africa? First results from Murge. – XX. General Assembly, IUGG Vienna, 11–24 August 1991, Abstract.

Márton, E., P. Pagác, I. Túnyi 1992: Paleomagnetic investigations on Late Cretaceous–Cenozoic sediments from the NW part of the Pannonian Basin. – Geol. Carpathica, 43, pp. 363–368.

Márton, E. D. Veljovic, 1987: Paleomagnetism of Cretaceous carbonate from the northwestern part of the Dinaric fold belt. – Tectonophysics, 134, pp. 331–338.

Odin, G.S., 1982: Numerical dating in Stratigraphy. – John Wiley, Chichester, 1094 p.

Ratschbacher, L., W. Frisch, F. Neubauer, S.M. Schmid, J. Neugebauer 1989: Extension in compressional orogenic belts. The eastern Alps. – Geology, pp. 404–407.

Savostin, L.A., J.C. Sibuet, L.P. Zonenshain, X. LePichon, M.J. Roulet 1986: Kinematic evolution of the Tethys belt from the Atlantic Ocean to the Pamir since the Triassic. – Tectonophysics, 123, pp. 1–35.

Tari, G., T. Báldi, M. Báldi-Beke : Paleogene retroarc foredeep basin beneath the Neogene Pannonian Basin: a geodynamic model. – Tectonophysics,

Vanden Berg, J. 1979: Paleomagnetism and the changing configuration of the Western Mediterranean area in the Mesozoic and Early Cenozoic areas. – Geologica Ultraiectina, 20, pp. 147–153.

Vanden Berg, J. 1983: Reappraisal of paleomagnetic data from Gargano (South Italy). – Tectonophysics, 98, pp. 29–41.

Vanden Berg, J., A.A.H. Wonders 1976: Paleomagnetic evidence of large fault displacement aroundf the Po-basin. – Tectonophysics, 33, pp. 310–320.

Vanden Berg, J., J.D.A. Zijderveld 1982: Paleomagnetism in the Mediterranean area. – In: Geodynamics series 7. Alpine–Mediterranean Geodynamics, final report of working group 3. Amer. Geophys. Union, Geol. Soc. Amer., pp. 83–112.

Acta Geologica Hungarica, Vol. 37/1–2, pp. 153–181 (1994)

The occurrence and morphology of sedimentary pyrite

Tamás Hámor
Hungarian Geological Survey, Budapest, Hungary

The five main morphotypes of sedimentary pyrite are framboidal, euhedral, equant, anhedral and ooidic. In anoxic sediments and sedimentary rocks, disseminated microscopic framboids and euhedral monocrystals occur dispersively. In dysoxic and oxic sediments where anoxic microenvironments are produced by organic matter, equant, framboidal and euhedral pyrites can form concentrated masses visible to the unaided eye.

Framboidal and euhedral pyrites precipitate by continuous uninterrupted surface-controlled crystal growth via sulphidation of iron monosulphides. Equant pyrites (which may be much larger) are formed by diffusion-controlled growth in pores where solutions are transported from external sources. The late diagenetic recrystallization of these three forms, or space restrictions during the early diagenetic precipitation of equant pyrites, results in the formation of "massive" anhedral or subhedral pyrites filling veins, nodules, etc. The rare ooidic pyrites indicate either cyclically changing anoxic–dysoxic conditions on the sea-floor or the encrustation activity of algae or bacteria.

The octahedron, hexahedron, pentagonal dodecahedron and their combinations make up the majority of pyrite crystal habits in both framboidal, euhedral and equant types. The octahedron is most frequent in organic-rich pelitic sediments, the cube in calcareous sediments, while the pyritohedron is commonly observed in evaporites or in sedimentary rocks as a late diagenetic precipitate.

Key words: sedimentary pyrite, framboid, diagenesis, anoxic, Pannonian basin

Introduction

Despite the numerous sedimentological, geochemical and mineralogical articles (Hudson 1982; Leventhal 1983; Sunagawa 1957; etc.), the morphological classification and the related genetic model of sedimentary pyrite have not been completed. Laboratory synthesis of pyrite has a limited validity, geochemical studies usually neglect morphological observations, and sedimentological data sets are often restricted to a few sections. Moreover, many authors do not distinguish the occurrence, morphology and crystallography of sedimentary pyrite.

The present study reviews the occurrences of sedimentary pyrite and proposes a new morphological system and general genetic model of its formation. The results are proven by the description and analysis of an approximately 20 km long core section of the Pannonian Basin and the accurate

Address: T. Hámor: 1440 Budapest, P.O. Box 117, Hungary
Received: 15 October, 1993

0236–5278/94/$ 4.00

revision of approx. 250 literary items. Except for the ooidic form, the sediments of the Pannonian Basin include all the main morphotypes ever published.

Methodology

Several hundred occurrences of sedimentary pyrite were found and described in the continuous core sections of the Pannonian Basin. The formations varied from basal marls to bauxites, from Permian to Pleistocene, from 2300 m depth to the surface. Seventy-seven representative samples were studied by scanning electron microscope. To avoid the loss of the smallest grain size fraction by washing out, we examined the surface of the whole rock. Some of the samples were analyzed by X-ray diffraction to determine the pyrite and to distinguish it from marcasite. Sulphur isotopic measurements are published elsewhere (Hámor and Hertelendi 1991).

The occurrences of sedimentary pyrite

Sedimentary pyrite is formed under anoxic conditions when sufficient decomposable organic matter, dissolved sulphate and reactive iron are present (Berner 1984). These conditions are accomplished in several sedimentary environments. To summarize the occurrences of sedimentary pyrite, the facies model elaborated by Rhoads and Morse (1971) was applied as a basis (Fig. 1). Pyrite occurring in peat and coal, and the weathering or metamorphosis of sedimentary pyrite, are beyond the scope of this study.

Dispersed, statiform lenses, cement

During early diagenesis most fine-grained marine and lacustrine sediments become anoxic a few decimetres below the sediment-water interface. Nevertheless, sedimentary environments are generally considered to be anoxic (sensu stricto) only when this process has been accomplished at the interface or in the overlying water ("inhospitable bottom", "dead layers", etc.). In the anoxic Oligocene Tard Clay Formation (Hungary) and in literature examples (Degens et al. 1972; Hudson 1982; Schallreuter 1984; Goodfellow 1987) single, disseminated framboids or framboidal aggregates, and small (<10 μm) euhedral pyrite crystals occur dispersively in sediments from anoxic depositional environments. Despite the fact that pyrite-sulphur content is generally high in these sediments (2–4%), the distribution of pyrite is homogeneous and almost invisible to the unaided eye. Leventhal (1983) and Raiswell and Berner (1985) suggest that the precipitation of such "syngenetic" pyrite begins in the water column below the O_2/H_2S boundary. The homogeneous distribution is not disturbed by any epi-, or infaunal activity or other local microenvironmental changes on the inhospitable seafloor. Pyrite may precipitate in the same way in periodically anoxic environments.

	sedimentary environment	occurrence of pyrite	dominant morphotypes
anoxic microenvironments of	oxic	fossils	framboidal (euhedral, equant)
		organic debris	framboidal (euhedral)
		concretions	equant (framboidal)
		cement	equant
	dysoxic	trace fossils	framboidal, anhedral (euhedral, equant)
		concretions	equant (framboidal)
		cement	equant
		shrinkage joints	equant (euhedral)
	anoxic	dispersed	framboidal (euhedral, ooidic)
		stratiform lenses	anhedral (equant, framboidal, ooidic)
		in situ reworked	equant

Fig. 1
The occurrences and related morphotypes of sedimentary pyrite

Small, isolated euhedral monocrystallites, larger (> 10 μm) equant pyrites and spheroidal framboids are often concentrated as stratabound masses or stratiform layers and lenses (McKibben & Eldridge, 1989). These layers and lenses are millimetre to decimetre thick, but can extend laterally for hundreds of metres. Sometimes a primary enrichment of framboids can result from a "rain" of sulphide cascading to the bottom, leading to the accumulation of layers (Goodfellow 1987). Schieber (1989) reported laminated pyrite beds on the mid-Proterozoic striped shales of the Newland Formation which he interpreted as resulting from the early diagenetic mineralization of microbial mats. In late diagenetic and metasediments, early diagenetic pyrite accumulations are modified by overgrowth and replacement of coarser equant or anhedral pyrite which results in the formation of stratiform lenses. Late diagenetic pyrite cements in siltstones and sandstones as euhedral and equant grains are well known (Kirchner 1985; Burley 1984); late framboids are less frequent.

In situ reworked

Erosional reworking of pyritized fossil steinkerns, burrow tubes, mineralized wood, irregular or tabular pyrite grains and geopetal stalactitic pyrites on a Devonian anaerobic seafloor was reported by Baird and Brett (1986). The widespread occurrence of the reoriented, aligned and mechanically broken pyrite grains, and the general absence of carbonate, indicated brief erosional episodes in an anoxic environment. Among the few thousand sulphide ooids (incl. pyrite and marcasite) that Binda and Simpson (1989) examined, three had a fragment of pyrite ooid as a nucleus, providing evidence of in situ reworking during the deposition of the Ordovician Winnipeg Formation. The relative instability of sedimentary pyrite does not allow long distance reworking under oxic conditions. However examples of the local reworking of sedimentary pyrite are recorded (Kirchner 1985).

Shrinkage joints, veinlets

Pyrite precipitation on the surface of shrinkage joints or fissures was observed in Pannonian delta plain sediments (this study). The decimetre long, thin, hair-like shrinkage joints and fissures oriented normal to the bedding are formed during early diagenetic consolidation or dewatering of the sediment. The thin pyrite film on the surface of joints consists of globules of twinned pyrite crystals and smaller euhedral ones (Fig. 2). A downward decrease of pyrite segregation suggests that super-saturated solutions infiltrated from the pore system of the overlying sediment. Pyrite segregations in the diagenetic collapse surfaces of claystones and tectonic slickensides or thick veinfills of massive, subhedral pyrite are late diagenetic features (Dill and Kemper 1990).

Concretions

Concretions are typical examples for the reducing microenvironment in oxic ("oxygenated", "normal") and dysoxic ("dysaerobic", "restricted") sediments. According to our observations and Carstens (1986), there are two types of pyrite concretion with different growth mechanisms: (1) cement-type concretions comprising passive precipitation of pyrite in the pore space of a host concretion, and (2) displacive-type concretion involving sediment-displacive growth of pyrite crystal-complexes. Both concretion types are precompactional, early diagenetic features, and display various shapes, although whilst displacive-type

Fig. 2
SEM image pyrite segregation on the surface of a diagenetic vertical fissure in clayey siltstone. Note the pyrite globules consisting of twinned octahedral crystals and the much smaller, disseminated euhedral pyrites. Scale bar = 10 μm

concretions rarely exceed centimetres, cement-type concretions are commonly decimetre-sized.

Pyrite segregations in carbonate (calcite, siderite, dolomite, ankerite), barite and chert nodules are well known (Coleman and Raiswell 1981; Curtis et al. 1986; Kortenski 1989). In the Jet Rock carbonate concretions, framboids are dominant in the centre, but towards the margin the number of euhedral (equant) pyrites increases (Coleman and Raiswell 1981). In Late Miocene carbonate concretions of the Pannonian Basin and in some from the Balkan Basin (Kortenski 1989) equant pyrites occur in the concretion centre and their concentration decreases towards the margins. Bacterial sulphate reduction provided sulphide ions but, with restrictions on the diffusive supply of iron and sulphate, especially in brackish-freshwater environments, only euhedral pyrite precipitated.

Displacive-type pyrite concretions are millimetre to decimetre sized subspherical, elongated ellipsoidal, or irregular crystal complexes that are sometimes flattened parallel to the bedding (Sultanov et al. 1989; Schmitz et al. 1988). Concretions generally have a radiating spherulitic texture, with anomalously elongated fibrous or tabular, pyrite or marcasite crystals evolving from the concretion centre where organic structures or inorganic detritus are occasionally preserved. Concretions sometimes have concentric zones suggesting breaks in crystal growth (White et al. 1991). Microscopic pyrite spherulites (Fig. 3) found in Late Miocene calcite concretions have a framboid as a nucleus and a rosette-like structure, showing great similarity to the famous "pyrite-sun" aggregates of Illinois (Baxter and Reinertsen, 1988) and the pyrite

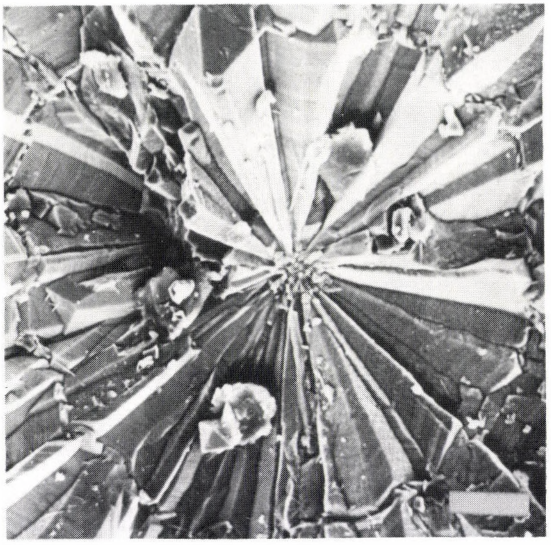

Fig. 3
Pyrite spherulites found in Late Miocene calcite concretion. The elongated radiating rows of zoned crystal-clusters grow epitaxially from the centre. The tips of crystal columns display octahedral habit. Scale bar = 20 μm

balls and discs of Hudson (1982). Other types of pyrite concretions e.g. aggregates, lenses, stars were reported by Hudson (1982) and Dill and Kemper (1990).

Trace fossils, fossils, organic debris

Many pyrite segregations are linked with trace fossils, particularly with the closed tubular or conical shaped dwelling structures of suspension feeder organisms (Thomsen and Vorren, 1984). For example 3–4 cm long, vertical, cone-shaped burrows with a concentric pyritic rim (*Skolithos* sp.?) are found in Late Miocene delta plain sediments. Digested organic refuse, readily decomposed by bacteria, is believed to have been transported to the margins where pyrite formation takes place. Support for this process comes from Harding and Risk (1986) who analyzed anomalous concentrations of trace elements at the margins of *Skolithos* sp. The smaller (2x10 mm), horizontal, tubular worm tracks in the dysaerobic, prodelta siltstones of the same Late Miocene sequence are filled completely with framboidal and euhedral pyrites. As in the previous example, axial symmetry can be observed here on a microscopic scale, as framboids are concentrated in the axis while euhedral crystals occur in the cylindrical mantle.

Precipitation of pyrite on remnants of coalified plant tissues, fecal pellets, or on other unidentifiable organic debris (algae, carcasses of fishes, etc.) is common in marine or brackish water sediments. The dominant forms are framboids, euhedral crystals and to a minor extent, coarse equant pyrites.

Pyrite has also been found in diatom frustuls, radiolarians, sponge-spicules, foraminifers (Schallreuter 1984), in gastropods (Kirchner 1985), brachiopods and crinoids (Loope and Watkins 1989), other molluscs (Brett and Baird 1986), and ammonites (Hudson 1982). The sheltered inner space of these shells becomes anoxic because easily decomposable organic substrate is generally found there. Under these circumstances pyrite formation may be limited by iron and sulphate supply. Besides framboidal and euhedral pyrites, a variety of crystal morphotypes is reported in literature (e.g. Hudson 1982). However, a general trend can be established. In microfossils framboids and euhedral crystals are dominant, whereas in macrofossils larger equant, twinned or cryptocrystalline crystals occur.

In conclusion, occurrences of sedimentary pyrite can be found in anoxic macro- or microenvironments that are directly or indirectly associated with organic matter and biological activity.

Morphology of sedimentary pyrite

Based on our observations and literature a new morphological classification of sedimentary pyrite is proposed (Fig. 4). The formation of the main morphotypes will be discussed in detail later.

Framboidal pyrites

The most common, and best-studied, form of sedimentary pyrite is the framboid (Figs 5, 6). This term was introduced in 1935 by G. W. Rust and is derived from the French for raspberry ("framboise"). Although later used to describe similar structures of other minerals (magnetite, digenite, etc.) the term framboid is principally applied to pyrite.

Framboids are more or less spheroidal aggregates of discrete, equigranular, euhedral pyrite microcrystals (Fig. 5). The diameter of framboids ranges from 5–100 μm but the mean size is 20–50 μm. A maximum diameter of 250 μm was reported by Sweeney and Kaplan (1973). The size and crystal habit of the constituent crystallites in a given framboid are essentially the same and the same crystal habits are found in framboids and in euhedral crystals. Within framboids the packing of microcrysts is usually irregular and disordered but, in more compacted sediments, pyritohedra may form ordered, closely-packed arrays. Framboids usually do not contain any matrix material but kaolinite, clay minerals and quartz are occasionally found within interstices and as thick coatings (Scheihing et al. 1978; Love et al. 1984; Fig. 6). Closely bound organic matter has been recognized inside a number of framboids (Love 1957; Love and Amstutz 1966). Framboids typically cluster together and form larger (100–300 μm) aggregates are often termed polyframboids (Love et al. 1971) although other terms are in use e.g.: "Roggenpyrits", "clusters of framboids", "framboid aggregate".

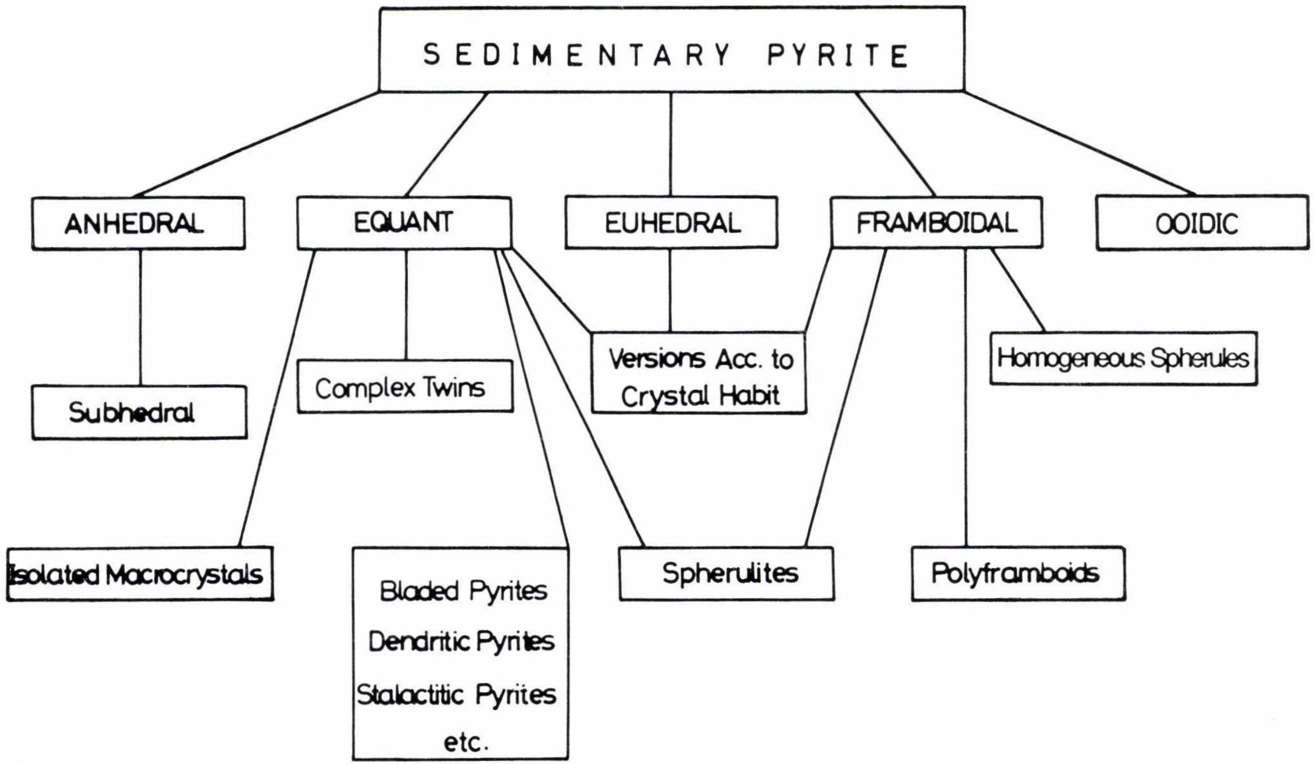

Fig. 4
Morphological classification of sedimentary pyrite. The lines leading to different morphotypes indicate both morphotypical and genetic connections

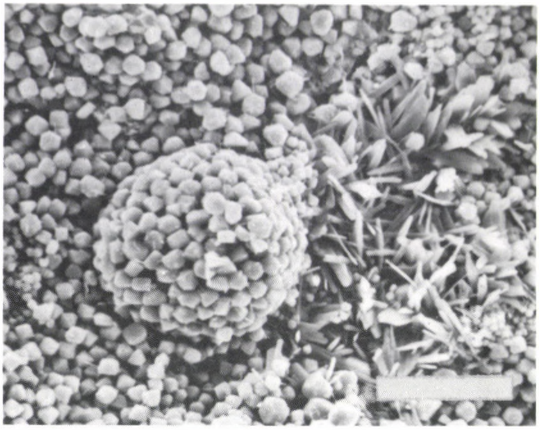

Fig. 5
Pyrite framboid and disseminated euhedral pyrites. The crystal habit is the combination of octahedron and cube in both morphotypes. The radial crystal cluster on the right consists of clay minerals. Scale bar = 5 μm

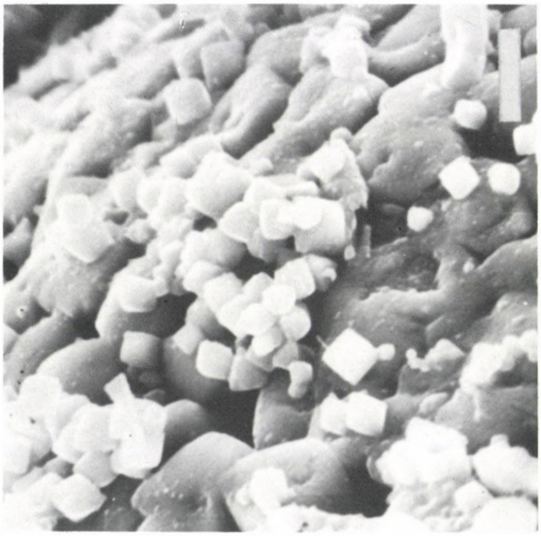

Fig. 6
Small euhedral pyrite crystals on the surface of a coated framboid. The thin coating is most probably clay mineral. Scale bar = 2 μm

In the finest (<5 μm) grain size fraction homogeneous cryptocrystalline pyrite spherules are observed (Rickard 1970; Sassano and Schrijver 1989; McKibben and Eldridge 1989). In the Pittsburgh coal, Renton and Bird (1991) interpreted such smooth spheres as completely coalesced framboids in which the intercrystallite voids are infilled by pyrite. Ordered islets or patches of euhedral pyrite crystals (Fig. 7) are possible initial, or transitional, forms towards framboids. The later recrystallization of framboids leads to the formation of equant complexes (Fig. 2; Schallreuter 1984; Ostwald and England 1979).

Framboids described from hydrothermal, volcanic exhalative formations are generally not equigranular (Love and Amstutz 1966). In hydrothermal

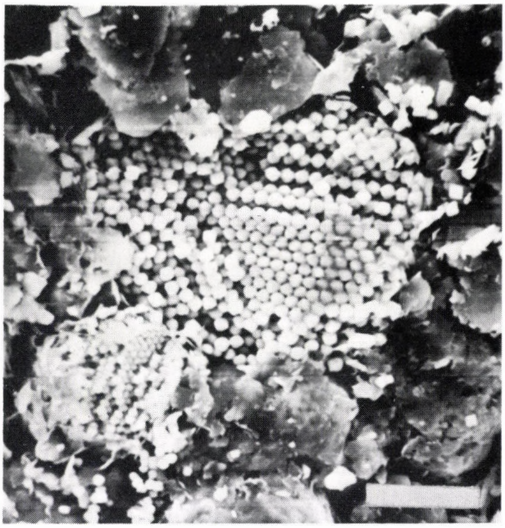

Fig. 7
Ordered islet euhedral pyrites in clay. A possible transition towards framboids. The crystals are combinations of octahedron and cube. Scale bar = 10 μm

laboratory experiments (Sunagawa et al. 1971) framboids increased in size and roundness with increasing duration of autoclaving but the size of microcrysts remained constant.

Euhedral pyrites

Euhedral pyrites are discrete isolated pyrite monocrystals generally occurring with framboids. Their size is usually between 0.1 and 5.0 μm (Figs 5–9) but at the highest values (10–30 μm) there is no sharp distinction from equant pyrites. In the literature euhedral pyrites are often referred to as "disseminated pyrites" together with framboids. Crystal faces are generally smooth, penetrating twins and crystal anomalies are rare. The crystal forms of euhedral pyrites are the same as in framboidal and equant pyrites (see below).

Equant pyrites

The term "equant" is, in general, synonymous with terms "equidimensional" or "isometrical", although anisometric, elongated crystals belong to this morphotype. Hudson (1982) first used this term to designate and distinguish those coarse-grained, well-developed crystals that do not form sub-spherical aggregates. In our formulation equant pyrites are relatively large (20 μm–2 cm), well-developed crystals which are usually twinned. Equant pyrites are generally characterized by a variety of crystal growth anomalies (Figs 10–15).

Equant pyrites show a particular tendency to form penetration twins and "rosette"-like complexes (Fig. 11). Crystal anomalies, e.g. like natural etchings on faces (Fig. 12) or on edges, negative forms with striated faces (Fig. 13),

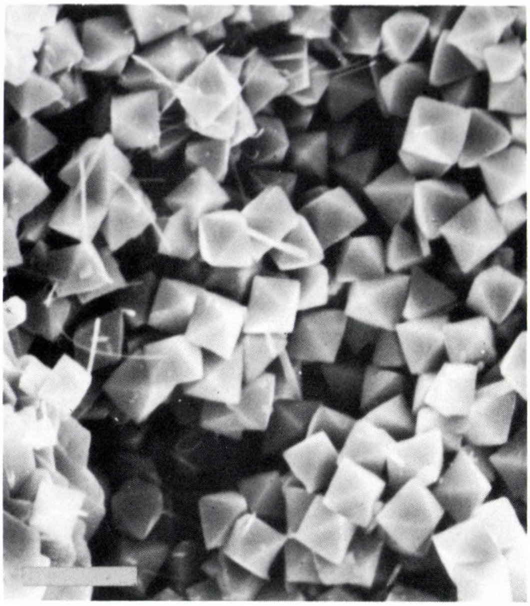

Fig 8
Pure octahedral crystals of euhedral type. The thin hair-like crystals are probably zeolites. Scale bar = 5 μm

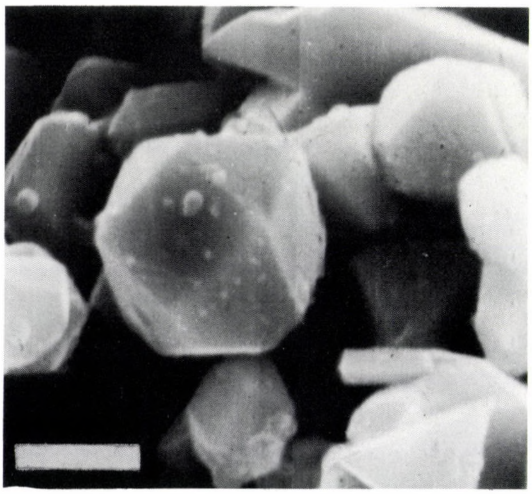

Fig. 9
The ideal, balanced combination of octahedron and cube. Euhedral pyrite. Scale bar = 1 μm

dendritic and skeletal crystals (Fig. 14; Strunz 1986) and arborescent grooves (Hudson 1982) are all frequent. None of these features can be observed on euhedral pyrites.

Unusual needle-like, acicular, cubic crystals found dispersively in a bauxite sample (Fig. 15) are rather similar to the pyrite needles that were grown synthetically by Murowchick and Barnes (1987), which were suggested to grow

Fig. 10
Equant cubic pyrite. The edges of the cube are modified by pyritohedral and the corners by octahedral faces. Scale bar = 10 μm

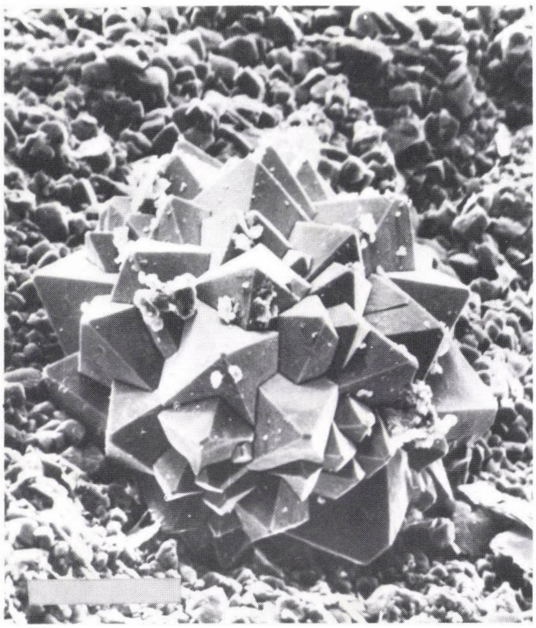

Fig . 11
Rosette-like penetration twin complex of octahedral equant pyrites. The corners are modified by small cubic faces. Scale bar = 50 μm

Fig. 12
Natural etching marks on the crystal face of equant, octahedral pyrite. Note the cubic faces on the corners. Scale bar = 10 µm

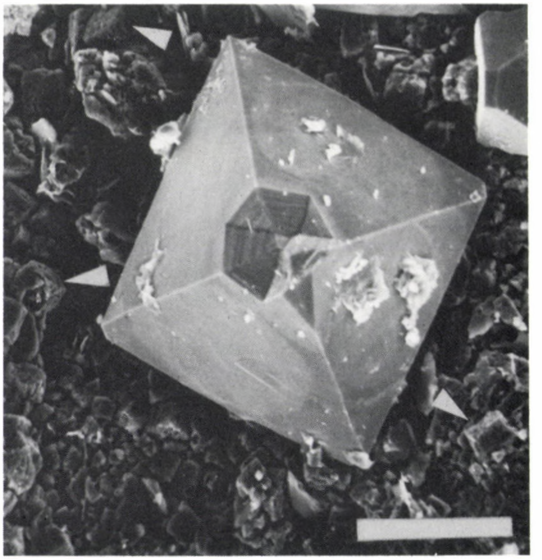

Fig. 13
Octahedral equant pyrite with negative forms at the corner. The striated faces inside are indicating polysyntethic twinning. Note the samll, arborescent cubes in the background (as shown by arrows). Scale bar = 40 µm

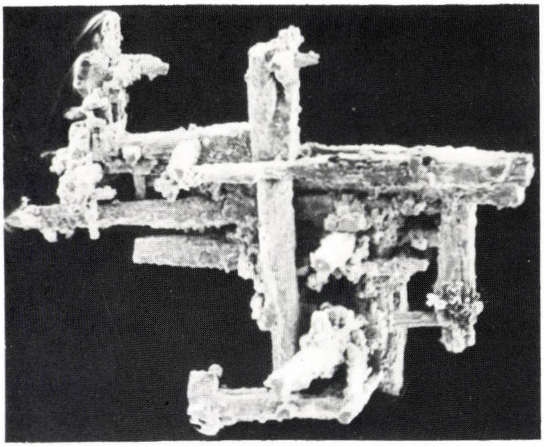

Fig 14
Skeletal pyrite found in the heavy mineral fraction of a clay. The size of the crystal is two millimetres

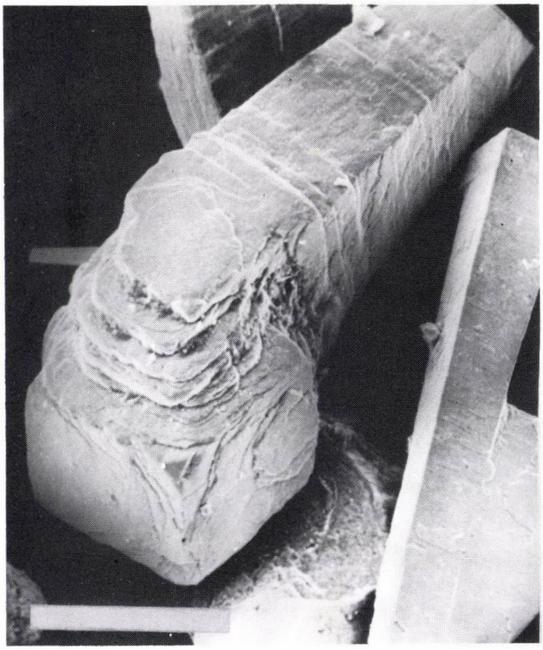

Fig. 15
Pin-like acicular pyrite growing from a cubic crystal. Note the layered faces and the octahedron on the corner of the cube. Scale bar = 20 µm. Late Cretaceous, washing residue of a bauxite sample

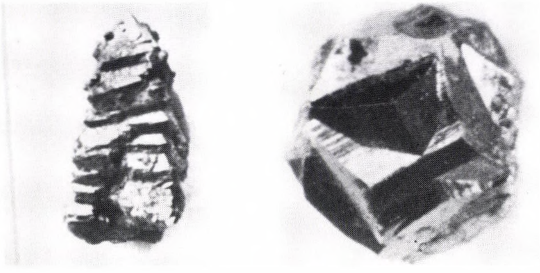

Fig. 16a,b
Sedimentary pyrite macrocrystals. a) Cone-in-cone structure of octahedral pyrite crystals; often described as "marcasite". Crystal size is seven millimetres. Late Miocene clay, Somlyó Formation. b) Penetration twin of two pentagonal dodecahedrons (Pyritohedron). The diameter of the crystal is four millimetres. Late Permian anhydrite, Perkupa Formation

by a screw dislocation mechanism. In contrast hydrothermal pyrite whiskers and platelets reported by Bonev et al. (1985) grew by a two-dimensional nucleation mechanism at the tips of the crystals through a unidirectional supply of material. Other elongated forms reported are: pyrite stalactites, rods of pyrite, chamber linings (Hudson 1982); pyrite stalactites (Baird and Brett 1986); rods of pyrite (Kirchner 1985); pyrite chimneys (Larter et al. 1981); columnar aggregates (Sassano and Shrijver 1989); filiform aggregates (Dill and Kemper 1990).

Pyrite spherulites can be interpreted as later overgrowths of elongated equant crystals on euhedral or framboidal pyrite (Fig. 3).

Isolated, large (1–20 mm) equant crystals are favoured subjects of traditional mineralogical studies (Sunagawa 1957; Carstens 1986; Penick 1987). Other common equant forms are hopper-shaped, and have striated faces, penetration intergrowths, and cone-in-cone structures (Fig. 16). The observation that "the large pyrite crystals differ from pore-filling (non-framboidal) pyrite with respect to growth morphology, internal structure, and growth mechanism" (Carstens 1986) seems applicable to most equant pyrites. All the other types of sedimentary pyrite having a definite morphology or crystal form not described here also belong to the equant pyrite category.

Marcasite and pyrrhotite are less common than pyrite and coexist with, or pseudomorph exclusively, equant, ooidic and anhedral pyrites (e.g. Baxter and Reinertsen 1988; Kortenski 1989; Binda and Simpson 1989; White et al. 1991).

Anhedral and subhedral pyrites

Anhedral and subhedral (or xenomorphic, cryptocrystalline, colloform) pyrites are often referred to as "massive pyrite". They generally fill veins, concretions, trace fossils or form stratabound layers. The diameter of individual grains, if recognizable, is the same as the equant forms. This morphotype lacks any obvious structure on a macro- and microscopic scale, although occasionally subhedral forms can be observed. Massive pyrites probably precipitated directly in an open system, as expressed in their generally light $\delta^{34}S$ values (Westgate and Anderson 1984), where there was an abundant supply of supersaturated solution causing rapid, multi-centered crystal-growth which, in a limited space, did not allow idiomorphic crystals to develop. In a few cases, anhedral pyrites formed by late diagenetic replacement of early pyrites. Thus, the experiments of Farrand (1970) showed that pyrite euhedra began to coalesce after one month and framboids became smooth and infilled with other sulphides. A year later only massive pyrite occurred.

Ooidic pyrites

Pyrite ooids (or ooliths) are the least frequent type of sedimentary pyrite, their occurrence being restricted to pre-Cenozoic formations. The ooids are small (0.1–4.0 mm) spheres consisting of concentric, onion-like layers that often have a fibrous character, radiating from the centre to the margins (Mitchell and Porter 1985). The concentric layers consist, besides pyrite, of phosphate, chalcopyrite and marcasite. Quartz grains, titanium oxide, fossil fragments, detrital pyrite or a fragment of pyrite ooid are frequently observed in the centre of ooids (Binda and Simpson 1989).

As for other ooidic textures, precipitation of such multi-layered spheres with a detrital nucleus suggests bottom water currents, cyclically changing conditions (anoxic to dysoxic) and/or the encrustation activity of algae or bacteria. One possible sedimentary environment is the anoxic upwelling system which develops seasonally or periodically on the western continental shelf close to the Equator (Demaison and Moore 1980). Cyclic conditions are suggested by the coexistence of phosphate and chamosite minerals and by the lithology of the host rock: clay-rich sandstones, pebbly sandstones (Mitchell and Porter 1985), organic-rich black shales containing graptolites (Hayes 1915) and transgressive clayey quartz-wacke (Binda and Simpson 1989). Additionally, direct biogenic activity cannot be neglected when considering the early and limited occurrence of pyrite ooids in the geologic record. Recent studies of biomineralization show pyrite and iron sulphides inside bacteria (Mann et al., 1990) and in prasinophyte algae (Hansen et al. 1986). The 150–1000 μm pyrite spherules that were found in the Fish Clay (C/T boundary, Denmark) and described by Hansen et al. (1986) differ from those of ooids by growing inward, but the lamellar structure is a possible remnant of algae.

Discussion

Genetic model

In the multi-factored, open-system sedimentary environments laws, genetic and facies models should be treated as "probable" or "mean" categories. This model (Figs 17, 18) can be considered to be of the same type. Although the environment has an impact on the formation of sedimentary pyrite, microenvironmental diagenetic changes are the determining factors in its morphology.

The role of monosulphides

The framboidal, euhedral, equant morphotypes are the most abundant authigenic mineral forming the anoxic-sulphidic sedimentary system. However, the joint occurrence of the three main morphotypes (Fig. 19) is very rare. Nevertheless, framboidal and euhedral forms do generally occur together and, despite their dissimilar shape, have common features in their formation, in contrast to equant pyrites. Laboratory syntheses of framboidal texture indicate inorganic precipitation during the slow reaction of iron monosulphides with intermediate sulphur species (Berner 1969a). Framboids may develop by the

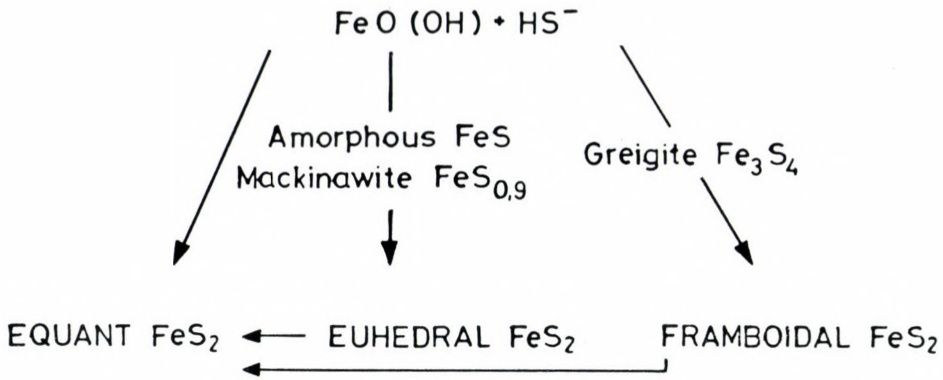

Fig. 17
Possible genetic pathways to framboidal, euhedral and equant pyrite (modified after Raiswell 1983)

direct precipitation of greigite (cubic Fe_3S_4), and mackinawite (tetragonal $FeS_{0.9}$) is not a necessary precursor (Sweeney and Kaplan 1973; Hallberg 1972). The formation of greigite from mackinawite requires traces of free O_2 or Fe^{3+}, the latter most probably being dissolved from goethite (Sweeney and Kaplan 1973). Greigite formation may thus be more difficult in environments where partially oxidized sulphur species cannot be produced; for example, thiosulphate is less abundant in very reduced solutions (Schoonen and Barnes 1991). In this sense framboid formation may occur in microenvironments that are not totally anoxic.

However, in previous genetic models (Sweeney and Kaplan 1973; Rickard 1975; Raiswell 1982) no distinction was made between the small, isolated crystals and the coarse-grained, intergrown pyrites. It seems possible that the reaction pathway through amorphous FeS and mackinawite leads to the formation of euhedral pyrites (sensu this paper), while direct precipitation produces equant pyrites. As emphasized earlier, framboidal and euhedral pyrites generally occur in the same pore space, their crystal size and habit are similar and the transitional form of the well-organized, closely-packed euhedral groups indicate a close genetic relationship to framboids (Figs 5, 7). Once greigite is formed, other monosulphides (e.g. mackinawite, as a precursor for greigite) may still remain; thus the dispersed, separated occurrence of the small, euhedral monocrystallites could occur by the crystallization of extremely finely-divided mackinawite or amorphous, minute iron monosulphide particles. Schoonen and Barnes (1991) have shown that, in solutions saturated with respect to both monosulphides and pyrite, the former nucleates and precipitates much faster due to a lower kinetic barrier for nucleation.

	FRAMBOIDAL	EUHEDRAL	EQUANT
mean size	$x \cdot 10^{1}\,\mu m$	$x \cdot 10^{0}\,\mu m$	$x \cdot 10^{2-4}\,\mu m$
precipitating	through monosulphides (greigite)	through monosulphides (mackinawite)	directly from solution
mode of solution supply	diffusion	diffusion	diffusion, pore solution flow
crystal growth	„surface – controlled"		„diffusion – controlled", sediment – displacive
formation	single event		long – lasting, repeatedly revival
reactants: organic matter	highly reactive, dispersed		less reactive, large mass
reactants: sulphate	internal and external sources		mainly external sources
reactants: iron	in situ, low concentrations		external, high concentrations
general sequence of precipitation	→	→	

Fig. 18
Relationship between pyrite morphology, formation and microenvironmental conditions

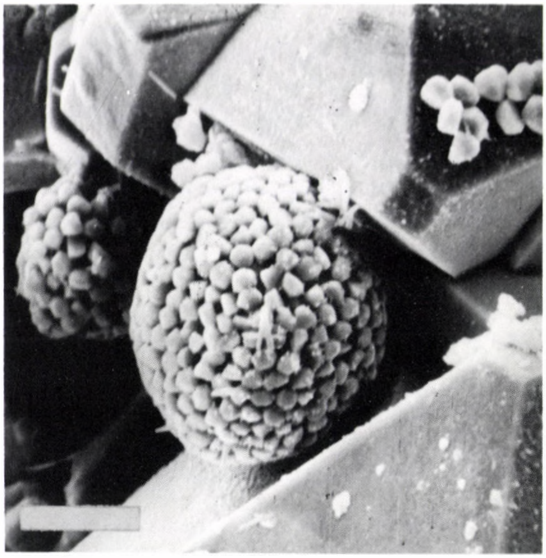

Fig. 19
The three main morphotypes of sedimentary pyrite in a porespace. The large equant octahedral crystals are modified by small cubic faces, the euhedral grains and the crystals in the framboid are more balanced combinations of octahedron and cube. Scale bar = 10 μm

Crystal growth and solution transport mechanisms

The crystal morphology of equant pyrites is obviously the result of direct precipitation from solution via direct nucleation. However, the continuous increase of crystal size from the 0.1–5.0 μm euhedral to 10–30 μm-sized equant pyrites in a given sample indicates a close relationship between the two morphologies. Euhedral pyrites may occasionally be precursors or nuclei for the subsequent growth of equant crystals. The late overgrowth or replacement of framboids can also lead to the formation of equant crystals (Fig. 3; Farrand 1970).

Crystal morphology is controlled by both growth rate and diffusion rate. Thus dendritic, spherulitic, skeletal crystals (or irregular crystal growth) result whenever the growth rate exceeds the diffusion rate (Kirkpatrick 1975). The hydrothermally-grown (250–500 °C), experimental pyrites of Murowchick and Barnes (1987) document that smooth cubic crystals form by surface-controlled growth. This experiment suggests layer-by-layer addition during the steady-state precipitation at low temperature and moderate supersaturation. At higher temperatures and a higher level of supersaturation, rougher, striated or dendritic crystals precipitate by diffusion-controlled growth. Where the diffusion rates are higher than solute incorporation rates into the crystal, corners and edges do not grow faster than flat faces, because nutrients are distributed evenly around the crystal. The balanced, smooth-faced euhedral pyrites and the crystals in framboids result from this surface-controlled growth. However, during the diffusion-controlled growth, the concentration of solute increases away from the surface of the crystal. Corners and edges then cross higher concentration contours, and growth at the ends of these protrusions is favoured over growth on the flat crystal faces. Arborescent grooves, etching marks, skeletal and dendritic pyrites will be produced, especially on the relatively anisometric octahedrons (Murowchick and Barnes 1987).

Carstens (1986) found two stages of concretionary pyrite growth in Lower Jurassic shales of Yorkshire, where a period of crystallization in the pore space was followed by a period of displacive growth, resulting in the formation of large columnar and dendritic crystals. In the Jet Rock concretions and in the Posidonia Shales, the second generation of crystals was columnar or hopper-shaped (Hudson, 1982) or twinned equant pyrites (Raiswell, 1982).

However, it is important to identify the driving force that provides a sufficient, long-term supply of solution for the sediment-displacive segregation of these coarse-grained crystals, despite the gradually closing system due to sediment burial. Organic matter-driven decay reactions may produce strong concentration gradients, which are suitable solute sources.

Berner (1969b) and Raiswell (1982) have pointed out that framboidal (and euhedral) pyrites are formed by decomposition of the most readily metabolized, dispersed, fresh organic matter that produced intensive bacterial sulphate reduction and hence light $\delta^{34}S$ values. Meanwhile, the mobile reduced products of bacterial decay (e.g. amines, aminoacids) solubilize iron from the host sediment, which can create a concentration gradient transporting iron and sulphate to the pore. The occurrence and paragenetic position of equant crystal complexes (Figs 11, 20) strongly support the existence of these "secondary" organic substrates. Zelibor et al. (1988) grew very similar spherical aggregates of vivianite in special redox cells. They conclude that the organic gel, formed by bacterial degradation of organic debris, can be a host matrix and a "gel-pump" to allow crystals to form a radiating pattern. Furthermore, "the electric field spanning the aerobic-anaerobic zones in the upper sediments may be an important driving force in addition to diffusion" (Zelibor et al. 1988).

Based on the studies of the preferred orientation of the large, hopper-shaped crystals to bedding, Carstens (1986) suggested that pore water flow along the bedding might act as a medium for solutes. Additionally, rates of pore water flow are orders of magnitude greater than diffusion rates. The differences in the H^+ ion concentration developed during the early framboidal–euhedral stage of pyrite formation should be considered as a possible factor inducing diffusion as well.

Raiswell (1982) has shown that framboids use in situ iron during their formation; this may also be true for euhedral pyrite. By contrast, in the case of equant pyrites (euhedral sensu Raiswell), iron is added to the system from external sources. The experiments of Farrand (1970), strongly support this model; at low iron concentrations pyrite particles form slowly and are idiomorphic, while at high iron concentrations flakes and flocculant precipitates develop. Iron is not a limiting factor in the formation of framboidal and

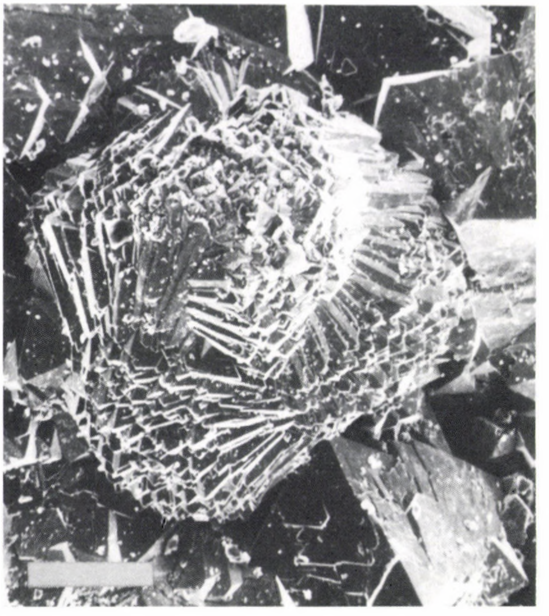

Fig. 20
Special triangular twin complex of octahedral equant pyrite crystals. Scale bar = 100 μm

euhedral pyrites on a microscale (in contrast to organic matter or sulphate), except in some euxinic (Raiswell and Berner 1985), and extremely iron-poor, sediments (e.g. limestones).

Open vs. closed system

Besides emphasizing that "completely open or closed systems are, however, endmember cases", Raiswell (1982) considered framboid formation as a prevailingly open system process based on their light $\delta^{34}S$ values. Sedimentary environmental factors such as sedimentation rate, salinity, quality and quantity of organic matter, and isotopic composition of dissolved sulphate in water, are generally closely related and control bacterial sulphate reduction, and thus the fractionation of sulphur isotopes (Kaplan 1983). The major factor in determining the isotopic composition of sedimentary pyrites is the open vs. closed character of the given sediment-pore system. Assuming that the environment was not an extreme isotopic pool (>>+30 ppm $\delta^{34}S$), and thermochemical reactions did not occur, then heavy (>>-5 ppm) $\delta^{34}S$ values of pyrites indicate precipitation in a prevailingly closed system. Closed systems are restricted for the egress of ^{34}S and characterized by the repeated redistribution of the previously formed remnant heavy ^{34}S isotopes.

However, light isotopic composition does not necessarily imply an open system in the case of small framboids and euhedral crystals. The simple reduction of normal seawater in a closed system results in a pyrite–sulphur content of approx. 0.3% (Berner 1984). The average pyrite–sulphur content of normal marine sediments five or six times this value (Berner 1984). The diffusive supply of sulphate from outside is obvious but the absolute volume of this sulphate, the distance of transport and thus the absolute openness of the pore space, compared with systems where equant pyrites were formed, is debatable. It is difficult to believe that the sometimes magnitudes larger equant pyrites were formed in a significantly more closed system than small framboidal and euhedral pyrites. The observed general sequence of precipitation of the three main types is framboidal to euhedral to equant (Figs 3, 6; Raiswel 1982; Hudson 1982; etc.). The formation of these is very close in space and time. Moreover, other paragenetic sequences also are known (Fig. 19). Hence equant pyrites do not necessarily indicate precipitation in the late diagenetic stage, since numerous coarse-grained pyrite concretions have been reported which formed in uncompacted sediments (see above). Pyrite formation can extend from the time of sedimentation until the present, and even compacted low-permeable pelitic rocks might be suitable, "open-enough" scenes for late diagenetic pyrite formation (Dill and Kemper 1990). In our samples (Hámor and Hertelendi 1991) and elsewhere (Hackley and Anderson 1986; Donelly and Jackson 1988; Maynard 1980; Westgate and Anderson 1984) small disseminated pyrite has heavier $\delta^{34}S$ values than massive, coarsely crystalline ones. The observation of Farrand (1970) that "the preservation of framboids demands protection from further access to a solvent within a few days of precipitation", and the occurrence of equant pyrites of different sizes and crystal habits in a given pore space (Fig. 13), provides further evidence for the open vs. closed debate.

Crystal habits

Most of the pyrite crystals described in the basic works of Dana (1903), Goldschmidt (1920), Hartman (1953), Sunagawa (1957) originated from hydrothermal ore deposits and veins. Similarly, attempts to demonstrate a correlation between crystal form and trace elements, mode of occurrence, crystal size, mineralization stages (Amstutz 1963; Sunagawa 1957; Bush et al. 1960), temperature and degree of supersaturation (Murowchick and Barnes 1987) are based on hydrothermal ore deposits and high-temperature laboratory experiments.

The three forms making up the majority of sedimentary pyrite crystals (in both framboidal, euhedral and equant types) are the octahedron {111}, the cube {100}, and the pyritohedron {210} (Fig. 21). The majority of the crystals in framboidal, euhedral and finer equant pyrites are built up from the unequal combinations of octahedron and cube or cube and pentagonal dodecahedron (Figs 5–16). The relative size of the modifying faces may vary within certain limits in a given pore space.

The combination of octahedron and pyritohedron is not known in sedimentary pyrites. The only exception is when the edges of the cube are

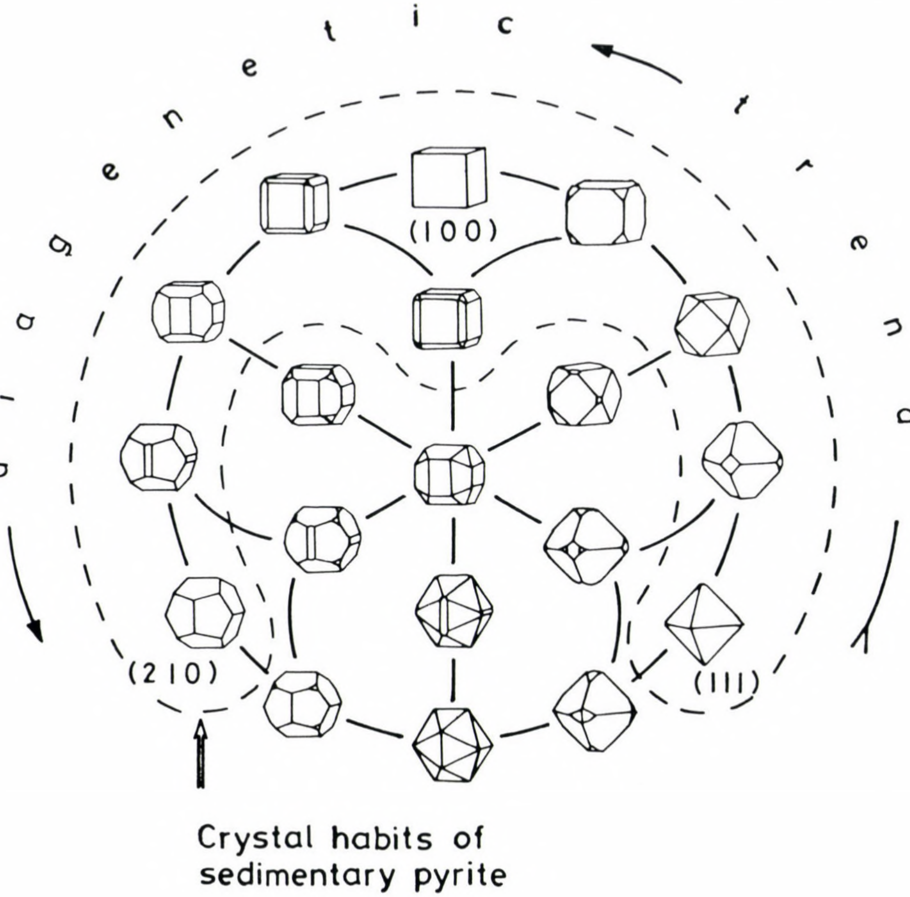

Fig. 21
Common pyrite habits (after Sunagawa 1957), crystal habits of sedimentary pyrite (indicated by dotted lines) and the general diagenetic trend

modified by small {210} faces and the corners by {111} faces (see Fig. 10); this 0.1 mm-sized equant crystal was found in dark grey Triassic calcareous marl of the Veszprém Formation. Trigonal trisoctahedron and trapezohedron were reported by Penick (1987), rhombic dodecahedron by Dill and Kemper (1990) and pseudohexagonal crystals by Sweeney and Kaplan (1973).

There is no obvious correlation between crystal size and habit. According to Smithson (1932) the largest crystals are cubes, but pyritohedra (Fig. 16b) and octahedra (Fig. 16a; Penick 1987; Carstens 1986) are just as frequently observed. Studying the hydrothermal veins in Japan, Sunagawa (1957) found that the cube was dominant among the smallest grain sizes, the octahedron in the middle sizes and the pyritohedron in the coarsest fraction. This is in keeping with the results of Murowchick and Barnes (1987), where (with increasing temperature and/or degree of supersaturation) the sequence produced was cube to octahedron to pyritohedron. Two of our samples, a Triassic marl and a Pannonian silt, contain disseminated cubes and octahedra but the different grain size fractions did not display any differences in crystal habit.

Pyritohedra always have an isometric, well-developed shape, while cubes frequently compose needle-like, elongated irregular crystals, due to their growth mechanism. Dendritic crystals are more often formed from octahedra, because this anisometric form has a preferred role during diffusion-controlled growth. Similarly, the {111} face receives dissolution most easily among the three major faces (Endo 1978).

The precipitation of a given crystal form is the function of the physical and chemical properties of the microenvironment, which depend on the macrosedimentary environment and subsequent diagenetic processes. In Pannonian organic-rich, pelitic sediments and lignites, the clear dominance of the octahedral form can be observed. However, marls and calcareous marls in deeper parts of the sequence, (below 800–1200 m depth) contain the cubic form. In these samples diagenesis is at an advanced stage (R_o –0.5%) but primary carbonate content is relatively high (20–40%). Similarly, large cubic crystals were found in several Triassic and Cretaceous limestones, calcareous marl and bauxite samples. Large (1 mm) pyritohedra were observed in anhydrite and its host-rocks in the Upper Permian–Lower Triassic sulphate evaporite sequence (Perkupa Formation, Fig. 16b).

Similar trends have been observed by other workers; thus the octahedron was dominant in C/T clay (Schmitz et al. 1988), in lacustrine silt (Kirchner 1985), in black shales (Love et al. 1971; Schallreuter 1984; Sassano and Schrijver 1989; Dill and Kemper 1990), in coal (Renton and Bird 1991), in ammonite-bearing shales (Hudson 1982), in peat (Altschuler et al. 1983). Cubic pyrites have been found in the biogenic mud of the Red Sea (Sweeney and Kaplan 1973), in methane-derived authigenic carbonate cemented mudstone (Ritger et al. 1987), in limestone (Penick 1987), and in sulphide–carbonate hydrothermal veins (Endo 1978). Pyritohedra and cubes were reported from a metamorphic gold-bearing sequence (Amaro et al. 1988), the host rock of hydrothermal anhydrite (Shanks and Niemitz 1982), coarse-crystalline marble (Whelan et al. 1990) and from epithermal replacement of gypsum deposits (Sunagawa 1957). Pure octahedral pyrites are not known from metasediments. These observations, and the hydrothermal experiments of Murowchick and Barnes (1987), prove the pyritohedron to be formed at the highest degree of supersaturation and temperature, in metasediments or in sulphates. Octahedral pyrite is believed to represent the other extreme, for simple empirical reasons. The pure combination of pyritohedron and octahedron has never been observed, in contrast with the octahedron-cube or cube-pyritohedron or the exceptional cube-pyritohedron–octahedron combination. Furthermore, pure octahedra do not occur in metasediments, nor do pyritohedra in recent or relatively young sediments. This is consistent with the results of Sunagawa (1957), where cubic crystals grow under "unsuitable conditions".

These conclusions are supported by the joint occurrence of cube with pyritohedra and by the occurrence shown in Fig. 13. In this picture, in the centre of a lime concretion, octahedral pyrites were concentrated, but as sulphate sources became exhausted and alkalinity increased, so smaller corroded cubic crystals precipitated in the same pore space. According to White et al. (1991) the octahedral face may be formed entirely of either Fe or S_2 ions, whereas cube face dominates if these ions are in equal concentrations in solution. Maybe the latter is the case in carbonates, or during late diagenesis in pelitic sediments.

Summary

Sedimentary pyrite precipitates in a wide range of sedimentary environments from the time of sedimentation, through diagenesis, until metamorphism. In strictly anoxic, H_2S-bearing environments its synsedimentary formation results in homogeneously-dispersed framboids and euhedral crystallites. In dysoxic and oxic environments, equant, framboidal and euhedral pyrites concentrate in reducing microenvironments produced by organic substance during early diagenesis.

Microscopic framboidal and euhedral pyrites precipitate through monosulphide intermediates with slow, continuous, uninterrupted, surface-controlled crystal growth, in a pore space where the easily decomposable, dispersed organic matter derives the diffusive supply of sulphate from outer pores, if the internal sources are already exhausted. Despite their dissimilar shape the only difference between framboids and euhedra probably arises from the mineralogy of the preceding iron monosulphides. Greigite seems to be an exclusive precursor for framboid, while euhedral crystallites precipitate from amorphous monosulphide or mackinawite, perhaps as a result of increased alkalinity (due to previous sulphate reduction), or when the oxidizing agents required to form greigite were exhausted. Both explanations are supported by the subsequent mode of euhedral pyrite formation.

The coarser-grained, occasionally magnitudes larger, irregular crystals of equant pyrites precipitate directly from solution by diffusion-controlled crystal growth and by a variety of growth mechanisms. These required the decomposition of less reactive, larger and concentrated masses of organic matter, with sufficient iron and sulphate being supplied from external sources.

Precipitation is a long-term process, occasionally interrupted, repeatedly revived. The largest crystals may even displace the host-sediment. The late diagenetic overgrowth and replacement of framboids and euhedral pyrites by equant types are quite frequent.

Sedimentary pyrite formation usually takes place during early diagenesis, preceding significant burial and compaction, when pore systems should be

regarded as prevailingly open. Here microenvironmental changes may lead to the precipitation of the three main morphotypes in a 100 µm wide pore space. The general sequence of precipitation is framboidal to euhedral to equant but exceptions do exist. Since the preserved organic matter itself remains reactive to an advanced stage of burial, the formation of low-temperature authigenic pyrites continues during the late diagenesis despite their less-permeable pelitic host sediments.

The octahedron (and its combination with the cube) in both morphotypes are the most frequently observed forms of sedimentary pyrites, probably because they are dominant in the common, organic-rich pelitic sediments. Crystals with predominantly cubic faces are characteristic of alkaline calcareous sediments or sedimentary rocks of a higher diagenetic stage. Pyritohedra, and the combinations of pyritohedron and cube, observed in slightly metamorphosed sedimentary rocks or in sulphate evaporites, indicate the highest degree of supersaturation.

Acknowledgements

The author would like to thank his former boss Áron Jámbor for the inspiration, Robert Raiswell, Stuart D. Burley and Kevin G. Taylor for their helpful and constructive comments, Ildikó Tiefenbacher for typing and processing the manuscript, Bjørn Buchardt and Henrik Friis for providing a peaceful place for writing this paper in Copenhagen and Aarhus, respectively. Acknowledgement is made to the Hungarian Scientific Research Fund (OTKA Project 7373) for the partial support of the research. This paper is a contribution to the IGCP Project No 254. "Metalliferous black shales".

References

Altschuler, Z.S., M.M. Schnepfe, C.C. Silber, F.O. Simon 1983: Sulfur diagenesis in Everglades peat and origin of pyrite in coal. – Science, 221, pp. 221–227.

Amaro, D., S.E. Ho, D.I. Groves N.J. MCnaughton, N. Dahl, N.J. Poll, M.W. Grigson 1988: The use of pyrite as an indicator of Archaean gold mineralization processes: Examples from Western Australia. – Bicentennial Gold 88. Melbourne, pp. 82–87.

Amstutz, G. C. 1963: Accessories on pyrite, pyrite zoning, and zoned pyrite. – Schweiz. Min. Pet. Mitteilungen, 33, pp. 111–122.

Baird, G. C., C.E. Brett 1986: Erosion on an anaerobic seafloor: significance of reworked pyrite deposits from the Devonian of New York State. – Palaeo., 57, pp. 157–194.

Baxter, J. W., D.L. Reinertsen 1988: The minerals of Illinois: an overview. – Rocks and Minerals, 63, pp. 194–200.

Berner, R. A. 1969a: The synthesis of framboidal pyrite. – Econ. Geol., 64, pp. 383–384.

Berner, R. A. 1969b: Migration of iron and sulfur within anaerobic sediments during early diagenesis. – Am. J. Sci., 267, pp. 19–42.

Berner, R. A. 1984: Sedimentary pyrite formation: An update. – Geochim. Cosmochim. Acta, 48, pp. 605–615.

Binda, P.L., E.L. Simpson 1989: Petrography of sulphide-coated grains from the Ordovician Winnipeg Formation, Saskatchewan, Canada. – Eur. J. Mineral., 1, pp. 439–453.

Bonev, I. K., M. Reiche, M. Marinov 1985: Morphology, perfection and growth of natural pyrite shiskers and thin platelets. – Phys. Chem. Mineral., 12, pp. 223–232.

Brett, C.E., G.C. Baird 1986: Comparative taphonomy: A key to paleoenvironmental interpretation based on fossil preservation. – Palaios, 36, pp. 207–227.

Burley, S.D. 1984: Patterns of diagenesis in the Sherwood Sandstone Group (Triassic), United Kingdom. – Clay Minerals, 19, pp. 403–440.
Bush, J.B., D.R. Cook, T.S. Lovering, H.T. Morri 1960: The Chief Oxide-Burgin area discoveries, East Tintic district, Utah; A case history. – Econ. Geol., 55, pp. 1116–1147.
Carstens, H. 1986: Displacive growth of authigenic pyrite. – J. Sedim. Petrol., 56, pp. 252–257.
Coleman, M.L., R. Raiswell 1981: Carbon, oxygen and sulphur isotope variations in carbonate concretions from the Upper Lias of N.E. England. – Geochim. Cosmochim. Acta, 45, pp. 329–340.
Curtis, C.D., M.L. Coleman, L.G. Love 1986: Pore water evolution during sediment burial from isotopic and mineral chemistry of calcite, dolomite and siderite concretions. – Geochim. Cosmochim. Acta, 50, pp. 2321–2334.
Dana, E.S. 1903: The system of mineralogy of James Dwight Dana. – Wiley, New York, 84 pp.
Degens, E.T., H. Okada, S. Honjo, J.C. Hathaway 1972: Microcrystalline sphalerite in resin globules suspended in Lake Kivu, East Africa. – Mineralium Deposita, 7, pp. 1–12.
Demaison, G.J., G.T. Moore 1980: Anoxic environments and oil source bed genesis. – A.A.P.G. Bull., 64, pp. 1179–1209.
Dill, H., E. Kemper 1990: Crystallographic and chemical variations during pyritization in the upper Barremian and lower Aptian dark claystones from the Lower Saxonian Basin (NW Germany). – Sedimentology, 37, pp. 427–444.
Donelly, T.H., M.J. Jackson 1988: Sedimentology and geochemistry of a mid-Proterozoic lacustrine unit from Northern Australia. – Sedim. Geol. 58, pp. 145–169.
Endo, Y. 1978: Surface microtopographic study of pyrite crystals. – Bull. Geol. Surv. Japan, 29, pp. 701–764.
Farrand, M. 1970: Framboidal iron sulphides precipitated synthetically. – Mineralium Deposita, 5, pp. 237–247.
Goldschmidt, V. 1920: Atlas der Kristallenformen, Bd. 6, Markasit–Pyrit.– pp. 179–208. Carl Winters Universitätbuchhandlung, Heidelberg.
Goodfellow, W.D. 1987: Anoxic stratified oceans as a source of sulphur in sediment-hosted stratiform Zn–Pb deposits (Selwyn Basin, Yukon, Canada). – Chem. Geol., 65, pp. 359–389.
Hackley, K.C., T.F. Anderson 1986: Sulfur isotopic variations in low-sulfur coals from the Rocky Mountain region. – Geochim. Cosmochim. Acta, 50, pp. 1703–1713.
Hall, A.J. 1986: Pyrite-pyrrhotine redox reactions in nature. – Min. Mag., 50, pp. 223–229.
Hallberg, R.O. 1972: Iron and zinc sulfides formed in a continuous culture of sulfate-reducing bacteria. – Neues Jahrb. Min., 11, pp. 481–500.
Hámor, T., E. Hertelendi 1991: Relationship between the early diagenetic evolution of sediment and the delta ^{34}S values of sedimentary iron sulfides. – Bull. Hung. Geol Soc., 121, pp. 133–151.
Hansen, H J., R. Gwozdz, R.G. Bromley, K.L. Rasmussen, E.W. Vogensen, K.R. Pedersen 1986: Cretaceous-Tertiary boundary spherules from Denmark, New Zealand and Spain. – Bull. Geol. Soc. Denmark, 35, pp. 75–82.
Harding, S C., M.J. Risk1986: Grain orientation and electron microprobe analyses of selected Phanerozoic trace fossil margins, with a possible Proterozoic example. – J. Sedim. Petrol., 56, pp. 684–690.
Hartman, P. 1953: Relation between structure and morphology of crystals. – Crystallogr. Inst. Univ. Groningen, pp. 95–106.
Hayes, A. O. 1915 Wabana iron ores of Newfoundland. – Canadian Geol. Survey, Memoir 78, 163 pp.
Hudson, J.D. 1982: Pyrite in ammonite-bearing shales from the Jurassic of England and Germany. – Sedimentology, 29, pp. 639–667.
Kaplan, I R. 1983: Stable isotopes of sulfur, nitrogen and deuterium in recent marine environments. – In: Stable isotopes in sedimentary geology (Ed. by M. A. Arthur, T. F. Anderson, I. R. Kaplan and J. Veizer). SEPM Short Course Notes 10, pp. 157–265.

Kirchner, J.G. 1985: Detrital and authigenic pyrite in an Illinoisan lacustrine silt, Central Illinois. – J. Sedim. Petrol., 55, pp. 869–873.
Kirkpatrick, R.J. 1975 Crystal growth from the melt, a review. – Am. Mineral., 60, pp. 798–814.
Kortenski, J. 1989: Mineral composition, geochemical features and genesis of sulphide–carbonate concretions in Balkan Coal Basin. – Rev. Bulgarian Geol. Soc., L, pp. 100–108.
Larter, R C.L., A.J. Boyce, M.J. Russel 1981: Hydrothermal pyrite chimneys from the Ballynoe barite deposit, Silvermines County, Tipperary, Ireland. – Mineralium Deposita, 16, pp. 309–318.
Leventhal, J.S. 1983: An interpretation of carbon and sulphur relationships in Black Sea sediments as indicators of environments of deposition. – Geochim. Cosmochim. Acta, 47, pp. 133–138.
Loope, D.B., D.K. Watkins 1989: Pennsylvanian fossils replaced by red chert: early oxidation of pyritic precursors. – J. Sedim. Petrol., 59, pp. 375–386.
Love, L.G. 1957: Micro-organisms and the presence of syngenetic pyrite. – Geol. Soc. London Quart. J., 113, pp. 429–440.
Love, L.G., G.C. Amstutz 1966: Review of microscopic pyrite from the Devonian Chattanooga Shale and Rammelsberg Bamderz. – Fortschr. Miner., 43, pp. 273–309.
Love, L G., C.D. Curtis, H. Brockley 1971: Framboidal pyrite: morphology revealed by electron microscopy of external surfaces. – Fortschr. Miner., 48, pp. 259–264.
Love, L G., A.T.H. Al Kaisy H. Brockley 1984: Mineral and organic material in matrices and coatings of framboidal pyrite from Pennsylvanian sediments, England. – J. Sedim. Petrol., 54, pp. 869–876.
Mann, S., N.H.C. Sparks, R.B. Frankel D.A. Bazylinski H.W. Jannasch 1990: Biomineralization of ferrimagnetic greigite (Fe_3S_4) and iron pyrite (FeS_2) in a magnetotactic bacterium. – Nature, 343, pp. 258–261.
Maynard, J. B. 1980: Sulfur isotopes of iron sulfides in Devonian-Mississippian shales of the Appalachian Basin: Control by rate of sedimentation. – Am. J. Sci., 280, pp. 772–786.
McKibben, M.A., C.S. Eldridge 1989: Sulfur isotopic variations among minerals and aqueous species in the Salton Sea geothermal system: A SHRIMP ion microprobe and conventional study of active ore genesis in a sediment-hosted environment. – Am. J. Sci., 289, pp. 661–707.
Mitchell, R.S., W.P. Porter 1985: Pyrite Ooliths in Sandstone in the Cayuga Group (Silurian), Wise County, Virginia. – Rocks and Minerals, 60, pp. 179–181.
Murowchick, J.B., H.L. Barnes 1987: Effects of temperature and degree of supersaturation on pyrite morphology. – Am. Mineral., 72, pp. 1241–1250.
Ostwald, J., B.M. England 1979: The relationship between euhedral and framboidal pyrite in base-metal sulphide ores. – Min. Mag., 43, pp. 297–300.
Penick, D.A. Jr. 1987: Pyrite and other Minerals from Bargers Quarry, Lexington, Virginia. – Rocks and Minerals, 62, pp. 109–113.
Raiswell, R. 1982: Pyrite texture, isotopic composition and the availability of iron. – Am. J. Sci., 282, pp. 1244–1263.
Raiswell, R., R.A. Berner 1985: Pyrite formation in euxinic and semi-euxinic sediments. – Am. J. Sci., 285, pp. 710–724.
Renton, J.J., D.S. Bird 1991: Association of coal macerals, sulfur, sulfur species and the iron disulphide minerals in three columns of the Pittsburgh coal. – Int. J. Coal Petrol., 17, pp. 21–50.
Rhoads, D.C, J.W. Morse 1971: Evolutionary and ecologic significance of oxygen-deficient marine basins. – Lethaia, 4, pp. 413–428.
Rickard, D.T. 1970: The origin of framboids. – Lithos, 3, pp. 269–293.
Rickard, D.T. 1975: Kinetics and mechanism of pyrite formation at low temperatures. – Am. J. Sci., 275, pp. 636–652.

Ritger, S., B. Carson, E. Suess 1987: Methane-derived authigenic carbonates formed by subduction-induced pore-water expulsion along the Oregon/Washington margin. – Geol. Soc. Am. Bull., 98, pp. 147–156.

Rust, G.W. 1935: Colloidal primary copper ores at Cornwall Mines, Southeastern Missouri. – J. Geol., 43, pp. 398–426.

Sassano, G.P., K. Schrijver 1989: Framboidal pyrite: Early-diagenetic, late-diagenetic, and hydrothermal occurrences from the Action Vale Quarry, Cambro-Ordovician, Quebec. – Am. J. Sci., 289, pp. 167–179.

Schallreuter, R.1984: Framboidal Pyrite in Deep-Sea Sediments. – Initial Rep. D. S. D. P., 75, pp. 875–891.

Scheihing, M.H., H.J. Gluskoter, R.B. Finkelman 1978: Interstitial networks of kaolinite within pyrite framboids in the Meigs Coal of Ohio. – J. Sedim. Petrol., 48, pp. 723–732.

Schieber, J. 1989: Pyrite mineralization in microbial mats from the mid-Proterozoic Newland Formation, Belt Supergroup, Montana, U.S.A. – Sed. Geol., 64, pp. 79–90.

Schmitz, B., P. Andersson, J. Dahl 1988: Iridium, sulfur isotopes and rare earth elements in the Cretaceous-Tertiary boundary clay at Stevns Klimt, Denmark. – Geochim. Cosmochim. Acta, 52, pp. 229–236.

Schoonen, M.A.A., H.L. Barnes 1991: Reactions forming pyrite and marcasite from solution: II. Via FeS precursors below 100°C. – Geochim. Cosmochim. Acta, 55, pp. 1505–1514.

Shanks, W.C., J. Niemitz 1982: Sulfur isotope studies of hydrothermal anhydrite and pyrite, Deep Sea Drilling Project Leg 64, Guaymas Basin, Gulf of California. – Initial Rep. D.S.D. P. LXIV, pp. 1137–1142.

Smithson, F. 1932: The habit of pyrite in some sedimentary rocks. – Min. Mag., 31, pp. 314–319.

Strunz, H. 1986: Mineralien aus Nordost-Bayern: Skelett-Pyrite, Manganomelan, Huntite. – Aufschluß, 27, pp. 69–76.

Sultanov, A., V. Kovachev, S. Dzhurano 1989: The Upper Cretaceous iron-sulphide concretions in Northeast Bulgaria — structure, composition and genesis. – Rev. Bulgarian Geol. Soc., L, pp. 65–71.

Sunagawa, I. 1957: Variation in the crystal habit of pyrite. – Geol. Surv. Japan Rep., 175, pp. 1–47.

Sunagawa, I., Y. Endo N. Nakai 1971: Hydrothermal synthesis of framboidal pyrite. – Soc. Min. Geol. Japan, Spec. Issue, 2, pp. 10–14.

Sweeney, R.E. I.R. Kaplan 1973: Pyrite framboid formation: Laboratory synthesis and marine sediments. – Econ. Geol., 68, pp. 618–634.

Thomsen, E., T.O. Vorren 1984: Pyritization of tubes and burrows from Late Pleistocene continental shelf sediments off North Norway. – Sedimentology, 31, pp. 481–492.

Westgate, L.M., T.F. Anderson 1984: Isotopic evidence for the origin of sulfur in the Herrin (No.6) Coal Member of Illinois. – Int. J. Coal Geol., 4, pp. 1–20.

Whelan, J.F., R.O. Rye, W. De Lorraine, H. Ohmoto 1990: Isotopic geochemistry of a mid-Proterozoic evaporite basin: Balmat, New York. – Am. J. Sci., 290, pp. 396–424.

White, G.N. J.B. Dixon, R.M. Weaver, A.C. Kunkle 1991: Genesis and morphology of iron sulfides in gray kaolins. – Clay and Clay Minerals, 39, pp. 70–76.

Zelibor, J.L. JR., F.E. Senftle, J.L. Reinhardt 1988: A proposed mechanism for the formation of spherical vivianite crystal aggregates in sediments. – Sed. Geol., 59, pp. 125–142

Acta Geologica Hungarica, Vol. 37/1–2, pp. 183 (1994)

Book review

O'Brien, N.R., Slatt, R.M. 1990: Argillaceous rock atlas

Springer, New York etc. With 242 illustrations, 46 in full colour

"Kein dankbares Thema" ("a thankless subject matter") – Professor Hans Füchtbauer of Bochum, Germany, told me, expressing the general opinion of geologists some 15 years ago, when I showed him my very uniform-looking shale samples. At that time the X-ray diffraction method was considered to be the fundamental procedure for demonstrating any eventual variability in the composition of clayey rocks. The book of O'Brien and Slatt shows us that for fine-grained clastic rocks, not only their mineralogical composition but their texture can also show substantial variation, thus providing essential information on their depositional environment and diagenetic history.

Because of the very fine overall size pattern, scanning electron microscopy proved to be the most suitable tool for demonstrating the arrangement of the plate-like clay particles. They can have an essentially oriented structure or can feature a random distribution pattern. Similar differences can be observed at two successive levels of resolution, as indicated by petrographic microscope and X-ray radiography. It is essential to show extreme care during the preparation of samples, in order to assure the correct interpretation of the pictures taken by these techniques.

The Atlas offers the review of a great number of significant shale and mudstone formations of the world, including the most prominent hydrocarbon source rocks (such as the Kimmeridge Clay of England or the Monterey Formation of California). In each case, microtextural illustrations are interpreted with a brief summary of the geological setting, depositional environment and mineralogical composition as determined by X-ray diffraction. Special chapters are devoted to discussing textural features of shales caused by compaction and geopressure (i.e. pore fluid pressures which are greater than hydrostatic pressure).

In addition to textural descriptions, current classification schemes of clayey rocks are also represented. The last part of the Atlas consists of a compositional summary, specifying the average mineralogical composition of argillaceous rocks formed in different geological ages. According to the authors, however, this kind of statistical summary can only be applied on a limited scale to the drawing of general conclusions, for the distribution of rocks based upon their age and their environment of formation does not show any uniform pattern.

The Atlas is intended to be a sequel of the famous "Sedimentology of Shale" published by Potter et al. in 1980. The authors were able to demonstrate the progress achieved in this field, especially as far as the techniques of textural analysis and the interpretation of the depositional environment of argillaceous rocks are concerned. Their study seems to show promising results which can eventually bring a solution to a number of still unresolved problems, specified at the end of the book.

István Viczián

ERRATA

Regrettably, in the number 35/1 of Acta Geologica Hungarica a misprint occurred in the paper of Bérczi-Makk, A.: Midian (Upper Permian) foraminifera from the large Mihalovits quarry at Nagyvisnyó (North Hungary). On page 29, in the first paragraph, in the fifth line Azerbaidzhan is correct instead of Ukraine. Sorry for the error.

PRINTED IN HUNGARY
Akadémiai Kiadó és Nyomda, Budapest

GUIDELINES FOR AUTHORS

Acta Geologica Hungarica is an English-language quarterly publishing papers on geological topics. Besides papers on outstanding scientific achievements, on the main lines of geological research in Hungary, and on the geology of the Alpine–Carpathian–Dinaric region, reports on workshops of geological research, on major scientific meetings, and on contributions to international research projects will be accepted.

Manuscripts are to be sent to the Editorial Office for refereeing, editing, in two typewritten copies, on floppy disk with two printed copies, or by E-mail. Manuscripts written by the following word processors will be accepted: MS Word, WordPerfect, or ASCII format. Authors are requested to sign and send to the Editor a Publishing Agreement after the manuscript has been accepted by the Editorial Board. Acceptance depends on the opinion of two referees and the decision of the Editorial Board.

Form of manuscripts

The paper complete with abstract, figures, tables, and bibliography should not exceed 25 pages (25 double-spaced lines with 3 cm margins on both sides).

The first page should include:

- the title of the paper (with minuscule letters)
- the full name of the author
- the name of the institution and city where the work was prepared
- an abstract of not more than 200 words
- a list of five to ten key words
- a footnote with the postal address of the author

The SI (System International) should be used for all units of measurements.

References

In text citations the author's name and the year of publication between brackets should be given. The reference list should contain the family name, a comma, the abbreviation of the first name, the year of publication, and a colon. This is followed by the title of the paper. Paper titles are followed – after a long hyphen – by periodical title, volume number, and inclusive page numbers. For books the title (English version), the name of the publisher, the place of publication, and the number of pages should be given.

Figures and tables

Figures and tables should be referred to in the text. Figures are expected in the size of the final type-area of the quarterly (12.6 x 18.6) or proportionally magnified 20–25% camera ready quality. Figures should be clear line drawings or good quality black-and-white photographic prints. Colour photographs will also be accepted, but the extra cost of reproduction in colour must be born by the authors (in 1995 US$ 260 per page). The author's name and figure number should be indicated on the back of each figure. Tables should be typed on separate sheets with a number.

Proof and reprints

The authors will be sent a set of proofs. Each of the pages should be proofread, signed, and returned to the Editorial Office within a week of receipt. Fifty reprints are supplied free of charge, additional reprints may be ordered.

Contents

Book review

Acta Geologica Hungarica

VOLUME 37, NUMBERS 3–4, 1994

Akadémiai Kiadó, Budapest

ACTA GEOL. HUNG. 37(3–4) 187–374 (1994) HU ISSN 0236-5278

ACTA GEOLOGICA HUNGARICA

A QUARTERLY OF THE HUNGARIAN ACADEMY OF SCIENCES

Acta Geologica Hungarica publishes original studies on geology, crystallography, mineralogy, petrography, geochemistry, and paleontology.

Acta Geologica Hungarica is published in yearly volumes of four numbers by

AKADÉMIAI KIADÓ
Publishing House of the Hungarian Academy of Sciences

H–1117 Budapest Prielle Kornélia u. 19–35

Manuscripts and editorial correspondence should be addressed to the

ACTA GEOLOGICA HUNGARICA

Dr. János Haas
Academical Research Group, Department of Geology, Eötvös Loránd University of Sciences
H–1088 Budapest, Múzeum krt. 4/a, Hungary
E-mail: haas@ludens.elte.hu

Orders should be addressed to

AKADÉMIAI KIADÓ
H–1519 Budapest, P.O. Box 245, Hungary

Subscription price for Volume 37 (1994) in 4 issues US$ 84.00, including normal postage, airmail delivery US$ 20.00.

Acta Geologica Hungarica is abstracted/indexed in Bibliographie des Sciences de la Terre, Chemical Abstracts, Chemie-Information, Hydro–Index, Mineralogical Abstract

PRINTED IN HUNGARY
Akadémiai Kiadó és Nyomda, Budapest

Acta Geologica Hungarica, Vol. 37/3–4, pp. 187–234 (1994)

No. 343:
"Stratigraphic Correlation of Epicratonic Peritethyan Basins"

Triassic facies types, evolution and paleogeographic relations of the Tisza Megaunit

Marcian Bleahu,
Ecological University, Bucharest

János Haas, Sándor Kovács, Csaba Péró
Geological Research Group, Eötvös Loránd University Budapest

Gheorghe Mantea, Sever Bordea, Ştefana Panin
Geological Institute of Romania, Bucharest

Anikó Bérczi-Makk
MOL Plc. Oil & Gas Laboratories, Budapest

Mihai Ştefănescu
Amoco Romania Petroleum Company, Bucharest

Gyula Konrád, Elemér Nagy, Erzsébet Rálisch-Felgenhauer
Hungarian Geological Survey, Budapest

Kresimir Sikić
Geological Institute, Zagreb

Ákos Török
Department of Engeneering and Geology, Technical University, Budapest

The Triassic facies patterns of the Tisza Megaunit bear witness to a transgression from S to N, i.e. from a southerly-lying open sea towards a northerly-lying continental hinterland. The distribution of the different facies is shown on fact maps and facies reconstructions for four major events of the Triassic sedimentary evolution: Upper Scythian (redbed stage and early stage of transgression), late Lower Anisian–early Middle Anisian ("Upper Wellenkalk", preceding the formation of intrashelf basins), Ladinian (Wetterstein platform stage) and Carnian–Norian in general (Keuper stage and Dachstein platform stage, respectively). These facies patterns prove that the block of the Tisza Megaunit was located on the North Tethyan margin adjacent to Europe in the Triassic, and was part of the Austroalpine domain which was deformed in Cretaceous.

Key words: Triassic, Tisza Megaunit, stratigraphy, facies, paleogeography, Carpatho-Pannonian region, Croatia, Hungary, Romania, Yugoslavia

Addresses: M. Bleahu: Ro–70119 Bucuresti, str. Dem. I. Dobrescu Nr. 4–6. Sect. 1, Romania
Gh. Mantea, S. Bordea, Şt. Panin: Ro–78344 Bucureşti, 32. Str. Caransebeş Nr. 1, Romania
M. Ştefănescu: Hotel Diplomat, Suite 201, 13–17. Sevastopol str. Bucuresti, 1, Romania
K. Sikić: 41000 Zagreb, Sachsova 2, Croatia
J. Haas, S. Kovács, Cs. Péró: H–1088 Budapest, Múzeum krt. 4/A, Hungary
A. Bérczi-Makk: H–1039 Budapest, Batthyányi u. 45, Hungary
Gy. Konrád, E. Nagy, E. Rálisch-Felgenhauer: H–1143 Budapest, Stefánia út 14, Hungary
Á. Török: H–1521 Budapest, Stoczek u. 2, Hungary
Received: 13 May, 1993

0236–5278/94/$ 5.00

Introduction

New investigations on surface outcrops of the Tisza Megaunit (Apuseni, Mecsek–Villány and Papuk Mts) and the rapidly increasing amount of borehole data (for summary see Bérczi-Makk 1986; Čanović and Kemenci 1988) made it possible to outline the distribution of Triassic facies types and the sedimentary evolution of the Tisza Megaunit. The present work is a late contribution to the topic of IGCP Project No. 198 ("Evolution of the Northern Margin of Tethys") and also to a new project No. 343 ("Stratigraphic Correlation of Epicratonic Peritethyan Basins") by geologists from three (more recently four) countries having worked on different parts of the megaunit. The Northern Bačka–Northern Banat region is described in more details in a separate contribution (Kemenci and Čanović, in press)

Boundaries and tectonic–facial subdivision of the Tisza Megaunit

The Tisza Megaunit (or "South Pannonian microplate" in sense of Balla 1982) constitutes the pre-Neogene basement of the southeastern half of the Pannonian Basin. The term was introduced by Fülöp et al. (1987) instead of the former "Tisia" proposed by Prinz in 1926 (see in Balogh 1972 and in Kovács 1982) of similar sound but having a very different connotation (for discussions see Fülöp et al. 1987; Fülöp 1989). The Tisza Megaunit, as shown in Fig. 1, is bordered on the NE by the Mid-Hungarian (cf. Szepesházy 1975; Fülöp et al. 1987) or Zagreb–Zemplín (cf. Grecula and Varga 1979) Lineament. To the NE the boundary is formed by the intermittent occurrences of the Pieniny Klippen Belt as far as Poiana Botizei (cf. Săndulescu et al. 1981; Săndulescu 1980). The eastern boundary is somewhat obscure, being hidden by the Tertiary fill of the Transylvanian Basin. Nevertheless, a few borehole data and geophysical interpretations indicate the presence of East Carpathian units in the basement of the basin (Săndulescu and Visarion 1978). Along the SE the megaunit is thrust over by the Mureş Ophiolite Belt (units of the Metaliferi Mountains), which forms the direct continuation of the innermost Vardar Subzone, of the Šumadija Zone (cf. Anđelković and Lupu 1967). To the south, the basement nappes of the megaunit, with thick pre-Alpine crystalline complexes, face the Inner Dinaric Ophiolite or Vardar units. Their boundary, according to borehole data, runs in a E–W direction in the central part of the Vojvodina (cf. Kemenci and Čanović 1975; Čanović and Kemenci 1988); further to the west, the border is formed by the Sava Lineament as far as Zagreb.

According to the structure of the outcrops in the Apuseni Mts (cf. Bleahu 1974, 1976; Ianovici et al. 1976; Istocescu and Dragastan 1978; Bleahu et al. 1981) and to borehole and seismic data, respectively, from the pre-Neogene basement of the Great Plain (cf. Istocescu and Ionescu 1970; Bérczi-Makk 1986; Balázs et al. 1986; Fülöp et al. 1987; Pap 1987, 1990; Grow et al. 1989, 1994; Kemenci 1991), the Tisza Megaunit is made up of basement nappe systems overthrust with northern vergency during the Cretaceous Austroalpine tectogenesis (Austrian, resp. Subhercynian tectonophases).

Views about the extent, boundaries and geotectonic role of the large unit presently called the "Tisza Megaunit" (or "Tisia terrane" in terms of the allochthonous terrane concept) have, however, basically changed in the last quarter century.

For a long time the pre-Neogene basement of the Great Plain, along with the surface outcrops of the Mecsek and Villány Mts, was considered as a rigid, cratonic median massif, the "Internide" of the Carpathian orogenic chain (for a historical review about this period see Balogh 1972). It was even recently considered as the rigid background ("Pannonian Median Massif") for the overthrusting of the Carpathian nappes and as the most internal zone of the West Carpathians (cf. Maheľ 1984, 1986; described as "Hungarian Massif" or "Tissia").

The recognition of its anomalously thin crust (Szénás 1968) and of the continuation of the structural–facial zones of the Apuseni Mts in the basement of the Great Plain, as far as the Mecsek and Villány Mts (Patrulius et al. 1971; Bleahu 1976, and in Ianovici et al. 1976; Patrulius 1976, and in Ianovici et al. 1976; Dimitrescu 1981), verified by an increasing number of deep-drilling data (Balázs et al. 1986; Bérczi-Makk 1986; Pap 1987, 1990; Kemenci 1991, shown on the maps by Fülöp and Dank et al. 1987; Dank and Fülöp et al. 1990) have, however, placed severe doubt upon its role as a median craton. Instead, it has been revealed that it represents an integral part of the Austroalpine orogenic domain, and that the classical "internide" concept should be completely abandoned. Applying the new mobilistic approach, Channel and Horváth (1976) considered first this unit as the "Tisia microplate", practically with the same extent and boundaries as the "Tisza Megaunit" is considered to have at present (cf. Fülöp 1989).

Independently of the experiences of the oil and gas exploration in the basinal areas, facies and structural characteristics of the Northern Apuseni Mountains permitted the recognition that it belongs to the Austroalpine orogeny, showing many common features with the Eastern Alps and West Carpathians (cf. Săndulescu 1972, 1975; Bleahu 1976; Patrulius 1976; and in Ianovici et al. 1976; Bleahu et al. 1981). Thus, this Austroalpine-type domain has been distinguished as the most internal part of the Carpathians in respect to the Outer Dacides and Median Dacides, as "Inner Dacides" (Săndulescu 1980, 1984b). Subsequent evaluation (Fülöp et al. 1987), connected also to terrane analysis (Csontos et al. 1992), have revealed the heterogeneity of this Inner Dacidic–Inner Carpathian–Pannonian ensemble. Recently three main units have been distinguished for this area (cf. partly also Kázmér 1986; Császár et al. 1990) which can be considered as main allochthonous terranes (see Fig. 1).

1. Inner West Carpathian or Tatro–Veporic Megaunit (=Slovakia terrane according to Plašienka 1991), between the Pieniny Klippen Belt and the Rába–Hurbanovo–Lubeník–Margecany lineament;

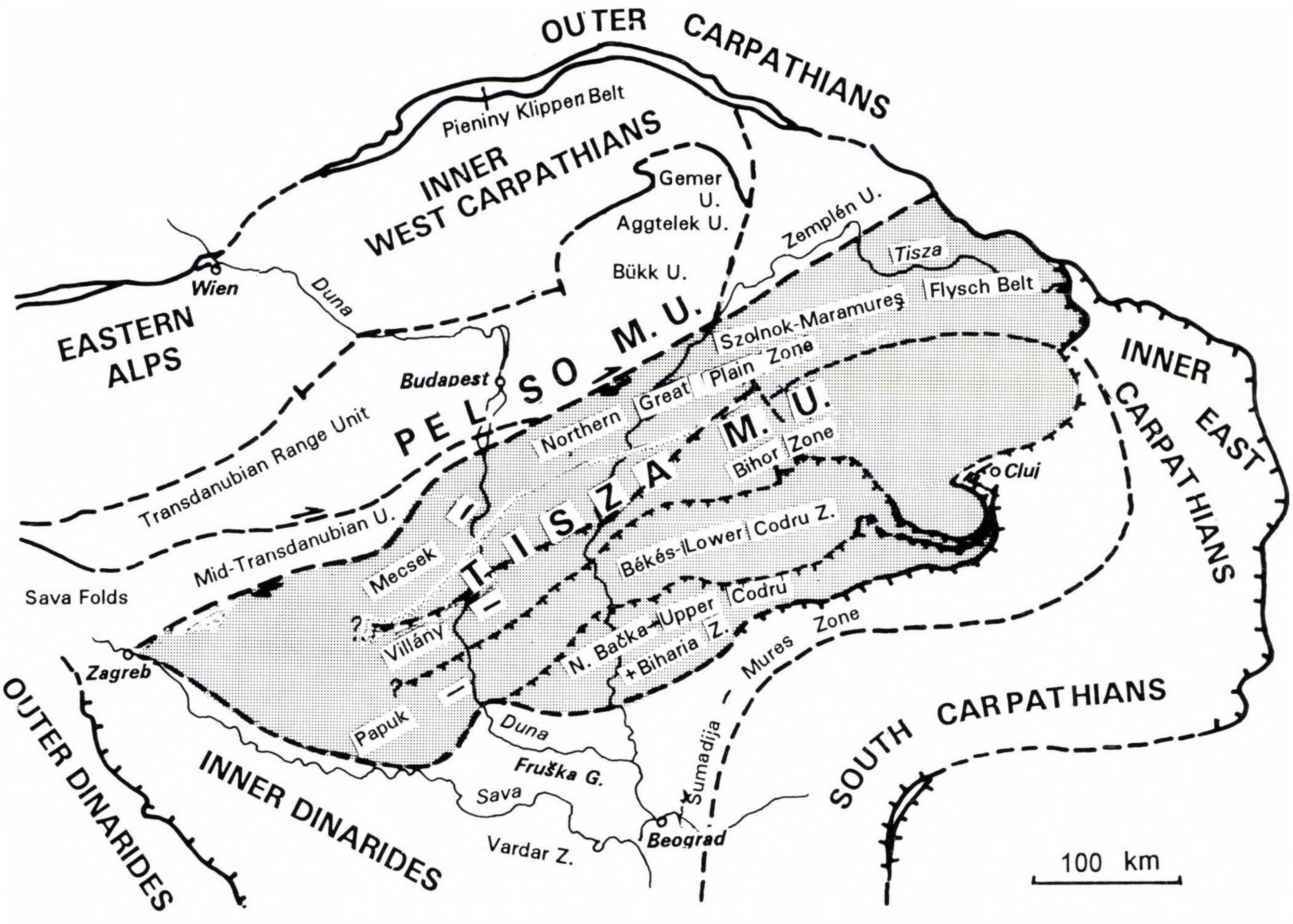

Fig. 1
Tectonic sketch of the Carpatho–Pannonian region, showing the position and tecto-facial zones of the Tisza Megaunit

2. Pelso Megaunit (Fülöp et al. 1987; Fülöp and Dank et al. 1987) between the Rába–Hurbanovo–Lubeník–Margecany (or Rába–Hurbanovo–Diósjenő: opinions are still varied) lineament and the Mid-Hungarian lineament; a composite terrane containing smaller terranes of mostly South Alpine–Dinaric origin (cf. also Haas et al. in print);

3. Tisza Megaunit (Fülöp et al. op. cit.) or "Tisia terrane" on the southern side of the Mid-Hungarian (or "Zagreb–Zemplín") lineament. Its extent and boundaries are described above (Fig. 1).

The thick polymetamorphic pre-Alpine complex of the Tisza Megaunit (within which considerable differences in metamorphic facies suggest also significant overthrustings; cf. Dimitrescu 1981; Szederkényi 1984; Szederkényi et al. 1991; Fülöp 1994); are overlain either by Late Paleozoic continental molasse sequences, deposited in intramontane basins, with bimodal volcanism, or the Mesozoic sedimentary cover rests directly on the metamorphic rocks. Based on the Mesozoic facies types, the following tecto–facial zones can be distinguished within the megaunit (see Fig. 1).

1. Mecsek–Northern Great Plain zone
2. Villány–Bihor zone
3. Papuk–Békés–Lower Codru zone
4. Northern Bačka–Upper Codru zone

The boundaries of the pre-Alpine metamorphic zones and of the Mesozoic facies zones do not necessarily coincide (cf. Balázs et al. 1986; Bérczi-Makk 1986).

The Upper Codru Nappes in the Apuseni Mountains are overthrust by the basement nappes of the Biharia Nappe System, the Mesozoic cover of which is unknown. Their corresponding crystalline rocks are also known from boreholes in Northern Bačka and Northern Banat (Kemenci 1991).

The *Mecsek–Northern Great Plain zone* (named in Bérczi-Makk 1986 as "Nagykőrös–Debrecen belt" for the Hungarian part of the Great Plain area) is characterized by the most proximal (nearest to the continental hinterland) type of Triassic, overlain by coal-bearing Liassic Gresten Facies, a thick "Fleckenmergel" sequence, deep-water carbonatic – siliceous late Dogger and Malm with basic volcanics (resembling the sedimentary sequence of the Pieniny Succession of the Klippen Belt; Birkenmajer, pers. comm.) and Lower Cretaceous basic volcanics.

The zone towards the NE constitutes the basement of the Late Cretaceous to Paleogene Szolnok–Maramureş Flysch Belt. Triassic rocks, however, are unknown below the flysch; even in the Hajdúszoboszló–Ebes region, the Liassic Gresten facies appears to directly overlie the crystalline basement (Szepesházy 1972). Basic volcanic and radiolaritic rocks found in several boreholes in Transcarpathia (Dolenko et al. 1976, 1981) are also considered to represent the continuation of this zone; such rocks of Middle–Upper Jurassic and Lower Cretaceous age are common in the basement of the Szolnok Flysch Zone (Bérczi-Makk 1986) and in the southwestern continuation of the zone. In Transcarpathia the mentioned rocks of related features but with no dating were supposed by several authors (e.g. Dolenko et al. op. cit) to be of Triassic age, and to represent remnants of Transylvanian nappes. Herein the alternative interpretation is put forward that they form the continuation along strike of the Mecsek–Northern Great Plain zone; however, the determination of their exact age and affiliation is indispensable.

The northeastern part of the zone is bordered on the south by the North Transylvanian (Somes) Fault against the mass of the Apuseni Mts. Bending to the SW, the continuation of the fault-line borders the Szolnok Flysch zone along its SSE edge. In the Transdanubian sector of the Tisza Megaunit the so-called "Mecsekalja" (=Foot of Mecsek) Lineament separates the Mecsek and Villány zones (Nagy 1969); it is considered to be a Variscan strike-slip zone (Szederkényi 1984) rejuvenated by younger movements. Further southwestern continuation of this boundary (as well as of the two zones discussed) in the basement of the Drava Basin is unclear.

The *Villány–Bihor zone* (named in Bérczi-Makk 1986 as "Bácska–Körös belt" for the Hungarian part of the Great Plain area) is also characterized by proximal-type Triassic of the Carpathian Keuper main facies zone. Locally, various hiatuses between the Middle Triassic and the Upper Dogger formation, carbonate platform facies in the Malm, Urgon-type Lower Cretaceous with bauxites and Albian flysch-type formations (Ianovici et al. 1976; Császár and Haas 1984; Császár and Haas et al. 1984; Baltreş and Mantea in press; Császár pers. com.) are also characteristic of this zone. The southern border of the zone is actually the front of the Lower Codru Nappes ("Békés Line" Fülöp et al. 1987). The entity of the Villány–Bihor zone was the first to be recognized among the tectofacial zones discussed here (see in Patrulius et al. 1971, p. 51).

Whereas the Bihor Unit, of large surficial extent, represents the "para-autochthone" (Săndulescu and Visarion 1978; Dimitrescu 1981) of the Apuseni Mts, the much smaller Villány Mts are made up by five overthrust scales (E. Nagy and I. Nagy 1976). Considerable facies differences in the Lower Cretaceous sequences of the latter may indicate that the amplitude of overthrusts might be of nappe dimensions (Császár 1992). The whole Villány Unit may even represent a nappe thrust over the Mecsek Unit. However, there are many similarities between the Lower and Middle Triassic rocks of the two mountain ranges, and transitional sequences were encountered in boreholes drilled in the area between them. Thus, a unified formation-rank lithostratigraphic subdivision has been proposed for the two units (Rálisch- Felgenhauer, in press; see Figs 21, 22).

The continuation of this zone under the Drava Basin is also problematic. It should be stressed, however, that in spite of different Mesozoic covers, the crystalline pre-Alpine basement complexes of the Papuk–Psunj Mts and of the Mecsek–Villány area (the latter known mostly from boreholes) show close similarities (cf. Pamić 1986).

The *Papuk–Békés–Lower Codru zone* (named in Bérczi-Makk 1986 as "Szeged – Békés belt" for the Hungarian part of the Great Plain area) is characterized by a predominantly dolomitic Middle–Upper Triassic development, corresponding (in facial position) to the Alpine "Hauptdolomit" facies zone; it thus represents the middle shelf domain. It should be stressed, however, that the true Alpine-type bituminous, cyclic "Hauptdolomit" is not known in the Tisza Megaunit and in the Apuseni Mts, where, due to the formation of the large Roşia intrashelf basin, the Triassic facies zones were shifted much more towards the continental hinterland than in the Eastern Alps and West Carpathians, respectively (see below). For this reason, among the Lower Codru Nappes only the Corbeşti outlier, assigned to the Arieşeni Nappe by Patrulius et al. (1979), or to the Finiş Nappe by Baltreş and Mantea (in press) corresponds to this dolomitic facies zone. Jurassic and Cretaceous rocks are poorly known, with the exception of the lowermost Vălani Nappe, the sequence of which is still closely related to that of the Bihor Unit. Characteristic development in this zone is the uppermost Jurassic to lowermost Cretaceous marly–shaly flysch-type sequence with Calpionellids, being present in the Finiş, Şeasa and Dieva Nappes (though the latter is attributable to the Upper Codru Nappes based on its Triassic sequence), in the Békés Unit (called here the Pusztaszőlős Marl Fm.) and also in the Papuk Mts.

The *Northern Bačka–Upper Codru zone*, at the southeastern margin of the Tisza Megaunit, is made up by outer shelf and shelf-margin type Middle and Upper Triassic sequences, with pelagic influence ("Wandkalk", "Schreyeralm–Hallstatt" limestones). It represents the Alpine Dachstein Limestone facies zone and includes the Dieva, Moma, Vaşcău and Coleşti Nappes in the Northern Apuseni Mts and Mesozoic basement of the northern part of the Vojvodina (or of Northern Bačka–Northern Banat). Jurassic rocks are mostly red pelagic limestones (usually as fissure fillings).

Facies distribution

The distribution of Triassic facies in the Tisza Megaunit is discussed below according to major stages of sedimentary-basin evolution. The stratigraphic columns of each tectonic units (Figs 1 and 2 respectively) are shown on Figs 3–20. Schematic facies reconstructions are made for four different evolutionary stages displaying the most characteristic facies patterns, together with the corresponding fact maps showing documented occurrences (Figs 23–30). These maps are generalized for certain time intervals because of scarcity or lack of detailed age data (this especially concerns the age of "Keuper" sediments within the Middle Carnian–Norian interval).

The borehole data concerning the Mecsek–Northern Great Plain and Villány–Bihor zones in the basement of the Great Plain are mentioned in the present paper only in cases where they differ from the development of the outcropping sequences; otherwise we only refer to the paper by Bérczi-Makk (1986).

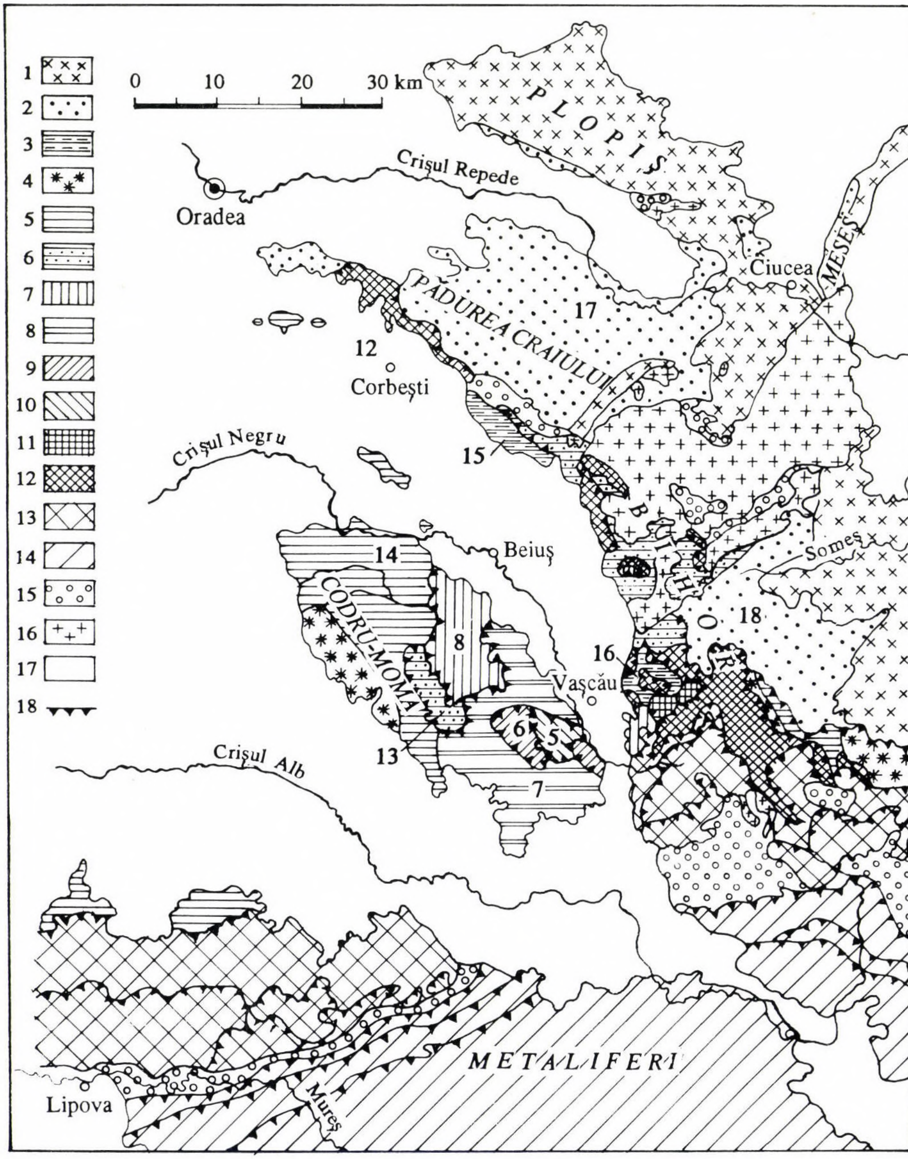

Fig. 2

Tectonic sketch of western part of the Apuseni Mts, with location of the reference sections (numbers are identical with figure numbers). *Northern Apuseni:* 1. Bihor Unit, cristalline basement; 2. Bihor Unit, Permomesozoic formations; 3. Vălani Nappe; 4. Finis–Gârda Nappe, crystalline basement; 5. Finis–Gârda Nappe, Permomesozoic formations. 6. Şeasa–Ferice Nappe; 7. Dieva–Bătrânescu Nappe; 8. Moma Nappe; 9. Vaşcău Nappe, 10. Coleşti Nappe. 11. Urmat and Vetre Nappes. 12. Arieşeni Nappe; 13. Biharia Nappe System; *Southern Apuseni*: 14. Metaliferi Nappe System; *Posttectonic formations:* 15. Senonian basins in Northern Apuseni; 16. Subhercynian and Laramian magmatites; 17. Neogene and younger formations (sedimentary formations and volcanics); 18. nappe boundaries

Besides the published materials (and in a few cases, unpublished research reports) mentioned in the text, our correlation is based furthermore on the following geological maps and excursion guides, as factual materials.

Geological maps:

Northern Apuseni Mts: Bleahu et al. 1979; Bleahu et al. 1980; Bleahu et al. 1981; Bleahu et al. 1984; Bleahu et al. 1985; Bordea et al. 1986; Bordea et al. 1988; Dimitrescu et al. 1977; Giuşcǎ and Bleahu 1965, 1967a, b; Mantea et al. 1987; Marinescu et al. 1982; Papaianopol et al. 1977; Patrulius et al. 1973; Rusu et al. 1977; Săndulescu et al. 1978; Ştefan et al. 1974.

Mecsek and Villány Mts: Chikán et al. 1984; Hetényi et al. 1982; Rakusz and Strausz 1953.

Excursion guides:

Northern Apuseni Mts: Bleahu et al. 1981; Patrulius et al. 1971; Patrulius et al. 1979.

Mecsek and Villány Mts: Császár et al. 1984; for key sections: Rálisch-Felgenhauer 1985a, b, 1986a, b, 1987a, b, c, d, 1988a, b, c, d, e, f.

Scythian: the continental redbed ("Buntsandstein") stage

In the classical Alpine (s.l.) Triassic the Scythian was the time of gradual transgression. While the innermost zones already belonged to the marine domain from the beginning of the Early Triassic, the external zones (with the exception of the outermost ones, which became parts of the Vindelician Ridge or its equivalents) had only been transgressed by the sea in the earliest Anisian. The continental redbeds are grouped into the "Alpiner Buntsandstein" megafacies, and the marine units into the "Werfen megafacies" ("Werfener Schichten") (cf. Tollmann 1976; Bystrický 1972, 1973). Their boundary is time-transgressive, showing gradual landward shifting.

The Early Triassic transgression reached only the southernmost zones of the Tisza Megaunit.

In the Northern Bačka–Upper Codru zone, marine Scythian sediments were found in a number of boreholes in the Northern Bačka and Northern Banat areas in the Vojvodina, and in the Dieva Nappe of the Codru-Moma Mts. In Northern Bačka and Northern Banat the Scythian ("Palić Series") is represented by a lower quartz sandstone–arkose sequence, and an upper siliciclastic–carbonatic one consisting of sandstones, siltstones, shales, marls, marly limestones and dolomites. The latter unit contains the Scythian foraminifer index species *Meandrospira pusilla* as well as other foraminifers and Myophoria-type bivalve shells. Fossil-free evaporite-bearing sequences ("Crna Bara Series") assigned to the Lower Triassic were found in two boreholes (for details see Kemenci and Čanović 1975; Čanović and Kemenci 1988; Kemenci and Čanović in press).

In the highest Codru Nappes (Vaşcău, Coleşti), the Scythian is not preserved. In the Dieva and Moma Nappes it can be subdivided into a lower, continental

"Werfen Quartzite" unit (="Alpiner Buntsandstein") and an upper, shallow marine "Werfen Shale" unit. In the latter, the Late Scythian index ammonite *Tirolites* sp. was found in the Dieva Nappe (Bleahu in Patrulius et al. 1979), whereas in the Moma Nappe *Costatoria costata* occurs (Ianovici et al. 1976; Patrulius et al. 1979). This bivalve may, however, range into the Lower Anisian, as well.

In the Papuk Mts the Lower Triassic is also bipartite. The lower unit consists of purple and white quartzites directly overlying the pre-Alpine granitic and metamorphic rocks, whereas the upper one is composed of "Werfen Shales" with marine macrofauna (mostly bivalves; Šikić 1975).

In the remaining part of the Tisza Megaunit the Scythian is continental, mostly fluviatile and deltaic, in part limnic (Patrulius et al. 1979; Bérczi-Makk 1986; Mader 1992; Barabás-Stuhl in press). Sediment transport directions and micromineralogical investigations indicate that the coarse-grained sediments (purplish-red, subordinately whitish quartzitic sandstones with conglomerate horizons; called "Jakabhegy Sandstone Formation" in the Mecsek, Villány and Békés zones or "Werfen Quartzite" in the Apuseni Mts, both correspond to the "Alpine Buntsandstein" megafacies) were transported southward from a northerly- located granitic-metamorphic source (cf. Nagy 1968, and in Kovács et al. 1988 for the Mecsek Mts, Popa 1981 for the Apuseni Mts). The age of the Jakabhegy Sandstone does not include the entire Scythian. In the Villány and Békés zones it overlies older Permian molasse (with a considerable hiatus) or pre-Alpine metamorphic and granitic rocks. On the other hand, in the Mecsek Mts the uppermost, grey sandstone member of the Kővágószőlős Sandstone Formation (Upper Permian for the most part) ranges up into the basal Triassic (Barabás-Stuhl 1981) and the Jakabhegy Sandstone overlies the latter with a basal conglomerate (the so-called "main conglomerate"). Only the uppermost part of the Jakabhegy Formation contains sporomorphs, which point to the Late Scythian *Densoisporites nejburgii* zone (Barabás-Stuhl 1981, 1993). The same palynozone (Antonescu et al. 1976) associated with *Triadispora crassa* zone has been detected in the marly shales of the Vălani Nappe (Antonescu et al. 1976; Antonescu, in Patrulius et al. 1979).

Early–Middle Anisian: the initial platform stage

By the Early Anisian all the external zones of the Alpine (s.l.) Triassic (with the exception of the Vindelician Ridge and its equivalents) were flooded by the sea. During this initial stage, the entire Tisza Megaunit became a carbonate shelf domain (with the possible exception of its northeastern marginal part, which may have remained emerged; Fig. 26).

Differentiation of this huge, mostly dolomitic ramp began in the Late Anisian (or in some areas probably in the latest Middle Anisian), and resulted in the formation of intrashelf basins, reef belts and back-reef lagoons. The reconstruction on Fig. 26 attempts to show the facies setting just prior to the differentiation. According to palynobiostratigraphic data the Villány–Bihor and Mecsek–Northern Great Plain zones were certainly not submerged before the Anisian. The lowermost Anisian fine detrital sequence (called Patacs Formation in the Mecsek and Villány Mts, and "Werfen Shales" in the Apuseni Mts), consisting of alternating red, subordinately greenish, fine-grained sandstones, siltstones and mudstones, with evaporitic intercalations in the higher part, reflects deposition in a flood plain to coastal lagoon environment. The "Werfen Shales" of the Lower Codru Nappes are also (or partly) of Early Anisian age.

The lowermost Anisian sequence of the Mecsek Mts shows a classical example of the gradual transgression changing from a purely siliciclastic depositional regime (Patacs Fm.), through a hypersaline lagoonal one (Magyarürög Evaporite Mb.), with decreasing clastic input into a carbonatic one (Hetvehely Dolomite Mb. and Viganvár Limestone Mb., the latter containing *Costatoria costata*). In the Villány Mts the Patacs Fm. is much thinner, and above the evaporitic member (Vokány Mb., which is considerably thicker than the Magyarürög Mb. in the Mecsek Mts), the basal part of the Rókahegy Dolomite Formation seems to replace the dolomitic and limestone members of the Mecsek Mts. (For detailed descriptions see Rálisch-Felgenhauer, in press; Rálisch-Felgenhauer and Török, manuscript) All these transitional, partly evaporitic units correspond to the Germanic "Röt" (occurring between the "Buntsandstein" and the "Muschelkalk") and indicate sabkha sedimentary environment.

After this sabkha stage in the northern zones, the entire Tisza Megaunit was subjected to carbonate shelf deposition. An outer shelf domain with a well-oxygenated lagoonal zone on the southeastern margin of the Tisza Megaunit is indicated by the algal Steinalm Limestone Formation of the Vaşcău nappe, with abundant, typical Anisian dasycladaceans in its upper part (*Physoporella pauciforata, Oligoporella pilosa* etc. Bleahu et al. 1972) and with the index foraminifer species *Meandrospira dinarica*. According to Alpine analogies, Gutenstein-type carbonates may be expected in its underlier; however, the deeper parts of the sequence of the nappe have been detached. On the other hand, the unusual thickness of the Steinalm Formation here (around 500 m), as compared with that in the Eastern Alps and West Carpathians (usually not more than 150–200 m), may indicate a replacement of a part of the Gutenstein Fm. In the Northern Bačka–Northern Banat area no borehole data are available to provide information for extension of Anisian platform carbonates.

The sedimentary environments of the two deeper Upper Codru Nappes (Dieva, Moma) and of the Papuk–Békés–Lower Codru zone were part of the huge dolomitic ramp built in the middle shelf zone during the entire Early and Middle Anisian (with the possible exception of the Lower Codru Units during the earliest Anisian; see above). In the Codru Nappes, two types of Anisian dolomites can be distinguished. The thick bedded to massive, coarse-grained, grey Sohodol Dolomite is considered to have been deposited on intermittently emergent shoals, while the medium to thin-bedded, finer-grained, dark grey to black Bulz Dolomite was formed in euxinic lagoons interspersed between the former (Patrulius et al. 1979). The dark grey dolomites of the Békés Basin (Szeged Dolomite Fm.) can be compared with the latter. Borehole documentations reported porphyrites in association with dolomites from one well (Csanádalberti). That was why Bérczi-Makk (1986, pp. 276 and 277, Fig. 7) mentioned and illustrated a porphyrite intercalation in the dolomite sequence. Revision of the cores has shown that these volcanics are, in fact, Miocene rhyolitic or dacitic tuffs at the base of the Neogene basin fill, resting on dolomite debris, probably also of Miocene age (Nusszer 1984; Bérczi-Makk 1987; and unpublished research reports).

In the western and eastern parts of the Papuk Mts the Upper Scythian Werfen Shales are overlain by dark grey to black, thickly bedded limestones, in some places with vermicular and megabreccia horizons (best comparable with the Alpine Annaberg Limestone). These are followed by light-coloured, thickly bedded dolomites. In the central part of the mountains, strongly tectonized Anisian rocks are represented by brecciated, rauhwacke-like, black Gutenstein-type dolomite, then by light-coloured, also brecciated, dolomites.

The Anisian dolomitic shelf deposits of the Villány–Bihor zone overlying the lowermost Anisian evaporite-bearing, fine detrital rocks are not as uniform as those of the Codru Nappes. In most areas of the Bihor Unit, the Crişul Repede Formation is divided by the dark-coloured Bucea Limestone into a Lower Dolomite member, dark grey in colour, and an Upper Dolomite one, which is light-coloured. The Padiş–Călineasa Fm. (new formation), recognized in the Vlădeasa–Bihor Mts, is made up of an alternation of grey dolomites and grey to black vermiculated limestones of Bucea-type (Baltreş and Mantea in press). The Lower Dolomite is medium-bedded and finer-grained than the upper one. It contains dark limestone intercalations with pseudomorphs after gypsum, indicating a hypersaline depositional environment. Crinoids (Dadocrinus) are characteristic in some places. The dark grey, usually vermicular Bucea Limestone indicates a sheltered, restricted lagoon environment, and represents a unit similar to the vermicular limestones of the adjacent Mecsek–Northern Great Plain zone. In the lower part it still contains *Costatoria costata*, while in the top part a bioclastic limestone horizon, with *Meandrospira dinarica* and a characteristic Anisian Dasycladacean flora (*Physoporella pauciforata, Oligoporella pilosa*, etc. Popa and Dragastan 1973; Popa 1981) occurs. Crinoids (Dadocrinus) may occur throughout it. The Upper Dolomite is thickly bedded to massive, coarse-grained and contains dolomitic limestone intercalations with a Dasycladacean assemblage (*Diplopora annulata* together with *D. annulatissima*), constraining it to a latest Anisian age. In the Villány Mts the Rókahegy Dolomite corresponds in its position to the Lower Dolomite, and the Gyüd Limestone to the Bucea Limestone of the Bihor Unit. The former is a greyish-brown, partly yellow or reddish coloured, thin bedded, often laminated dolomite, with ooidal and peloidal intercalations.

The Gyüd Limestone, in its lower part, is thin-bedded, with dolomite intercalations; higher up it is generally vermicular and becomes thickly bedded in its uppermost part. Its colour becomes lighter up sequence, being grey in the lower part, often with a greenish shade, passing to pinkish and light grey higher up. Encrinites and laminated intercalations may also occur. Characteristic fossils are bivalves (*Entolium discites* etc.) and crinoids (*Dadocrinus gracilis, Encrinus liliiformis*).

The "Muschelkalk" sequence of the Mecsek Mts also begins with dolomites: the Vöröshegy Dolomite, consisting of red, pinkish or yellowish dolomites, dolomitic marls and rarely, clayey laminated interbeds. Small recrystallized coral mounds, up to a few metres in diameter, may also occur. The Vöröshegy Dolomite and the above discussed Rókahegy Dolomite are united now into a single formation, as two members (Rálisch-Felgenhauer, in press; see Figs 21, 22). The most characteristic unit of the Mecsek "Muschelkalk" is the Lapis Limestone Formation, a typical vermicular limestone sequence, equivalent to the Germanic "Wellenkalk". Its main part (including the former Báránytető and Lapis Limestone Members of Nagy 1968, and Balogh 1981) is made up mostly by strongly bioturbated grey limestone beds, with intercalations of slump beds, encrinites and biogenic beds rich in bivalve shells, as well as of laminated horizons. The slump beds can be interpreted as seismically triggered, and the encrinites and bivalve-bearing bioclastic beds as tempestites, while the laminated beds were deposited during intertidal cycles. The upper part of the formation is formed by thickly bedded grey limestones, partly also vermicular ones (Tubes Limestone Member). In the top part crinoidal limestone "lenses" occur, containing the index foraminifer species *Glomospira densa*. Characteristic faunal elements of the formation are *Entolium discites, Velopecten albertii, Modiola triquetra, Naticella* sp., *Dadocrinus gracilis, Encrinus liliiformis* and the trace fossil Rhizocorallium. The formation was deposited in a restricted lagoon zone behind the above-discussed, back-stepping wide dolomite platform. It also partly represents an equivalent of the Bucea Limestone of the Bihor Unit.

Late Anisian–Early Carnian: the main carbonate platform stage with intrashelf basins

Simultaneously with Middle Triassic rifting in the northwestern termination of the Tethys, associated with sea-level rise at the Anisian/Ladinian boundary interval, the former, rather uniform dolomite ramp was differentiated into large intrashelf basins and reef–lagoon complexes. In the North Alpine Triassic, the Wetterstein carbonate platform complexes and the Reifling intrashelf basins formed during this evolutionary stage. In the eastern part of the Tisza Megaunit, in the Codru–Bihor section, the situation was rather different due to formation of the very large embayment-like Roşia basin (see below).

Short-lived basins preceding the main platform stage

Apart from this general pattern persisting throughout this time, relatively short-lived basins formed in some areas, which were later overgrown by carbonate platforms. Because these cases deviate from the general trend, they will be discussed first.

In Northern Bačka and Northern Banat, dark grey micritic limestones, containing foraminifers, radiolarians, filaments and *Globochaete alpina*, were found in several boreholes. They are attributed to the Upper Anisian or Lower Ladinian (Čanović and Kemenci 1988). The microfacies types indicate pelagic connections.

The Triassic sequences of the Mecsek and Villány areas show a deepening-upward tendency, as indicated by the deposition of shallow basinal (e.g. deep distal ramp) sediments, which are included now in the Zuhánya Limestone Formation (Rálisch-Felgenhauer, in press). The Zuhánya Limestone s.s. of the Villány Mts is usually grey to greenish grey, medium-bedded, sometimes marly, nodular, spotty limestone. Its best-known variety, however, which is exploited for ornamentation stone in the Zuhánya quarry at Siklós, is an intra-conglomerate-like, thickly bedded limestone, redeposited still in a semi-consolidated stage by slumps and mud-flows. This type is characteristically varicoloured, greenish-brownish grey, often with a purplish-reddish shade and brown-yellow patches. Brachiopods are common in some places. The Bertalanhegy Limestone Member of the Mecsek Mts is composed of grey, nodular limestones and marls, rich in brachiopods and crinoids. The overlying Dömörkapu Limestone Member is a dark grey, medium-bedded limestone with characteristic yellow or yellowish red marly infillings, which originated by gentle slumping and by disintegration of the original sediment (Konrád 1990; Rálisch-Felgenhauer in press). The prevailing microfacies type is mudstone or (in the Bertalanhegy and Zuhánya Limestones) brachiopodal floatstone. Up to now only the Pelsonian/Illyrian boundary interval has been proven by ammonoids (*Paraceratites binodosus*; Detre 1973) and by conodonts (*Gondolella bifurcata bifurcata, G. bifurcata hanbulogi; G. bulgarica;* Kovács and Papšová 1986). Brachiopods (*Coenothyris vulgaris, Tetractinella trigonella, Punctospirella fragilis*) are common but less age-diagnostic. The low diversity of the fauna and the extreme predominance and morphological variations of *C. vulgaris* strongly suggest Germanic connections rather than Alpine ones (Pálfy and Török 1992). Lithologically, the brachiopod limestones can be compared with the "Terebratulenkalk" of the Germanic Triassic, and the Dömörkapu Limestone with the "Schaumkalk"; the shell accumulations can be interpreted as storm deposits, similar to those described from the Germanic equivalents (Török 1993a, b). In the Bihor Unit of the Apuseni Mts, unlike in the Codru Nappes, the Upper Anisian basinal formations are replaced by the Upper Dolomite of the Crişul Repede Formation (described in the previous chapter), or by the alternation of grey dolomites with grey to black limestones of the Padiş–Călineasa Formation.

The main platform stage and intrashelf basins

In the Codru–Bihor section of Tisza Megaunit the facies zones shifted considerably towards the continental hinterland due to the formation of the Roşia embayment; it will therefore be discussed separately from the rest of the megaunit.

In the Northern Bačka–Northern Banat part of the Northern Bačka–Upper Codru Zone a Wetterstein carbonate platform was built with reef and lagoon facies, marking the outer shelf domain of the Tisza Megaunit. These units have been exposed by boreholes at Velebit, the reef facies being indicated by calcareous sponges, the lagoonal one by dasycladaceans (*Teutloporella herculea*) and codiaceans, as well as by foraminifers. Carnian platform facies has been found by boreholes at Bajša and Bački Monoštor, where it contained dasycladaceans (*Poikiloporella* sp.), codiaceans, solenoporaceans and foraminifers (Čanović and Kemenci 1988).

The Ladinian–Early Carnian(?) platform stage is represented in most of the Papuk Mts by thick bedded, light-coloured dolomites, in some places with *Diplopora annulata*. In the upper part of the sequence shale intercalations up to a few metres thick may occur, containing *Daonella lommeli*. In the westernmost part of the mountains the light-coloured dolomites are replaced by dark grey to black dolomites, in some places also with *Diplopora annulata*. The upper part of the dark dolomite sequence contains an unusual greenish and reddish marl horizon of a few tens of metres thickness. On the other hand, in the north-central part of the mountains, basinal dark grey, bedded, Reifling-type limestones with chert nodules and lenses occur above the Anisian dolomites. They contain crinoid debris at the base. Biostratigraphic data are not yet available from them. In the Békés Basin brownish grey, fine-grained dolomites were found in the Csanádapáca-2 borehole, containing the dasycladacean algae *Gyroporella* aff. *ampleforata* (Kurucz 1977; Bérczi-Makk 1986). *Gyroporella ampleforata* is also known from the Apuseni Mts (Popa and Dragastan 1973) and points to a Lower Ladinian age. White and light grey, coarse grained dolomites found in other boreholes may be of Upper Triassic age (see below).

The Ladinian dolomites of the Mecsek–Villány region are now included in the Csukma Dolomite Formation. In the Villány Mts its lower member, just above the basinal Zuhánya Limestone, is the Csukma Dolomite Member s.s.: brownish or yellowish grey to greyish white, thickly bedded to bedded, sometimes platy dolomite. The upper member, called Templomhegy Dolomite, showing an upward-increasing clay content, consists of yellowish, brownish or light grey, thickly bedded to platy dolomite, calcareous or marly dolomite and dolomitic marl. Both members are almost devoid of fossils; only a few brachiopods (Lingula) and poorly-preserved forams were found. Both members were deposited in an ultra-back-reef, inner shelf lagoonal environment showing upward-increasing pelitic input. This environment was in more of an ultra-back-reef position than that of the contemporaneous Diplopora-dolomites of the Papuk Mts.

In the western and northern part of the Mecsek Mts the Kozár Limestone Member is replaced by the Kán Dolomite Member (Konrád, in Chikán and Konrád 1982), which represents a transition to the dolomite members in the Villány Mts. It consists of grey, brownish or yellowish grey, saccharoidal dolomites, in its higher part with laminitic and oolitic intercalations. The Kozár Limestone Member consists of grey to light grey, thickly bedded limestones, in the lower part with oolitic and crinoidal beds. Selective dolomitization in irregular patches is common. The microfacies changes from microsparite (mudstone) to intrapelsparite, crinoidal biosparite and oosparite (grainstone). The top part of the member is formed by an oncolitic horizon of a few metres thickness, with oncoids up to 20 cm in diameter, usually with small gastropod cores (Kókai and Rálisch-Felgenhauer 1981). In the very top the "Trigonodus horizon" occurs in 1–2 m thickness, composed of a large amount of thick bivalve shells, also microbially encrusted (oncoids) as a rule. Characteristic fauna of the horizon contains (according to Vadász 1935): *Trigonodus* cf. *sandbergeri, T.* aff. *problematicus, T. sandbergeri* var. *hungaricus* and seems to be correlative with the Trigonodus dolomite at the top of the Germanic Muschelkalk (Balogh 1981). In the basement of the Great Plain, in the "Körös region" (in the sense of Bérczi-Makk 1986, to the East of the Tisza River) of the Villány–Bihor belt, Ladinian–Carnian dark grey, clayey limestones and calcareous marls were found by the Biharugra-3 and Doboz-I boreholes, near the Romanian border, containing a Wetterstein-type foraminifer fauna (Bérczi-Makk 1985, p. 306; 1986, p. 275). We relate these rocks to the Raming Limestone known in several units of the Apuseni Mts.

The Codru–Bihor area differed considerably at this time from the rest of the Tisza Megaunit, and particularly from the classical North Alpine–West Carpathian Triassic. This was caused by the formation of a large, embayment-like Roşia intrashelf basin in the Late Anisian, which resulted in extreme narrowing of the platform facies zones and their shifting towards the continental hinterland. This situation persisted until the Early Carnian.

The sedimentary zone of the Vaşcău Nappe belonged to the shelf margin, where reddish–pinkish, thickly bedded, sometimes wavy pelagic limestones were deposited, with scarce intercalations of thin red shales ("Schreyeralm Limestone"; Patrulius et al. 1971, 1979). Though not quite identical with the nodular, mostly red, typical Schreyeralm Limestone, it is very similar to the Nádaska Limestone of the Silica Nappe in Northern Hungary and to the "Ladinian Hallstatt Limestone" of the Mürztal Nappe in the SE part of the Northern Limestone Alps, both being deposited in a shelf margin to slope setting. The basal part of the formation contains ammonoids pointing to Upper Anisian age (among other *Flexoptychites* cf. *flexuosus*), while from its upper part conodonts of the *Gondolella auriformis* zone were reported by Mirăuţa, in Patrulius et al. (1979). *G. auriformis*, according to more recent investigations in Epidauros, Greece (Krystyn 1983) and in its type section in the Rudabánya Mts, North Hungary (Kovács 1991) is indicative of the Middle Carnian.

The Upper Anisian–Middle Carnian Izbuc Formation of the Moma Nappe represents a typical slope sediment of platform-basin transitional setting, with autochthonous basinal limestones and redeposited platform-derived carbonates. It consists of variegated, light grey to black, sometimes pinkish or yellowish cherty limestones, in part with wavy bedding (Reifling- or Roşia- type), or thick-bedded to massive, bioclastic limestones or breccias, in part with echinoderm debris (Raming- and Wetterstein reefal-type) and violet, or grey shales.

The basinal limestones contain pelagic elements, such as radiolarians and "filaments". The age is proven by conodonts, a few ammonoids, and daonellids.

Since the Late Anisian the depositional environment of the lowermost Upper Codru Nappe (Dieva Nappe), and of all the Lower Codru Nappes, have belonged to the Rosia intrashelf basin. The Roşia Limestone Formation is megascopically similar to the Alpine Reifling Limestone: dark grey to black, thin to medium bedded, cherty (especially in its upper part) micritic limestone, with wavy or nodular bedding planes and yellow or red clay coatings. It differs, however, from the latter in its microfacies: typical pelagic elements, such as radiolarians and "filaments" (shells of juvenile pelagic bivalves) are missing or are very rare. Several argillaceous to marly "Daonella Shale" intercalations occur in the Ladinian part of the formation (with *D. taramellii, D. tyrolensis, D. lommeli*, etc.), their thickness reaching, or even exceeding, 10 m. They may correspond to the Partnach Marl interbeds of the Alpine Reifling Limestone. The Roşia Limestone of the Vălani Nappe, Corbesti Outlier and a part of the Finiş Nappe was overlain in the Early Carnian by platform carbonates, which prograded towards the basin. These begin with Raming Limestone type transitional sediments, followed by Wetterstein-type reefal limestones and dolomites. In the Pădurea Craiului and Bihor Mts parts of the Finiş Nappe, and the Şeasa Nappe the Roşia Limestone reaches up to the Norian (Bordea and Bordea 1973; Gheorghian 1976).

The Bihor Unit has an Upper Anisian to Lower Carnian sequence different from the other units. The Upper Anisian "Upper Dolomite" of the Crisul Repede Formation was discussed above. The uppermost Anisian Lugaş Formation, wedging between the "Upper Dolomites" and the Wetterstein Limestone, is divisible into three members. The dark coloured, rarely in places red, Peştiş Shale includes ooidic-bioclastic and coquina limestone intercalations with brachiopods (*Coenothyris vulgaris, Punctospirella fragilis*), crinoids (*Encrinus liliiformis*), bivalves and remnants of reptiles (Jurcsak 1973, 1975, 1976, 1977, Nothosaurus, Tanystropheus). The Vida Limestone is a dark grey, medium-bedded, micritic limestone with conodonts, nodosariid foraminifers and rare ammonites (Ptychites). The medium to thick-bedded, bio- and intraclastic, shallow-water Butan Limestone and the massive, light-coloured Butan Dolomite replaced the upper part of the basinal Vida Limestone along the margins of the Upper Anisian embayment. The top part of the Butan Limestone contains echinoderms (*Encrinus liliiformis*, Cidaris radiolas) and dasycladaceans (*Teutloporella triasina*). It is worth mentioning that, in the Peştiş Shale, "the occurrence of reptiles of poor swimming capacity known also from the Germanic Basin such as Nothosaurus and Tanystropheus points to connections with the latter by the way of not far apart standing islands" or "to an insular extension of the Vindelician land deep into the Alpine territory" (Patrulius et al. 1979, p. 6).

The Bihor Wetterstein carbonate platform was very different from those of the North Alpine and West Carpathian domains, because the extensive dolomite belt characterizing the northern units of the latter two is missing here. Together with the ultra-back-reef inner shelf lagoonal zone, where these dolomites were formed, the original width of the North Alpine–West Carpathian Ladinian–Lower Carnian carbonate platform zone was of the order of hundreds of kms. In the Bihor area, however, the platform was formed in the proximity of the continental hinterland. Its reefal facies is characterized above all by calcareous sponges and corals, and the lagoonal one by dasycladaceans. At the base *Diplopora annulata* is still associated with *D. annulatissima*, indicating uppermost Anisian age, while the main part of the platform is Ladinian, where the dominating *Diplopora annulata* is associated with *Teutloporella herculea* and *T. nodosa*. The Lower Carnian age of the top part of the platform is proven by *Poikiloporella duplicata* and *Clypeina besici* (cf. Bleahu et al. 1970; Diaconu and Dragastan 1969, 1970; Patrulius 1970; Popa and Dragastan 1973; Popa 1981; Dragastan et al. 1982; Mantea 1985). The most interesting formations are the detrital Zugăi and Ordâncusa Formations, interfingering with the Wetterstein Limestone. The Zugăi Formation is a fluviatile-continental, chaotic formation, which is made up of red or grey argillaceous shales, siltstones, red-violet quartzitic sandstones with flat, chip-like, varicoloured limestone megabreccias (in places with boulders of Wetterstein Limestone) and also of dark Anisian limestone, with limy–argillaceous–silty matrix. It occurs as huge lenticular bodies, both underlain and overlain by Wetterstein Limestone.

The occurrence of Wetterstein Limestone blocks indicates that this formation is younger than the base of the Wetterstein Fm. The Ordâncuşa Formation replaces a part of the Wetterstein Limestone in the southern part of the Bihor Mts (see Dimitrescu et al. 1977; Bleahu et al. 1980). It consists of several megacycles, each of them several hundreds metres thick, and is composed, in ascending order, of red sandstone, red shale and laminated limestone. The first cycle contains thick beds of organodetrital limestones of Wetterstein-type. The sedimentary environment of the formation could correspond to marginal lagoons between the Wetterstein carbonate platform and the "Bihor Land", with periodical influxes of continental sediments (Baltreş in Patrulius et al. 1979).

The close relationship between the Wetterstein Limestone and the continental-influenced Zugăi and Ordâncuşa Formations shows that the Bihor Wetterstein carbonate platform was actually a fringing platform, formed immediately around the continental hinterland and surrounding the large Roşia embayment. This paleogeographic setting explains the differences in the facies zonation (extremely narrowed lagoonal zone) compared to that in the Eastern Alps and West Carpathians.

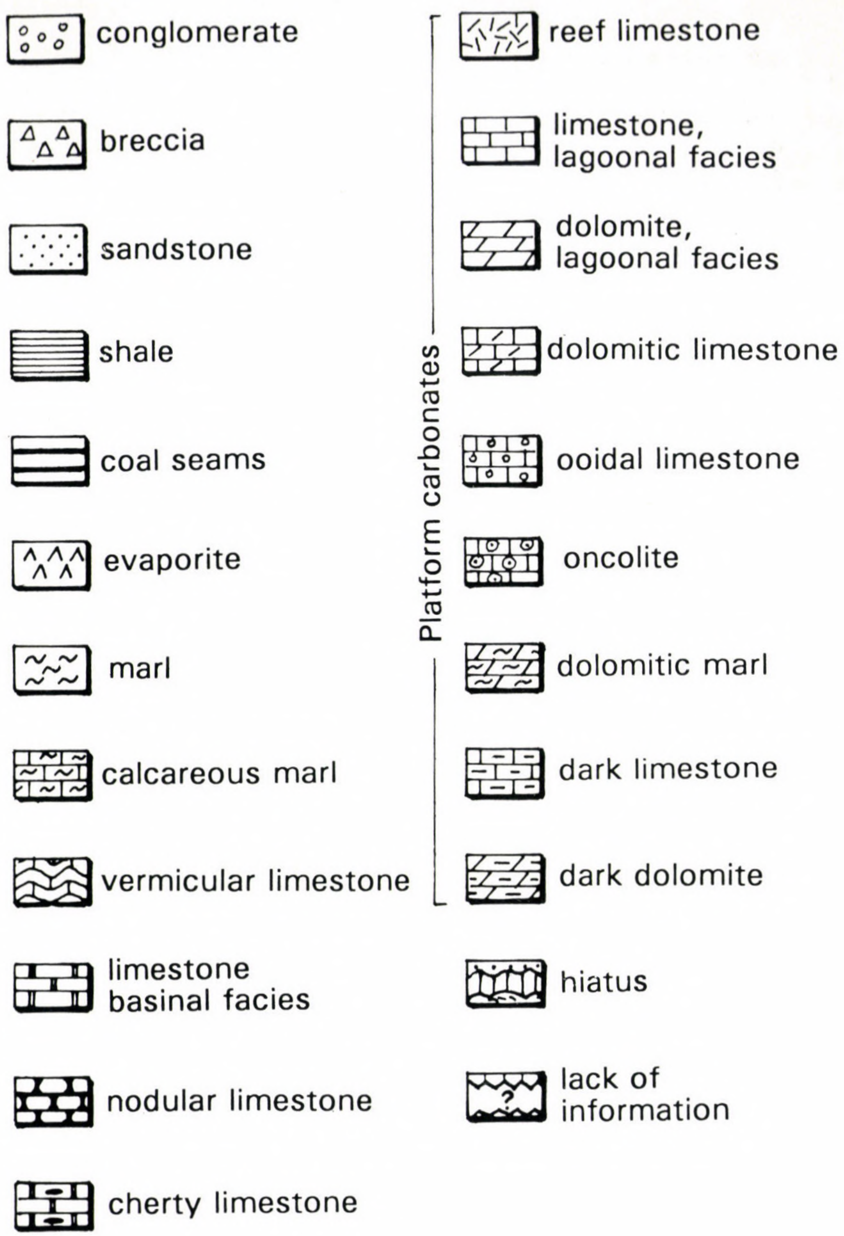

Fig. 3
Legend for the stratigraphic columns

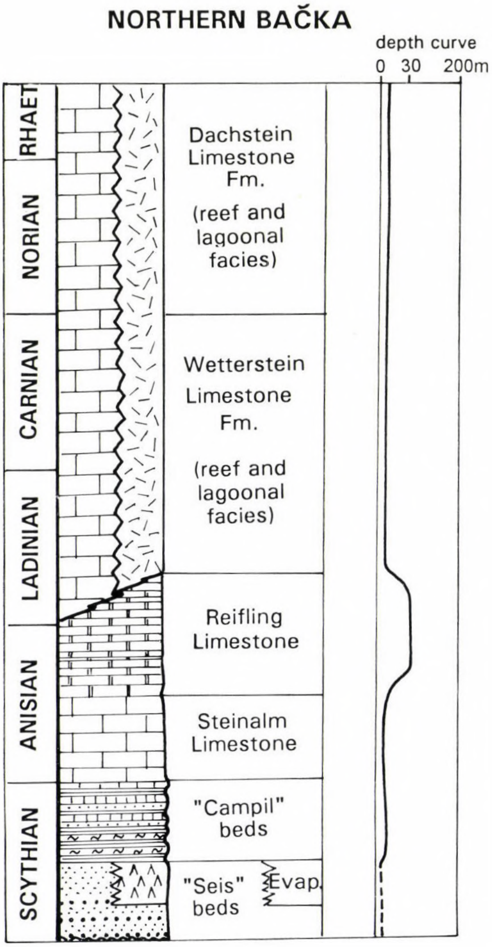

Fig. 4
Northern Bačka–Upper Codru Zone: Northern Bačka–Northern Banat area (after Čanović and Kemenci 1988; Kemenci and Čanović, in press)

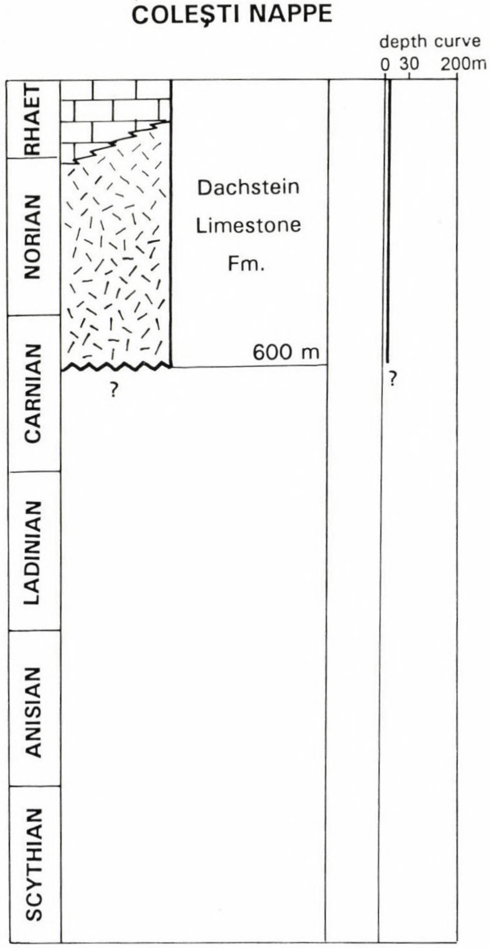

Fig. 5
Northern Bačka–Upper Codru Zone: Coleşti Nappe (after Bleahu et al. 1979)

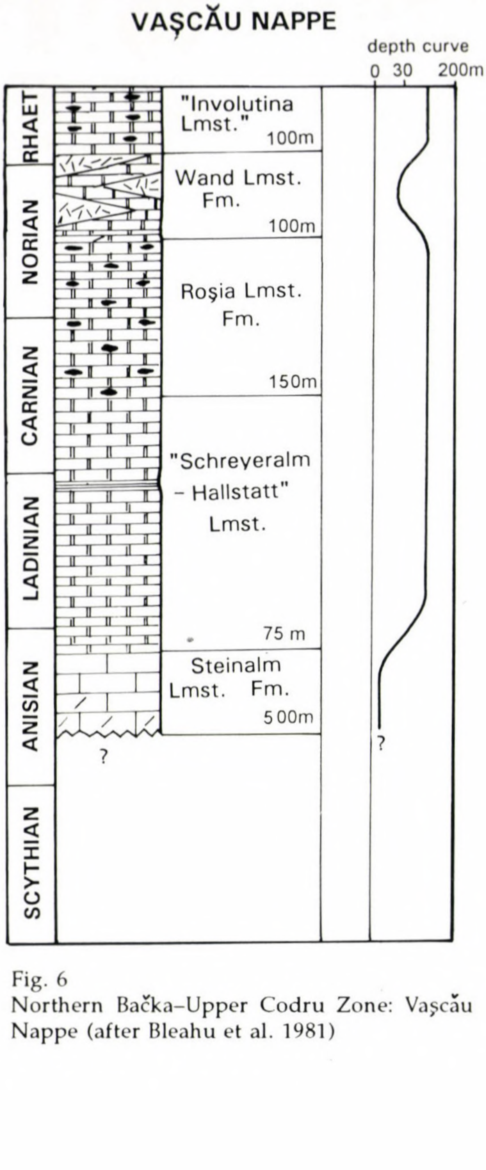

Fig. 6
Northern Bačka–Upper Codru Zone: Vaşcău Nappe (after Bleahu et al. 1981)

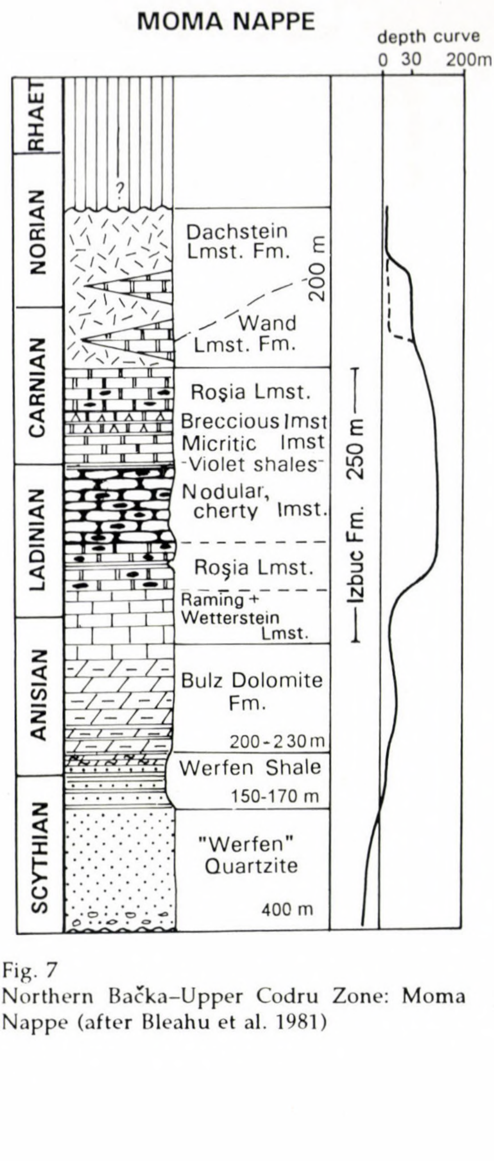

Fig. 7
Northern Bačka–Upper Codru Zone: Moma Nappe (after Bleahu et al. 1981)

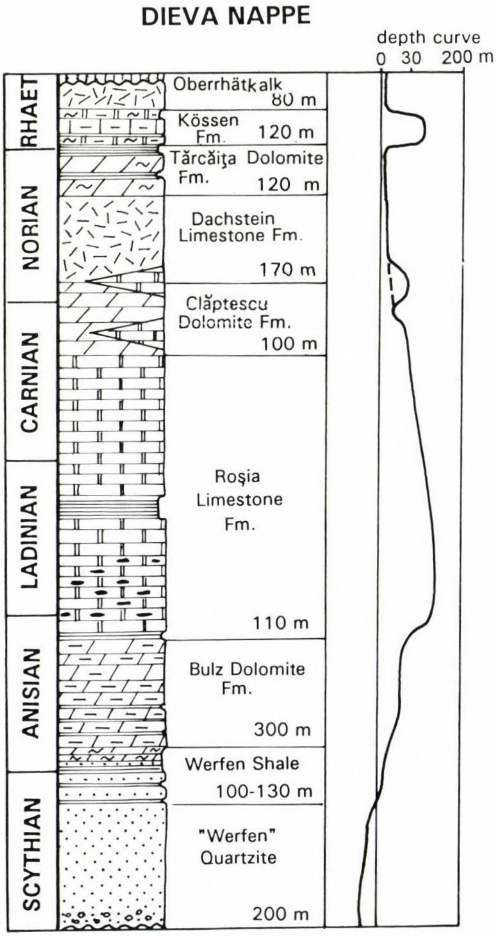

Fig. 8
Northern Bačka–Upper Codru Zone: Dieva Nappe (after Patrulius et al. 1979)

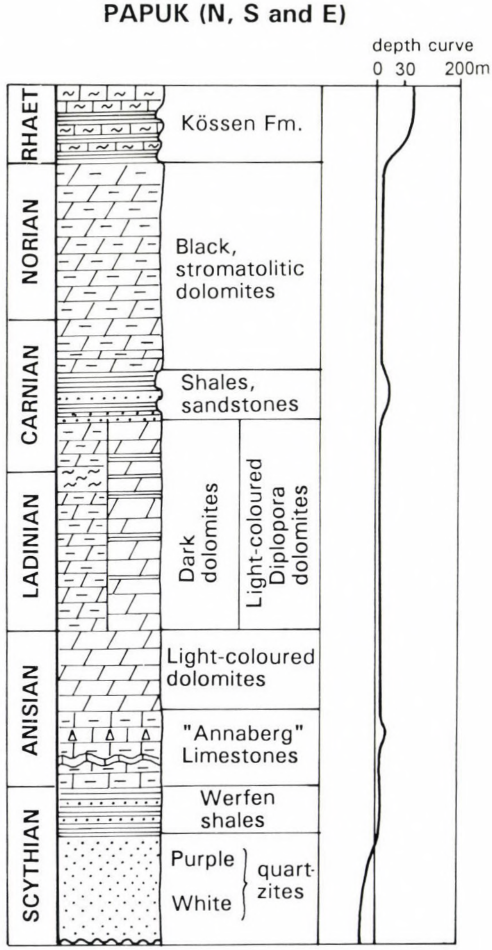

Fig. 9
Papuk–Békés–Lower Codru Zone: Papuk Mts, western, southern-central part and eastern part (Šikić et al. 1975)

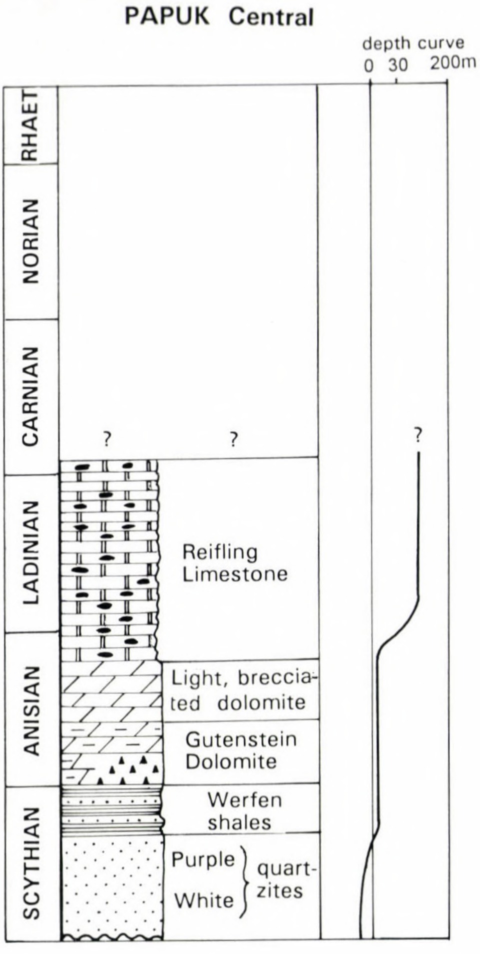

Fig. 10
Papuk–Békés–Lower Codru Zone: Papuk Mts, northern–central part (Šikić et al. 1975)

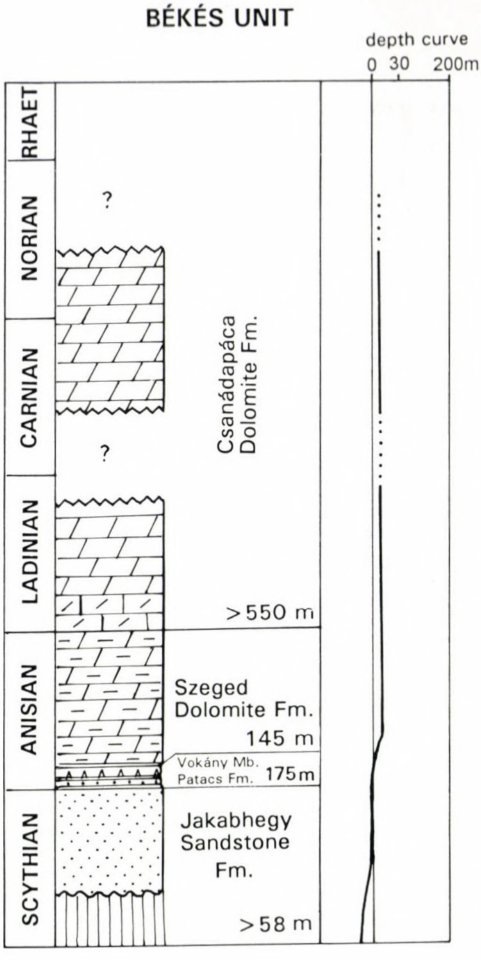

Fig. 11
Papuk–Békés–Lower Codru Zone: Békés Unit (after Bérczi-Makk 1986)

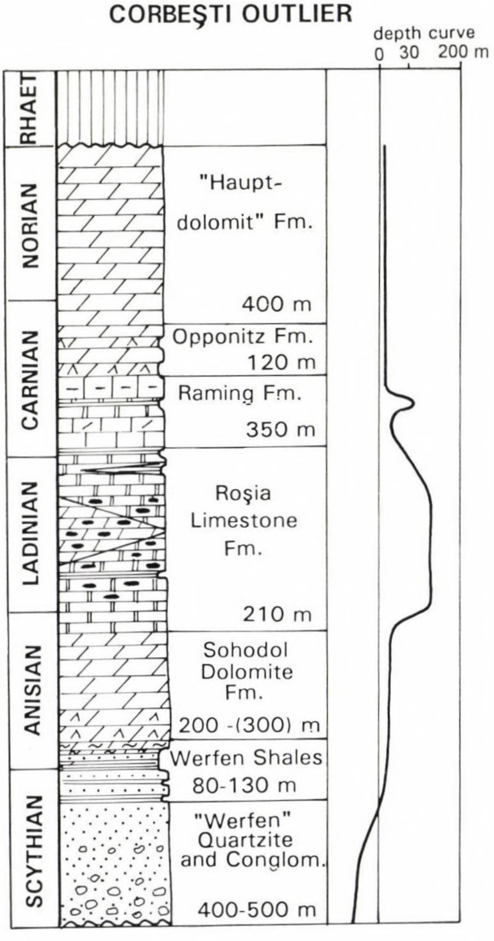

Fig. 12
Papuk–Békés–Lower Codru Zone: Corbeşti outlier (after Patrulius in Patrulius et al. 1979)

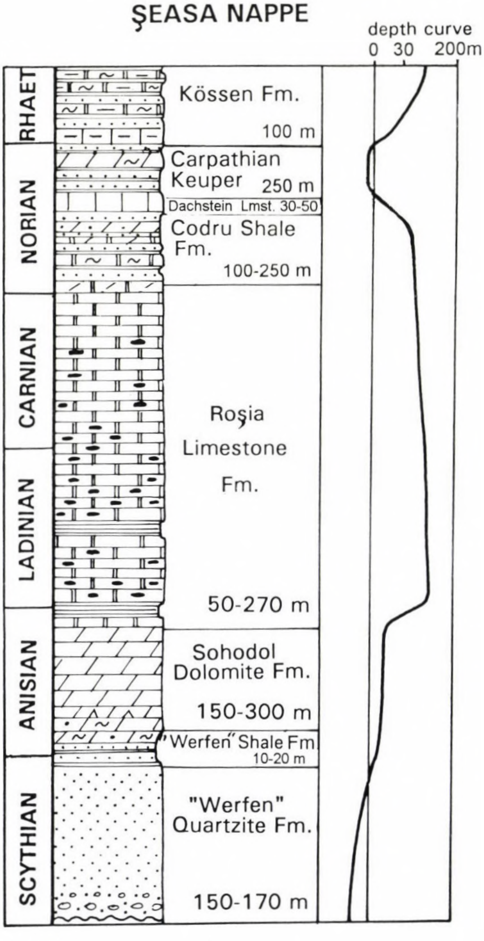

Fig. 13
Papuk–Békés–Lower Codru Zone, Lower Codru Nappes: Şeasa Nappe (after Ştefǎnescu et al. 1983)

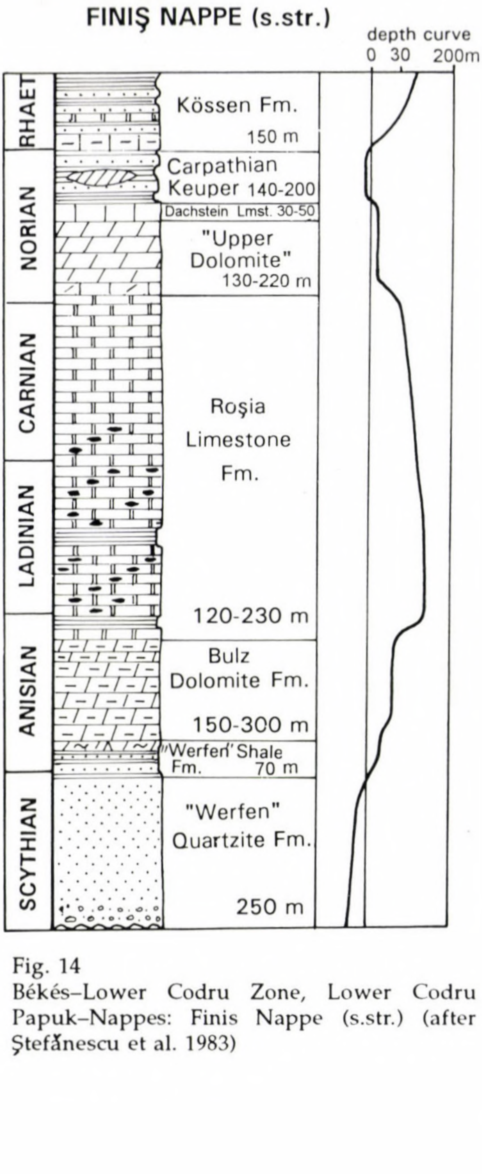

Fig. 14
Békés–Lower Codru Zone, Lower Codru Papuk–Nappes: Finis Nappe (s.str.) (after Ştefănescu et al. 1983)

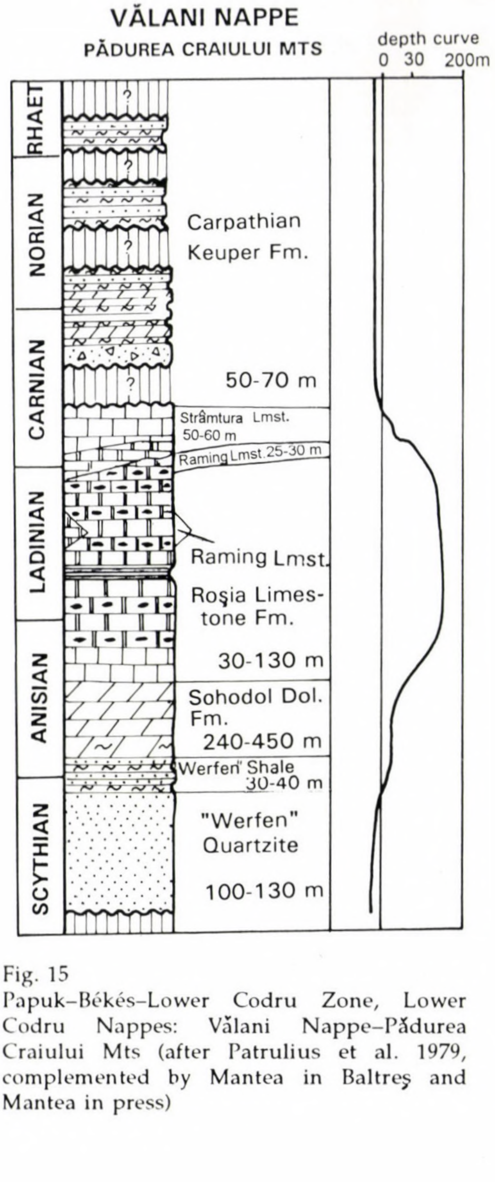

Fig. 15
Papuk–Békés–Lower Codru Zone, Lower Codru Nappes: Vălani Nappe–Pădurea Craiului Mts (after Patrulius et al. 1979, complemented by Mantea in Baltreş and Mantea in press)

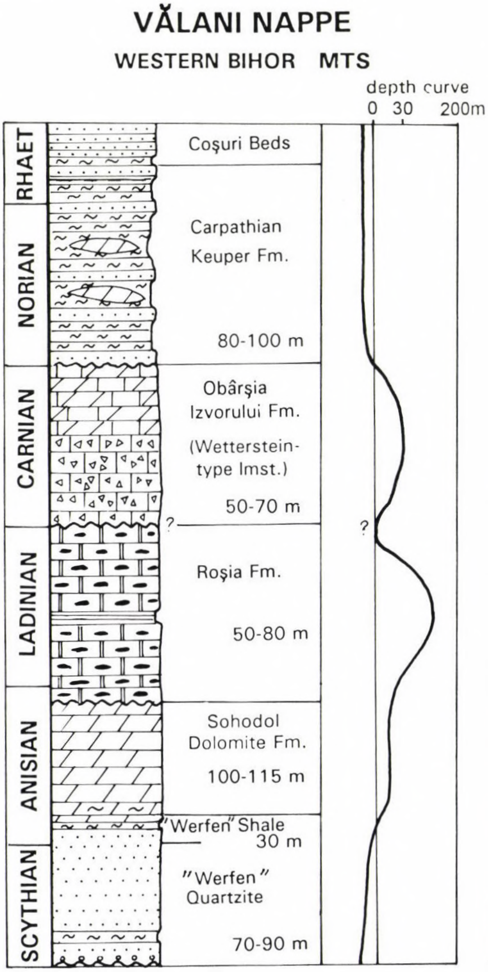

Fig. 16
Papuk–Békés–Lower Codru Zone, Lower Codru Nappes: Vălani Nappe–Western Bihor Mts (after Bordea et al. 1975)

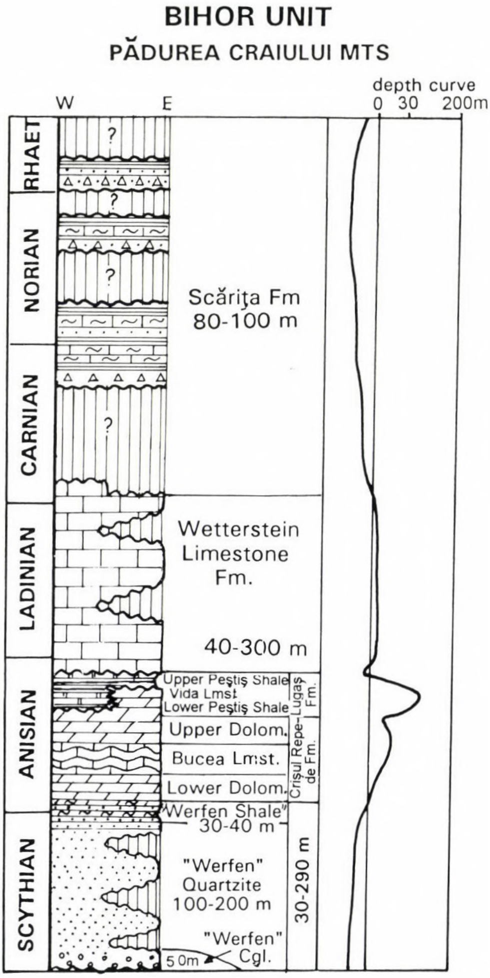

Fig. 17
Villány–Bihor Zone: Bihor Unit–Pădurea Craiului Mts (after Patrulius et al. 1979, complemented by Mantea in Baltreş and Mantea in press; S. Bordea., J. Bordea and Mantea)

Middle Carnian–Norian: the "Keuper" stage

During this time the sea retreated from epicontinental Europe and also from the northern zones of the Tisza Megaunit.

The Upper Triassic of the Northern Bačka–Upper Codru zone still reflects an outer shelf to shelf margin position, as during the Middle Triassic. Boreholes in the Northern Bačka region (primarily in the vicinity of the village of Bajša) have drilled

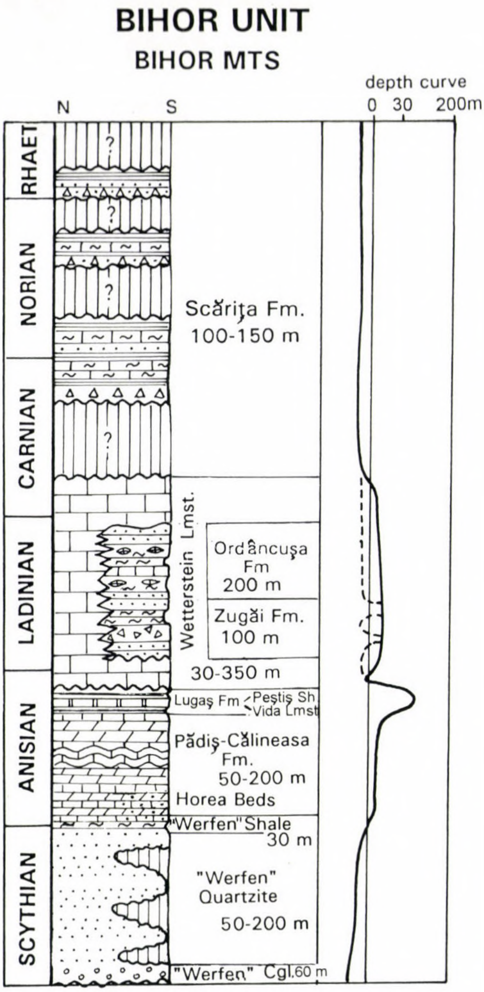

Fig. 18
Villány–Bihor Zone: Bihor Unit–Bihor Mts (after Patrulius et al. 1979, complemented by Mantea in Baltres and Mantea in press)

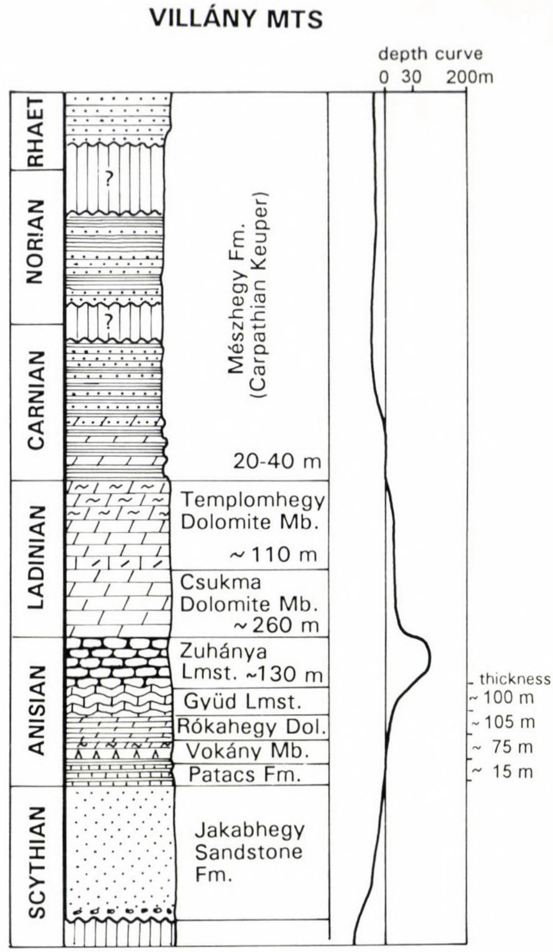

Fig. 19
Villány–Bihor Zone: Villány Mts. (Rálisch-Felgenhauer, Nagy, Konrád, Török)

Dachstein-type reef limestones with corals, calcareous sponges and hydrozoans, and lagoonal facies deposits with calcareous algae (among others the Norian–Rhaetian *Diplopora muranica*). The thick, Upper Triassic sequences of the Upper Codru Nappes (from the lowermost Dieva Nappe to the uppermost Colesti Nappe) correspond to an outer shelf carbonate platform showing pelagic influence. The Colesti Nappe is built up by Norian Dachstein reef limestone (with corals and calcareous sponges), at the base with halobians (e.g. Bleahu et al. 1972; Panin et al. 1982) indicating connections to pelagic environments, and Rhaetian loferitic

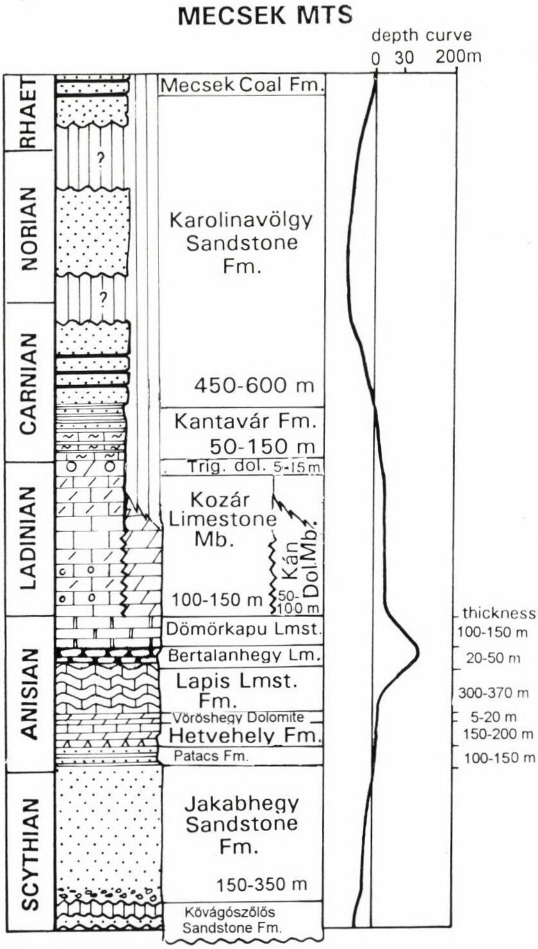

Fig. 20
Mecsek–Northern Great Plain Zone: Mecsek Mts (Rálisch-Felgenhauer, Nagy, Konrád, Török)

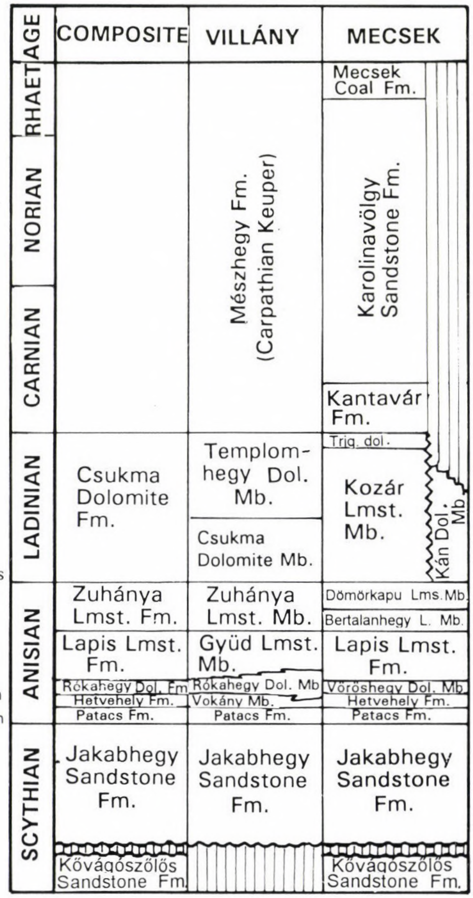

Fig. 21
Composite stratigraphic table of Triassic of the Mecsek and Villány Mts (Rálisch-Felgenhauer, Nagy, Konrád, Török)

Lapis Lmst. Fm. ("Wellenkalk")	Tubes Lmst. Mb.
	Lapis Lmst. Mb.
	Báránytető Lmst. Mb.
Rókahegy Dol. Fm.	Vöröshegy Dol. Mb.
Hetvehely Fm.	Víganvár Lmst. Mb.
	Hetvehely Dol. Mb.
	Magyarürög Ev. Mb.
Patacs Fm.	Patacs Fm.

Ev. = Evaporite

Fig. 22
Detailed lithostratigraphy of the Lower–Middle Anisian of the Mecsek Mts (Rálisch-Felgenhauer, Nagy, Konrád, Török)

Dachstein Limestone with megalodontids belonging to the genus Conchodon. In the sedimentation area of the Vaşcău Nappe, intrashelf basinal conditions lasted up to the Middle Norian: the "Schreyeralm" Limestone is overlain by Roşia Limestone, in the top with the conodont *Gondolella steinbergensis* indicating already the Alaunian substage. In the Moma Nappe the platform/basin transitional facies of the Izbuc Formation is followed by the reef facies of the Wand/Dachstein Limestone, with pelagic influence indicated by pinkish or greyish, micritic limestones containing halobians and (in the top) monotids (Panin and Tomescu 1974). The light coloured, thickly bedded to massive Upper Carnian–Lowermost Norian Clăptescu Dolomite Formation of the Dieva Nappe represents a completely dolomitized platform facies, in which pelagic influence is indicated by intercalations of red dolomitic limestones with conodonts and halobians. It is overlain by reefal Dachstein Limestone with corals and calcareous sponges, and replaced in the upper part by lagoonal facies with dasycladaceans (genus Heteroporella) and megalodontids. The Tărcăiţa Dolomite above the Dachstein Limestone represents a heteropic facies of the Carpathian Keuper: thick bedded dark grey, fine grained dolomites, with intercalations of greyish or pinkish Megalodon-bearing limestone beds and thin beds of grey or red argillites.

The Papuk–Békés–Lower Codru zone would correspond to the "Hauptdolomit" facies zone of the Eastern Alps and West Carpathians, with, however, certain differences in development. In the Papuk Mts the Diplopora-bearing dolomites are overlain by grey to dark grey sandstones and shales of a few tens of metres of thickness, most probably corresponding to the East Alpine and West Carpathian Lunz Sandstone event. These clastic rocks are followed by black, thickly bedded stromatolitic dolomites of Upper Carnian(?)–Norian age, of about 200 m thickness.

In the Békés Basin white or light grey, coarse-grained dolomites can be assigned to the Upper Triassic (Bérczi-Makk 1986). From among the Lower Codru Nappes, only the sequence penetrated by the Corbeşti borehole may represent the "Hauptdolomit" facies zone. The sequence was formerly attributed to the Arieşeni Nappe (Patrulius et al. 1979), but recently, Baltreş and Mantea (in press), assigned it to the Finiş Nappe. The Upper Carnian light, massive limestones, dolomitic limestones, vuggy dolomites and anhydritic dolomites may represent a facies equivalent of the East Alpine Opponitz Formation, of hypersaline lagoonal facies. The Norian dolomites are represented first by brown, fine-grained dolomites, and then by white, coarse-grained dolomites.

The Norian sequence of the Şeasa Nappe shows a deviation from the classical North Alpine–West Carpathian Triassic. In the latter sedimentary region, namely in the zone of the Bajuvarikum and Choč Nappe, the Reifling basins were filled up by the Middle Carnian Lunz Sandstone and Reingraben Shale; here the basinal carbonate sedimentation (Roşia Limestone) continued until the Early Norian (Patrulius 1976; Patrulius et al. 1976). Later it was filled up by the clastic Codru Formation, consisting of dark grey argillaceous-silty shales, light grey marly shales, silty marls, subordinately interbedded quartzitic sandstones and dark grey, thickly bedded limestones and sandy limestones. In the Finiş Nappe the Codru Formation is missing and substituted by a platform dolomite ("Upper Dolomite"). Both the Codru Formation and the "Upper Dolomite" are overlain by a relatively thin sequence (30 m) of Dachstein lagoonal facies with megalodontids. The terrigenous detrital supply requires a northerly-lying continental hinterland in Norian time, with erosion, and probable deposition of Carpathian Keuper-type sediments, in the low-lying areas, from which these clastics could be transported into the basin, probably through intraplatform channels. The infilled former basin of the Şeasa Nappe was site of terrigeneous clastic sedimentation in the Upper Norian (Carpathian Keuper, in about 250 m thickness) in the Codru Mts (Ştefănescu et al. 1983), whereas in the Bihor Mts interfingering of the Carpathian Keuper and the Dachstein Limestone is visible (Valea Frunzei Formation).

Following the Early Carnian carbonate platform stage, the zone of the Vălani Nappe became part of a continental domain and, together with the Villány– Bihor zone, was a site of Carpathian Keuper-type sedimentation (Patrulius 1971). The exact age of these red clastics is still an open question, due to paucity or lack of biostratigraphic data. These clastics always occur between the Ladinian–Lower Carnian carbonates and the lowermost Jurassic Gresten-type clastics (or even younger Jurassic rocks cf. Császár et al. 1984); in many areas they may be missing due to long-lasting denudation. The age of the Carpathian Keuper could be confined (taking into consideration the general trends of the Alpine, resp. European Late Triassic evolution) by two events: the Early–Middle Carnian "Raibl" (or "Reingraben") and the latest Triassic "Kössen" events.

The Mészhegy Formation of the Villány Triassic (red and greenish grey shales, siltstones and fine-grained sandstones, with thin dolomite intercalations in the basal part, Rálisch-Felgenhauer 1985b) and the Scăriţa Formation of the Bihor Unit (red shales, in the lower part with interbedded grey or red, micritic and pelletal limestones, and with red sandstones in the upper part) developed gradually from the underlying carbonate formations. Whether they comprise the entire Middle Carnian–Rhaetian interval, or only a part of it, or whether the sequences enclose hidden hiatuses, cannot be determined at the present stage of knowledge. For this reason these units are simply regarded as "Upper Triassic". The basal breccia and conglomerate in the Carpathian Keuper of the Vălani Nappe suggest an erosional disconformity. For discontinuous Carpathian Keuper-type sequences another event may determine a possible lower boundary: the base of the Codru Formation (Middle Lacian), e.g. the appearance of the clastic input in the depositional zone of the Şeasa Nappe. The basal part of the Codru Formation in the Codru Mts (Şeasa Nappe) even contains red shales (Patrulius et al. 1979).

In the pre-Tertiary basement of the Great Plain, Carpathian Keuper-type sediments were found by drilling in the "Körös region" of the Villány–Bihor zone, in the boreholes Biharugra-3 and Doboz-I. They consist of red siltstones and sandstones, with grey limestone intercalations, attributable to the Scăriţa Formation (Bérczi-Makk 1985, 1986).

As opposed to the red Carpathian Keuper (s.l.) of the Villány–Bihor zone, the Mecsek–Northern Great Plain zone is characterized in the Upper Triassic by grey detrital rocks. The Kozár Limestone Member with the "Trigonodus Dolomite Bed" in its topmost part is followed by the Kantavár Formation, consisting of black, bedded to medium-bedded, argillaceous limestones with intercalations of thin, black argillaceous marls and coal measures (vitrite, up to 2 cm thickness). The upper part contains an increasing amount of dark sandstones and shales. Ostracod lumachelles with 1 or 2 species of the genus Darwinula (Kristan-Tollmann, and Monostori pers. comm.), pointing to a freshwater environment, small gastropods and coalified plant remnants (Equisetites, Anatopteris) are common. The formation was deposited in brackish to fresh water lagoons and is comparable to the Lettenkeuper of the Germanic Triassic (Balogh 1981).

Based on this correlation, and on the basis of sporomorphs contained in the unit (the same association as in the lower member of the overlying Karolinavölgy Sandstone Formation; Bóna 1983, 1984a, b, and in press), its age may correspond to the uppermost Ladinian–Lower Carnian. At the base of the formation argillaceous ironstones occur, either as thin intercalations or as up to 10–15 m thick bodies, consisting of kaolinites and siderites. Formerly these rocks were believed to be of volcanic origin (Nagy and Ravasz-Baranyai 1968), but now they are considered to be swamp deposits (Rálisch-Felgenhauer in press).

The Kantavár Formation is overlain by the Karolinavölgy Sandstone Formation, made up by grey, coarse-grained or fine-grained sandstones, siltstones and shales, sometimes with greenish, brownish or reddish shade. The sandstones are of arkosic type. The formation can be subdivided into three parts. The lower member (in 120–150 m thickness) is of lagoonal and lacustrine, subordinately deltaic facies and contains thin coal seams and carbonaceous shales. Its Carnian age is proven by a rich sporomorph association (Bóna 1983, 1984a, b, and in press). The middle member (of 140–160 m thickness) is predominantly lacustrine, subordinately lagoonal. It contains only a few plant remnants, but no determinable sporomorphs; therefore its assignment to the Norian relies merely on its stratigraphic position. The often greenish-grey coloured upper member is fluviatile at its base and deltaic and lacustrine in its higher parts. It contains thin coal seams again. Its Rhaetian age has been proven by a rich sporomorph association (Bóna op. cit.). The first two members belong to the regressive wing of the cycle, and the upper one to the new transgressive one. It is possible that the three members are separated by hiatuses. Chamositic beds occur in the middle and upper members, in the latter together with argillaceous ironstones. The transport of detritic material, similarly to the Liassic Gresten facies, was from north to south, from a northerly-lying granitoid provenance (Nagy 1968, 1969, 1971; and in Kovács et al. 1989).

In the subsurface continuation of the Mecsek–Northern Great Plain zone, the Karolinavölgy Sandstone was found in several boreholes in the vicinity of Nagykőrös (Bérczi-Makk and Cserepes 1985; Bérczi-Makk 1986). Further to the NE, to the east of the Tisza River, no Triassic rocks are known in the basement of the Hungarian part of the Szolnok–Maramures flysch zone (with the exception of the

Endrőd boreholes on the SE margin, where the Scythian Jakabhegy Sandstone was found; cf. Bérczi-Makk 1986, Fig. 8). On the other hand, the Jurassic–Lower Cretaceous sequence is known there from many boreholes (see Bérczi-Makk 1986, Fig. 3). Therefore, according to Szepesházy (1972), it is not excluded that the Liassic Gresten facies lies directly upon the crystalline basement, similarly for example, to the lower Infrabucovinian Nappes of the East Carpathians (cf. Săndulescu et al. 1981).

Rhaetian[1]: the "Kössen event"

The "Kössen event" is marked by renewed transgression in the Central and West European epicontinental Triassic (Ziegler 1982), as well as in the Alpine Triassic (Lein 1987). At the same time the clastic input was also renewed in the Alpine Triassic.

In the southernmost Northern Bačka–Upper Codru Zone, with the exception of the Dieva Nappe, this event cannot be recognized. The Dachstein-type carbonate platform accretion certainly continued until the end of the Triassic in the depositional areas of the Vaşcău and Coleşti Nappes. The presence of the Rhaetian within the Dachstein-type platform is assumed in Northern Bačka, on the basis of foraminifers (Čanović and Kemenci 1988), while the topmost Triassic is not known in the Moma Nappe sequence. In the Dieva Nappe dark, thickly bedded limestones represent the Kössen event, followed by light massive limestones, an equivalent of the North Alpine "Oberrhätkalk". The Papuk–Békés–Lower Codru Zone (especially in the Papuk Mts), is characterized by a typical Kössen Formation although the topmost part of the Triassic sequence has not been exposed by boreholes in the Békés Basin and in the Corbeşti outlier of the Finiş Nappe. In the Papuk Mts black shales (mainly in the lower part) and thick beds of black marly limestones (mainly in the upper part) represent the Kössen Formation, with the same rich fauna as in the North Alpine and West Carpathian equivalents (Šikić et al. 1975). In the western part of the Finiş and Şeasa Nappes (Codru Mts) the Kössen Formation consists mainly of black shales and black, bedded limestones, with interbedded organodetritic limestones (with corals, megalodonts, brachiopods and gastropods); in the eastern part (Bihor Mts) the proportion of thick limestone beds is higher and in the upper part of the formation black shales prevail, with intercalations of fine-grained sandstones and silty to sandy limestones (Bleahu and Mantea 1964; Bordea et al. 1975; Patrulius et al. 1979)

The "Bihor Land" (including the sedimentary zone of the Vălani Nappe) remained either emerged during the time of the latest Triassic transgression, or sediments of the "Kössen event" had been eroded prior to the deposition of the Liassic Gresten clastics. (The clastics of the Gresten Formation may rest on the Scăriţa Formation, on the Wetterstein Limestone, on the Anisian dolomites or directly on the crystalline Arada Series; cf. Mantea 1985.) In the Mészhegy Formation of the Villány Mts the topmost two beds (both of them 0.6–0.7 m thick) can probably be attributed to the

1 The "Rhaetian", the status and content of which are presently widely disputed by Triassic stratigraphers, is used "sensu lato" in the present contribution.

Rhaetian (Birkenmajer, pers. comm.), based on analogies: the lower sandstone bed contains plant remnants (stems and leaves), and the upper microconglomerate bed frequent bone fragments.

In the Mecsek Mts the first few, thin coal seams of the Mecsek Coal Formation, indicating a swamp environment, are still of Rhaetian age, as proven by sporomorphs (Bóna 1983, and in press; Lachkar et al. 1984).

Conclusions

Based on surface and subsurface data, the setting of Triassic facies zones within the Tisza Megaunit indicates transgression from a southerly-lying (according to present coordinates) open sea domain towards a northerly-lying continental hinterland made up of granitoid and crystalline rocks, from which the detrital material was supplied.

The evolutionary stages are summarized as follows:

– *Scythian*: "Buntsandstein" stage, with gradual flooding by the sea from the south (represented by the "Werfen megafacies").

– *Earliest Anisian*: final stage of transgression; the entire area of the Tisza Megaunit became flooded by the sea (with a probable exception in its northeastern part – the "Bihor Land"). Carbonate platform evolution was initiated in the southern zones, whereas an evaporitic sabkha belt was formed in the northern zones (the "Reichenhall event", Schlager and Schöllnberger 1974; or the "Röt" stage of the Germanic Triassic).

– *Late Early Anisian– Early Middle Anisian:* the early carbonate platform stage, with the formation of a huge, mostly dolomitic ramp, bounded to the north by a restricted lagoonal zone with vermicular limestones (corresponding to the Germanic "Wellenkalk" facies).

– *(Late Middle Anisian)–Late Anisian:* disruption of the uniform ramp, formation of intrashelf basins fringed partly by carbonate platforms (the "Reifling event", Schlager and Schöllnberger 1974).

– *Ladinian–Early Carnian:* the main platform stage; in the eastern section the large Rosia basin was formed, bordered to the north by a zone of Wetterstein carbonate platforms directly fringing the continental "Bihor Land", as indicated by the interfingering of the Wetterstein carbonates with the predominantly siliciclastic Zugai, and Ordancusa Formations, respectively.

In the Early Carnian the extent of the Rosia basin was reduced due to the basinward progradation of the Wetterstein platforms.

To the north, in the Mecsek zone, the fresh water–lagoonal Kantavár Formation was formed in the uppermost Ladinian–Early Carnian, in a basin separated from the Tethyan Sea. It resembled the "Lettenkohle" of the Germanic Triassic (Balogh 1981).

– *Middle Carnian:* Due to the initiation of tectonic differentiation and approximately coeval climatic change ("Reingraben" or "Raibl event" in the Alps; cf. Schlager and Schöllnberger 1974), the carbonate sedimentation was complemented by deposition of siliciclastics in the northern zones. The sharp

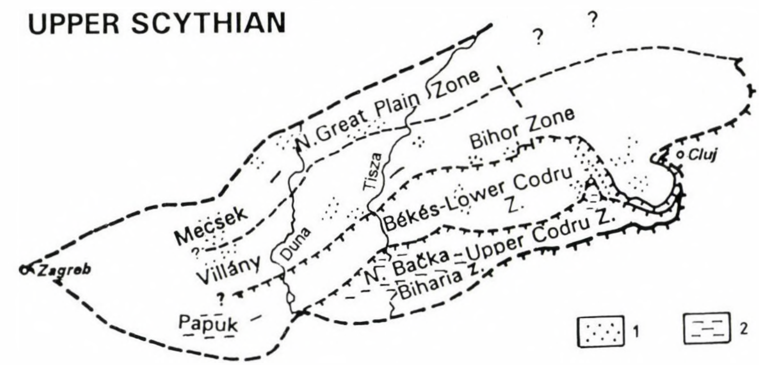

Fig. 23
Distribution of the Upper Scythian lithofacies in the Tisza Megaunit. 1. Continental deposits (Jakabhegy Sandstone + "Werfen" Quartzite); 2. Marine deposits (Werfen beds)

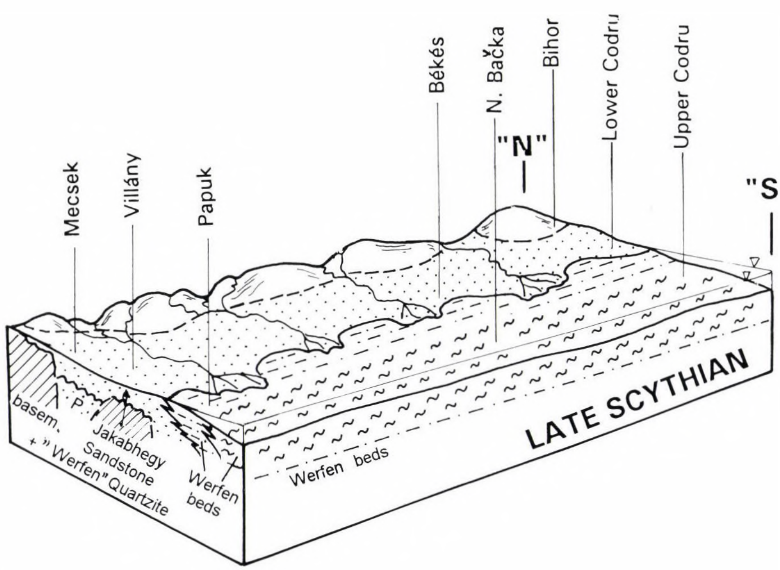

Fig. 24
Paleogeographic reconstruction for the Late Scythian

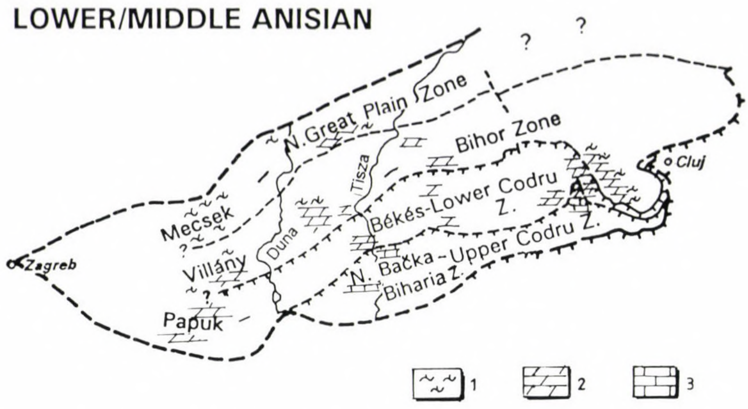

Fig. 25
Distribution of the Lower/Middle Anisian lithofacies in the Tisza Megaunit. 1. Restricted lagoonal facies (vermicular limestone and/or dolomite); 2. Inner shelf dolomite (Bulz + Sohodol Dolomite + others); 3. Outer shelf facies (Steinalm Limestone)

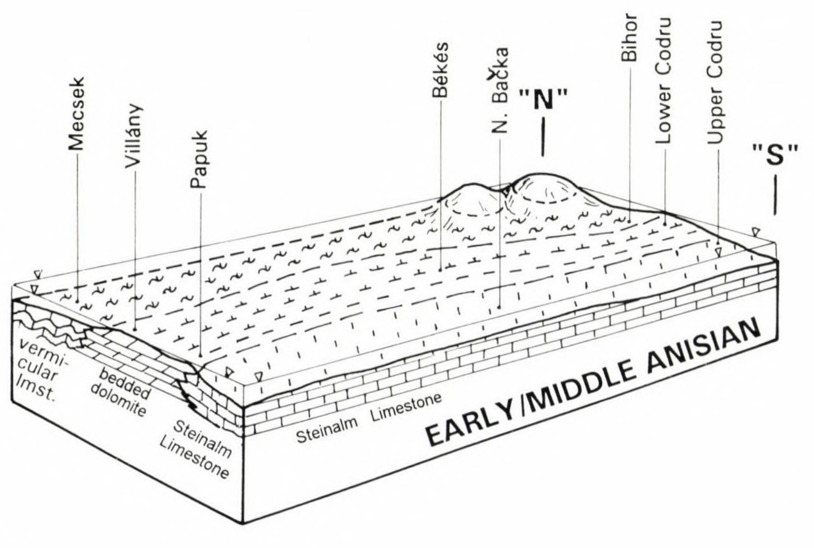

Fig. 26
Paleogeographic reconstruction for the Early–Middle Anisian

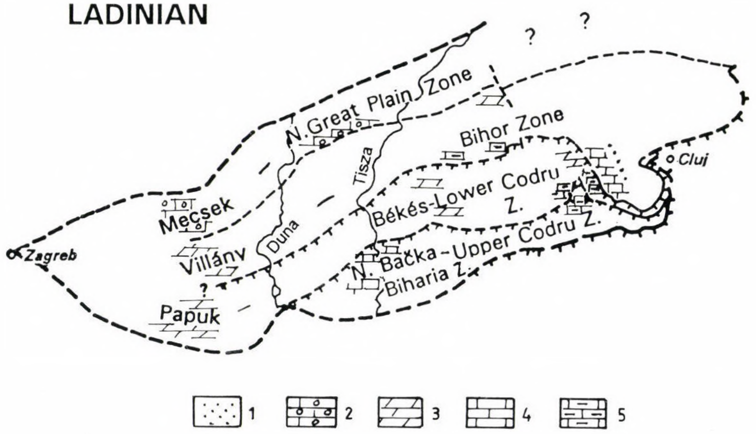

Fig. 27
Distribution of the Ladinian lithofacies in the Tisza Megaunit. 1. Continental deposits (Zugai+ Ordancusa Fm.); 2. Ooidic limestone (Kozár Limestone); 3. Inner shelf dolomite; 4. Outer shelf facies (Wetterstein Limestone); 5. Basin facies (Rosia Limestone, "Schreyeralm–Hallstatt" Limestone)

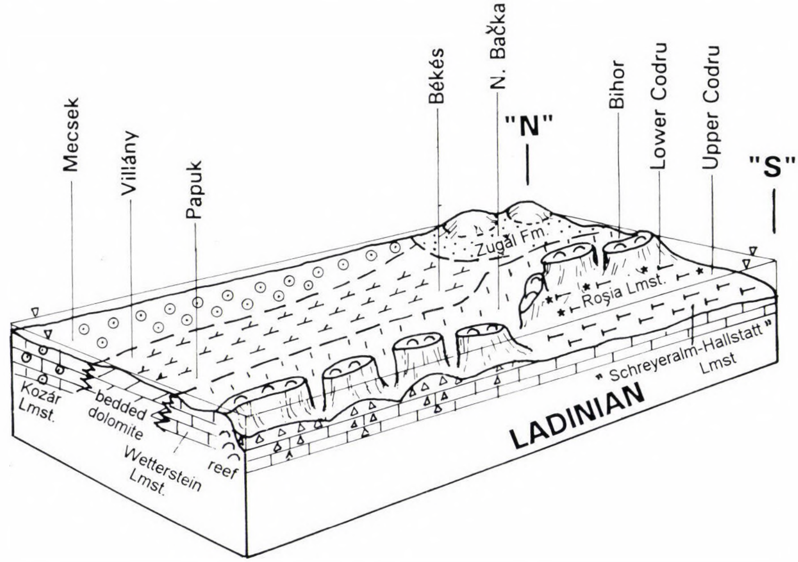

Fig. 28
Paleogeographic reconstruction for the Ladinian

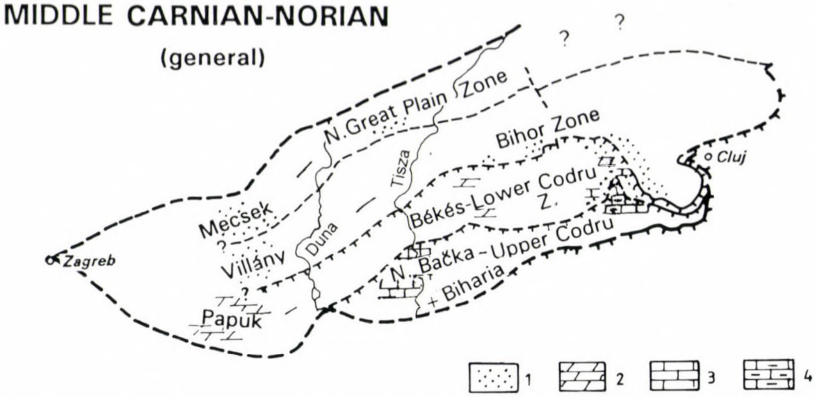

Fig. 29
Distribution of the Middle Carnian–Norian (in general). 1. Continental deposits ("Keuper" megafacies); 2. Inner shelf ("Hauptdolomit" megafacies); 3. Outer shelf (Dachstein Limestone megafacies); 4. Basin facies (Rosia Limestone)

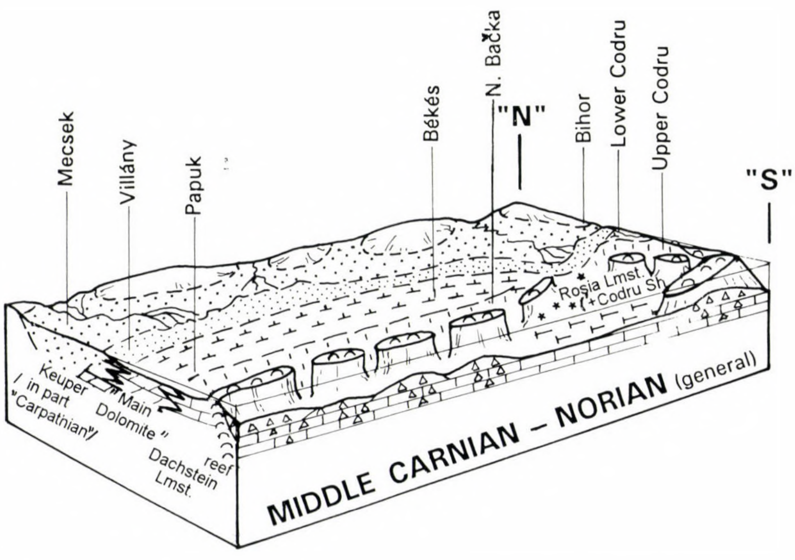

Fig. 30
Paleogeographic reconstruction for the Middle Carnian–Norian (general)

difference between the Mecsek and Villány Mesozoic began already at this time: in the former zone grey, coarse-grained sediments with thin coal seams were accumulated, and in the adjacent Villány–Bihor zone red, fine-grained continental clastics, gradually replacing the underlying carbonates. This is explained by the assumption that the formation of the half-graben structure in which the anomalously thick Liassic Gresten facies of the Mecsek unit was accumulated (E. Nagy 1969, Fig. 8; Szente 1992), had already begun at this time (or even during the deposition of the Kantavár Formation).

In the Papuk Mts the "Reingraben event" is most probably represented by the clastics which occur between the Diplopora-bearing dolomites and the black, stromatolitic dolomite (the *Daonella lommeli*-bearing shale interbeddings in the upper part of the Diplopora–dolomite possibly indicate their forerunners or equivalents of the North Alpine Partnach beds).

– *Late Carnian–Early Norian:* Pelagic influence can be recognized in the lower part of carbonate platforms of the lower Upper Codru Nappes (Dieva and Moma Nappes) in the form of reddish, conodont- and Halobia-bearing intercalations. They can be assigned to the same event, which caused the break-down of the North Alpine (Mürztal Facies; Lein 1987) and West Carpathian (Silica Nappe; Kovács 1984) shelf margin and resulted in the deposition of Hallstatt Limestones. Such a pelagic influence is common in the southern part of the North Alpine–West Carpathian Dachstein platforms.

– *Middle Early Norian* (beginning with Lacian-2)–*Early Middle Norian:* Infilling of the Roşia basin of the Şeasa sedimentary zone with clastics (Codru Formation). The fact that it did not begin immediately after the sea-level fall at the end of the Early Carnian (= Cordevolian), or that the Reingraben Shales and Lunz Sandstones are missing here, can be explained by the low tectonic activity in the hinterland. Due to low relief, the clastic supply was rather low, the sediments were trapped in the coastal lagoons (e.g. during the deposition of the lower part of Scăriţa Formation), and/or a slightly emerged land zone may have formed a barrier, hampering the transport into the Roşia basin. (This barrier was most probably the Villány–Bihor ridge, the morphological separation of which from the Mecsek half-graben began already in the early part of the Carnian; cf. Galácz and Vörös, lecture.) A tectonic uplift in the hinterland during the middle part of the Lacian could have produced a higher relief and the beginning of clastic input into the Roşia basin.

– *Late Middle Norian–Late Norian:* The red clastics of the Carpathian Keuper were able to be transported across the filled Şeaşa zone, episodically as far as the sedimentary zone of the Dieva Nappe (Tărcăiţa Dolomite).

– *Rhaetian*: the Kössen transgression. More or less typical Kössen beds (with characteristic fauna) were deposited in the central zones. In the Villány–Bihor zone and in the Vălani Nappe there is no record of it, or only a poor one, whereas in the Mecsek zone formation of the thick Liassic coal sequence already began in the Late Rhaetian. On the southeastern margin (Vaşčau–Coleşti Nappes) the Dachstein-type platform accretion continued.

To sum up the above review: during the Triassic the Tisza Megaunit was undoubtedly adjacent to a northerly-lying (according to present-day coordinates) continental hinterland, and was part of the North Tethyan Margin (cf. Dercourt et al. 1990, pls 1–2). It was split off from there in the Middle Jurassic, as indicated in the Mecsek– Northern Great Plain zone, by the cessation of siliciclastic input and the beginning of hemipelagic sedimentation in the Bathonian, as reflected by the replacement of "Fleckenmergel" deposits by "ammonitico rosso"–type calcareous marls (Galácz 1984; Bérczi-Makk 1986). Together with the Eastern Alps and the Inner Carpathian chain, it was part of the Austroalpine orogeny (as expressed already by a number of authors, e.g. Patrulius et al. 1971; Săndulescu 1972, 1984b, 1989; Bleahu 1976; Ianovici et al. 1976; Patrulius 1976; Wein 1978; Bleahu et al. 1981; Kovács 1980, 1982 and others; for the Jurassic position of the Mecsek–Villány region, Géczy 1973 a, b and his students), that was folded during the Albian Austrian and/or Late Turonian–Early Senonian Mediterranean (Pregosau) tectonophase. Paleo- magnetic data show the same European directions during the Triassic, Jurassic and Lower Cretaceous, and rotation of the region (and, consequently, separation from the Austroalpine orogenic belt) occurred only in post-Aptian times (cf. Balla 1986). Whether the Triassic oceanic domain, which was adjacent to the outer shelf domain of the Tisza Megaunit on the south, had only one branch (as postulated by Bleahu 1976, Fig. 1 and Kovács 1984, Fig. 4; Fuchs 1985; Tollmann 1987) or was bifurcated (as supposed by Săndulescu 1984a, Fig. 4 and Lupu 1984, Fig. 1), is beyond the scope of the present paper. It should be noted, however, that in the latter case the other branch could only be to the east of the Bihor Unit (see in Săndulescu 1990, Figs 1–2) and not to the north of it (again: according to present coordinates!).

Various opinions (e.g. Mišík 1987; Mišík et al. 1989a, b) placing the Tisza Megaunit on the South Tethyan margin, adjacent to the Outer Dinaric shelf (which shows, however, a very different evolution[2]), as done by Mišík et al. (1989b, Fig. 4), or considering it as an island, must face a major contradiction in transport direction of the terrigenous clastics: from (or across) a northerly (resp. northeasterly)-lying open sea domain! The latter authors have carefully summarized all the differences between the individual units of the West Carpathians and of the Tisza Megaunit,

2 The diagnostic differences of the South Tethyan Outer Dinaric margin as against the North Tethyan one are as follows (see Dimitrijević 1982; Grubić 1980; Pamić 1982):

– Absence of a polymetamorphic crystalline basement with granitoids (the pre-Alpine rocks are represented by non to very low grade metamorphosed, in most part carbonatic Paleozoic sequences, in places with marine fossils);

– Marine sedimentation throughout the Late Permian–Early Triassic ("Bellerophon Kalk" and Werfen Facies);

– Intense island-arc-type volcanism, especially in the Ladinian (up to a few hundred metres thick volcanic suite);

– Intense synsedimentary tectonism; emerged blocks in the Middle Triassic are indicated by conglomerates and breccias, which are very characteristic for this shelf: Richthofen conglomerates in the South Alpine sector, Uggowitz breccias in the NW Dinarides;

– In the High Karst Nappe continuous platform carbonate accretion (locally interrupted by hiatuses) from the Middle–Late Triassic to the Cretaceous.

but these can be explained by local factors (e.g. different rocks in the continental hinterland or the presence of the large Rosia intrashelf basin).

Acknowledgements

Prof. Krzysztof Birkenmajer (Cracow) and Dr. Jozef Michalík (Bratislava) reviewed an earlier draft of the manuscript. Their suggestions and corrections are greatly acknowledged. The authors are very grateful for Acad. Mircea Sandulescu (Bucharest) for his critical remarks. Thanks are due to Dr. Ruza Kemenci and Dr. Miruna Canovic (Novi Sad) for their contribution to the stratigraphic column of the Northern Backa–Northern Banat region (which appears in more details in a separate paper).

For the Hungarian part the preparation of this article was supported by National Research Fund (OTKA) No. 2671.

References

Anđelković, M., M. Lupu 1967: Die Geologie der Šumadija und Mureş-Zone. – Carp.-Balk. Geol. Assoc. 8th Congr., Rep. Geotect., 1, pp. 15–28.

Antonescu, E., D. Patrulius, I. Popescu 1976: Corrélation palynologique préliminaire de quelques formations de Roumanie attribuées au Trias inférieur. – D. S. Inst. geol. geof., 62, 5, pp. 3–30.

Balázs, E., B. Cserepes-Meszéna, A. Nusszer, Gy. Szili, P. Gyémánt 1986: An attempt to correlate the metamorphic formations of the Great Hungarian Plain and the Transylvanian Central Mountains (Munţii Apuseni). – Acta Geol. Hung., 29, pp. 317–320.

Balla, Z. 1982: Development of the Pannonian basin basement through the Cretaceous–Cenozoic collision: a new synthesis. – Tectonophysics, 88, 1–2, pp. 61–102.

Balla, Z. 1986: Analysis of the anti-clockwise rotation of the Mecsek Mountains (Southwest Hungary) in the Cretaceous: interpretation of paleomagnetic data in the light of the geology. – Geoph. Transactions, 32, 2, pp. 147–181.

Balogh, K. 1972: Historical review of conceptions referring to the Pannonian Mass. – Geol. Práce, Správy, 58, pp. 5–28.

Balogh, K. 1981: Correlation of the Hungarian Triassic. – Acta Geol. Hung., 24, 1, pp. 3–48.

Baltreş, A., Gh. Mantea in press: Sedimentologic evolution of Bihor carbonate platform (Northern Apuseni Mountains–Romania). – Travaux ICSOBA, 22, 24, pp. 43–59 Zagreb.

Barabás–Stuhl, Á. 1981: Microflora of the Permian and Lower Triassic sediments of the Mecsek Mountains (South Hungary). – Acta Geol. Hung., 24, 1, pp. 49–97.

Barabás-Stuhl, Á. 1993: Palynological revaluation of Lower Triassic and Lower Anisian formations of Southeast Transdanubia. – Acta Geol. Hung., 36, 4, pp. 405–458.

Barabás-Stuhl, Á., A. Barabás (in press): Sedimentology of the Jakabhegy Sandstone Formation. – Acta Geol. Hung.,

Bérczi-Makk, A. 1985: Triász mikrofauna kelet-magyarországi szénhidrogénkutató mélyfúrásokból (Triassic microfauna from hydrocarbon exploratory wells in eastern Hungary) – Földt. Közl., 115, 3, pp. 303–313.

Bérczi-Makk, A., B. Cserepes-Meszéna 1985: A nagykőrösi preneogén aljzat földtani felépítése (Geology of the pre-Neogene basement of Nagykőrös [Central Hungary]) – Földt. Közl., 115, 3, pp. 249–266.

Bérczi-Makk, A. 1986: Mesozoic formation types of the Great Hungarian Plain. – Acta Geol. Hung., 29, 3–4, pp. 261–282.

Bleahu, M. 1974: The Apuseni Mountains, in Mahel', M. (ed.): Tectonics of the Carpathian–Balkan Regions. – Inst. Geol. Dionýs Stúr, pp. 221–243.

Bleahu, M. 1976: Structural position of the Apuseni Mountains in the Alpine system. – Rev. Roum. géol. géophys. géogr., Ser. Géol., 20, pp. 7–19.

Bleahu, M. 1976: Structure géologique des Apuseni septentrionaux. – Rev. roum. géol. géophys., géogr., Ser. Géol., 20, 1, pp. 27–39.

Bleahu, M., Gh. Mantea 1964: Le Rhétien des Monts Apuseni. – Colloque du Jurassique, 1962. C. R. Mém. pp. 663–674.

Bleahu, M., D. Patrulius, C. Tomescu, J. Bordea, Şt. Panin, S. Rădan 1970: Date noi asupra depozitelor triasice din Munţii Apuseni (New data on the stratigraphy of the Triassic deposits from the Apuseni Mountains). – D.S. Inst. Geol. Geof., 66, 4, pp. 29–41.

Bleahu, M., Şt. Panin, C. Tomescu 1972: Contribuţii la biostratigrafia depositelor triasice din Platoul Vaşcău (Munţii Apuseni) (Contributions on the Triassic deposits biostratigraphy of Vaşcău Plateau [Apuseni Mountains]). – D.S. Inst. Geol. Geof., 58, 3, pp. 5–25.

Bleahu, M., Şt. Panin, C. Tomescu, A. Ştefan, Gh. Istrate, M. Ştefănescu 1979: Harta geologică a R.S. România, scara 1:50 000, Foaia Vaşcău, 55d. – Inst. Geol. Geof., Bucureşti.

Bleahu, M., R. Dimitrescu, S. Bordea, J. Bordea, Gh. Mantea 1980: Harta geologica a R.S. România, scara 1:50 000, Foaia Poiana Horea, 56b. – Inst. Geol. Geof., Bucureşti.

Bleahu, M., S. Bordea, M. Lupu, A. Ştefan, D. Patrulius, Şt. Panin 1981: The structure of the Apuseni Mountains. – XII. Cong. Carp. Balk. Geol. Assoc. Guide to excursion B3, 107 p. Bucharest.

Bleahu, M., Şt. Panin, Fl. Marinescu, M. Ştefănescu, A. Popescu, I. Nicolae 1981: Harta geologică a R. S. România, scara 1:50 000, Foaia Dr. Petru Groza, 55b. – Inst. Geol. Geof., Bucureşti.

Bleahu, M., Şt. Panin, M. Ştefănescu, N. Stan, A. Popescu, C. Tomescu, A. Stefan 1984: Harta geologică a R.S. România, scara 1:50 000, Foaia Dumbrăviţa, 55a. – Inst. Geol. Geof. Bucureşti.

Bleahu, M., J. Bordea, Gh. Mantea, G. Cioflică, A. Ştefan, A. Popescu, Fl. Marinescu, S. Bordea 1985: Harta geologică a României, scara 1:50 000, Foaia Pietroasa, 56a. – Inst. Geol. Geof., Bucureşti.

Bóna, J. 1973: Palynological practice in the investigation of Liassic coal measures in the Mecsek Mountains. – Ősl. Viták, 21, pp. 65–71, Budapest.

Bóna, J. 1983: A mecseki felsőtriász és alsóliász palynológiai vizsgálata (Palynological studies on the Upper Triassic and Lower Liassic of the Mecsek Mountains). – Ősl. Viták, 29, pp. 47–57, Budapest

Bóna, J. 1984a: Adatok a mecseki felső-triász és alsó-liász palynológiai szintezéséhez (Contributions to the palynostratigraphic division of the Upper Triassic and Lower Liassic in the Mecsek Mts). – MÁFI. Évi Jel., 1982, pp. 203–216.

Bóna, J. 1984b: Szintjelző spórák és virágporszemek a kelet-mecseki felsőtriász kőszén-fekü rétegekből (Index spores and pollens from the Upper Triassic coal footwall layers in the Eastern Mecsek Mts). – Folia Comloensis, 1, pp. 3–25, Komló.

Bóna, J. (in press): Palynobiostratigraphy of the Upper Triassic formations in the Mecsek Mts. – Acta Geol. Hung.,

Bordea, S., J. Bordea 1973: Noi date stratigrafice şi structurale în nord-vestul Munţilor Bihor (New Stratigraphic and Structural Data in the North–West of the Bihor Mountains). – D. S. Inst. Geol. Geof., 69, 5, pp. 5–12.

Bordea, S., M. Bleahu, J. Bordea 1975: Date noi stratigrafice şi structurale asupra Bihorului de vest. Unitatea de Următ şi unitatea de Vetre (New Stratigraphic and structural Data on the Western Bihor Mountains. Următ and Vetre Units). – D. S. Inst. Geol. Geof., 61, 5, pp. 61–83.

Bordea, S., J. Bordea, Gh. Mantea, C. Costea 1986: Harta geologică R. S. România scara 1:50 00, Foaia Zece Hotare 40b. – Inst. Geol. Geof., Bucureşti.

Bordea, S., R. Dimitrescu, Gh. Mantea, A. Ştefan, J.Bordea, M. Bleahu, C. Costea 1988: Harta geologică R. S. România, scara 1:50 000, Foaia Biharia 56c. – Inst. Geol. Geof., Bucuresti.

Bystrický, J. 1972: Faziesverteilung der mittleren und oberen Trias in den Westkarpaten. – Mitt. Ges. Geol. Bergbaustud., 21, 1, pp. 289–310.

Bystrický, J. 1973: Triassic of the West Carpathian Mountains – Guide to Excursion D. X. Congr. Carpath.-Balk. Geol. Ass., 137 p. Bratislava.

Čanović, M., R. Kemenci 1988: Mezozoik podine Panonskog basena u Vojvodini. – Stratigrafija i facije, magmatizam, paleogeografija. 339 p., Matica srpska, Odeljenje za prirodne nauke, Novi Sad.
Channel J.E.T., F. Horváth 1976: The African/Adriatic promontory as a paleogeographical premise for Alpine orogeny and plate movements in the Carpatho-Balkan region. – Tectonophysics, 35, 1–3, pp. 71–102.
Chikán, G., Gy. Konrád 1982: A nyugat-mecseki földtani térképezés újabb eredményei (Latest results of geological mapping in the W Mecsek Mountains [S Hungary]). – MÁFI Évi Jel. 1980-ról, pp. 169–186.
Chikán, G., Chikán G-né, A. Kókai A. 1984: A Nyugati-Mecsek földtani térképe. 1:25 000 (Geological map of the W Mecsek). – MÁFI Budapest.
Császár, G. 1992: Urgonian facies of the Tisza Unit. – Acta Geol. Hung., 35, 3, pp. 263–285.
Császár, G., J. Haas 1984: The Cretaceous in Hungary: a review. – Acta Geol. Hung., 23, 3–4, pp. 417–428.
Császár, G., J. Haas et al. 1984: Mesozoic formations in Hungary. – Guidebook to Excursion 104 of the XVIIth International Geological Congress. 92 p. Budapest.
Császár, G., A. Galácz, J. Haas, M. Kázmér, S. Kovács, A. Nagymarosy, K. Szentgyörgyi, A. Vörös 1990: Paleogeography of the Pannonian Basin. – In: Evolution of the northern margin of Tethys: The Results of IGCP Project 198. vol. 3. Rakús, M., Dercourt, J., Nairn, A. (Eds) Mém. Soc. Géol. France, Nouv. Ser. No. 154 (III.) pp. 63–89.
Csontos, L., A. Nagymarosy, F. Horváth, M. Kováč 1992: Tertiary evolution of the Intra-Carpathian area: a model. – Tectonophysics, 208, pp. 221–241.
Dank, V., J. Fülöp et al. 1990: Magyarország szerkezetföldtani térképe. 1:500 000 (Tectonic map of Hungary). – MÁFI, Budapest
Dercourt, J., L.E. Ricou, S. Adamia, Cs. Császár, H. Funk, J. Lefeld, M. Rakús, M. Săndulescu, A. Tollmann, P. Tchoumachenko 1990: Paleogeographical maps 1:10 000 000 IGCP 198 "Northern Margin of Tethys", – Geol. ústav Dionýza Stúra, Bratislava.
Detre, Cs. 1973: A mecseki triász legjobb megtartású és első rétegtanilag értékelhető Ammonoidea lelete (Über die ersten, stratigraphisch auswertbaren Ammonoiden-Fund von bester Erhaltung der Mecseker Trias). – MÁFI Évi Jel., 1971, pp. 277–282.
Diaconu, M., O. Dragastan 1969: Triassic Calcareous Algae from the Apuseni Mountains (Romania). – Rev. of Paleobot. and Palynol., 19, pp. 63–101.
Diaconu, M., O. Dragastan 1970: Date noi asupra depozitelor triasice din Pădurea Craiului (Munţii Apuseni) (New data on Triassic deposits of Pădurea Craiului Mts). – D.S. Inst. Geol. Geof., 56, pp. 43–50.
Dicea, O., P. Duţescu, F. Antonescu, G. Mitrea, R. Botez, I. Donose, V. Lungu, I. Moroşanu 1980: Contribuţii la cunoaşterea tectonicii zonei transcarpatice din Maramureş (Contribution concerning the tectonics of the Maramureş Transcarpatian Zone). – D.S. Inst. Geol. Geof., 65, pp. 35–53, Bucuresti.
Dimitrescu, R. 1981: Hypothéses sur la structure du soubassement du secteur sud-oriental de la Dépression Pannonique. – Rev. roum. Géol. Géophys. Géogr., Ser. Géol. 25, pp. 31–35.
Dimitrescu, R., M. Bleahu, M. Lupu 1977: Harta geologică a R.S. România, scara 1:50 000, Foaia Avram Iancu, 56d, Inst. Géol. Geof., Bucureşti.
Dimitrijević, M.D. 1982: Dinarides: An Outline of the Tectonics. – Earth Evol. Sci., 2, 1, pp. 4–23, Braunschweig–Wiesbaden.
Dolenko, G.N., L.G. Danhilovits 1976: Novoye utsenhie a geosinklinaliah i yivo primenhenie k Ukranskim Karpathem. – Geol. Zborn. Geol. Carpath., 27, 1, pp. 1–10.
Dolenko, G.N., I.T. Boitsevskaia, L.G. Danhilovits, A.P. Medvediev, P.N. Tsarnhenko 1981: Ophioliti i razvithie Ukranskih Karpat v planhe thektonhiki litosphernih plit. – Geol. Zborn. Geol. Carpath., 32, 4, pp. 449–464.
Dragastan, O., M. Diaconu, E. Popa, R. Damian 1982: Biostratigraphy of the Triassic formations in the East of the Pădurea Craiului Mts. – D. S. Inst. Geol. Geof., 67, 4, pp. 29–61.

Fuchs, W. 1985: Grosstektonische Neuorientierung in den Ostalpen und Westkarpaten unter Einbeziehung plattentektonischer Gesichtspunkte. – Jb. Geol. B.A., 127, 4, pp. 571–631.
Fülöp, J., K. Brezsnyánszky, J. Haas 1987: The new map of basin basement of Hungary. – Acta Geol. Hung., 30, 1–2, pp. 3–20.
Fülöp J., V. Dank, et al. 1987: Magyarország földtani térképe a kainozóikum elhagyásával. 1:500 000 (Geologic map of Hungary without the Cenozoic). – MÁFI, Budapest.
Fülöp, J. 1989: Bevezetés Magyarország geológiájába (Introduction to the geology of Hungary). – Akadémiai Kiadó, 246 p, Budapest.
Fülöp, J. 1994: Magyarország geológiája. Paleozóikum II. (Geology of Hungary. Paleozoic II). – Akadémiai Kiadó, 447 p, Budapest.
Galácz, A. 1984: Jurassic of Hungary: a review. – Acta Geol. Hung., 27, 3–4, pp. 359–377.
Géczy, B. 1973a: The origin of the Jurassic faunal provinces and the Mediterranean plate tectonics. – Ann. Univ. Sci. Budapestiensis, Sect. Geol., 16, pp. 99–114.
Géczy, B. 1973b: Plate tectonics and paleogeography in the East-Mediterranean Mesozoic. – Acta. Geol. Hung., 17, pp. 421–428.
Gheorghian, D. 1976: Contribuţii la cunoaşterea unor microfauna triasice din Munţii Apuseni (Pădurea Craiului) [Contributions to knowledge of same Triassic microfauna from Apuseni Mountains (Pădurea Craiului)]. – D. S. Inst. Geol. Geofiz., 62, 3, pp. 25–38.
Giuşcă, D., M. Bleahu 1965: Harta geologică a R.S. România, scara 1:200 000, Foaia Arad, 16. – Inst. Geol. Geof., Bucureşti.
Giuşcă, D., M. Bleahu 1967a: Harta geologică a R.S. România, scara 1:200 000, Foaia Şimleul Silvaniei, 9. – Inst. Geol. Geof., Bucureşti.
Giuşcă, D., M. Bleahu 1967b: Harta geologică a R. S. România, scara 1:200 000 Foaia Brad, 17. – Inst. Geol. Geof., Bucureşti.
Grecula, P., I. Varga 1979: Main discontinuity belts on the inner side of the Western Carpathians. – Miner. Slovaca, 11, 5, pp. 389–404, Spišská Nová Ves.
Grow, J.A., Gy. Pogácsás, A. Bérczine-Makk, P. Várnai, D. Hajdú, E. Varga, Cs. Péró 1989: A Békési medence tektonikai és szerkezeti viszonyai (Tectonic and structural conditions of the Békés Basin). – Magyar Geofiz., 30, 2–3, pp. 63–97.
Grow, J.A., R.E. Mattick, A. Bérczi-Makk, Cs. Péró, D. Hajdú, Gy. Pogácsás, P. Várnai, E. Varga 1994: Structure of the Békés Basin Inferred from Seismic Reflection, Well and Gravity Data. – In: P.G. Teleki et al. (Eds): Basin Analysis in Petroleum Exploration, 1–38. Kluwer Academic Publishers, Netherlands.
Grubić, A. 1980: An Outline of geology of Yugoslavia. – In: Grubić, A. (Ed.): Yugoslavia. 26th International Geological Congress, Guidebook to Excursions 201A–202B, pp. 5–49. Paris–Beograd.
Haas, J., S. Kovács, L. Krystyn, R. Lein (in press): Significance of Late Permian–Triassic facies zones in terrane reconstructions in the Alpine–North Pannonian domain. – Tectonophysics, 242, 1–2, pp. 19–40.
Hetényi, R., G. Hámor, M. Földi, I. Nagy, E. Nagy, I. Bilik 1982: A Keleti-Mecsek földtani térképe. 1:25 000 (Geological map of the E-Mecsek Mts). – MÁFI Budapest.
Ianovici, V., M. Borcoş, M. Bleahu, D. Patrulius, M. Lupu, R. Dimitrescu, H. Savu 1976: Geologia Munţilor Apuseni. – Edit. Acad. R.S.R., 631 p. Bucureşti.
Istocescu, D., G. Ionescu 1970: Geologia părtii de nord a Depresiunii Pannonice (Sectorul Oradea – Satu Mare) [The Geology of the Northern part of the Pannonian Depression (Oradea–Satu Mare Zone)]. – D.S. Inst. Geol. Geof., 55, 5, pp. 73–84.
Istocescu, D., O. Dragastan 1978: Les occurences triassiques du bassin de Beiuş (Monts Apuseni). – D. S. Inst. Geol. Geof., 64, 4, pp. 137–145.
Istocescu, D., A. Mihai, M. Diaconu, F. Istocescu 1970: Studiul geologic al regiunii cuprinse între Crişul Repede şi Crişul Negrru (Geological study of the region between the Crişul Repede and Crişul Negru). – D. S. Inst. Geol. Geof., 55, 5, pp. 89–106, Bucuresti.
Jurcsak, T. 1973: Date noi asupra reptilelor fosile de vîrstă mesozoică din Transilvania (New Data on the Mesozoic reptilians from Transilvania). – Nymphaea I, pp. 245–261, Oradea.

Jurcsak, T. 1975: Tanystropheus biharicus n. sp. (Reptilia, Squamata), o nouă specie pentru fauna triasică diu România ([Tanystropheus biharicus n. sp. {Reptilia, Squamata}, a new species for Triassic fauna from Romania). – Nymphaea III, pp. 45–52, Oradea.
Jurcsak, T. 1976: Noi descoperiri de reptile fosile in Triasicul de la Aleşd (New discoveries of Triassic reptiles of the Aleşd locality). – Nymphaea, IV, pp. 67–91. Oradea
Jurcsak, T. 1977: Contribuţii noi privind placodontele si sauropterygienii din Triasicul de la Aleşd (Bihor, România) [New contributions regarding the Placodonts and Sauropterygiens of the Triassic from Aleşd (Bihor, Romania)]. – Nymphaea V., pp. 5–30. Oradea.
Kázmér, M. 1986: Tectonic units of Hungary: Their boundaries and stratigraphy (a bibliographic guide). – Ann. Univ. Sci. Budapest, Sect. Geol. pp. 45–120.
Kemenci, R. 1991: The Magmatites and Metamorphites in the Regional, Structural Units of the Tertiary Basement in Vojvodina. Yugoslavia. – In: Karamata, S. (Ed.): Geodynamic evolution of the Pannonian Basin. Serb. Acad. Sci. and Arts. Acad. Conf. 62. Dept. of Nat and Math. Sci., 4, pp. 227–242.
Kemenci, R., M. Čanović 1975: Preneogena podloga Vojvodanskog dela Pannonskog basena. – Radovi Znan. sav. za naftu JAZU, Sekc. Geol. Geof. Geokem., 5, pp. 248–256, Zagreb.
Kemenci, R., M. Čanović (in press): Geologic setting of the pre-Tertiary Basement in Vojvodina (Yugoslavia) Part I, The Tisza Megaunit. – Acta Geol. Hung. (in press).
Kókai A., E. Rálisch 1981: Újabb adatok a mecseki anizuszi képződmények ismeretéhez (Contributions to the knowledge of the Mecsek Mountains' Anisian). – MÁFI Évi Jel. 1979, pp. 201–209.
Konrád, Gy. 1990: A mecseki és villányi középső-triász betétes mészköveinek keletkezéséről (Middle Triassic mudstone-inserted limestones in the Mecsek and Villány Mountains). – MÁFI Évi Jel. 1988, I. pp. 81–86.
Kovács, S. 1980: Paleogeographical significance of the Triassic Hallstatt limestone facies in the North Alpine facies region. – Földt. Közl., 110, pp. 360–381.
Kovács, S. 1982: Problems of the "Pannonian Median Massif" and the plate tectonic concept: Contributions based on the distribution of late Paleozoic–early Mesozoic isopic zones. – Geol. Rundsch., 71, pp. 617–640.
Kovács, S. 1984: North Hungarian Triassic facies types: a review. – Acta Geol. Hung., 27, 3–4, pp. 251–264.
Kovács, S., J. Papšová 1986: Conodonts from the Paraceratites binodosus zone (Middle Triassic) from the Mecsek Mountains, southern Hungary, and from the Choč Nappe of the Low Tatra Mountains, Czechoslovakia. – Geol. Zborn. Geol. Carpath., 37. pp. 59–74.
Kovács, S., G. Császár, A. Galácz, J. Haas, E. Nagy, A. Vörös 1989: The Tisza Superunit was originally Part of the North Tethyan (European) Margin. – In: Rakús, M., K. Dercourt, A. Nairn (Eds) Evolution of the Northern margin of Tethys: the results of IGCP project 198. Vol. 2. Mém. Soc. Géol. France, Nouv. Ser. No. 154 (II), pp. 81–100 Paris.
Kovács, S. 1991: Rudabánya Mts., Varbóc, Telekes-völgy, NW tributary No.8. Bódvalenke Limestone Fm., Hallstatt Limestone Fm. – In: Geological key-sections of Hungary, No. 91/163, MÁFI, Budapest.
Krystyn, L. 1983: Das Epidauros-Profil (Griechenland) ein Beitrag zur Conodonten–Standard-zonierung des tethyalen Ladin und Unterkarn. – In: Zapfe, H. (Ed.) Neue Beiträge zur Biostratigraphie der Tethys–Trias, Schriftenr. Erdwiss. Komm. Österr. Akad. Wiss., Band 5, pp. 231–258, Wien.
Kurucz, B. 1977: A Pusztaföldvár–Battonya közötti terület medencealjzatának képződményei és hegységszerkezete (Formations and structure of the basement of the Pusztaföldvár-Battonya area). – JATE Szeged. Doctor Univ. theses. Manuscript.
Lachkar, G., J. Bóna, M.J. Pavillon 1984: The Liassic Gresten Facies: palynological data and paleogeographical significance. – Acta Geol. Hung., 27, 3–4, pp. 409–416.
Lein, R. 1987: Evolution of the Northern Calcareous Alps during Triassic times. – In: Flügel, H. W., P. Faupl (Eds) Geodynamics of the Eastern Alps, pp. 85–102, Wien.

Lupu, M. 1984: Problems of the European Continental Margin in the Transylvanian–Pannonian Area. – An. Inst. Geol. Geofiz., 64, pp. 323–332, Bucureşti.

Mader, D. 1992: Mecsek Mts. and Balaton Highlands (Hungary): Permian and Triassic. – In: Evolution of Paleoecology and Paleoenvironment, Permian and Triassic fluvial basins in Europe, Vol. I, Western and Eastern Europe, pp. 739–852, Gustav Fischer Verlag, Stuttgart–New York

Mahel', M. 1984: The West Carpathians. – In: Mahel', M., Malkovský, M.(Eds): Explanations to Tectonic Map of Czechoslovakia 1:500 000, pp. 29–49, GÚDŠ Bratislava.

Mahel', M. 1986: Geologická stavba ceskoslovenských Karpát. 1. – Paleoalpinské jednotky. 503 p. VEDA, Vyd. slov. Akad. Vied, Bratislava.

Mantea, Gh. 1970: Geologia pǎrtii de nord a Muntilor Bihor (regiunea Ferice) [The geology of the northern part of the Bihor Mts (Ferice Zone)] – St. cerc. geol. geofiz. geogr., Ser. Geol. 14, 2, pp. 511—522.

Mantea, Gh., A.Ştefan, A. Rusu, R. Dimitrescu 1987: Harta geologicǎ a R. S. România, scara 1:50 000 Foaia Rǎchiţele 41d – Inst. Geol. Geof. Bucureşti.

Marinescu, Fl., I. Papaianopol, A. Popescu, V. Moisescu, A. Rusu, A. R. Horvath, St. Cîmpeanu, C. Tomescu 1982: Harta geologicǎ a R. S. România, scara 1:50 000 Foaia Tusa, 28d – Inst. Geol. Geof. Bucureşti.

Misík, M. 1987: On relationship of the Central West Carpathians and the Northern Apuseni Mts. – Geol. Zborn. Geol. Carpath., 38, 6, pp. 643–650.

Misík, M., R. Mock., M. Rakús, A. Biely 1989a: The area of Mesozoic sedimentation of the Mecsek and Northern Apuseni Mountains was not situated in the West Carpathians. – In Rakús, M., J. Dercourt,A. E. M. Nairn, (Eds) Evolution of the Northern Margin of Tethys, Vol. 2, Mém. Soc. Géol. France, N. S. 152, 2, pp. 69–79. Paris.

Misík, M., R. Mock, M. Rakús, A. Biely 1989b: The sedimentation area of the Mecsek Mts was not in the West Carpathians. – Geol. práce, Správy 90, pp. 7–22.

Nagy, E. 1968: Triasbildungen des Mecsek Gebirges. – Ann. Inst. Geol. Hung., 51, 1, pp. 1–239.

Nagy, E. 1969: Paläogeographie. In: Unterlias–Kohlenserie des Mecsek Gebirges (Geologie). – Ann. Inst. Geol. Hung., 51, 2, pp. 289–317.

Nagy, E. 1971: Der unterliassische Schichtenkomplex von Grestener Fazies im Mecsek Gebirge (Ungarn). – Ann. Inst. Geol. Hung., 54, 2, pp. 155–159.

Nagy E., L. Ravasz-Baranyai 1968: Tufás kaolinit- és sziderit-telepek a mecseki ladini összlet alján (Tuffige Kaolinit–und Sideritlager im Mecsek Gebirge an der Basis des ladinischen Komplexes). – Földt. Közl., 98, 2, pp. 213–217.

Nagy, E., I. Nagy 1976: Triasbildungen des Villányer Gebirges. – Geol. Hung. Ser. Geol., 17, pp. 111–227.

Pálfy, J., Á. Török 1992: Comparison of Alpine and Germano-type Middle Triassic Brachiopod faunas from Hungary, with remarks on Coenothyris vulgaris (Schlotheim, 1820). – Ann. Univ. Sci. Budapest., Sect. Geol., 29, pp. 303–323.

Pamić, J. 1982: Trijaski magmatizam Dinarida. – 236 p., Nafta, Zagreb.

Pamić, J. 1986: Magmatic and metamorphic complexes of the adjoining area of northernmost Dinarides and Pannonian Mass. – Acta Geol. Hung., 29, 3–4, pp. 203–220.

Panin, Şt., C. Tomescu 1974: Noi contribuţii la biostratigrafia depozitelor triasice din Platoul Vaşcǎu (New contributions to the Triassic deposits biostratigraphy from the Vaşcǎu Plateau). – D. S. Inst. Geol. Geof., 60, 4, pp. 51–57.

Panin, Şt., M. Bleahu, C. Tomescu, E. Mirǎuţa, M. Ştefǎnescu 1982: Structure of the Vaşcǎu Plateau. – D. S. Inst. Geol. Geof., 67, 5, pp. 109–124.

Pap, S. 1987: Kelet-Magyarország 4500 méternél mélyebb fúrásainak földtani eredményei. (Geological results of boreholes below 4500 m depth in East-Hungary) – In: Alföldi Tanulmányok, XI, pp. 7–43, Békéscsaba.

Pap, S. 1990: Felpikkelyezett rétegsorok a Közép–Tiszántúlon (Upthrusted sequences in the middle part of the territory east of the Tisza). – MÁFI Alkalmi Kiadv., 36 p., Budapest.

Papaianopol, I., A. Popescu, St. Cîmpeanu 1977: Harta geologică a R. S. România, scara 1:50 000 Foaia Plopiş, 28c. – Inst. Geol. Geof. Bucureşti.
Patrulius, D. 1970: Inventar sumar al algelor Dasycladaceae triasice din Carpaţii Românesti (Summary the Triassic Dasycladacean algae of Romanian Carpathians). – D.S. Inst. Geol. Geof., 55, 3, pp. 187–200.
Patrulius, D 1971: Unitatea de Vălani: un nou element structural al sistemului pînzelor de Codru (Munţii Apuseni) [The Vălani Unit: a new structural element of the Codru Nappes System (Apuseni Mountains)]. – D. S. Inst. Geol. Geof., 57, 5, pp. 155–171.
Patrulius, D. 1976: Les formations mésozoiques des Monts Apuseni septentrionaux: corrélation chronostratigraphique et faciale. – Rev. roum. Géol., géophys, géogr., Ser. Géol., 20, 1, pp. 49–57.
Patrulius, D., Bleahu, M. 1967: Le Trias des Monts Apuseni. – Geol. Sborn. 18, 2, pp. 245–255.
Patrulius, D., M. Bleahu, I. Popescu, S. Bordea 1971: The Triassic Formations of the Apuseni Mountains and of the East Carpathian Bend. – Guidebook to Excursions of the IInd Triassic Colloquium, Carpatho–Balkan Assoc., 86 p. Bucharest.
Patrulius, D., E. Popa, St. Cîmpeanu, Th. Orasanu 1973: Harta geologica a R. S. România, scara 1:50 000, Foaia Remeţi, 41a – Inst. Geol. Geof., Bucureşti.
Patrulius, D., D. Gheorghian, E. Mirăuţa 1976: Corrélation biochronologique du Calcaire de Roşia, formation triassique du systéme des nappes de Codru (Monts Apuseni). – D. S. Inst. Geol. Geof., 62. 4., pp. 121–133.
Patrulius, D., M. Bleahu, E. Antonescu, A. Baltreş, S. Bordea, J. Bordea, D. Gheorghian, M. Iordan, E. Mirăuţa, Şt. Panin, E. Popa, C. Tomescu 1979: The Triassic Formations of the Bihor Autochton and Codru nappe–system (Apuseni Mountains). – IIIrd Triassic Colloquium of the Carpatho–Balkan Geol. Assoc, Guidebook to Field Trips, 21 p., Bucharest.
Plašienka, D. 1991: Mesozoic tectonic evolution of the epi-Variscan continental crust of the Central Western Carpathians – a tentative model. – Miner. slov., 23., 5–6, pp. 447–457.
Popa, E. 1981: La biostratigraphie des formations Mésozoiques de la partie orientale de Pădurea Craiului (Monts Apuseni). – An. Inst. géol. géophys., géogr., 58, pp. 203–282.
Popa, E., O. Dragastan 1973: Alge şi foraminifere triasice (Anisian–Ladinian) din estul Pădurii Craiului (Munţii Apuseni) [Triassic alagae and forams from Eastern Pădurea Craiului (Apuseni Mts)]. – St. cerc. geol. geof. geogr., Ser. Geol., 18, 2, pp. 425–442.
Rakusz, Gy., L. Strausz 1953: A Villányi hegység földtana (La Géologie de la Montagne de Villány). – MÁFI Évk. 41, 2, 44 p.
Rálisch-Felgenhauer, E. 1985a: Mecsek, Pécs, Exposure of Lapisi street. Misina Formation, Lapis Limestone Member. – In: Geological key-sections of Hungary. No. 85/855 MÁFI, Budapest.
Rálisch-Felgenhauer, E. 1985b: Villány Mountains, Villány, Sikló–cut of Templomhegy. Mészhegy Sandstone Formation, Somsicshegy Formation. – In: Geological key-sections of Hungary. No. 85/855 MÁFI, Budapest.
Rálisch-Felgenhauer, E. 1986a: Mecsek, Pécs, Lapisi street, 7 km. Misina Formation, Báránytető Limestone Member. – In: Geological key-sections of Hungary. No. 86/166 MÁFI, Budapest.
Rálisch-Felgenhauer, E. 1986b: Mecsek, Pécs, Exposure of Misina street. Misina Formation; Bertalanhegy Limestone Member, Dömörkapu Limestone Member. – In: Geological key-sections of Hungary. No. 86/166 MÁFI, Budapest.
Rálisch-Felgenhauer, E. 1987a: Kisrét, park–lane to Dömörkapu, "U"-bend of Misina road, Pécs. Misina Formation. – In: Geological key-sections of Hungary. No. 87/254 MÁFI, Budapest.
Rálisch-Felgenhauer, E. 1987b: Lower quarry of Templom-hegy, Villány, Villány Mountains. Siklós Formation, Templomhegy Dolomite Member. – In: Geological key-sections of Hungary. No. 87/254 MÁFI, Budapest
Rálisch-Felgenhauer, E. 1987c: Mecsek, Pécs, Kis-Tubes, Rotary-promenade. Misina Formation. Tubes Limestone Member. – In: Geological key-sections of Hungary. No. 87/301 MÁFI, Budapest.

Rálisch-Felgenhauer, E. 1987d: Villány Mountains, Siklós, Rigó quarry. Siklós Formation; Zuhánya Limestone Member, Csukma Dolomite Member. – In: Geological key-sections of Hungary. No. 87/301 MÁFI, Budapest.

Rálisch-Felgenhauer, E. 1988a: Exposure at Abaliget Street, Pécs, Mecsek Mountains. Misina Formation, Viganvár Limestone Member. – In: Geological key-sections of Hungary. No. 88/49 MÁFI, Budapest.

Rálisch-Felgenhauer, E. 1988b: Mecsek Mountains, Hetvehely, Sásvölgy. Hetvehely Dolomite Formation. – In: Geological key-sections of Hungary. No. 88/211 MÁFI, Budapest.

Rálisch-Felgenhauer, E. 1988c: Mecsek Mountains, Pécs, Kantavár, Lámpás–valley. Karolina Valley Sandstone Formation. – In: Geological key-sections of Hungary. No. 88/176 MÁFI, Budapest.

Rálisch-Felgenhauer, E. 1988d: Remete-rét, S slope of Vörös-hegy, Pécs, Mecsek Mountains. Misinai Formation, Vöröshegy Dolomite Member. – In: Geological key-sections of Hungary. No. 88/49 MÁFI, Budapest.

Rálisch-Felgenhauer, E. 1988e: Villány Mountains, Csarnóta quarry. Siklós Formation, Gyűd Limestone Member. – In: Geological key-sections of Hungary. No. 88/211 MÁFI, Budapest.

Rálisch-Felgenhauer, E. 1988f: Villány Mountains, Siklós, Oliva quarry. Siklós Formation, Gyűd Limestone Member. – In: Geological key-sections of Hungary. No. 88/49 MÁFI, Budapest.

Rálisch-Felgenhauer, E. (in press): A Mecsek–Villány vonulat triász litosztratigráfiája (Triassic lithostratigraphy of the Mecsek–Villány range). – Földt. Közl., (in press)

Rálisch–Felgenhauer, E., Á. Török (1990): Triász. Mecsek- és Villányi-hegység. In: Bérczi-Makk et al.: A Tiszai–egység magyarországi részének mezozóikuma (Triassic. Mecsek and Villány Mts. In: Mesozoic of the Hungarian part of Tisza Unit). – Manuscript, MÁFI.

Rusu, A., B. Popescu, V. Moisescu, V. Ignat, Fl. Marinescu, A. Popescu 1977: Harta geologică a R. S. România, scara 1:50 000, Foaia Mezeş, 29c. – Inst. Geol. Geof. Bucureşti.

Săndulescu, M. 1972: Consideraţiuni asupra posibilităţilor de corelare a structurii Carpaţilor Orientali şi Occidentali (Considerations on the correlation possibilities of the Eastern and Western Carpathians structure). – D. S. Inst. Geol. Geofiz., 58, 5, pp. 125–150, Bucureşti.

Săndulescu, M. 1975: Essai de synthèse structurale des Carpathes. – Bull. Soc. Géol. France, 7, 17, 3, pp. 299–358.

Săndulescu, M. 1980: Sur certains problèmes de la corrélation des Carpathes Orientales roumaines avec les Carpathes ucrainiennes. – D. S. Inst. Geol. Geofiz., 65, pp. 163–180. Bucureşti.

Săndulescu, M. 1984a: Compared Alpine Geotectonic Models. – An. Inst. Geol. Geofiz., 64, pp. 343–351, Bucureşti.

Săndulescu, M. 1984b: Geotectonica României. – Editura Technica, 336 p., Bucureşti.

Săndulescu, M. 1989: Structure and tectonic history of the northern margin of Tethys between the Alps and the Caucasus. – In: Rakús, M., Dercourt, J., Nairn, A. E. M. (Eds) Evolution of the Northern Margin of Tethys, Vol. II, Mém. Soc. Géol. France, Nouv. Série, No. 154 (II), pp. 3–16, Paris.

Săndulescu, M. 1990: Paleogeography of the Romanian Carpathians and Foreland. In: Rakús, M., Dercourt, J., Nairn, A. E. M. (Eds) Evolution of the Northern Margin of Tethys, Vol. III., Mém. Soc. Géol. France, Nouv. Série No. 154, (III), pp. 91–100, Paris.

Săndulescu, M., M. Visarion 1978: Considérations sur la structure tectonique du soubassement de la dépression de Transylvaniae. – D. S. Inst. Geol. Geofiz., 64, 5, pp. 153–173.

Săndulescu, M., H.G. Kräutner, M. Borcoş, S. Năstăseanu, D. Patrulius, M. Ştefănescu, C. Ghenea, M. Lupu, H. Savu, I. Bercia, Fl. Marinescu 1978: Harta geologică a R. S. România, scara 1:1 000 000, Foaia 1. – Inst. Geol. Geof. Bucureşti.

Săndulescu, M., H.G. Kräutner, I. Balintoni, D. Russo-Săndulescu, M. Micu 1981: The structure of the East Carpathians (Moldavia–Maramureş area). – 12th Congr. Carpatho- Balkan Geol. Assoc., Guidebook series 19. 95 p., Bucharest.

Schlager, W., W. Schöllnberger 1974: Das Prinzip stratigraphischen Wenden in den Schichtfolge der Nördlichen Kalkalpen. – Mitt. Geol. Ges. Wien, 66–67, pp. 165–193. Wien.

Šikić, K., M. Brkić 1975: Donji trijas u Papuku i Krndiji. – Geol. vjesn., 28, pp. 133–141. Zagreb.
Šikić, K., M. Brkić, A. Šimunić, M. Grimani 1975: Mezozojske naslage Papučkog gorja. – Radovi Znan. sav. za naftu JAZU, Sekc. Geol. Geof. Geokem., 5, pp. 87–96, Zagreb.
Ştefan, A., V. Ignat, St. Cîmpeanu, B. Popescu, Gh. Istrate, Th. Orăşanu 1974: Harta geologică a R. S. România, scara 1:50 000, Foaia Ciucea, 41b. – Inst. Geol. Geof. Bucureşti.
Ştefănescu, M., Şt. Panin, C. Tomescu 1983: A new tectonic image of the Mesozoic deposits of the Codru–Moma mountains between Crişu and Rîpoasa valleys (Northern Apuseni). – D. S. Inst. Geol. Geof., 69, 5, pp. 105–107.
Szederkényi, T. 1984: Az Alföld kristályos aljzata és földtani kapcsolatai (Crystalline basement of the Great Hungarian Plain and its geologic relations). – D. Sc. theses. Manuscript.
Szederkényi, T., P. Árkai, Gy. Lelkes-Felvári 1991: Crystalline Groundfloor of the Great Hungarian Plain and South Transdanubia, Hungary. – In: Karamata, S. (Ed.) Geodynamic evolution of the Pannonian Basin. – Serb. Acad. Sci. and Arts, Acad. Conf. 62. Dept. of Nat. and Math. Sci., 4, pp. 261–273, Beograd.
Szente, I. 1992: Early Jurassic Molluscs from the Mecsek Mountains, (S. Hungary). A preliminary study. – Ann. Univ. Sci. Budapest., Sect. Geol., 29, pp. 325–343.
Szénás, Gy. 1968: A Kárpát-medence kéregszerkezete a földtan és a geofizika tükrében (The crustal structure of the Carpathian Basin). – Geofiz. Közlem., 17, 4, pp. 17–37, Budapest.
Szepesházy, K. 1972: A Tiszántúl középső részének júra időszaki képződményei, a szénhidrogénkutató fúrások adatai alapján (Der Juragesteine des mittleren Teiles von Tiszántúl auf Grund von Schürfbohrungen auf Erdöl und Erdgas). – MÁFI Évi jel. 1970, pp. 67–78.
Szepesházy, K. 1975: Az Északkeleti-Kárpátok földtani felépítésének és a kárpáti térségben való nagyszerkezeti helyzetének vázlata (Geological setting of the NE Carpathians and their position in the Carpathian system). – Ált. Földt. Szemle, 8, pp. 25–60.
Tollmann, A. 1976: Analyse des klassischen nordalpinen Mesozoikums. – Franz Deuticke, 580 p., Wien.
Tollmann, A. 1987: Neue Wege in der Ostalpengeologie und die Beziehungen zum Ostmediterran. – Mitt. Österr. geol. Ges., 80, pp. 47–113, Wien.
Török, Á. 1993a: Storm influenced sedimentation in the Hungarian Muschelkalk. – In: Hagdorn, H. Seilacher A. (Eds) Muschelkalk. Schöntaler Symposium 1991 (Sonderbände der Gesellschaft für Naturkunde in Württemberg 2). Korb (Goldschneck). pp. 133–142, Stuttgart
Török, Á. 1993b: Brachiopod beds as indicators of storm events: an example from the Muschelkalk of Southern Hungary – In: Pálfy, J., A. Vörös (Eds) Mesozoic Brachiopods of Alpine Europe. pp. 161–172. Hungarian Geological Society. Budapest.
Vadász, E. 1935: Mecsek hegység (Mecsek Mountains). – Magyar Tájak Földt. Leírása. 1. pp. 1–180. Budapest.
Wein, Gy. 1978:A Kárpát-medence alpi tektogenezise (Alpine-type tectogenesis of the Carpathian Basin). – MÁFI Évi Jel., 1976, pp. 245–256, Budapest.
Ziegler, P.A. 1982: Triassic Rifts and Facies Patterns in Western and Central Europe. – Geol. Rundsch., 71, 3., pp. 747–772, Stuttgart.

Acta Geologica Hungarica, Vol. 37/3–4, pp. 235–268 (1994)

Tectonic and magmatic effects on amphibole chemistry in mylonitized amphibolites and amphibole-bearing enclaves associated with granitoid rocks, Mecsek Mountains, Hungary

Péter Árkai, Géza Nagy
Laboratory for Geochemical Research,
Hungarian Academy of Sciences, Budapest

Changes in mineral chemistry were determined in a mafic series represented by mylonitized amphibolite and amphibole-bearing gneiss enclaves in contact with or embedded in the Hercynian granitoid complex of the Mecsek Mts, Hungary. The main trend of isomorphic substitutions in amphibole is intermediate between the tremolite ↔ tschermakite and tremolite ↔ pargasite, being the same both in the mylonitized amphibole and in the enclaves. Mineral associations and chemical changes in amphibolite and plagioclase suggest that mylonitization proceeded in prograde, amphibolite facies conditions. No signs of migmatite formation were found in the mylonitized complex. The variations in modal composition, amphibole chemistry and compositional zoning of porphyroclasts are explained by local differences in lithology, shearing and metasomatic effects. In mafic enclaves of the granitoids the amphibole is represented by actinolite, actinolitic hornblende and subordinately, magnesio-hornblende. The combination of prograde (growth and diffusional) zoning and actinolite-hornblende exsolution in calcic amphibole is a consequence of complex, subsolidus crystallization of the enclaves.

Key words: amphibole, amphibolite, mylonite, granitoid, mineral chemistry, amphibolite facies, greenschist facies, thermobarometry, Mecsek Mts, Hungary

Introduction

Although migmatites and anatectic granitoids are commonly associated with amphibolites and often contain mafic enclaves, termed mesosomes or paleosomes (=restites) following the classification of Ashworth (1985), relatively few data refer to the crystal chemical evolution of amphibole in such settings. Because the solidus temperatures of these mafic rocks are significantly higher than those of the metaclastic rocks which are apparently the major component of the S-type anatectic granitoids, amphibolite seems to be a suitable "refractory" rock type for identifying the different, earlier episodes of metamorphic and magmatic processes, the effects of which have been obliterated in metaclastic rocks due to their intense melting and magmatic mobilization. On the other

Address: P. Árkai, G. Nagy: H–1112 Budapest, Budaörsi út 45, Hungary
Received: 10 Jun, 1994

0236–5278/94/$ 5.00

hand, shearing (mylonitization) is also a common phenomenon in metamorphic complexes which surround the granitoid massifs.

Microstructural, mineral paragenetic, bulk chemical and mineral chemical investigations were carried out in order to supply new data on the effects of mylonite formation and granitoid magmatism on the chemistry of amphibole in amphibolites and mafic enclaves deriving from the metamorphic–granitoid complex of the Mecsek Mountains (Hungary).

Geologic outline

The area investigated forms part of the Tisza Unit (Fig. 1a). The Tisza Unit, which originated from the northern, stable European margin of Tethys by horizontal microplate displacements (Kovács 1982; Kázmér and Kovács 1985; Balla 1988; Haas et al. 1990), proved to be one of the most stable blocks of the Pannonian Basin during its Alpine tectonometamorphic evolution (Árkai 1991).

The basement of the Tisza Unit is characterized by regional pre-Hercynian(?) or early Hercynian medium thermal gradient amphibolite facies metamorphism. This was overprinted by a high thermal gradient Hercynian event, with grades ranging from subgreenschist facies up to amphibolite facies. The formation of syn- and late-kinematic migmatites and granitoids was connected to the axes and centres of thermal maxima of this low-pressure event, as typified by the Mecsek granitoids. In certain zones the second phase of metamorphic recrystallization was preceded by cataclastic or mylonitic deformation. Locally, Alpine retrograde (subgreenschist and greenschist facies) metamorphic overprints have also been demonstrated (Lelkes-Felvári and Sassi 1981; Árkai 1984; Szederkényi 1984; Árkai et al. 1985; Szederkényi et al. 1991).

The Eastern Mecsek Mountains (Mórágy Hills) are built up mainly by granitoids containing mafic restites (Fig. 1b). According to Buda (1985) the U–Pb, Rb–Sr and K–Ar isotopic ages measured on zircon, biotite and amphibole of the collision-type, K-rich, slightly alkaline and monzonitic granitoids scatter between 365 and 311 Ma. Main and trace element compositions indicate that they are S-type granitoids of anatectic–metasomatic origin, while the restites are remnants of basic magmatic rocks. The granitoid melt crystallized in a water-saturated system with low f_{O_2} buffered by ilmenite. The composite order disorder relations of the potash feldspar (intermediate ordering in the matrix and maximal ordering in the porphyroblasts) was interpreted by Buda in terms of an anatectic–metasomatic model, outlined originally by Szádeczky-Kardoss (1959).

The petrogenetic interpretation of the metamorphic surroundings and the enclaves of the granitoids is hindered by insufficient petrographic data. Ghanem and Ravasz-Baranyai (1969) described greenschist, epidote–amphibolite and subordinate amphibolite facies rocks, which were derived from basic–intermediate volcanics (greenschist, actinolite schist, amphibolite). Rocks of sedimentary origin (marble, phyllite, paragneiss) are relatively rare. According

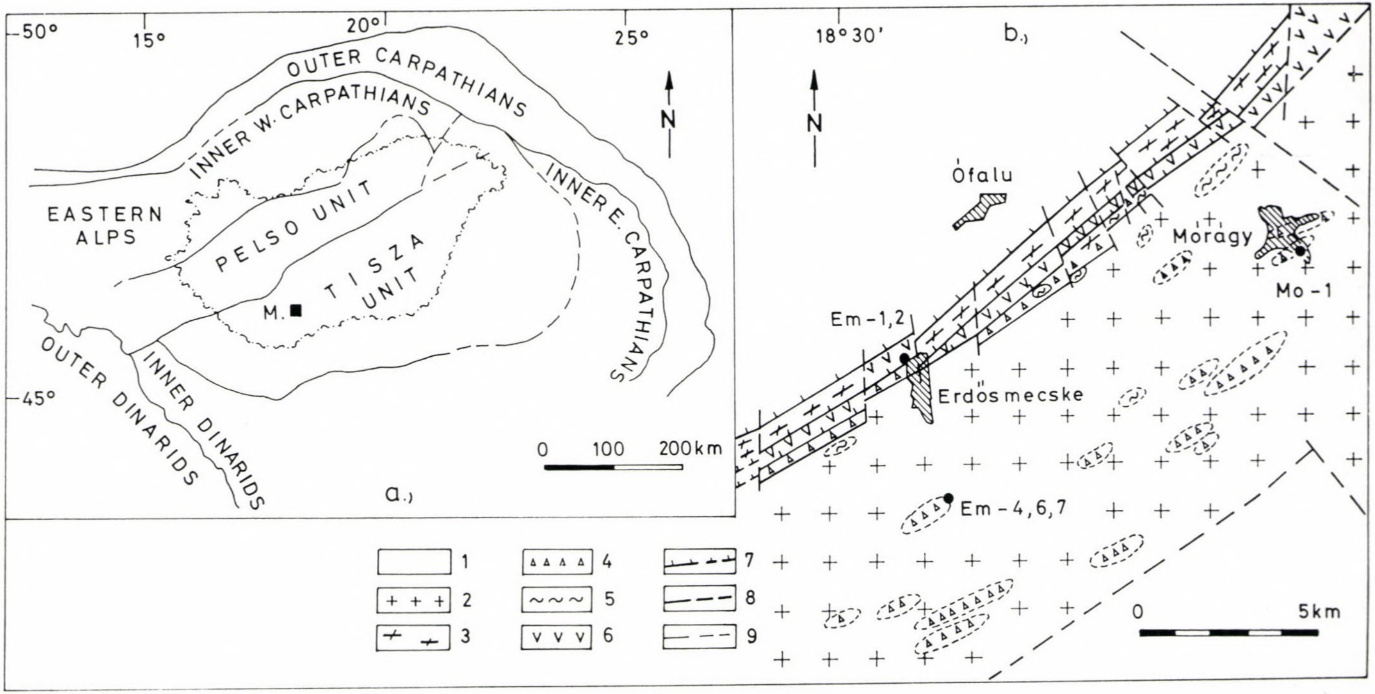

Fig. 1
a) Tectonic position of the Mecsek Mountains (M) in the Alpine–Carpathian system after Haas et al. (1990); b) Geological map of the pre-Permian metamorphic and granitoid formations of the eastern Mecsek Mountains after Jantsky (1979) and Szederkényi (1975, 1987), with the locations of the investigated samples. 1. unknown pre-Permian basement; 2. granite–granodiorite; 3. mylonite zone with traces of partial anatexis and K-metasomatism; 4. agmatite; 5. cordierite–sillimanite gneiss; 6. mylonitized amphibolite, locally with phyllite and marble intercalations; 7. overthrust; 8. fault; 9. boundary of the formations

to the above-mentioned authors and Szádeczky-Kardoss et al. (1969) this complex, and the intrusive equivalents of the volcanic rocks, were the starting materials for the granitoids' formation. Many of the metamorphic rocks were interpreted by Szederkényi (1975) as mylonites formed during early Variscan transcurrent faulting striking ENE-WSW. Locally, the mylonite formation was followed by partial melting, although the narrow (1.5–2 km wide) zone should not be regarded as the true migmatitic border of the granitoid mass (see Fig. 1b).

Based on assumed lithostratigraphic analogies, Jantsky (1979) distinguished an older amphibolite facies and granitized sequence of pelitic-psammitic and "ophiolitic" origin, from a younger, greenschist facies sequence containing phyllite, amphibolite, marble and serpentinite.

Lelkes-Felvári and Sassi (1981) considered that the high-grade metamorphism and anatexis developed under a relatively high (>34 $^{\circ}C\ km^{-1}$) thermal gradient indicated by the occurrence of cordierite + sillimanite + staurolite.

It can therefore be stated that the metamorphic rocks in the Eastern Mecsek Mountains were in the main subjected to shearing (mylonitization), Hercynian anatectic granitization and subsequent K-metasomatism. However, the spatial, temporal and genetic relations of the mostly greenschist facies rocks, forming a continuous narrow belt at the northern margin of the granitoid massif and the amphibolite facies rocks found mostly as enclaves in granitoids, are rather uncertain.

Methods

In addition to macro- and microscopic observations, bulk chemical, XRD and electron microprobe analyses were performed.

Elemental concentrations were determined by AAS (Perkin-Elmer 5000) using a flame technique after digesting the rock samples in lithium metaborate. Gravimetric (SiO_2, H_2O^+ and H_2O^-), spectrophotometric (SiO_2, TiO_2 and P_2O_5), permanganometric (FeO) and volumetric (CO_2) methods completed the major element analyses.

The XRD powder analyses were undertaken using a Philips PW-1730 diffractometer with CuK_{α} radiation. Measuring conditions were: 45 kV, 35 mA, proportional counter, graphite monochromator, 1° divergence and detector slits, 2°/min goniometer and 2 cm/min chart speeds and 2 s time constant.

Chemical analyses of minerals were carried out by a JEOL JCXA-733 electron microprobe equipped with 3 WDS, using the measuring program of Nagy (1984, 1990). The measuring conditions were: 15 kV, 30 nA, defocused electron beam with a diameter of 5–10 μm, measuring time 5x5 s. Matrix effects were corrected by using the method of Bence and Albee (1968). The following standards were used for quantitative analysis: orthoclase (Si, Al and K), synthetic glass (Fe, Mg and Ca), spessartine (Mn), rutile (Ti) and albite (Na). Statistical errors expressed as 1 σ are as follows: SiO_2: ± 0.3, TiO_2: ± 0.05, Al_2O_3: ± 0.05, FeO: ± 0.2, MgO: ± 0.1, MnO: ± 0.05, CaO: ± 0.1, Na_2O: ± 0.03, and K_2O: ± 0.02%.

Cation numbers per amphibole unit cell and T, M1–M3, M4 and A site occupancies were calculated following the scheme of Robinson et al. (1982) suggested for Ca-amphiboles: the sum of the cations (excluding Ca, Na and K) was normalized to 13, and then the total cation content was normalized to 23 oxygens by sharing the total iron between Fe^{3+} and Fe^{2+}.

Petrography

The localities from which samples were collected are show in Fig. 1b, and are listed together with the rock types in Table 1. Table 2 lists the minerals of samples determined by microscopic, XRD and electron microprobe methods.

At the northern and of the village of Erdősmecske the granitoid mass is in fault contact with mylonitized amphibolite and its phyllonitic, hydrothermally-altered, strongly weathered equivalents. The amphibolite belongs to the Silurian(?)-Devonian(?) Ófalu Formation, the presumed age of regional metamorphism being Lower Carboniferous (Szederkényi 1987). Based on the albite+amphibole assemblage, the amphibolite has been thought to reflect greenschist facies regional metamorphism (Jantsky 1979).

Table 1
List of investigated samples

sample	rock type	locality
Em-1/A	mylonitized amphibolite (foliated, with crenulation)	150 m from the northern end of Erdősmecske village: outcrop in the watercourse
Em-1/B	mylonitized amphibolite with plagioclase + kalifeldspar-rich, diffuse lenses	
Em-2/A1	mylonitized amphibolite with thin, felsic (plagioclase + K-feldspar) bands	northern end of Erdősmecske village: samples from the well of the last garden
Em-2/A2	brecciated, mylonitized amphibolite with plagioclase + K-feldspar ± quartz fissure fillings	
Em-4/1	agmatite (amphibole-biotite gneiss enclaves in granodiorite)	quarry at the railway station at Erdősmecske village
Em-6		
Em-7		
Mo-1	melanosome enclave in granodiorite	quarry in Mórágy village

In samples Em-1/A, Em-1/B, Em-2/A1 and Em-2/A2 (i.e. with decreasing distance from the tectonic contact with the granitoid mass), continuous changes in microstructure and modal composition can be observed. The schistose, microcrenulated sample (Em-1/A) contains only very rare feldspar-rich lenses or bands (< 1mm thick), while in more massive samples (Em-1/B and Em-2/A1) local enrichment of feldspars can often be observed. Samples Em-2/A2 represents a brecciated variant which contains mylonitized amphibolite fragments of several mm (maximum 1–2 cm) diameter preserving their original orientation. These mafic fragments are cemented by several mm thick, often disconnected fissure fillings of feldspars.

Sample Em-1/A contains amphibole porphyroclasts with a maximum diameter of about 1500 μm in the micro-crenulated matrix, which is composed mainly of amphibole with an average grain size of ca. 150–200 μm (Fig. 2a). Other constituents are: titanite (30–40 μm, max. 320 μm) forming individual grains, aggregates, bands and locally, inclusions in larger amphibole grains; epidote, which forms quasi-monomineralic bands (Fig. 2b) arranged parallel to the crenulated foliation surfaces, similarly to titanite; and chlorite, which forms large flakes or aggregates. Xenoblastic plagioclase and K-feldspar are found rarely, while ilmenite is present only in trace amounts.

In sample Em-1/B the plagioclase-rich bands and lenses with diffuse borders are observed (Fig. 2c). Amphibole porphyroclasts with a maximum diameter of ca. 500 μm are present in the matrix, which is composed predominantly of amphibole, abundant plagioclase, subordinate chlorite, ilmenite, quartz, K-feldspar and titanite (Fig. 2d). The average diameter of the matrix grains varies between 40 and 100 μm.

Table 2
Modal composition of mylonitized amphibolites and amphibole-bearing enclaves

sample	Qtz	Pl	Kfs	Am	Bt	Chl	Ep	Ttn	Ilm	Hem	Ap	Py	Cal	Sm
Em-1/A		o	o	+		o	o	o	tr					tr
Em-1/B	tr	x	tr	+		o		tr	o					o
Em-2/A1	tr	x	o	+	tr	o	tr	o	o	tr				o
Em-2/A2	tr	x	o	x	tr	o	tr	o	tr	tr				o
Em-4/1	o	x	x	x	x	o					o	o	o	
Em-6	o	x	x	x	x	tr		o		tr	tr	o	tr	
Em-7	o	x		x	x	o	o	tr	tr	tr			o	
Mo-1	o	o	0	x	x	o		o			o			

Symbols: Qtz– quartz; Pl – plagioclase; Kfs – K-feldspar; Am – amphibole; Bt – biotite; Chl – chlorite; Ep – epidote; Ttn – titanite; Ilm – ilmenite; Hem – hematite; Ap – apatite; Py – pyrite; Cal – calcite; Sm – smectite; + – dominant; x – abundant; o – subordinate; tr – trace

Fig. 2 →
Microstructures of mylonitized amphibolite and amphibole-biotite gneiss enclaves. Unless indicated microphotographs are in plane polarized light. Abbreviations also in Figs 3 and 4: Am– amphibole; Act – actinolite; Hbl – hornblende; Bt – biotite; Chl – chlorite; Ep – epidote; Pl – plagioclase; Kfs – K-feldspar; Qtz – quartz; Ms – muscovite; Ti – titanite. a – Mylonitized amphibolite with foliation, micro-crenulation and amphibole porhyroclasts (sample Em-1/A); b – epidote- and titanite-rich bands in mylonitized amphibolite (sample Em-1/A); c – mylonitized amphibolite with amphibole porphyroclasts and feldspar-rich parts (sample Em-1/B); d – matrix of mylonitized amphibolite Em-1/B; e – feldspar-rich lenses and bands in mylonitized amphibolite (samples Em-2/A1); f – transition between the amphibole-rich and feldspar-rich parts of sample Em-2/A1, showing the presence of biotite; g – amphibole-rich and feldspar-rich parts in brecciated, mylonitized amphibolite (sample Em-2/A2); h – microtexture of amphibole-biotite gneiss enclave enclosed by granitoid (sample Em-4/1)

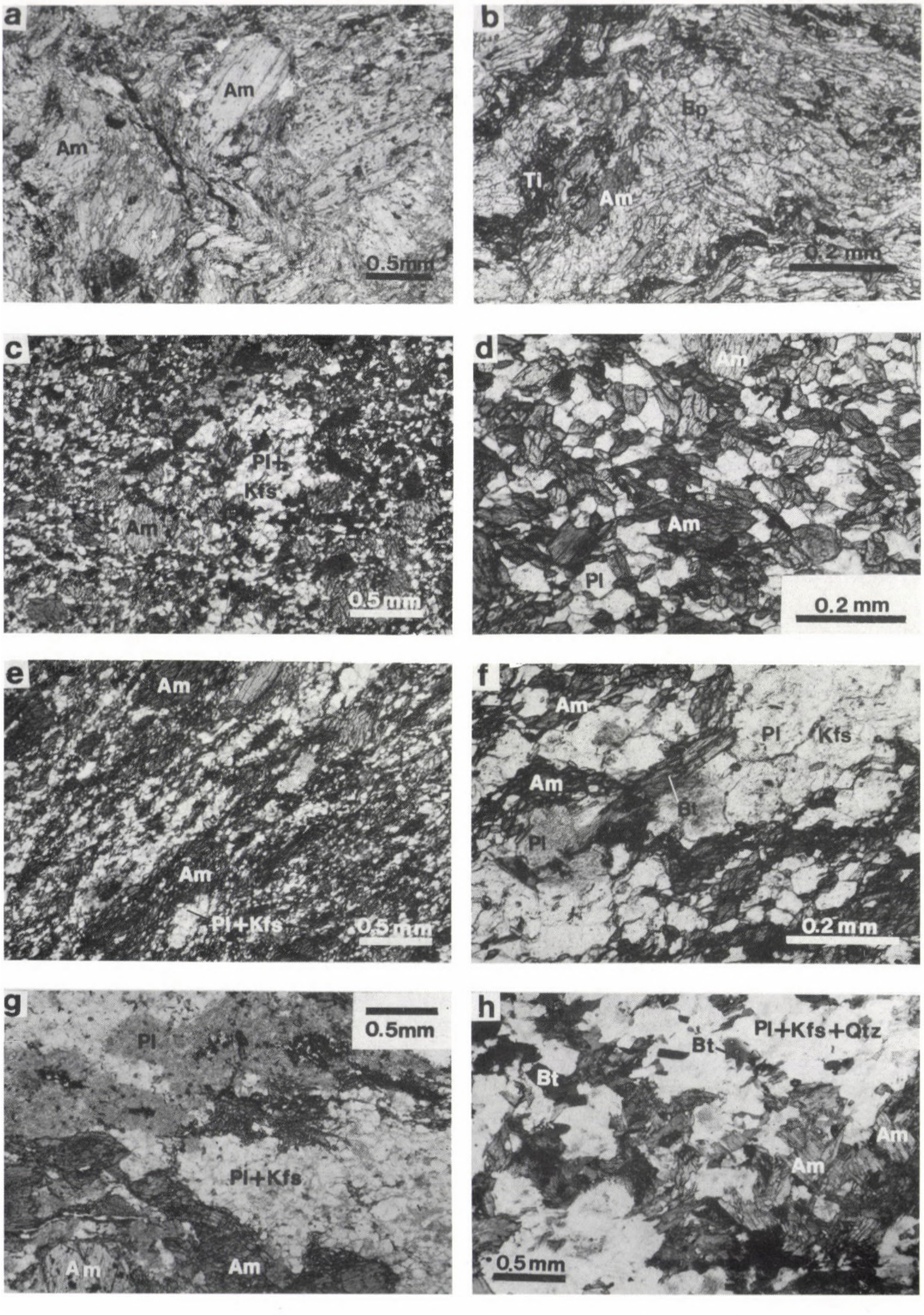
a
Am
Am
0.5mm
b
Ep
Ti
Am
0.2 mm
c
Pl+
Kfs
Am
0.5 mm
d
Am
Am
Pl
0.2 mm
e
Am
Am
Pl+Kfs
0.5 mm
f
Am
Pl
Kfs
Am
Bt
Pl
0.2 mm
g
0.5mm
Pl
Pl+Kfs
Am
Am
h
Pl+Kfs+Qtz
Bt
Bt
Am
Am
0.5 mm

Sample Em-2/A1 contains feldspar-rich (plagioclase >K-feldspar) layers and lenses (Fig. 2e). In the feldspar-rich parts biotite also occurs (Fig. 2f). The dominant part of the rock is mylonitized amphibolite. Optical zoning of amphibole porphyroclasts (average diameter 300–450 μm, maximum diameter ca. 600 μm) indicates chemical inhomogeneity. The matrix constituents (with an average grain size of about 40–50 μm) are amphibole, plagioclase, K-feldspar, chlorite, titanite, ilmenite and, in trace quantities, quartz, epidote and hematite.

In sample Em-2/A2 fragments of partially mylonitized amphibolite are embedded in fine- to medium-grained, plagioclase + K-feldspar-rich cement (Fig. 2g). In the amphibolitic parts large (max. 2000 μm) amphibole clasts are found in the fine-grained mylonitic matrix containing isometric grains of amphibole, plagioclase, K-feldspar, chlorite, titanite, and in trace amounts, quartz, epidote, ilmenite and hematite.

Samples Em-4/1, Em-6 and Em-7 are dark-grey, fine-grained (average grain diameter ca. $\leq$ 1 mm) mafic enclaves with gneissose structure embedded in light-grey, equigranular, medium-grained (average grain size 5–6 mm) granitoid. Boundaries between the granitoid and its enclaves are diffuse. In addition, leucocratic (quartz + feldspar) aggregates lacking sharp boundaries can be found also within the enclaves. Average grain-sizes of the enclave minerals are significantly greater than those in the mylonitized amphibolites. There is a gradual transition between the mafic (biotite + amphibole-rich) and the felsic (feldspars + quartz-rich) parts of the enclaves (Fig. 2h). Compositional growth zoning of plagioclase in felsic parts indicates crystallization from a melt (Fig. 3a). Feldspars contain biotite and amphibole inclusions. Based on the textural features simultaneous crystallization (or recrystallization) of amphibole, biotite and titanite can be determined (Fig. 3b, c). However, local transformations of amphibole to biotite and vice versa can also be observed. In some places the boundaries between amphibole and biotite are sharp, and are determined by crystal faces; elsewhere, diffuse, irregular boundaries are interpreted as reaction fronts. Inclusions of amphibole in biotite and biotite in amphibole are equally present. Rarely, muscovite is also found.

Similar conclusions can be drawn from the textural features of sample Mo-1 (Fig. 3d), which represents a medium-grained (average grain size 2–6 mm), dark-grey melanosome enclave, rich in biotite and amphibole and showing no signs of preferred orientation. It contains amphibole, biotite, quartz, plagioclase, K-feldspar, chlorite, titanite, and apatite.

Variations in modal composition of the various types of mylonitized amphibolites are also reflected in the bulk chemical compositions (Table 3). With increasing amounts of feldspars (from sample Em-1/A to Em-2A/2) the SiO_2, Na_2O and K_2O contents increase, and the TiO_2, Fe_2O_3, FeO and CaO contents decrease significantly. The bulk chemistry of amphibole-bearing enclaves (samples Em-4/1 and Mo-1) differs primarily from the mylonitized amphibolites by their higher K_2O content.

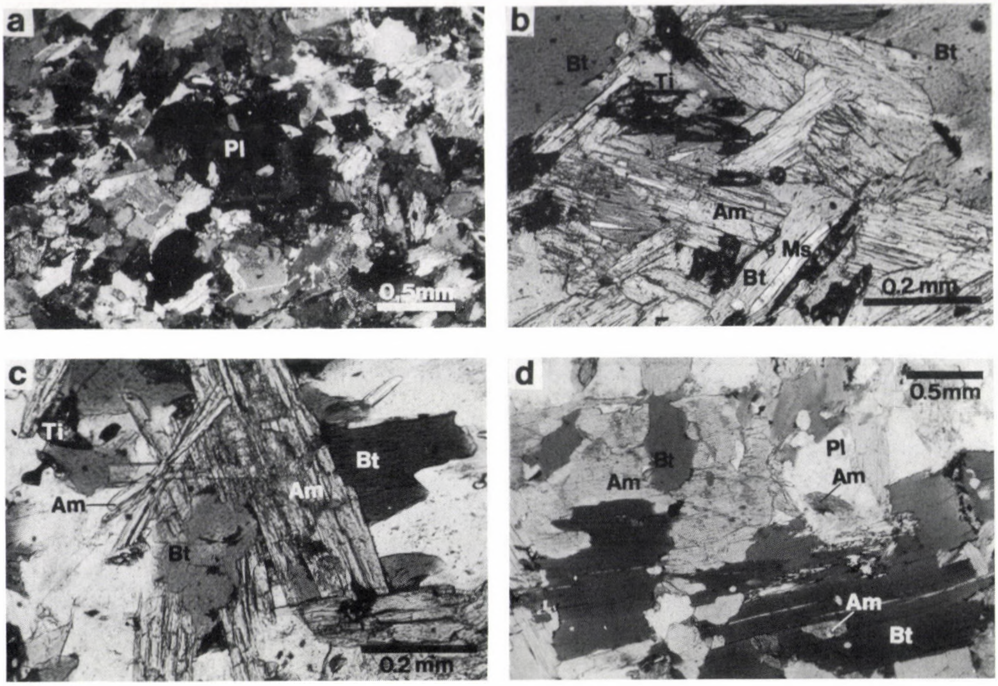

Fig. 3
Microstructures of mylonitized amphibolite and amphibole-biotite gneiss enclaves. Unless indicated microphotographs are in plane polarized light. a – zoned plagioclase in felsic part of the enclave (sample Em-4/1). Crossed polarizers; b–c – textural relations of biotite and amphibole in enclave in sample Em-4/1; d – amphibole inclusions in biotite, and plagioclase and biotite inclusion in amphibole (melanosome enclave in granitoid, sample Mo-1)

Table 3
Chemical composition of mylonitized amphibolites and amphibole-bearing enclaves

	Em-1/A	Em-1/B	Em-2/A1	Em-2/2	Em-4/1	Mo-1
SiO_2	40.15	48.32	48.80	52.92	51.60	54.36
TiO_2	3.90	2.78	2.18	0.98	1.35	1.13
Al_2O_3	15.09	14.43	14.76	14.66	14.57	8.71
Fe_2O_3	5.47	3.49	3.25	2.18	0.62	1.64
FeO	9.26	8.12	7.54	5.45	7.14	7.52
MnO	0.20	0.21	0.19	0.19	0.20	0.14
MgO	7.26	7.08	7.32	8.30	6.43	9.89
CaO	14.62	9.40	9.81	8.25	7.39	7.14
Na_2O	1.19	3.46	2.91	3.43	3.26	0.95
K_2O	0.39	0.41	0.64	0.98	2.81	4.67
$^{+}H_2O$	3.02	2.23	2.41	2.53	2.02	1.39
$^{-}H_2O$	0.10	0.22	0.30	0.20	0.28	0.02
CO_2	0.00	0.00	0.00	0.11	1.84	0.14
P_2O_5	0.29	0.28	0.22	0.08	0.31	0.85
total	100.94	100.43	100.337	100.31	99.82	98.55

Mineral chemistry

Amphibole

Figure 5 illustrates the variation of cations as a function of Si, based on a unit cell containing 23 (0). There is a strong, negative correlation between Si and total Al contents. Total Fe, Fe^{3+}, Fe^{2+}, Ti, (Al^{VI}+Fe^{3+}+Ti), Na, K and (Na+K)A contents decrease, while Mg, (Fe^{2+}+Mg+Mn) contents and the Mg/(Mg+Fe^{2+}) ratio increase with increasing Si contents. Neither the Mn and Ca contents nor the Fe^{3+}/(Fe^{3+}+Fe^{2+}) ratio correlate with Si. Considering the agmatic enclaves as having approximately similar Si contents, sample Mo-1 differs by its higher Mg, and lower Fe and Mn contents from samples Em-4/1, -6 and -7. Comparing the compositions of amphiboles with similar Si values, the amphibole-bearing enclaves in granitoid (samples Em-4/1, -6, -7 and Mo-1) have higher K values than those of mylonitized amphibolites (samples Em-1/A, -1/B and -2/A1).

Larger grains (porphyroclasts or -blasts) of amphibole are compositionally zoned both in mylonitized amphibolites and in amphibole-bearing enclaves. The compositions of the smaller, matrix-forming grains usually correspond to those of the outer parts (rims) of the larger ones. In samples Em-1/A and -1/B Si and Mg contents decrease and Al, Fe and Na contents increase passing from the centre towards the edges of the crystals. Compositional variations along a profile across a porphyroclast (Fig. 4a) are shown in Fig. 6a. Porphyroclasts from samples Em-2/A1 and -2/A2 are characterized by more complicated variations. From the centre outward Si and Mg initially increase, and Al, Fe and Na initially decrease, but after poorly defined maxima and minima, opposite trends occur towards the rim (Figs 4b, c and 6b, c).

Prograde compositional zoning similar to that in mylonitized amphibolites was also found in larger amphibole grains of the enclaves, with Si and Mg contents decreasing and Al, Fe, Na, K and Ti contents increasing towards the margins. The character of the changes varies, however. In places it is continuous, implying growth zoning (samples Em-6 and -7), whereas elsewhere discontinuous zoning occurs (Figs 4d and 6d). Composite zoning was also observed (Figs 4e–h and 6e). In the latter case the early growth zoning of the amphibole (signs of which can be seen near the margin of an idioblastic grain, see Fig. 4f) was disturbed by later exsolution producing magnesio-hornblende (thin, spindle-like, lighter forms in Figs 4g–h) and actinolite (major, darker part

Fig. 4 →
Back-scattered electron images of mylonitized amphibolites and amphibole-bearing enclaves. Solid lines indicate the approximate direction of the analysed profiles plotted in Fig. 6. Amphibole porphyroclasts in mylonitized amphibolites from samples Em-1/B (a), Em-2/A1 (b) and Em-2/A2 (c), (d) diffusion-type zoning in amphibole from enclave Em-4/1, (e)–(h) – hypidioblastic amphibole grain with idioblastic and partially resorbed biotite inclusions (sample Mo-1). Amphibole grain displays growth-zoning (outer parts, pictures (e), (f) and (h)); darker (actinolitic) haloes around certain biotite inclusions and contacting biotite grains (pictures (e) and (h)); and actinolite-hornblende exsolutions (picture (g))

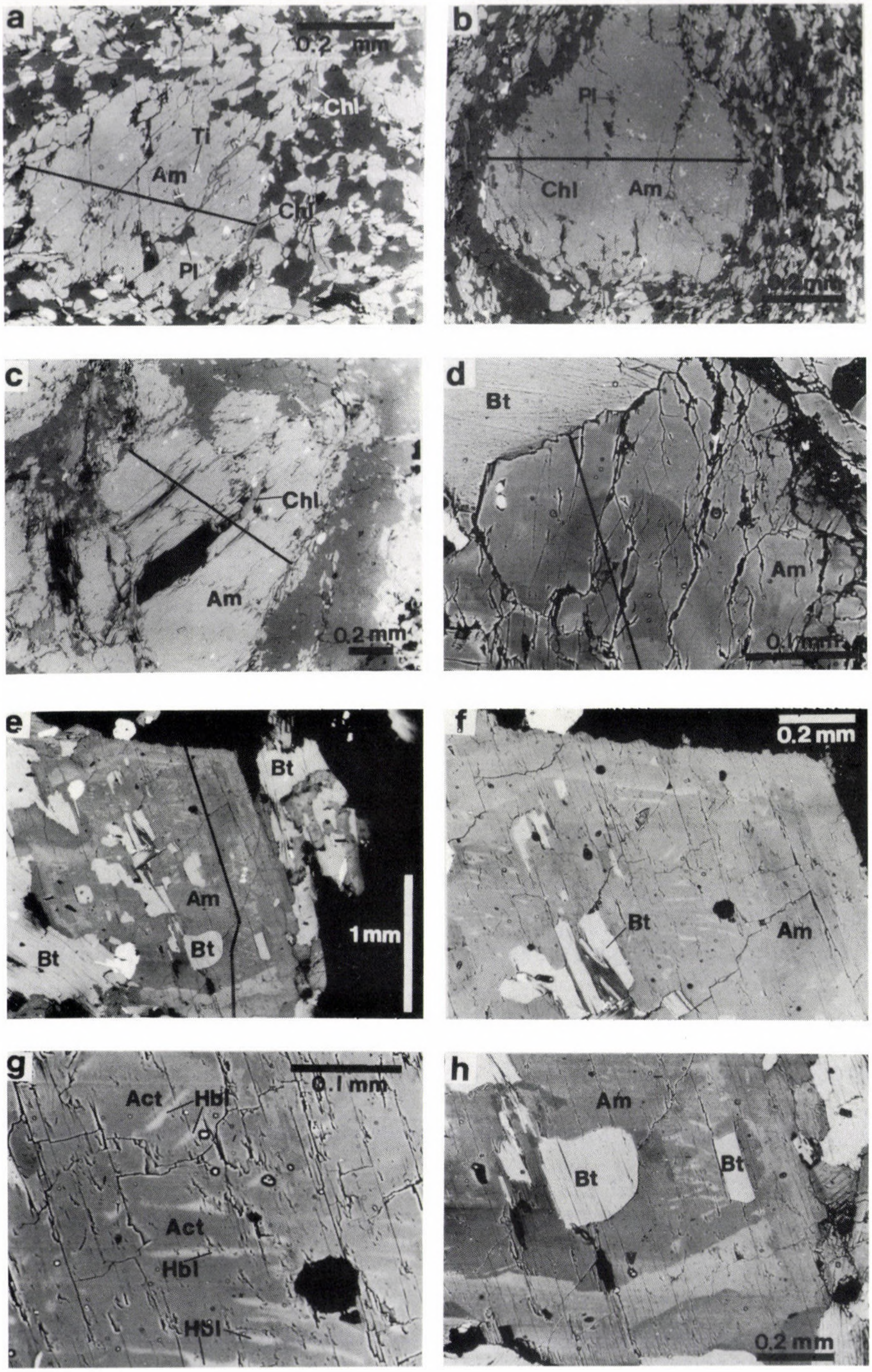
a
0.2 mm
Chl
Ti
Am
Chl
Pl
b
Pl
Chl
Am
c
Chl
Am
0.2 mm
d
Bt
Am
0.1 mm
e
Bt
Am
Bt
Bt
1 mm
f
0.2 mm
Bt
Am
g
0.1 mm
Act
Hbl
Act
Hbl
Hbl
h
Am
Bt
Bt
0.2 mm

of the crystal). Similar, but very fine-scale, pervasive exsolution within the calcic amphibole series was proven recently by Smelik et al. (1991). Reaction haloes are seen around biotites (darkest, Fe-poor actinolitic parts around certain biotite inclusions and adjoining biotite flakes, see Fig. 4h).

In order to interpret the chemical evolution of the investigated amphiboles, average compositions of the inner, transitional and outer parts of crystals were calculated (Table 4). The "outer part" also represents grains in the matrix. The mylonitized amphibolites consist mainly of magnesio-hornblende with subordinate tschermakitic hornblende and ferroan pargasite, while the agmatic enclaves contain actinolite, actinolitic hornblende and magnesio-hornblende, usually showing a continuous trend from actinolite to magnesio-hornblende from the centre towards the margin of crystals.

In both mylonitized amphibolites and amphibole-containing enclaves, the nature of the isomorphic substitution is the same for the entire Si content range of the amphiboles (Figs 7 and 8). The main trend represents a substitution between tremolite and an intermediate member between pargasite and

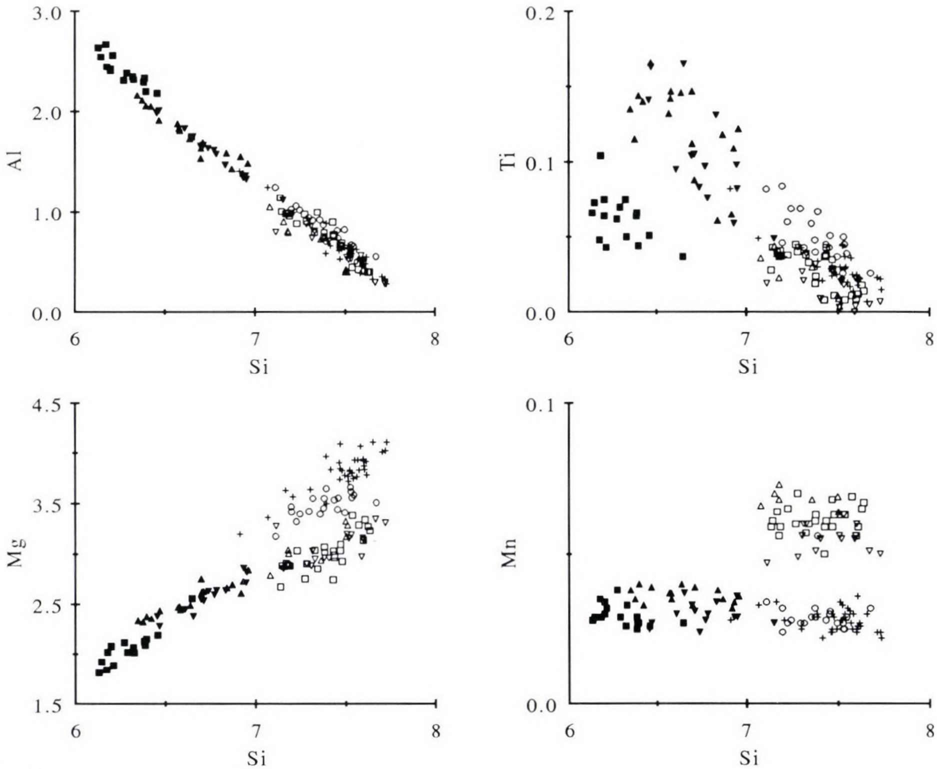

Fig. 5
Variation diagrams of the chemical compositions of amphiboles (numbers of cations per unit cell containing 23 0). ■ – sample Em-1/A, ▼ – sample Em-1/B, ▲ – sample Em-2/A1, ○ --sample Em-2/A2, ❑ – sample Em-4/1, ▿ – sample Em-6, △ –sample Em-7, + –s ample Mo-1

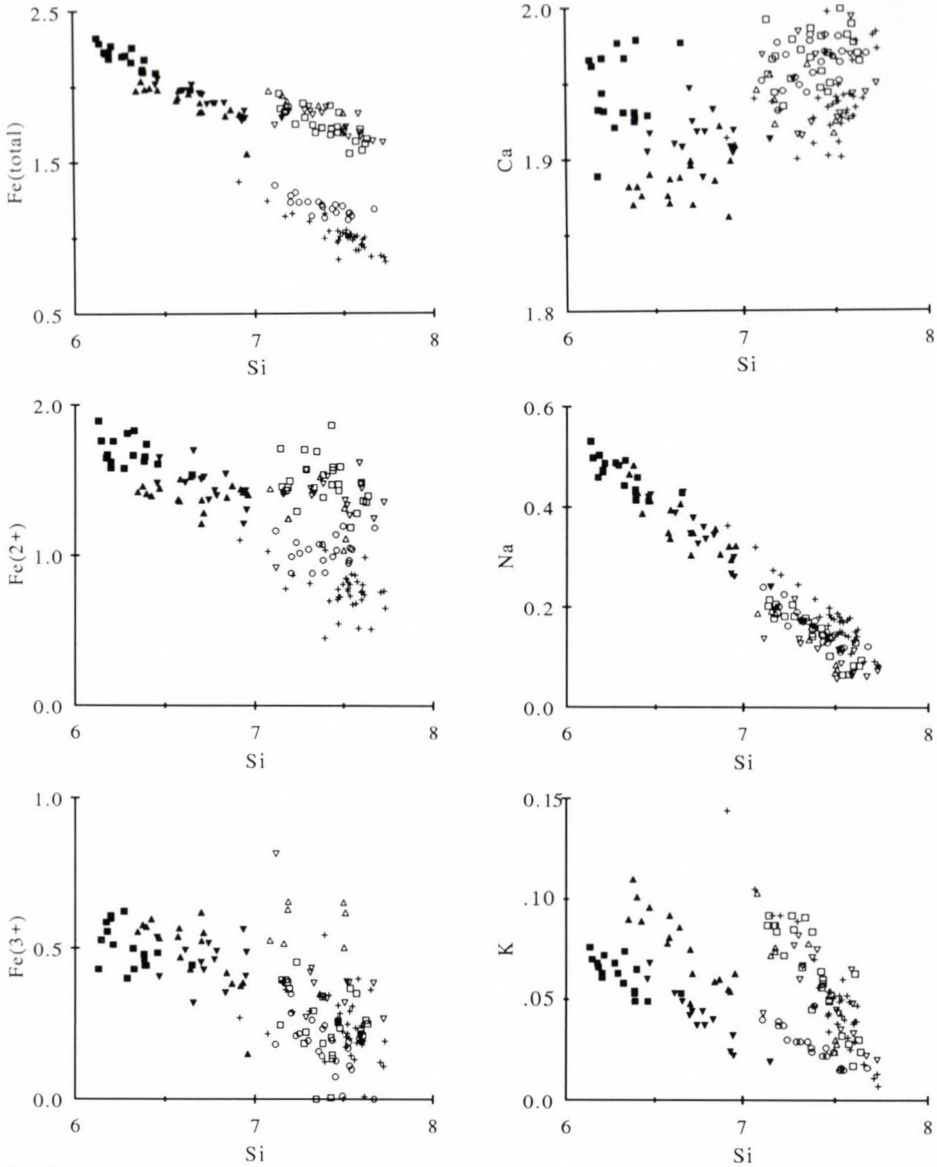
2.5
1.5
0.5
Fe(total)
6
7
8
Si
2.0
1.9
1.8
Ca
6
7
8
Si
2.0
1.0
0.0
Fe(2+)
6
7
8
Si
0.6
0.4
0.2
0.0
Na
6
7
8
Si
1.0
0.5
0.0
Fe(3+)
6
7
8
Si
0.15
.10
.05
0.0
K
6
7
8
Si

Fig. 5 cont.

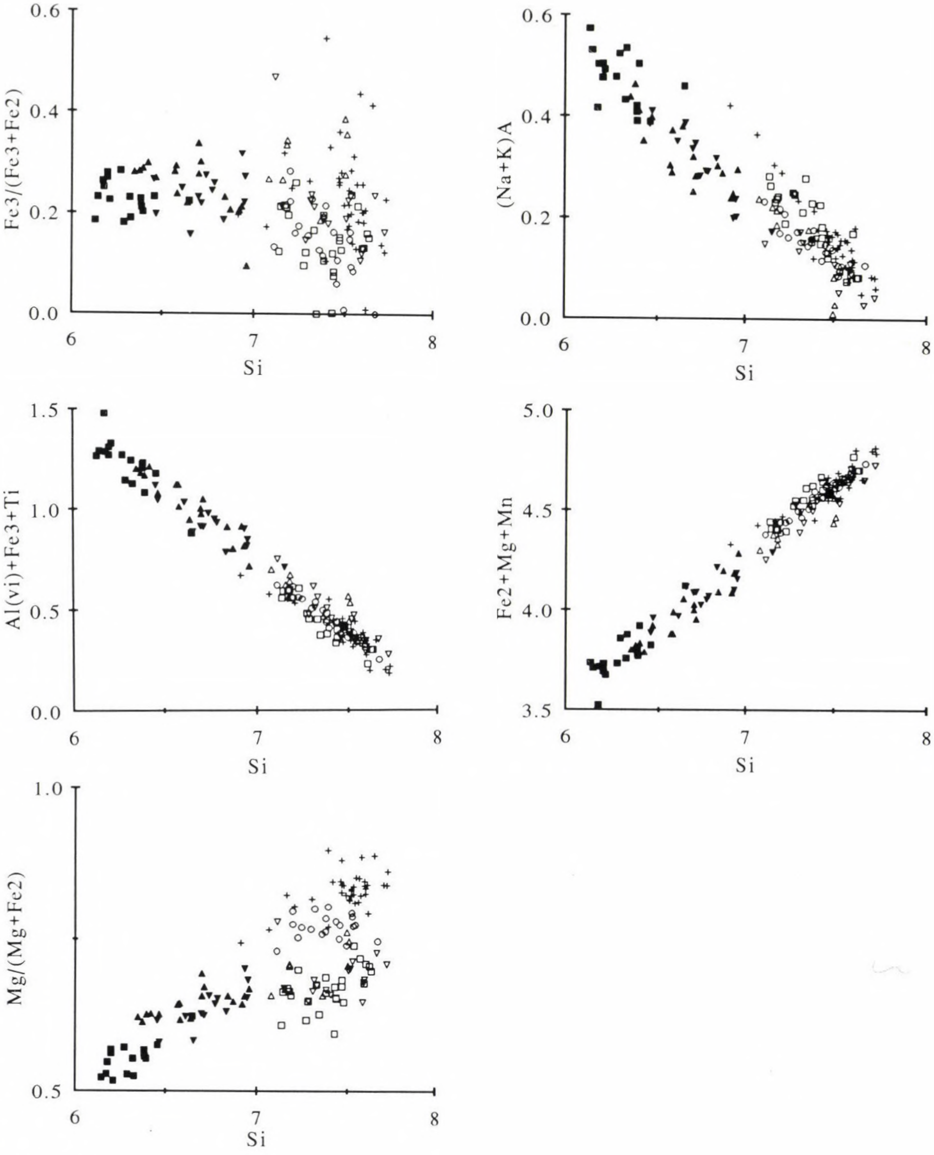

Fig. 5 cont.

tschermakite (approximately 55% pargasite and 45% tschermakite). The amount of the pargasitic/tschermakitic component increases towards the edges of crystals.

The isomorphic substitution of the investigated amphiboles can be described by the following main types:

(1) tschermakitic: $(Mg,Fe^{2+})+Si = Al^{IV}+(Al^{VI}, Fe^{3+})$ and

(2) edenitic: $[\ ]\,A+Si = [Na,K]A+Al^{IV}$.

Within type (1) simple ionic substitutions of $Mg \leftrightarrow Fe^{2+}$ and $Al^{VI} \leftrightarrow Fe^{3+}$ also occur.

The relative importance of the two main substitutions can be estimated by comparing the slopes of the corresponding Si-substitutions, i.e., comparing $\Delta(Mg+Fe^{2+})/\Delta Si$ and $\Delta(Na+K)A/\Delta Si$. In the present case these ratios are 0.71 and 0.26, respectively. This means that the tschermakitic type is 2.7 times more important than the edenitic one. (In case of pargasitic substitution the rate of (1) and (2) equals 1:1, see Ague, 1989.)

Plagioclase and K-feldspar

The An content in plagioclase in mylonitized amphibolites varies between 15 and 42% and in enclaves between 24 and 43% (Table 5), indicating non-equilibrium conditions in both cases. The An content of plagioclase crystals in matrix and especially in the feldspar-rich parts of the mylonitized amphibolites, however, is higher than in crystals enclosed by or being in contact with amphibole porphyroclasts (samples Em-1/B and -2/A1). In sample Em-2/A2 at least two generations of plagioclase were distinguished, An=33–37% and An=15%. An amphibole-bearing gneiss enclave (sample Em-7) contains andesine porphyroblasts and oligoclase matrix crystals.

The K-feldspar (microcline) has Or content varying between 92 and 98%, and An content=0%.

Biotite

Biotite was found in amphibole-bearing enclaves of the granitoid mass (Table 6). Using Foster's (1960) chemical classification, it corresponds usually to Mg=Fe-biotite, in sample Mo-1 to Mg-biotite. Biotite grains closely associated with amphibole are characterized by higher Al^{VI} and lower Ti contents than those which form inclusions in plagioclase.

Chlorite

Chlorite was found only in amphibolites. Biotite-bearing enclaves do not contain chlorite. Thus, the occurrences of biotite and chlorite are contrasting (Table 2). According to the nomenclature of Foster (1962), the compositions of chlorite (see Table 7) correspond to brunsvigite, less frequently to ripidolite.

Table 4

Chemical compositions (weight%) and ionic formulae of amphiboles from mylonitized amphiboles and amphibole- bearing enclaves

sample	Em- 1/A		Em- 1/B		Em-2/A1			Em- 2/A2			
part in grain	b	e	b	e	a	b	e	a	c	d	e
n	8	9	5	9	1	8	8	1	5	11	3
SiO_2	43.35	41.70	47.66	45.06	46.28	46.80	44.22	49.89	52.79	51.30	49.89
TiO_2	0.54	0.57	0.76	1.03	0.81	1.00	1.28	0.42	0.35	0.48	0.70
Al_2O_3	12.81	14.10	7.68	10.02	9.90	8.98	11.46	6.04	3.72	4.98	6.46
*FeO	17.16	18.04	14.88	15.88	15.15	14.90	16.15	10.61	9.64	9.95	10.75
MnO	0.22	0.25	0.25	0.23	0.32	0.29	0.30	0.20	0.23	0.26	0.25
MgO	9.87	8.86	12.75	11.32	12.16	12.32	11.03	15.90	16.81	16.27	15.49
CaO	12.28	12.17	12.23	12.09	12.03	12.13	11.99	12.78	12.82	12.74	12.59
Na_2O	1.53	1.70	1.00	1.32	1.24	1.18	1.44	0.72	0.42	0.56	0.80
K_2O	0.29	0.36	0.15	0.26	0.34	0.34	0.49	0.21	0.08	0.15	0.21
total	98.05	97.75	97.36	97.21	98.23	97.94	98.36	96.77	96.86	96.69	97.14

numbers of cations in unit cell containing 23(O)

Si	T	6.40	6.21	6.96	6.66	6.71	6.82	6.47	7.20	7.56	7.38	7.18
Al^{iv}		1.60	1.79	1.04	1.34	1.29	1.18	1.53	0.80	0.44	0.62	0.82
Al^{vi}	M1- -M3	0.62	0.69	0.29	0.40	0.41	0.36	0.44	0.23	0.19	0.23	0.28
Ti		0.06	0.06	0.08	0.11	0.09	0.11	0.14	0.05	0.04	0.05	0.08
Fe^{3+}		0.48	0.52	0.44	0.46	0.55	0.41	0.55	0.28	0.11	0.17	0.22
Mg		2.18	1.97	2.78	2.49	2.63	2.68	2.41	3.42	3.59	3.49	3.33
Fe^{2+}		1.63	1.73	1.38	1.51	1.28	1.41	1.42	1.00	1.04	1.03	1.06
Mn		0.03	0.03	0.03	0.03	0.04	0.03	0.04	0.02	0.03	0.03	0.03
Ca	M4	1.94	1.95	1.91	1.92	1.87	1.90	1.88	1.98	1.96	1.97	1.94
Na		0.06	0.05	0.09	0.08	0.13	0.10	0.12	0.02	0.04	0.03	0.06
Na	A	0.38	0.44	0.20	0.29	0.22	0.23	0.29	0.18	0.08	0.12	0.17
K		0.06	0.07	0.03	0.05	0.06	0.06	0.09	0.04	0.02	0.03	0.04
total		15.44	15.51	15.23	15.34	15.28	15.29	15.38	15.22	15.10	15.15	15.21
Al		2.23	2.48	1.33	1.74	1.70	1.54	1.97	1.03	0.63	0.85	1.10
Na		0.44	0.49	0.28	0.38	0.35	0.33	0.41	0.20	0.12	0.16	0.23
A		0.44	0.51	0.23	0.34	0.28	0.29	0.38	0.22	0.10	0.15	0.21
		Ts-Hbl	Fe-Prg	Mg-Hbl	Mg-Hbl	Mg-Hbl	Mg-Hbl	Mg-Hbl	Mg-Hbl	Act	Act-Hbl	Mg-Hbl

sample		Em- 4/1		Em- 6		Em- 7		Mo-1		
part in grain		b	e	b	e	b	e	b	e	f
n		6	19	4	11	3	5	28	5	4
SiO_2		52.02	49.78	52.68	50.50	51.38	48.33	53.18	49.52	54.43
TiO_2		0.11	0.30	0.12	0.18	0.07	0.30	0.26	0.46	0.14
Al_2O_3		2.48	4.96	2.36	4.03	2.37	4.88	3.48	6.48	2.00
*FeO		13.32	14.51	13.76	14.60	14.33	15.39	8.38	9.99	7.44
MnO		0.51	0.49	0.44	0.44	0.53	0.55	0.23	0.24	0.22
MgO		15.05	13.36	15.00	13.94	15.00	13.21	18.20	16.22	19.41
CaO		12.65	12.47	12.51	12.47	12.37	12.19	12.77	12.47	12.97
Na_2O		0.31	0.59	0.33	0.43	0.27	0.63	0.59	1.05	0.34
K_2O		0.17	0.38	0.16	0.33	0.15	0.42	0.25	0.57	0.09
total		96.62	96.84	97.36	96.92	96.47	95.90	97.34	97.00	97.04
numbers of cations in unit cell containing 23(O)										
Si	T	7.60	7.33	7.63	7.40	7.50	7.19	7.53	7.13	7.67
Al^{iv}		0.40	0.67	0.37	0.60	0.50**	0.81	0.47	0.87	0.33
Al^{vi}	M1--M3	0.03	0.19	0.04	0.10	0.00	0.06	0.11	0.23	0.02
Ti		0.01	0.03	0.01	0.02	0.01	0.03	0.03	0.05	0.01
Fe^{3+}		0.27	0.25	0.30	0.37	0.50	0.53	0.22	0.29	0.25
Mg		3.28	2.93	3.25	3.05	3.27	2.93	3.84	3.48	4.08
Fe^{2+}		1.35	1.54	1.35	1.41	1.16	1.38	0.77	0.92	0.61
Mn		0.06	0.06	0.05	0.05	0.06	0.07	0.03	0.03	0.03
Ca	M4	1.98	1.97	1.94	1.96	1.94	1.95	1.94	1.92	1.96
Na		0.02	0.03	0.06	0.04	0.06	0.05	0.06	0.08	0.04
Na	A	0.07	0.13	0.03	0.08	0.02	0.13	0.10	0.22	0.05
K		0.03	0.07	0.03	0.06	0.03	0.08	0.04	0.10	0.02
total		15.10	15.20	15.06	15.14	15.05	15.21	15.14	15.32	15.07
Al		0.43	0.86	0.41	0.70	0.41	0.86	0.58	1.10	0.34
Na		0.09	0.17	0.09	0.12	0.08	0.18	0.16	0.30	0.09
A		0.10	0.21	0.06	0.14	0.05	0.21	0.14	0.32	0.07
		Act	Act-Hbl	Act	Act-Hbl	Act	Mg-Hbl	Act	Mg-Hbl	Act

* – total Fe calculated as FeO; ** – including 0.09 Fe^{3+}; a – centre, b – inner part, c – transitional inner part, d – transitional outer part, e – outer part (rim) of the porphyroclasts, f – near to biotite. The composition of the grains of matrix usually corresponds to that of the outer part of the porphyroclasts. n – number of measurements. Nomenclature of amphiboles fter Hawthorne (1981), modified from Leake (1978): Ts-Hbl – tschermakitic hornblede, Fe-Prg – ferroan pargasite, Mg-Hbl – magnesio-hornblende, Act – actinolite, Act-Hbl – actinolitic hornblende

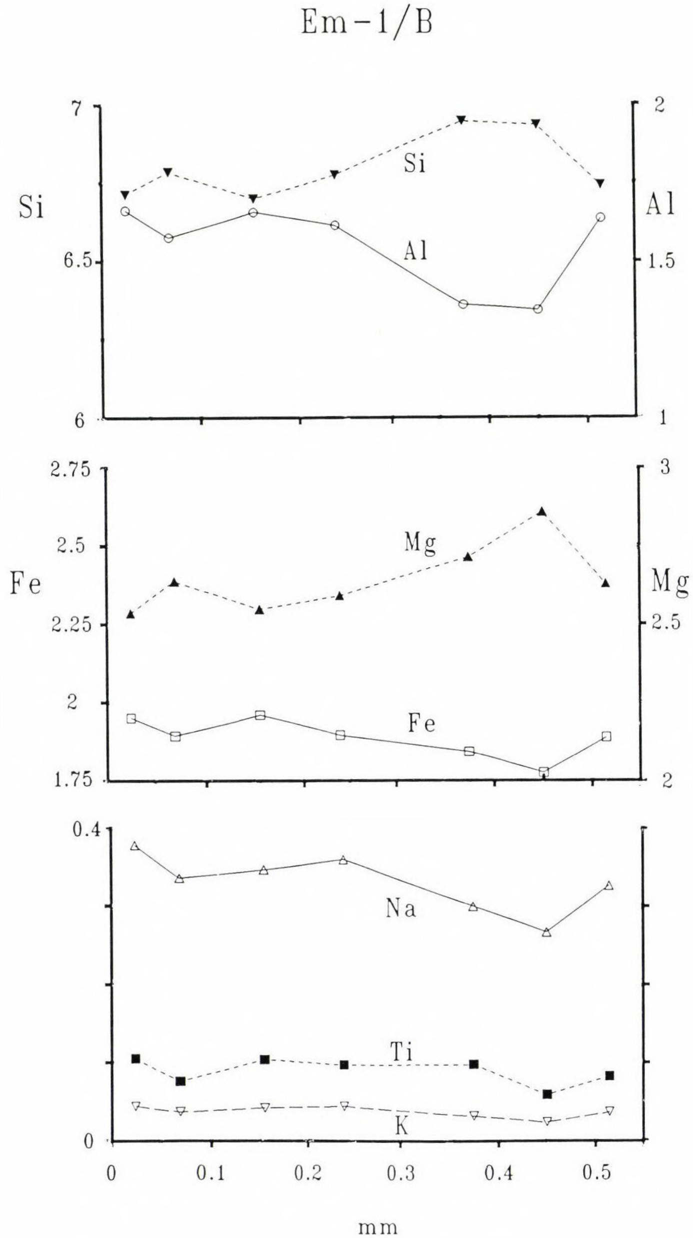

Fig. 6a
Types of compositional zoning in amphibole from mylonitized amphibolites and amphibole-bearing enclaves (changes in cation numbers per 23 0 from edge to edge of the crystals). a – prograde zoning in amphibole porphyroclast in sample Em-1/B, see Fig. 4a

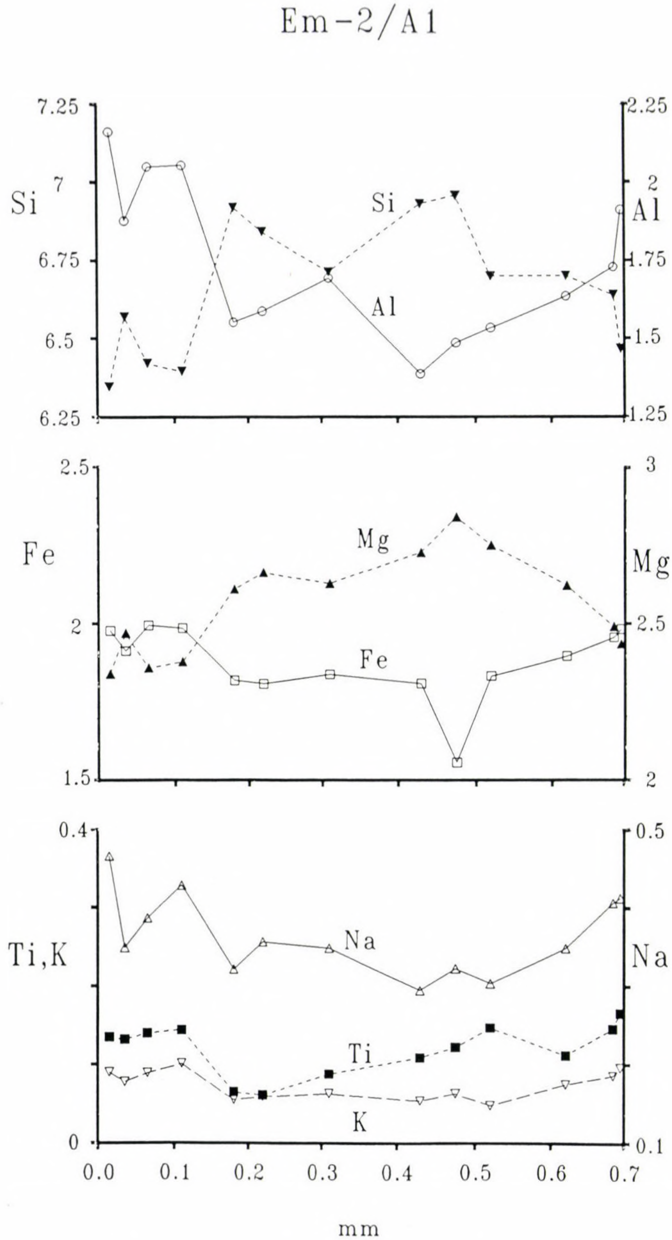

Fig. 6b
Complex zoning in amphibole porphyroclast in sample Em-2/A1, see Fig. 4b

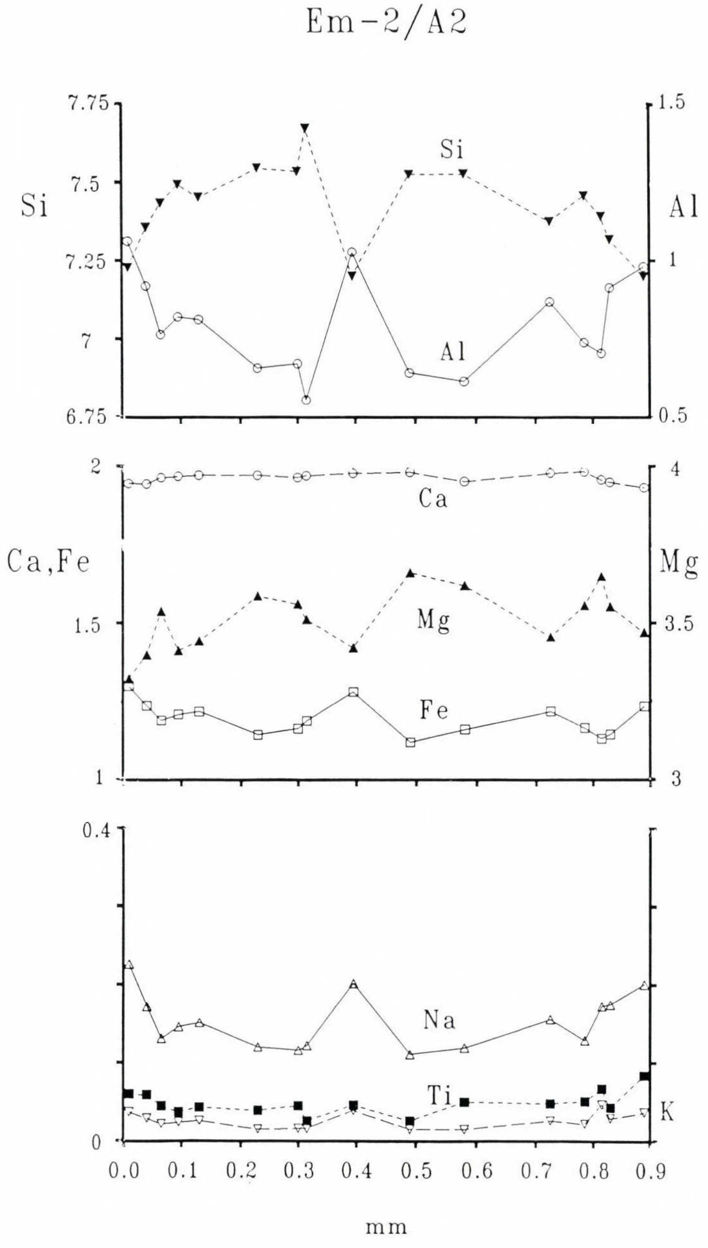

Fig. 6c
Complex zoning in amphibole porphyroclast in sample Em-2/A2, see Fig. 4c

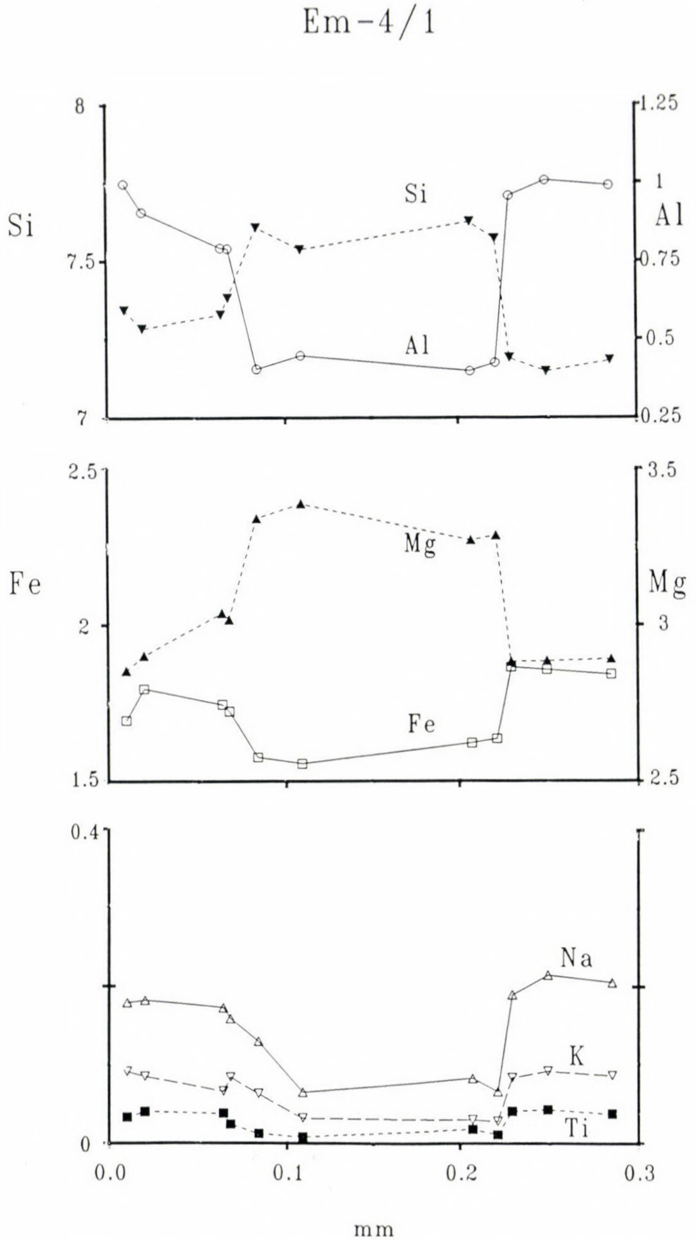

Fig. 6d
Diffusion type secondary zoning in amphibole in enclave Em-4/1, see Fig. 4d;

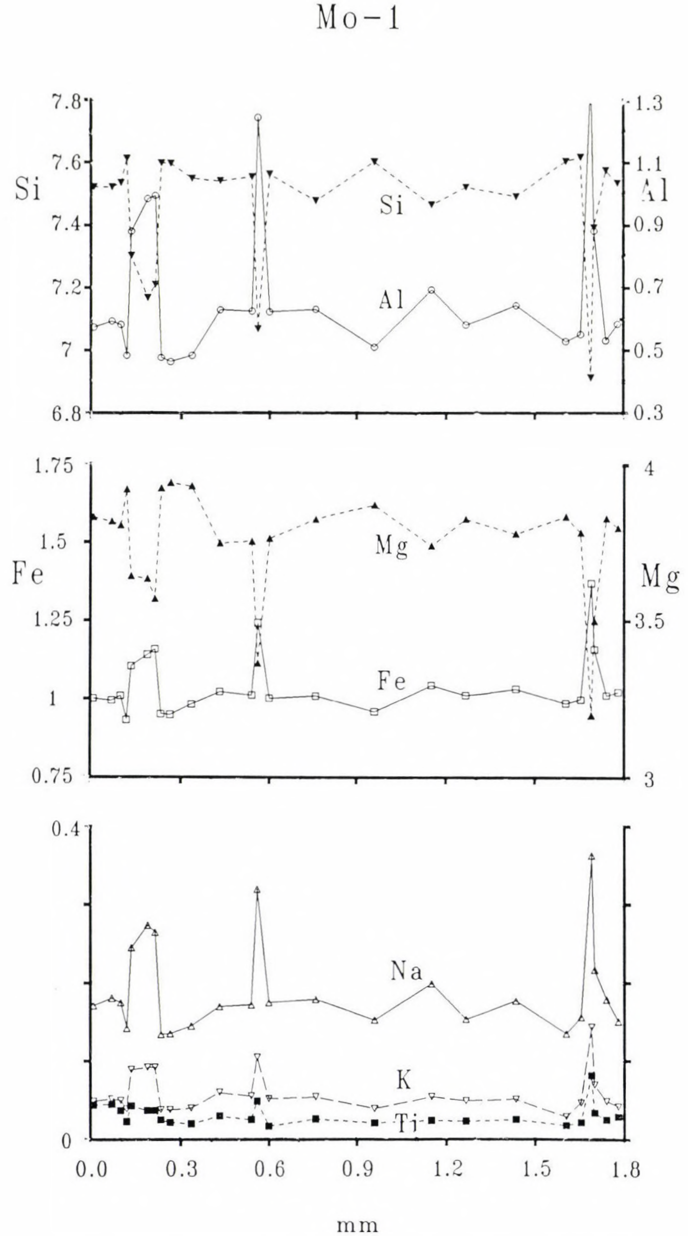

Fig. 6e
Superposition of growth zoning and hornblende–actinolite exsolution in an enclave sample Mo-1, see Fig. 4e

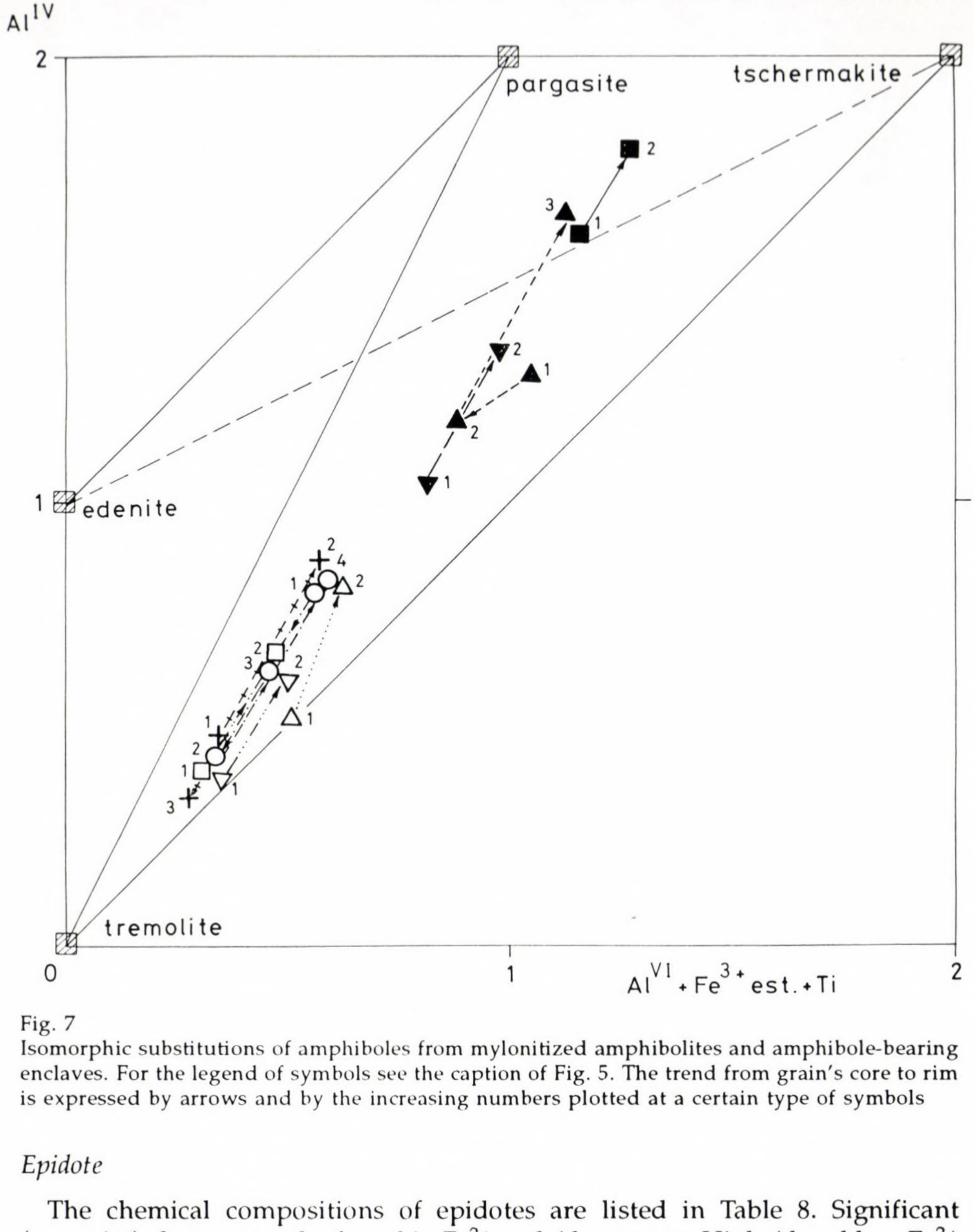

Fig. 7
Isomorphic substitutions of amphiboles from mylonitized amphibolites and amphibole-bearing enclaves. For the legend of symbols see the caption of Fig. 5. The trend from grain's core to rim is expressed by arrows and by the increasing numbers plotted at a certain type of symbols

Epidote

The chemical compositions of epidotes are listed in Table 8. Significant (opposite) changes can be found in Fe^{3+} and Al contents. High Al and low Fe^{3+} contents were measured in mylonitized amphibolite (sample Em-1/A) as compared to those of the amphibole gneiss enclave (sample Em-7). The Fe^{3+}/Al ratio of the feldspar-rich, mylonitized amphibolite (sample Em-2/A1) is intermediate between the ratios of the two above-mentioned samples.

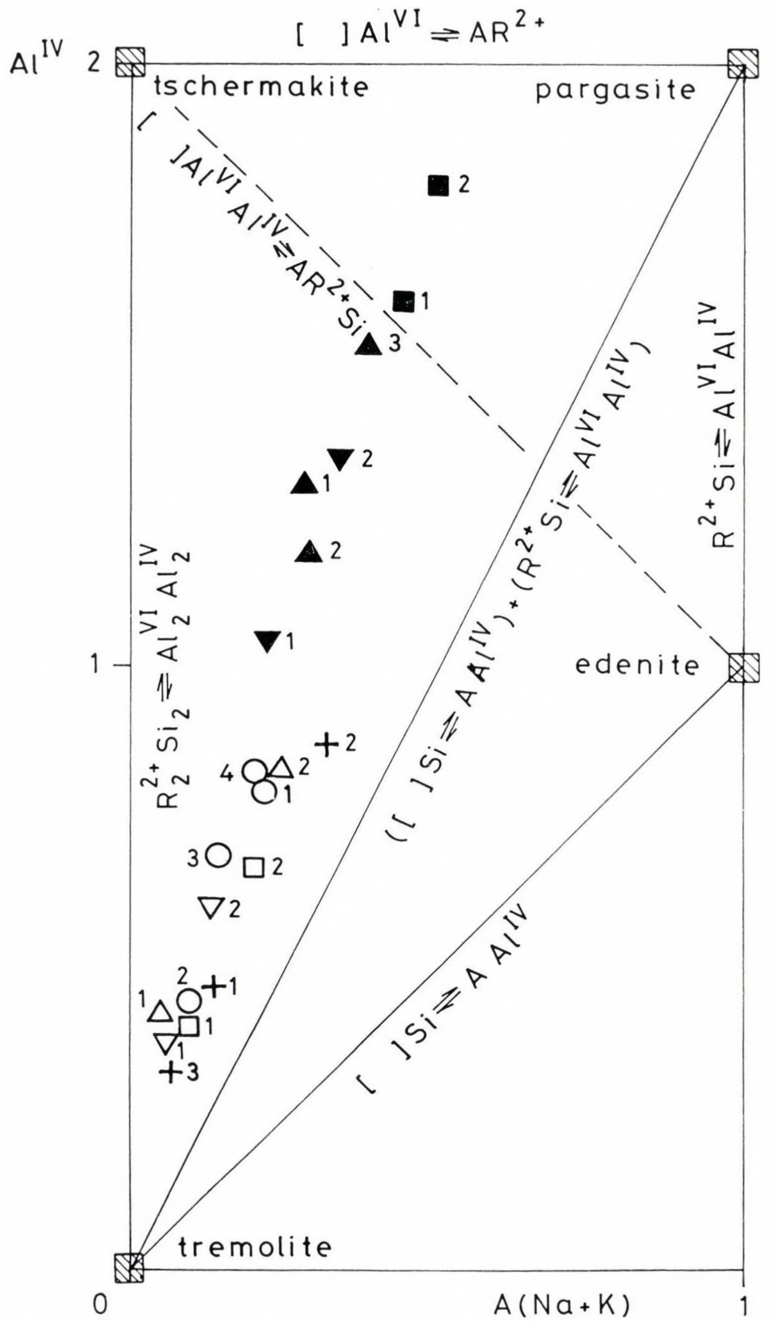

Fig. 8
Isomorphic substitutions of amphiboles. For the legend of symbols see Fig. 5

Table 5
Average chemical compositions of plagioclase and K feldspar

sample	Em-1/A	Em-1/B			Em-2/A1			
grain type	a+c	a	b	c	a	b	d	d
n	5	1	2	4	2	3	3	3
SiO_2	62.05	61.36	59.69	59.65	61.00	58.18	57.91	63.95
Al_2O_3	23.15	25.02	25.55	25.58	24.49	26.62	26.98	19.03
CaO	4.20	5.98	6.09	7.46	6.35	8.19	8.60	0.18
Na_2O	9.21	8.31	7.99	7.57	7.80	6.83	6.61	0.89
K_2O	0.08	0.07	0.08	0.05	0.09	0.05	0.05	14.90
total	98.69	100.74	99.40	100.31	99.73	99.87	100.15	98.95
numbers of cations in unit cell containing 8(O)								
Si	2.77	2.70	2.66	2.65	2.71	2.60	2.58	2.97
Al^{iv}	1.22	1.30	1.34	1.34	1.28	1.40	1.42	1.04
Ca	0.20	0.28	0.29	0.36	0.30	0.39	0.41	0.00
Na	0.80	0.71	0.69	0.65	0.67	0.59	0.57	0.08
K	0.00	0.01	0.01	0.00	0.01	0.00	0.00	0.88
total	4.99	5.00	4.99	5.00	4.97	4.98	4.98	4.97
	An(20)	An(28)	An(29)	An(36)	An(31)	An(40)	An(42)	Kfs

sample	Em-2/A2				Em-4/1		Em-6		Em-7		Mo-1
grain type	c(I)	c(II)	d	d	c	c	c	c	c	e	c
n	5	2	1	3	11	6	10	8	9	3	3
SiO_2	59.17	63.33	59.57	63.40	60.29	63.54	61.80	65.18	61.90	57.69	61.95
Al_2O_3	26.19	23.34	26.23	18.60	24.94	18.40	24.39	18.39	24.66	27.63	23.03
CaO	6.93	3.19	7.72	0.03	6.54	0.00	5.80	0.01	5.70	9.01	4.92
Na_2O	7.47	9.72	7.24	0.20	7.83	0.71	8.32	0.76	8.33	6.48	8.84
K_2O	0.20	0.09	0.06	15.96	0.17	15.65	0.14	15.63	0.17	0.14	0.17
total	99.96	99.59	100.82	98.19	99.77	98.30	100.45	99.97	100.76	100.95	98.91
numbers of cations in unit cell containing 8(O)											
Si	2.63	2.79	2.63	2.98	2.69	2.98	2.74	3.00	2.73	2.56	2.77
Al^{iv}	1.37	1.37	1.37	1.03	1.31	1.02	1.26	1.00	1.28	1.45	1.22
Ca	0.33	0.15	0.37	0.00	0.31	0.00	0.27	0.00	0.27	0.43	0.24
Na	0.64	0.83	0.62	0.02	0.68	0.07	0.72	0.07	0.71	0.56	0.77
K	0.02	0.00	0.00	0.96	0.03	0.94	0.01	0.92	0.01	0.01	0.01
total	4.99	5.14	4.99	4.99	5.02	5.01	5.00	4.99	5.00	5.01	5.01
	An(33)	An(15)	An(37)	Kfs	An(30)	Kfs	An(27)	Kfs	An(27)	An(43)	An(24)

a - inclusion in amphibole porphyroclast, b - grain contacting amphibole porphyroclast, c - grain in the matrix, d - grain in the feldspar-rich part, e - porphyroblast, n - number of the measurements

Table 6
Average chemical compositions of biotite

sample	Em-4/1		Em-6	Em-7	Mo-1
part in grain	a	b	a	a	a
n	6	3	7	10	11
SiO_2	37.37	37.48	37.56	36.05	38.29
TiO_2	1.70	2.75	2.35	1.77	2.49
Al_2O_3	15.37	13.84	14.93	15.48	14.67
*FeO	18.39	19.08	19.42	19.24	12.47
MnO	0.31	0.28	0.31	0.37	0.10
MgO	11.91	11.48	11.46	12.27	16.34
CaO	0.09	0.02	0.04	0.05	0.02
Na_2O	0.09	0.05	0.07	0.10	0.10
K_2O	9.38	9.63	9.85	9.29	9.75
total	94.61	94.62	95.99	94.62	94.23
	numbers of cations in unit cell containing 22 (O)				
Si	5.71	5.76	5.70	5.55	5.71
Al^{IV}	2.29	2.24	2.30	2.45	2.29
Al^{VI}	0.48	0.27	0.37	0.36	0.29
Ti	0.19	0.32	0.27	0.20	0.28
$*Fe^{2+}$	2.35	2.45	2.46	2.48	1.56
Mn	0.04	0.04	0.04	0.05	0.01
Mg	2.71	2.63	2.59	2.82	3.63
Ca	0.02	0.00	0.01	0.01	0.00
Na	0.03	0.02	0.02	0.03	0.03
K	1.83	1.89	1.91	1.82	1.86
total	15.65	15.62	15.67	15.77	15.66

Symbols: * – total Fe calculated as FeO and Fe^{2+}, respectively; a – associated with amphibole; b – inclusion in feldspar; n – number of measurements

Discussion

Mylonitized amphibolites

Both microstructural and mineral chemical data refer to non-equilibrium crystallization conditions of mylonitized amphibolites. The chemical composition of the cores of amphibole porphyroclasts may refer to the physical parameters of regional metamorphism which preceded the mylonite formation. Using the discrimination diagrams of Laird and Albee (1981), the projection points of these cores correspond to the biotite zone. Considering also the composition of plagioclase (oligoclase) coexisting with amphibole cores, regional metamorphic conditions of high-T greenschist facies or low-T amphibolite facies can be deduced.

Table 7
Average chemical compositions of chlorite

sample	Em-1/A	Em-1/B	Em-2/A1	Em-2/A2	
grain type	a	b	a	b	a
n	5	6	7	5	4
SiO_2	25.50	26.41	27.14	27.28	27.61
TiO_2	0.08	0.05	0.07	0.04	0.11
Al_2O_3	20.62	20.75	20.66	20.58	19.37
*FeO	23.06	24.14	21.60	17.90	17.88
MnO	0.28	0.30	0.27	0.24	0.26
MgO	16.02	15.31	17.18	19.82	18.68
CaO	0.10	0.20	0.18	0.15	0.21
Na_2O	0.03	0.03	0.01	0.04	0.03
K_2O	0.04	0.03	0.04	0.02	0.03
total	85.73	87.22	87.15	86.07	84.18
numbers of cations in unit cell containing 28 (O)					
Si	5.45	5.56	5.63	5.62	5.82
Al^{IV}	2.55	2.44	2.37	2.38	2.18
Al^{VI}	2.63	2.70	2.68	2.62	2.63
Ti	0.01	0.01	0.01	0.01	0.02
$*Fe^{2+}$	4.13	4.25	3.75	3.09	3.15
Mn	0.05	0.05	0.05	0.04	0.05
Mg	5.09	4.80	5.31	6.09	5.87
Ca	0.02	0.04	0.04	0.03	0.05
Na	0.01	0.01	0.00	0.02	0.01
K	0.01	0.01	0.01	0.00	0.01
total	19.95	19.87	19.85	19.90	19.79

Symbols: * – total Fe calculated as FeO and Fe^{2+}, respectively; a – grains in the matrix; b – inclusion in amphibole; n – number of measurements

Based on the chemical zoning of porphyroclasts and the chemistry of matrix-forming amphibole and plagioclase grains, these amphibolites were mylonitized in a prograde system as compared to the preceding regional metamorphism. The decrease of Si and Mg and the increase of Al, Fe and Na in amphibole relates to increasing metamorphic grade (see Wiseman 1934; Liou et al. 1974; Laird and Albee 1981; Tournon et al. 1989; Räumer et al. 1990; Poli 1991). The variations observed in the chemistry of amphibole porphyroclasts of the amphibolites of the Mecsek Mountains agree with the changes in amphibole chemistry [i.e., the decrease of $Mg/(Mg+Fe^{2+})$ and Si, and the increase of $(Na+K)A$, $Al^{VI}/(Al^{VI}+Fe^{3+})$] described earlier by Brodie (1981) in a 5 m wide Alpine shear zone producing mylonite from amphibolite-facies metagabbro. In addition to the well-known microstructural changes (grain-size reduction, foliation), increase of the amphibole and decrease of the plagioclase contents were also observed by Brodie in the central part of the shear zone.

Table 8
Chemical compositions of epidote

sample	Em-1/A	Em-2/A1	Em-7
n	3	1	2
SiO_2	38.7	37.64	37.50
TiO_2	0.03	0.15	0.07
Al_2O_3	28.49	24.72	24.19
* Fe_2O_3	6.26	9.18	10.36
MnO	0.16	0.11	0.19
MgO	0.03	1.45	0.08
CaO	24.47	21.51	23.19
Na_2O	0.03	0.01	0.00
K_2O	0.00	0.06	0.02
total	98.17	94.83	95.60
numbers of cations in unit cell containing 25 (O)			
Si	5.97	6.03	6.01
Al^{VI}	5.18	4.67	4.57
Ti	0.00	0.02	0.01
*Fe^{3+}	0.81	1.23	1.39
Mn	0.02	0.02	0.03
Mg	0.01	0.35	0.02
Ca	4.05	3.69	3.98
Na	0.01	0.00	0.00
K	0.00	0.01	0.00
total	16.05	16.02	16.01

Symbols: * – total Fe calculated as Fe_2O_3 and Fe^{3+}, respectively; n – number of measurements

Because of the extensive Quaternary-Holocene cover deposited on the surface of the eroded metamorphic–magmatic complex, neither the position and extension of the shear zone, nor the relations of the investigated samples to this zone could be detected exactly in the field. Based on the observations of Brodie (1981), sample Em-1/A may derive from the central part of the shear zone, while in the order of samples Em-1/B, -2/A1 and -2/A2, i.e., approaching the tectonic contact of the mylonitized amphibolite/granitoid, the amphibolite becomes richer in feldspars either because of the decreasing effect of shearing or the original lithological inhomogeneity of the rock mass.

With increasing feldspar (plagioclase > microcline) content of the mylonitized samples, i.e., with the presumed decreasing effect of shearing, the Si, Mg, (Fe^{2+}+Mg+Mn) contents and the Mg/(Mg+Fe^{2+}) ratio of the amphibole increase, and the total Fe, Fe^{3+}, Fe^{2+}, Ti, (Al^{VI}+Fe^{3+}+Ti), Na, K and (Na+K)A contents decrease. In the sequence of samples from Em-1/A to Em-2/A2, more and more complicated compositional zoning profiles were found in the amphibole porphyroclasts. In order to explain these trends, the following possibilities can be taken into consideration:

(i) the observed shift in amphibole chemistry reflects the differences in bulk rock compositions (see Table 3);

(ii) the intensity of the prograde recrystallization associated with shearing decreased in the given order of the samples (the highest temperature might have been reached in sample Em-1/A, i.e., in the supposed central part of the shearing zone);

(iii) as magmatism postdates mylonitization and the given sequence of samples represents decreasing distance from the tectonic contact between the mylonitized amphibolite and the granitoid, magmatic–postmagmatic fluids, migrating along this fault and infiltrating the surrounding tectonite might cause the changes mentioned above.

Despite the detailed mineral chemical characterization, there is no possibility of discriminating between the above-mentioned mechanisms. In the case of samples Em-1/A, -1/B and -2/A1 factors (i) and (ii), and in the brecciated sample Em-2/A2, factor (iii) might be significant. Considering the complicated forms of compositional zoning in amphibole porphyroclasts, the combination of the above-mentioned factors also seems to be an acceptable explanation. Taking into account the retrograde trend of changes in amphibole chemistry towards the contact with granitoid, the modal composition (andesine-oligoclase + microcline) of the felsic parts ("mobilizates") of the rocks, the lack of real migmatite structures and the tectonic character of the contact zone itself, the prograde heat effect of the granitoid magmatism causing embryonal form of partial melting of the mylonitized amphibolite can be ruled out with high probability.

Since the microstructural and mineral chemical features refer to no-equilibrium conditions, the interpretation of the results of thermobarometric calculations requires special precaution. Applying the amphibole–plagioclase thermobarometer of Plyusnina (1981, 1982) for a porphyroclast of sample Em-2/A1, the above-mentioned prograde changes were justified: 540°C/3.2 kbar for the core and 580°C/4 kbar for the rim. Similar temperatures, but significantly lower ($\leq$ 2 kbar) pressures, were obtained for brecciated, mylonitized amphibolite (Em-2/A2). The pressure values calculated by the method of Fershtater (1990) agree fairly well with those obtained by Plyusnina's method. Low (<3, usually <2 kbar) pressures can also be established using the amphibole NaM4–Al^{IV} barometer of Brown (1977). As the composition of the amphibole and chlorite differs significantly from those used by Triboulet and Audren (1988) for P–T-path calculations, this method could not be used in the present study.

Amphibole-bearing enclaves

According to Jantsky (1979) the majority of the agmatites originated from cordierite- and sillimanite-bearing paragneiss and mica schist of high-T amphibolite facies by partial melting. This process was accompanied by mineral transformation of biotite(I) + plagioclase(I) $\rightarrow$ green amphibole + titanite + rutile + biotite (II) + epidote, and by increasing the amount of felsic minerals (plagioclase(II), microcline, quartz). This reaction, considered as characteristic of migmatization by Mehnert (1968), was also proposed by Jantsky (1979) for granitized metabasites which form agmatic remnants of ancient dykes and smaller intrusions in the sedimentary complex, the anatexis of which presumably produced the granitoid melt.

Árkai et al. (1985) explained the compositional zoning of amphibole (actinolite $\rightarrow$ actinolitic hornblende) by prograde recrystallization of actinolite-bearing enclaves, which presumably derived from the greenschist facies Ófalu Formation of the Mecsek Mts. The prograde recrystallization was caused by the thermal effect of the enclosing granitoid melt. The calculated T–P values (535°C/<2 kbar) refer to the non-equilibrium character of the thermal transformation.

According to Buda (1985) the volumes of the individual enclaves called amphibole–biotite "resistites" (properly: restites) vary from several hundred m to several cm. Their amphibole content varies between 1–40 vol.%. Relic diopsidic augite, indicative of their basic magmatic origin, was also found in certain cases. Mg content decreases and Fe content increases both in amphibole and biotite with advancing transformation caused by the granitoid melt. The average compositions of the amphibole correspond to the Mg- or Fe-rich actinolitic hornblende. Non-equilibrium transformation of amphibole to biotite was proven by microtextural observations and element distribution ratios. Two (magmatic and metasomatic) generations of biotite were distinguished. However, no information was given by Buda on the genesis of amphibole.

As partially dissolved biotite inclusions can be found in idioblastic amphiboles and vice versa, and the character of the contacts between the two minerals changes within short distances, the contrasting opinions of Jantsky (1979) and Buda (1985) about the relation of amphibole and biotite may both be valid, supposing near-equilibrium crystallization of the two minerals and local fluctuations in the chemistry of the enclosing–infiltrating medium.

The main changes in amphibole chemistries of amphibole-bearing enclaves can be described by the same exchange reaction already observed in zoned crystals in mylonitized amphibolite (see Figs 7 and 8). Within the general trend certain deviations caused by simple element substitutions were also demonstrated. In enclaves the higher K contents of amphiboles as compared to the amphiboles of similar Si values from mylonitized amphibolites (see Fig. 5), may be the result of a K-rich fluid infiltration. The variations in Fe, Mg and Mn contents and their ratios may relate to differences in original bulk chemistry of the various enclaves. Compared to the mylonitized amphibolites, the amphiboles of the enclaves are enriched in tremolitic (actinolitic) component, which, taking the well-known prograde chemical changes of amphibole into account, seems to be a contradiction, since the temperature within the granitoid melt should have been considerably higher than in the neighbouring metamorphic aureole (mylonitized amphibolite).

Interestingly, strongly differing compositions (pargasitic hornblende, pargasite) were reported by Sorensen (1988) and Kotopouli et al. (1991) for prograde transformations associated with migmatization. Consequently, it seems very unlikely that the mineral chemical differences between mylonitized amphibolites and enclaves are related to advancing migmatization, because the enclaves have indications of lower metamorphic grade (actinolitic amphiboles). The observed mineral association of enclaves may form by subsolidus reactions at a late stage in the cooling of the granitoid complex.

Amphiboles in the enclaves of the Mecsek Mts are also zoned. The main trend is similar to that described in mylonitized amphibolites. The amounts of the tschermakitic/pargasitic components increasing from cores towards the crystal's edges imply prograde changes in physical conditions. This prograde zoning requires a special geological explanation. A late, regional re-heating, or movements of granitoid magma (emplacement of late intrusion), or re-heating combined with chemical effects of late K-metasomatism described by Buda (1985) may be acceptable candidates for an explanation. The combination of different types of zoning (prograde growth-zoning, diffusional zoning, and recurrent zoning caused by actinolite–hornblende exsolution) found in certain enclaves refers to the complex evolutionary path of the subsolidus mineralogy of the enclaves.

Thermobarometric data (530–550 °C/< 2 kbar by Plyusnina's (1982) method) support the genetic model outlined above. The empiric barometer of Hammarstrom and Zen (1986), improved by Hollister et al. (1987) and Johnson and Rutherford (1989), can only be applied to amphiboles crystallized from calc-alkaline melts. The high Si content of the amphiboles in enclaves of the Mecsek Mts, however, relate to their formation by subsolidus reactions (see Wones and Gilbert, 1982); thus, the above-mentioned amphibole–Al geobarometers were not applied in this work, although their results (usually < 2 kbar) conform with those obtained by methods established for metamorphic rocks. The amphibole–plagioclase thermometer of Blundy and Holland (1990) for both magmatic and metamorphic rocks yields erroneously high (>700 °C, usually >800 °C) temperatures for amphibolites and enclaves, contradicting the mineral assemblages and mineral chemical data.

Conclusions

Summarizing the microstructural, mineral paragenetic and mineral chemical data, it can be concluded that the low-P type, high-T greenschist/low-T amphibolite facies amphibolite complex contacting tectonically the granitoid massif of the Mecsek Mountains mylonitized in prograde (amphibolite facies) conditions preceding the emplacement of granitoids. Compared to the mylonitized amphibolite, the agmatic amphibole–biotite enclaves in granitoids show lower T mineral assemblages which might have formed by subsolidus reactions at a late stage of cooling, by re-heating, combined presumably with the chemical effects of K-metasomatism.

The nature of isomorphic substitutions of amphiboles, both within a single grain and between grains of different rock types, proved to be the same, being intermediate between the tremolite ↔ tschermakite and tremolite ↔ pargasite series, with the tschermakitic substitution dominant. Total Fe, Fe^{3+}, Fe^{2+}, Ti (Al^{VI}+Fe^{3+}+Ti), Na, K and (Na+K)A contents decrease, while Mg (Fe^{2+}+Mg+Mn) contents and the Mg/(Mg+Fe^{2+}) ratio increase with increasing Si content of the amphibole.

Porphyorclasts or -blasts of amphibole are usually zoned. In mylonitized amphibolite simple prograde zoning (decrease of Si and Mg, increase of Al, Fe and

Na) was detected. Approaching the tectonic contact between the mylonitized amphibolite and the granitoid, the feldspar (oligoclase-andesine > microcline) content of the amphibolite and the actinolitic component of the amphibole increase, and the zoning in amphibole becomes more complex. Acceptable explanations for these phenomena are: differences in original bulk rock compositions, changes in recrystallization associated with shearing of varying intensity, and effects of infiltrating metasomatic fluids acting along the tectonic contact, or – most probably – combinations of the above-mentioned processes.

While the amphibole in mylonitized amphibolites is mainly magnesio-hornblende with subordinate tschermakitic hornblende and ferroan pargasite, the enclaves are characterized by actinolite, actinolitic hornblende and subordinately by magnesio-hornblende. The tschermakitic/pargasitic components increase from cores towards the grains' rims. The combination of prograde growth zoning, diffusional zoning and recurrent zoning caused by actinolite-hornblende exsolution points to the complex subsolidus crystallization history of the enclaves.

No signs of real migmatite formation were found in the mylonitized amphibolite. The low-T subsolidus reactions obliterated the original (pre-granitoid) features of the mafic enclaves and the eventual early (prograde) changes caused by the physical and chemical effects of the granitoid melt. Thus, despite the fact that the planar metamorphic microstructure was preserved in most cases, these mafic rock fragments have lost any evidence for their early history to a much greater extent than could be anticipated.

Acknowledgements

The authors are indebted to Mr. A. Incze (Laboratory for Geochemical Research, Hungarian Academy of Sciences) for providing the bulk chemical main component analyses. The present work forms parts of one of the authors' (P. Á.) metamorphic petrological research programmes Nos 284/1987–1991 and T007211/1993-1996, sponsored by the Hungarian Scientific Research Fund (OTKA).

References

Ague, J.J. 1989: The distribution of Fe and Mg between biotite and amphibole in granitic rocks: Effect of temperature, pressure and amphibole composition. – Geochem. J., 23, pp. 279–293.

Ashworth, J.R. 1985: Introduction. In: J.R. Ashworth (Ed.): Migmatites. Blackie, Glasgow, pp. 1–35.

Árkai, P. 1984: Polymetamorphism of the crystalline basement of the Somogy-Dráva Basin (Southwestern Transdanubia, Hungary). – Acta Miner. Petr. Szeged., 26, pp. 129–153.

Árkai, P. 1991: Alpine regional metamorphism of the different tectonic domains in the Hungarian part of the Pannonian Basin. – In: A. Baud, P. Thelin, G. Stampfli (Eds): Paleozoic geodynamic domains and their alpidic evolution in the Tethys. – IGCP Project No. 276 Newsletter No. 2. Mémoires de Géologie (Lausanne) 10, pp. 5–13.

Árkai, P., G. Nagy, G. Dobosi 1985: Polymetamorphic evolution of the South-Hungarian crystalline basement, Pannonian Basin: geothermometric and geobarometric data. – Acta Geol. Hung., 28, pp. 165–190.

Balla, Z. 1988: On the origin of the structural pattern of Hungary. – Acta Geol. Hung., 31, pp. 53–63.

Bence, A.E., A. Albee 1968: Empirical correction factors for electron microanalysis of silicates and oxydes. – J. Geol., 76, pp. 382–403.
Blundy, J.D., T.J.B. Holland 1990: Calcic amphibole equilibria and a new amphibole–plagioclase geothermometer. – Contrib. Mineral. Petrol., 104, pp. 208–224.
Brodie, K.H. 1981: Variation in amphibole and plagioclase composition with deformation. – Tectonophysics, 78, pp. 385–402.
Brown, E.H. 1977: The crossite content of Ca-amphibole as a guide to pressure of metamorphism. – J. Petrol., 18, pp. 53–72.
Buda, Gy. 1985: Origin of collision-type Variscan granitoids as exemplified by the granitoids of Hungary, the Western Carpathians and the Central Bohemian Massif. – C.Sc. Thesis, Budapest (in Hung.).
Fershtater, G.B. 1990: Empiritsheskij plagioklaz-rogovoobmankovyj barometr (empirical plagioclase–amphibole barometer). – Geokhimija, 3, pp. 328–335.
Foster, M.D. 1960: Interpretation of the composition of trioctahedral micas. – U.S. Geol. Surv. Prof. Paper, 354-B, pp. 11–48.
Foster, M.D. 1962: Interpretation of the composition and a classification of the chlorites. – U.S. Geol. Surv. Prof. Paper, 414-A, pp. 1–33.
Ghanem, M.A.E.A., L. Ravasz-Baranyai 1969: Petrographic study of the crystalline basement rocks, Mecsek Mountains, Hungary. – Acta Geol. Acad. Sci. Hung., 13, pp. 191–219.
Haas, J., G. Császár, S. Kovács, A. Vörös 1990: Evolution of the western part of the Tethys as reflected by the geological formations of Hungary. – Acta Geod. Geoph. Mont. Hung., 25, pp. 325–344.
Hammarström, J.M., E-an Zen 1986: Aluminium in hornblende: An empirical igneous geobarometer. – Amer. Mineral., 71, pp. 1297–1313.
Hawthorne, F.C. 1981: Crystal chemistry of the amphiboles. – In: Veblen, D.R. (ed.): Amphiboles and other hydrous pyriboles – Mineralogy. – Reviews in Mineralogy, 9A, pp. 1–102. Miner. Soc. Amer., Washington.
Hollister, L.S., G.C. Grissom, E.K. Peters, H.H. Stowell 1987: Confirmation of the empirical correlation of Al in hornblende with pressure of solidifications of calc-alcali plutons. – Amer. Mineral., 72, pp. 231–239.
Jantsky, B. 1979: Géologie du socle cristallin granitise de la montagne Mecsek. – Annals Hung. Geol. Inst., 60, pp. 1–385.
Johnson, M.C., M.J. Rutherford 1989: Experimental calibration of the Al-in-hornblende geobarometer with application to Long Valley Caldera (California) volcanic rocks. – Geology, 17, pp. 837–841.
Kázmér, M., S. Kovács, 1985: Permian–Paleogene paleogeography along the Eastern part of the Insubric–Periadriatic lineament system: evidence for the continental escape of the Bakony-Drauzug Unit. – Acta Geol. Hung., 28, pp. 71–84.
Kotopouli, C.N., G. Pe-Piper, C.G. Katagas 1991: The metamorphism and migmatization of the Xanthe-Echinos metamorphic complex, Central Rhodope, Greece. – Lithos, 27, pp. 79–93.
Kovács, S. 1982: Problems of the "Pannonian Median Massif" and the plate tectonic concept. Contributions based on the distribution of Late Paleozoic–Early Mesozoic isopic zones. – Geol. Rundschau, 71, pp. 617–640.
Laird, J. 1980: Phase equilibria in mafic schists from Vermont. – J. Petrol., 21, pp. 1–37.
Laird, J., A.L. Albee 1981: Pressure, temperature, and time indicators in mafic schists: their application to reconstructing the polymetamorphic history of Vermont. – Amer. J. Sci., 281, pp. 127–175.
Leake, B.E. 1978: Nomenclature of amphiboles. – Canad. Mineral., 16, pp. 501–520.
Lelkes-Felvári, Gy., F.P. Sassi 1981: Outlines of the pre-Alpine metamorphism in Hungary. – In: Karamata, S., F.P. Sassi (eds): IGCP Project No. 5 Newsletter No. 3, pp. 89–99.
Liou, J.G., S. Kuniyoshi, K. Ito 1974: Experimental studies of the phase relations between greenschist and amphibolite in a basaltic system. – Amer. J. Sci., 274, pp. 613–632.
Mehnert, K.R. 1968: Migmatites and the origin of granitic rocks. – Elsevier, Amsterdam.

Nagy, G, 1984: Computer programs for quantitative electron microprobe analysis developed for geological applications. – EUREM '84: Proc. 8th Eur. Congr. on Electron Microscopy, Budapest, pp. 1041–1042.
Nagy, G. 1990: Quantitative analysis by electron microprobe: Methods and applications in the Laboratory for Geochemical Research. – Izotóptechnika, Diagnosztika 33, pp. 133–139 (in Hungarian).
Plyusnina, L.P. 1981: Eksperimental'noe izutshenie zavisimosti glinozemistosti rogovykh obmanok ot PT-uslovij ikh obrazovanija. – Izv. Akad. Nauk SSSR, Ser. Geol., No. 7, pp. 19–28.
Plyusnina, L.P. 1982: Geothermometry and geobarometry of plagioclase–hornblende-bearing assemblages. – Contrib. Mineral. Petrol., 80, pp. 140–146.
Poli, S. 1991: Reaction spaces and P-T paths: from amphibole eclogite to greenschist facies in the Austroalpine domain (Oetztal Complex). – Contrib. Mineral. Petrol., 106, pp. 399–416.
Räumer, J.F., G. Galetti, H.J. Pfeifer, R. Oberhänsli 1990: Amphibolites from Lake Emosson/Auguilles Rouge, Switzerland: Tholeiitic basalts of a Paleozoic continental rift zone. – Schweiz. mineral. petrogr. Mitt., 70, pp. 419–435.
Robinson, P., F.S. Spear, J.C. Schumacher, J. Laird, C. Klein, B.W. Evans, B.L. Doolan 1982: Phase relations of metamorphic amphiboles: Natural occurrence and theory. – In: D.R.Veblen, P.H. Ribbe (Eds): Amphiboles: Petrology and experimental phase relations. – Reviews in Mineralogy, 9B, pp. 1–227. Miner. Soc. Amer., Washington.
Smelik, E.A., M.W. Nyman, D.R. Veblen 1991: Pervasive exsolution within the calcic amphibole series: TEM evidence for a miscibility gap between actinolite and hornblende in natural samples. – Amer. Mineral., 76, pp. 1184–1204.
Sorensen, S.S. 1988: Petrology of amphibolite-facies mafic and ultramafic rocks from the Catalina Schist, southern California: metasomatism and migmatization in a subduction zone metamorphic setting. – J. Metamorphic Geol., 6, pp. 405–435.
Szádeczky-Kardoss, E. 1959: On the magmatic mechanisms of the Carpathian Median Massif. – Proc. Internat. Geochem. Conf., Budapest (in Hungarian).
Szádeczky-Kardoss, E., Á. Juhász, E. Balázs 1969: Erläuterung zur Karte der Metamorphiten von Ungarn. – Acta Geol. Acad. Sci. Hung., 13, pp. 27–34.
Szederkényi, T. 1975: Rare element research of the Early Paleozoic formations in SW-Transdanubia. – C.Sc. Thesis, Budapest (in Hungarian).
Szederkényi, T. 1984: Crystalline basement of the Great Hungarian Plain and its geological connections. – D.Sc. Thesis, Budapest (in Hungarian).
Szederkényi, T. 1987: Geological key sections of Hungary: Mórágy quarry, Erdősmecske, Ófalu. – Hungarian Geological Institute, Budapest.
Szederkényi, T. P. Árkai, Gy. Lelkes-Felvári 1991: Crystalline basement of the Great Hungarian Plain and South Transdanubia, Hungary. In: Karamata, S. (ed.): Geodynamic evolution of the Pannonian Basin. – Serb. Acad. Sci. Arts, Acad. Conf., 62, Dept. Nat. and Math. Sci., 4, pp. 261–273, Beograd.
Tournon, J., C. Triboulet, J. Azema 1989: Amphibolites from Panama: anticlockwise P–T paths from a pre-upper Cretaceous metamorphic basement in Isthman, Central America. – J. Metamorphic. Geol., 7, pp. 539–546.
Triboulet, C., C. Audren 1988: Controls on P-T-t deformation path from amphibolite zonation during progressive metamorphism of basic rocks (estuary of the River Vilaine, South Britanny, France). – J. Metamorphic Geol., 6, pp. 117–133.
Wiseman, J.D.H. 1934: The central and south-west Highland epidiorites: A study in progressive metamorphism. – Geol. Soc. London, Quart. J., 90, pp. 354–417.
Wones, D.R., M.C. Gilbert 1982: Amphiboles in igneous environment. – In: Veblen, D.R., P.H. Ribbe, P.H. (eds): Amphiboles: petrology and experimental phase relations. – Reviews in Mineralogy, 9B, pp. 355-390. Miner. Soc. Amer., Washington.

Acta Geologica Hungarica, Vol. 37/3–4, pp. 269–280 (1994)

Morphotectonic studies of the Eastern Mecsek Mountains, South Hungary

Mohamed Tolba and Géza Császár
Hungarian Geological Institute, Budapest

This paper presents some morphotectonic studies of the eastern part of Mecsek Mountains, which represents a window of the Mesozoic sequence within the Pannonian Basin. Morphometrically, the drainage system is tectonically controlled in the mountainous area, which means that the tectonic lines were rejuvenated in recent times, while it is topographically (slope) controlled in the surrounding area. Fracture analysis shows that the fracture pattern visible on air photo within the mountainous area is similar – to a certain extent – to the fault pattern seen on the geological map, reflecting the post-Mesozoic stresses more or less along the originally Mesozoic tectonic lineaments; within the surrounding area, the pattern reflects only drainage lineation traces or neotectonic lines. Finally, it is clear that the major tectonic lines of the area are expressed morphologically and could be seen from space.

Key words: remote sensing, drainage, fractures, morphotectonics, Mecsek Mts

Introduction

The Mecsek Mountain range represents a fractured and fragmented fault block of a fold system, principally originated by the Alpine movement. It is a combination of a relict mountain of old crystalline rocks situated mainly in the basement, on which a Permian to Lower Cretaceous sequence was deposited unconformably; it was then intruded by Lower Cretaceous volcanics, and covered by Neogene sediments and even some Neogene volcanic products (Fig. 1).

The interpretation of the studied area using remote sensing data was carried out by Chikán (1975), Kókai (1980), Joó and Stogicza (1984), Stogicza and Csillag (1986), Stogicza (1987), and Brezsnyánszky and Sikhegyi (1987). Geomorphologically, the area was studied by Pécsi (1970) as a part of the evaluation of the entire territory of Hungary, and by Ádám et al. (1981) as a part of South Transdanubia.

Using a series of aerial photographs in stereopairs, together with a Landsat image in hard copy format and a radar image covering only the western part of the area, the drainage and the fracture traces, as well as the detectable major tectonic lineaments, have been traced and analyzed, focusing on their morphotectonic applications.

Address: M. Tolba, G. Császár: H–1442 Budapest, Stefánia út 14.
Received: 28 May, 1994

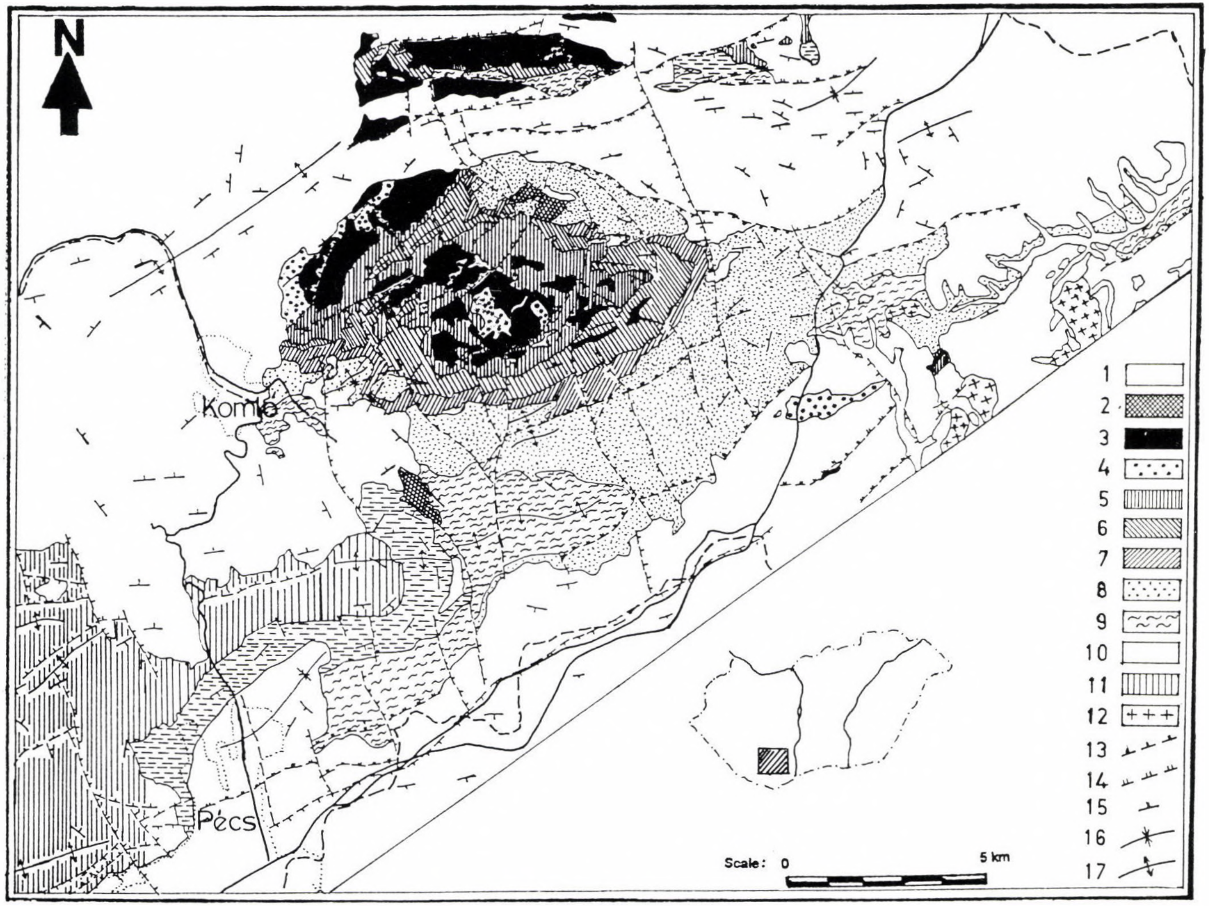

Fig. 1

Geological map of the area simplified after Szederkényi and Kassai (1974). 1. Neogene sediments; 2. Lower Cretaceous phonolite; 3. Lower Cretaceous volcanics; 4. Lower Cretaceous sedimentary rocks; 5. Upper Jurassic; 6. Middle Jurassic; 7. Toarcian; 8. Pliensbachian; 9. Upper Sinemurian; 10. Lower Sinemurian–Hettangian; 11. Triassic; 12. Proterozoic–Early Paleozoic; 13. normal faults; 14. reversed faults; 15. strike and dip of strata; 16. axis of a syncline; 17. axis of an anticline

Drainage analysis

Along the axis of the Mecsek Mountains, a NE–SW-oriented drainage divide separates the drainage to the north and to the south (Fig. 2). The Eastern Mecsek Mountains area is divided into two separate drainage basins (Fig. 3); the first (A), within the mountainous area, flows eastward within the mountains and continues to the north, while the second (B), in the surrounding area, flows to the south.

Qualitatively the first basin (A) is characterized by a subdendritic to angulate pattern, which is mainly interpreted as a structurally-controlled pattern reflecting a high tectonic effect of that area. The second basin (B) is characterized by a subparallel to trellis pattern, which may indicate moderate to steep slope but is also found in areas of parallel and elongate landforms. Also, basin (A) shows a finer texture relative to the second one (B). The texture is a function

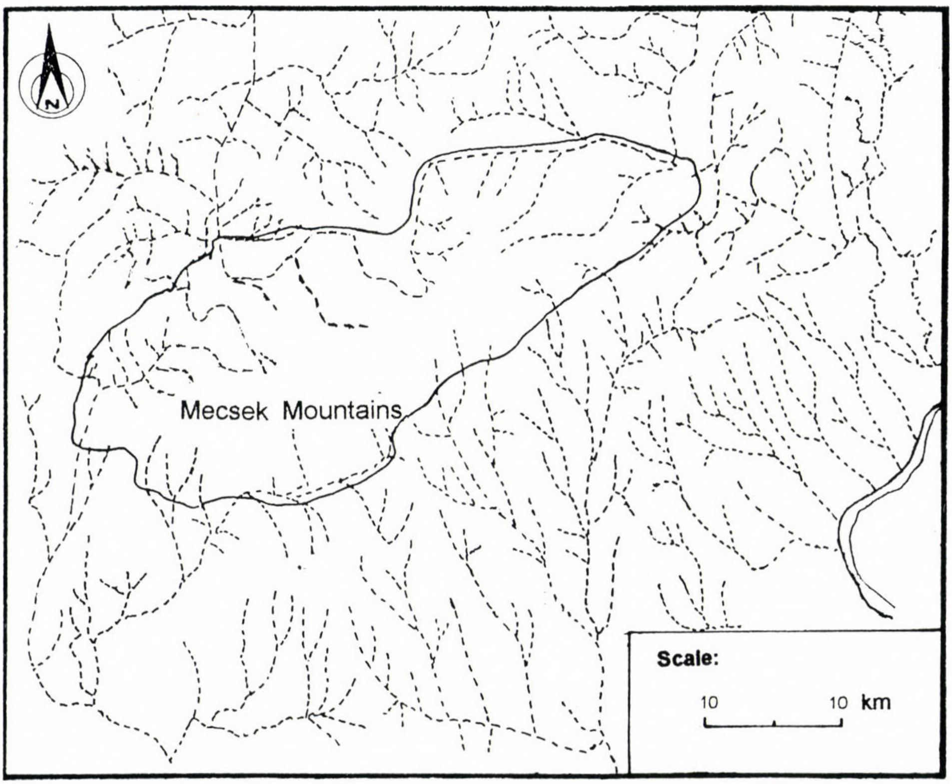

Fig. 2. The drainage network around Mecsek Mountains simplified after Ádám *et al* (1981)

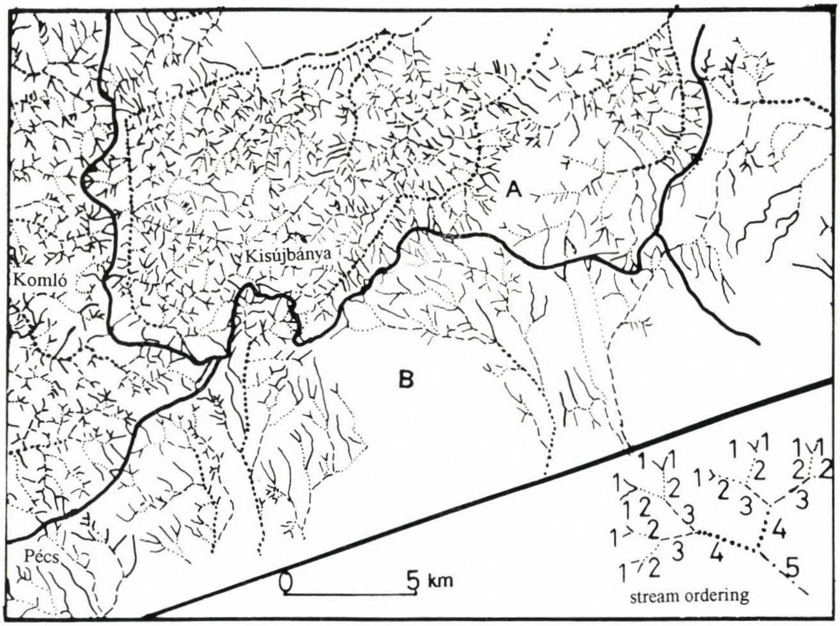

Fig. 3
The drainage map of the area: drainage traces; drainage divide; A – mountainous area; B – surrounding area

of many factors such as climate, rock characteristics, infiltration capacity, topography, and number of erosional cycles (Howard 1987). The mountainous area is characterized by relatively competent, less permeable rocks units. Drainage anomalies are only recognized in the bending of drainage traces in the northern part of the area, showing a preferred flowing of the tributaries in Mesozoic-covered areas to NE–SW, and NNE–SSW; while in the Miocene-covered areas, the trend is N–S, reflecting tectonic control.

Quantitatively, the stream network in both basins was examined according to Horton's laws (Horton 1945) and its modifications (Strahler 1952) in terms of stream order, stream number, bifurcation ratio, stream frequency, drainage density, relief ratio (Schumm 1956), and elongation ratio. The measurements and different relationships are presented in Figs 4 and 5. In the mountainous area the cummulative percentage of the stream numbers within higher stream orders are less than that in the surrounding area. That means that more streams of a given order are collected in the higher order stream. So, the mountainous area has higher bifurcation ratios (see below) which is used as a clue to predict uplifting of that mentioned area in the younger times. The average stream length is longer at the higher stream orders within the mountainous area while the lower stream orders are shorter realative to the surrounding area reflecting the different patterns detected within both of the studied basins. The patterns

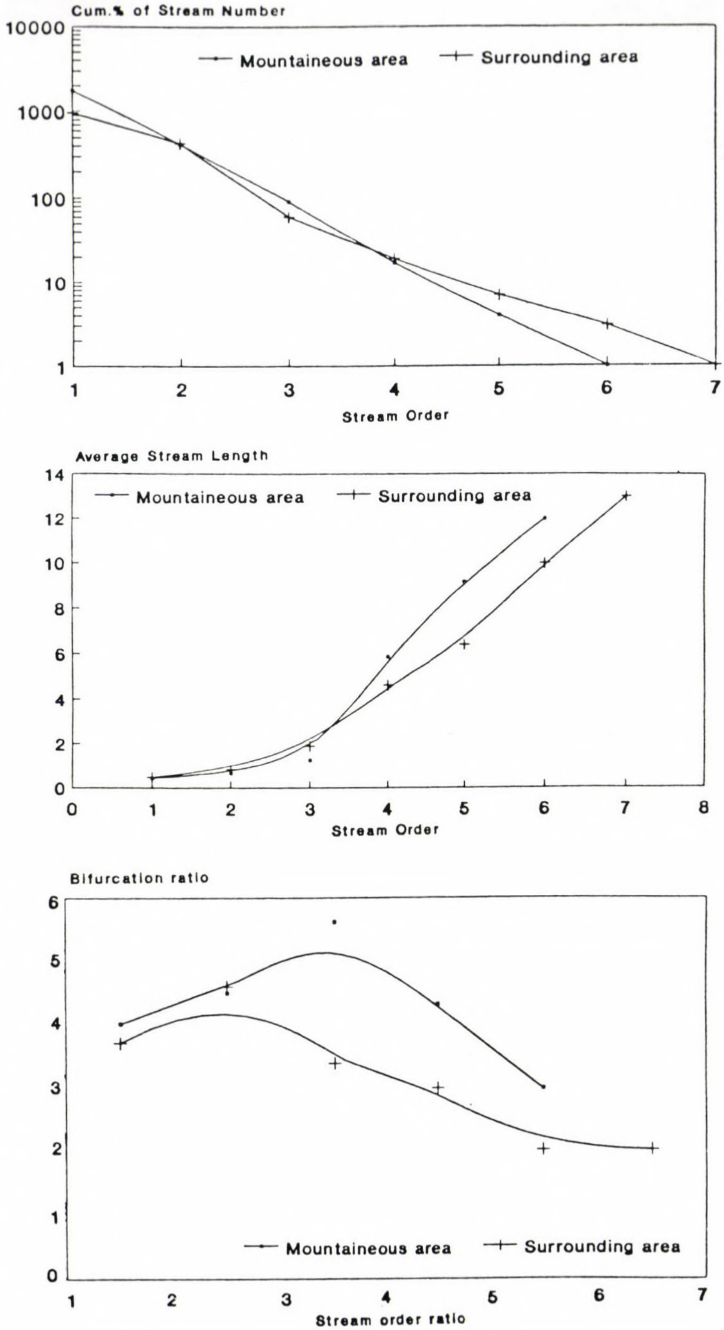

Fig. 4
Relationships between different linear characteristics of the drainage basins

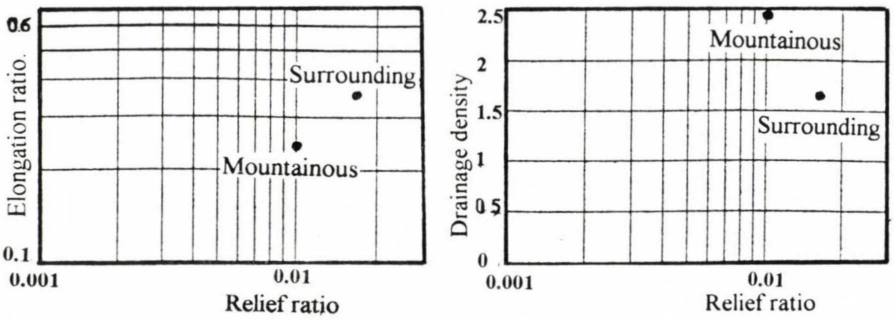

Fig. 5
Relationships between relief ratio, and both elongation ratio and drainage density

and its interpretations have been discussed earlier. The average bifurcation ratio (R_b) in the mountainous area of the Mecsek Mountains is higher (4.3) than that in surrounding area (3.1) reflecting the uplifting of the mountainous area in the younger times (Zuchiewicz 1989) than that in the surrounding area. The mountainous area shows lower relief ratio and elongation ratio that means that the topographic factor was minimized. On the other hand the higher relief ratio and elongation ratio of the surrounding area reflected the topographic control. The relation between relief ratio and the drainage density shows a higher drainage density and lower relief ratio of the mountainous area convincing the absence of the topographic factors. The drainage density also important because of its implication for runoff (Chorley 1971) and climate (Gregory 1976).

Fracture analysis

The air photo fractures were traced and measured (using different remote sensing data) in terms of number (N) percent and length (L) percent for each class of 10° of arc. These measurements are separated for the total area, the mountainous area, and the surrounding area. Azimuth-frequency (rose) diagrams are plotted for those measurements (Fig. 6). The fracture analysis showed differences in pattern and frequency of these diagrams. The total area (A) diagram configures a dominance of NNW–SSE to NW–SE orientation of fractures. These orientations are characteristic for Late Neogene tectonism and may be a neotectonic phenomenon. The mountainous area (B) diagram expresses the dominance of NE–SW to NNE–SSW orientation of fractures. These orientations are coincide with the tectonic lines in the Mesozoic formations. The surrounding area diagram shows the same as in the total area. The fracture characteristics of the area are summarized as follows:

	N	L	N/L	Dominant orientations	
Total area	523	528.8	0.89	N5, 25W	N5–15, 45, 65E
Mountainous area	279	256.8	1.08	N5–25, 75W	N5–25, 35–55E
Surrounding area	244	272.0	0.90	N15, 45W	N5, 45, 65E

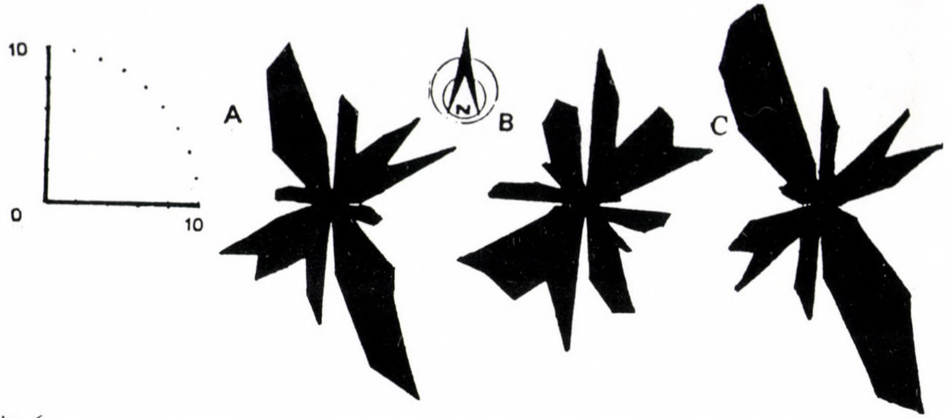

Fig. 6
The azimuth–frequency (Rose) diagrams of the traced fractures within the area. A – total area; B – mountainous area; C – surrounding area

In comparison with the fault pattern using the geological map (Hetényi et al. 1981) data, it is clear that the fracture pattern of the mountainous area shows some similarities to the fault pattern, which means that the air photo fractures in the mountainous area reflect more or less real tectonic lineaments (Fig. 7).

Geomorphological overview

The area of the Mecsek Mountains is a horst-type mountain island constituting a cornerstone of South Transdanubia. The highest peak is Zengő (681 m). The tectonic effect is clear on the topography. The orographic map (Fig. 8) compiled from the topographic maps shows the levelling of the area. Also the contour map (Fig. 9), together with the three-dimensional overview (Fig. 10), was compiled using the elevation and triangulation points and plotted with the SURFER software to give an idea about the geomorphological

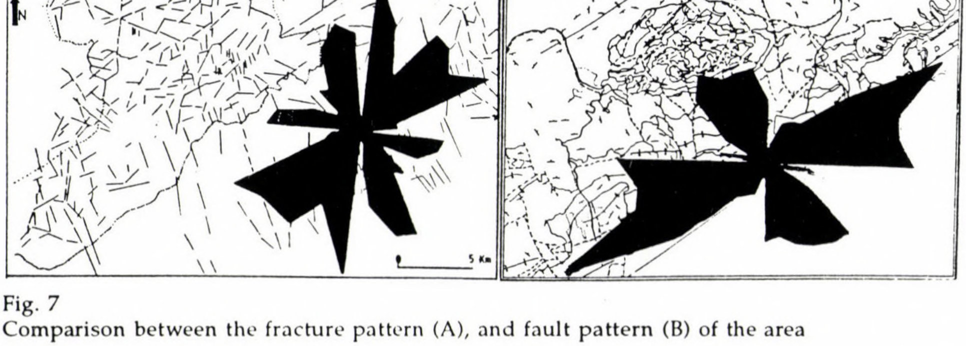

Fig. 7
Comparison between the fracture pattern (A), and fault pattern (B) of the area

Fig. 8
Orographic map of the studied area

characteristics of the area. The valleys are almost deep and narrow, with rather steep slope sides, and sometimes with angular bending, reflecting tectonic effects.

These figures give an impression about the unity of the area during the youngest uplifting that is supposed to be occurred in post-Pannonian time. The area was uplifted as one block to form an island-like position from its Transdanubian position. Uplifting during younger times is also convinced by the bifurcation ratio (see earlier). The uplift took place along the main tectonic lines that bounded the area.

Morphotectonic setting

Morphotectonic analysis is the study of landforms of regional or tectonic significance, and as such is the basis for the interpretation of geologic structure from remotely sensed images (Gold 1980). The Mecsek Mountains represent a good example of such areas in which the major tectonic lineaments are well exposed on the surface, affecting the topography and the drainage. The

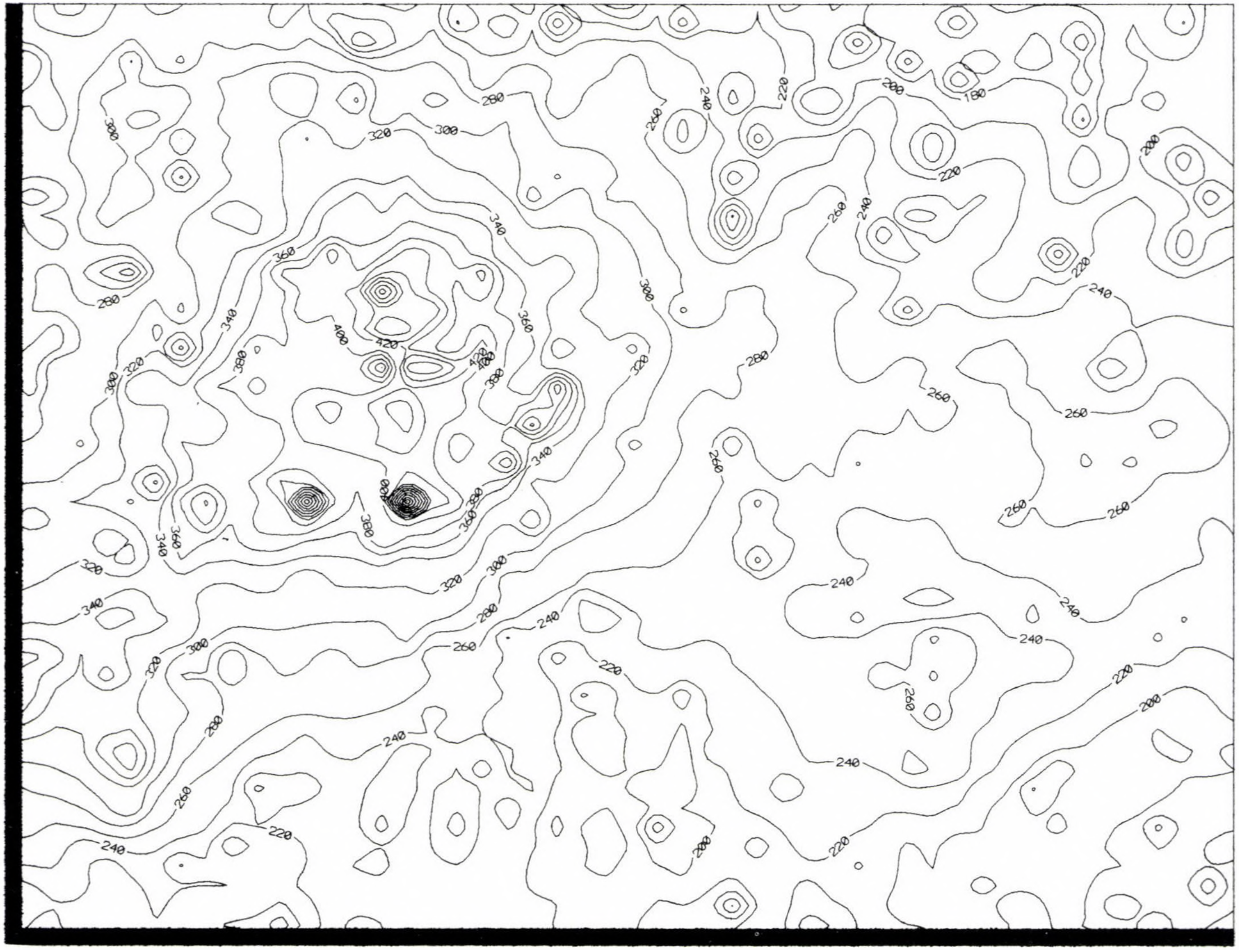

Fig. 9
Contour map of the studied area smoothed regardless to the drainage network

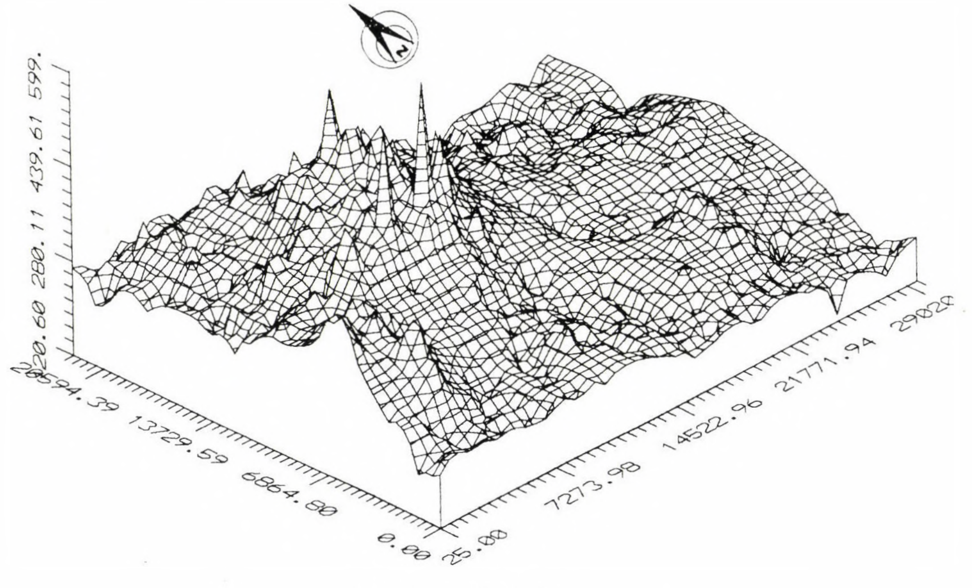

Fig. 10
Three-dimensional view of the studied area looking to N45E

Fig. 11
Morphotectonic map showing the major tectonic lines of the area as it is seen from space

Mecsekalja(1), Magyaregregy–Nagymányok(2), Magyaregregy–Komló(3), Hosszúhetény(4) and Márévár(5) valley lineaments are examples of these lines which are detectable from space as well as other major tectonic fractures in the area (Fig. 11).

Conclusion

The morphotectonic studies of the eastern part of the Mecsek Mountains show tectonic control of the drainage network within the mountainous area. The drainage analysis both qualitative and quantitative show the tectonic factors that have affected the mountainous area. On the other hand the topographic factors are dominant in the surrounding area. The stream segments are deep and narrow convincing the tectonic control. The bifurcation ratio is reflecting an uplifting of the mountainous area as a result of rejuvenation of older lines during younger times. The last compressive episode shows a detectable difference along east-west direction that is reflected by the decrease of bending of drainage segments from east to west. The airphoto fracture pattern of the mountainous area is similar – to certain extent – to the real tectonic pattern. The boundaries of the mountains to the north and to the south and many of the major fractures are easily seen from space.

References

Ádám, L., Gy. Lovász, S. Marosi, M. Pécsi, L. Rétvári, J. Szilárd 1981: Déldunántúli-dombság geomorfológiai térképe (Geomorphological map of the South Transdanubian Hill Range). –

Brezsnyánszky, K., F. Sikhegyi 1987: Neotectonic interpretation of Hungarian Lineaments in the light of Satellite imagery. – In: I. Joo (Ed.) Recent Crustal Movement in the Carpatho–Balkan Region. Journ. of Geodyn., 8, pp. 193–203.

Chikán, G. 1975: A Keleti-Mecsek aerofotogeologiai értékelése (Aerophotogeological evaluation of the Eastern Mecsek Mts). – MÁFI Évi Jelentés 1975-ről., pp. 319–332.

Chorley, R.J. 1971: The drainage basin as a fundamental geomorphic unit. – In: R. Chorley (Ed.) Introduction to fluvial processes, pp. 29–52, Mechnen, London.

Gold, D. 1980: Structural Geology. – In: Siegal and Gillespie (Eds) Remote sensing in geology, pp. 419–483. John Wiley & Sons, New York.

Gregory, K.J. 1976: Drainage networks and climate. – In: E. Derbyshire (Ed.) Geomorphology and climate. pp. 290–315, Wiley, New York.

Hetényi, R., G. Hámor, M. Földi, I. Nagy, E. Nagy, I. Bilik 1981: The geological map of the Eastern Mecsek Mountains. Scale 1:25 000. – Hungarian Geological Institute, Budapest.

Horton, R.E. 1945: Erosional development of streams and their drainage basins: hydrophysical approach to quantitative morphology. – Amer. Geol. Soc. Bull., 56, pp. 275–370.

Howard, D.A. 1967: Drainage analysis in geologic interpretation. – AAPG Bull., 51/11, pp. 2246–2259.

Joó, T., F. Stogicza 1984: Távérzékelési módszerek gyakorlati alkalmazása a Máza-Dél kutatási területen (Practical application of remote sensing methods in the research area Máza-South). – BKL-Bányászat, 117, 8, pp. 539–544.

Kókai, A. 1980: DK–Dunántúl földtani-szerkezeti viszonyai a Landsat-1 műhold felvétel kiértékelése alapján (Geological–structural conditions of SE Transdanubian on the basis ofg evaluating the Landsat–1 satellite image). – MÁFI Évi-Jelentés 1980-ról. pp. 501–508.

Pécsi, M. 1970: Geomorphological Regions of Hungary. – Budapest 45 p.
Schumm, S.A. 1956: Evolution of drainage systems and slopes of bad lands at Perth Amboy, New Jersey. – Geol. Soc. Am. Bull., 67, pp. 497–646.
Stogicza, F. 1987: Űrfelvételek alapján végzett tektonikai vizsgálatok a Mecsek hegység területén (Tectonical investigations carried out on the basis of aerial photographs in the area of the Mecsek Mts). – BKL-Bányászat, 120, 3, pp. 187–196.
Stogicza, F., G. Csillag 1986: Űrfelvételek számítógépes feldolgozása a Mecsek hegység tektonikai értékeléséhez (Computer processing of aerial photographs to the tectonical evaluation of the Mecsek Mts). – BKL-Bányászat, 119, 7, pp. 470–475.
Strahler, A.N. 1952: Dynamic basis of geomorphology. – Amer. Geol. Soc. Bull., 63, pp. 923–938.
Zuchiewicz, W. 1989: Morphotectonic phenomena in the Polish Flysch Carpathians: a case study of the eastern Beskid Niski Mountains. – Quaestiones Geographicae, Spec. Issue 2, Adam Mickiewicz University Press, Poznan 1989, pp. 155–167.

Acta Geologica Hungarica, Vol. 37/3–4, pp. 281–296 (1994)

Outlines of geology of the metamorphic basement of the Sălaj (Szilágy) Basin, Romania

János Kalmár
Hungarian Geological Institute, Budapest

The basement of the Sălaj (Szilágy) basin outcrops in North Transylvanian Crystalline Islands; it was also investigated in some boreholes. In the surficial occurrences such as Erdőd (Ardud), Bükk (Bâc), Cikó (Ţicau), Hegyes (Heghieş), Szilágysomlyói Măgura (Magura Şimleului) and the Meszes (Mezeş) and Réz (Rez) Mts, the various types of metamorphic rocks were described (magmatic rocks such as orthogneisses and amphibolites, and terrigenous ones such as mica-schists, paragneisses and quartzites, rare marble lenses, together with small alcaline intrusions, migmatites and pegmatites). Similar rock types were found in boreholes. The basement is made up of two different domains: the first is characterized by the presence of amphibolites, leptinites and migmatic belts, and was correlated with the Autochthonous Unit of the basement of the Hungarian Plain (Kőrös and Szeghalom Formations); the second, without amphibolites and with intensive shearing processes and low pressure associations, is a unit split off from Southern Tisia (South Hungarian Nappe).

Key words: basement, metamorphic rocks, amphibolites, gneisses, Szilágy (Sălaj) basin, Transylvania, polymetamorphism, retrogressive processes, mylonites, neomorphic biotite, phengite, staurolite, andalusite

Introduction

The Sălaj (Szilágy) Basin is one of the Eastern Gulfs of the Pannonian Basin. The knowledge concerning the deep zones of this area has increased in the past years, both through Romanian and Hungarian drilling activity and through petrographic studies of the metamorphic rocks of the Northwestern Transylvanian Islands, as well through re-interpretation of geophysical data.

The northern border of the Szilágy Basin coincides with the southern margin of the Szolnok–Maramureş Flysch Belt. In the eastern part, the Szilágy Basin is separated from the Szamos Platform by the Para-Meszes fault system. Southward, the basin is bordered by the Meszes (Mezeş) and Réz (Rez, Plopis) Mts, which are part of the Erdélyi-középhegység (Munţii Apuseni) range. Westward, the Szilágy Basin is largely opened toward the Pannonian one, through the Békéscsaba–Nagykároly deep zone (Fig. 1).

Address: J. Kalmár: H–1142 Budapest, Stefánia út. 14, Hungary
Received: 12 February, 1994

0236–5278/94/$ 5.00

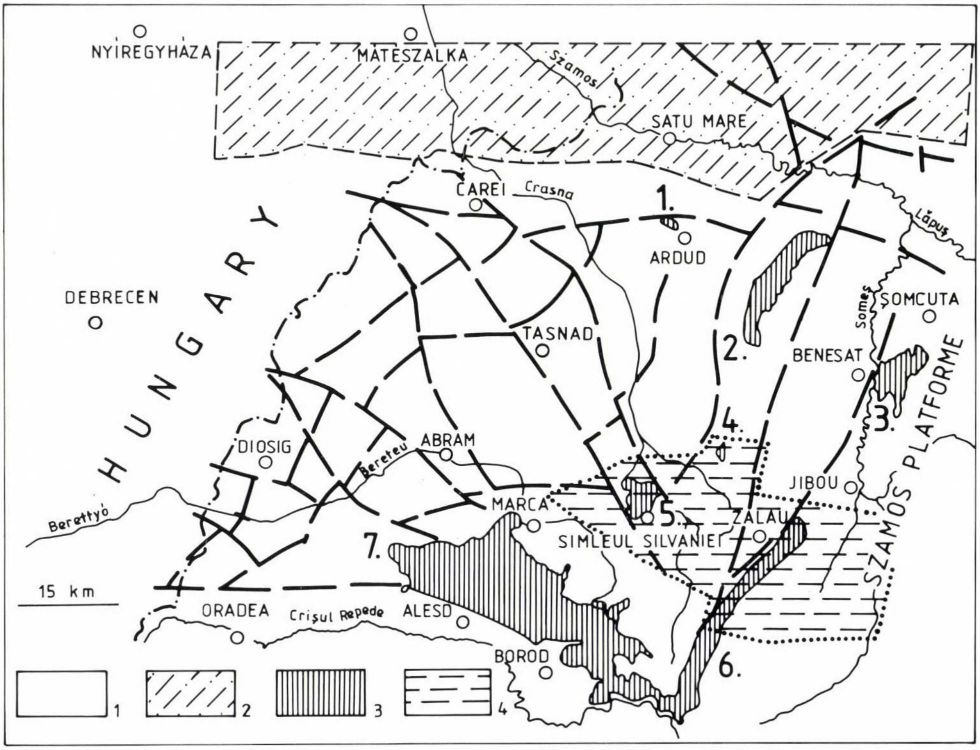

Fig. 1
The crystalline islands from Szilágy Basin: 1. Erdőd (Ardud); 2. Bükk (Bâc); 3. Cikó (Ţicau); 4. Hegyes (Heghieş); 5. The Magura from Szilágysomlyó (Măgura Şimleului); 6. Meszes (Mezeş); 7. Réz (Rez); a – Sedimentary cover deposits; b – Szolnok–Máramaros Flysch Belt; c – Outcropping metamorphic rocks; d – SE-Szilágy Domain

Short history

Before the Ist World War, the oldest formations of the Szilágyság were known only in the outcrops in the crystalline islands (Hofmann 1879, 1883; Mattyasovszky 1879; Telegdi-Róth 1912). Beginning in 1910, a few boreholes were deepened in the central and eastern parts of the basin, which penetrate the entire stratigraphic column as far as the metamorphic basement.

Between the Ist and IInd World Wars, Szádeczky (1925), Szádeczky-Kardoss (1925) and Kräutner (1938, 1940) published papers on the petrography of the North-Transylvanian Crystalline Islands. After 1944, the metamorphic rocks were studied by Ciornei (1953), Dimitrescu (1962, 1963), Ignat and Ignat (1964–1972), Câmpianu (1964), Kalmár (1972) and Zincenco et al. (1990). The regional geologic and geophysical considerations concerning the Szilágy Basin and the surrounding territories were supplied by Cristescu et al. (1957), Paucă (1964), Dicea et al. (1981) and Visarion et al. (1992).

Outcropping basement: the metamorphic formations in the crystalline islands

The Pre-Variscan basement outcrops in Erdőd (Ardud), Bükk (Bâc), Cikó (Ţicău), Hegyes (Heghieş) and Szilágysomlyói Măgura (Magura Şimleului), as well in the Meszes (Mezeş) and Réz (Rez) Mts.

The Castle Hill (Dâmbul Cetăţii) at Erdőd

The metamorphic nature of this 1 km^2-large hill was discovered by a pedology researcher, H. Asvadurov, in 1969. Our latest sampling established that the Várdomb is made up of various types of weathered and fresh micaschists and quartzitic schists containing thin leptinite levels (Plate I: 1), which are correlated with the Prihodiste Formation of the Bükk Mts.

The Bükk (Bâc, Codru) Mts

The Bükk (Bâc) Mts are a 45 km long, 5–15 km wide, NE–SW and N–S oriented ridge, which was raised out of the surrounding Neogene sedimentary area by two parallel faults.

In the Bükk Mts an asymmetric anticline is developed, centered on the ridge of the mountains. In the core of this anticline occurs the Lespezi Formation; in its wings, the Prihodişte Formation appears (Fig. 2).

According to Kalmár et al. (1989), the Lespezi Formation consists of quartzose micaschists, quartzitic schists and paragneisses. In the upper section of the formation, thin, discontinuous leptinite lenses appear. With their rhythmical schistosity and alternating mica-rich and mica-poor levels, these rocks were probably formed from flysch-like sedimentary rocks.

The base of the Prihodiste Formation is marked by a quasi-continuous amphibolite level, followed by garnet-rich mica-schists, leptinites, amphibolites, actinolites, biotitic gneisses with graphitic quartzite and marble lenses. The petrographical, chemical and structural peculiarities of this succession suggest a metamorphosed volcano-sedimentary origin.

The grade of the metamorphism in the Bükk Mts is highest in the area located between Lespezi (575 m) and Tarniţa peaks. Typical minerals here are biotite, almandine, An_{30} plagioclase and kyanite, and in amphibolic rocks, hornblende and An_{40} plagioclase appear. S and N of this central area, staurolite was found in metapelites. In the extremities of the mountains, plagioclase contains less than 20% An; also, ferrotremolite and iron-rich epidote appear.

In the entire Bükk Mts, especially in the mica-rich rocks, a retrogressive mineral assemblage is developed: albite, chlorite, phengite (replacing biotite). The last progressive metamorphic event was the formation of neomorphic biotite and muscovite, 1–2 cm large ferrotremolite and euhedral garnet porphyroblasts with albite and chlorite filling the pressure shadows.

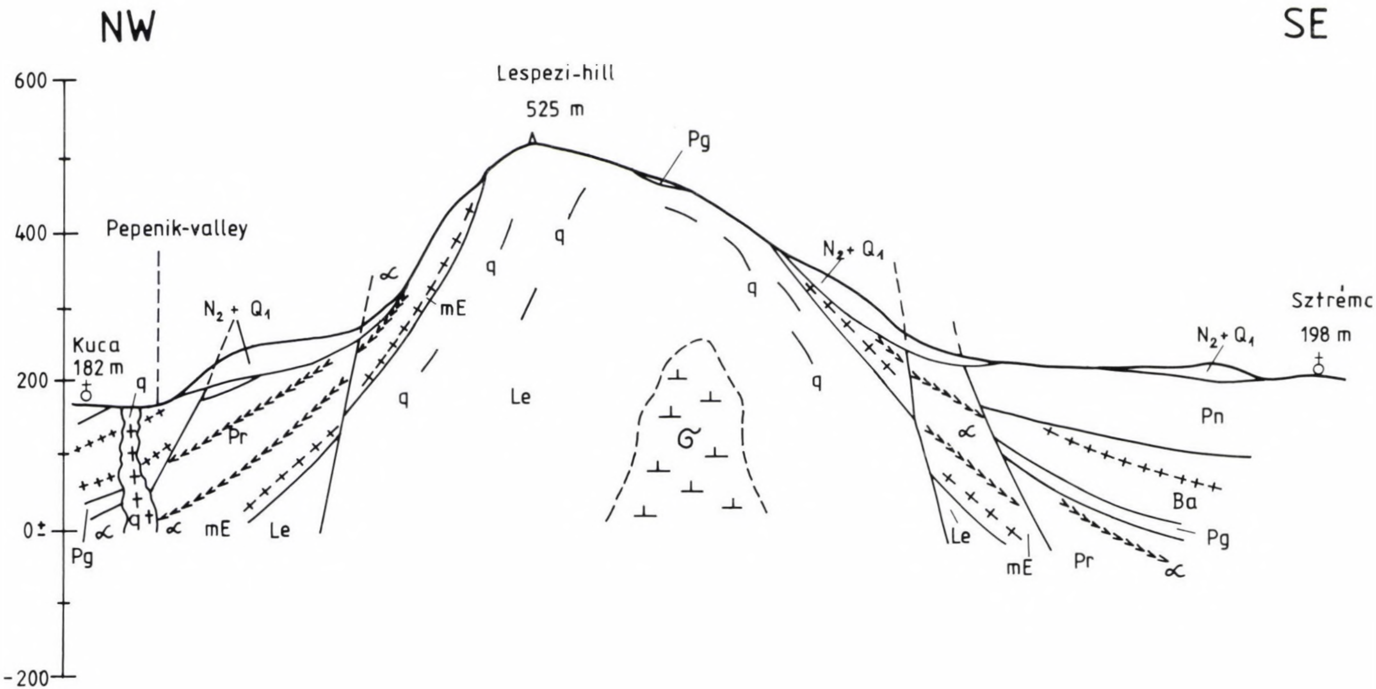

Fig. 2
Cross-section through the Bükk Mts. N_2+Q_1 – Upper Pliocene–Lower Pleistocene continental deposits; Pn – Pannonian; Ba – Badenian; Pg – Paleogene; Metamorphic rocks: Pr – Prihodiste Magmatic Formation; α – amphibolites; mE – gneisses and leptinites; Le – Lespezi Terrigenous Formation; q – quartz lenses; Magmatic rocks: q – Badenian rhyolite neck; σ– hypothetical syenite or monzogranite intrusion

In the Bükk Mts the small alcaline intrusions had been previously described by Mattyasovszky (1878) and partly studied by Dimitrescu (1962). We have mapped 15 gneissic granite, monzo-granite and syenite bodies not larger than 2 km, and some migmatite zones. At the contact between syenite and surrounding mica-schists, a cordierite-tourmaline-epidote-albite contact zone was formed. Pegmatites, gold-bearing quartz lodes and lens-like bodies are also known.

The Cikó (Ţicău) Hills

Eastward of the Szamos (Someş) gorge, in a 15–25 km^2 large, irregular triangular area, crystalline rocks occur which are part of the Szamos Platform (Platforma Someşană). The summit of the hill is Prisaca Peak (661.6 m). These "mountains" are built up of an acid, magmatic, lower member and by an upper, terrigenous member, forming a N–S-oriented, northward-opened syncline.

The magmatic Stejera Member is well-developed in the eastern and southern parts of the Cikó Hills. It is made up of five ortho-gneissic and garnet-rich mica-schist levels (Kalmár and Kovács-Pálffy 1993). The uppermost one also contains three small amphibolite intercalations. In some mica-schist levels, leptinites, graphitic quartzites and almandinites were identified (Fig. 3). The petrographic and petrochemical studies demonstrated that the biotitic gneisses and the leptinites of the Stejera Member were initially acidic, dacite- and rhyolite-type igneous rocks or pyroclastites, and that the mica-schists were formed from iron-rich clayey deposits, as products of submarine decomposition of the lavas and tuffs (Kalmár 1986).

The terrigenous Glod-Hagau Member is built up by quartzitic mica-schists, quartzitic schists, quartzites and paragneisses, including two garnet-rich mica-schist horizons and a leptinite one.

In the Cikó Hills, the original metamorphic assemblage is biotite, almandine, zoned An_{20-25} plagioclase and hornblende. Staurolite (Plate I: 3) is known in the SE corner of hill and in boreholes. The retrogressive phase is represented by albite, epidote, chlorite and phengite. Neomorphic cross-biotite and muscovite, An_{20}-plagioclase, idioblastic almandine, tourmaline and ferrotremolite represent the last, progressive phase.

The Hegyes (Heghieş) Hill

Southward of the Bükk Mts, a small, 5 km long, 1–1.5 km wide hill range is located. This is Hegyes Hill (521 m), which represents the summit of a large tectonic block, covered by thin Badenian epi- and pyroclastic deposits.

The metamorphic rocks of Hegyes Hill form an anticline and a syncline consisting of paragneisses, quartzitic schists and mica-schists, and a thick marker-horizon of orthogneiss (Plate I: 4). These rocks present a characteristic silky feature, and are strongly micro-folded. The first metamorphic mineral assemblage is represented by muscovite, biotite, almandine and

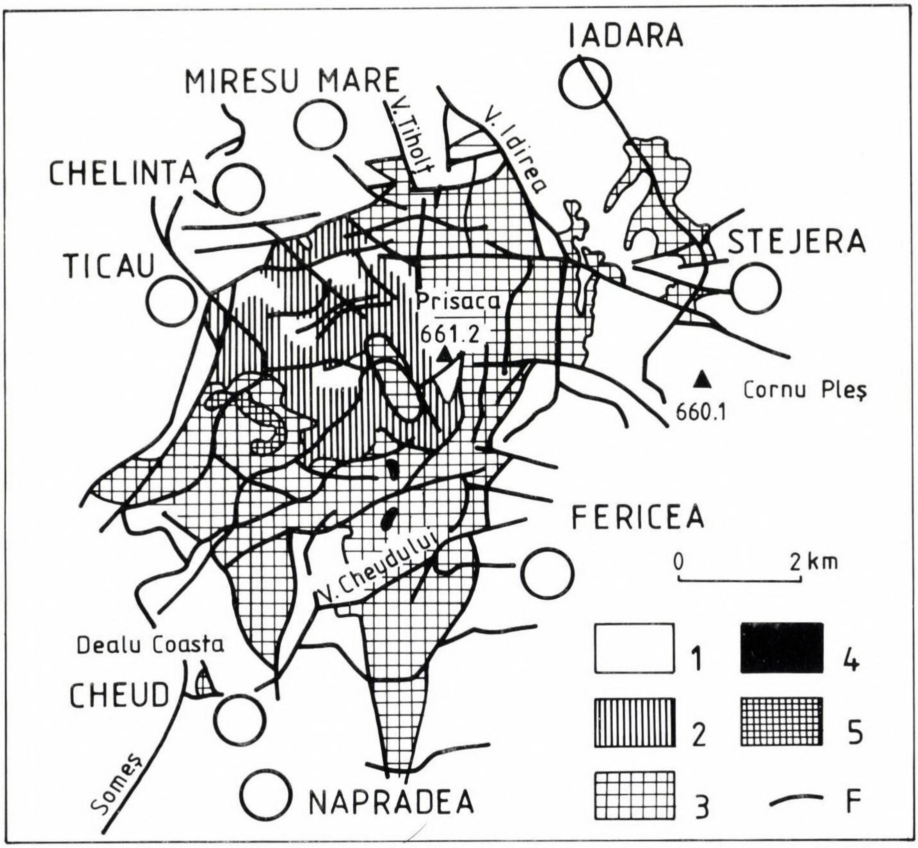

Fig. 3
Geologic sketch of the Cikó Mts. 1. Paleogene and Neogene sedimentary cover; Metamorphic rocks: 2. Terrigenous Member; 3. Magmatic Member; 4. Meta-granodiorite lenses; 5. Amphibolite lenses; F – Faults

An_{20}-plagioclase. After mylonitic deformation, a retrogressive association was developed: phengite, chlorite, sericite, epidote and carbonate. In some samples, neomorphic biotite was found.

The Szilágysomlyói Magura (Măgura Simleului)

The Măgura (574.6 m), which dominates the little town of Szilágysomlyó (Şimleul Silvaniei), is built up by strongly folded metamorphic rocks. It is subdivided into three stratigraphic units: a lower, terrigenous, biotitic-muscovitic member, a middle, magmatic (orthogneissic horizon) and an upper, terrigenous muscovitic member. Quartzitic schists, mica-schists and paragneisses constitute the terrigenous members of Magura (Kalmár 1993).

As in those of Hegyes, in metamorphic rocks of the Magura the first metamorphic mineral-assemblage can be recognized only in non-mylonitised,

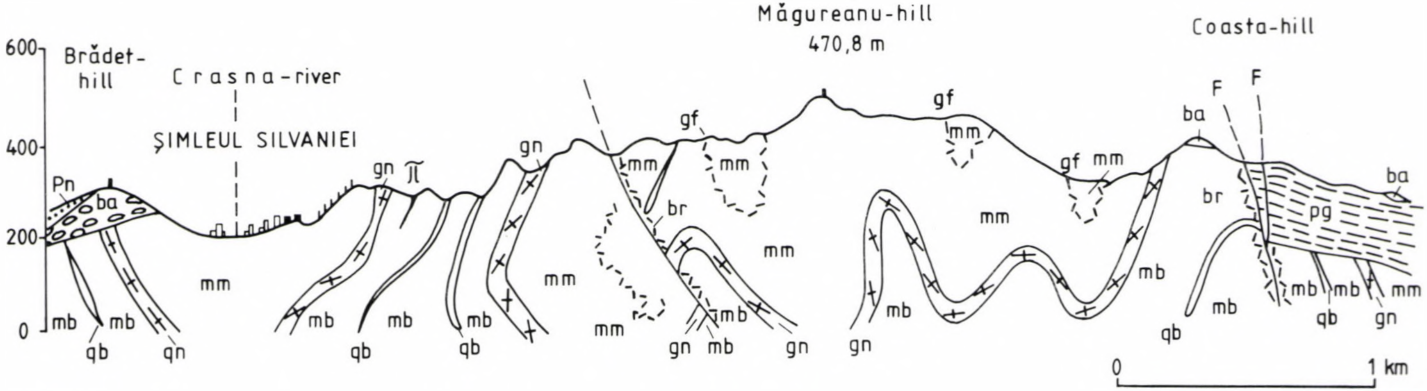

Fig. 4
Geologic section through the Szilágysomlyói Magura. Pn – Pannonian; ba – Badenian; pg – Paleogene; Metamorphic rocks: mm – Upper Muscovitic Member; gf – Graphitic Mica-schist Level; gn – Acid Magmatic Level; mb – Lower Biotito-muscovitic Member; qb – Biotitic Quartzite Level; – Pegmatite, F – Faults

unsheared samples. This assemblage is: almandine, biotite, muscovite and plagioclase. In the SE, in Szenthegy (Dealu Sfânt), small, sericitised relics of andalusite appear. The retrogressive assemblage develops along the sheared wings of the microfolds, forming a secondary schistosity (crenulation cleavage) and the minerals phengite, chlorite, iron-poor epidote and fine-grained quartz. After the formation of these minerals, the rocks were subjected to mylonitisation, and finally, to neo-formation of cross-biotite, muscovite and staurolite (Plate II: 1). The clear edges of the garnet porphyroblasts were formed in this phase.

The Meszes (Mezeş) Mts

The Meszes is a 50 km long, 3–10 km wide mountain range, the altitude of which increases from N to S (Druiu Peak, 546 m; Măgura Priei, 1024 m). Its geological structure is quite complicated; it is made up of strongly asymmetrical and sheared folds and is intensively fragmented by a great number of faults.

In the Northern Meszes, the upper, muscovite-rich and the lower, two-mica bearing member accompanied by a few leptinite lenses were mapped by Ignat and Ignat (1972). Some similarity with the Szilágysomlyói Magura can be detected, including the presence of the mylonitic rocks (Plate II: 2). The index-minerals of the first metamorphic association are biotite, almandine, staurolite, An_{20-25}-plagioclase, and small andalusite fragments (Kalmár et al. unpubl. report, 1975).

The structure of the southern part of Meszes is mostly undisturbed. In the terrigenous succession (paragneisses, quartzitic schists, mica-schists) representing the uppermost part of the Szamos Series, some amphibolite lenses were identified by Ionescu (1964) and Nedelcu (1968). Between the Gumbei and Ragului valleys, and southward to Măgura Priei hill, they are covered by the greenschists of the Arada Formation (albite-chlorite-epidote schists, chlorite-sericite schists, sericitic quartzites) which forms some shallow synclines.

The boundary between these two different domains of the metamorphic formations cross-cuts the mountain range south of the Zilah (Zălau)–Kolozsvár (Cluj-Napoca) road (Şura Dacilor Motel), along an intensively tectonised zone.

The Réz (Rez) Mts

The Réz Mts is the largest metamorphic mountain range of NW Transylvania, extending between the Báród Basin (Bazinul Borodului) and the Szilágy Basin, covering approx. 1600 km^2.

According to the geological maps of Ciornei (1953) and Câmpianu (1964), they consist of a NE–SW oriented anticlinorium, with few secondary folds on its wings. The stratigraphic column of the Réz Mts consists of a monotonous terrigenous succession in which amphibolites, leptinites, garnet-bearing mica-schists and graphitic quartzites appear. They can be considered as one or more metamorphosed volcano-sedimentary complexes. A migmatitic zone between Fekete-patak (Valea Neagra) and the gorge of the Berettyó (Barcău) river near Márkaszék (Marca) can be followed.

In samples collected from the outcrops of the western side of the Réz Mts I have found three mineralogical assemblages: the first, a progressive association (biotite, staurolite, almandine, An_{25}-plagioclase, hornblende), followed by a retrogressive chlorite-phengite-albite-epidote association and, finally, by the development of neomorphous micas.

The metamorphic basement in boreholes

The first systematic description of the borehole cores was carried out by Ghiurca (1973), and later by Dicea et al. (1981). Stratigraphic columns, petrographic analyses and geophysical logs can be consulted in unpublished documentations. Their correlation gives sufficient data about the constitution and spatial arrangement of the metamorphic rock-types in the basement of the Szilágy Basin.

In the ISEM's boreholes from the western foreland of the Bükk Mts (Chilia, Homorod, Solduba, Soconzel, Bicaz, Ciuta) garnet-bearing mica-schists, amphibolites, leptinites and some pegmatite lenses were found, which correlate with the Prihodişte Formation.

In boreholes located at greater distances from the Bükk Mts [Madaras (Mădăras), Piskolc (Piscolţ), Ákos (Acâs), Nagykároly (Carei)] the depth of the metamorphic basement increases continuously to 4000 m. Mica-bearing grey quartzites and quartzose mica-schists are the prevailing rocks, but a few amphibolite-levels (Plate II: 3) were also traversed. It is very probable that the formations known in the Bükk Mts are present here.

Along the Romanian–Hungarian state border, at Selénd (Şilindru) and Székelyhíd (Secuieni), the oil-prospecting boreholes were stopped in quartzitic schists, in micro-folded mica-schists and paragneisses which are identical with the cores from Álmosd-1, Nyírábrány-1 and 3 boreholes from E Hungary (Szederkényi 1984)

In the northern foreland of the Réz Mts, in the Széplak (Suplacul de Barcău) – Ip (Ipu) Area, approx. 1800 shallow oil wells recovered weathered and brecciated garnet-bearing mica-schists and paragneisses, which outcrop at the northern border of the mountains, between the Fekete river (Valea Neagra) and Derna. In the boreholes from the inner area of the Szilágy Basin, as well as between Érábrány (Abram) and Tasnád (Tăşnad), biotite-staurolite-almandine micaschists appear, with thin leptinite and amphibolite intercalations. They are correlated with the metamorphic rocks both of the Bükk and Réz Mts.

In boreholes which prospected the upper Pliocene lignite deposits from Bobota, Szilágysámsod (Şamşud) and Chieşd, as well in hydrogeological wells from the Hereclean and Zilah (Zălau) area, the metamorphic rocks are silky, fine-grained, often mylonitised and are similar to the metamorphic rocks from

Magura and Hegyes. Neomorphic biotite, muscovite and albite porphyroblasts are also frequent. Similar rock-types were described eastward of Meszes (Lujerdiu, Surduc) by Soroiu et al (1985).

Age of metamorphic rocks

In the North Transylvanian area, Pb–Pb age dating only performed at the Macskamező (Răzoare) manganese deposit, outside of the Szilágy Basin (in the eastern Preluca Mts), resulting 1.6 ± 0.3 Ga. This demonstrates that the first palyngenetic processes are no older than Middle Algonkian. The first sediments and the rocks formed by their metamorphism must be considerably younger.

In the cover of the Tisia-realm (Tázlár Formation) and in the Erdélyi-középhegység (Munţii Apuseni), slightly metamorphosed Carboniferous sedimentary rocks are known. Permian sedimentary and volcanic rocks were identified south of the Réz Mts and in boreholes in the southern Szilágy Basin (Istocescu and Ionescu 1970). Consequently, the rocks forming the actual basement of the Szilágy Basin were metamorphosed in the first phases of the Hercynian orogenesis or earlier (the age of the Arada Formation is considered to be Upper Devonian and it covers the Szamos Series).

From the Bükk, Cikó and Szilágysomlói Magura 12 samples for K–Ar age-dating were collected and analysed (Soroiu and Popescu 1986; Zincenco et al. 1990). The values vary between 94 and 106 Ma. The authors explain the rejuvenation of the metamorphic ages by a thermal event which took place between the Lower and Upper Cretaceous, produced by the collision between the Tisia realm (micro-plate?) and the basement of the Transylvanian Domain. According to the borehole and geophysical data, Soroiu et al (1990) draw the suture line 50–60 km eastward of Szilágyság.

Two samples show a "hybrid" age (172 and 252 Ma, the last value for a syenite sample from the Bükk Mts), suggesting either that the rocks were subjected to thermal events before the Alpine orogenesis, or that the determinations were imprecise.

According to the petrographic observations, the metamorphic recrystallisation of the rocks forming the basement of the Szilágy Basin occurred in two or three successive or independent phases. In further studies, the accurate P–T determination for all of the mineral associations, using adequate thermobarometers (see Árkai 1987) and Rb-Sr dating, are considered necessary.

Structure of the Basement of the Szilágy Basin

Dimitrescu (1963) considered the metamorphic rocks which outcrop in the Réz, Meszes and in the NW Transylvanian Crystalline Islands to be the continuation of the metamorphic rocks described by himself (1957) in the Could Szamos (Someşul Rece) source area. For these rocks he proposed the lithostratigraphic megaunit called Szamos Series (Seria de Someş), or using modern terminology, the Szamos Group. In recent papers, the northern area of this group was separated (Zincenco et al. 1990), as the Silvanide Group.

In this paper it is possible to subdivide the Silvanide Group into two different domains, according to the succession of the metamorphic events and the tectonic behaviour of the described rocks.

The first described domain outcrops at Erdőd, Bükk and Cikó, and traverses the basin [Madaras (Mădăras), Ákos (Acâs), Érábrány (Abram), Széplak (Suplacul de Barcău)], continuing in the Réz and South-Meszes Mts. This domain correlates with the Hungarian Kőrös and Szeghalom Formations of the Autochthonous Unit. In spite of difficulties in detailed stratigraphic correlation, the lithostratigraphic units of this domain present common features, such as a complete series of magmatic (basic, intermediate and acid) rock-types and their subaqueous alteration products, the presence of carbonatic rocks (marbles), the migmatite lenses and the syn- and postkinematic intrusions. The metamorphic events began with high-pressure and medium-temperature associations, followed by a weak retrogressive phase. The tectonic effect was weak to medium-strong; no mylonitized or sheared zones were developed.

The second domain, extending over a small area in the SE corner of the Szilágy Basin and eastward, in the Szamos Platform, is characterized by the absence of the magmatic levels, except for thin acidic ones. These rocks were subjected to intensive shearing, resulting in mylonites. Low pressure, middle or low temperature mineral association was identified (andalusite, etc.). This domain is comparable to the metamorphic rocks which were described by Szederkényi (1984) in the SW of the Hungarian Plain, as the South Hungarian Nappe, extending eastward as the Codru–Arieseni Nappe from the Erdélyi-középhegység.

In our conception, the second domain represents an alien unit, the tectonic relations of which are unknown in the present day.

After the closure of these domains, a new metamorphic event was produced: the progressive blasthesis of neomorphous biotite and muscovite, the overgrowth of some minerals, and, finally, the crystallization of albite and chlorite in pressure shadows. This event was recognized in both domains. The most probable age of this recrystallisation is Alpine.

The formation of the actual configuration of the Szilágy Basin began after the Cretaceous orogenic events (according the approximative K–Ar ages, Subhercynic or Late Kimmerian phases). The movement of the tectonic blocks continued during the Tertiary until the present, which is demonstrated by seismic activity along some regional faults and the disturbance of the hydrographic network.

Acknowledgements

Financial support for this paper, including expenses of the investigations in Romanian libraries and core deposits, was provided by the Hungarian Research Fund OTKA, theme T 7636.

The author is indebted to Drs. J. Andrei and N. Mihailescu, Institutul de Geologie al României, Bucureşti, for their help in consultation of unpublished Romanian documents, and to Prof. Dr. T.

Szederkényi for permission to examine the Hungarian core collection of JATE University, Szeged, from the Great Hungarian Plain.

Plate I

1. – Weathered, phaneroblastic leptinite from Castle Hill of Erdőd (Dealul Cetăii, Ardud). + Nichols, 16 x
2. – Syenite from Somoteşului valley, Hutaszelestye (Poiana Codrului), Bükk (Bâc) Mts, with microcline, albite, quartz and biotite. + Nichols, 16 x
3. – Gneiss with "check-board albite" and rare biotite sheetlets, Silvania Quarry, Erked (Archid), Hegyes (Heghieş) Hill. + Nichols, 16 x
4. – Staurolite crystals in quartz-rich mica-schist, Rom. Cath. Cemetery, Szilágysomlyó (Şimleul Silvaniei). + Nichols, 16 x

Plate II.

1. – Mylonitized gneiss, with a plagioclase porphyroblast relics. Druiu hill, Roman Limes way, Northern Meszeş (Mezes) Mts + Nichols, 16 x
2. – Neomorphic biotite porphyroblast displacing the older muscovite sheetlets. 32. Corond borehole, 443 m. + Nichols, 16 x
3. – Amphibole gneiss, 4405 Ákos (Acâş) borehole, 2230 m. + Nichols, 16 x
4. – Microfolded mica-schist. 1 Tasnád (Tăşnad) borehole, 2235 m. + Nichols, 24 x

Plate I

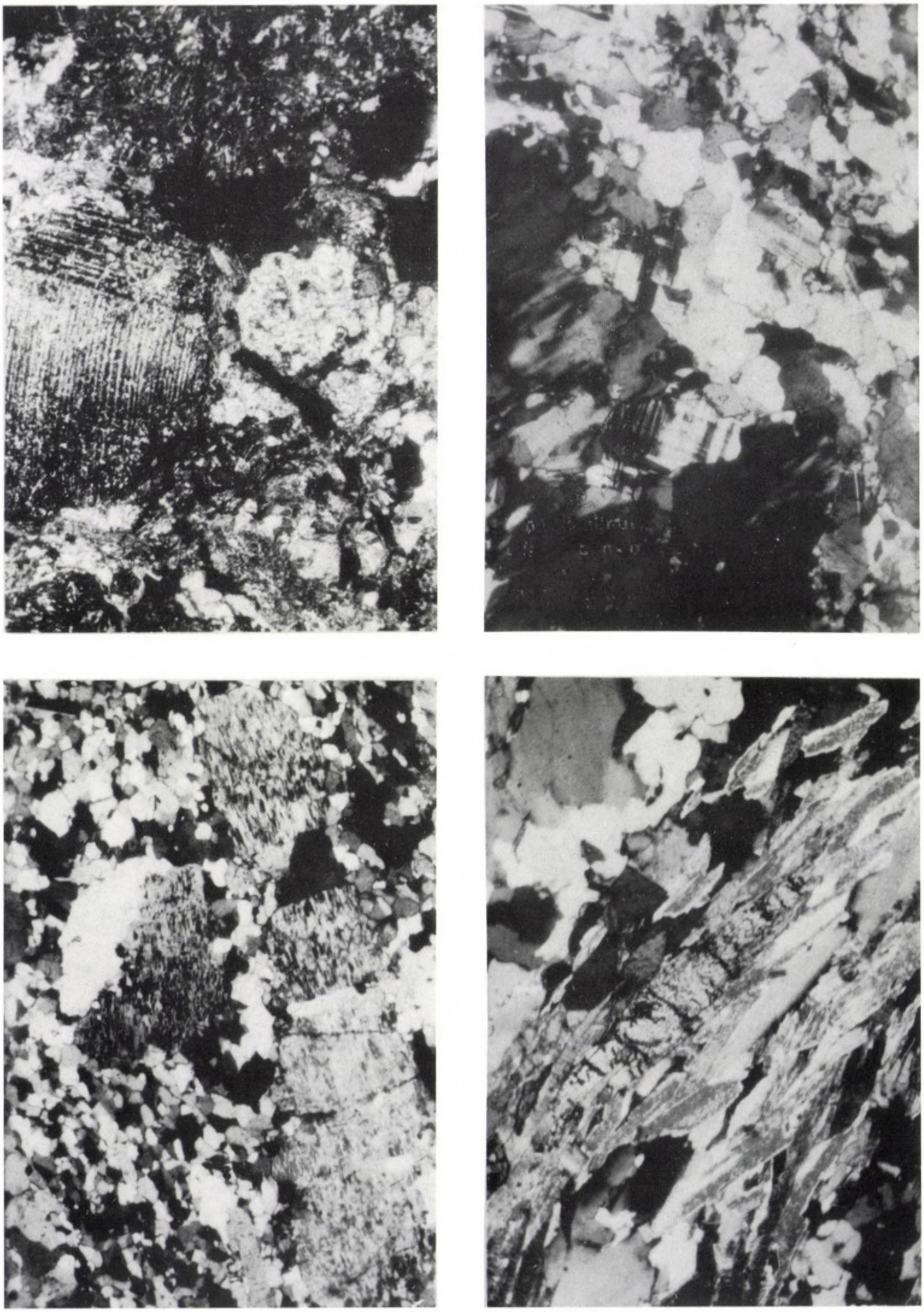

Plate II

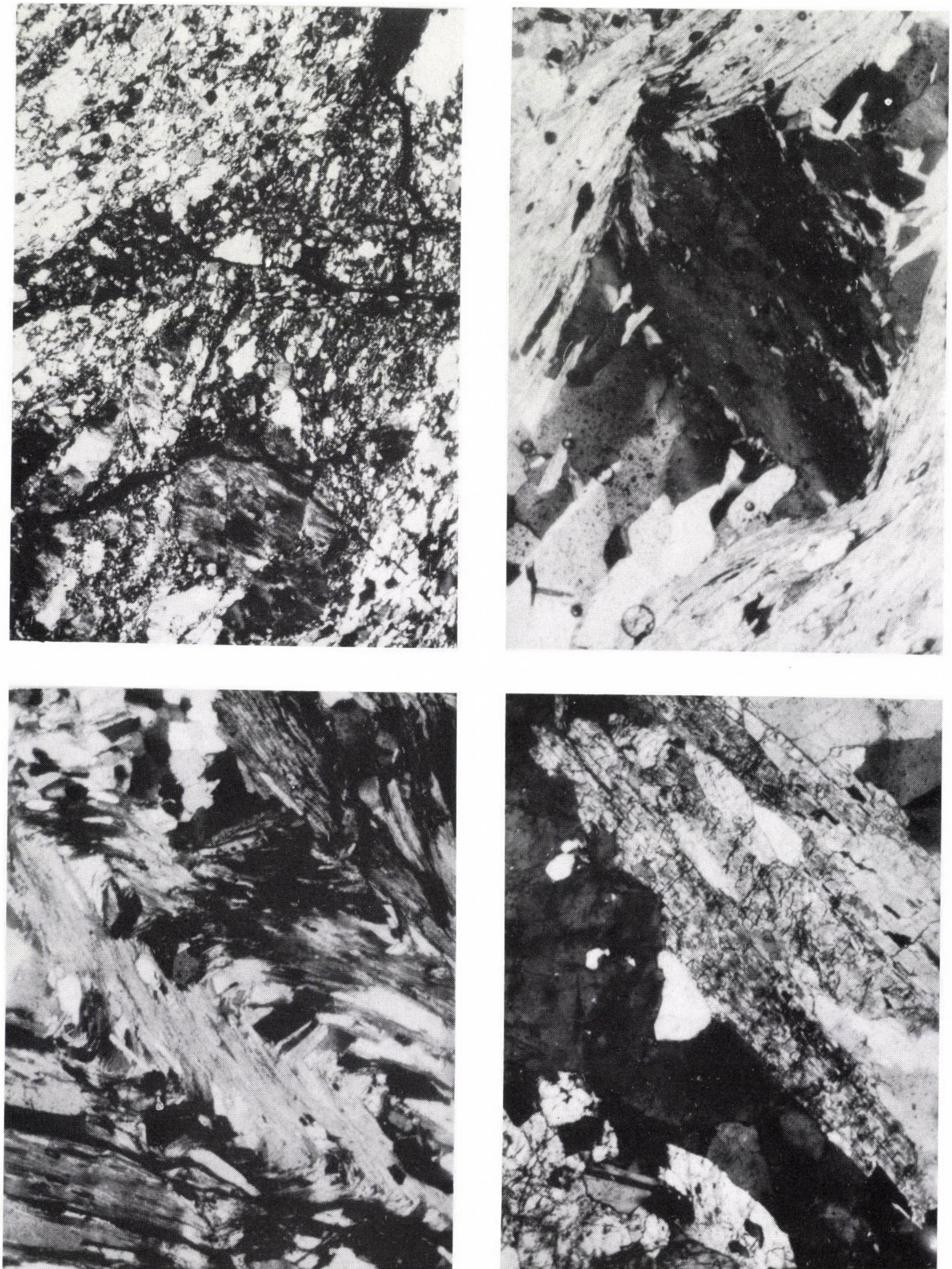

References

Asvadurov, H. 1969: O nouă insulă de cristalin în nord-vestul Transilvaniei. (A new crystalline island in NW Transylvania). – D. S. Inst. Geol. LX/1, pp. 12–17, Bucureşti

Árkai P. 1987: Contribution to the knowledge of the polymetamorphic basement of the Great Plain (Pannonian Basin, East Hungary): the environment of the Derecske Depression. – Fragmenta Min., Petr., 13, pp. 7–20.

Câmpianu, Şt. 1964: Raport geologic pentru minereuri neferoase în cristalinul Munţilor Rez (Ciucea–Valea Drăganului şi Bucea–Făgadău) [Geologic Report concerning the Pb–Zn–Cu ores in crystalline formations of the Rez (Réz) Mts]. – Unpubl. Report, IPGG Bucureşti.

Ciornei, P. 1953: Raport asupra şisturilor cristaline din partea centrala si vestica a Muntilor Rezului (Report concerning the crystalline schists fron the central and western parts of the Réz Mts). – Unpubl. Report, IG Bucureşti.

Cristescu, T., D. Romanescu, A. Soare, A. Stefănescu 1957: Asupra unor rezultate obinute de prospectiunea gravimetica şi magnetometrica în R.P.R., III. Zona Lăpuş–Oaş–Sălaj–Cîmpia de Vest (About some results obtained in gravimetric and magnetometric prospections in Romanian People's Republic, III. Lăpus (Lápos)–Oas (Avas)–Salaj (Szilágyság)–Western Plain (Alföld) Zone). – Unpubl. Report, IGG Bucureşti.

Dicea, I., I. Zah, Gh. Georgescu 1981: Raport geologic asupra forajelor executate în NV Transilvaniei, zona Jibou–Vima–Goştila–Măgoaja [Geologic Report concerning the boreholes executed in NW Transylvania, Jibou (Zsibó)–Vima (Drágavilma)–Gostila–Magoaja (Hollómező) Zone]. – Unpubl. Report, MMPCh Bucuresti.

Dimitrescu, R. 1962: Notă asupra unor roci eruptive din cristalinul Bîcului (Codrului) [Note concerning the igneous rocks from the crystalline formations of the Bâc (Bükk) Mts]. – D. S. Com. Geol. XLVIII., pp. 62–68, Bucureşti.

Dimitrescu, R. 1963: Asupra Şisturilor cristaline din NV Transilvaniei (Outline of the crystalline rocks from NW Transylvania). – SSNG, Comunic. Geol., II., pp. 33–45, Bucuresti.

Ghiurca, V. 1973: Foraje de cercetare în cuprinsul bazinului Salaj (Research drillings in the area of the Sălaj Basin). – IDT–MMPG., Studii de Geologie, pp. 3–25. Bucuresti.

Hofmann, K. 1879: Jelentés az 1878 nyarán Szilágymegye keleti részében tett földtani részletes felvételekről (Report concerning the detailed geological mapping followed in the eastern parts of the Szilágy (Sălaj) district in the summer of the 1878th year). – Földt. Közl., 9, 5–6, pp. 167–213.

Hofmann, K. 1883: Bericht über die im Sommer 1882 im südlichen Theile der Szathmárer Comitate ausgeführten geologischen Spezialaufnahmen. – Földt. Közl., 13, 1–3, pp. 104–113.

Ignat, V., D. Ignat 1972: Raport de sinteză asupra prospecţiunilor pentru minereuri neferoase în cristalinul muntilor Mezes [Synthetic report concerning the prospections for Pb–Zn–Cu ores in crystalline formations of the Meses (Meszes) Mts]. – Unpubl. Report, IPGG Bucureşti.

Ionescu, D. O. 1964: Raport geologic asupra prospectiunilor pentru minereuri neferoase în sectorul Stârci–Valea Ragului (Geologic Report concerning the prospections for Pb–Zn–Cu ores followed in Stârci–Ragului valley area). – Unpubl. Report, IPGG Bucuresti.

Kalmár I. 1972: Strarigrafia terenurilor metamorfice şi sedimentare din insulele cristaline Inău, Preluca şi Ţicău [Stratigraphy of the metamorphic and sedimentary formations from the Inău (Ünő), Preluca (Preluka) and Ţicău (Cikó) crystalline islands]. – Unpubl. Univ. Dr. Thesis, Inst. Petrol, Gaze, Geol., Bucureşti.

Kalmár, I. 1986: Gneisele feldspatice dela Stejera–Ţicău [The feldspar gneisses from Stejera (Sztezsera)–Ţicău (Cikó)]. – D. S. Inst. Geol. Rom. LXX/1. pp. 288–295 Bucuresti.

Kalmár, I., P. Kovács-Pálffy, P. Paulini, I. Angelescu 1989: Nota preliminara privind structura geologica a masivului Codru (Bâc) [Preliminary note about the geological structure of the Codru-Bâc (Bükk) Mts]. – D. S. Inst. Geol. Rom., LXXIII/1. pp. 73–87 Bucuresti.

Kalmár, J. 1993: A Szilágysomlyói Magura földtani szerkezete [Geological structure of the Szilágysomlyói Măgura (Măgura Şimleului)]. – In print, Földt. Közl. 125.

Kräutner, Th. 1938: Recherches géologiques et pétrographiques dans les massifs cristallins du NW de la Transilvanie. – C. R. Inst. Géol. Roum., XXII, pp. 133–138.

Kräutner, Th. 1940: Observations géologiques et pétrographiques dans les massifs de Bâcul, Heghieş et dans l'île cristalline de la Măgura, prés de Simleul Silvaniei. – C. R. Inst. Géol. Roum., XXIII, pp. 37–45. Bucureşti

Mattyasovszky, J. 1879: Jelentés az 1879 évben Szilágymegyében eszközölt földtani felvételről (Report concerning the geological surveying executed in Szilágy (Salaj) district in the 1879th year). – Földt. Közl., 9, pp. 292–300.

Nedelcu, L. 1968: Raport geologic asupra prospectiunilor pentru mineralizaţii neferoase în Munţii Mezeş, perimetrul V. Gumbei–Măgura Priei [Geologic report concerning the prospections for Pb-Zn-Cu ores in Meses (Meszes) Mts, Gumbei valley–Magura Priei area]. – Unpubl. Report, IPGG Bucuresti

Pauca, M. 1964: Bazinul Silvaniei [The Sylvania (Szilágy) Basin]. – Ann. Com. Geol., XXXII, pp. 3–130. Bucuresti

Soroiu, M., I. Balintoni, A. Voda 1985: A model of the basement of the Transylvanian Basin as revealed by K-Ar dating. – R. Roum. Géol., Géophys., Géogr., 29., pp. 29–35 Bucuresti.

Soroiu, M., D. Popescu 1986: Rezultatele deterninărilor de vîrsta radiogena K/Ar pe esantioane de roci cristaline, Munţii Maramuresului, Preluca, Bâc şi Şimleul Silvaniei [Results of K/Ar age determinations on some crystalline rock samples from Maramures (Máramaros) Mts, Preluca (Preluka), Bâc (Bükk) and Şimleul Silvaniei (Szilágysomlyó)]. – Unpubl. Report, IPEG Maramureş, Baia Mare.

Szádeczki, Gy. 1925: Munţii ascunsi ai Transilvaniei de Est (Covered mountains of the Eastern Transylvania). – D. S. Inst. Geol. Rom. XIII, pp. 35–41.

Szádeczki-Kardoss, E. 1925: Contributii la geologia Ardealului de nord-vest (Contributions to the geology of the NW Transylvania). – D. S. Inst. Geol. Rom. XIV, pp. 22–30.

Szederkényi, T. 1984: Az Alföld kristályos aljzata és földtani kapcsolatai (The crystalline basement of the Great Hungarian Plain and its geological connections). – Ac. D. Thesis, JATE Szeged.

Telegdi-Róth, K. 1912: A Réz-hegység északi oldala Paptelek és Kazáncs között és a Szilágysomlyói Magura déli része (The northern slope of the Réz (Rez) Mts between Paptelek (Popeşti) and Kazáncs (Cuzap) and the southern parts of the Szilágysomlyói Magura (Măgura Simleului). – M. Kir. Földt. Int. Évi Jel. 1911-ről. pp. 110–120.

Visarion, M., M. Săndulescu, P. Constantinescu, L. Atanasiu, A. Ivanov 1992: Studiul structural privind posibilităile de acumulare a hidrocarburilor în depozitele sedimentare din substratul bazinului Panonic. Partea I. Sect. Crişu Repede–Someş [Structural study on the possibility of accumulation of the hydrocarbons in the sedimentary deposits from depth of the Pannonian Basin. Ist parts: Crişu Repede (Sebes Kőrös)–Someş (Szamos) Area]. – Unpubl. Report, IG Bucureşti

Zincenco, D. G., M. Soroiu, S. Cuna 1990: Cretaceous thermal front on Pre-Mesozoic continental crust, documented by K-Ar data: on example, the Sylvanic belts, NW Transylvania, Romania. – Rev Roum. Géol., Géophys., Géogr., 34, pp. 95–105, Bucureşti.

Acta Geologica Hungarica, Vol. 37/3–4, pp. 297–309 (1994)

Palynological investigation of Albanian Upper Cretaceous formations

Ágnes Siegl-Farkas

Hungarian Geological Institute, Budapest

Vangjel Kici, Agim Pirdeni, Abedin Xhomo

Instituti i Studimeve dhe Projektimeve te Gjeologjise Tirana

The authors present the results of palynologic investigation of Upper Cretaceous (Cenomanian, Maastrichtian) formations belonging to the Krasta–Cukali tectonic zone of Albania. The foraminifers, assigned to the *G. gansseri–A. mayaroensis* foraminifer taxon-zone, were deposited on the north coast of Tethys, in the area of the Normapolles geobotanic province. At the end of the Maastrichtian, the mixing of Boreal and Mediterranean flora elements can be well traced, followed by their gradual transition into the younger vegetation dominated by Postnormapolles, with their acme in the Palaeogene. The palynologic and palaeoenvironmental evaluation was carried out on the basis of the examination of 23 samples and the determination of 24 sporomorph taxa.

Key words: IGCP-262, -287, Albania, Krasta-Cukali tectonic unit, Upper Cretaceous, N margin of Tethys, palynology, Normapolles province, Postnormapolles, palaeoenvironment

Introduction

The working sessions of projects IGCP-262 (Tethyan Cretaceous Correlation, held in 1991 in Albania) and IGCP-287 (Tethyan Bauxites, held in 1993 in Albania), followed by field trips, renewed Albanian–Hungarian geological co-operational relations. In the framework of this co-operation, the present paper presents the results of palynologic investigations of Upper Cretaceous samples collected from outcrop. The geologic description of the formations and the results of the micropalaeontologic investigations were published by the Albanian colleagues in the form of an excursion guide and an abstract collection, prepared for the working sessions of the above-mentioned projects.

Geological setting

Albania is a small but geologically highly interesting country, due to its complicated geologic structure. Located between the Dinarides in the north and the Hellenides in the south, the Albanides are in a key position.

Cretaceous deposits occur in different tectonic zones and are characterized by various facies (Fig. 1). Palynologic examinations were carried out in Upper Cretaceous sediments in the area of the Krasta–Cukali zone.

Addresses: Á. Siegl-Farkas: H-1442 Budapest, P.O. Box 106, Hungary
V. Kici, A. Pirdeni, A. Xhomo: Instituti i Studimeve dhe Projektimeve te Gjeologjise, Blloku Vasil Shanto, Tirana
Received: 15 April, 1994

0236–5278/94/$ 5.00 © 1994 *Akadémiai Kiadó, Budapest*

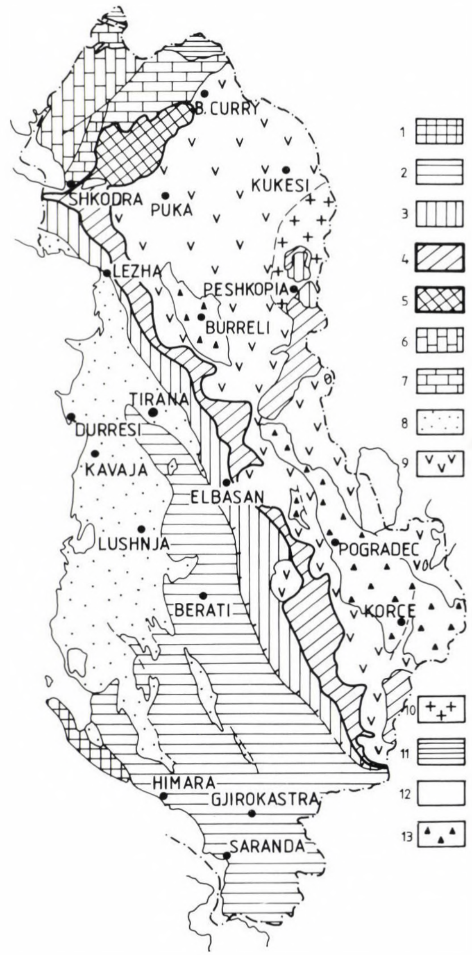

Fig. 1

Tectonic scheme of Albanides. 1. Sazani zone; 2. Ioniane zone; 3. Kruja zone; 4–5. *Krasta–Cukali zone:* 4. Krasta subzone; 5. Cukali subzone; 6–7. *Albanian Alps zone:* 6. Maiesia e Madhe subzone; 7. Valbona subzone; 8. Vermoshi unit; 9. Mirdita zone; 10. Korabi zone; 11. Gashi zone; 12. Preadriatic depression; 13. Albana–Thessalian depression

Two subzones, the Krasta and the Cukali, are distinguished within the Krasta–Cukali zone. Based on its peculiar tectonic development, the Lisne-Spiteni unit can be separated within the Krasta subzone (Fig. 2). This unit represents a permanently elevated ridge which existed during the Jurassic and the Cretaceous. One of the most reduced sequences of the Tethyan area was formed on this ridge.

The Cukali subzone represents the northeastern branch of the Krasta–Cukali zone. Differences in the development of the Lower Cretaceous deposits of the Krasta and Cukali subzones made it possible to distinguish them in terms of their different palaeogeographic setting.

Senonian sections of the Krasta and Cukali subzones are identical. They consist of well-stratified limestones with Globotruncana, but in the Cukali subzone the thickness is reduced. The Upper Maastrichtian is represented by flysch deposits in both sub-units, with a transitional marl-limestone unit at the base.

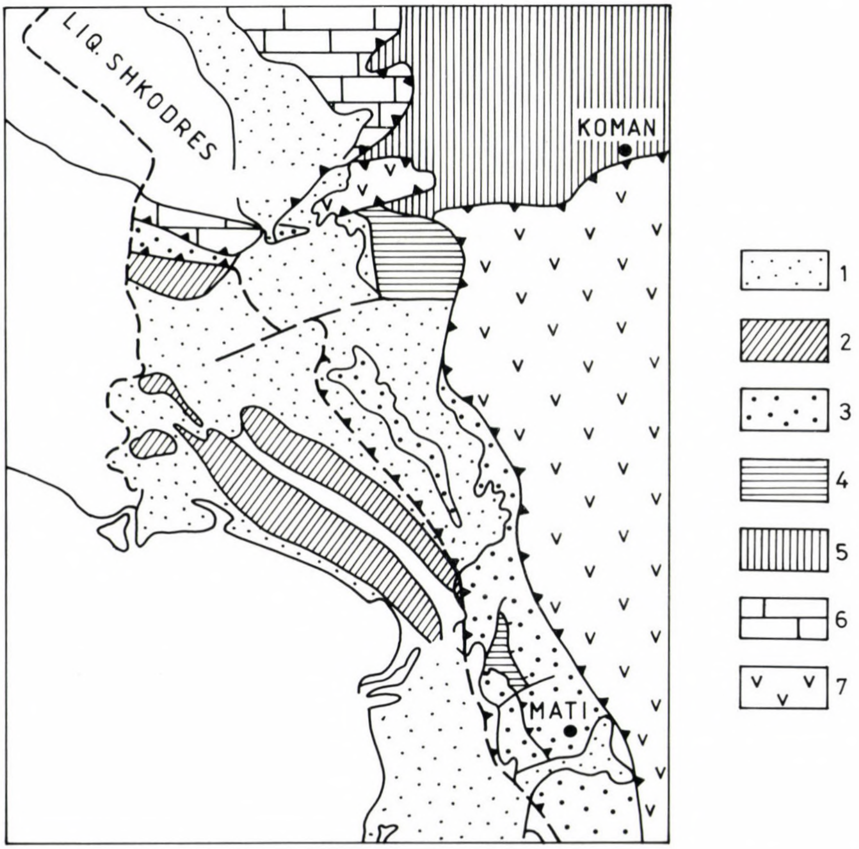

Fig. 2

Scheme showing the setting of Lisne-Spiteni unit. 1. Quarter; 2. Kruja zone; 3. Krasta subzone; 4. Lisne–Spiteni unit; 5. Cukali subzone; 6. Albanian Alps zone; 7. Mirdita zone

Krasta-subzone

Cenomanian-Maastrichtian exposure near the bridge at Mati (Fig. 3).

The outcrop exposes the Cretaceous succession of the Krasta subzone. Six samples were taken from marl and siltstone layers of the Cenomanian flysch and transitional beds of Upper Maastrichtian age.

The Cenomanian flysch sequence

The Cenomanian flysch sequence consists of an alternation of siltstones, reddish biomicritic marls with planktonic microfossils, biomicritic marly limestones, and calcarenitic turbidites. Rarely, debris flow deposits occur as well.

Pithonella ovalis and Calcisphaerulidae are present in the limestones. *Rotalipora appeninica* and *Praeglobotruncana stephani* were found in the topmost part of this sequence in other sections.

Palynological investigations

One sample each from both the lower and upper marl intercalations of the flysch-type formation, assigned to the Albo-Cenomanian on the basis of foraminifer investigations, was subjected to palynologic investigation.

Both samples were rich in organic matter, mostly of colloidal size; however, sporomorphs were encountered only in the lower section of the exposure.

The sporomorphs represented by a few specimens were highly carbonized and badly preserved (Plate I).

Tricolpites sp. (1)
cf. *Teneria* sp. (1)
Triporopollenites div. sp. (3)

On the basis of the determined association, which consisted of angiosperms only (taking into consideration also the lack of so-called "early angiosperms"), it is most likely that the deposition of the formation took place during the Late Cenomanian.

The transitional unit

The transitional unit consists of biomicritic marly limestones, calcarenitic turbidites and sandstone–siltstone–claystone strata (the latter predominates in the topmost part of the section) overlain by flysch of the Krasta subzone. Based on the globotruncanids, the transitional unit is of Middle–Upper Maastichtian age (*G. gansseri* and *A. mayaroensis* zones).

Palynological investigations

In the marl intercalation of the exposure, the palynologic investigation of four samples was carried out, all of which contained a great amount of organic matter. Sporomorphs could be determined only in two samples. These were:

Micrhysridium sp. (1)
cf. *Foveolatisporites* sp. (1)

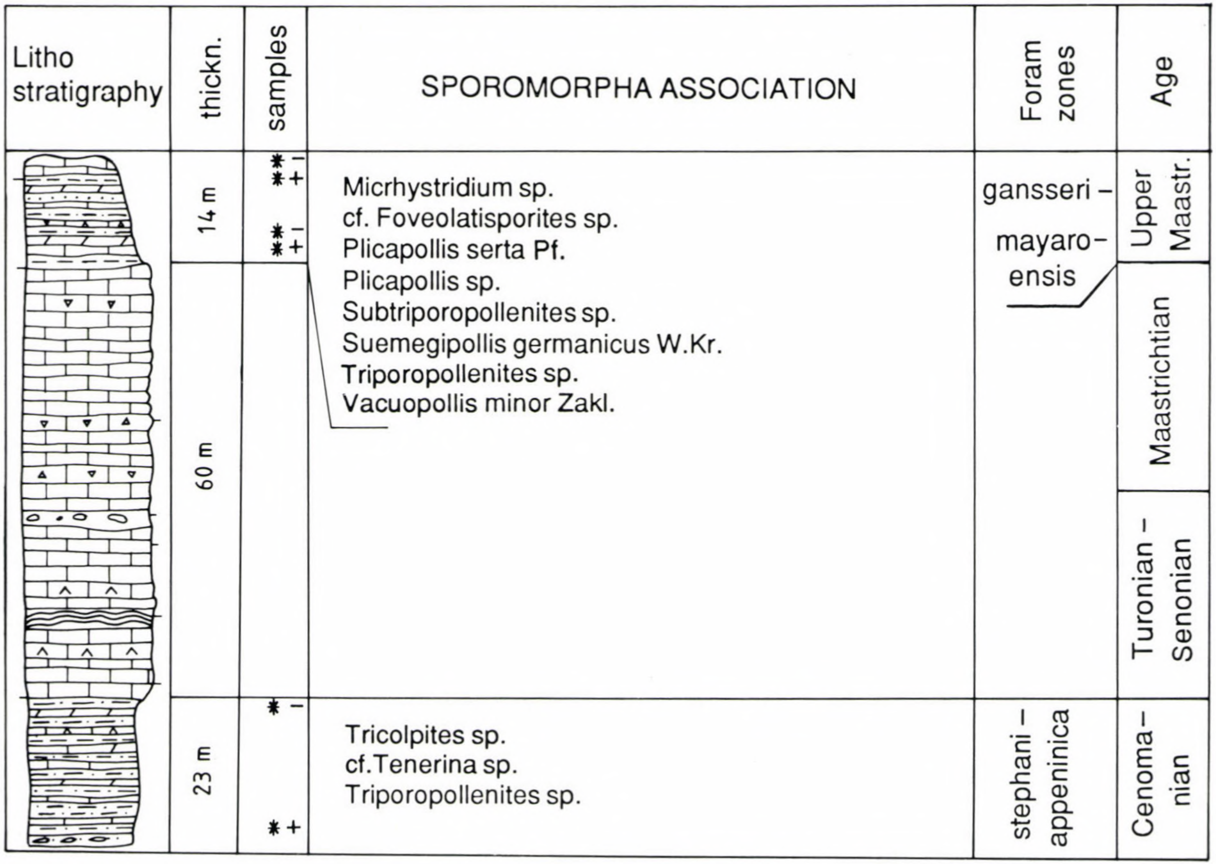

Fig. 3
Palynology of Cenomanian–Maastrichtian outcrop near bridge of Mati

Plicapollis serta Pf. (1)
Plicapollis sp. (minor typ.)(1)
Subtriporopollenites sp. (1)
Suemegipollis cf. *germanicus* W.Kr (1)
Triporopollenites sp. (2)
cf. *Vacuopollis minor* Zakl. (1)

This sporomorph association, containing Postnormapolles elements as well, is characteristic of the vegetation of the Late Maastrichtian. The only phytoplankton (*Micrhystridium* sp.) occurring in the fossil assemblage indicates a pelagic marine sedimentation area.

Cukali-subzone

Upper Maastrichtian exposure, north of Koman (Fig. 4).

North of Koman, in a roadcut, the Upper Maastrichtian transitional unit was studied (Fig. 5).

Based on *G. conica, G. aegyptica, R. contusa, G. gansseri, R. rugosa,* the thin-bedded biomicritic limestones intercalated with shales were assigned to the Middle–Upper Maastrichtian (*G. gansseri –A. mayaroensis* Zones).

Palynological investigations

In the shale intercalations of the outcrop, seven samples were collected, badly preserved and hardly determinable.

Each sample contained a large amount of organic matter. Due to the undiversified nature of the sporomorph associations, we present a merged flora list below:

Intratriporopollenites sp. (1)
Interpollis sp. (3)
Interpollis velum W. Kr. (2)
Interpollis cf. *microsupplingensis* W. Kr. (1)
Interporopollenites sp. (1)
Interporopollenites cf. *proporus* Weyl. et Krieg. (1)
cf. *Minorpollis minimus* W. Kr. (1)
cf. *Nudopollis* sp. (2)
Oculopollis sp. (3)
Plicapollis sp. (6)
Plicapollis serta Pf. (2)
Plicapollis pseudoexcelsus (W. Kr.) W. Kr. (1)
cf. *Semioculopollis* sp.(3)
Subtriporopollenites sp. (5)
Triporopollenites div. sp. (11)
Tricolporopollenites cf. *rotundiformis* W. Kr. (1)
Trudopollis sp. (2)
Vacuopollis minor Zakl. (2)
Pseudopapillopollis praesubhercynicus Góczán

In the fossil assemblage, neither fern spores indicating the proximity of the coast, nor phytoplankton indicative of a marine environment, were found. The association, consisting mostly of Postnormapolles species, appears to prove the Late Maastrichtian age of the formation.

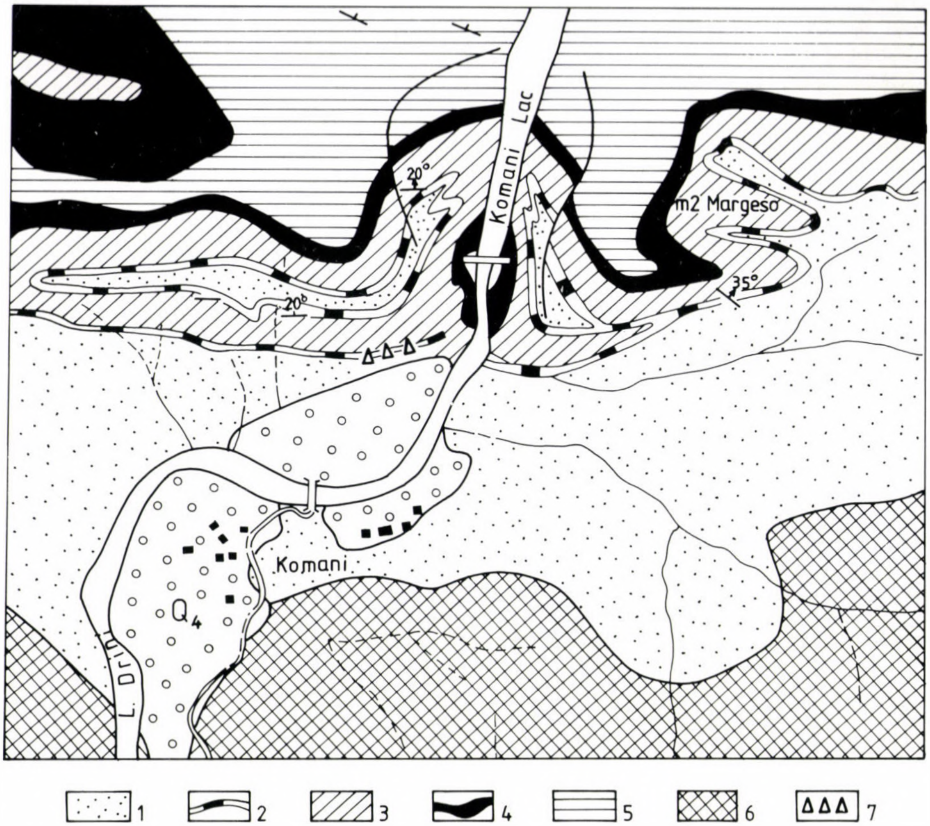

Fig. 4
Schematic map of Koman region and setting of sampling points. 1. Maastrichtian–Eocene flysch of Cukali subzone; 2. Upper Maastrichtian transitory pack; 3. Cretaceous Limestones; 4. Kimmeridgian–Valanginian radiolarites; 5. Lower–Upper Jurassic limestones; 6. Mirditas zone; 7. sampling

In comparing the sporomorph associations of the Krasta and Cukali Subzones' formations, assigned to the *gansseri-mayaroensis* foraminifer zones, the following conclusions can be drawn:

The amount of organic matter accompanying the sporomorph associations, as well as the richer sporomorph association, indicate that the formations of the Cukali subzone were deposited in proximity of the coast;

– The sporomorph association determined here contains more Postnormapolles elements (Interpollis species); this, and the presence of Intratriporopollenites species (deriving from a dendroid angiosperm similar to the here-appearing Tilia), indicates the moderately warm Late Maastrichtian climate;

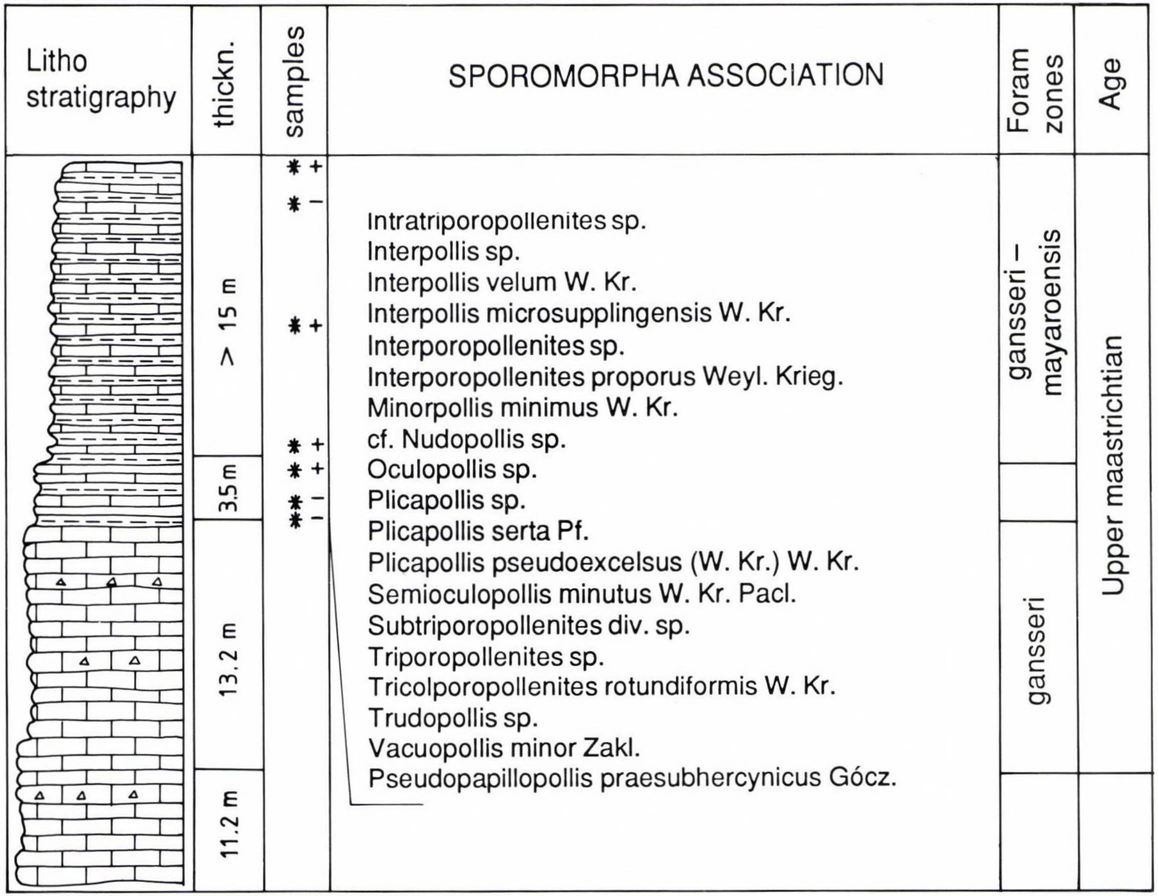

Fig. 5
Palynology of Upper Maastrichtian sediments, North of Koman, Cukali subzone

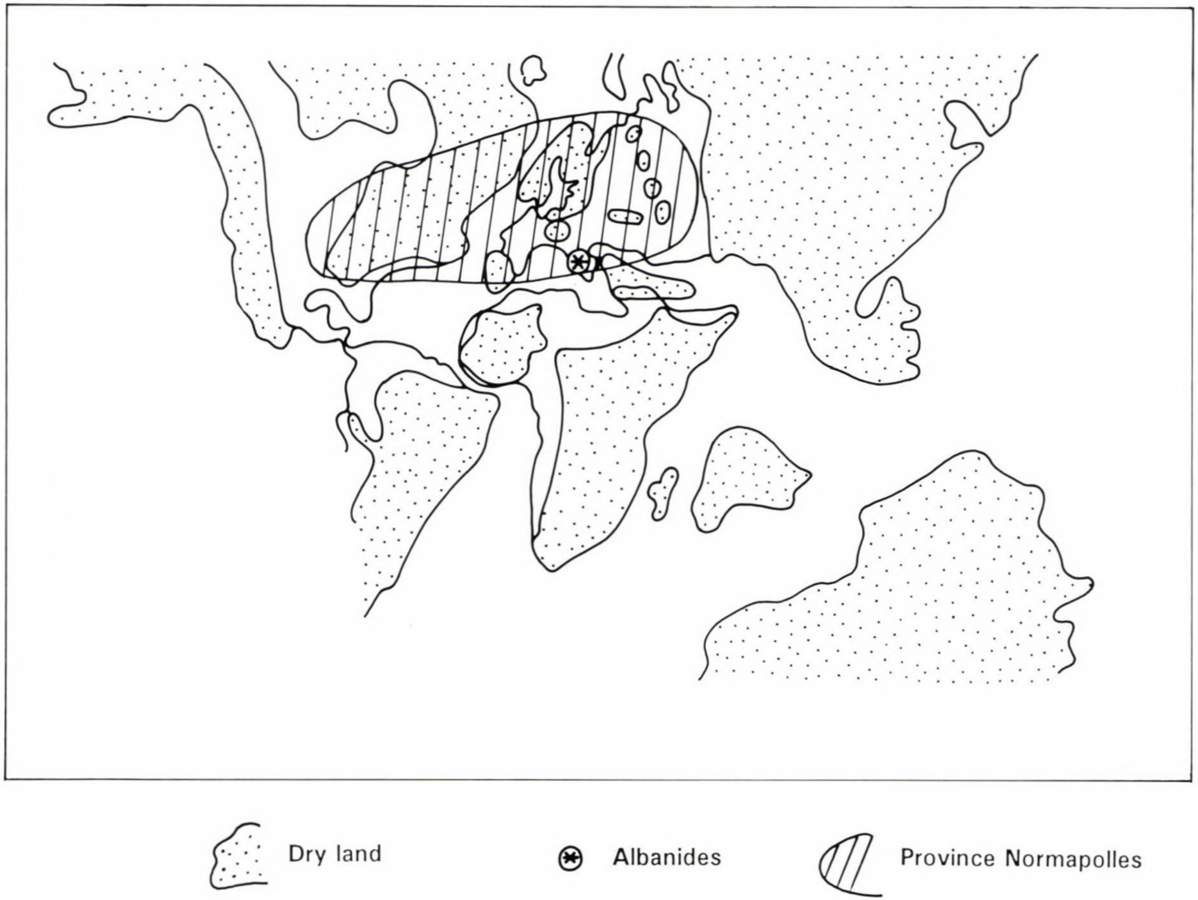

Fig. 6
Senonian palaeogeography of Normapolles province (after Smith and Briden 1977)

– *Pseudopapillopollis praesubhercynicus*, represented in the association of the subzone by a single specimen, has so far been found only in the Upper Campanian–Maastrichtian formations of Mediterranean areas (Slovakia, Slovenia, Romania, Hungary – Snopková (in Koráb and Snopková 1972), Antonescu 1973, Góczán 1964, 1967 (in Góczán et al. 1967), 1973, Siegl-Farkas 1986, 1991, 1993;

– The *Micrhystridium* species determined in the Krasta Subzone association, indicates pelagic marine sedimentation;

– The species *Suemegipollis* cf. *germanicus* determined here is known from Boreal (N Germany, Bohemia) and Mediterranean (France, Hungary, Romania) Senonian areas (Góczán et al. 1967, Antonescu 1973, Siegl-Farkas 1986).

Palaeoenvironmental conclusions

The palynologic data presented here provide the first factual evidence that the territory of Albania belonged to the area of the Normapolles geobotanic province during the Upper Cretaceous (Fig. 6). During the Late Maastrichtian, besides the Normapolles genera, the members of the Postnormapolles genera appeared in great numbers, having their acme in the Palaeogene, indicating the moderation of the tropical climate of Senonian by the end of Cretaceous. The fossil assemblages lacked the gymnospermous pollen grains usually occur only rarely in the area of the Normapolles province.

The fern spore, represented only by a single specimen, appears to prove a pelagic marine sedimentary environment, assumed on the basis of the finding of also a single phytoplankton.

Thus, in the area of the Albanides belonging to the north margin of Tethys, at the end of the Maastrichtian the mixing of certain Boreal and Mediterranean flora elements can be traced, as well as the gradual transition of the Normapolles group into the younger vegetation dominated by Postnormapolles.

Acknowledgements

My thanks go to the leaders of the IGCP projects Dr. Andrea Mindszenty and Dr. Géza Császár, as well as to Dr. Endre Dudich and Dr. Dëfrim Shkupi, for allowing me to take part in the working sessions.

Pate I

1–3. – Plicapollis serta Pf.
4. – cf. Minorpollis minimus W.Kr.
5–6. – Suemegipollis cf. germanicus W.Kr.
7. – cf. Nudopollis sp.
8–9. – Interpollis cf. velum W.Kr.
10. – cf. Vacuopollis minor Zakl.
11–12. – Interpollis cf. velum W.Kr.
13. – Plicapollis sp.
14–15. – cf. Tenerina sp.
16–17. – Trudopollis sp.
18–19. – Pseudopapillopollis praesubhercynicus Góczán
20. – cf. Nudopollis sp.
21–22. – Subtriporopollenites sp.
23. – Trudopollis sp.
24. – Semioculopollis sp.
25. – cf. Interpollis sp.
26. – Subtriporopollenites sp.
27. – Triporopollenites sp.
28. – cf. Semioculopollis sp.
29. – Plicapollis sp.
30–31. – cf. Semioculopollis sp.
32–33. – Intratriporopollenites sp.
34–35. – Triporopollenites sp.
36–37. – Interporopollenites cf. proporus Weyl. et Krieg.
38–39. – Plicapollis cf. serta Pf.
40. – Tricolporopollenites cf. rotundiformis W.Kr.
41–42. – Interpollis cf. microsupplingensis W.Kr.
43–44. – Michrystridium sp.

1, 5–6, 10, 13, 14–15, 21–22, 27, 43–44, from Krasta subzone, others are from Cukali subzone. Magnification: x 1000

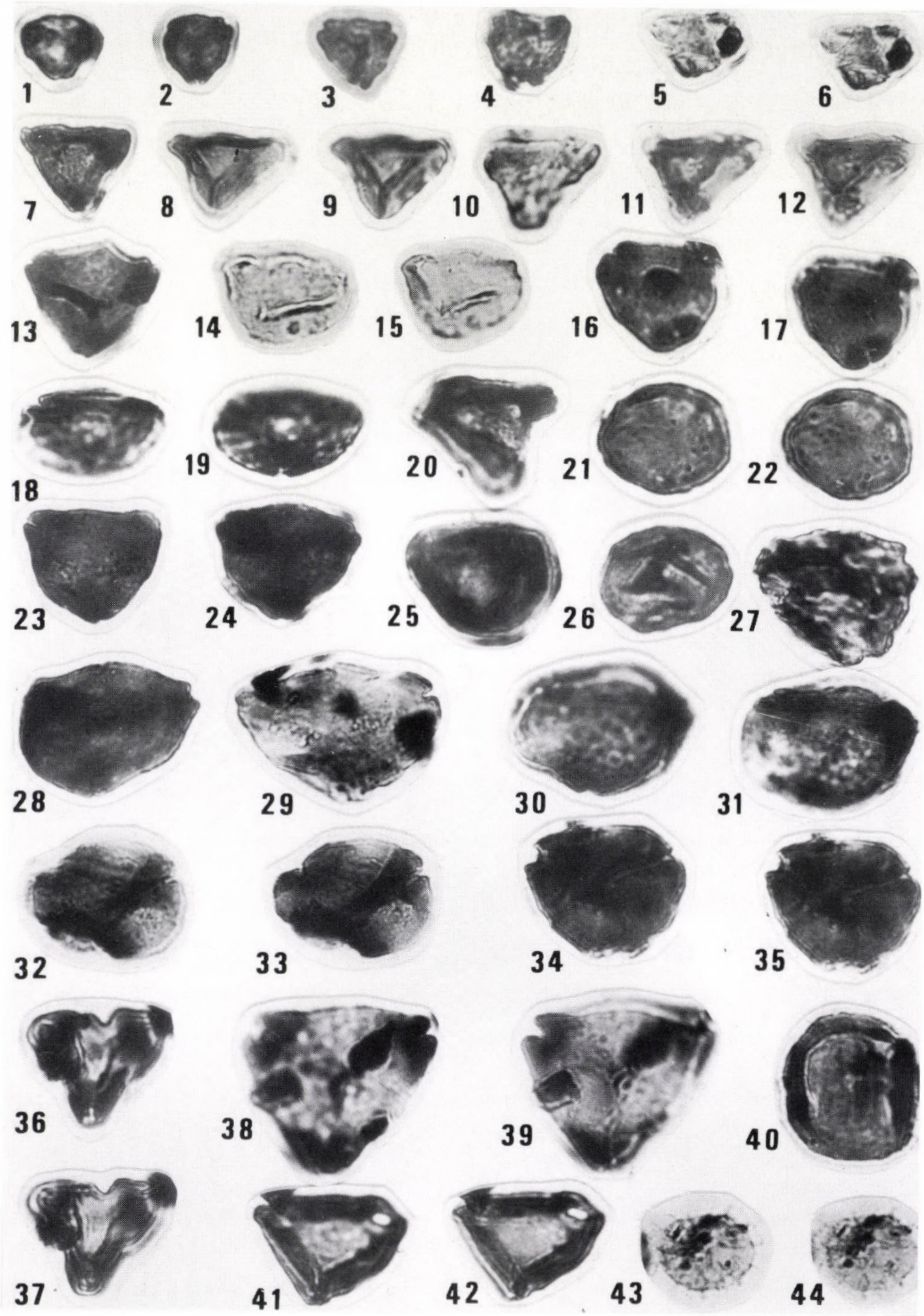
1
2
3
4
5
6
7
8
9
10
11
12
13
14
15
16
17
18
19
20
21
22
23
24
25
26
27
28
29
30
31
32
33
34
35
36
38
39
40
37
41
42
43
44

References

Antonescu, E. 1973: Asociatii palynologice caracteristice Cretacice din Muntii Metaliferi. – Dari de Seama Sedintelor, 59, pp. 115–169.

Góczán, F. 1964: Stratigraphic palynology of the Hungarian Upper Cretaceous. – Acta Geol. Hung., 8, 1–4, pp. 229–264.

Góczán, F. 1973: Ober Kretazische Kohlenbildung in Ungarn im lichte der Palynologie. – Proc. of the III. Int. Palyn. Conf. 1971, Moscow, The Palynology of Cenophytic, Publ. Off., "Nauka", pp. 28–35.

Góczán, F., J.J. Groot, W. Krutzsch, B. Pacltová 1967: Die Gattungen des "Stemma Normapolles Pflug 1953b" (Angiospermae). – Paläontologische Abhandlungen B, 11, 3, pp. 427–633.

Góczán, F., Á. Siegl-Farkas 1990: Palynostratigraphical zonation of Senonian sediments in Hungary. – Review of Paleobot. and Palynol., 66, pp. 361–377.

Kici, V. 1991: Main distinguished characteristics between Cretaceous deposits of Cukali and Krasta are distinguished paleogeographic expression. –IGCP 262. Field symposium on Tethyan cretaceous formations and related mineral resources. Abstracts, Tirana.1991.

Kici, V., L. Peza, S. Guranjaku, A. Xhomo 1993: Overview of the Mesozoic–Tertiary Bauxites of Albania. – IGCP–287. Correlation of Mesozoic–Tertiary bauxites and related paleokarst phenomena in the Tethyan Realm. – Field guide, Final Meeting, Tirana, 1993.

Koráb, T., P. Snopková 1972: Palynologické a Stratigrafické zhodnotenie Lupkovskych Vrstiev a ich Paleogeografická interpretácia. – Geol. prac. Správy, 58, pp. 79–101.

Peza, L., A. Xhomo, P. Sadushi, A. Pirdeni, P. Theodori, F. Arkaxhiu, V. Kici, G. Brahimi 1991: IGCP–262. Field symposium on Tethyan Cretaceous formations and related mineral resources. – Excursion guide, Tirana, 1993.

Siegl-Farkas, Á. 1986: Palynostratigraphy of the Senonian from Borehole Bácsalmás–1 (S. Great Hungarian Plain). – MÁFI Évi Jel. 1984-ről, pp. 429–459.

Siegl-Farkas, Á. 1991: Bauxite deposits and Senonian formations in Hungary. – Cret. Res., 14, pp. 663–668.

Siegl-Farkas, Á. 1993: A contribution to the palynology of Central European areas of the Normapolles province. – Paleofloristic and Paleoclimatic changes during Cretaceous and Tertiary. – Proc. of the Int. Symp. Bratislava pp. 39–42.

Smith, A.G., J.C. Briden 1977: Mesozoic and Cenozoic Paleocontinental Maps. – Cambridge Earth Sci. Ser., 63 p.

Acta Geologica Hungarica, Vol. 37/3–4, pp. 311–325 (1994)

Physiography and Quaternary sedimentation of the coastal zone in the South Sinai, Egypt

Ebtehal Fathy
Hungarian Geological Institute
Budapest

János Haas
Geological Research Group, Eötvös Loránd University
Budapest

Quaternary and Recent sediments of the coastal zone in the southernmost part of the Sinai are characterized by close association of biogenic carbonates, siliciclastic sediments and evaporites. The arid conditions influence the grain size and quantity of terrigenous sediments entering the Gulf of Aqaba through numerous wadis. Due to the limited amount and the relatively coarse grain-size of terrigenous input, the development of reefal carbonates has been continuous. The water circulation pattern of the gulf has also been favourable for reef growth.

The evolution of the Quaternary reef terraces along the western coast of the Gulf of Aqaba was controlled by eustatic sea-level changes, recent faulting and erosional processes.

Key words: Quaternary, modern sedimentation, coral reef, coastal environments, sea level changes, physiography, South Sinai, Egypt

Introduction

Aim of this paper is to describe the physiography and sedimentation of the coastal zone of the southeastern part of Sinai Peninsula. The recently performed work is based exclusively on field observations and takes into consideration data of previous works from literature. The results of laboratory studies (microfacies analysis, X-ray, SEM, geochemical studies, etc.) are to be published in another paper.

The study area comprises the southernmost part of the Sinai Peninsula, on the western coast of the Gulf of Aqaba (Fig. 1). It extends from the mouth of Wadi Kid in the northeast to the tip of Ras Muhammed in the south (Fig. 2). Most of the coastal area is made up of Quaternary formations. Alluvial sediments of the major wadis coming from the interior of the igneous and metamorphic hinterland cover large parts of the coastal area. The Miocene sedimentary rocks are confined to the southeastern part of the area.

Recent carbonate sediments have been studied for more than a century in the region. Walther (1888) was the first to describe the reefs of the Sinai Peninsula. Friedman (1965, 1968) pointed out a systematic series of zones characterized by different sediments and organisms along a traverse from the shore into the gulf south of Elat. He also studied beach rocks and fossil reefs along the shore. In the last two decades investigations have been carried out

Addresses: E. Fathy: H-1143 Budapest, Stefánia út 14, Hungary,
J. Haas: H-1088 Budapest, Múzeum krt. 4/a, Hungary
Received: 14 September, 1993

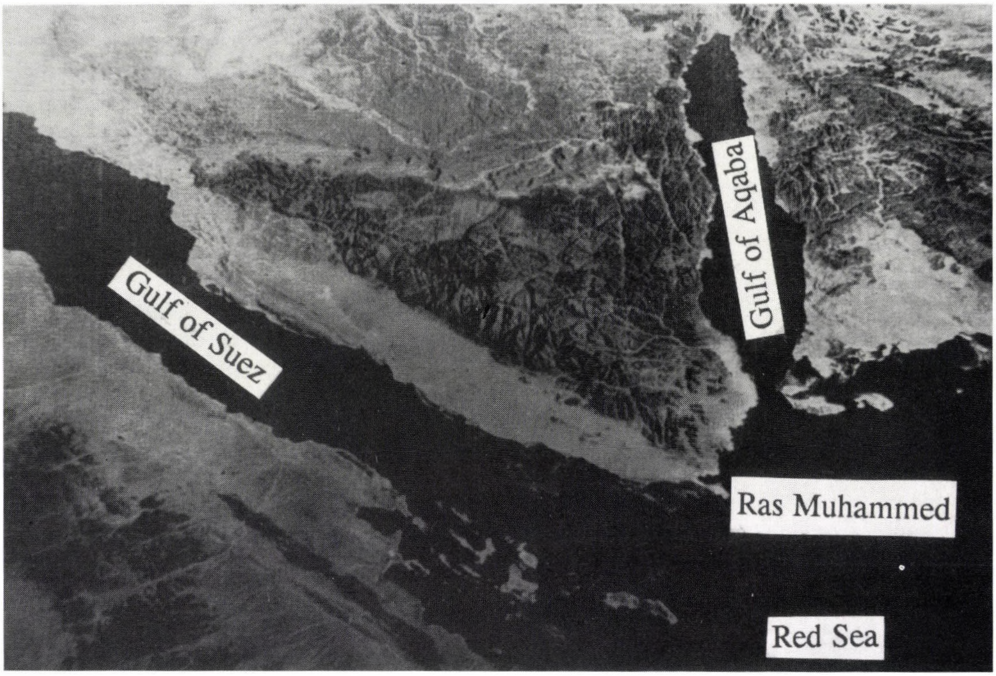

Fig. 1
Sinai Peninsula between the Gulf of Suez and Gulf of Aqaba (Landsat image)

on diagenesis of Pleistocene reef terraces (Gvirtzman et al. 1973; Gvirtzman and Friedman 1977) and on the geology and sedimentology of the Gulf of Aqaba region (Gvirtzman et al. 1977; Friedman 1985). Little attention has been given so far to factors governing geomorphological characteristics of the coastal zone.

Quaternary and Recent sedimentary environments of the Gulf of Aqaba coast comprise an association of pure carbonates generally accumulated in the form of reefs and their related carbonate detritus, and pure siliciclastics deposited mainly in the form of alluvial fans covering the coasts in front of the main wadis. Occasionally, evaporite sedimentation also occurs in the sabkha environments.

Onshore there is a series of faults which raised the fossil reef terraces, controlling their present-day setting. These reefs began to develop in the region at least 350 000 years ago.

Geologic Setting and Structure Evolution

The southern Sinai was a part of the continuous and stable Arabo-African platform. Rifting of the Red Sea system (continental break-up) began in the Late Oligocene, reactivating late Precambrian zones of structural weakness

(Makris and Rihm 1991). At the northern end of the Red Sea the rift system bifurcates, the western branch having been occupied by the Gulf of Suez, and the eastern one by the Gulf of Aqaba (Fig. 1). The Gulf of Suez was formed during the Early Miocene by extension and subsidence. In the Middle Miocene, the extension of the Gulf of Suez slowed down. At its junction with the Gulf of Aqaba, the Red Sea spreading center is thought to come to an end; the plate motions continued in a left-lateral transform zone, along which the Dead Sea and the Gulf of Aqaba began to form as pull-apart basins (Freund et al. 1970; Makris and Rihm 1991). Since the Pliocene, however, E-W extensional tectonics have been active in the Gulf of Aqaba (Lyberis 1988).

The developing rift basin was filled up mainly by: a) an older series of deformed and tilted synrift sediments, Miocene–Early Pliocene (?) in age; and b) a younger series of subhorizontal, only weakly disturbed postrift sediments, Quaternary in age.

Outcrops expose marine sandy limestones and coral reef limestones, designated as "raised reefs", as well as a variety of continental, mainly alluvial, beds.

Physiography and Sedimentation

The coastal plain

The coastal plain extends southwestward from the mouth of Wadi Kid to the Ras Muhammed. The coast is a relatively narrow strip. Slightly but irregularly, it widens northward, reaching a maximum width of 7 km in some places. The seaward edge of the coastal plain is traversed by several narrow embayments (locally called sharms) which always form outlets of ephemeral wadis. The most important of them are Marsa Breika, Sharm El Sheikh, Marsa El At and Marsa Um Merikha.

The southern part of the coastal plain disappears. Here the mountainous hinterland, consisting mainly of alkaline plutonic and marine Miocene rocks, is located in the vicinity of the shore. The Miocene rocks are frequently capped by uplifted Pleistocene reefs.

In the area north of Marsa Abu Minesel, crystalline basement rocks retreat 5–10 km from the shoreline; consequently, the coastal zone becomes wider.

On the other hand, at the northern boundary of the study area a broad, flat coastal zone has been developed, showing lateral facies changes within a few tens of metres. The area located at the mouth of Wadi Kid serves as a typical example of the coexistence of reefs, alluvial fans and coastal supratidal sabkhas (e.g. at Shurat El Mongtah and El Ghargana). It exhibits an intimate association of pure carbonate sedimentation, in the form of flourishing reef growth and related carbonate detritus accumulation, and deposition of terrigenous clastics, mainly in the form of alluvial fans. There is also local evaporite sedimentation in the form of sabkha deposits. The coastal sabkha of Wadi Kid is composed essentially of fine, loose siliciclastic sediments, including thin intercalations of

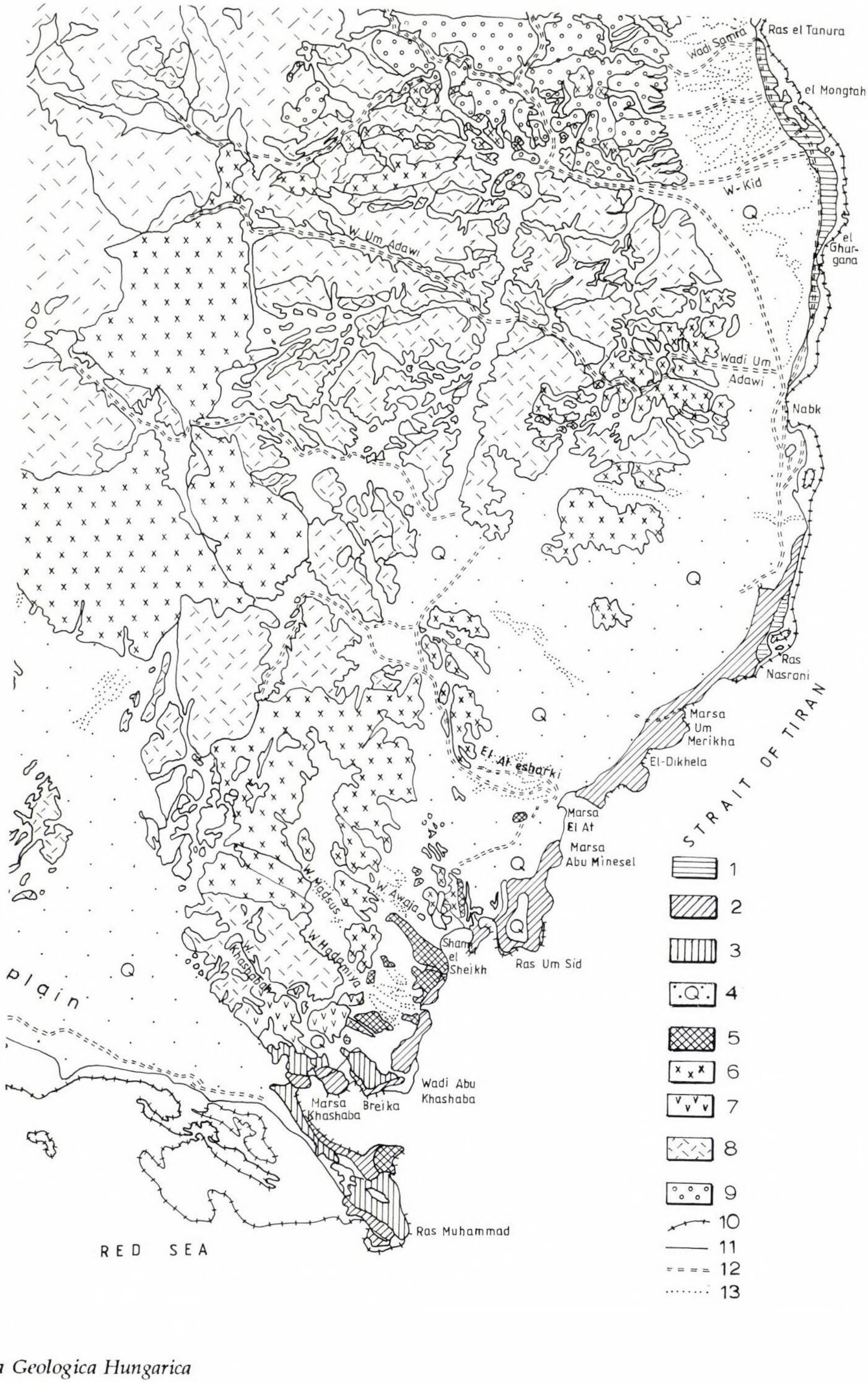
Ras el Tanura
Wadi Samra
el Mongtah
W-Kid
Q
el Ghur-gana
W. Um Adawi
Wadi Um Adawi
Nabk
Q
Q
Ras Nasrani
STRAIT OF TIRAN
Marsa Um Merikha
El-Dikhela
El-At esharki
Q
Marsa El At
Marsa Abu Minesel
Q
W. Nadsus
W. Awaja
W. Hadamiya
W. Khashaba
Sharm el Sheikh
Ras Um Sid
plain
Q
Wadi Abu Khashaba
Marsa Khashaba
Breika
Ras Muhammad
RED SEA
1
2
3
Q
4
5
6
7
8
9
10
11
12
13

gypsum crystals. Pits dug into the sabkha exposed well-bedded, fine sand, containing abundant scattered, millimetre-size gypsum crystals, which were formed in the substratum of a very shallow marine facies showing evidence of frequent emersions.

Minor dunes exist in the distal portion of Wadi Kid. These dunes are fixed and stabilized by abundant and well-adapted coastal vegetation, which probably prevents their large-scale landward migration. The strike of these dunes is approximately East–West and the highest ones do not exceed 1 m.

The morphology of the coastal zone continues under the sea, forming the modern reef flat just below the present-day sea level. It is capped by loose skeletal and terrigenous sediments with extensive growth of seagrass, especially on the leeward side. Coral growth becomes more intense toward the reef margin, to form the reef crest and reef slope. Occasionally channels or narrow lagoons can be found between the reef flat and the beach. In these cases, lagoons act as a trap, cutting off potential supplies from the coast to the reef flat and vice versa.

In the study area the beaches are narrow and poorly developed. Three types of beaches can be distinguished:

1. Where the coastal plain approaches the shoreline, the width of the beach is limited (from less than one meter to about 50 m). These beaches are generally sandy. They are bordered by raised Pleistocene terraces of reefal limestone (Fig. 3a). The skeletal carbonate sediments, derived partly from the erosion of the fossil reefal sediments, form a very thin veneer. Dunes are absent.

2. At one locality (Marsa Um Merikha), the beach sediments consist of coarse pebbles covering a small patch on the beach (Fig. 3b). Most probably they are not related to the present-day hydraulic regime. The pebbles may have been reworked from the mouth of Wadi Um Merikha.

3. The beaches of the low-lying coastal plains are relatively wide and usually surrounded by clastic continental sediments, including flood plain deposits with well-developed dunes less than 2 m high (Fig. 4a, b) and salt-encrusted fine sand and silt in the transitional belt to the recent sabkha sediments. They are represented in the north by Shurat El Ghargana and El Mongtah. At Marsa El At, the character of the sedimentation is very similar, showing an association of pure carbonates, siliciclastics, and evaporites.

Sub-environments of particular importance are characteristical below:

A) Wadis

Wadi Kid is one of the largest wadis in the Sinai. It is located in the northernmost tip of the studied region. Its catchment area lies within the adjacent uplifted basement rocks to the west of the coast. In its lower course

← Fig. 2
Geological map of the coastal area of the southern part of the Sinai Peninsula (after Y. Bentor and M. Eyal 1987). 1. reef flat (Q_3), partially covered with alluvial deposits; 2. reef terrace (Q_2); 3. reef terrace (Q_1); 4. terrestrial alluvium (Q); 5. Miocene; 6. alkaline plutonics; 7. volcanic rocks; 8. calcalkaline plutonics; 9. metamorphic rocks; 10. living reefs; 11. geological boundary; 12. drainage line; 13. alluvial fan or wadi deposits

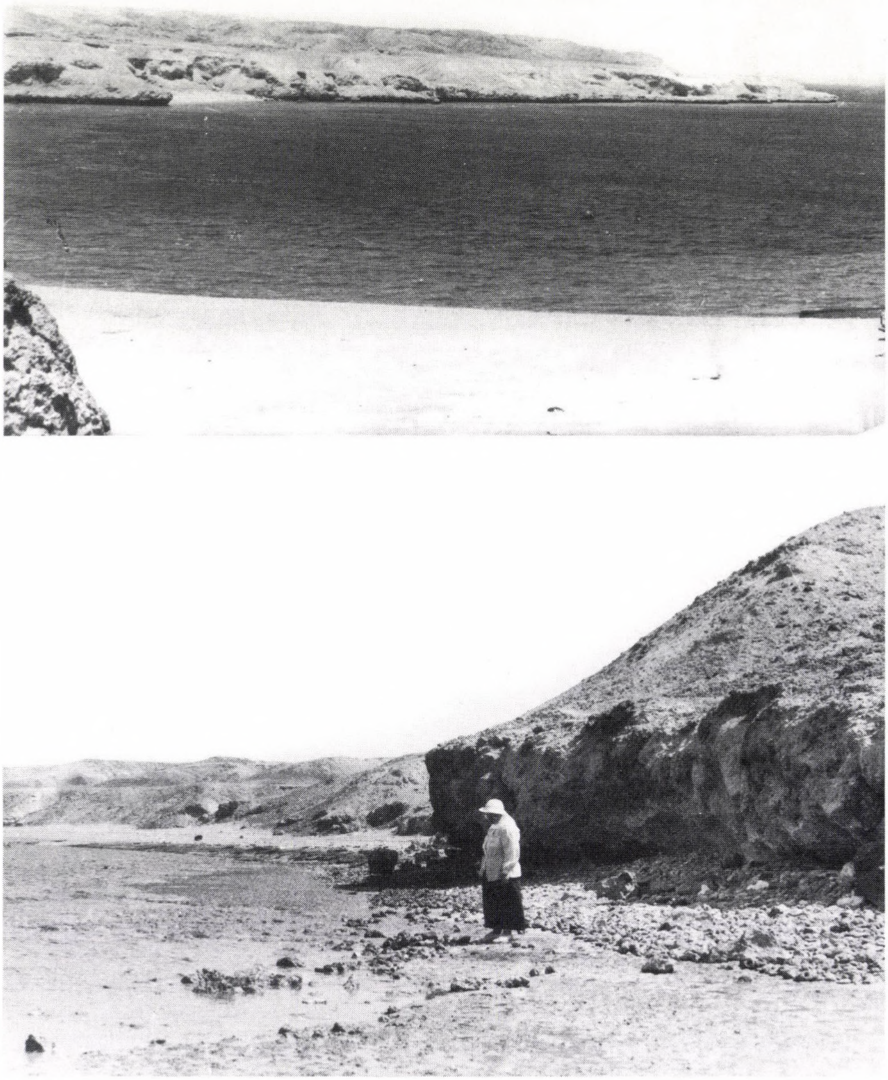

Fig. 3a, b
Photographs showing typical features of the shore zone. a) Thin veneer of sand covering the reef flat in the foreground and reef terraces in the background, b) Sandy, narrow beach backed by raised reef terraces. The sediments derived partly from the erosion of terraces and gravels sparsely spread over the beach

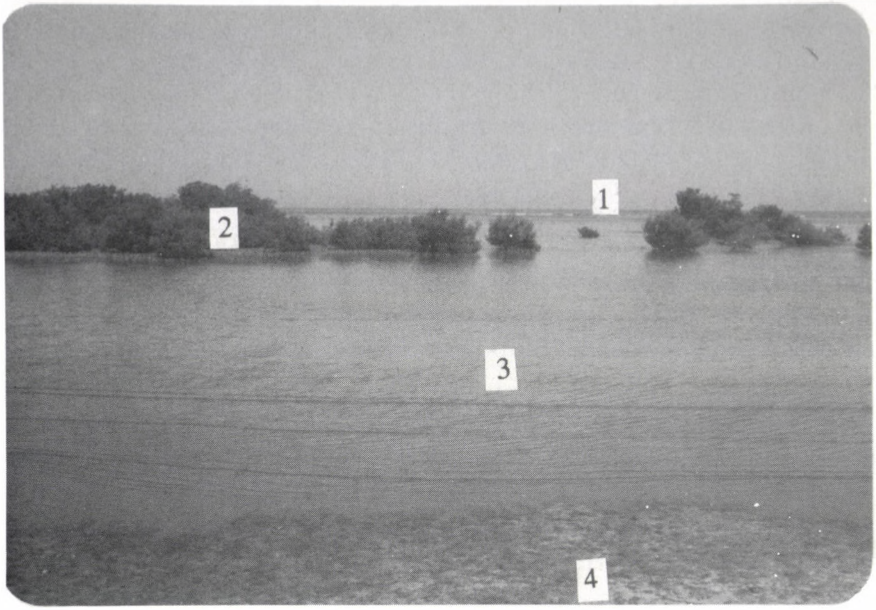

Fig. 4a, b
Sedimentary environments in the coastal zone of Shurat el Ghargana area, showing: 1. Open sea, 2. Mangrove forests around a closed lagoon on the reef flat, 3. Reef flat in the intertidal zone, 4. Sabkha along the shore line, 5. Flood plain deposits with well-developed dunes, less than 2 m high

it has a flood plain about one kilometer wide. South of it are located the drainage basins of Wadis Um Adawi and El At Esharki, and further to the south Wadis Awaja and Madsus.

The southernmost part of the crystalline massif is drained by narrow the artery of the Wadi Khashaba. The origins of the alluvial fans are closely related to the Plio-Pleistocene peripheral uplift of the hinterland areas (Sellwood and Netherwood 1984).

The entire hinterland area is characterized by the predominance of Miocene and Pleistocene faulting, in addition to left-lateral horizontal movements following the Aqaba system. The form and trend of the drainage basins are largely controlled by these faults. Many wadis consist of straight sections extending at an angle of 60–70 to each other. The typical examples are Wadis Madsus and El At Esharki.

B) Pleistocene marine terraces

From Marsa Khashaba to Ras Nasrani, the coastal plain is covered by two Quaternary marine terraces. The maximum height of the older terrace is 30 m, whereas that of the younger one is 15 m above the recent sea level (Figs 5, 6). The total width of the terraces does not exceed 2 km. These terraces generally consist of reefal coral limestones with carbonate cement. In some cases the younger terrace has been eroded, exposing the superbly preserved original shape of the older coral platforms. By contrast, if the upper terrace has been preserved, the corals in it have commonly been destroyed, as well as dissolved by recent surface leaching and erosion. Apart from corals, other skeletal debris, e.g. molluscs, echinoderms, forams and red algae are common in many parts of the reefal terraces. Coralline algae also play the most important role as frame-building organisms in the studied sequences.

The surface of the uppermost reefal unit has been covered by sediments of sabkhas, alluvial plains and braided streams, a characteristic continental facies under arid climatic conditions. The older (Q_1) emergent terraces, which are located very close to the hinterland area, can be found as isolated erosional remnants, or they form small patches in the area north of Marsa Khashaba, along the border of the El Qa'a plain and along the northern shore of Marsa Breika, where the tipped Miocene sandstones and conglomerates form the basis of these reefal sediments.

The physiography of the area is determined mainly by the younger (Q_2) terrace. It forms coastal cliffs at an altitude of 15 m above sea level, extending along a distance of 35 km. They transit laterally into alluvial sediments towards the land, and sometimes into beach rocks or beach sediments seaward. These terraces are cut by many wadis, e.g. Wadi Madsus, Awaja and El At Esharki.

Locally notches, formed predominantly by bioerosion, are cut into the uplifted reef sequences at 1–2 m above the present sea level. Equivalent sediments on the Farasan Islands have been dated between 4 200 and 6 500 yrs B.P. (Dullo 1990) and correspond to the Flandrian transgression.

C) The reef flat

In the coastal zone between Wadi Kid and Ras Nasrani, a broad, pitted reef flat (Q3) is exposed in the lower intertidal zone (Figs 5, 7). The landward part of the flat is covered with alluvial deposits, whereas its seaward edge is populated by the living corals. Large cavities were formed in the substratum. Some cavities are surrounded by a dense forest of mangroves (Fig. 8). Mangroves were developed along a stretch of coast extending 20 km in length. They all correspond to the alluvial fan of Wadi Kid, located to the north of the small Oasis of Nabk. From south to north they are (1) Shurat El Ghargana, (2) Marsa Abu Labad, (3) Shurat Arwashi and (4) Shurat El Mongtah.

Between Shurat El Ghargana and Shurat El Mongtah a discontinuous line of fossil reefs is exposed in the intertidal zone, and is overlain by beach rock (Figs 5, 9). This setting suggests that these reefs were formed prior to the last glaciation in the latest Pleistocene.

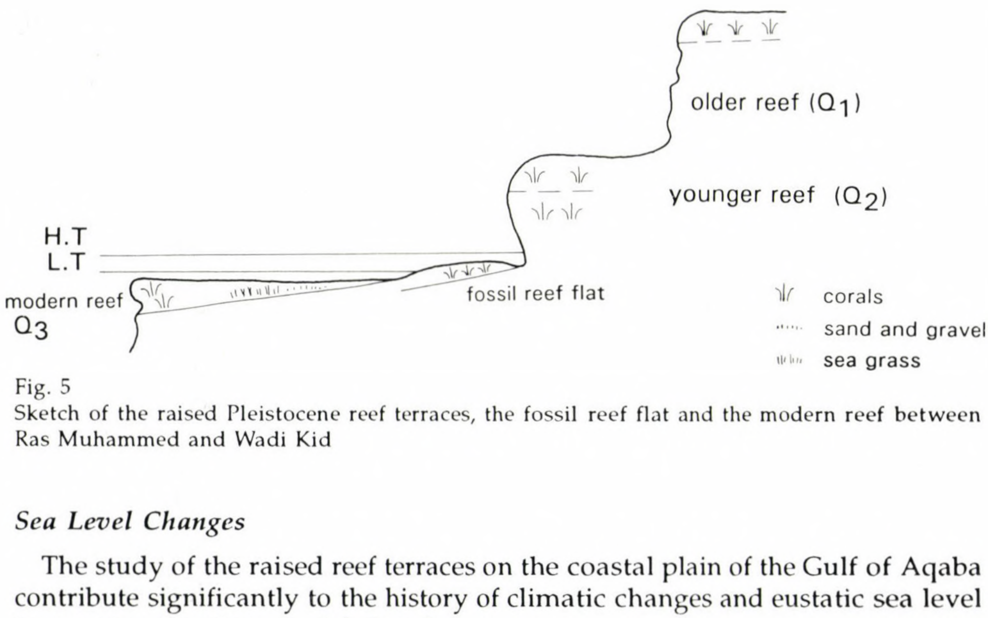

Fig. 5
Sketch of the raised Pleistocene reef terraces, the fossil reef flat and the modern reef between Ras Muhammed and Wadi Kid

Sea Level Changes

The study of the raised reef terraces on the coastal plain of the Gulf of Aqaba contribute significantly to the history of climatic changes and eustatic sea level in a regional and even global scale.

230Th/234U dating of the emerged coral limestone terraces of the southern Sinai were recently reported by Strasser et al. (1992). Measurements on some well-preserved corals, and mostly on thick shells of the bivalve Tridacna, indicate three groups of ages:

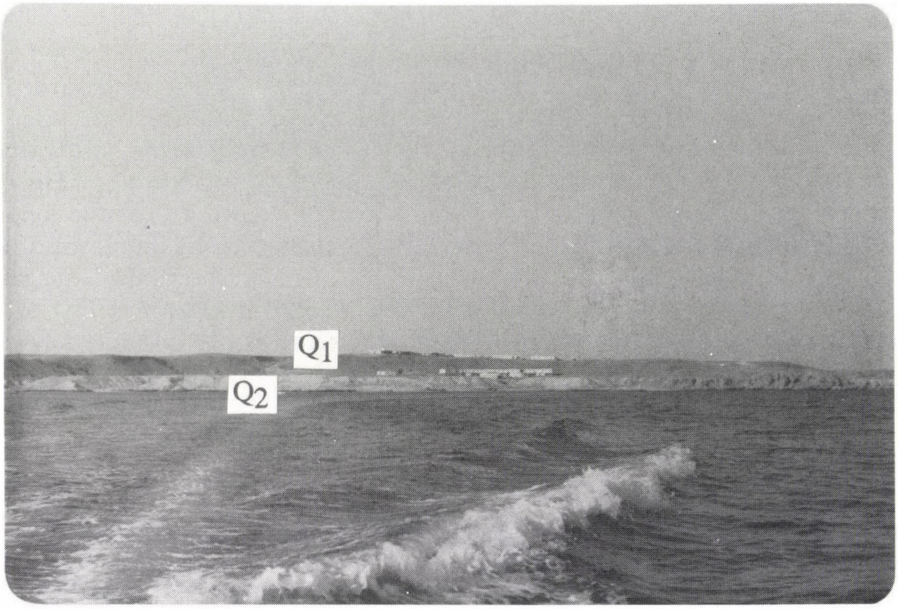

Fig. 6
The two reef terraces in Marsa el Atrea. The older terrace is marked by Q_1, the younger one by Q_2

Fig. 7
Modern reef flat in the intertidal zone at low tide; Wadi Kid area

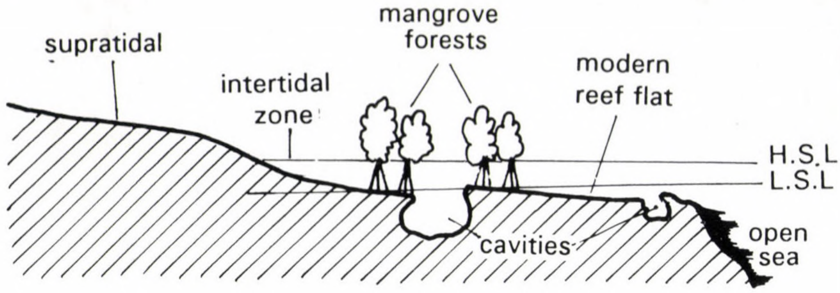

Fig. 8
Sketch illustrating sedimentary environments in the coastal zone of Shurat el Ghargana area

a) the best-developed terraces, at about 10 to 15 m above the shore, yielded ages from 140 000 to 60 000 yrs B.P., indicating the last interglacial period.

These carbonate formations may be contemporaneous with the lower reef unit in two Red Sea islands (Zabarged and Northern Brother), dated at 138 000 to 125 000 yrs B.P. by Hoang and Taviani (1991). Similar ages have been published from the Saudi Arabian coast of the Gulf of Aqaba (Dullo 1990). In contrast, Friedman (1972) dated the same cycle between 108 000 and 140 000 yrs B.P. and Gvirtzman and Friedman (1977) at about 110 000 yrs B.P.

b) In the southern Sinai, only one outcrop yielded an age of 190 000–250 000 yrs B.P. This cycle may correlate with the middle terrace recognized in Jordan (Al-Rifaiy and Cherif 1988), on the Saudi Arabian side of the Gulf of Aqaba (Dullo 1990), on Zabarged Island (Hoang and Taviani 1991); it has also been identified in the Sinai (200 000–250 000 yrs B.P., in Gvirtzman and Friedman, 1977).

The very restricted present-day extension of this reef cycle can be attributed to local tectonic activity of the coastal belt and/or to intense erosion.

c) Terraces at an altitude of more than 25 m yielded ages of 270 000–350 000 yrs B.P., probably corresponding to an earlier interglaciation. This unit has been

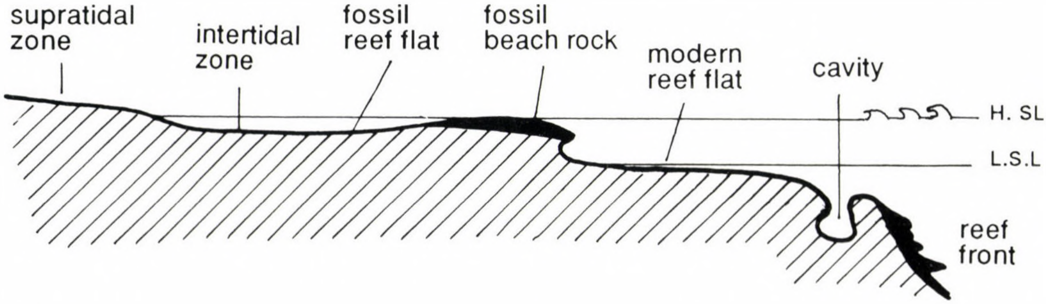

Fig. 9
A generalized cross-section showing setting of the fossil reef flat, fossil beachrock and modern reef flat at Shurat el Mongtah; Wadi Kid area

found at higher altitudes (up to 120 m) in the southern part of the peninsula, and indicates lowering northward (30–50 m). The same cycle has been recorded from the southern Sinai with an age older than 250 000 yrs B.P. (Gvirtzman and Friedman 1977), and in the Red Sea Islands from 290 000 to 300 000 yrs B.P. (Hoang and Taviani 1991).

The temperature curves based on oxygen isotope measurements and calculations of the orbital parameters of the Milankovitch cycles indicate the warmest period (and highest sea level) at about 330 000 yrs B.P. (Hays et al. 1976).

The ages of studied coral reef terraces show an apparent correlation with the ages close to, or slightly younger than, the global sea level highstands of the last three interglacial periods which, according to the model by Milankovitch (1941) were orbitally controlled. In addition, the climatic models (Prell 1984) revealed that in the interglacial periods of the past 150 000 yrs B.P., increased insolation resulted in summer monsoonal winds of SW direction and great precipitation, i.e. rainy periods over South Asia and North Africa.

The hydrographic conditions in the Red Sea were also strongly controlled by regional fluctuations of the climatic conditions, related to changes in monsoon intensity and the restricted water exchange with the Gulf of Aden (Indian Ocean). During the last glacial maximum (18 000 yrs B.P.), high water salinity prevailed, due to high aridity and a glacial-eustatic drop in sea level of as much as 130 m. This sea-level drop resulted in a change in circulation pattern which induced changes in the foraminiferal fauna and mineralogical composition of the sediments (Locke and Thunell 1988).

This significant sea-level drop also led to the extinction of the coral population, and to the formation of deep canyons cut into the pre-existing reefs (Gvirtzman et al. 1977).

The increased runoff and more humid climate at the beginning of the Holocene resulted in a further decrease in surface salinity of the Red Sea. The connection between the Red Sea and Gulf of Aden was reestablished. New fringing reefs were formed, and the canyons were flooded to form embayments or sharms (Gvirtzman et al. 1977).

Climatic and hydrographic conditions and their relation to Quaternary sedimentation

The present-day climate of the study area is hot and dry, and rainfall is scarce. The average annual rainfall ranges between 5–25 mm, with an air temperature which reaches 40 °C in summer and 22 °C in winter (Friedman 1968).

The arid nature of the Sinai climate tends to influence the grain size of terrigenous sediments entering the sea from the many wadis. Due to low humidity, the chemical weathering of the hinterland area is limited; therefore, the terrigenous sediments tend to be coarse. The homogeneous sediment input does not prevent reef growth, since due to the coarse grain-size, deposition is rapid and the re-establishment of a clear marine water condition is rapid.

Climatic and depositional conditions similar to the present-day ones may have prevailed in the gulf during the development of the fossil reefs. Crystalline rock fragments, interlayering within the fossil reefal carbonates, strongly support this idea.

Wind and wave energy also play an important role in the coexistence of carbonate and siliciclastic sediments. The predominant northern and north-eastern winds generate waves which approach the shoreline of the gulf diagonally, thus creating southward longshore currents (Friedman 1968). These currents redistribute terrigenous material from the submarine slopes into the deep basins. The alluvial fans protect the supratidal environments, including sabkhas, by blocking waves and currents (Friedman 1985). The reefs and, locally the mangroves, also play an important role in the protection of the sabkhas.

A warmer and less saline surface current flows into the gulf from the Red Sea, keeping the surface-water temperature in the gulf 5 °C above its equilibrium value. Water circulation in the Red Sea and the Gulf of Aqaba is changed seasonally by the oceanic currents in the Indian Ocean (Fig. 10). In winter, during the northeast Monsoon, surface water flows northward into the Red Sea, while saline Red Sea deep water flows into the Gulf of Aden. In summer, a reverse motion takes place (Locke and Thunell 1988). These conditions are necessary for a flourishing reef growth.

Conclusions

During the Quaternary, in the coastal belt of the southernmost part of the Sinai Peninsula a) biogenic carbonates, i.e. reefs and related carbonate detritus, b) siliciclastics of alluvial fan origin and c) sabkha evaporites were deposited, in a geographically close relationship.

This facies association reflects the sea level history and climatic changes of the area. The hot and arid climate of the Sinai played a decisive role in the development of this sedimentary pattern. Terrigenous supply, entering the gulf from numerous wadis, consists of coarse siliciclastic sediments. Due to rapid deposition they do not prevent reef growth.

Waves being generated by the predominantly northerly and northeasterly winds, diagonally approaching the shoreline of the gulf, induce southward longshore currents. These characteristic currents redistribute the terrigenous debris, transporting them into deep basins. At the same time the warm, less saline surface current flowing from the Red Sea into the gulf maintains the conditions necessary for a flourishing reef growth.

Supratidal sabkhas are associated with alluvial fans (they are located on the distal fans as a rule), and are also controlled by local environmental conditions. They developed in areas protected from waves and currents by reefs and locally by mangroves.

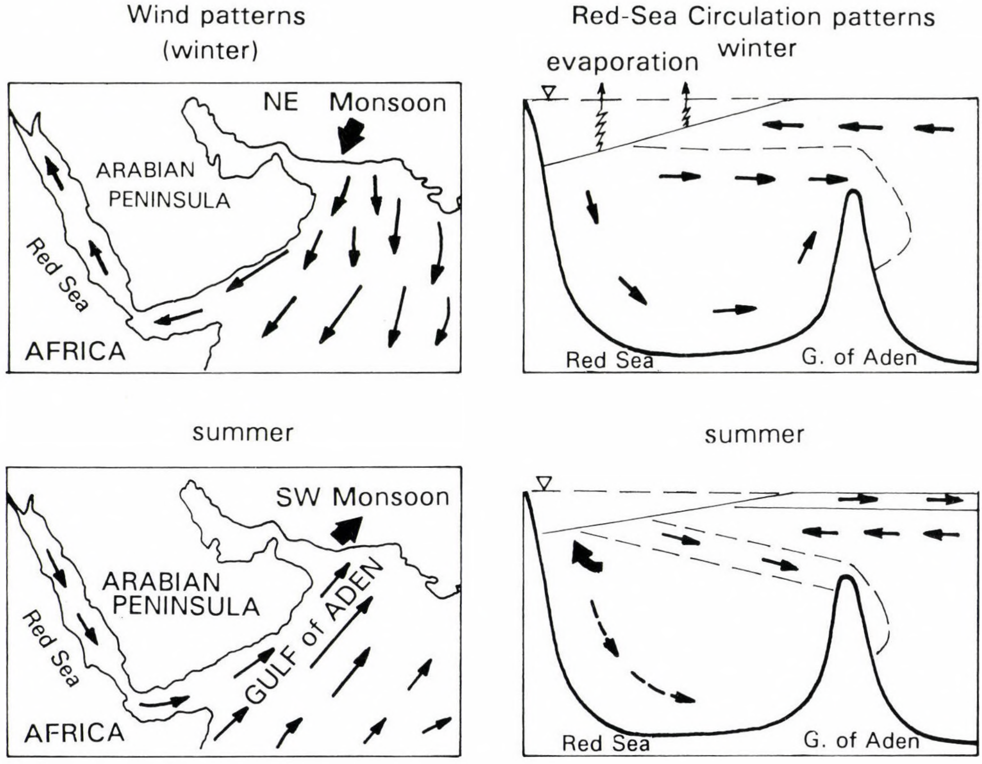

Fig. 10
Wind and circulation patterns between the Indian Ocean and the Red Sea (after Locke and Thunell 1988)

The relationship between sedimentation and sea level history is reflected by raised coral reef terraces along the western coast of the Gulf of Aqaba. The evolution of these terraces corresponds to glacial and interglacial episodes in the Late Pleistocene. The sea level rise favoured the formation of reefal and lagoonal systems, while in the periods of sea level lowering, marine terraces became subaerially exposed, and siliciclastics prograded. The physiography of the terraces was also governed by the recent coastal erosional processes, and by post-depositional faulting as well.

Acknowledgements

This paper is related to Ms Ebtehal Fathy's PhD dissertation which was supported by the Hungarian Geological Institute in a great degree. Mr. M. Hassan added considerably to the field works. Thanks of the authors go to the special readers, Dr Géza Csészár and Dr. György Lelkes for their substantial work and helping intent.

References

Al-Rifaiy, I.A., O.H. Cherif 1988: The fossil coral reefs of Al-Aqaba, Jordan. – Facies, 18, pp. 219–230.

Bentor, Y.K., M. Eya 1987: Jebel Sabbagh Sheet. – Israel Academy of Sciences and Humanities, Jerusalem.

Dullo, W.C. 1990: Facies, Fossil record, and age of Pleistocene reefs from the Red Sea (Saudi Arabia). – Facies, 22, pp. 1–46.

Freund, R., Z. Garfunkel, I. Zak, M. Goldberg T. Weissbrod, B. Derin 1970: The shear along the Dead Sea rift. – Philos. Trans. Roy. Soc. London, A 267: pp. 107–130.

Friedman, G.M. 1965: A fossil shoreline reef in the Gulf of Aqaba (Elat). – Israel J. Earth Sciences, 14, pp. 86–90.

Friedman, G.M. 1968: Geology and geochemistry of reefs, carbonate sediments and waters, Gulf of Aqaba (Elat), Red Sea. – J. Sediment. Petrol., 38, pp. 895–919.

Friedman, G.M. 1972: Coral reef rock from Red Sea: sequence and time scale for progressive diagenesis and its effect on porosity and permeability. – Am. Assoc. Pet. Geol. Bull., 56, p. 678.

Friedman, G.M. 1985: Gulf of Elat (Aqaba): Geological and sedimentological framework. – In: G.M. Friedman and W.E.Krumbein, Ecological Studies, 53: Hypersaline Ecosystems, Springer-Verlag Berlin, pp. 39–41.

Gvirtzman, G., B. Buchbinder, A. Sneh, Y., Nir, Y., G.M. Friedman 1977: Morphology of the Red Sea fringing reefs: A result of the erosional pattern of the last glacial low-stand sea level and the following Holocene recolonization. – 2nd Symp. Intern sur les coreaux recifs coralliens fossils, Paris, Sept. 1974, Mem. B.R.G.M., 89, pp. 480–491.

Gvirtzman, G., G.M. Friedman, D.S. Miller 1973: Control and distribution of Uranium in coral reefs during diagenesis. – J. Sediment. Petrol., 43, pp. 985–997

Gvirtzman, G., G.M. Friedman 1977: Sequence of progressive diagenesis in coral reefs. – Am. Assoc. Pet. Geol., Stud. Geol., 4, pp. 357–380.

Hays, J.D., J. Imbrie, N.J. Shackleton 1976: Variations in the Earth's orbit:: pacemaker of the ice ages. – Science, 194, pp. 1121–1132.

Hoang, C.T., M. Taviani 1991: Stratigraphic and tectonic implications of Uranium-series-dated coral reefs from uplifted Red Sea Islands. – Quat. Res., 35, pp. 264–273.

Locke, S., R.C. Thunell 1988: Paleoceanographic record of the last glacial/interglacial cycle in the Red Sea and Gulf of Aden. – Palaeogeogr., Palaeoclimatol., Palaeoecol., 64, pp. 163–187.

Lyberis, N., 1988: Tectonic evolution of the Gulf of Suez and the Gulf of Aqaba. – Tectonophysics, 153, pp. 209–220.

Makris, J., R. Rihm 1991: Shear-controlled evolution of the Red Sea: pull apart model. – Tectonophysics, 198, pp. 441–466.

Milankovitch, M. 1941: Kanon der Erdbestrahlung und seine Anwendung auf das Eiszeitenproblem. – Acad. R. Serb. Spec. Ed., pp. 133, 633.

Prell, W.L. 1984: Monsoonal climate of the Arabian Sea during the late Quaternary: a response to changing solar radiation. – In: A.I. Berger et al. (Eds), Milankovitch and climate, Part 1. Reidel, Hingham, Mass., pp. 349–366.

Sellwood, B.W., R.E. Netherwood 1984: Facies evolution in the Gulf of Suez area: sedimentation history as an indicator of rift initiation and development. – Modern Geol., 9, pp. 43–69.

Strasser, A., C. Strohmenger, E. Davand, A. Bach 1992: Sequential evolution and diagenesis of Pleistocene Coral reefs (South Sinai, Egypt). – Sediment. Geol., 78, pp. 59–79.

Walther, J., 1888: Die Korallenriffe der Sinai Halbinsel. Geologische und biologische Betrachtungen. – Abh. math.-natur-wiss. Kl. Konigl. Sachs. Gesellsch. Wissensch., 14, pp. 439–506.

Acta Geologica Hungarica, Vol. 37/3–4, pp. 327–350 (1994)

The Karakaya Basin: a Palaeo-Tethyan marginal basin and its age of opening

Okan Tüysüz, Erdinç Yiğitbaş
ITÜ Maden Fakültesi Jeoloji Bölümü, Istanbul

The Ilgaz-Kargi Massif in NW Turkey is one of the rare places where the Palaeozoic-Early Mesozoic tectonic units forming the basement of the Rhodope-Pontide Fragment and their interrelationships can be observed from under a Late Jurassic and younger cover. The pre-Malm rocks of the massif constitute three tectonostratigraphic units, and include Middle Jurassic granitoids that cut across them. These three tectonostratigraphic units are the following:

1. The *Karakaya Unit*, consisting of, from base to top: a metaclastic unit and Permian metacarbonates (İbi Formation), an olistostromal complex containing carbonate blocks (Aktaş Formation), a lava-pyroclastic-carbonate-clastic alternation produced in a deep and tectonically active marine environment (Kunduz Formation) and a fairly homogeneous carbonate-lava-pyroclastic alternation deposited in a deep but relatively quiet marine environment (Gümüşoluğu Formation);
2. *The Elekdağ Unit*, formed from an ophiolitic sequence (the Yilanli Group) and a mélange complex (Domuzdağ complex);
3. *The Küre Unit*, formed from a pelagic lava-pyroclastic-clastic sedimentary rock alternation (Bekirli Formation) and an overlying Liassic flysch (Akgöl Formation). The Elekdağ Unit represents a fragment of the floor of the Palaeo-Tethys and a mélange generated during its south dipping subduction. The record preserved in the Karakaya Unit indicates the presence of a Permian carbonate platform constructed on a granitic foundation and the subsequent disintegration of this platform with the accompanying volcanism heralding the opening of the Karakaya Basin. The Küre Unit, forming the common stratigraphic cover of both the Elekdağ and the Karakaya Units, indicates a direct connection between the Palaeo-Tethys and the Karakaya Basin. Relationships between these two oceanic realms possibly resembled that between the present Indian Ocean and the Andaman Sea.

Key words: Palaeo-Tethys, Karakaya Basin, Cimmerides, Turkey

Introduction

The main tectonic units of northern Turkey are the Rhodope-Pontide and the Sakarya continental fragments, separated by the Neo-Tethyan Intra-Pontide suture (Fig. 1). Within these two tectonic units a widespread metamorphic rock association is present which extends from the Aegean shores in the west (Bingöl et al. 1973; Okay et al. 1990) to the city of Erzincan (Fig. 1) in the east (Tekeli 1981; Koçyiğit 1991). The protoliths of this association are sedimentary and igneous rocks which in some places display an ordered internal succession (Okay 1984; Tüysüz 1990), in others a chaotic internal structure including blocks (Tekeli 1981; Tüysüz and Dellaloğlu 1992). This association is known in the

Address: O. Tüysüz, E. Yiğitbaş: ITU Maden Fakültesi, Glotek Ünitesi, 80626 Ayazaga, Istanbul, Turkey
Received: 25 October, 1993

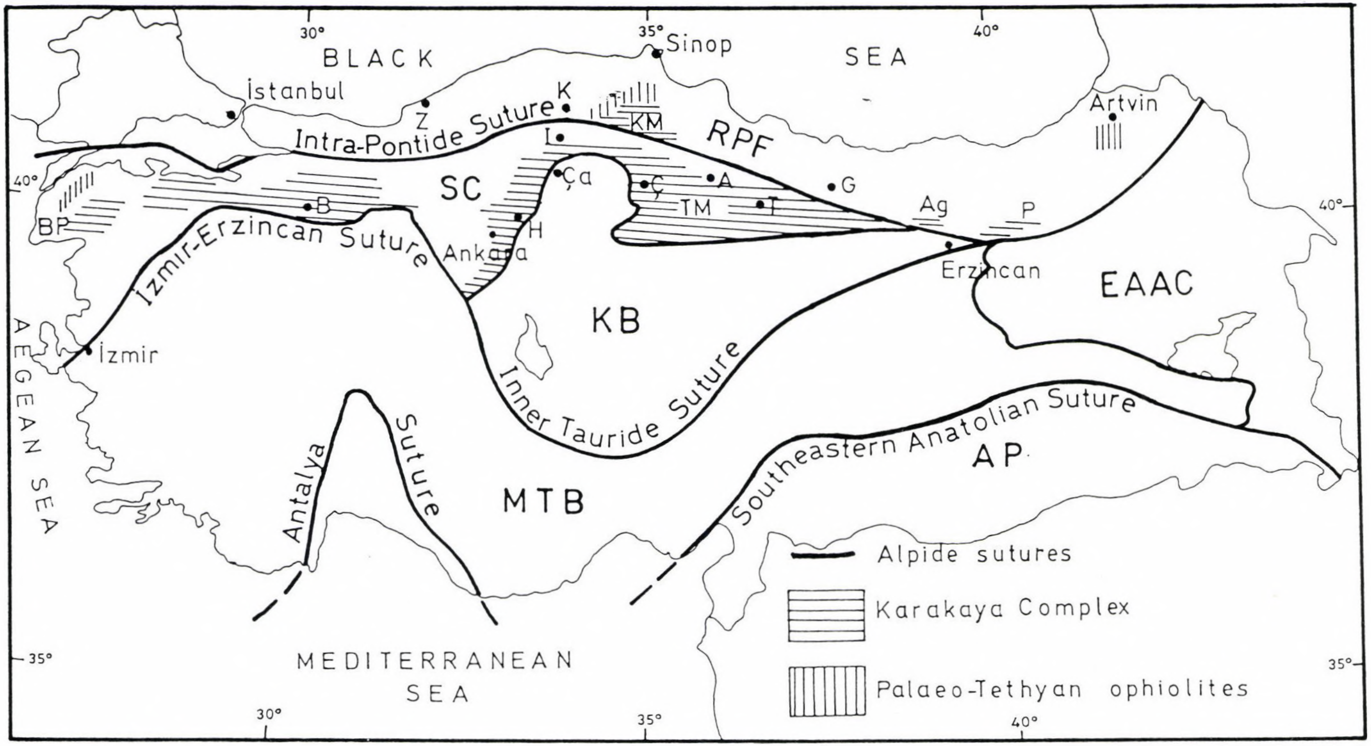

Fig. 1
Map showing the areal distribution of the Palaeo-Tethyan ophiolites and the Karakaya complex. The map also shows Alpide sutures and continental blocks of the country. Continental blocks : RPF – Rhodope–Pontide Fragment; SC – Sakarya Continent; KB – Kirsehir Block; MTB – Menderes Taurus Block; AP – Arabian Platform; EAAC – Eastern Anatolian Accretionary Complex; Z – Zonguldak; K – Kastamonu; KM – Kargi massif; G –Gümühane; Ag – Agvanis massif; P – Pulur massif; BP – Biga peninsula; B – Bilecik; H – Hasanoǧlan; Ça – Çankiri; I – Ilgaz; Ç – Çorum; A – Amasya; T – Tokat; TM – Tokat massif

literature under such designations as the Karakaya Formation (Bingöl et al. 1973), the Karakaya Complex (Şengör et al. 1984) or the Karakaya Unit (Tüysüz 1990). There is a general agreement that the Karakaya Basin was a tectonic environment which existed in the Late Palaeozoic up to the beginning of the Mesozoic in the Mediterranean Tethysides in Northern Turkey. Although the presence of the remnants of this tectonic environment in Northern Turkey has long been known (Wijkerslooth 1942; Blumenthal 1945; Blumenthal 1948), their significance in the geological evolution of the country has been recognized only recently (Şengör and Yılmaz 1981; Tüysüz 1990; Okay et al. 1990).

The palaeogeographic setting of the Karakaya Basin, its age of opening and closing and its relationships with the Palaeo-Tethys remain controversial. Triassic (Bingöl et al. 1973), Permian (Yilmaz 1981), Carboniferous (Tekeli 1981) and Devonian (Bingöl 1983) ages of opening, and Pre-Liassic in general (Yilmaz 1981) or in the west Late Triassic and in the east Liassic (Tekeli 1981) ages of closing have been proposed. Bingöl et al. (1973) have interpreted the Karakaya Basin as a short-lived, deep and narrow trough, genetically related to a larger ocean to the south; Tekeli (1981) and Bingöl (1983) regarded it as a major ocean; Şengör and Yılmaz (1981) viewed it as a back-arc basin located to the south of Palaeo-Tethys and Okay et al. (1990) considered it a Permian fore-arc basin of the Palaeo-Tethys.

These widely divergent views have resulted from the prevalent paucity of the field data and could not be rigorously tested; therefore, no consensus of opinion has emerged as to the age and location of opening of the Karakaya Basin and its relationship with the Palaeo-Tethys. Recent field work carried out in the middle part of the Rhodope-Pontide Fragment (Figs 1 and 2) has led to results which have an important bearing on these questions. The purpose of this paper is to summarize these new data and to discuss their implications for the palaeogeography of the Palaeo-Tethys and the Cimmerian continent.

Geologic setting

In the Central Pontides (Rhodope–Pontide Fragment + Sakarya Continent) Middle Jurassic sedimentary rocks un- and non-conformably cover early Jurassic and older rocks and the contacts between them (Fig. 2). A major portion of the rocks beneath this unconformity is metamorphic, and was effected by at least two phases of penetrative deformation. By contrast, sedimentary rocks above the unconformity were deformed by long wavelength folds with east-trending fold axes. We thus call all the rocks below the Middle Jurassic unconformity "basement rocks", and those above the unconformity "cover rocks", which form a transgressive sequence from the Late Jurassic to the end of the Early Cretaceous (Yılmaz and Tüysüz 1988; Tüysüz et al. 1989). These basement and cover units were imbricated during a Late Cretaceous south-vergent deformation in the southern part of the Central Pontides (Fig. 2).

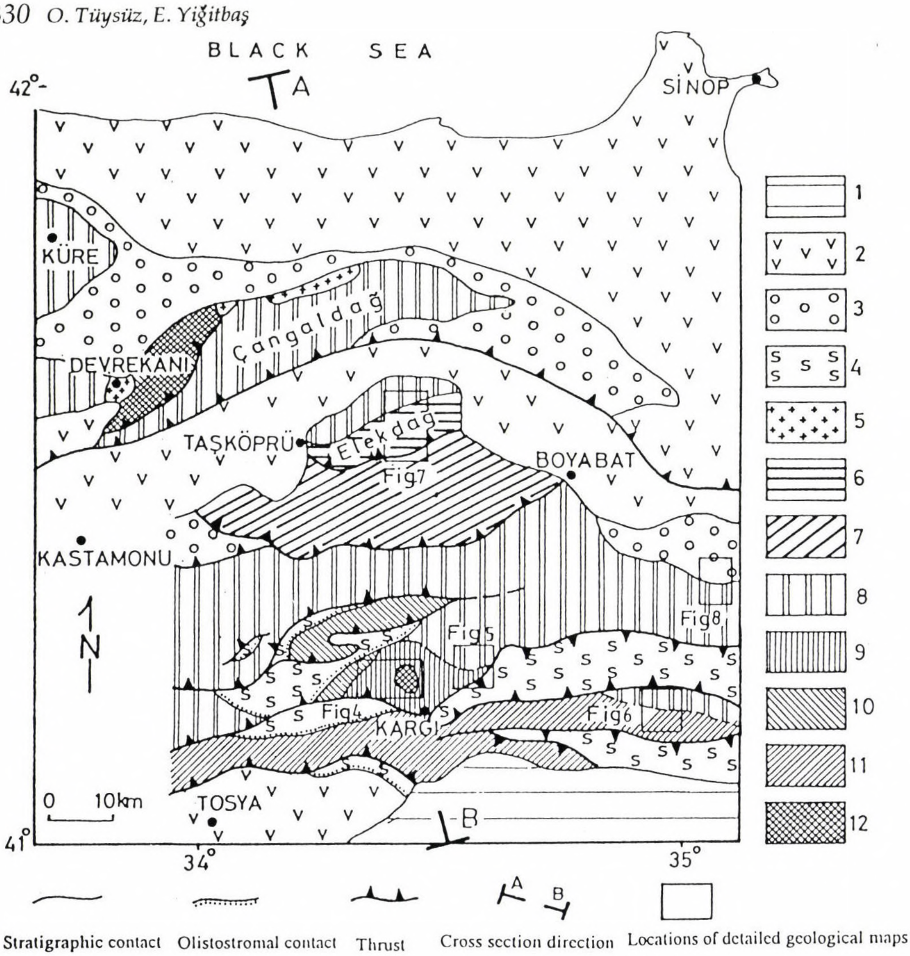

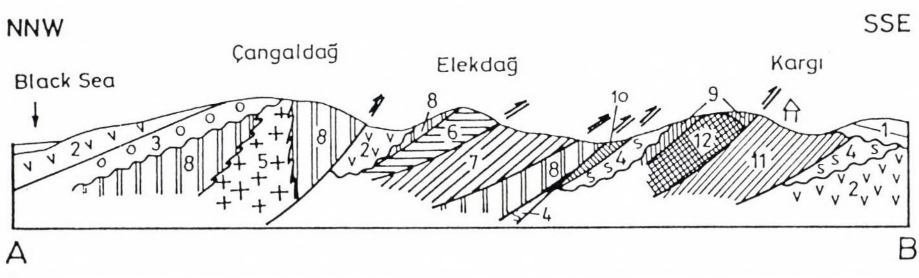

Fig. 2

Geological map and cross-section of the Central Pontides. The map is simplified by the elimination of Neogene and younger sediments and structures. The "olistostromal contact" implies an unconformity which developed during the tectonic imbrication of the region. 1. post-tectonic clastics and volcanics (Eocene); 2. arc- magmatics (Upper Cretaceous); 3. clastic rocks and platform carbonates (Malm–Lower Cretaceous); 4. Ophiolite and ophiolitic melange (Upper Cretaceous); 5. post-collisional granitoids (Dogger); 6. Yilanli group (Carboniferous--Triassic); 7. Domuzdağ melange (Triassic); 8. Bekirli Formation (Triassic); 9. Aktaş Formation (Triassic); 10. Gümüşoluğu Formation (Triassic); 11. Kunduz Formation (Triassic); 12. İbi Formation (Permian)

Syntectonic olistostromal mélange wedges of Campanian age (Yigitbas et al. 1990) developed between the individual slices.

This imbricate zone is seen in wide areas in the southern part of the Kargi Massif (Fig. 2). Despite the imbrication and deformation, the internal order and even, locally, stratigraphic and structural relationships between and within these very thick slices which form the imbricated zone, can be recognized. Both on the basis of such preserved relationships and on the basis of data gathered from the unimbricated northern areas the basement is divided into three tectonostratigraphic units, namely the Karakaya, the Elekdağ, and the Küre Units.

The Karakaya Unit (Figs 2 and 3)

This unit includes the İbi, Aktaş, Gümüşoluğu and Kunduz Formations that are in stratigraphic contact with one another and that developed on a continental basement.

Ibi Formation (Figs 2, 3 and 4): This formation crops out within the imbricated zone in the core of the İbi Anticline, which is decapitated by a fault; its stratigraphic base is not exposed (Fig. 4). This sequence was metamorphosed in greenschist facies, and in its lowest visible parts commences with a gneissic metaconglomerate with lensoid quartz clasts. Upward in the section, grain size decreases and the metaconglomerate passes successively into metasandstones, schists and phyllites, in which the primary bedding can commonly be recognized. Upsection the sequence contains thin metacarbonate lenses. Through an increase in the frequency of such lenses, metaclastic rocks are progressively replaced by a metacarbonate section. These metacarbonate rocks are thickly bedded, heavily calcite-veined and are locally interlayered with thin phyllites and calcschists. They contain the following fossils indicating a neritic environment and an Upper Carboniferous–Permian age.

Benthonic foraminifera:
Geinitzina sp.
Globivalvulina sp.
Futuberitina sp.
Archaesphaera sp.
Farlandia sp.
Dislosphaerina sp.
Agathammina sp.
Schubertella sp.
Pseudovermiporella sp.

Algae:
Barinella sp.
Mizzia velebitana

The carbonates are also locally rich in corals, indicating a shelf to reefal environment.

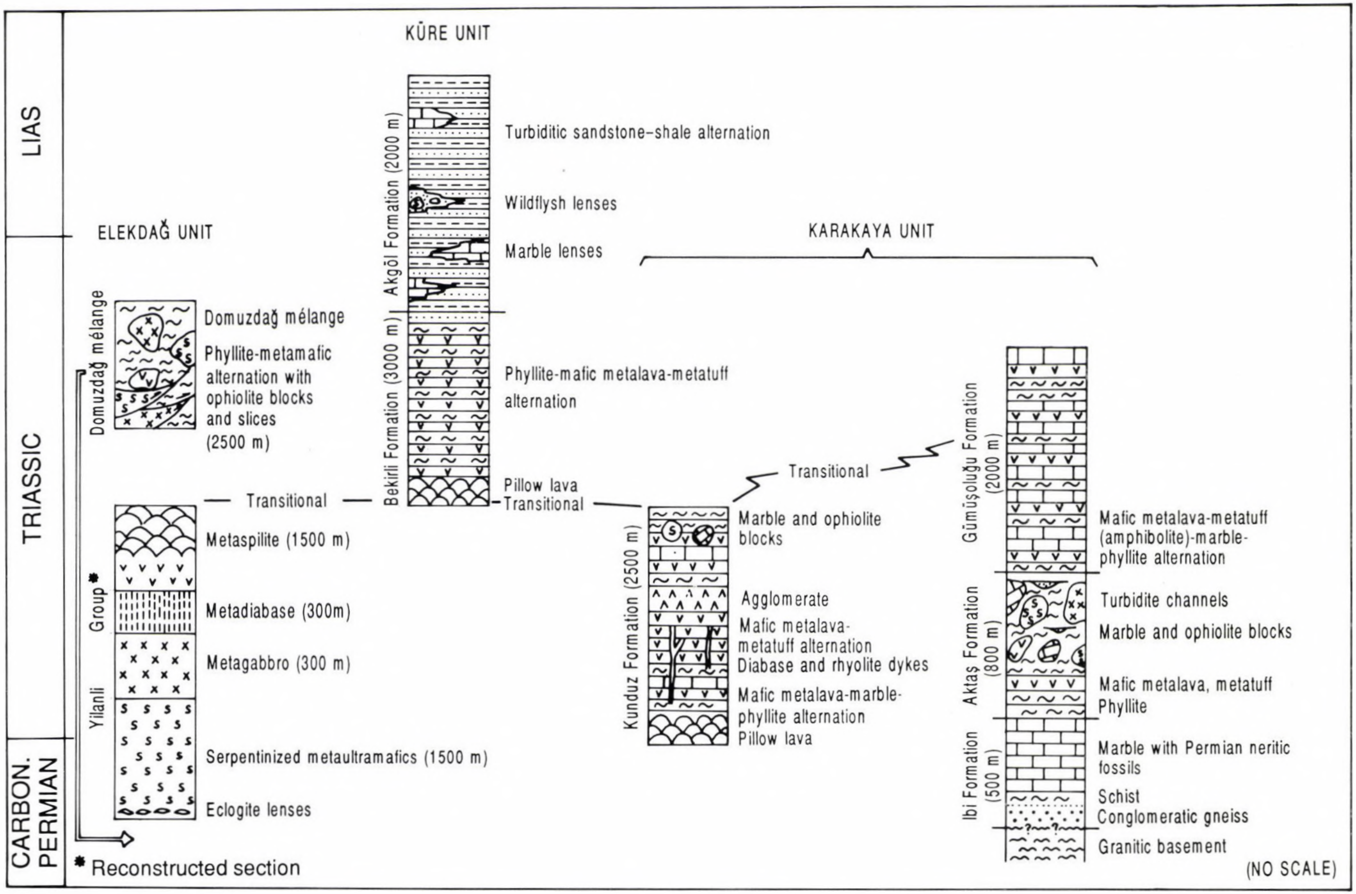

Fig. 3
Columnar stratigraphic sections of pre-Dogger units of the Central Pontides

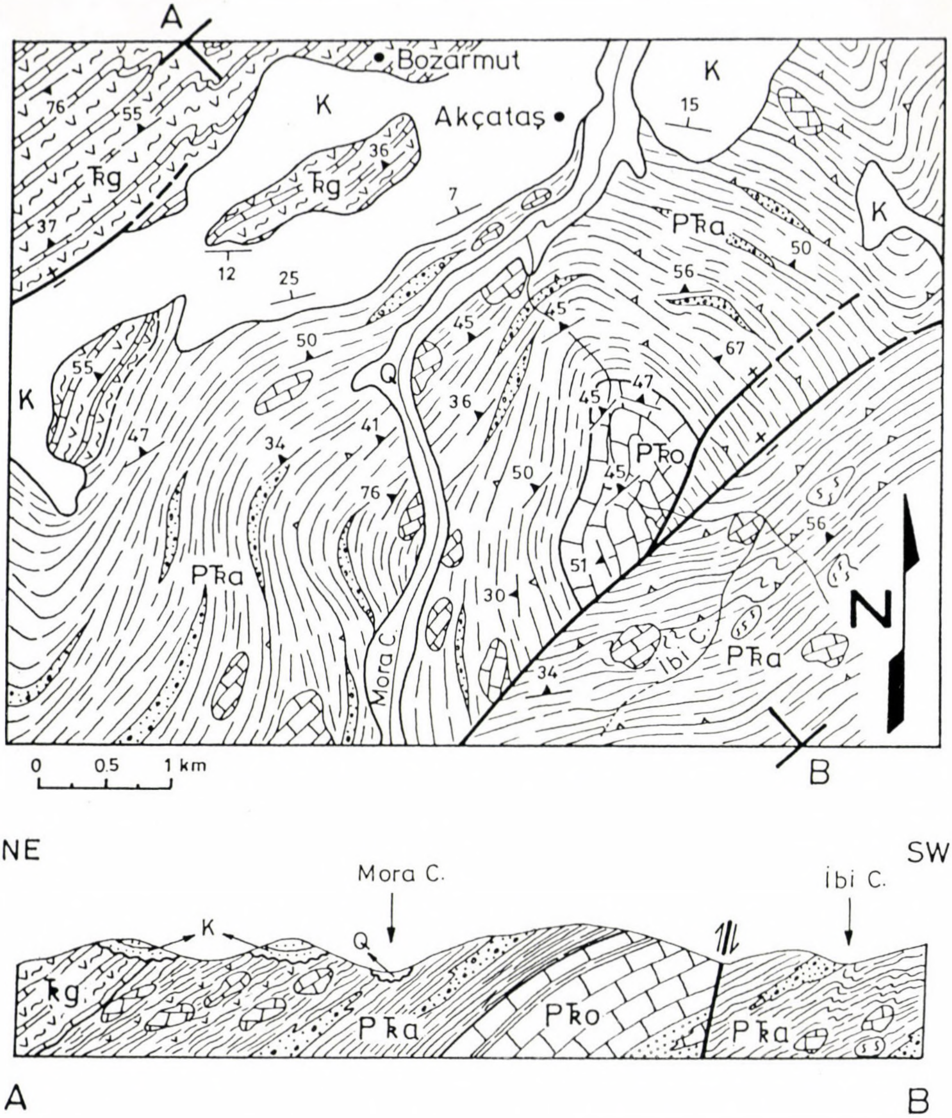

Fig. 4
Detailed geological map and cross-section of the İbi Anticline and surroundings. PTo – İbi Formation; Pta – Aktaş Formation; Tg – Gümüşoluğu Formation; K – Upper Cretaceous sediments. The location of this map is shown in Fig. 2; for the age and stratigraphy of the formations, see Fig. 3

Aktaş Formation (Figs 2, 3 and 4): This formation exhibits transitional contacts with the Permian carbonates forming the upper levels of the İbi Formation. It contains numerous blocks and was metamorphosed in greenschist facies. The Permian carbonate rocks seen in the core of the İbi anticline pass upwards into a phyllite-carbonate intercalation through a progressive increase in phyllite interlayers, and finally into a homogeneous phyllite. The thickness of this phyllite varies between hundred metres and one kilometer repeatedly, and each time within a few hundred metres at most. In the light of the progressive deepening of the environment of deposition through time, this suggests normal fault control during the deposition. In the upper levels of the phyllite there are lens-shaped, coarse metaclastic channels with thicknesses of up to 5–10 meters and a minimum of 30–100 meters length. Although the coarse-grained channel-fill material acquired a gneissic texture by the elongation of the clasts, as a result of deformation coeval with metamorphism, it can still be recognized that they were coarse-grained turbidites. Indeed, both above and beside these channels there are some coarse-grained metasandstone interlayers, indicating that the whole sequence was probably a flysch.

Angular to subrounded, poorly sorted, 5–50 cm large metacarbonate pebbles and blocks, most probably derived from the neritic carbonates in the lower parts of the sequence, occur in the channels or as debris flows within the phyllites and metasandstones. They are associated with mafic metalavas and metapyroclastics whose frequency increase upsection. The presence of active volcanicity accompanying faulting further supports the inference of an extensional environment. The geochemical characteristics of these magmatics are not known. Despite metamorphism their tuff, lapilli and agglomerate origin can be recognized under the microscope and in places in the field. This implies a volcanic source providing material to this tectonically active sedimentary basin. Upsection, thickness and lateral extension of these pyroclastic rocks increase and 5–10 metres thick mafic lava horizons are also seen. The size of the blocks also increases upwards reaching diameters of hundreds of meters or even a kilometer. At this level diverse rock types such as metaspilite, metagabbros, and metaserpentinites begin to appear among the blocks, indicating an ophiolitic source, probably the ophiolite of the Elekdağ Unit to be described below. In places where blocks predominate the unit acquires a typical mélange appearance, while in others, individual blocks lie embedded in an ordered and very thick phyllitic matrix. Sections with complex internal structure have lensoidal shapes within the relatively ordered section. Between the internally complex lenses and the ordered sequences there is no discontinuity in foliation and fold axis, suggesting that these two sections became juxtaposed during deposition, possibly through debris flow mechanisms resulting from episodic failure of steep slopes and before metamorphism.

No age diagnostic fossils have been found in the Aktaş Formation in the study area. It succeeds fossiliferous carbonates of the İbi Formation and is

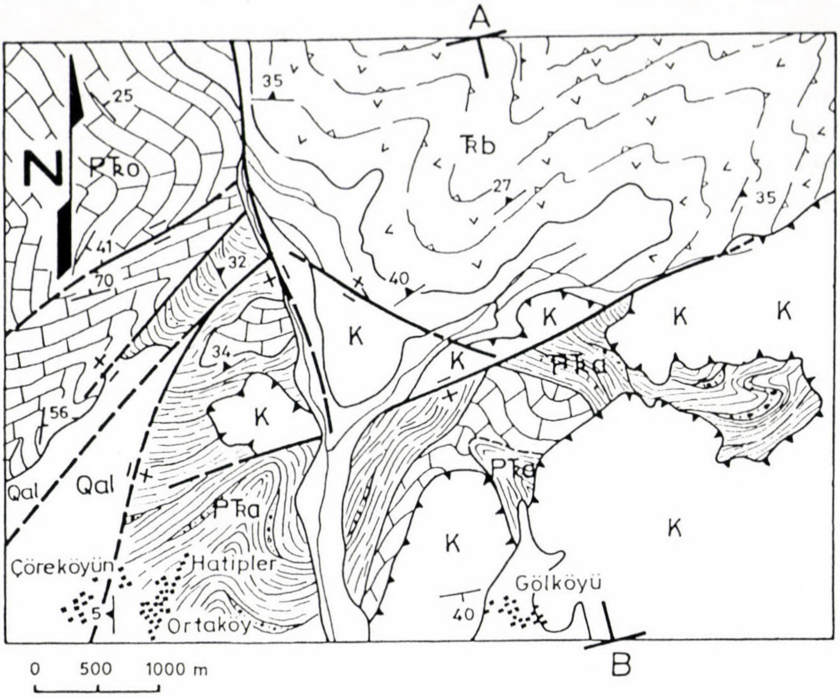

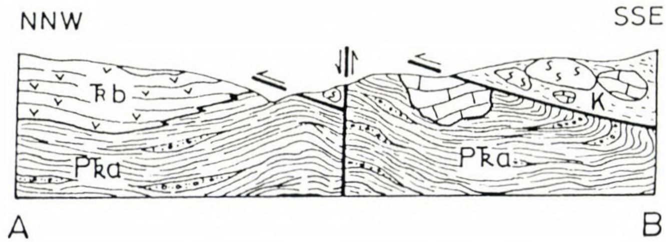

Fig. 5
Detailed geological map and cross-section of the Gölköyü–Hatipler area, NE of Kargi. PTo – Permian limestone marble of the İbi Formation; Tb – Bekirli Formation; Tk – Kunduz Formation; K – Upper Cretaceous ophiolites, ophiolitic mélange; Qal – Quaternary alluvium. The location of this map is shown in Fig. 2; for the age and stratigraphy of the formations, see Fig. 3

unconformably overlain by Upper Cretaceous rocks. It is thus temporally bracketed between the Permian and the Late Cretaceous. Around Ilgaz (Tüysüz and Dellaloğlu 1992), Hasanoğlan (Akyürek et al. 1984), Amasya and Çorum (Tüysüz in prep.) (Fig. 1) the Aktaş Formation has a wide areal distribution and is unconformably overlain by Liassic clastic rocks. In these areas Permo-Triassic fossils have also been found within the blocks of this formation (Şengör and Yılmaz 1981; Tekeli 1981; Akyürek et al. 1979, 1984; Okay et al.

1990; Tüysüz and Dellaloğlu 1992; Tüysüz, in prep.). These data indicate a probable Triassic age.

To the north of the İbi Anticline (i.e. upsection) the Aktaş Formation passes gradually into the Gümüşoluğu Formation (Fig. 4), and to the east it passes into the Bekirli Formation of the Küre Unit.

Gümüşoluğu Formation (Figs 2 and 3): This formation consists of a regular metasedimentary–metavolcanic alternation. It has a wide areal distribution and underwent two or three phases of penetrative deformation, characterized by the following: A penetrative foliation, S_1, defined by amphiboles and micas, is the earliest recognizable structure. Although locally S_o is visible where metamorphism was of low grade, no fold closures could be detected. D_2 is characterized by kink folds, which fold the S_1. Locally a crenulation cleavage, S_2, is associated with these. A weakly developed D_3 is expressed by a second generation of kink folds. No foliation developed during the D_3. As the other formations of the Karakaya Unit, the Gümüşoluğu Formation also has an imbricated internal structure. In different slices of this formation which thrusted over each other, different metamorphic grades can be seen, ranging from low-pressure greenschist facies up to high-pressure greenschist or epidote–amphibolite facies.

Metacarbonates consisting of white, saccaroidal marble or calcschist are the most widespread rocks. The phyllites and the schists consist of quartz, calcite, white mica and, locally, sodic amphibole, garnet, epidote and chlorite. Amphibolites interlayered with the metacarbonates and metaclastics contain mainly hornblende, glaucophane, epidote and albite. Petrographic studies of these metabasic rocks imply that their protoliths were mafic lava and tuff (Tüysüz 1985). In places where metamorphism was weak, pillowed mafic metalavas, alternating with carbonates and clastics, mafic tuffs, agglomerates, red hemipelagic mudstones, and rare manganese nodules are seen. In the Gümüsolugu Formation there are fairly sparse marble olistoliths that are found either as solitary blocks or in the form of olistostromal horizons.

No fossil of biostratigraphic value has been found in the Gümüşoluğu Formation. However, because it passes without a break into the underlying Aktaş Formation (Fig. 4), and because it is unconformably overlain by early Cretaceous sedimentary rocks we infer a Triassic age for it.

Kunduz Formation (Figs 2 and 3): This formation consists of alternating sedimentary, magmatic and pyroclastic rocks, all of which were affected by greenschist facies metamorphism. The formation is lithologically similar to the Gümüsolugu Formation and distinguished from it by rapid vertical and horizontal lithological variations, abundant block content and the presence of coarse pyroclastic material.

The stratigraphic base of the formation is not exposed. Its lowest visible rocks are pillowed mafic metalavas. The pillows were elongated in a NW–SE direction by deformation and interpillow spaces are filled with carbonates and pelagonite tuff. Despite metamorphism, these lavas have largely preserved their primary structure and texture. They display epidote and chlorite characteristic of greenschist spilite facies. Locally these pillow lavas were traversed by 30–70 cm thick diabase dikes exhibiting a blastoophitic texture. More rarely they were also cut by andesite dikes. These probably formed the feeders of the lavas and pyroclastic rocks further upsection. Upwards pillow lavas contain sedimentary interlayers. Most of these are carbonates, calcareous phyllites and red pelagic mudstones. The section passes upwards into a lava-sediment intercalation by an increase in the number, and in the thickness, of the sedimentary interlayers and by the replacement of the pillow lavas with massive flows. The metaclastic layers are rich in quartz and white mica, and the metalavas in albite, epidote and chlorite. This unit has a well-developed cleavage dipping gently to the NW and contains red and violet metamudstones and turbiditic conglomerate lenses, containing equant, rounded clasts. In these coarse-grained horizons bedding and some sole marks are still recognizable despite metamorphism.

Further upsection is a mafic metalava-phyllite alternation dominated by the former component. Within this there are metacarbonate horizons which are a few tens of meters thick and laterally continuous for many kilometers. Upwards, the metacarbonate horizons become sparser, and metatuff and meta-agglomerate interlayers appear. Meta-agglomerates appear as thick lenses (Fig. 6) which entirely preserved their structure despite metamorphism. They consist largely of mafic and partly felsic lava fragments and a tuff matrix. A weak generally gently NW dipping cleavage has developed in the matrix. This part of the section is also cut by mafic and felsic dikes. In this section of the Kunduz Formation lithologies vary rapidly both vertically and horizontally. This rapid variation is interpreted to document frequent and swift changes of the depositional conditions. In the uppermost part of the Kunduz Formation there is a metalava, phyllite and metatuff intercalation. Within this intercalation are dispersed mostly marble, and more sparsely and of smaller size, metaspilite, metagabbro and metaserpentinite blocks. These blocks show the same lithologic character as those in the Aktaş Formation, and similarly are thought to have been derived from the neritic Permian carbonates and the ophiolitic rocks of the Elekdağ unit.

Main oxides, trace and rare earth element analyses of the magmatic rocks of the Kunduz Formation were undertaken by Doğan (1990). According to her, the basic lavas of this formation are tholeiitic and alkalic in character. Main element oxides show that they are olivine tholeiitic low- and high-magnesium basalts, ferrobasalts and basaltic andesites. According to the results of the trace element analyses, they typify an enriched mantle source. On the discrimination diagrams, they fall between the oceanic island and MORB fields, and thus show a transitional character. Saunders and Tarney (1984) showed that transitional magma types from oceanic island to MORB field are typical of magmatics of marginal basins. REE analyses of the magmatics of the Kunduz Formation also support this idea.

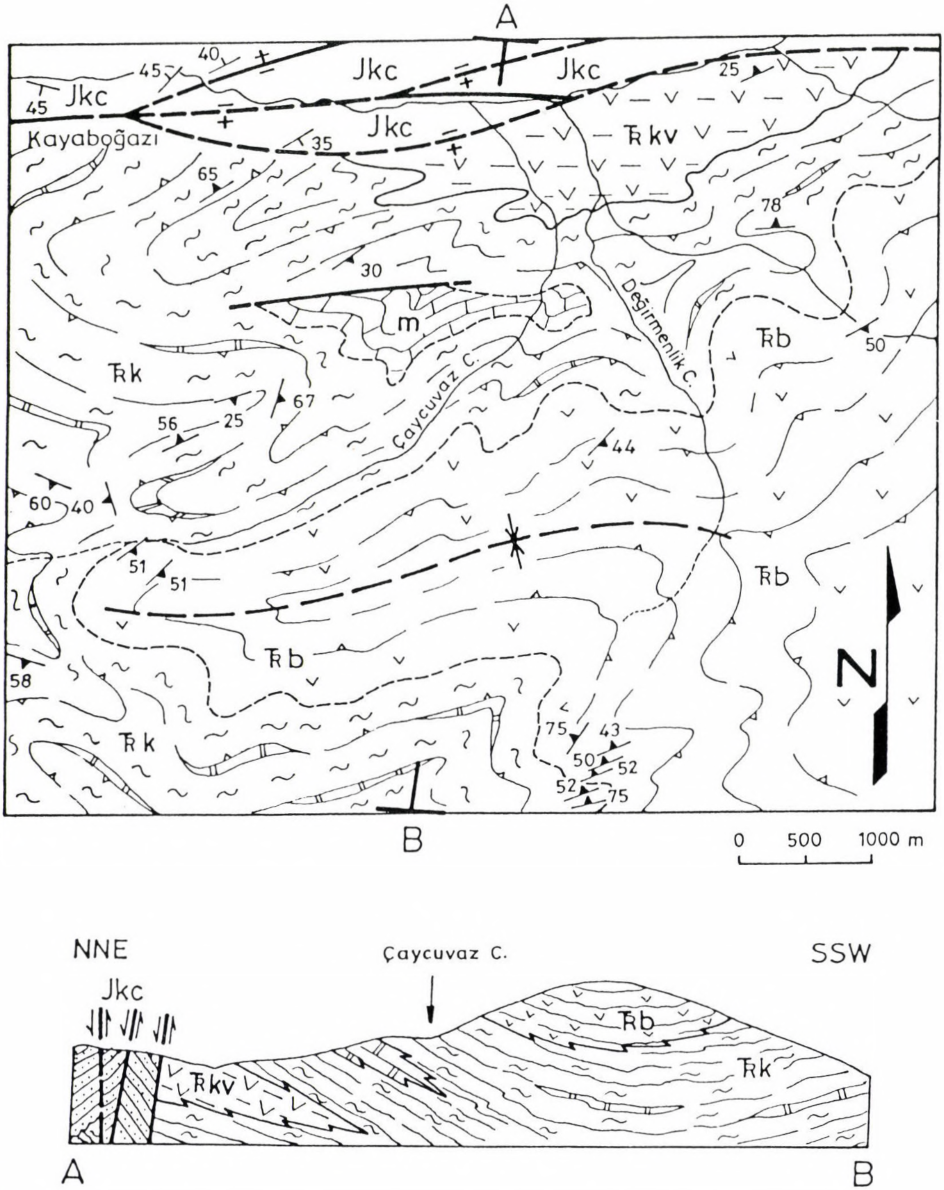

Fig. 6
Detailed geological map and cross-section of the Çaycuvaz area. Tk – Kunduz Formation; m – marble lenses; Tkv – agglomerate lense within the Kunduz Formation; Tb – Bekirli Formation; Jkc – Lower Cretaceous sediments. The location of this map is shown in Fig. 2; for the age and stratigraphy of the formations, see Fig. 3

The formation gradually passes vertically into the Bekirli Formation of the Küre Unit by the disappearance of the blocks (Fig. 6). The stratigraphic base of the Kunduz Formation was obliterated during Late Cretaceous tectonism. It has yielded no evidence to indicate its age except the fact that it is unconformably covered by Early Cretaceous sediments. Its content of blocks displaying a lithological character similar to those in the Ibi Formation and its gradual passage upwards into the Bekirli Formation of the Küre Unit lead us to think that it is of Triassic (pre-Carnian) age. If our parallelization of its neritic carbonate blocks with those of the Ibi Formation is valid, then this correlation provides another age constraint.

The Elekdağ Unit (Figs 2 and 3)

This unit consists of an ophiolitic sequence and an ophiolitic mélange.

Ophiolitic sequence (The Yılanlı group) (Figs 2, 3 and 7): This sequence consists of serpentinized metaultramafics, metagabbro, metadiabase, and metalavas (Tüysüz 1990). Its constituent rock units compose a number of south verging imbricate slices within which such transitional contacts as gabbro to diabase, or diabase to spilitic lavas may be recognized in spite of metamorphism. Thus the Yılanlı group has been interpreted as an imbricated ophiolite sequence. (Tüysüz 1990). Geochemical data from these rocks (major, trace and REE) support its identification as parts of MORB ophiolite (Yılmaz 1979; Eren 1979; Güner 1980; Tüysüz 1985; Yılmaz and Şengör 1985; Doğan 1990).

Within the pseudostratigraphy of the Yılanlı metaophiolite the uppermost unit is made up of pillowed and massive lavas. These metalavas contain sedimentary interlayers in their upper parts. A major part of these interlayers consists of fine-grained clastics, and the rest are carbonates. Through an increase in the sedimentary interlayers the ophiolite sequence passes upward either into the Bekirli Formation of the Küre Unit or into the Akgöl Formation. This passage is seen both on the northern slope of the Elekdağ (Fig. 7) and further north in the core of the Çangaldağ Anticline (Yılmaz 1979; Yılmaz and Tüysüz 1984, 1991; Tüysüz 1985; Aydın et al. 1986) and around the town of Küre (Fig. 2) (Güner 1980; Yılmaz and Tüysüz 1984). Owing to their small sizes, outcrops of this unit are not shown on the map in Fig. 2, except in the Elekdağ. The Bekirli and the Akgöl Formations overlying metaophiolite are unconformably covered by Malm and younger deposits. The lowermost parts of the ophiolite were affected by blueschist metamorphism and locally include eclogite blocks and lenses (Fig. 7).

The ophiolitic mélange (Domuzdağ Complex) (Figs 2 and 3): This mélange occurs tectonically beneath the Yılanlı ophiolite described above. The matrix of the mélange consists of an alternation of metamafics derived from lavas and tuffs (Tüysüz 1985) and fine-grained metaclastics, whereas the blocks themselves represent the various lithologies of the metaophiolite. The blocks are mainly formed from metaserpentinite, metagabbro, metadiabase, metaspilite and

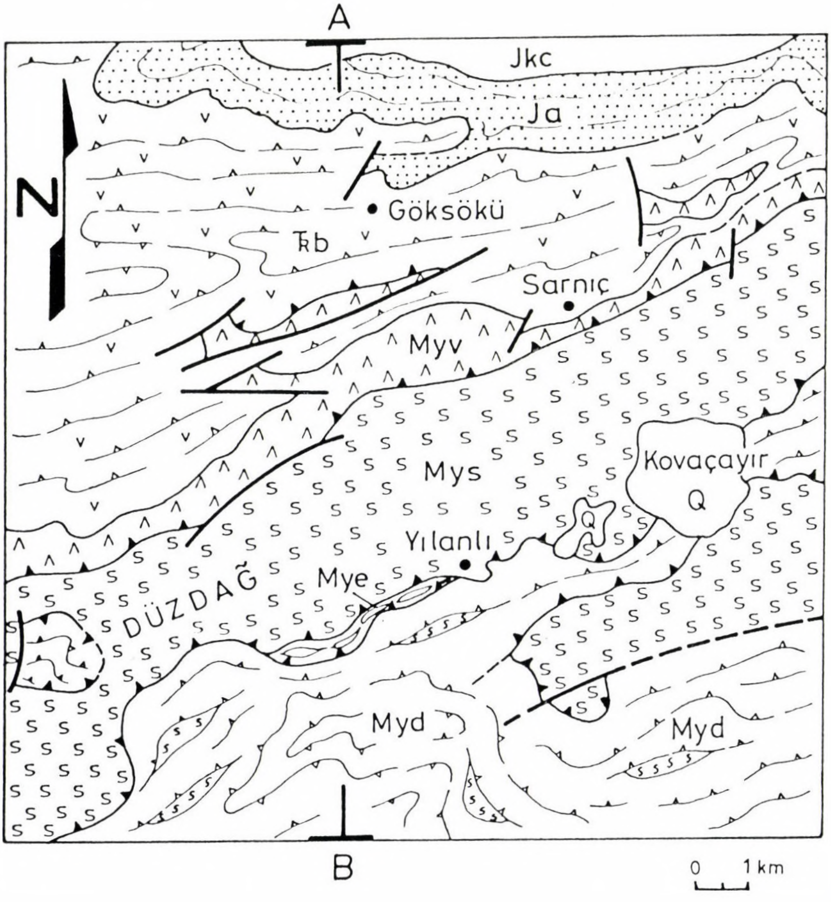

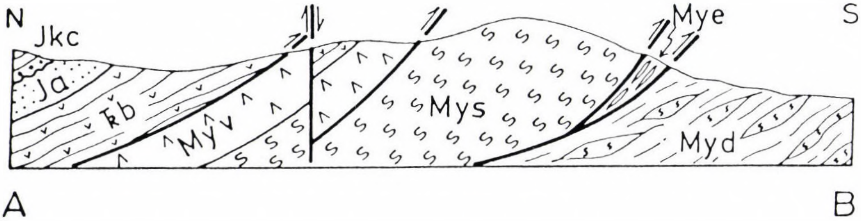

Fig. 7
Detailed geological map and cross-section of the Düzdag–Kovaçayir area. Myd – Domuzdag mélange; Mye – eclogite lenses; Mys – metaserpentinite; Myv – metagabbro-metadiabase; Tb – Bekirli Formation; Ja – Akgöl Formation; Jkc – Lower Cretaceous sediments; Q – Quaternary alluvium. The location of this map is shown in Fig. 2; for the age and stratigraphy of the formations, see Fig. 3

metachert. All of the meta-igneous blocks show identical petrography and geochemical characteristics (Tüysüz 1985) with the metaophiolitic sequence described above. In addition to the blocks of clearly oceanic origin there are also abundant marble blocks.

Block size varies from a few tens of cm to a few hundreds of meters. Despite metamorphism some of the blocks show evidence of synsedimentary emplacement. During the flattening of the matrix these blocks have become elongated in a roughly E–W direction and underwent boudinage, but did not acquire a cleavage. The number of such blocks increases northwards towards the ophiolite. This is interpreted to indicate syntectonic sedimentation coeval with the emplacement of the ophiolite onto the mélange. In the south where the blocks are few, the mélange acquires the appearance of an olistostromal metaflysch with volcanic and volcanogenic interlayers. Some of the blocks exhibit tectonic contacts with the matrix, and/or with one another. This shows that both tectonic and sedimentary processes influenced the origin and growth of the mélange.

Similar to the lower parts of the ophiolites, the mélange was also affected by blueschist metamorphism. The blueschist metamorphism is replaced by greenschist metamorphism across tectonic contacts as distance from the ophiolite-mélange contact increases (e.g. Fig. 7). Our inference that the metamorphic mélange was fed by the ophiolitic sequence, the observation that it is unconformably overlain by the Early Cretaceous sedimentary rocks and the great similarity of the volcanic and the sedimentary material forming its matrix to the similar rocks in the Küre Unit lead us to ascribe a pre-Liassic to Triassic age to the mélange.

Küre Unit (Figs 2 and 3)

This unit is divided into the Bekirli and the Akgöl Formations.

Bekirli Formation (Figs 2 and 3): This formation is a metamorphic unit, the protoliths of which formed an alternation of lavas, tuffs and fine-grained clastics. As mentioned above it lies in stratigraphic contact both upon the Karakaya unit to the south (Figs 5 and 6), and on the Elekdağ Unit to the north (Fig. 7). It thus forms a common cover to these two units.

In the northern areas, the Bekirli Formation stratigraphically follows the diabases and the spilitic lavas of the Elekdağ Unit, and appears as an alternation of homogeneous lava and fine-grained clastics. Upsection it turns into a flysch by progressive elimination of the igneous interlayers.

In the southern areas, the Bekirli Formation rests upon the Aktas and the Kunduz Formations of the Karakaya Unit along stratigraphic contacts. Here pyroclastic rocks are dominant, with fine-grained, thin, clastic interlayers. A large portion of the pyroclastics consist of tuffs with interlayers of volcanogenic clastics and some lapilli and agglomerates. These pyroclastics attain thicknesses of hundreds of meters in the south, whereas in the north they are very thin or

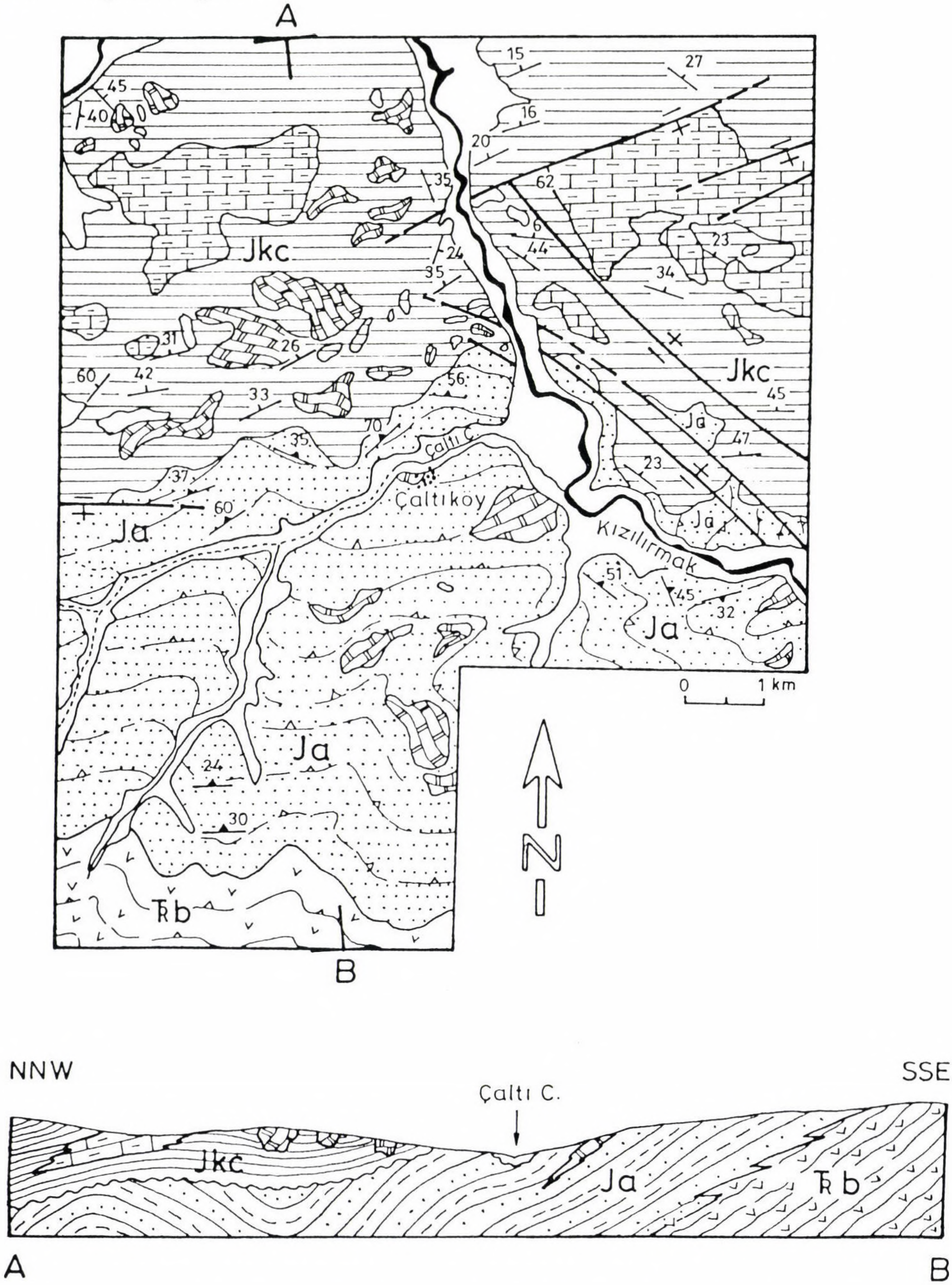

Fig. 8
Detailed geological map and cross-section of the Çaltiköy area. Tb – Bekirli Formation; Ja – Akgöl Formation and marble lenses within this formation; Jkc – Late Cretaceous clastic sediments including marble blocks and limestone lenses. The location of this map is shown in Fig. 2; for the age and stratigraphy of the formations, see Fig. 3

absent. Most of the pyroclastics are mafic and some are felsic. In places they contain likely pelagic recrystallized carbonate horizons. These horizons have yielded a *P. foliata* fauna indicating an age range from Upper Ladinian to Lower Carnian (Chatalov et al. in prep).

Above both types of its stratigraphic basement, the Bekirli Formation passes upwards into a flysch known as the Akgöl Formation, by the elimination of its magmatic interlayers (Fig. 8). The Bekirli Formation was affected mostly by greenschist, and locally by blueschist, metamorphism.

The Akgöl Formation (Figs 2 and 3): The Akgöl Formation is a flysch sequence and is commonly found stratigraphically above the Bekirli Formation or its non-metamorphic equivalents (Figs 3, 7 and 8). In the northern parts of the Central Pontides it is a homogeneous sandstone-shale intercalation, containing wild- flysch lenses with ophiolite and Triassic neritic limestone blocks in its lower horizons. This flysch has largely been regarded as a trench fill turbidite on the basis of its sedimentologic characteristics (Yılmaz and Tüysüz 1984, 1988; Tüysüz et. al. 1989). In this region the Akgöl Formation has not been affected by metamorphism, except for its lowermost parts, and contains fossils indicating a Lias to Dogger age (Chatalov et al. in prep; Ketin 1962; Kutluk and Bozdoǧan 1981; Aydin et al. 1986).

In the southern part of the Central Pontides the flysch character of the Akgöl Formation persists and contains marble lenses in its visible upper horizons. Here the unit is affected by greenschist metamorphism.

Although not analysed in detail by sedimentologic and structural studies, the presence of neritic environments in the more southerly sections of the Akgöl Formation, as suggested by the interlayering of coarsely crystalline white marble lenses (Fig. 8), has given us the feeling that, within the Akgöl Formation, a multitude of trench and forearc environments, ranging from forearc basins through inner slope basins to trench turbidites, appear to be represented, not unlike the situation observed both in the Andaman trench–Andaman forearc couple (Curray et al. 1982, Fig. 4) and in the trench–forearc couple to the south of Central Java (Curray et al. 1982, Fig. 9).

Environmental evaluation and evolutionary model

Although mapped on a 1:25 000 reconnaissance basis, and later supplemented by spot checks for fossil localities, the data we present allow the following gross picture to be painted about the Cimmeride evolution of the Central Pontides.

The Ibi Formation of the Karakaya Unit of Late Carboniferous to Permian age is the oldest palaeontologically dated rock unit in the Central Pontides. It shows the presence of a shallow marine, locally reefal carbonate platform established on an inferred granitic foundation. The lowermost clastic units beneath the platform carbonates (gneisses and schists) were probably shallow marine, or possibly even terrestrial, deposits. The basement of these clastics is not exposed in the Central Pontides, but in the Sakarya zone further west (around Bilecik Fig. 1) a granitic basement underlies them (Yılmaz 1981), which forms the basis of our inference.

The Permian carbonates are followed by the clastics and volcanics and the olistoliths of the Aktaş Formation. That some of the blocks are derived from the underlying Permian carbonates suggests the disintegration of the platform coevally with the onset of volcanism. In addition, the presence of ophiolitic blocks indicates a nearby ophiolitic source, feeding ocean-floor clasts into a juvenile intracontinental rift. The two succeeding formations of the Karakaya Unit (Gümüşoluğu and Kunduz Formations) bear witness to the development of a deep and tectonically active extensional environment, accompanied by an explosive volcanism that produced their pyroclastic components.

Frequent and abrupt thickness changes of the formations forming the Karakaya Unit are interpreted here to reflect synsedimentary faulting. We believe that this extensional deep sea environment corresponds to what has been termed the Karakaya Ocean in Northern Anatolia (Şengör and Yılmaz 1981; Tüysüz 1990; Okay et al. 1990).

The Elekdağ Unit is a pre-Malm ophiolite, including an ophiolitic mélange which it fed. This ophiolite has been considered a remnant of Palaeo-Tethys (Sengör et al. 1980, 1984; Tüysüz 1990).

The Permian carbonate platform, located to the south of Palaeo-Tethys, is here considered a part of the Permian Gondwanaland, in accordance with its extensions in the Sakarya zone (Şengör et al. 1984; Şengör 1990, Okay et al. 1990). Palaeo-Tethys separated Laurasia and Gondwanaland as a huge triangular east-facing embayment of Panthalassa (Şengör 1984; Şengör et al. 1980, 1984). Indeed today the Elekdağ ophiolite, representing the remnants of the Palaeo-Tethys, is located to the north of the Karakaya remnants (Figs 1 and 2); this supports the inference that the Permian platform, in which the Karakaya Basin had opened, was located to the south of the main branch of the Palaeo-Tethys. Pyroclastic rocks and lavas on the platform carbonates of the Karakaya Unit, such as the Aktaş metalavas and metatuffs, the locally agglomeratic metalavas with rich clastic sediment debris-flow deposit intercalations and the andesite dykes of the Kunduz Formation, interpreted as related to a magmatic arc, are thought that have evolved above the south-dipping subduction zone of Palaeo-Tethys postulated by Şengör et al. (1980, 1984). Indeed, trace and REE geochemistry of these rocks support this conclusion (Doğan 1990). Westphalian B and C andesitic volcanics (Tokay 1954) in the Zonguldak basin, as well as the Gümüşhane granitoids (Fig. 1) (Baykal 1952; Yılmaz 1974) have been interpreted as the products of this same arc magmatism (Şengör et al. 1984).

That pyroclastic material increases southward in the Bekirli Formation may be considered to point to the presence of the volcanic source to the south.

The disintegration of the Permian carbonate platform, and the assumption that it supplied blocks to younger, deeper marine sediments, was also noticed in the Sakarya zone, and interpreted as an indication for the initial opening of the Karakaya Basin (Şengör and Yılmaz 1981; Yılmaz 1981; Okay et al. 1990 and references there in). According to Şengör and Yılmaz (1981) this opening occurred as a consequence of the rifting of a back-arc basin above the south-dipping Palaeo-Tethyan subduction zone. An unexpected observation is the presence of abundant ophiolite blocks in the block-bearing section above the carbonate platform, which were derived from the Elekdağ Unit, i.e. from the floor of the ocean, the subduction of which is here believed to have given rise to the opening of the basin. This observation suggests the presence of a compressional environment immediately adjacent to an extensional one. A present-day analogue of such a situation is encountered in the Nicobar and Andaman Islands Compressional High/Andaman Basin Extensional Deep couple in NE Indian Ocean (Fig. 9). A mélange belt has developed along the Andaman and Nicobar Islands to the east of the Andaman Trench as a consequence of the easterly subduction of the Indian Ocean floor. Immediately behind this mélange belt is a magmatic arc, represented by Narcodam and Barren Islands. Behind this arc is the Andaman Basin, the opening of which is controlled by a series of pull-aparts nucleated between right-stepping en-echelon strike-slip fault segments, connecting the Sagaing Fault in Burma with the Semangko Fault in Sumatra. The maximum depth of the Andaman Basin reaches 4 km, and it is at least partly floored by juvenile oceanic crust. A broad carbonate platform along the Mergui terrace in the Malayan Peninsula borders the Andaman Sea to the East (Hamilton 1979). The presence of compressional and extensional environments existing side-by-side in a long and narrow zone may be interpreted in two ways. One is to assume the presence of an extensional arc immediately behind the trench. In such cases, however, oceanic rocks hardly ever rise above sea-level in order to provide persistent sediment, even olistolith sources as for example in the Marianas. The other way is to assume the presence of a major strike-slip system coincident with the arc axis. Pull-aparts will then create basins, and push-ups the sediment sources. We prefer this second model, because it also explains the great shuffling of the pre-existing tectonic units.

In the block diagram prepared on the basis of the geographic locations, petro-tectonic characteristics, and the environment of evolution of the pre-Malm units of the Central Pontides, we see the same tectonic environments as those in the Andaman Sea in similar relationships (Fig. 10). The south-dipping subduction of Palaeo-Tethys created a mélange belt and a magmatic arc to the north of a deep-sea environment, most likely formed in a transtensional setting and receiving material from the arc volcanism.

It is a matter of current debate whether this back-arc basin was ever floored by oceanic crust. Although Tekeli (1981) claimed that it had been, on the basis of the presence of ophiolitic blocks, we think that such blocks were all derived from the main Palaeo-Tethys, as inferred in the present paper. Moreover, in the eastern Central Pontides and further east, the Karakaya Basin merges with

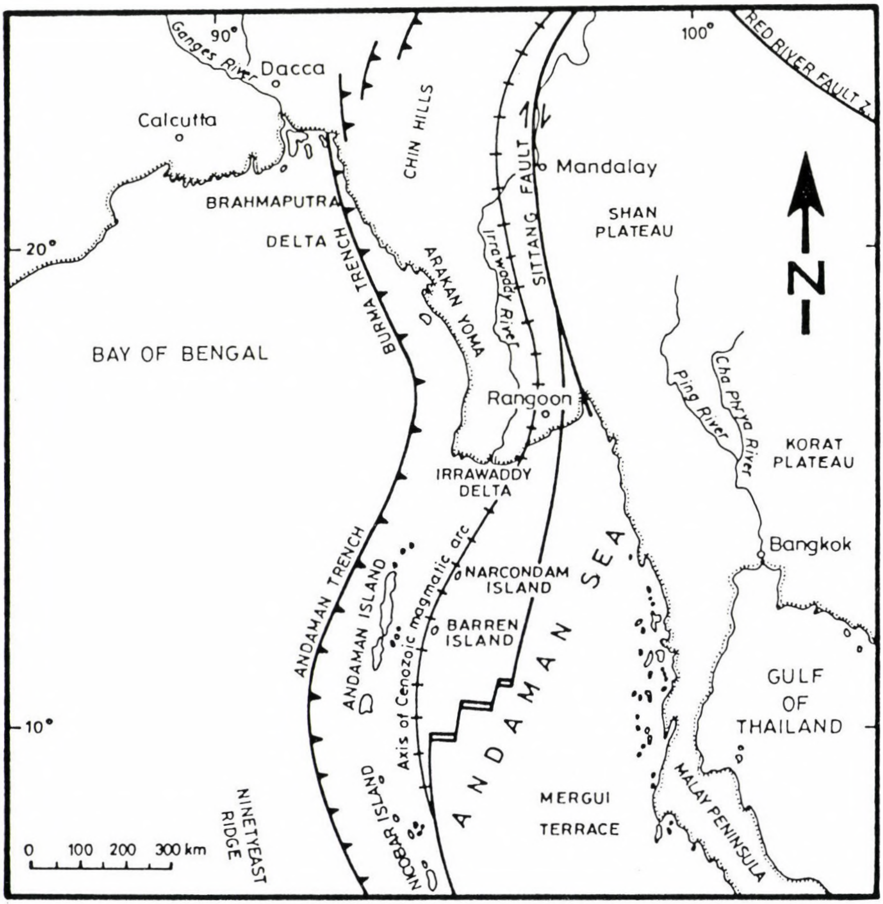

Fig. 9
Tectonic map of the Andaman Sea and surroundings (after Hamilton 1979)

Palaeo-Tethys. The Küre Unit was interpreted as a common cover to the Karakaya and the Elekdağ Units, suggesting a direct link between the Karakaya Basin and Palaeo-Tethys. In the area here described, the nature of the floor of the Karakaya Basin remains unclear. Only if one considers that the high-pressure metamorphism of the Gümüşoluğu Formation necessitates an oceanic anchor to pull the continental environment it represents into the subduction zone, our inferred location of the Gümüsolugu Formation along the margin of the Karakaya Basin implies that the latter had an oceanic floor. We believe this to be a strong argument for the oceanic nature of the floor of the Karakaya, as was directly proven by the presence of a Karakaya ophiolite much further east near Erzincan (Koçyiğit, 1990).

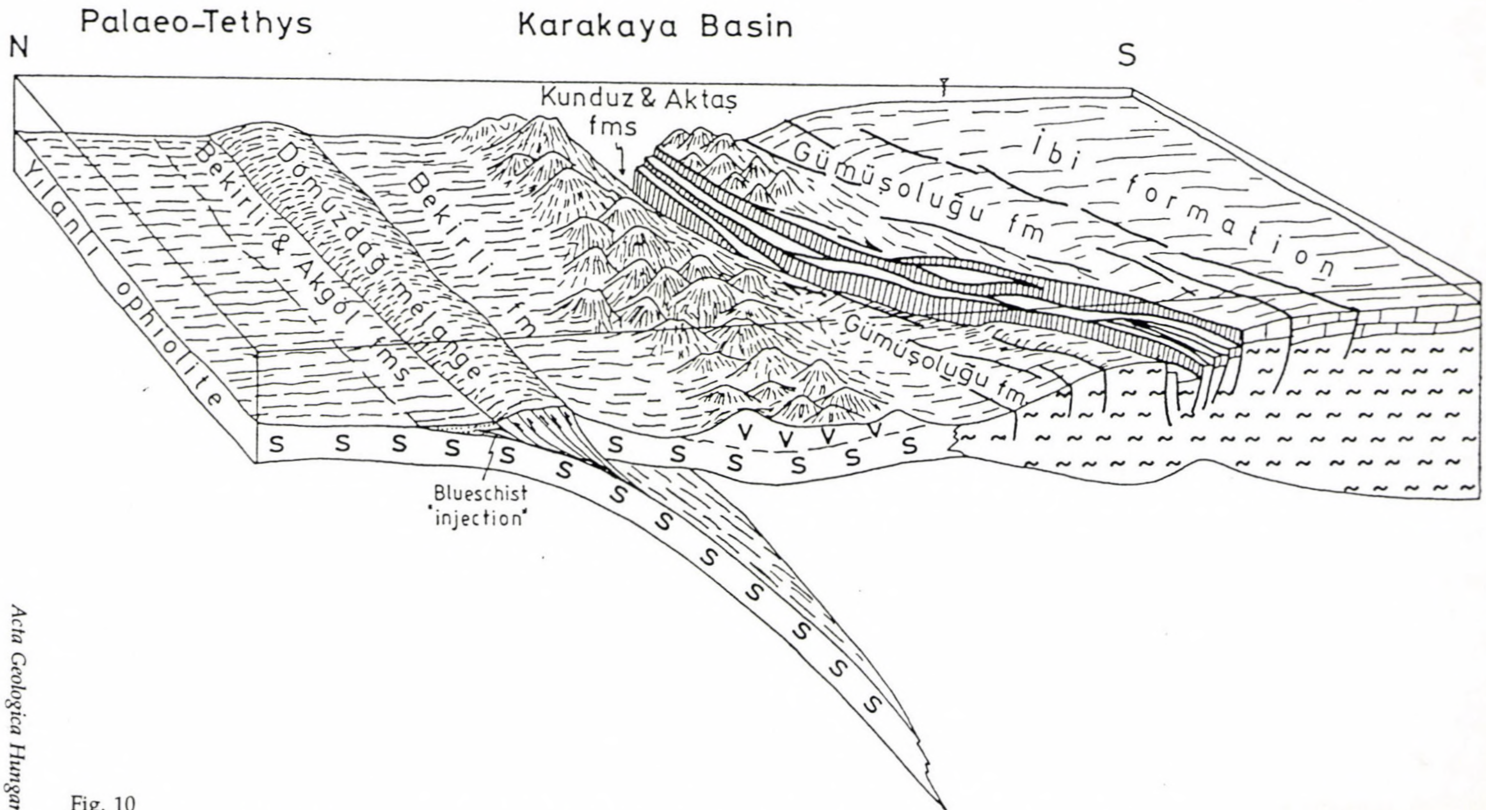

Fig. 10
Interpretative block diagram showing the tectonic settings of the pre-Dogger units of the Central Pontides

Owing to the unconformable Lias, the age of the closure of the Karakaya Basin in the Biga peninsula (Fig. 1), in the western part of the Sakarya zone, has been considered latest Triassic–Liassic (Yılmaz 1981; Okay et al. 1990). In contrast, in the Central Pontides the oldest unit unconformably covering the remnant of Palaeo-Tethys and the Karakaya Basin are Malm clastics and carbonates. Moreover, rocks belonging to the Küre Unit are tectonically overlain by rocks belonging to continental basement across a north-vergent thrust, later cut by post-orogenic Dogger granitoids (Tüysüz 1990). These data indicate that the Karakaya and Palaeo-Tethys closed during late Lias or Early Dogger. This closure was brought about by the collision of Laurasia with the Cimmerian continent, and the remnants of Palaeo-Tethys and the Karakaya Basin were sandwiched between them. It was during the Lias that the northern branch of Neo-Tethys rifted, internally disrupting the Cimmerian Continent (Görür et al. 1983), and the ruins of the orogenic collage formed from the remnants of the Karakaya Basin, the Palaeo-Tethys Ocean and the Cimmerian Continent form the basement of the northern margin of this Neo-Tethys branch.

Conclusions

This study demonstrates the Late Permian–Triassic opening by back-arc rifting of the Karakaya mini-ocean in Northern Turkey. It also suggests that this ocean merged with the main body of Palaeo-Tethys in the central part of the present Rhodope–Pontide fragment, in a manner analogous to the Andaman Sea/Indian Ocean communication through the Andaman/Nicobar Islands, north of Sumatra. The coexistence of compressional and extensional deformations throughout the history of the Karakaya Basin is through to suggest a significant strike-slip control during its evolution, similar to the situation in the Andaman Sea. This strike-slip component must be taken into account in the palaeotectonic evolution schemes of the Cimmerides.

Acknowledgements

This paper is based on data collected during the project "the geology of the Kargi Massif", jointly undertaken by the Turkish Petroleum Co. (TPAO) and the Istanbul Technical University. The late Mr. O. Sungurlu conceived the project and supported it, both financially and intellectually, by field visits and discussions until his sudden and premature death. Our gratitude to him is more then can be expressed in mere words.

For field support and discussions we are also grateful to H.S. Serdar and K. Saka. We thank A.M.C. Şengör, A.I. Okay, J.F. Dewey, A.H.F. Robertson and S. Kovács for constructive criticism on this manuscript.

References

Akyürek, B., E. Bilginer, E. Çatal, Z. Dağer, Y. Soysal, O. Sunu 1979: Eldivan-Şabanözü (Çankırı dolayında ofiyolit yerlesmesine iliskin bulgular. – Jeoloji Mühendisligi, 9, pp. 5–11.

Akyürek, B., E. Bilginer, B. Akbas, N. Hepsen, S. Pehlivan, O. Sunu, Y. Soysal, Z. Dağer, E. Çatal, B. Sözeri, H. Yıldırım, Y. Hakyemez 1984: Ankara– Elmadag–Kalecik dolayinin temel jeolojik özellikleri. – Jeoloji Mühendisligi, 20, pp. 31–46.

Aydın, M., Ö. Sahintürk, H.S. Serdar, Y. Özçelik, I. Akarsu, A. Üngör, R. Çokugras, S. Kasar 1986: Ballıdag–Çangaldağı (Kastamonu) arasındaki bölgenin jeolojisi. – Türkiye Jeol. Kur. Bült., 29, 2, pp. 1–16.

Baykal, F., 1952: Recherches géologique dans le Région de Kelkit-Şiran (NE l'Anatolie). – Rev. Fac. Sci. de l'Univ. d'Istanbul, Serie B, XVII, 4, pp. 289–304.

Bingöl, E., 1983: Prekambriyen–Jura arasında Türkiyenin olasılı jeotektonik evrimi. – Türkiye Jeol. Kur., 37. Bilimsel ve Teknik Kurultaiy Bildiri Özetleri, pp. 36–38.

Bingöl, E., B. Akyürek, B. Korkmazer 1973: Biga yarimadasının jeolojisi ve Karakaya Formasyonunun bazı özellikleri. – Cumhuriyetin 50. Yili Yerbilimleri Kongresi Tebligleri, . MTA Enst., Ankara, pp. 70–72.

Blumenthal, M.M. 1945: Kuzey Anadolunun bazı ofiolit mıntıkaları Liastan evveli devreye mi aittir? – MTA Mecm., 1–33, pp. 115–124.

Blumenthal, M.M. 1948: Bolu civarı ile Asağı Kizilirmak mecrasi arasindaki Kuzey Anadolu silsilelerinin jeolojisi. – MTA Yayınları, Ankara, Seri. B, 13, 265 p.

Curray, J.R., F.J. Emmel, D.G. Moore, R.W. Raitt 1982: Structure, Tectonics, and Geological History of the Northeastern Indian Ocean. – In: The Ocean Basins and Margins, A.E.M. Nairn, F.G. Stehli (Eds) v.6. The Indian Ocean, Plenum Press, New York, pp. 399–450.

Doğan, M. 1990: Pontid kuşağı Paleotetis ofiyolitlerinin jeokimyasal verilerle petrolojik, magmatik ve tektonik modellemesi (Unpublished Ph.D. Thesis). – Istanbul Univ. Fen Bil. Enst., 201 p.

Eren, R. 1979: Kastamonu–Taşköprü bölgesi metamorfitlerinin jeolojik, petrografik etüdü. (PhD thesis) – ITÜ Mim. Müh. Fak., 143 p.

Görür, N., A.M.C. Sengör, R. Akkök, Y. Yılmaz 1983: Pontidlerde Neotetisin kuzey kolunun açılmasına ilıkin sedimentolojik veriler. – Türkiye Jeol. Kur. Bült., 26, 1, pp. 11–20.

Güner, M. 1980: Küre civarının masif sülfit yataklari ve jeolojisi, Pontidler (Kuzey Türkiye). – MTA Enst. Derg., 93/94, pp. 65–109.

Hamilton, W. 1979: Tectonics of Indonesian Region. – Geol. Surv. Professional Paper 1078, 345 p.

Ketin, I. 1951: Über die Geologie der Gegend von Bayburt in Nordost Anatolien. – Fac. Sci. of Univ. Istanbul Rev., Ser.B, 16, pp. 113–127.

Ketin, I. 1962: 1:500 000 ölçekli Türkiye Jeoloji Haritas izahnamesi (Sinop). – MTA Enst. Yayını, Ankara, 111 p.

Koçyiğit, A. 1990: Structural relationships of three suture zones to the west of Erzincan (NE Turkey): Karakaya, Inner Tauride, and Erzincan sutures. – 8th Petroleum Congress of Turkey, Proceedings (Geology), pp. 152–160.

Kutluk, H., N. Bozdoğan 1981: IV. Bölge Üst Paleozoyik-Alt Mesozoyik çökelleri palinoloji ön raporu. TPAO (Turkish Petroleum Co.) – Internal Report, No. 1545.

Okay, A.I. 1984: The geology of the Agvanis metamorphic rocks and neighbouring Formations. – Bull. Min. Res. Expl. Inst. Turkey, 99/100, pp. 16–36.

Okay, A.I., M. Siyako, K.A. Bürkan 1990: Geology and Tectonic Evolution of the Biga Peninsula, northwest Turkey. – Bull. Tech. Univ. Istanbul, Special Issue on Tectonics, 44, pp. 191–256.

Saunders, A.D., J. Tarney 1984: Geochemical characteristics of basaltic volcanism within back-arc basins. – In Marginal Basin Geology: Volcanic and Associated Sedimentary and Tectonic Processes in Modern and Ancient Marginal Basins (Eds Kokelaar and Howells). Geol. Soc. London Spec. Publ., 16, pp. 59–76.

Şengör, A.M.C. 1984: The Cimmeride orogenic system and the tectonics of Eurasia. – Geol. Soc. America, Spec. Paper, 195, pp. 1–77.

Şengör, A.M.C. 1990: A new model for the late Palaeozoic-Mesozoic tectonic evolution of Iran and implications for Oman. – Robertson, Searle, Ries (Eds), Geol. Soc. London Spec. Publ., 49, pp. 797–831.

Şengör, A.M.C., Y. Yılmaz 1981: Tethyan evolution of Turkey: A plate tectonic approach. – Tectonophysics, 75, pp. 181–241.

Şengör, A.M.C., Y. Yılmaz, I. Ketin 1980: Remnants of a pre-Late Jurassic ocean in northern Turkey: Fragments of Permian-Triassic Palaeo-Tethys. – Geol. Soc. Am. Bull., Part I, 91, pp. 599–609.

Şengör, A.M.C., Y. Yılmaz, O. Sungurlu 1984: Tectonics of the Mediterranean Cimmerides. – In: Nature and evolution of the western termination of Palaeo-Tethys. Dixon, Robertson (Eds), Geol. Soc. London Spec. Publ., 14, pp. 117–152.

Tekeli, O. 1981: Subduction complex of pre-Jurassic age, northern Anatolia, Turkey. – Geology, 9, pp. 68–72.

Tokay, M. 1954: Filyos çayı agzı-Amasra-Bartın-Kozcağız-Çaycuma bölgesinin jeolojisi. – MTA Enst. Derg., 46–47, pp. 58–73.

Tüysüz, O. 1985: Kargi masifi ve dolayındaki tektonik birliklerin ayırdı ve araştırılması (Petrolojik inceleme). (Unpublished Ph. D. thesis). – Istanbul University, Fen Bil. Enst., 431 p.

Tüysüz, O. 1990, Tectonic evolution of a part of the Tethyside orogenic collage: The Kargı Massif, Northern Turkey. – Tectonics, 9, 1, pp. 141–160.

Tüysüz, O., E. Yığıtbaş, H.S. Serdar 1989: Orta Pontidlerin güney kesiminin jeolojisi. – TPAO internal report, 2596, 291 p.

Tüysüz, O., A.A. Dellaloğlu 1992: Çankırı havzasının tektonik birlikleri ve jeolojik evrimi. – Türkiye 9. Petrol Kongresi, Bildiriler, Jeoloji, pp. 333–349.

Wijkerslooth, P. de, 1942: Türkiye ve Balkanlardaki krom cevheri zuhuratı ile bunlarin bu ülkelerin büyük tektoniğine olan münasebetleri. – MTA Enst. Derg., 26, pp. 35–75.

Yılmaz, O. 1979: Daday–Devrekani masifi kuzeydogu kesimi metamorfik petrolojisi.– (Thesis) Hacettepe Üniv., Yerbilimleri Enst., 176 p.

Yılmaz, Y. 1974: Geology of the Gümüshane granite (Petrography). – Istanbul Univ. Fen Fak Mecm., Ser. B, 39, (3-4), pp. 157–172.

Yılmaz, Y. 1981: Sakarya kıtası güney kenarının tektonik evrimi Istanbul Yerbilimleri, 1, 1–2, pp. 33–52.

Yılmaz, Y., O. Tüysüz 1984: Kastamonu-Boyabat-Vezirköprü-Tosya arasindaki bölgenin jeolojisi (Ilgaz-Kargı masiflerinin etüdü). – MTA (Mineral Research Inst. of Turkey) internal report, 275 p.

Yılmaz, Y., O. Tüysüz 1988: Kargi masifi ve dolaylarında Mesozoyik tektonik birliklerin düzenlenmeleri sorununa bir yaklasim. – TAPG Bull., 1–1, pp. 73–86.

Yılmaz,Y., O. Tüysüz 1991: Anatomy of an imbricated zone: Geology of the Kargi Massif, Central Pontides. – Bull. Tech. Univ. Istanbul, 44, pp. 279–299.

Yılmaz, Y., A.M.C. Sengör 1985: Palaeo-Tethyan ophyolites in northern Turkey: Petrology and tectonic setting. – Ofioliti, 10, 2/3, pp. 485–504.

Yiğitbaş, E., O. Tüysüz, H.S. Serdar 1990: Geologic characteristics of Late Cretaceous active continental margin in the Central Pontides. – 8th Petroleum Congress of Turkey, TAPG and UCTEA-CPE, Proceedings (Geology), pp. 141–151.

Acta Geologica Hungarica, Vol 37/3–4, pp. 351–367 (1994)

Mineral resources of Estonia and the problems of their exploitation

Anto Raukas
Institute of Geology, Estonian Academy of Sciences
Tallinn

In spite of its small area and relatively simple geological structure, Estonia is rich in mineral resources, the mining of which has caused severe environmental damage. Estonian phosphorite deposits are the largest in Europe (about 750 million tons of P_2O_5). Reserves of limestone, dolomite and clay are practically unlimited. 22.3% of the territory is covered by bogs with the maximal thickness of peat of 16.7 m. Mineral waters with differing degrees of mineralization and balneological properties are used in many parts of the Republic. Curative sea muds have been used since the beginning of the 19th century. Serious ecological problems have arisen in connection with the world's largest exploited (14.9 million tons in 1993) oil shale deposits in NE Estonia, supporting the generation of electric power (80% of the total mined) and the chemical (20%) industry. Proven reserves are estimated at 3800 million tons,and possible reserves are considered much larger, as are the reserves of alum shale (up to 60 billion tons), rich in uranium and other (Mo, V, Th, Re a.o.) valuable microelements. As a result of mining activities, both air and water are highly polluted, and natural landscapes have been spoilt in about 8% of the republic's territory.

Key words: mineral resources, oil shale, alum shale, phosphorites, peat, clay, building materials, curative mud, mineral waters, human impact

Geological structure

Estonia, the northernmost of the Baltic Republics, is situated on the southern slope of the Fennoscandian Shield, in the northwestern part of the East European Platform. The boundary between the Fennoscandian Shield and its buried southern slope which runs through the Gulf of Finland is determined by the northern limit of sedimentary rocks. From the Vendian to and including the Devonian, the Estonian area was mainly one of sinking, whereas regions to the north were predominantly subjected to uplift. As a result, both the surface of the crystalline basement and the overlying Vendian and Palaeozoic sedimentary cover have a gentle dip (7–15′) to the south (az. 179°); bedrock of different age crops out in the form of more or less W–E-striking belts (Figs 1, 2).

The depth of the crystalline basement ranges from 100 m in North Estonia up to 600 m in the south-eastern part of the Republic (Fig. 2). In the Valmiera–Lokno uplift (in the SE area) the basement reaches a depth of – 232 m (Puura et al. 1983). This basement is composed of Lower Proterozoic rocks, such as gneisses, migmatites, amphibolites, shales and quartzites which were folded,

Address: A. Raukas: Estonia Ave 7, Tallinn EE 0001 Estonia
Received: 23 October, 1993

0236–5278/94/$ 5.00

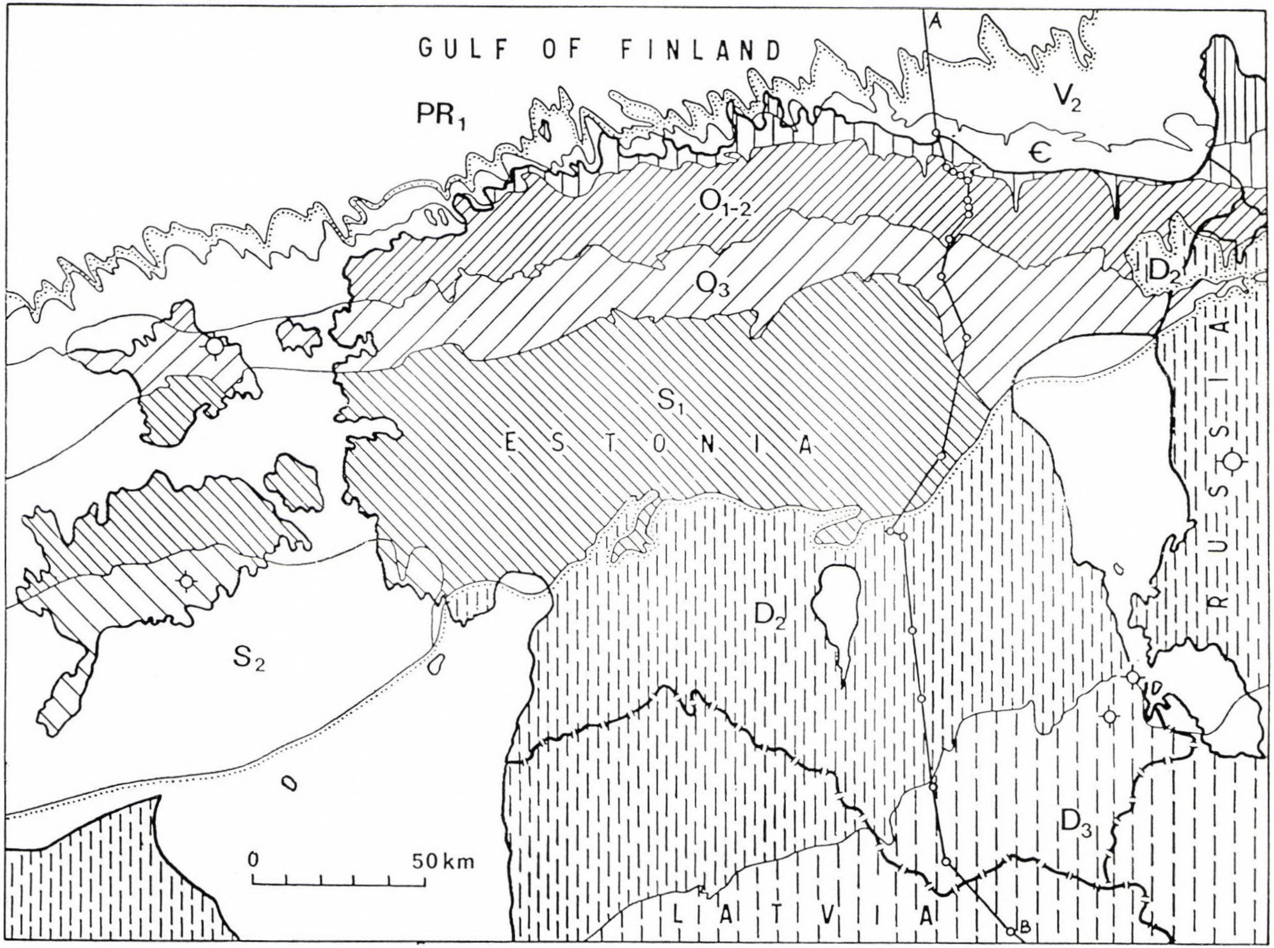

Fig. 1
Geological Sketch Map of Estonian Bedrock. Meteoritic craters and astroblems are marked with circles O. Compiled by R.Vaher

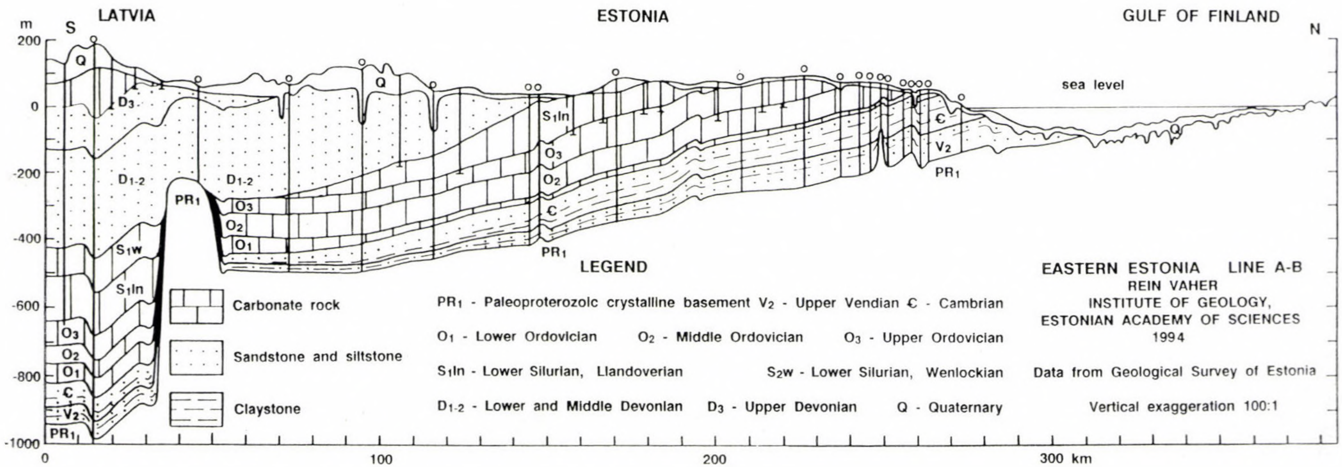

Fig. 2
Geological cross-section of Eastern Estonia. For location of the section see Fig.1

divided into blocks by faults and interspersed with pegmatite veins. Intrusions of rapakivi or mafic rocks occur in limited areas, and iron metallization is observed in faulted zones.

In 1931, a strong anomaly was discovered during magnetometric investigations near the town of Jõhvi. Before World War II two boreholes were drilled. In the first core, ferriferous quartzites were found at depths of 368–505 m, and in the second core at 667–721 m (Luha 1946). Recent investigations (Raudsep et al. 1993) have demonstrated that iron ore occurs to a depth of 700 m; its reserves are estimated at approximately 629 million tons. Iron content is varied (25–34.4%).

The sedimentary bedrock is composed of Ordovician and Silurian carbonate sedimentary rocks in North and Central Estonia, and of Devonian sandstones in South Estonia (Fig. 1). The total thickness of Vendian rocks (mainly clays and sandstones) amounts to 155 m; Cambrian clays, siltstones and sandstones are up to 125 m, Ordovician rocks 180 m and Silurian up to 435 m thick. The maximum thickness of Devonian rocks was estimated in the Hino borehole at 448.5 m (Rõõmusoks 1983).

Quaternary deposits are of uneven distribution (Raukas 1978). In North Estonia, on the Ordovician and Silurian carbonate rocks the thickness of the Quaternary cover is usually less than 5 metres. Occasionally, on alvars, it is virtually absent. The Quaternary cover is at its thickest in the Haanja and Otepää Heights (often more than 100 m) and in South Estonian buried valleys (up to 207 m).

Historical background

Estonian mineral resources were already used before written records began (The history..., 1986). Erratic boulders were used in the Mesolithic (7500–3000 B.C.), when prehistoric man learnt to make weapons from them. At around 6000 B.P., people discovered that clay made good earthenware. About 5000–4000 B.P. carbonate rocks were applied to the building of townlets and fortified settlements. The birth of local metallurgy – smelting of iron from bog ore – goes back to at least the beginning of our era. Since 1230, lime has been widely used as a binder, and bricks made of local clays have served as building material for strongholds and churches.

We have good reason to believe that in the Lõhavere stronghold, lead was smelted from galena of the Adavere Stage as early as the beginning of the 13th century. In 1803 in the Arusaare limestone quarry a galenite block 4 poods in weight was found. Every pood contained 9 kg of Pb and 5.3 kg of Ag. Galena is probably of hydrothermal origin and it is found in many places all over Estonia (Navesti, Viivikonna etc.), but commercial reserves have not yet been estimated (Raudsep et al. 1993).

The manufacture of glass from surface sands was introduced in the 17th century. By the end of the 18th century travertine and lake chalk had found an application as fertilizers, and peat as a fuel. The first evidence of the use of curative muds in Estonia dates from this period. The first industrial enterprises to produce cement, bricks and glass in Estonia were established in the 1870s (The history..., 1986).

The mining of kukersite oil shale began in 1916 at Kohtla–Järve. The processing of oil shale was carried out by a state-owned enterprise founded in 1919, and by several private companies. In 1920 a phosphorite mine was opened at Ülgase, and since 1939 an open pit has been operating at Maardu.

After the presence of uranium in Estonian alum shale (dictyonema argillite) was discovered in the spring of 1945, a high-level meeting attended by L. Beria, K. Voroshilov, G. Malenkov and some other high-ranking members of the Soviet Government, as well as leading scientists (P. Kapitsa, M. Althausen) took place in the Kremlin, where the problems of uranium production from Estonian alum shale were discussed. Three main methods for the separation of metals from the shale were subsequently utilized:

1. the autoclaving-based technology developed in the Moscow Institute of Chemical Technology;
2. the biochemical technology developed in the Institute of Mineral Resources in Moscow; and
3. the combined power–hydrometallurgical technology developed in the Estonian Academy of Sciences (Althausen 1992).

Production of uranium concentrate was undertaken at Sillamäe, NE Estonia. The data concerning this production technology and wastes were kept top secret. It was only in April of 1992 that the Ministry of Atomic Energy of the former USSR for the first time informed the Chairman of the Presidium of the Estonian Supreme Soviet of what was occurring in this region.

Main mineral resources

Kukersite oil shale

Kukersite is light to dark brown in colour and consists of organic, carbonate and terrigenous components. The material of the oil shales accumulated in the marginal part of the shallow epicontinental Baltic Palaeobasin. Its organic matter contains the algal microphytofossils *Cloeocapsomorpha prisca*. Thin interlayers of kukersite are spread throughout the entire section of the Ordovician carbonate rocks, from the Volkhov to the Porkuni Stage (Table 1). The Kukruse Stage is known to be the richest in kukersite, as regards both its areal distribution (5000 km^2) and the thickness of the layer (max. 60–70 cm). Here the commercial seams have been identified at two levels. The lower seam is referred to as the Kiviôli Formation, and it is also exploited in the Leningrad District (the Estonian and Leningrad mining areas, respectively). The upper seam is related to the Peetri Formation.

Table 1
Stratigraphy of the Estonian bedrock

System	Sub-system	Series	Regional stage	Some important local units: substages (st), formations (f), beds (b), stratas (s)
DEVONIAN	Upper	Frasnes	Sargajevo	Dubniki (b) Chudovo (b) Pskov (b) Snetnaja Gora (b)
	Middle	Givet	Amata Gauja Burtniek	
		Eifel	Aruküla	
			Narva	Kernavé (st) Leivu (st) Vadja (st)
			Pärnu	Tamme (b) Tori (b)
	Lower	Ems	Rezekne	
		Prague		
		Lochkov		
			Tilze	
SILURIAN	Upper	Pridoly	Ohesaare	
			Kaugatuma	
		Ludlow	Kuressaare	
			Paadla	
	Lower	Wenlock	Rootsiküla	
			Jaagarahu	
			Jaani	
		Llandovery	Adavere	
			Raikküla	
			Juuru	

ORDOVICIAN	Upper	Ashgill	Porkuni	
			Pirgu	
			Vormsi	
			Nabala	
	Middle	Caradoc	Rakvere	
			Oandu	
			Keila	
			Jõhvi	
			Idavere	
			Kukruse	
		Llandeil	Uhaku	
		Llanvirn	Lasnamägi	
			Aseri	
			Kunda	
	Lower	Arenig	Volkhov	
			Latorp	
		Tremadoc	Ceratopyge	
			Pakerort	
CAMBRIAN	Upper			Kallavere (f) Tsitre (f) Ülgase (f)
	Middle	Deimena		Paala (s) Ruhnu (s)
	Lower	Aisčiai		Irben (f) Soela (f)
		Liivi	Talsi	Tiskre (f) Lükati (f) Sôru (f)
		Baltic		Lontova (f)
VEND.	Upper	Valdian	Kotlin	Voronka (f) Kotlin (f) Gdov (f)

The commercial seam of kukersite is of a cyclical structure due to the alternation of the layers of kukersite and limestone; this phenomenon is traceable over an extensive area (Geology..., 1986). Kukersite layers thin or die out towards the peripheral parts of the deposits. This is accompanied by a decrease in kerogen content. The highest productivity (conditional fuel per 1 m^2 of the deposit) has been noted in the northern part of the Estonian mining area, between Kukruse and Jôhvi (1.5 t/m^2). Here the calorific value of oil shale is 10–12 MJ/kg. At the outer boundary of the deposit the calorific value is 1.7 times, and the yield about 3 times, lower. With the southward dip of the layers the depth of the commercial seam increases to 100 m. As a result the prime cost grows abruptly towards the periphery of the area.

The kukersite oil shale is the most important mineral resource in Estonia; some of its characteristics are shown in Table 2. Of the total mined, 80 per cent is used by electrical power plants and 20 per cent by the chemical industry. Kukersite is produced in six underground mines (7.8 million tons in 1993) and four open-pit mines (7.1 million tons). The depth of quarries is 15–20 m, whereas that of mines is 20–60 m. The thickness of the commercial seam attains 2–3 m. The total output of kukersite in 1980 has increased sixteen times in comparison to 1940 (or 1946) (Fig. 3). The Estonian deposit currently mined is estimated to hold commercial- quality kukersite reserves of 3.8 billion tons. In adjacent areas, reserves of a lower-quality kukersite are estimated at 3.9 billion tons. Superficially investigated kukersite reserves in the Tapa deposit are 2.5 billion tons (Fig. 4). In view of the current level of output and related losses (27.8% in mines and 12.3% in quarries in 1993), the reserves of kukersite will, in all probability, be exhausted in the next hundred years.

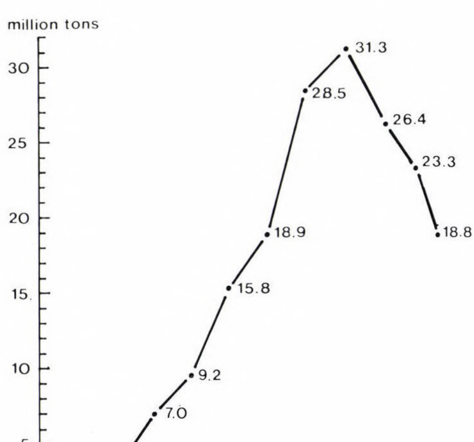

Fig. 3
Dynamics in the production of Oil Shale between 1940 and 1992

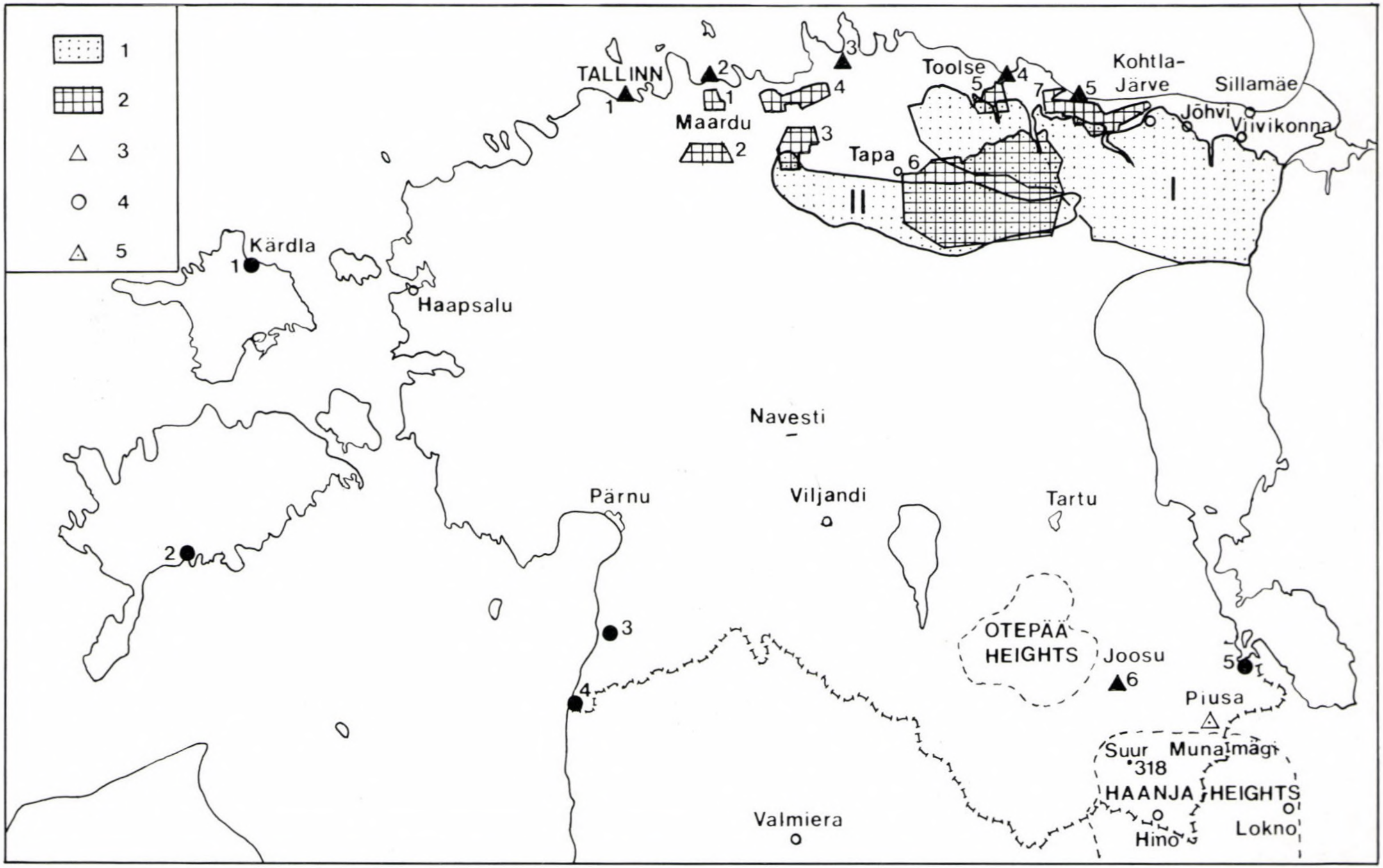

Fig. 4
Main mineral deposits mentioned in the text: (1). *oil shale*: I – Estonian Deposit; II – Tapa Deposit; (2). *phosphorite*: 1. Maardu; 2. Raasiku; 3.. Kehra; 4. Tsitre; 5. Toolse; 6. Rakvere; 7. Aseri; (3). *clay*: 1. Kopli; 2. Kallavere; 3. Kolgaküla; 4. Kunda; 5. Aseri; 6. Joosu; (4). *mineral water*: 1. Kärdla; 2. Kuressaare; 3. Häädemeeste; 4. Ikla; 5. Värska; (5). *sand for glass*: Piusa

Table 2
Some characteristics of Estonian kukersite oil shale (After Geology... 1986 with complements)

Indices of the oil shale seam	Unit of measure	Index
Depth of the base	m	5–120
Thickness of the seam	m	1.6–3.2
Total thickness of oil shale layers	m	1.2–2.6
Organic matter content	%	25–40
Ash content	%	35–49
Specific calorific value of commercial oil shale	MJ/kg	6.3–12.2

Alum shale (Dictyonema argillite)

Estonian alum shale is dark brown to brownish black oil shale with a low calorific value (6.1–6.7 MJ/kg) and a low organic matter content (up to 18 per cent). It is related to the Lower Ordovician Pakerort and Ceratopyge Stages (Table 1) and covers an area of 12 000 km^2. The thickness of the bed varies from 3–6 m in the western part of the area to 3 m in the eastern part. It overlies sandstone, thin interlayers of which can also be observed in places in the shale. Alum shale is an offshore clayey sediment of the shallow epicontinental Baltic Palaeobasin. It contains graptolites and therefore is often called graptolitic or kerogenic argillite. The origin of the organic matter is unknown.

The reserves of alum shale have not yet been precisely evaluated, but , they are expected to amount to 60 billion tons. The rock contains about 20 valuable elements, such as vanadium, molybdenum, strontium and rare trace elements. As alum shale is rather rich in pyrite (2 per cent), with its burning abundant sulphur compounds are emitted with smoke, making it a source of atmospheric pollution.

According to the data of the Estonian Geological Survey and some other research institutions, the average chemical composition of Estonian alum shale is as follows:

SiO_2: 48–50%, Al_2O_3: 10–12%, K_2O: 6–7%, Fe_2O_3 4–5%, S: 3–5%, CaO and MgO: 1–2%, TiO_2, Na_2O, P_2O_5 and CO_2 less than 1% (Raudsep et al. 1993).

The mean content of some valuable elements in the Toolse deposit (g/t) is:

U: 192 (3–850), V: 800, Mo: 430, Pb: 118, Zn: 85, Cu: 80, Cr: 42, Ni: 92, Co: 23, Th: 13 (in some places up to 500), Y: 45, Cd: 20 (Raudsep et al. 1993 a.o.).

Within the limits of the North Estonian phosphorite deposits (Maardu, Toolse), alum shale overlies a layer of Obolus phosphorite. In the case of its surface mining, alum shale is removed and mixed in the waste dump with other rocks of the overburden (glauconitic sandstone, quartz sand and limestone). However, if they lie above the water table in the waste dump, the loosened layers of shale are subject to self-ignition, which may occur even several decades after the mining.

In 1989 open cast phosphorite mining at Maardu covered an area of 6.36 km^2. According to Veski (Institute of Chemistry, Estonian Acad. Sci.), 4.15–23.54 kg of U and up to 1.95 kg of Th enter Lake Maardu from every square km. Waste hills at Maardu contain about 73 million tons of alum shale. If there were only 30 g of U per ton of alum shale, then 2.19 million kg of U would leach into the surface and groundwaters and enter the Gulf of Finland.

Because of the contamination of the environment and the destruction of forested areas due to underground burning, the elimination of self-ignition of alum shale, as well as the elaboration of comprehensive mining and utilization technologies, have become the most important targets of investigations (Viiding and Raukas 1984).

Phosphorites

Estonian phosphorites (the so-called Obolus phosphorites) are the near-shore accumulations of shells and detritus of lingulate brachiopods of the families Ungula, Schmidtites, Keyserlingia, etc. (10–90 per cent, 35 per cent average) in quartzitic sandstone. The content of shells in sandstones probably depends on tidal movements. In comparison with other kinds of phosphorite, Obolus phosphorite is poor in P_2O_5 (less than 10 per cent on average), but it serves as a valuable raw material for the manufacture of fertilizers as it can be easily concentrated by flotation, and besides, it is favourably located from economic and geographical points of view (Viiding and Raukas 1984).

Shells of brachiopods consist of the mineral francolite, with about 36 per cent content of P_2O_5. Hence, the quality of phosphorite as a raw material depends on its shell content. Enrichment yields a concentrate with up to 27 per cent P_2O_5 content.

Obolus phosphorite is found in North Estonia in the Lower Ordovician Pakerort Stage (Table 1), where in places it forms a stratum ranging from 1 to 3 m in thickness (Maardu, Toolse, Aseri deposits). The thickest phosphorite layers (5 m on the average) occur in the Lääne-Virumaa District in the vicinity of Rägavere and Assamalla, where the P_2O_5 content is also high (10–11 per cent). In these areas the phosphorite layers lie at a depth of 50–250 m. According to the present forecasts the Rakvere phosphorite deposit would be, in all likelihood, the largest in Europe (Raudsep 1991, The Geology... 1987). Resources of the deposit are estimated at about 750 million tons of P_2O_5, i.e. ca. 1–2% of the total phosphorite (P_2O_5) supplies in the world.

Commercial phosphorite reserves have been studied in seven (Maardu, Raasiku, Kehra, Tsitre, Toolse, Aseri and Rakvere) deposits (Fig. 4). Of those, the Toolse deposit, where the depth of the phosphorite layer is favourable for exploitation, will undoubtedly be of the greatest significance in the nearest future. Phosphorite reserves there are estimated at 330 million tons.

Surface mining in Maardu has given rise to several problems concerning the utilization of some ancillary minerals contained in the overburden. The possibilities of comprehensive mining of the overburden have been studied for the Toolse deposit. For every ton of phosphorite mined, the overburden will yield 0.5 tons of alum shale, 0.2 tons of glauconitic sandstone, 2.0 m^3 of high-quality building and cement limestone, 1.0–1.5 m^3 of lower-quality limestone and 0.4 m^3 of quartz sand (Kivimägi and Teedumäe 1971).

In open cast mining at the Toolse deposit, the disposal of alum shale in waste dumps must be avoided. The argillite of Toolse is much richer in pyrite than that of Maardu, and tends even more to self-ignition, thus posing a great threat to the environment.

The opening of new phosphorite deposits requires supplementary studies for the purpose of the rational use of mineral resources and observation of the principles of environmental protection. All perspective deposits are located in densely populated agricultural areas. Technological, economic, social, hydrogeological and other studies suggest that the realization of the opening of new phosphorite mines in Estonia under the current difficult economic situation would not be expedient. In 1987 the government of the Republic decided not to proceed with mining phosphorites in Estonia in this century. The last functioning mine at Maardu, close to Tallinn (with the annual output of 0.5 million tons), was closed in 1991, because the greater part of the deposit had been exhausted and the ecological situation of the region was catastrophic.

Peat

Mires (fens, bogs, swamps), which partly coincide with forest areas, occupy about 22.3% of Estonia's territory. At present, total peat reserves are estimated at 2.2 billion tons. About 0.4 billion tons of peat are suitable as animal litter, and 1.8 billion tons can be used for fuel and for soil improvement. Within Estonia as a whole there are 165 000 mires and peatlands with an area of more than 1 hectare, of which 1,500 are of commercial importance (Fig. 5). The largest bogs are Puhatu (468 sq. km), Epu-Kakerdi (417 sq. km), Lihula-Lavassaare (383 sq. km) and Sangla (342 sq. km). The greatest thickness of peat (16.7 m) was measured in the Võllamäe bog on the foot of Suur-Munamägi Hill (318 m), which is the highest point of the Baltic States. The mean annual peat output was for a long time about 5 million tons; about 0.9 million tons were used for making briquettes, 1.6 million tons for animal litter and 2.4 million tons for soil improvement. Now peat production is decreasing: in 1991 the total output was 1.8 million tons, in 1992 1.36 million tons and in 1993 only 621 thousand tons. Part of the production (some 110 000 tons in 1991) is exported to foreign countries (Italy, Netherlands, Germany, etc.) as a substrate for horticulture.

There would be sufficient reserves here for an additional 150 years if waste in production were avoided. In fact, production losses amount to 35–40% (Orru 1987), which complicates the situation considerably. Besides, by January 1, 1987, 28% of the area of Estonian mires had been drained (15% as forests, 12% for agricultural use and 1% for peat production), and therefore more mires should be taken under state protection. At present about a third of undrained mires are under such protection.

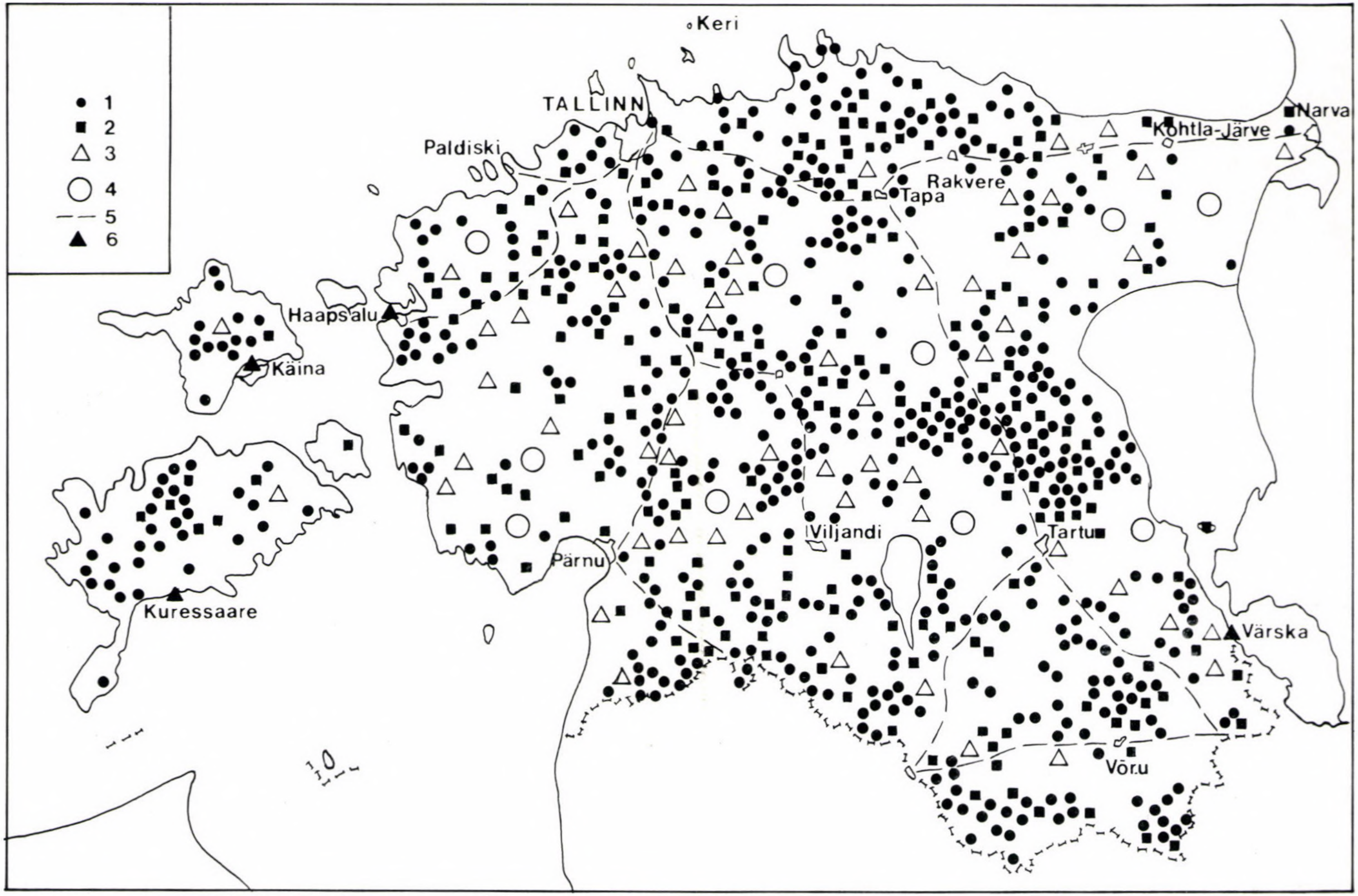

Fig. 5
The most important peat bogs (1–4) in Estonia according to data of the Estonian Geological Survey and the Estonian Research Institute of Agriculture and Land Improvement (Raukas 1992) and main deposits of curative mud (I–IV). Conventional signs: 1. bogs of 100–500 ha; 2. 500–2000 ha; 3. 2000–10 000 ha; 4. more than 10 000 ha; 5. railways; 6. mud deposits: I – Käina; II – Kuressaare III – Haapsalu; IV – Värska

Mineral resources of secondary importance

Sand and gravel

As Estonian landforms have mostly been shaped by continental glaciers, resources of sand and gravel are fairly abundant. Partly due to this, the value of such material has often been underestimated, and therefore they have frequently been wasted. As a result of this practice, resources of sand and gravel are already practically exhausted in some parts of the Republic.

In Estonia there are altogether more than 900 gravel and sand deposits, whose commercial reserves are evaluated at about 250 million cu m. Inferred reserves amount to about one billion cu m (Raudsep et al. 1993). 6.9 million cu m of sand and gravel were mined in 1991, 2.2 million cu m in 1992 (Paalme 1993), which is much less than in previous years. Nevertheless, a new increase is predicted at the turn of the century.

The only glass and foundry sand deposit is located at Piusa in SE Estonia. In the Upper Devonian sandstones reserves are estimated at about 4.5 million tons.

In terms of mineral wealth protection, the main problems to be solved involve the exploitation of construction sand and gravel: a rational network of large, highly-mechanized quarries must be established, the purposeful and depleting use of reserves must be controlled, and mined-out quarries must be reclaimed. Since a great number of sand and gravel relief forms are unique objects of scientific research and/or places for recreation, the interests of industry and nature protection frequently collide. An important undertaking of the Estonian geologists is the compilation of a detailed "red data book" on landforms and other unique geological objects (Viiding 1985) which will be published under the title of "Ürglooduse raamat" ("The book of Primeval Nature").

Clay

Clays occurring in Cambrian, Devonian and Quaternary sediments are mostly easily fusible, and their resources are practically unlimited. They are used mainly as a raw material for ceramics (output in 1992: 165 000 cu m and in 1993: 75 000 cu m) and cement. Refractory clay has been found only in the Devonian clay deposit at Joosu.

Limestone and dolomite

Commercial reserves of limestone and dolomite deposits are estimated at about 750 million cu m. Limestone is used as a raw material in producing lime, cement, building stone and glass; it also has applications in the chemical, pulp and paper industries (Teedumäe 1988). Dolomite is suitable for making facing stones. Of the total annual output (3.1 million cu m in 1991 and 950 000 cu m in 1993), the greater part is used for construction work.

Curative mud

Curative mud has been used in health resorts since the beginning of the 19th century. Although Estonia borders on the sea, the usable deposits of sea mud are not extensive (Fig. 5),and the reserves of the three major deposits (Haapsalu, Kuressaare and Käina) are estimated to be 2.6 million cu m. The explored deposits of lake muds (gyttja) occur in 121 lakes. The largest deposits of curative lake mud are situated at Värska (45 million tons). Lake mud can be used not only for medical purposes, but also as fertilizer, fodder for livestock, fuel, etc. Total reserves of lake mud are estimated at 2.5–3 billion cu m.

Mineral water

Mineral water with different degrees of mineralization and balneological properties is in use in many parts of Estonia. The total yield of the five larger mineral water aquifers of Häädemeeste, Ikla, Kärdla, Kuressaare and Värska (Fig. 4) is 4 700 cu m per day. Hydrogeologically, these are artesian waters, and are connected with different ground water complexes; chemically they belong to the chloric calcium-sodium or sulphatic-sodium type.

Other mineral resources

Other mineral resources, mainly of local interest, are lake chalk (utilized as an additive to concentrated fodder, as a neutralizer of heightened acidity in silage, and crayon), pyrite (resources about 100–200 million tons), ocher, glauconite sand (as fertilizer, colour earth, water purifier) and diatomite (as isolation material).

In several places in Estonia, mainly in the northern part of the mainland and on the islands of the Gulf of Finland, natural gas (methane) occurrences are known. In 1905–1912 local gas was used in the lighthouse and for heating on the Island of Keri.

Crystalline erratic boulders (about 2 million cu m) and rocks from the basement, which near Tallinn are at a depth of about 170-200 m can be used as road metal. At the Maardu deposit these reserves are estimated at about 258 million cu m (Raudsep et al. 1993).

Human impact

The territory of Estonia has been inhabited throughout the Holocene. Land cultivation did not begin to dominate in the life of ancient people until the beginning of the Early Iron Age, about 600 years B.C. Since that time, man has inflicted incurable wounds on nature. The vigorous intensification of agriculture and industry during the Soviet occupation was accompanied by a sharp increase in the exploitation of mineral resources and by an ever worsening impact on the environment. Over the past 50 years, the population of Estonia has increased some 1.4 times, the number of workers and employers 3.8 times, industrial output 4.2 times, the production of mineral resources 15 times, and the generation of electric power 100 times.

Human activities have spoilt the natural landscape in about 8% of the territory of Estonia, and drawing up recommendations for land improvement is one of the most important tasks facing Estonian geologists today. This will not be easy, because annual exploitation in the mining industry alone amounts to over 70 million tons of solid mineral resources, which makes up over 50 tons per capita. Moreover, it should be noted that these figures do not include the sand used as a ballast material and the overburden removed from open pits. In 1991 the territory of the mined area increased by 344 hectares in mines and by 269 hectares in open pits (Paalme 1993). Every year, about 600 ha of land are lost to oil-shale pits. In northeastern Estonia about 250 ha are covered by ash-fields and waste hills (Raukas 1992).

As a result of oil shale mining alone, the area of the quarries covered with waste rocks increases by several hundred hectares annually. Out of the total area of 10 000 hectares spoiled by mining activities, 8330 hectares had been reclaimed by January 1, 1992. Most of these areas have been reforested and 110 hectares returned to agricultural use, but such areas are far from being of top quality.

In the future, alongside the designing of new mining enterprises, much more attention should be paid to the elaboration of technologies that are environmentally safe. The main targets of mineral wealth protection include not only the exhaustive mining with minimum losses and rational utilization of mineral resources, but also the disposal of processing wastes. In some cases it seems cheaper to use old waste hills in the oil shale basin than to open new mines. At present, Estonian geologists are engaged in solving these complicated problems and elaborating scientifically motivated recommendations for the economic and social development of their homeland. It is well known that in the Soviet system the Estonian economy was centralized under Moscow's control, and that nature conservation was a matter of secondary importance. In independent Estonia nature conservation and mineral wealth protection will presumably gain first-rate importance. In the beginning of April, 1992, all the countries of the Baltic Sea catchment area approved the Baltic Sea Joint Comprehensive Environmental Action Programme, which besides the commitment made by the individual states for improving the state of the sea, includes plans for international participation in the liquidation of "hot spots" within economically less-well-off states (National..., 1992).

Much hope is placed on the support of and cooperation with the countries of the European Community. Already significant financial and technological support has been received from Sweden and Finland. This is understandable in part, because Estonia is one of the greatest polluters per capita of European air and waters. According to the "National Report of Estonia to UNCED 1992" (National..., 1992) Estonia is among the worst European countries in the production of SO_2 per capita (140 kg). The production of CO_2 in Estonia in 1990 was 35.8 million tons, one of the highest per capita all over the world.

Serious environmental problems are caused by some 300 000 tons of dust emitted into the atmosphere annually, approximately 200 000 tons of which originates from the chimneys of the power plants processing the oil shale and containing mostly oxides of alkali and alkaline-earth metals. The pH of precipitation is thus highly alkaline in the vicinity of these plants. In addition to this, fly ash contains heavy metals, including toxic ones, in relatively high concentrations: for instance, some 50 tons of lead, 30 tons of mercury, 30 tons of zinc and 20 tons of copper are emitted annually. About 90% of the pollutants remain within 30 km of the pollution sources via dry and wet deposition, causing critical ecological conditions.

Another 15 million tons of industrial waste are added yearly. In Sillamäe, radioactive waste from the chemical and metal production plant, which formerly belonged to the Soviet military industrial complex (and was earlier involved in concentration of uranium), has been dumped in a tailing which lies on the coast of the Gulf of Finland. The tailing includes an estimated 1200 tons of uranium, 750 tons of thorium; the activity of radium exceeds 7 kCi. The radioactively polluted area covers over 100 ha, having an impact on the health of local inhabitants (National..., 1992). To all of that, we should add the military pollution by former Soviet Army regiments. This includes the pollution of surface water, groundwater, soils and bottom sediments of the sea and lakes, as well as damage of picturesque landscapes, all of which needs the participation of geologists in resolving the resultant acute problems.

Environmental and nature protection have a long tradition in Estonia. The Nature Investigators' Society has already been active since 1853. In 1910 a bird sanctuary was established on the Vaika islets in the West-Estonian (Moonsund) archipelago. The first nature protection law was approved in 1935 and 47 nature reserves were established before 1940. In 1957 the new Nature Protection Law of Estonia was approved, being the first of its kind in the Soviet Union and occupied Baltic countries. In 1976 Lahemaa National Park was established on the northern coast, as the first national park within the USSR. On February 23, 1990 the Law on the Protection of Nature in Estonia was approved. At present there are three National Parks, one Biosphere Reserve, 5 State Nature Reserves, one Hydrological Reserve, 14 Landscape Reserves, 6 Botanical-Zoological Reserves, 30 Mire Reserves, four Botanical Reserves, 20 Ornithological Reserves, one Geological Reserve (Kaali Meteorite Craters), one Nature Park and 53 locally protected areas, covering a total of 12% of the Estonian territory.

Decline in mining activities and the introduction of new technologies together with economic measures (resource charges, pollution taxes) inspire us with hope that the situation will improve in the nearest future.

References

Althausen, M. 1992: Vendian-Lower Paleozoic metalliferous black shales. – Oil Shale, 9, 3, pp. 194–207 (in Russian with English summary).

Geology of the Kukersite-bearing Beds of the Baltic Oil Shale Basin. 1986 – V. Puura (Ed.). "Valgus", Tallinn. 84 p. (in Russian with English and Estonian summaries).

Kivimägi, E., A. Teedumäe 1971: Result of a complex estimation of the rocks in the phosphorite deposit of Toolse. – Eesti NSV Teaduste Akadeemia Toimetised. Keemia, Geoloogia, 20, 3, pp. 243–250 (in Russian with English and Estonian summaries).

Luha, A. 1946: Mineral resources of the Estonian S.S.R. RK – "Teaduslik Kirjandus", Tartu. 180 p. (in Estonian).

National Report of Estonia to UNCED 1992 – (compiled by M. Lahtmets). Ministry of Environment, Republic of Estonia. Tallinn. 40 p.

Orru, M. 1987: How many bogs are there in Estonia? – Eesti Loodus, 10, pp. 646–652 (in Estonian with English and Russian summaries).

Paalme, G. 1993: Mineral resources. – Estonian Environment 1992 Environmental Report 6. Environmental Data Centre. National Board of Waters and Environment. Helsinki, pp. 11–15.

Puura, V.A., R.M. Vaher, V.M. Klein, H.J. Koppelmaa, M.I. Niin, V.V. Vanamb, J.E. Kirs 1983: The Crystalline Basement of Estonian territory. – "Nauka", Moscow. 208 p. (in Russian with English summary).

The Geology and Mineral Resources of the Rakvere Phosphorite Basin, 1987. (Ed. Puura). "Valgus", – Tallinn. 211 p. (in Russian with English and Estonian summaries).

The History of Geological Sciences in Estonia, 1986 (Ed. Viiding, Kaljo). – "Valgus", Tallinn, 360 p. (in Russian).

Raudsep, R. 1991: The biggest phosphorite deposit of Europe. – Bulletin of the Geological Survey of Estonia, 1–1, p. 39.

Raudsep, R., V. Räägel, L. Savitskaja, M. Orru, V. Kattai 1993. Estonia's Mineral Wealth. – Eesti Geoloogiakeskus, Tallinn. 64 p. (in Estonian).

Raukas, A. 1978: Pleistocene Deposits of the Estonian S.S.R. – "Valgus", Tallinn. 310 p. (in Russian with English and Estonian summaries).

Raukas, A. 1992: Applied Quaternary Geology in Estonia. – In: Glacial stratigraphy, engineering geology and earth construction (Ed. Kauranne). Geological Survey of Finland, Spec. Paper, 15, pp. 89–96.

Rôômusoks, A. 1983: The Bedrock Geology of Estonia. – "Valgus", Tallinn. 224 p. (in Estonian).

Teedumäe, A. 1988: Mineral Reserves Supply in the Estonian S.S.R. for the Manufacture of Construction Materials. – "Valgus", Tallinn. 43 p. (in Russian with English and Estonian summaries).

Viiding, H. 1985: Estonian Book of Primeval Nature. – Eesti Loodus, 3, pp. 138–145 (in Estonian with English and Russian summaries).

Viiding, H., A. Raukas 1984: Main Mineral Resources and Protection of Mineral Wealth. – In: Estonia. Nature, Man, Economy (Ed. Punning). Estonian Geographical Society, Tallinn, pp. 88–96.

Acta Geologica Hungarica, Vol. 37/3–4, pp. 369–374 (1994)

Bauxites of the Northern and Southern Ural Mountains as an additional source of scandium

Arnold Fedorovich Yeremeev,
Vladimir Nikolaevich Lavrenchuk
Kamensk-Uralsky, Russia

Earlier literature reported very low scandium contents from bauxite: 5–7 ppm (the clark value being 10 ppm). The values found by the authors by means of quantitative optical spectrography are higher by one order of magnitude: 80.4 ppm as the average of 53 samples of Northern Ural bauxites and 73.1 as the average of 29 samples of Southern Ural bauxite. Its positive correlation with the aluminium content has been stated. During the Bayer processing of bauxite, scandium goes into the red mud (up to 150–200 ppm), while during reductive melting it follows aluminium and titanium into the slag (up to 300–400 ppm). Therefore, it could be economically extracted from the dumped slags of the two Ural aluminium factories.

Key words: bauxite, scandium, Ural Mts

Introduction

It was repeatedly pointed out in the pertinent literature (Borisenko 1961, 1964; Schcherbina 1964 etc.) that bauxites represent an important source of scandium. However, this has been stated only in general terms. In addition, even nowadays the data published by Goldschmidt and Peters in 1939 are incorrectly cited. In fact, they had obtained low contents of scandium (Sc_2O_3 ≤ 5 ppm) not for the bauxites in general, but for eleven (11) samples from France, the USA, Dutch Guyana, and British Guyana. For the Arkansas bauxites, for instance, Gordon and Murata (1952) obtained a similarly low value: 6.9 ppm scandium as the average of 14 analyses of bauxites and bauxitic clays. The coefficient of enrichment (Ce), calculated in comparison to the nepheline syenites considered to be the source rock, is 2.1 ($C_eAl=2.7$).

According to the data obtained by the present authors, the content of scandium in the gibbsitic bauxites of the Arkalykh deposit of Kazakhstan is about 10 ppm, while in the diasporic-boehmitic bauxites of the Ural Mountains (Northern and Southern bauxite districts) it is higher by almost an order of magnitude.

The statement made by Goldschmidt and Peters that the scandium is removed during bauxite formation does not apply to all cases.

Addresses: A.F. Yeremeev, V.N. Lavrenchuk: Kamensk–Uralski, Sverdlov region Oktiabrskaya 75, kv. 6, 623417 Russia
Received 25 October, 1993

0236–5278/94/$ 5.00

Although there are scandium data published concerning the Northern Ural bauxite deposits (Gutkin 1968, 1970), they do not merit serious consideration, due to the small number of samples analysed and the specific exploration tasks they served.

Regularities of distribution

We have studied, on the basis of a sufficiently large factual basis, the distribution of scandium in the bauxites of the Northern and Southern Ural, in order to distinguish the possibility of its recovery during the industrial transformation of bauxite into alumina.

The bauxites of the Northern and the Southern Ural are mineralogically similar. Consequently, they are processed by means of very similar technologies, in the Ural Aluminium Factory and the Bogoslovo Aluminium Factory, respectively.

The Bayer-grade bauxites contain about 53.5 per cent alumina and 3.5 to 4 per cent silica. The sinter-grade bauxites contain 1 to 3 percent less alumina and 2 to 4 per cent more silica. In a paper dealing with beryllium (Lavrenchuk and Yeremeev 1979) we have shown that the Be/Al ratio indicates that the Northern Ural bauxites are genetically related to mafic rocks, and the Southern Ural bauxites to intermediary ones. The coefficients of enrichment for aluminium and beryllium are close to each other, within the range of 3.2–3.5.

The same procedure was used for the calculation of scandium enrichment.

According to Vinogradov (1949, 1962), the clark value of scandium is about 6–10 ppm. It had already been established by Eberhard in 1908 and it was confirmed by Goldschmidt and Peters in 1931 that "scandium is mainly an element of the mafic rocks".

The scandium content of mafic rocks is 24 ppm, according to Vinogradov (1962), and 30 ppm according to Turekian and Wedepohl (1961). The corresponding values for intermediary rocks are 25 and 14 ppm, respectively.

The considerable discrepancy may be due to the low level of geochemical knowledge about scandium.

For the calculation of the C_e we have adopted the data of Turekian and Wedepohl (Table 1). Since they are orientative only, the resulting C_e is, too.

The average scandium content of 53 samples of Northern Ural bauxite is 80.4 ppm, while that of 29 samples of Southern Ural bauxites 73.1 ppm. These values are rather high, and they suggest an enrichment of scandium concomitant with aluminium.

The Northern Ural bauxites, with alumina content up to 50 per cent (21 samples), have an average scandium content of 68.6 ppm. The $Sc.10^4/Al$ ratio is 3.00, the average of Al being 22.86 percent. With increasing alumina (over 50 per cent) the scandium content also increases. Their ratio stays virtually the same. The average values of 32 samples are 88.1 ppm scandium, 30.90 per cent aluminium, and $Sc.10^4/Al=2.85$.

Disregarding the samples which contain less than 5 percent CaO and FeS_2, the average values of 28 samples turned out to be 91.8 ppm scandium, 30.60 percent aluminium, and $Sc.10^4/Al=3.00$ (see Table 3).

Table 1
Scandium in the Uralian bauxites and in two types of possible source rocks. Scandium was determined by quantitative spectrometry (± 10–15 rel%), in the Polevo Laboratory of the Ural Regional Geological Direction.

	Northern Ural			Southern Ural		
	bauxites 53 samples	mafic rocks	C_e	bauxites 29 samples	intermediary rocks	C_e
Scandium, ppm	80.4	30	2.68*	73.1	14	5.22**
Sc_2O_3, ppm	123.3	46		112.1	21.5	
Aluminium, %	27.72	7.8	3.55	25.86	8.2	3.15
Alumina, %	52.39	14.74		48.88	15.50	
Sc 10^4/Al	2.90	3.85*		2.83	1.71	
Sc_2O_3/Al_2O_3	1/4250	1/3200		1/4360	1/7200	

* In case of 24 ppm scandium content in mafic rocks the C_e would be 3.35, i.e: very close to that of aluminium, and the Sc 10^4:Al ratio would be lowered to 3.08. Consequently, the Sc_2O_3/Al_2O_3 ratio would increase to 1:4000.

** This value seems a bit too high. It is possible that the scandium content of the source rocks differs significantly from the average given by Turekian and Wedepohl.

Table 2
Scandium in the Northern and Southern Ural bauxites in function of their alumina content and other components

	All 53 samples	Al_2O_3 <50 (21)	Al_2O_3 >50 (32)	FeS_2 <5 (36)	FeS_2 >5 (17)	CaO + FeS_2 <5 (28)
Northern Ural						
Sc, ppm	80.4	68.6	88.1	96.0	47.4	91.8
Al, per cent	27.72	22.86	30.90	29.72	23.32	30.60
Sc 10^4/Al	2.90	3.00	2.85	3.23	2.03	3.00
Southern Ural						
Sc, ppm	73.1 (29)	63.9 (14)	81.7 (15)			80.6 (18)
Al, per cent	25.86	21.73	29.71			28.05
Sc 10^4/Al	2.83	2.94	2.75			2.87

When the sample set was split into two groups (pyrite content less/more than 5 percent), it was found that the difference in scandium content is twofold, and in alumina only 6 per cent:

	FeS_2 less than 5 per cent (36 samples)	FeS_2 more than 5 per cent (17 samples)
Scandium, ppm	96.00	47.40
Al, per cent	29.72	23.32
Total Fe_2O_3, percent	18.15	15.04 (of which 11.45 in pyrite)
$Sc.10^4/Al$	3.23	2.03 (This last value needs to be checked on a larger set of samples.)

Table 3
Scandium in the Northern Ural bauxites with CaO and FeS_2 contents less than 5 per cent

Sample number	Al %	Sc ppm	Sc 10^4/Al	Sample number	Al %	Sc ppm	Sc 10^4/Al
6	22.65	70	3.09	69	30.88	100	3.24
34	25.54	80	3.13	1	30.99	85	2.74
38[a]	25.62	55	2.15	75	31.03	90	2.90
27[a]	25.86	110	4.25	127	31.23	105	3.36
37	26.70	100	3.75	115	31.54	85	2.69
131	27.95	85	3.04	82	31.78	110	3.46
42[a]	28.45	140	4.92	53	31.83	90	2.83
52	28.57	100	3.50	4	32.14	80	2.49
119	29.54	90	3.05	33[b]	32.19	85	2.64
59	30.52	70	2.29	56	33.85	80	2.36
113	30.63	85	2.78	129	36.29	120	3.31
27[b]	30.66	110	3.59	20	37.39	120	3.21
45	30.84	110	3.57	12	40.43	60	1.48
5	30.86	90	2.92				
97	30.87	65	2.11	Average (28)	30.60	92	3.00

If it is confirmed, it would mean that during the formation of high-grade bauxites scandium becomes partially separated from aluminium (on the whole, in the process of lateritic weathering, the behaviour of these two elements is virtually identical). Our data do not support the conclusion drawn by Terentieva (1959) that scandium in the bauxites is bound not to the aluminium, but to the ferrous iron and the magnesium present in the form of siderite and leptochlorites.

The Southern Ural bauxites display the same assemblages of elements and minerals as the Northern Ural ones. The generalized numerical data are presented in Table 2.

In a paper by Gipronickel the average scandium content was indicated as 24.4 ppm, in contrast to our 80 ppm. The data obtained from samples taken in different years from different deposits are rather divergent. In the deposits of the district, the scandium content ranges from 17.4 to 82.3 ppm. The average value of 24.4, however, seems to be too low.

The bauxites of the Northern and the Southern Ural represent, in our view, a valuable source of scandium. Their scandium content is 7–8 times higher than the clark value (10 ppm). It should be noted that the content of gallium, which is already being extracted from bauxites, is only 2.5–3 times higher than its clark value (19 ppm according to Vinogradov 1962). In absolute terms, one metric ton of Southern Ural bauxite contains twice as much scandium than gallium.

During the processing of bauxite the entire amount of scandium goes into the red mud, which shows scandium contents of up to 150–200 ppm. During reductive melting scandium follows titanium and aluminium into the slag. According to Zazubin et al. (1967) the scandium content of the slag is 1.9 times higher than that of the original red mud. Accordingly, the scandium content of the dumped slags of the Ural Aluminium Factory and the Bogoslovo Aluminium Factory might be 300 to 400 ppm.

We assume that such a considerable content of scandium is sufficient to make its recovery economically viable. Accordingly, the dumped slags of the two aluminium factories are genuine concentrates for the extraction of scandium.

Tsvetmetinformatsiya (1977) gives no information about the production of scandium in foreign countries. However, it is known that research is being conducted in this direction. In the USA there is a factory producing scandium metal and its compounds. The raw material for this factory is being imported.

For new technologies of the future, considerable amounts of scandium may be needed. This makes the investigation of the behaviour of this element and of its recovery from the red mud particularly important. The success of this task depends on the concentrated and co-operative efforts of all interested institutions.

References

Borisenko, L.F. 1961: Scandium (in Russian). – Ed. Ac. Sc. USSR, Moscow, 1961 Ed. Nauka, Moscow.

Borisenko, L.F. 1964: Scandium (in Russian). – In Geochemistry, mineralogy and genetical types of rare element deposits, Vol. 1, Ed. Nauka, Moscow,

Goldschmidt, V.M., K. Peters 1931: On the geochemistry of scandium (1938, in Russian). – Collection of papers on the geochemistry of rare elements, GONTI NKTP SSSR, Moscow–Leningrad.

Gordon, M. Jr., K.J. Murata 1952: Minor elements in Arkansas bauxite. – Economic Geology, 47, 2.

Gutkin, E.S. 1968: On the geochemistry of scandium in bauxites (in Russian). – Geokhimiya. 1,

Gutkin, E.S. 1970: Gallium, scandium, niobium and tantalum in the bauxites of the Northern Ural Basin (in Russian) - Litologiya i poleznye iskopaemye, 3.

Lavrenchuk, V.N., A.F. Yeremeev 1979: Beryllium in the diasporic-boehmitic bauxites of the Ural Mts (in Russian). – Geokhemiya, 2.

Schcherbina, V.V. 1964: Scandium in the sedimentary rocks. – In Metals in sedimentary formations, 3 (in Russian) Ed. Nauka, Moscow

Terentieva, K.F. 1959: Rare elements in bauxites (in Russian). – Geol. mestorozhd. redkykh elementov, 6. – Gosgeoltekhizdat, Moscow.
Turekian, K.K., Wedepohl, K.H. 1961: Distribution of the elements in some major units of the Earth's crust. – Bull. Geol. Soc. Amer., 72.
Vinogradov, A.P. 1962: Average concentrations of the chemical elements in the main types of eruptive rocks of the Earth's crust (in Russian). – Geokhimiya, 7.

ACTA GEOLOGICA HUNGARICA

Editor-in-Chief

J. Haas

Volume 37

ACTA GEOLOGICA HUNGARICA

Vol. 37

Contents

Numbers 1–2

Book review

Numbers 3–4

GUIDELINES FOR AUTHORS

Acta Geologica Hungarica is an English-language quarterly publishing papers on geological topics. Besides papers on outstanding scientific achievements, on the main lines of geological research in Hungary, and on the geology of the Alpine–Carpathian–Dinaric region, reports on workshops of geological research, on major scientific meetings, and on contributions to international research projects will be accepted.

Manuscripts are to be sent to the Editorial Office for refereeing, editing, in two typewritten copies, on floppy disk with two printed copies, or by E-mail. Manuscripts written by the following word processors will be accepted: MS Word, WordPerfect, or ASCII format. Authors are requested to sign and send to the Editor a Publishing Agreement after the manuscript has been accepted by the Editorial Board. Acceptance depends on the opinion of two referees and the decision of the Editorial Board.

Form of manuscripts

The paper complete with abstract, figures, tables, and bibliography should not exceed 25 pages (25 double-spaced lines with 3 cm margins on both sides).

The first page should include:

- the title of the paper (with minuscule letters)
- the full name of the author
- the name of the institution and city where the work was prepared
- an abstract of not more than 200 words
- a list of five to ten key words
- a footnote with the postal address of the author

The SI (System International) should be used for all units of measurements.

References

In text citations the author's name and the year of publication between brackets should be given. The reference list should contain the family name, a comma, the abbreviation of the first name, the year of publication, and a colon. This is followed by the title of the paper. Paper titles are followed – after a long hyphen – by periodical title, volume number, and inclusive page numbers. For books the title (English version), the name of the publisher, the place of publication, and the number of pages should be given.

Figures and tables

Figures and tables should be referred to in the text. Figures are expected in the size of the final type-area of the quarterly (12.6 x 18.6) or proportionally magnified 20–25% camera ready quality. Figures should be clear line drawings or good quality black-and-white photographic prints. Colour photographs will also be accepted, but the extra cost of reproduction in colour must be borne by the authors (in 1995 US$ 260 per page). The author's name and figure number should be indicated on the back of each figure. Tables should be typed on separate sheets with a number.

Proof and reprints

The authors will be sent a set of proofs. Each of the pages should be proofread, signed, and returned to the Editorial Office within a week of receipt. Fifty reprints are supplied free of charge, additional reprints may be ordered.

Contents